Lecture Note and Document

Of

434353 RESERVOIR ENGINEERING I

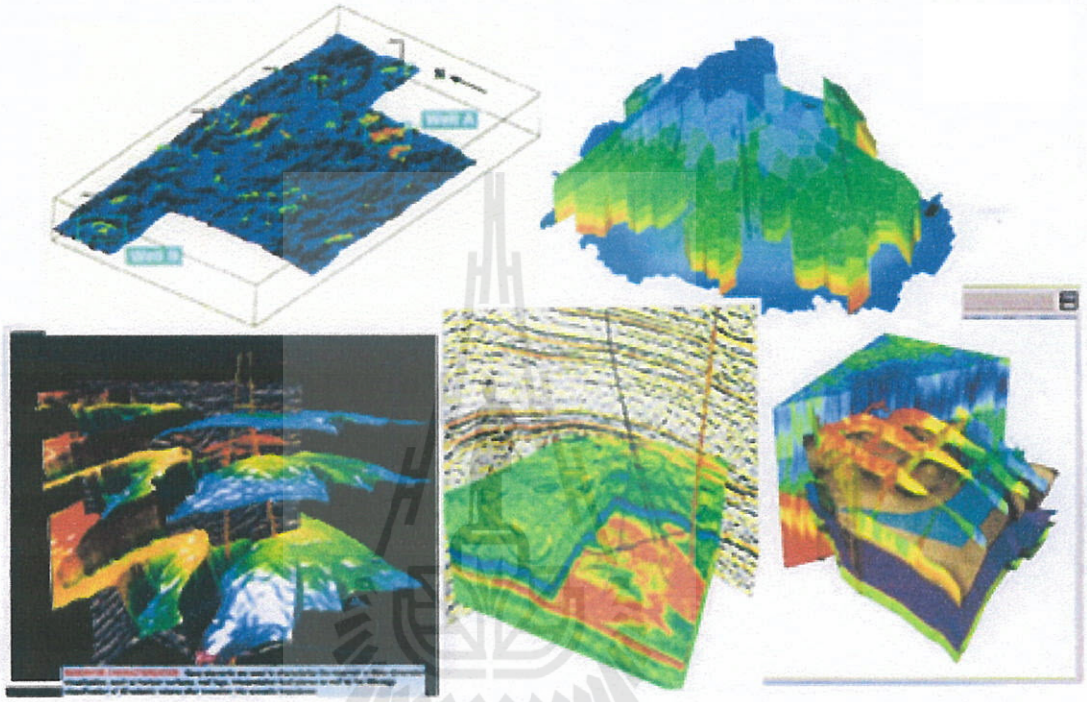

Prepared by

Kriangkrai Trisarn

Petroleum Engineering
School of Geotechnology
Institute of Engineering

434 353 PETROLEUM RESERVOIR ENGINEERING @ 2012(1/2555)

by Kriangkrai Trisarn

Course Contents

1. Introduction to Petroleum Geology (2 hrs.)
2. Rock and Fluid Properties (4 hrs.)
3. Reserve Estimation Methods (2 hr.)
4. Reservoir Volumetric (2 hrs.)
5. Material Balance & Drive Mechanism(2 hrs)
6. Gas Reservoir (4 hrs.)
7. Gas-Condensate Reservoir (6 hrs.)
8. Undersaturated Oil Reservoir (4 hrs.)
9. Saturated Oil Reservoir (4 hrs.)
10. Fluid Flow in Porous Media (6 hrs.)
11. Introduction to Well Testing(2 hrs)
12. Water Influx (4 hrs.)
13. The Displacement of Oil and Gas(2 hrs)

GRADING

Homework	20 %
Quiz I, II = 10+10 =	20 %
Mid-term	25 %
Final Exam	35 % by Kriangkrai Trisarn

TEXTS

1. CRAFT, B.C. and Hawkins, M.F. : ***Applies Reservoir Engineering,@1996 revised***, PRENTICE-HALL, INC., ENGLEWOOD, N.J.

REFERENCES

1. Gian Luigi Chierici, 1994 : Principles of Petroleum Reservoir Engineering., Springer-Verlag, New York ,1994.
2. NORMAN J. CLARK, : ***Element of Petroleum Reservoir.***, SPE,1969, Dallas, Texas.
3. J.S. ARCHER & C.G. WALL ,: ***Petroleum Engineering,*** Kluwer Academic Publishers 1996, Boston, USA.
4. Dr. CHARLES R. SMITH & G.M. TRACY : ***Applies Reservoir Engineering Manual,*** OGCI, INC., Tulsa, Oklahoma, USA.
5. M.A. MIAN : ***Petroleum Engineering*** Handbook for the Practicing Engineer. PennWell Books 1995, Tulsa, Oklahoma, USA.
6. Tarek Ahmed : ***RESERVOIR ENGINEERING HANDBOOK,@2006***, Gulf Publishing Company, Houston, Texas, USA.

Lecture Plan

1st week ; ***1. Introduction and Basic Petroleum Geology*** (2 hrs.)

2. Rock and Fluid Properties (2 hrs.)

- Rock Properties
- Fluid Properties

2nd week ; ***2. Rock and Fluid Properties***(2 hrs.)

- Rock Properties
- Fluid Properties

3. Reserve Estimations (2 hrs.)

- Volumetric.
- Material Balance
- Reservoir Performance
- Stochastic & Deterministic
- Reservoir Simulation

3rd week ; ***4. Reservoir Volumetric (4 hrs)***

- In-Place Volume,
- Areal Extent of resesrvoir, Structural Contour Map
- Rock Volume Estimation.
- Thickness Map, Isopach Map.
- Isoporosity, Isocapacity Maps.
- Hydrocarbon Pore Volume Maps
- Probabilistic, Stochastic & Deterministic
- Recovery Factors and Reserves.

4th week ; ***5. Material Balance & Drive Mechanism*** (3hrs)

- Drive Mechanism

Solution Gas(Depletion) Drive, Gas Cap Drive, Water Drive, and Combination Drive.

- Derivation of Material Balance Equation.
- Uses and Limitations of the Material Balance Method.
- The Havlena and Odeh Method of Applying The Material Balance Equation(as a straight-line equation)

5th week ; ***QUIZ NO.1***

6. Gas Reservoir (4 hrs.)

- Calculating Gas In Place by the Volumetric Method
- Calculation of Unit Recovery from Volumetric Gas Reservoir.
- Material Balance.
- The Gas Equivalent of Produced Condensate and Water
- Gas Reservoirs as Storage Reservoirs
- Abnormally Pressured Gas Reservoir.
- Limitations of Equations and Errors.

6th week ; *7. Gas Condensate(4 hrs.)*

- Mole Compositions and Other Properties.
- Calculation of Initial Gas and Oil(Condensate).
- The Performance of Volumetric Reservoir.
- Use of Material Balance
- Lean Gas Cycling and Water Drive
- Use of Nitrogen for Pressure Maintenance

7th week ; 7 *Gas Condensate cont.(2 hrs.)*

8. Undersaturated Oil Reservoir Fluid (2hrs.)

- Compositions and Other Properties.
- Calculation of Initial Oil In Place by Volumetric Method and Estimation of Oil Recoveries.
- Material Balance in Undersaturated Reservoirs.
- Calculations Including Formation and Water Compressibilities.

8th week 9 *Undersaturated Oil Reservoir Fluid (2hrs.*)

- Calculation of Initial Oil In Place by Volumetric Method and Estimation of Oil Recoveries.
- Material Balance in Saturated Reservoirs.
- Calculations Including Formation and Water Compressibilities.

9 th week ; *QUIZ NO 2*

10. Fluid Flow in Porous Media(3 hrs.)

- Darcy's Law and Permeability.
- The Classification of Reservoir Flow System.
- Steady State Flow System.

10th week ; *10 . Fluid Flow in Porous Media cont.(4 hrs..)*

- Development of the Radial Differential Equation.
- Transient flow Systems.
- Pseudosteady-State Flow System.
- Productivity Index(PI)
- Superposition.

11th week ; *11. Introduction to Well Testing*(3 hrs)

- Pressure Drawdown Testing.
- Pressure Buildup Testing.

12th week ; *12. The Displacement of Oil and Gas*(2 hrs)

- Microscopic Displacement Efficiency
- Relative Permeability.
- Macroscopic Displacement Efficiency.

RESERVOIR ENGINEERING I 2012

By Assoc. Prof. Kriangkrai Trisarn

CHAPTER I and II

1.Introduction to Petroleum geology.

2. Rock and Fluid Properties

How Does Plate Tectonics Contribute to the Creation of Oil?

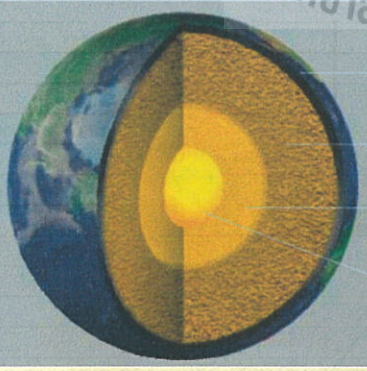

Structure of the Earth consists of

1.1.1 Lithosphere consists of rigid, solid rock from 65 to 100 km. thick and includes oceanic crust and continental crust in its upper layers and the uppermost part of the mental.(Fig. 1.1). SIMA (silicon and magnesium) and SIAL (silicon and aluminum) combine to form the crust, it has specific gravity of 2.6- 2.65.

1.1.2 Mantle is beneath the lithosphere and approximately 2900 km. thick and includes in its upper part the asthenosphere, which is about 200 km. thick. Temperature and pressure are balanced so that the asthenosphere is very near the melting point and can flow when subjected to stress. Iron and magnesium-bearing silicate mineral make up the mantle, which has a specific gravity of 4.5-5.0.

1.1.3 Core Iron and nickel (gravity of 10.5) are the predominant constituents of the core of the earth. The core is approximately 7,000 km. in diameter and consists of an outer liquid portion about 2,200 km thick and a solid inner core with the diameter of 2,600 km. Rotation of the earth is thought to create circulation currents within the liquid core that generate the magnetic field around the earth.

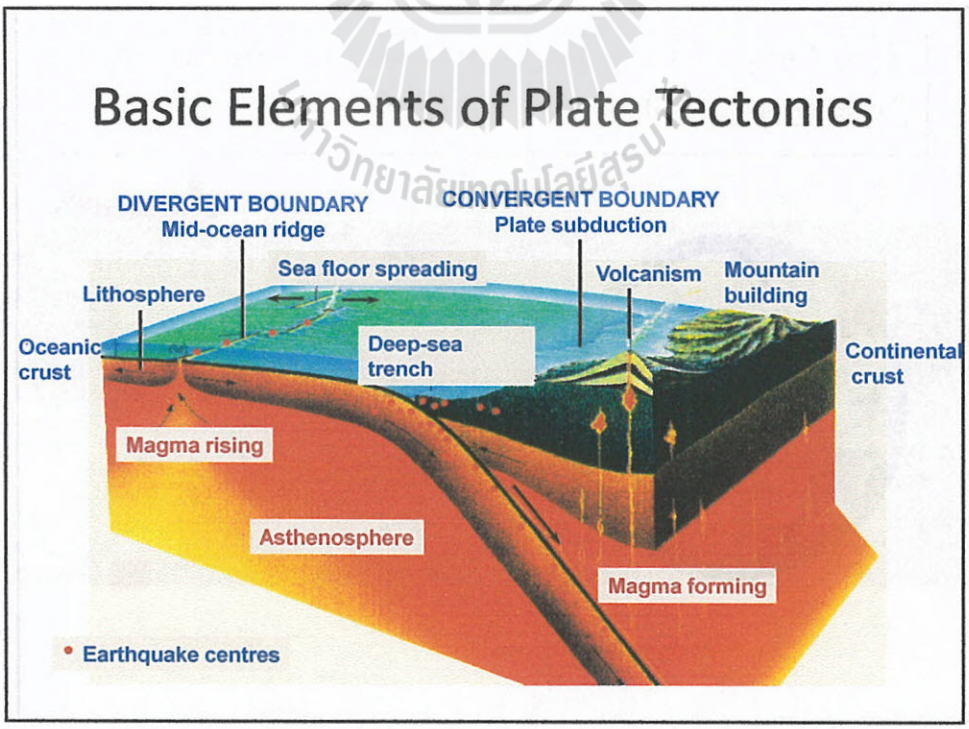

Causes of Continental Motion

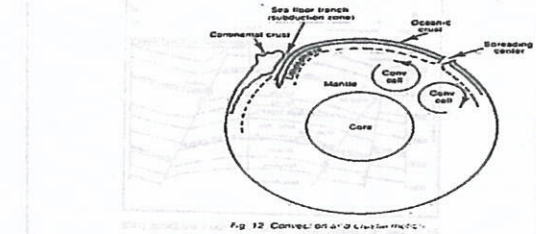

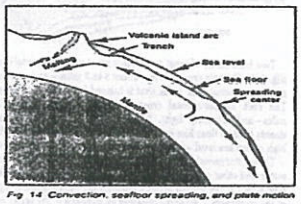

Fig. 14 Convection, seafloor spreading, and plate motion

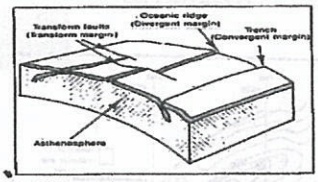

Fig. 20. Plate margins

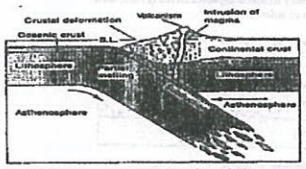

Fig. 21. Convergent trench continental margin

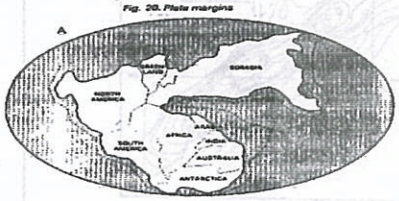

The relative positions of the continents are shown 200 million years ago (A) and today (B).

Continental & Plate Margin

- Divergent Continental Margins
- Convergent Continental Margins
- Transform Continental Margins

Fig. 1.4. Oceanic crust is thinner but heavier than continental crust.-

Two basic kinds of crust are *oceanic crust* and *continental crust* (fig. 1.4). Oceanic crust is thin—about 5 to 7 miles—and made up of heavy igneous rock (rock that is formed from cooled magma). The rock of continental crust, however, is thick—20 to 30 miles—and relatively light. Because of these differences, continents tend to float like icebergs in a "sea" of heavier rock, rising high above sea level where they are thickest—in the mountains.

These continental heights are gradually worn away by running water and other agents. Particles of rock are carried into the sea, where they are deposited in thick sedimentary beds along the edges of the continents. Cemented together by minerals in the water and by the pressure of more sediments deposited on top of them, these beds become layers of *sedimentary* rock.

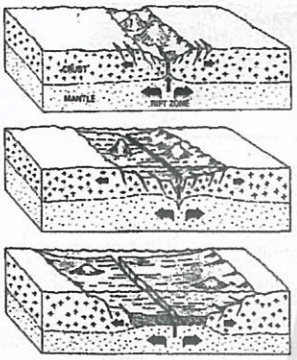

Fig. 1.5. Oceanic crust forms in the rift between two diverging plates.

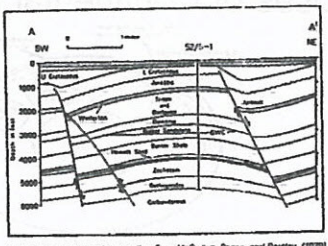

Fig. 27. Hewett Field, geologic section. From McQuillan, Bacon, and Barclay, (1970). Permission to publish by Graham & Trotman Limited.

USA

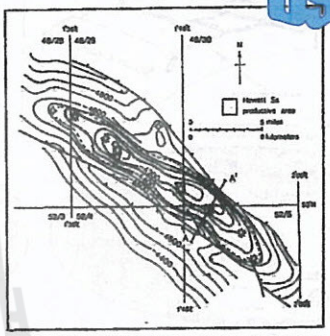

Fig. 28. Hewett Field, structure map on Hewett Sandstone. From McQuillan, Bacon, and Barclay, (1970). Permission to publish by Graham & Trotman Limited.

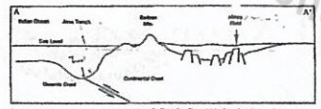

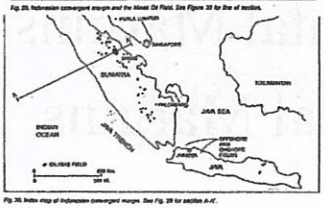

Figure 1.4 Convergent Margins

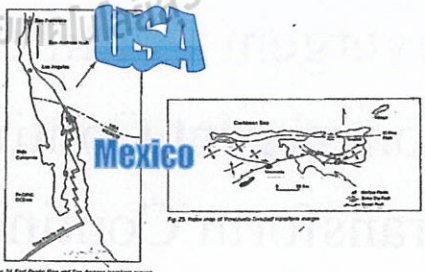

USA

Figure 1.5 Transform Margins

Venezuela

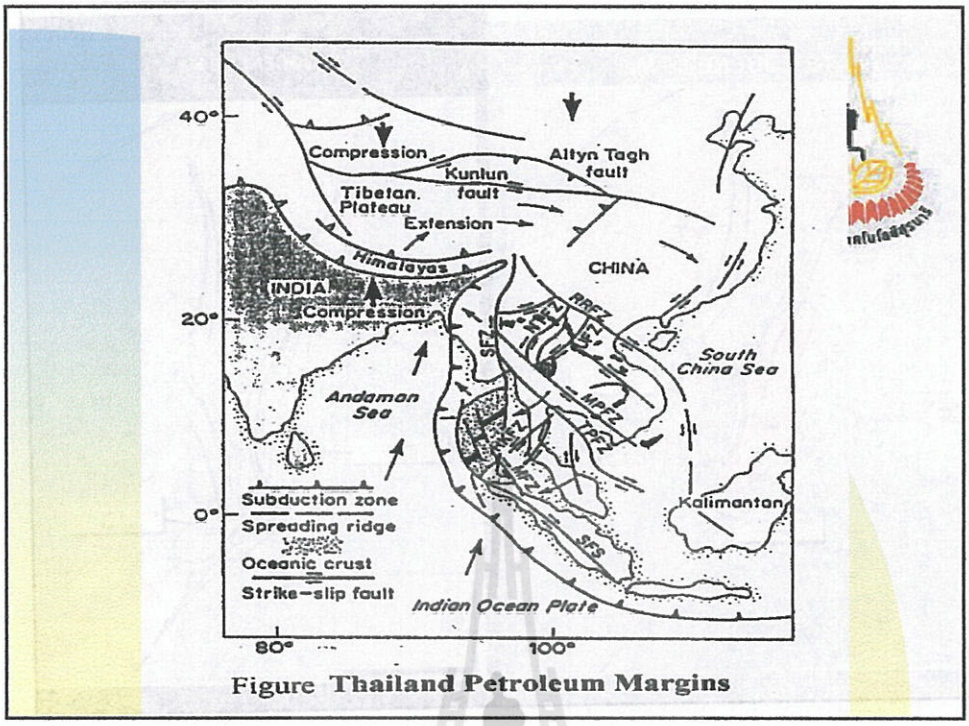

Figure Thailand Petroleum Margins

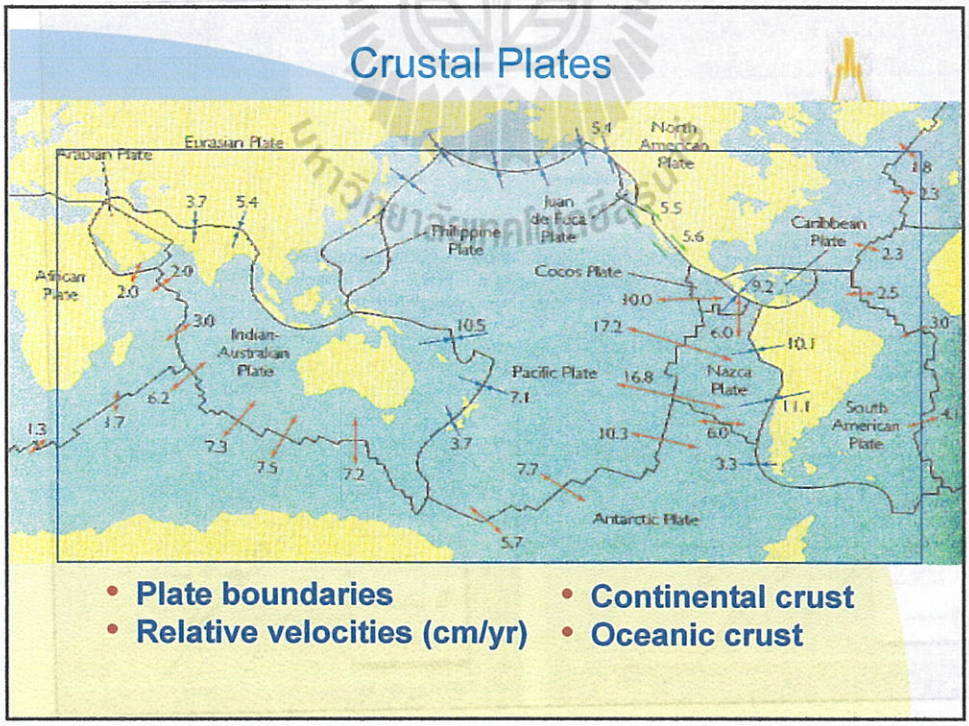


ANDAMAN SEA
LATE EOCENE 38 Ma
SHAN PLATE
BURMAN PLATE
INDIAN PLATE
SHALLOW SAG
KHLONG MARUI FAULT
SUNDA CRATON MAGIN
ANDAMAN SEA
OLIGOCENE 30 Ma
BURMAN PLATE
SHAN PLATE
PLATE ROTATION
INDIAN PLATE
SLOW
LATE OLIGOCENE REEFS
MERGUI & NORTH SUMATRA BASINS
Volcanics

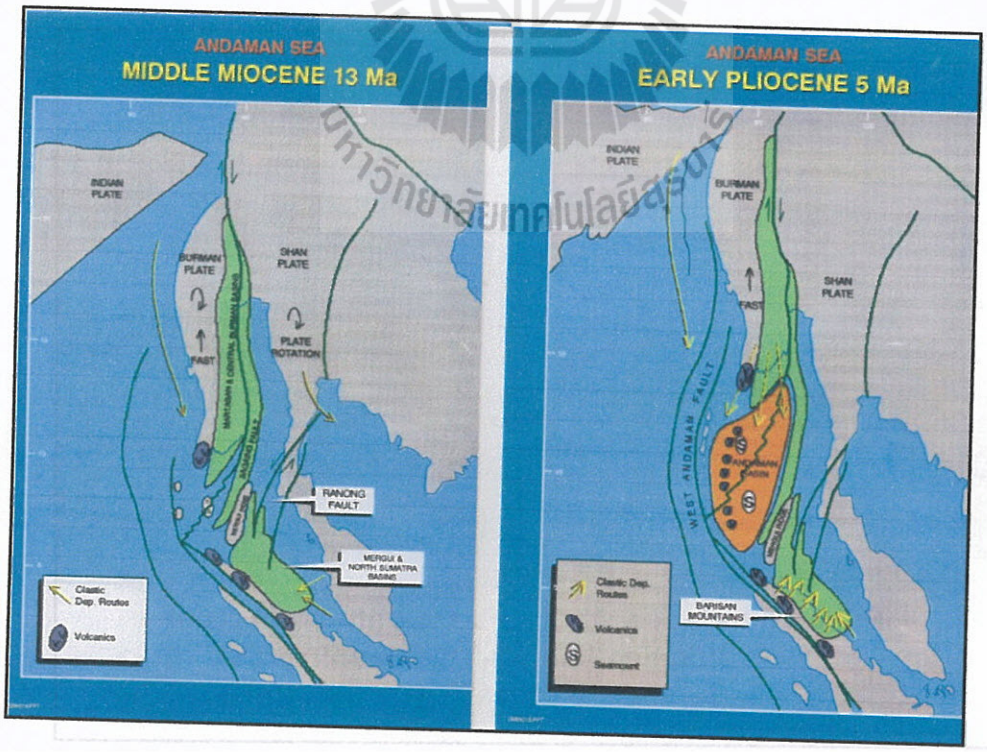
ANDAMAN SEA
MIDDLE MIOCENE 13 Ma
INDIAN PLATE
BURMAN PLATE
SHAN PLATE
FAST
PLATE ROTATION
RANONG FAULT
MERGUI & NORTH SUMATRA BASINS
Clastic Dep. Routes
Volcanics
ANDAMAN SEA
EARLY PLIOCENE 5 Ma
INDIAN PLATE
BURMAN PLATE
SHAN PLATE
FAST
WEST ANDAMAN FAULT
ANDAMAN BASIN
Clastic Dep. Routes
Volcanics
Seamount
BARISAN MOUNTAINS

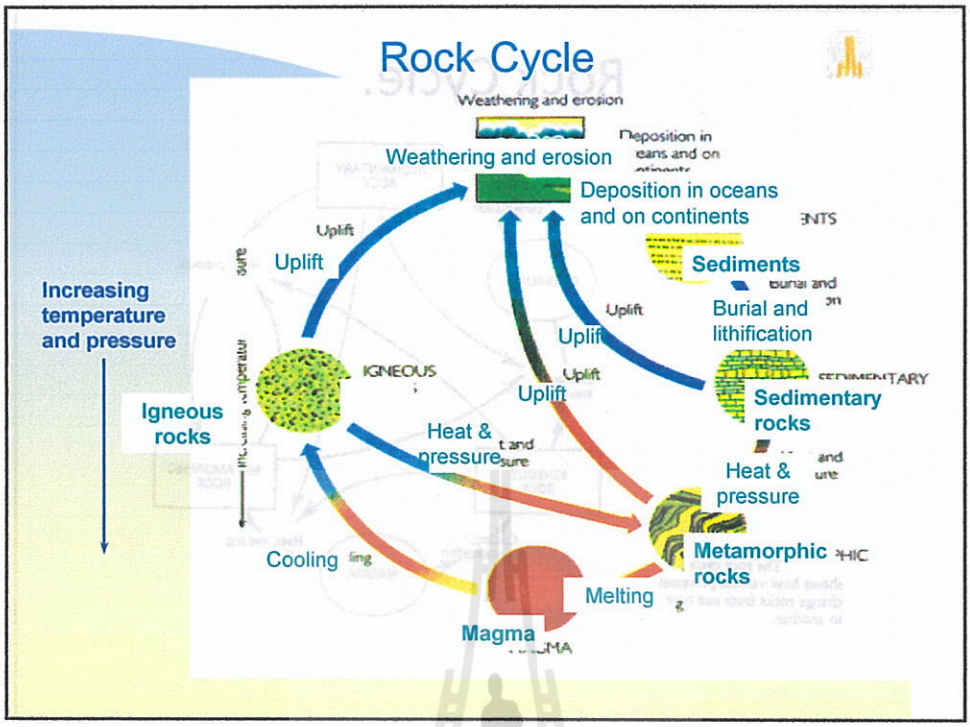
Rock Cycle
Weathering and erosion
Deposition in oceans and on continents
Sediments
Burial and lithification
Sedimentary rocks
Heat & pressure
Metamorphic rocks
Melting
Magma
Cooling
Uplift
Igneous rocks
Increasing temperature and pressure

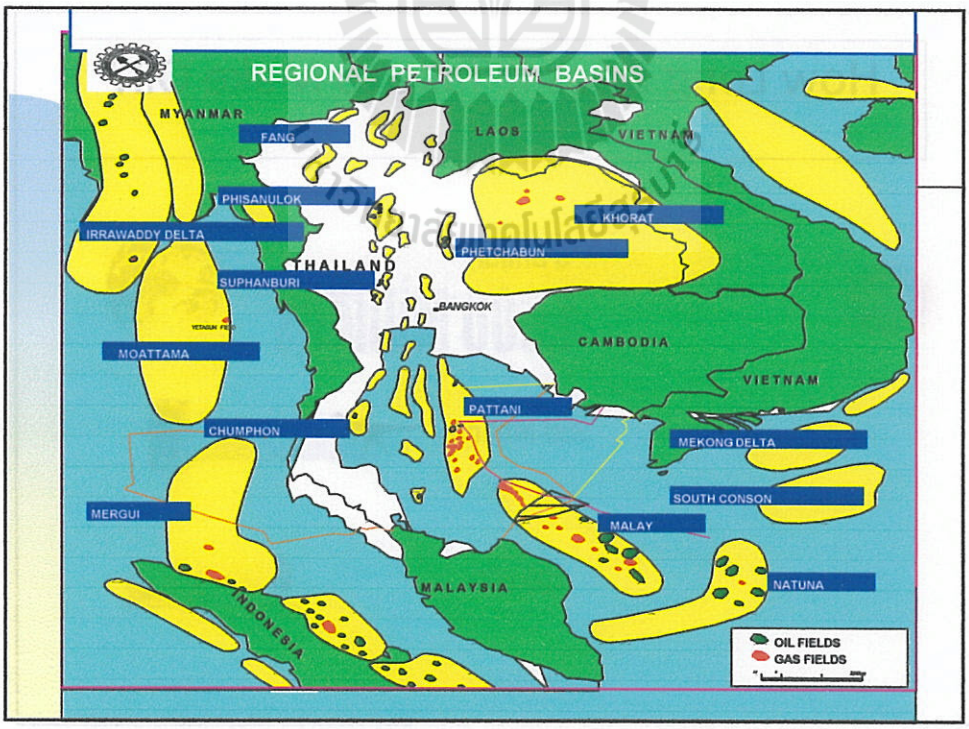
REGIONAL PETROLEUM BASINS
MYANMAR
FANG
LAOS
VIETNAM
PHISANULOK
KHORAT
IRRAWADDY DELTA
PHETCHABUN
THAILAND
SUPHANBURI
BANGKOK
CAMBODIA
MOATTAMA
VIETNAM
PATTANI
CHUMPHON
MEKONG DELTA
SOUTH CONSON
MERGUI
MALAY
MALAYSIA
NATUNA
INDONESIA
OIL FIELDS
GAS FIELDS

Rock Cycle.

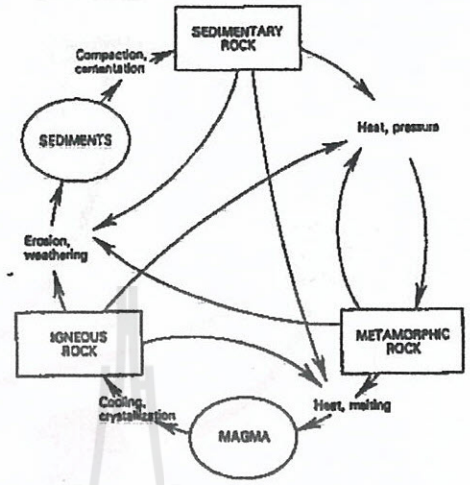

. The rock cycle shows how various processes change rocks from one type to another.

How Long Does It Take to Make Oil?

Geologic Time Scale - Biostratigraphy

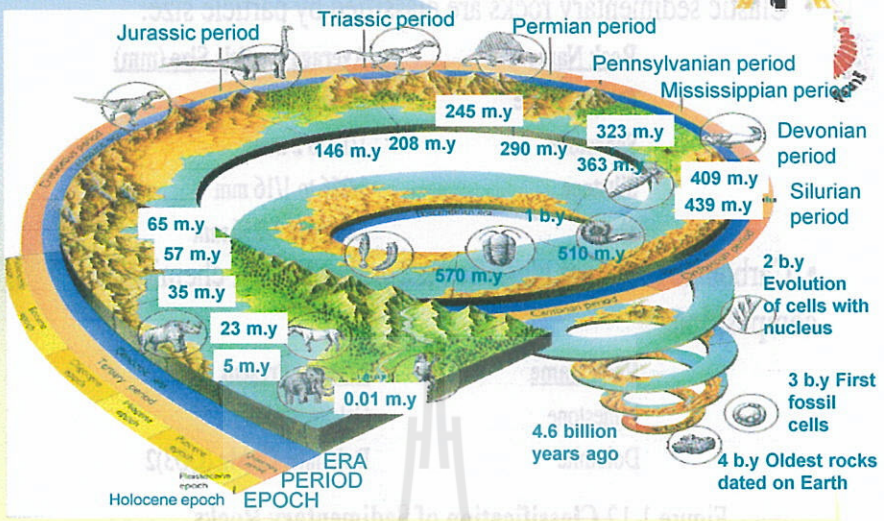

Classification of Rocks

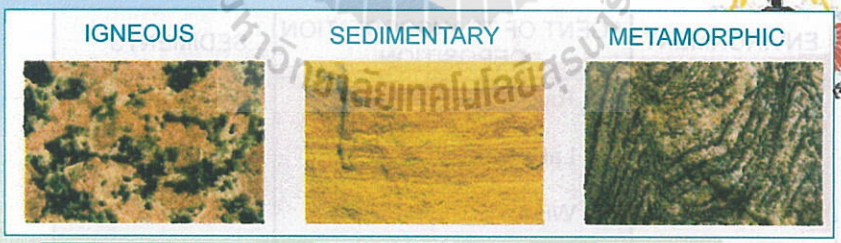

	IGNEOUS	SEDIMENTARY	METAMORPHIC
Source of material	Melting of rocks in hot, deep crust and upper mantle	Weathering and erosion of rocks exposed at surface	Rocks under high temperatures and pressures in deep crust
Rock-forming process	Crystallization (Solidification of melt)	Sedimentation, burial and lithification	Recrystallization in solid state of new minerals

Classification of SEDIMENTARY Rocks

- Clastic sedimentary rocks are classified by particle size:

Rock Name	Average Particle Size (mm)
Conglomerate	Greater than 2mm
Sandstone	1/16 to 2 mm
Siltstone	1/256 to 1/16 mm
Shale	Less than 1/256 mm

- Carbonate rocks are classified according to their chemical composition:

Rock Name	Mineral Present
Limestone	Calcite, $CaCO_3$
Dolomite	Dolomite, $Ca\,Mg\,(CO_3)_2$

Figure 1.12 **Classification of Sedimentary Rocks**

Clastic Sedimentary Environments

ENVIRONMENT	AGENT OF TRANSPORTATION DEPOSITION	SEDIMENTS
Alluvial	Rivers	Sand, gravel, mud
Lake	Lake currents, waves	Sand, mud
Desert	Wind	Sand, dust
Glacial	Ice	Sand, gravel, mud
Delta	River + waves, tides	Sand, mud
Beach	Waves, tides	Sand, gravel
Shallow shelf	Waves, tides	Sand, mud
Deep sea	Ocean currents, settling	Mud

Classification of SEDIMENTARY Rocks

- Clastic sedimentary rocks are classified by particle size:

Rock Name	Average Particle Size (mm)
Conglomerate	Greater than 2mm
Sandstone	1/16 to 2 mm
Siltstone	1/256 to 1/16 mm
Shale	Less than 1/256 mm

- Carbonate rocks are classified according to their chemical composition:

Rock Name	Mineral Present
Limestone	Calcite, CaCO3
Dolomite	Dolomite, Ca Mg (CO3)2

Figure 1.12 **Classification of Sedimentary Rocks**

Clastic Sedimentary Environments

ENVIRONMENT	AGENT OF TRANSPORTATION DEPOSITION	SEDIMENTS
Alluvial	Rivers	Sand, gravel, mud
Lake	Lake currents, waves	Sand, mud
Desert	Wind	Sand, dust
Glacial	Ice	Sand, gravel, mud
Delta	River + waves, tides	Sand, mud
Beach	Waves, tides	Sand, gravel
Shallow shelf	Waves, tides	Sand, mud
Deep sea	Ocean currents, settling	Mud

The Origin of Sedimentary Rocks

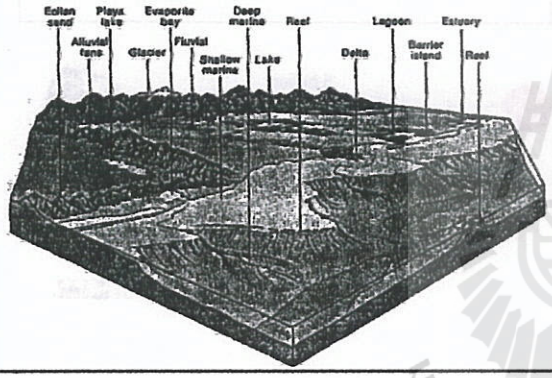

Origin of Petroleum

Figure 1.15
—*Sources of organic material.*

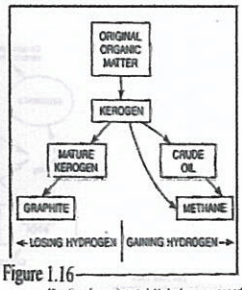

Figure 1.16
Alteration of organic material to hydrogen-poor and hydrogen-rich compounds. From Barker, 1979. Permission to publish by AAPG.

Kerogen Types

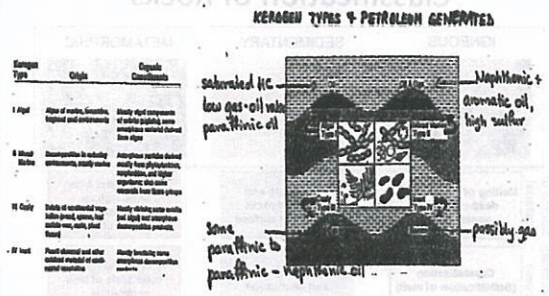

Figure 1.17 Kerogen types, Origin , and Organic Constituents

1. *Source* : material from which oil is formed, and matured.
2. *Reservoir rocks*: porous and permeable beds in which the petroleum may migrate and accumulate after being formed.
3. *Migration path*: connecting source rock to reservoir rock.
4. *Traps*: subsurface condition restricting further movement of oil and gas such that it may accumulate in commercial quantities.(as the following figures)

Figure 2.1 Requirements for Commercial Petroleum Accumulations

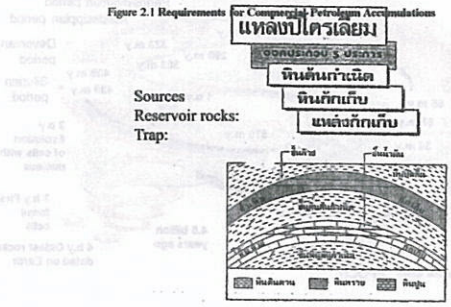

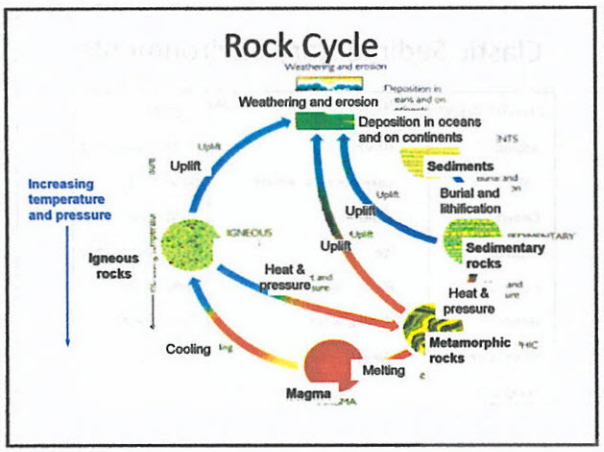

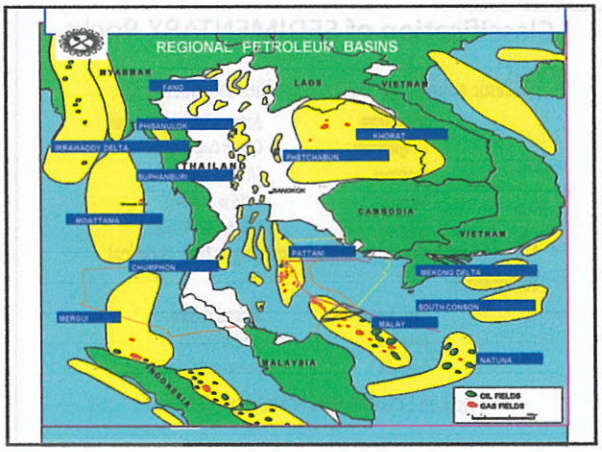

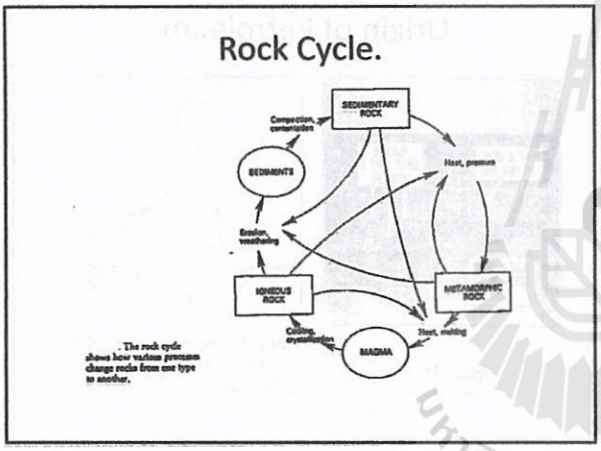

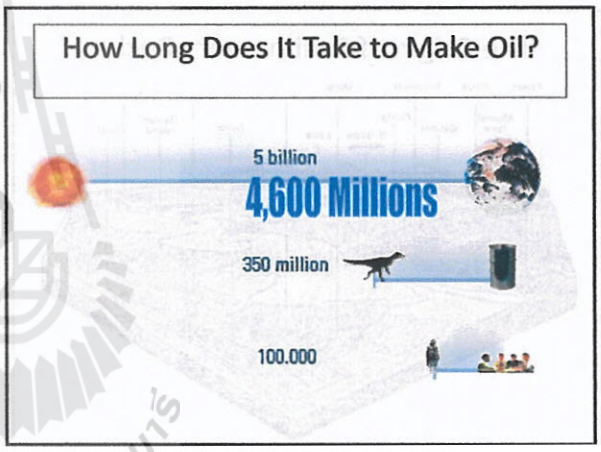

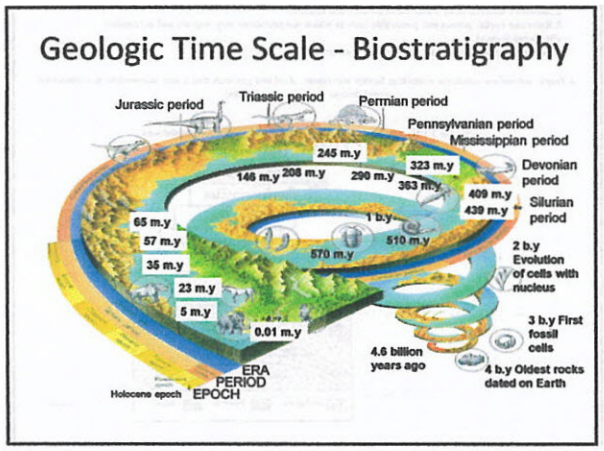

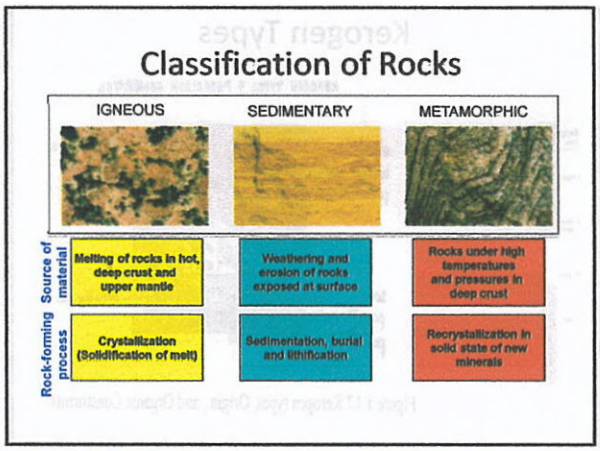

Reservoir Fluid Properties

1. *Paraffins* ; which have the general formula C_nH_{2n+2}. These chemical compounds are chemically stable and have either straight and branched chains.

2. *Naphthenes* (Cycloparaffins) having the general formula C_nH_{2n}. These compounds have a rings structure as shown in the following figure.

3. *Aromatics*(Benzene series) having the general formula C_nH_{2n-6}. These compounds are chemically active and contain the benzene ring

In addition to hydrocarbons, petroleum may contain numerous impurities such as carbon dioxide , hydrogen sulfide, and other complex compounds of nitrogen, sulphur, and oxygen.

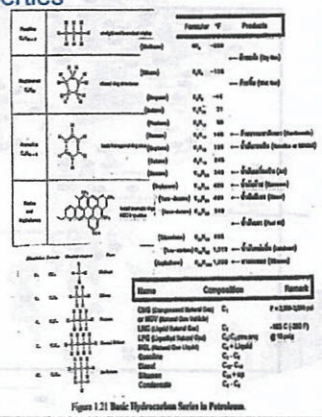

Figure 1.21 Basic Hydrocarbon Series in Petroleum.

Hydrocarbon Maturation

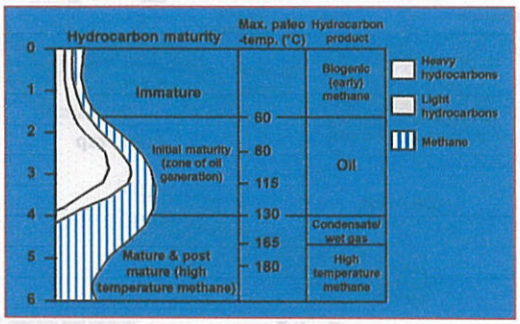

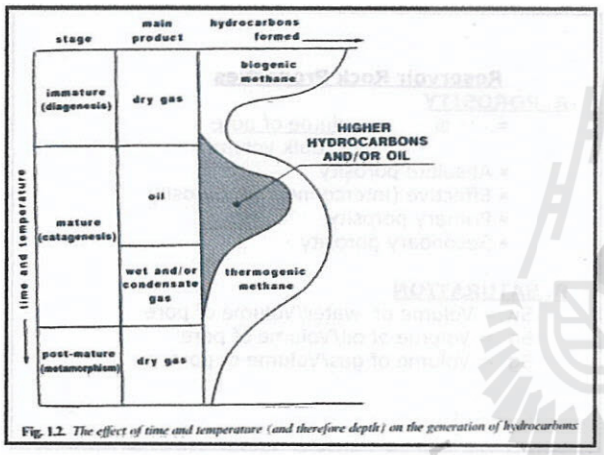

Fig. 1.2. *The effect of time and temperature (and therefore depth) on the generation of hydrocarbons*

Origin of Natural Gas

The major sources of the hydrocarbon gases are

(1) METHANOGENETIC BACTERIA
(2) ALL TYPES OF KEROGENS
(3) COAL
(4) OIL IN SOURCE AND RESERVOIR ROCKS

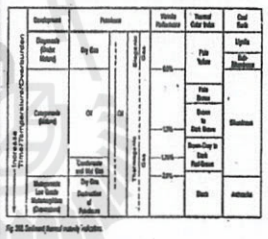

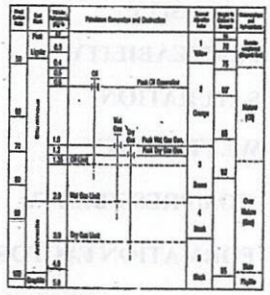

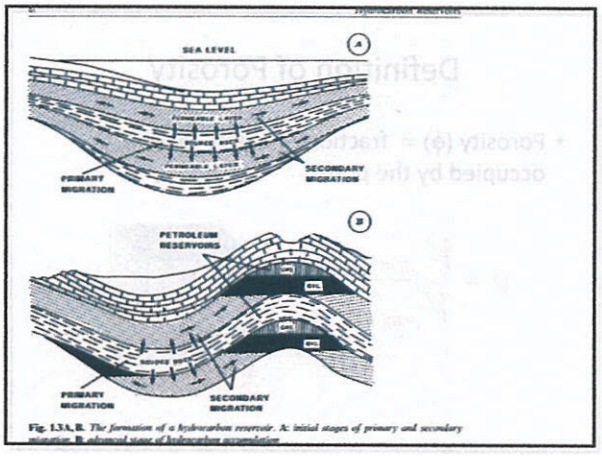

Fig. 1.3 A, B. *The formation of a hydrocarbon reservoir. A: initial stages of primary and secondary migration. B: advanced stage of hydrocarbon accumulation*

From Source to Reservoir

SOURCE ➡ **MIGRATION** ➡ **RESERVOIR**

- Rock Types
  - Shales 65%
  - Carbonates 21%
  - Marl 12%
  - Coal 2%
- Compaction
- Aquathermal pressure
- Buoyancy
- Hydrodynamic regime
- Rock Types
- Porosity
- Permeability

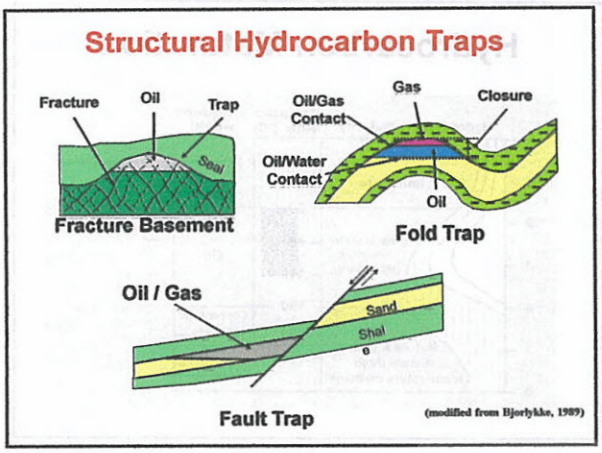

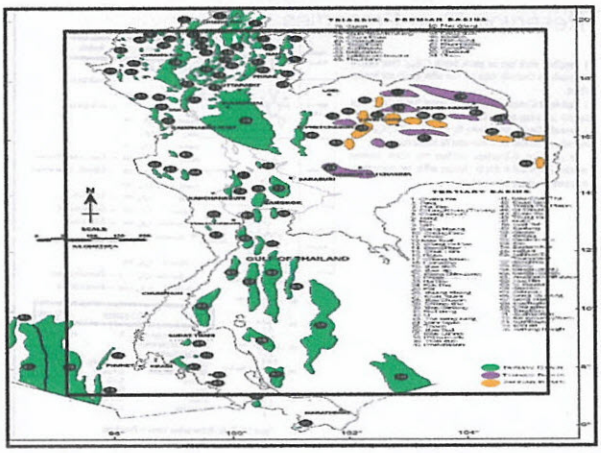

1.11 Reservoir ROCK PROPERTIES

- POROSITY
- PERMEABILITY
- SATURATION
- WETTABILITY
- COMPRESSIBILITY
- FORMATION FACTOR

Reservoir Rock Properties

A. POROSITY

= φ = volume of pore / Bulk volume

- Absolute porosity
- Effective (interconnected) porosity
- Primary porosity
- Secondary porosity

B. SATURATION

Sw = Volume of water/Volume of pore
So = Volume of oil/Volume of pore
Sg = Volume of gas/Volume of pore

1. Porosity
   - A. Absolute porosity
   - B. Effective porosity
1. Primary porosity
2. Secondary porosity

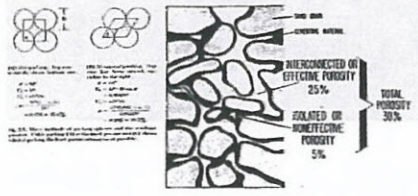

Figure 1.18 Effective, non-effective and total porosity

Definition of Porosity

- Porosity (ϕ) = fraction of a unit volume occupied by the pores

$$\phi = \frac{V_{fluid}}{V_{total}}$$

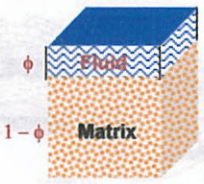

Porosity

- Porosity depends on grain packing, not grain size
- Rocks with different grain sizes can have the same percentage porosity

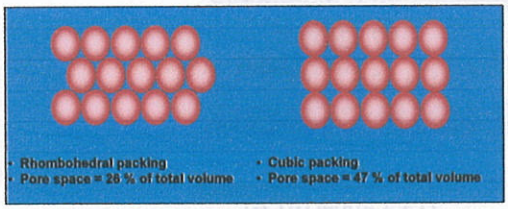

Fluid Saturation

- Fluid saturation is defined as the fraction of pore volume occupied by a given fluid

$$saturation = \frac{V_{specific\ fluid}}{V_{pore\ space}}$$

Definitions

S_w = water saturation

S_o = oil saturation

S_g = gas saturation

S_h = hydrocarbon saturation = $S_o + S_g$

Permeability

- The rate of fluid flow through a reservoir depends on
  - –Pressure drop
  - –Fluid viscosity
  - –Permeability
- Permeability is a measure of the ease at which a fluid can flow through the reservoir
  - –Large grains lead to high permeability and large flow rates
  - –Small grains lead to low permeability and small flow rates
- Permeability and porosity are related

Darcy's Law

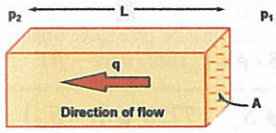

$$k = \frac{q\mu}{A} \bullet \frac{L}{(p_1 - p_2)}$$

k = permeability (measured in darcies)

L = length
q = flow rate
P_1, P_2 = pressures
A = surface area
μ = viscosity

Figure 1.24 **Permeability**

Q = Rate of Flow, cc/sec.
ΔP = Pressure Differential, Atmospheres
A = Area, cm^2
μ = Fluid Viscosity, Centipoise
L = Length, cm
K = Permeability, Darcies

$$Q = \frac{K\Delta PA}{\mu L}$$

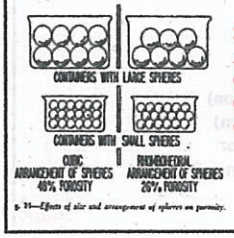

Size + shape
Arrangement
Compaction
Cementation
Grain kind

C. PERMEABILITY $K = \frac{Q\mu\Delta L}{A\Delta P}$

- Absolute one fluid phase in pore = k = 413 md ; k_w @ S_w = 1.0 or k_o @ S_o = 1.0
- Effective 2-3 phases in pore; k_{ew} @ S_w = 0.7, k_{ew} = 248 md, k_{eo} =50 md.
- Relative: Krw =  .Kro = 

D. WETTABILITY

- Water wet
- Oil wet

E. FORMATIOM COMPRESSIBILITY

Cf = $1.87 \times 10^{-6} \times \phi^{-0.415}$ by Hall Humble

$= -\left(\frac{1}{V}\right)\left(\frac{dV}{dp}\right)$

F. FORMATION FACTORS

$F = Ro/Rw = a/\phi^m$

Rock Properties

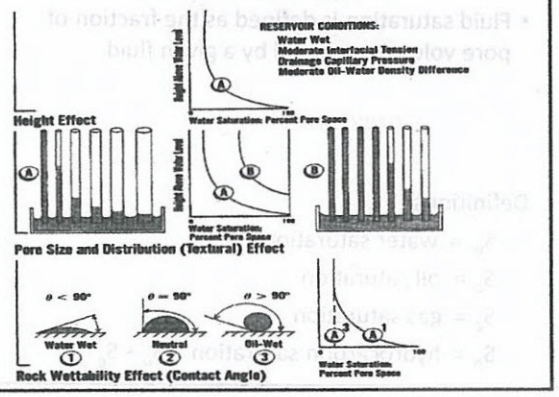

E. FORMATIOM COMPRESSIBILITY

Cf = $1.87 \times 10^{-6} \times \phi^{-0.415}$ by Hall Humble

$$C_f = -\left(\frac{1}{V}\right)\left(\frac{dV}{dp}\right)$$

Consolidated Sandstone

$$C_f = \frac{97.32(10)^{-6}}{(1+55.8721\phi)^{1.42859}}$$

Limestone

$$C_f = \frac{0.853531}{(1+2.4664(10)^6\phi)^{0.9299}}$$

1 acre ≡ 43,560 ft

1 acre-ft = 43,560 ft

1 bbl = 42 gal = 5.61 cu ft

1 acre-ft = $\frac{43,560}{5.61}$ = 7758 bbl

It is then obvious that the pore space within a rock is equal to

$$7758 \times \phi = V_p\,(bbl/acre-ft)$$

where ϕ = porosity of the rock in question. Further reasoning as shown by Figure 2.6 results in the well-known Volumetric Equation of Oil in Place:

$$N = \frac{7758\ \phi\ S_o}{B_o} = \frac{7758\ \phi\ (1-S_w)}{B_o}$$

where

N = Tank oil in place, bbl/acre-ft

S_o = Fraction of pore space occupied by oil (the oil saturation)

S_w = The water saturation

B_o = The formation volume factor for the oil at the reservoir pressure barrels reservoir space/barrel tank oil.

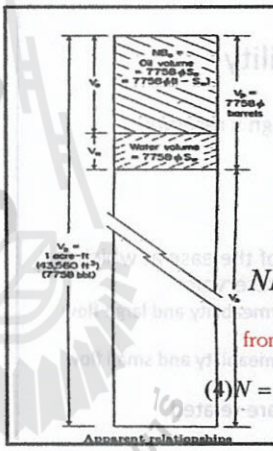

$$(1) S_o = \frac{V_o}{V_p}$$

$$(2) S_w = \frac{V_w}{V_p}$$

$$\Big\} S_o + S_w = 1$$

$$(3) V_o + V_w = V_p$$

or

$$NB_o + 7758\ \phi\ S_w = 7758\ \phi$$

from which

$$(4) N = \frac{7758\ \phi\ (1-S_w)\ barrels/acre-ft}{B_o}$$

Reserves Estimation Methodology

Volumetric Calculation

Reserves = Bulk Volume . ϕ . So . Bo . Rf

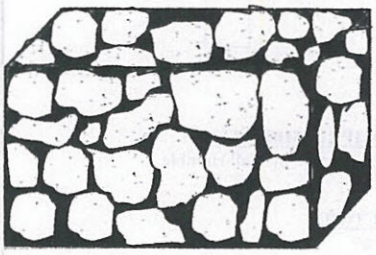

ϕ = Porosity

So = Saturation

Bo = Volume Factor

Rf = Recovery Factor

Volumetric Estimates

- Reserves = Reservoir Volume x Porosity x Oil Saturation x Recovery Factor x Shrinkage to Surface Conditions
- In oilfield units:

Reserves = [7758 x A x h x ø x (1-S_w) x R]/Bo

where Or 43560 for gas or Bg

- 7757 = bbls/acre-ft
- A = area (sq. ft) or Acre
- h = net thickness (ft)
- ø = porosity (fraction)
- S_w = water saturation (fraction)
- R = recovery factor (fraction)
- Bo = formation volume factor
- Bg = Gas formatiom volume factor

Reservoir Fluid Properties

- KEOGEN TYPES & PETROLEUM GENERATED
- TYPE I Saturated HC + low gas – oil Ratio paraffinic oil
- TYPE II Naphthenic + aromatic oil high sulfur
- TYPE III Some Paraffinic to Paraffinic – napthenic oil
- TYPE IV Possibly gas

GAS PROPERTIES,

1.GAS LAW
- PV = nzRT
- PVT or PHASE Diagram

2. GAS DENSITY
- SG = Molecular Wt./ 28.97(air = 1)
- Density = M.W.* P/(z*R*T)

3. GAS COMPRESSIBILITY FACTOR

4..GAS FORMATION VOLUME FACTOR

$$B_g = \frac{V_{Reservoir}}{V_{Std.Cond.}}$$

= 0.02829 z*T/P cu.ft./SCF
= 0.00504 z*T/P bbl/SCF
= 35.35 P/(z*T) SCF/cu.ft.
= 198.4 P/(z*T) SCF/bbl.

5. GAS COMPRESSIBILITY

6. GAS VISCOSITY μ_g

7. STANDARD CONDITION
P = 14.7 psia, t = 60° F

8.GAS Gradient

$$P_{ws} = P_{wh} e^{\frac{0.1875*SG*D}{Z_{avg}T_{avg}}} \approx 0.25*\frac{P_{wh}}{100}\frac{D}{100}$$

8.DRY GAS (CH_4> 90%), WET GAS

9.SOUR GAS(H2S, CO2, NO2), SWEET GAS

10. HEATING VALUE

11.THERMODYNAMIC PROPERTY

IDEAL GAS LAW

Pressure-Volume-Temperature (PVT) behavior of gases are called ***Equations of State.***

$$p*V = n*R*T$$

where,
p is absolute pressure (psia) (P1*V1/T1)=(P2*V2/T2)
V is total volume, cubic feet
n is moles, lb- moles(pound-moles)
T is absolute temperature in degree Rankine(460+°F)
R is gas constant = 10.73

From Boyle's and Charles's laws,

REAL GAS LAW

$$p*V = z*n*R*T$$

(P1*V1/Z1*T1)=(P2*V2/Z2*T2)

Supercompressibility Factor, usually shortened to the ***Compressibility Factor***, or Gas ***Deviation Factor.***

Phase Behavior PVT Diagram

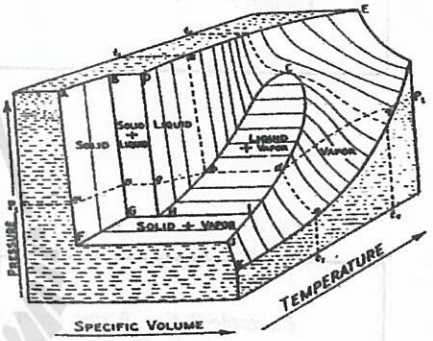

PSEUDOCRITICAL PROPERTIES

Fig. 2.3. Pressure-temperature phase diagram of a reservoir fluid.

IDEAL GAS LAW

$$p*V = n*R*T$$

where,
p is absolute pressure (psia)
V is total volume, cubic feet
n is moles, lb- moles(pound-moles)
T is absolute temperature in degree Rankine(460+°F)
R is gas constant = 10.73

The ideal gas law was developed from Boyle's and Charles's laws, which were formed from experimental observations.

The petroleum industry works with a set of Standard Conditions—usually 14.7 psia and 60°F. When a volume of gas is reported at these conditions, it is given the units of SCF(standard cubic feet). Sometimes the letter *M* will appear in the units, e.g *MCF* or *MSCF*, this refers to *1,000* standard cubic feet.

Example 1.1. Calculating the contents of a tank of ethane in moles.

Initial condition:

$$p = p_i \text{ for all values of } r$$

Outer boundary condition:

For an infinite aquifer:

$$p = p_i \text{ at } r = \infty$$

For a finite aquifer:

$$\frac{\partial p}{\partial r} = 0 \text{ at } r = r_e$$

this point, we rewrite the diffusivity equation in terms of the following dimensionless parameters:

$$\text{Dimensionless time: } t_D = 0.0002637\frac{kt}{\phi\mu c_t r_R^2} \tag{8.6}$$

$$\text{Dimensionless radius: } r_D = \frac{r}{r_R}$$

$$\text{Dimensionless pressure: } p_D = \frac{p_i - p}{p_i - p_{wf}}$$

where k = average aquifer permeability, md; t = time, hours; ϕ = aquifer porosity, fraction; μ = water viscosity, cp; c_t = aquifer compressibility, psi^{-1}; r_R = reservoir radius, feet. With these dimensionless parameters, the diffusivity equation becomes:

$$\frac{\partial^2 p_D}{\partial r_D^2} + \frac{1}{r_D}\frac{\partial p_D}{\partial r_D} = \frac{\partial p_D}{\partial t_D} \tag{8.7}$$

van Everdingen and Hurst converted their solutions to dimensionless, cumulative water influx values and made the results available in a convenient form here given in Tables 8.1 and 8.2 for various ratios of aquifer to reservoir size, expressed by the ratio of their radii, r_e/r_R. Figures 8.7 to 8.10 are plots of some of the tabular values. The data are given in terms of dimensionless time, t_D, and dimensionless water influx, W_D, so that one set of values suffices for all aquifers whose behavior can be represented by the radial form of the diffusivity equation. The water influx is then found by using Eq. (8.8):

$$W_e = B'\Delta p W_D \tag{8.8}$$

where

$$B' = 1.119\phi c_t r_R^2 h\frac{\theta}{360} \tag{8.9}$$

B' is the water influx constant in barrels per pounds per square inch and θ is the angle subtended by the reservoir circumference, (i.e., for a full circle, $\theta = 360°$ and for a semicircular reservoir against a fault, $\theta = 180°$). c_t is in psi^{-1} and r_R and h are in feet.

Example 8.1 shows the use of Eq. (8.8) and the values of Tables 8.1 and 8.2 to calculate the cumulative water influx at successive periods for the case of a constant reservoir boundary pressure. The infinite aquifer values may be used for small time values even though the aquifer is limited in size.

Example 8.1. Calculate the water influx after 100 days, 200 days, 400 days, and 800 days into a reservoir the boundary pressure of which is suddenly lowered and held at 2724 psia ($p_i = 2734$ psia).

Given:

$\phi = 0.20$	$k = 83$ md
$c_t = 8(10)^{-6}$ psi^{-1}	$r_R = 3000$ ft
$r_e = 30{,}000$ ft	$\mu = 0.62$ cp
$\theta = 360°$	$h = 40$ ft

SOLUTION: From Eq. (8.6):

$$t_D = \frac{0.0002637(83)t}{0.20(0.62)[8(10)^{-6}](3000^2)} = 0.00245t$$

From Eq. (8.9):

$$B' = 1.119(0.20)[8(10)^{-6}](3000^2)(40)\left(\frac{360}{360}\right) = 644.5$$

At 100 days $t_D = 0.00245(100)(24) = 5.88$ dimensionless time units. From the $r_e/r_R = 10$ curve of Fig. 8.8 find corresponding to $t_D = 5.88$, $W_D = 5.07$ dimensionless influx units. This same value may also be found by interpolation of Table 8.1, since below $t_D = 15$ the aquifer behaves essentially as if it were infinite, and no values are given in Table 8.2. Since $\Delta p = 2734 - 2724 = 10$ psi, and water influx at 100 days from Eq. (8.8) is

$$W_e = B'\Delta p W_D = 644.5(10)(5.07) = 32{,}680 \text{ bbl}$$

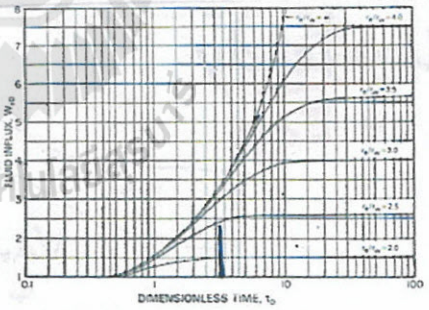

Fig. 8.7. Limited aquifer values of dimensionless influx W_D for values of dimensionless time t_D and aquifer limits given by the ratio r_e/r_R.

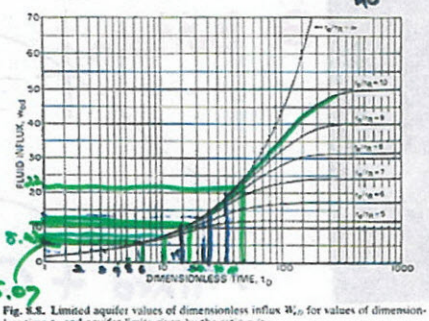

Fig. 8.8. Limited aquifer values of dimensionless influx W_D for values of dimensionless time t_D and aquifer limits given by the ratio r_e/r_R.

TABLE 8.1.
Infinite aquifer values of dimensionless water influx W_{eD} for values of dimensionless time t_D

Dimensionless time t_D	Fluid influx W_{eD}	Dimensionless time t_D	Fluid influx W_{eD}	Dimensionless time t_D	Fluid influx W_{eD}	Dimensionless time t_D	Fluid influx W_{eD}	Dimensionless time t_D	Fluid influx W_{eD}	Dimensionless time t_D	Fluid influx W_{eD}
0.00	0.000	79	35.697	455	150.249	1190	340.843	3250	816.090	35.000	6780.247
0.01	0.112	80	36.058	460	151.640	1200	343.308	3300	827.088	40.000	7650.096
0.05	0.278	81	36.418	465	153.029	1210	345.770	3350	838.067	50.000	9363.099
0.10	0.404	82	36.777	470	154.416	1220	348.230	3400	849.028	60.000	11,047.299
0.15	0.520	83	37.136	475	155.801	1225	349.460	3450	859.974	70.000	12,708.358
0.20	0.606	84	37.494	480	157.184	1230	350.688	3500	870.903	75.000	13,531.457
0.25	0.689	85	37.851	485	158.565	1240	353.144	3550	881.816	80.000	14,350.121
0.30	0.758	86	38.207	490	159.945	1250	355.597	3600	892.712	90.000	15,975.389
0.40	0.898	87	38.563	495	161.322	1260	358.048	3650	903.594	100.000	17,586.284
0.50	1.020	88	38.919	500	162.698	1270	360.496	3700	914.459	125.000	21,560.732
0.60	1.140	89	39.272	510	165.444	1275	361.720	3750	925.309	$1.5(10)^5$	$2.538(10)^4$
0.70	1.251	90	39.626	520	168.183	1280	362.942	3800	936.144	2.0"	3.308"
0.80	1.359	91	39.979	525	169.549	1290	365.386	3850	946.966	2.5"	4.066"
0.90	1.469	92	40.331	530	170.914	1300	367.828	3900	957.773	3.0"	4.817"
1	1.569	93	40.684	540	173.639	1310	370.267	3950	968.566	4.0"	6.267"
2	2.447	94	41.034	550	176.357	1320	372.704	4000	979.344	5.0"	7.699"
3	3.202	95	41.385	560	179.069	1325	373.922	4050	990.108	6.0"	9.113"
4	3.893	96	41.735	570	181.774	1330	375.139	4100	1000.858	7.0"	$1.051(10)^1$
5	4.539	97	42.084	575	183.124	1340	377.572	4150	1011.595	8.0"	1.189"
6	5.153	98	42.433	580	184.473	1350	380.003	4200	1022.318	9.0"	1.326"
7	5.743	99	42.781	590	187.166	1360	382.432	4250	1033.028	$1.0(10)^6$	1.462"
8	6.314	100	43.129	600	189.852	1370	384.859	4300	1043.724	1.5"	2.126"
9	6.869	105	44.858	610	192.533	1375	386.070	4350	1054.409	2.0"	2.781"
10	7.411	110	46.574	620	195.208	1380	387.283	4400	1065.082	2.5"	3.427"
11	7.940	115	48.277	625	196.544	1390	389.705	4450	1075.743	3.0"	4.064"
12	8.457	120	49.968	630	197.878	1400	392.125	4500	1086.390	4.0"	5.313"
13	8.964	125	51.648	640	200.542	1410	394.543	4550	1097.024	5.0"	6.544"

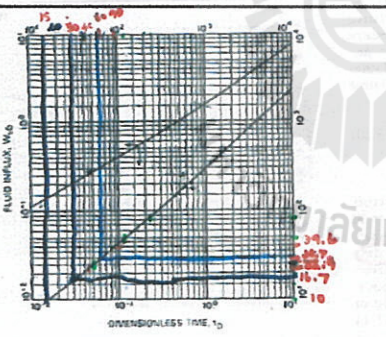

Fig. 8.9. Infinite aquifer values of dimensionless influx W_{eD} for values of dimensionless time t_D.

Similarly at

t = 100 days	200 days	400 days	800 days
t_D = 5.88	11.76	23.52	47.04
W_{eD} = 5.07	8.43	15.00	22.75
W_e = 32,680	54,330	89,500	146,600

For aquifers 99 times as large as the reservoirs they surround, or $r_e/r_R = 10$, this means that the effect of the aquifer limits are negligible for dimensionless time values under 15, and that it is some time before the aquifer limits affect the water influx appreciably. This is also illustrated by the coincidence of the curves of Figs. 8.7 and 8.8 with the infinite aquifer curve for the smaller time values. It should also be noted that unlike a steady-state system, the values of water influx calculated in Ex. 8.1 fail to double for a doubling of the time.

While water is entering the reservoir from the aquifer at a declining rate, in response to the first pressure signal $\Delta p_1 = p_i - p_1$, let a second, sudden pressure drop $\Delta p_2 = p_1 - p_2$ (not $p_i - p_2$) be imposed at the reservoir boundary at a time t_1. This is an application of the principle of superposition, which was discussed in Chapter 7. The total or net effect is the sum of the two as illustrated in Fig. 8.11 where, for simplicity, $\Delta p_2 = \Delta p_1$ and $t_2 = 2t_1$. The upper

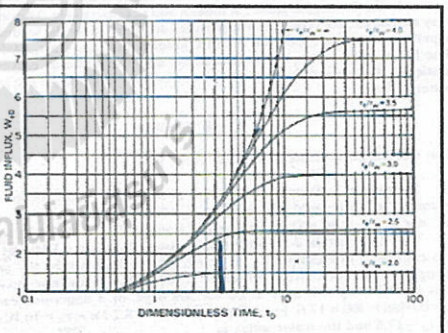

Fig. 8.7. Limited aquifer values of dimensionless influx W_{eD} for values of dimensionless time t_D and aquifer limits given by the ratio r_e/r_R.

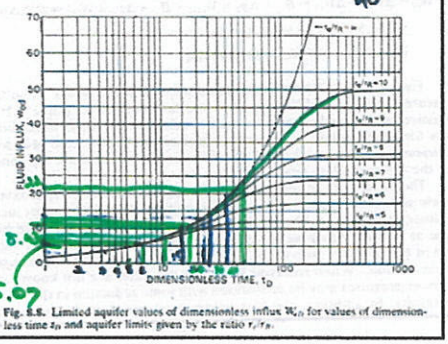

Fig. 8.8. Limited aquifer values of dimensionless influx W_{eD} for values of dimensionless time t_D and aquifer limits given by the ratio r_e/r_R.

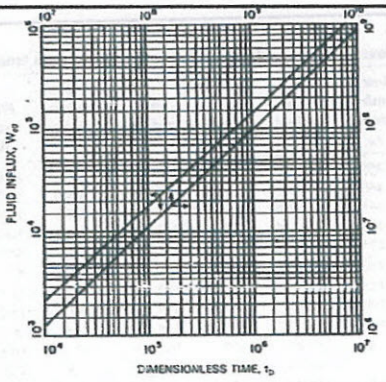

Fig. 8.10. Infinite aquifer values of dimensionless influx W_{eD} for values of dimensionless time t_D.

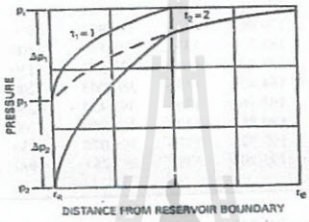

Fig. 8.11. Pressure distributions in an aquifer due to two equal pressure decrements imposed at equal time intervals.

and middle curves represent the pressure distribution in the aquifer in response to the first signal alone, at times t_1 and t_2, respectively. The upper curve may also be used to represent the pressure distribution for the second pressure signal alone at time t_2 because in this simplified case $\Delta p_2 = \Delta p_2$, and $\Delta t_2 = \Delta t_1$. The lower curve, then, is the sum of the upper and middle curves. Mathematically, this means that Eq. (8.10) can be used to calculate the cumulative water influx:

$$W_e = B' \Sigma \Delta p W_{eD} \tag{8.10}$$

This calculation is illustrated in Ex. Prob. 8.2.

Example 8.2. Suppose in Ex. 8.1 at the end of 100 days the reservoir boundary pressure suddenly drops to $p_2 = 2704$ psia (i.e., $\Delta p_2 = p_1 - p_2 = 20$ psi, *not* $p_i - p_2 = 30$ psi). Calculate the water influx at 400 days total time.

The water influx due to the first pressure drop $\Delta p_1 = 10$ psi at 400 days was calculated in Example 8.1 to be 89,590 bbl. This will be the same even though a second pressure drop occurs at 100 days and continues to 400 days. This second drop will have acted for 300 days, or a dimensionless time of $t_D = 0.0588 \times 300 = 17.6$. From Fig. 8.8 or Table 8.2 for $r_e/r_R = 10$ $W_{eD} = 11.14$ for $t_D = 17.6$ and the water influx is

$$\Delta W_{e2} = B' \times \Delta p_2 \times W_{eD} = 644.5 \times 20 \times 11.14 = 143{,}600 \text{ bbl}$$

$$W_{e2} = \Delta W_{e1} + \Delta W_{e2} = B' \times \Delta p_1 \times W_{eD1} + B' \times \Delta p_2 \times W_{eD2} = B' \Sigma \Delta p W_{eD}$$

$$= 644.5\,(10 \times 13.90 + 20 \times 11.14)$$

$$= 89{,}590 + 143{,}600 = 233{,}190 \text{ bbl}$$

Example 8.2 illustrates the calculation of water influx when a second pressure drop occurs 100 days after the first drop in Example 8.1. A continuation of this method may be used to calculate the water influx into reservoirs for which boundary pressure histories are known, and also for which sufficient information is known about the aquifer to calculate the constant B' and the dimensionless time t_D.

The history of the reservoir boundary pressure may be approximated as closely as desired by a series of step-by-step pressure reductions (or increases), as illustrated in Fig. 8.12. The best approximation of the pressure history is made as shown by making the pressure step at any time equal to half of the drop in the previous interval of time plus half of the drop in the succeeding period of time.[6] When reservoir boundary pressures are not known, average reservoir pressures may be substituted with some reduction in the accuracy of the results. In addition, for best accuracy, the average boundary pressure

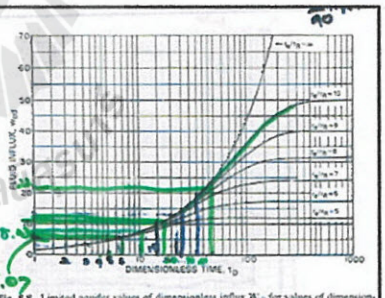

Fig. 8.8. Limited aquifer values of dimensionless influx W_{eD} for values of dimensionless time t_D and aquifer limits given by the ratio r_e/r_R.

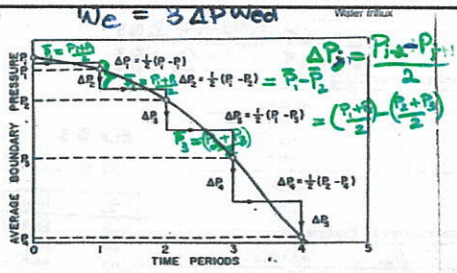

Fig. 8.12. Sketch showing the use of step pressures to approximate the pressure-time curve.

Example 8.3 illustrates the calculation of water influx at two successive time values for the reservoir shown in Fig. 8.13.

Example 8.3. Calculate the water influx at the third and fourth quarter years of production for the reservoir shown in Fig. 8.13. Use $\phi = 0.209$; $k = 275$ md (average reservoir permeability, presumed the same for the aquifer); $\mu = 0.25$ cp; $c_t = 6 \times 10^{-6}$ psi^{-1}; $h = 19.2$ ft; area of reservoir = 1216 ac; estimated area of aquifer = 250,000 ac; $\theta = 180°$.

SOLUTION: Since the reservoir is against a fault $A = \frac{1}{2}\pi r_R^2$ and:

$$r_R^2 = \frac{1216 \times 43{,}560}{0.5 \times 3.1416}$$

$$r_R = 5807 \text{ ft}$$

For $t = 91.3$ days (one-quarter year or one period):

$$t_D = \frac{6.323 \times 10^{-3} \times 275 \times 91.3}{0.209 \times 0.25 \times 6 \times 10^{-6} \times (5807)^2} = 15.0$$

$$B' = 1.119 \times 0.209 \times 6 \times 10^{-6} \times (5807)^2 \times 19.2 \times (180°/360°)$$

$$= 455 \text{ bbl/psi}$$

Since the aquifer is 250,000/1216 = 206 times the area of the reservoir, for a considerable time the infinite aquifer values may be used. Table 8.3

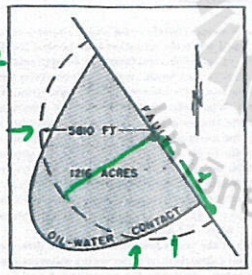

Fig. 8.13. Sketch showing the equivalent radius of a reservoir.

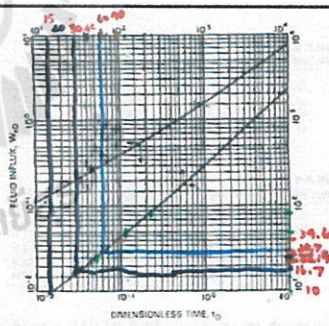

Fig. 8.9. Infinite aquifer values of dimensionless influx W_{eD} for values of dimensionless time t_D.

TABLE 8.3.
Boundary step pressures and W_{eD} values for Ex. 8.3

Time Period t	Time in Days t	Dimensionless Time, t_D	W_{eD}	p, Avg. Reservoir Pressure, psia	p_B, Avg. Boundary Pressure, psia	Δp, Step Pressure, psi
0	0	0	0.0	3793	3793	0.0
1	91.3	15	10.0	3786	3788	2.5
2	182.6	30	16.7	3768	3774	9.5
3	273.9	45	23.0	3749	3758	20.0
4	365.2	60	28.7	3699	3709	32.5
5	456.5	75	34.3	3657	3680	34.0
6	547.8	90	39.6	3613	3643	33.0

[a] Infinite aquifer values from Fig. 8.9 or Table 8.1.

shows the values of boundary step pressures and the W_{eD} values for the first six periods. The calculation of the step pressures Δp is illustrated in Fig. 8.12. For example,

$$\Delta p_3 = \tfrac{1}{2}(p_2 - p_4) = \tfrac{1}{2}(3788 - 3748) = 20.0 \text{ psi}$$

Tables 8.4 and 8.5 show the calculation of $\Sigma \Delta p \times W_{eD}$ at the end of the third

TABLE 8.4.
Water influx at the end of the third quarter for Example 8.3

t_D	W_{eD}	Δp	$\Delta p \times W_{eD}$
45	22.9	2.5	57.3
30	16.7	9.5	158.7
15	10.0	20.0	200.0

TABLE 8.5.
Water influx at the end of the fourth quarter for Example 8.3

t_D	W_{eD}	Δp	$\Delta p \times W_{eD}$
60	28.7	2.5	71.8
45	22.9	9.5	217.6
30	16.7	20.0	334.0
15	10.0	32.5	325.0

and fourth periods, the values being 416.0 and 948.0, respectively. Then the corresponding water influx at the end of these periods is

$$W_e \text{ (3rd quarter)} = B' \Sigma \Delta p \times W_{eD} = 455 \times 416.0 = 189{,}300 \text{ bbl}$$

$$W_e \text{ (4th quarter)} = B' \Sigma \Delta p \times W_{eD} = 455 \times 948.4 = 431{,}500 \text{ bbl}$$

In calculating the water influx in Ex. 8.3 at the end of the third quarter, it should be carefully noted in Table 8.4 that since the first pressure drop, $\Delta p_1 = 2.5$ psi, had been operating for the full three quarters ($t_D = 45$), it was multiplied by $W_{eD} = 22.9$, which corresponds to $t_D = 45$. Similarly, for the fourth quarter calculation in Table 8.5, the 2.5 psi was multiplied by $W_{eD} = 28.7$, which is the value for $t_D = 60$. Thus the W_{eD} values are inverted so that the one corresponding to the longest time is multiplied by the first pressure drop, and vice versa. Also, in calculating each successive value of $\Sigma \Delta p \times W_{eD}$, it is not simply a matter of adding a new $\Delta p \times W_{eD}$ term to the former summation, but a complete recalculation, as shown in Tables 8.4 and 8.5.

You should show that the water influx values at the end of the fifth and sixth quarters are 773,100 and 1,201,600 bbl, respectively.

Ex 8.3

At the end of fifth quarter

t_D	W_{eD}	ΔP	$\Delta P \times W_{eD}$
75	34.3	2.5	85.75
60	28.7	9.5	272.65
45	22.9	20.0	458.00
30	16.7	32.5	542.75
15	10.0	34.0	340.00
		Σ	1699.15

W_e (5th quarter) $= B' \cdot \Sigma \Delta P \times W_{eD}$
$= 455 \times 1699.15 = 773{,}100$ bbl

At the end of sixth quarter

t_D	W_{eD}	ΔP	$\Delta P \times W_{eD}$
90	39.6	2.5	99.0
75	34.3	9.5	325.85
60	28.7	20.0	574
45	22.9	32.5	744.25
30	16.7	34.0	567.8
15	10.0	33.0	330
		Σ	2639.65

W_e (6th quarter) $= B' \cdot \Sigma \Delta P W_{eD}$
$= 455 \times 2639.65 = 1{,}201{,}600$ bbl

TABLE 8.4.
Water influx at the end of the third quarter for Example 8.3

t_D	W_{eD}	Δp	$\Delta p \times W_{eD}$
45	22.9	2.5	57.3
30	16.7	9.5	158.7
15	10.0	20.0	200.0

TABLE 8.5.
Water influx at the end of the fourth quarter for Example 8.3

t_D	W_{eD}	Δp	$\Delta p \times W_{eD}$
60	28.7	2.5	71.8
45	22.9	9.5	217.6
30	16.7	20.0	334.0
15	10.0	32.5	325.0

and fourth periods, the values being 416.0 and 948.0, respectively. Then the corresponding water influx at the end of these periods is

$$W_e \text{ (3rd quarter)} = B' \Sigma \Delta p \times W_{eD} = 455 \times 416.0 = 189{,}300 \text{ bbl}$$

$$W_e \text{ (4th quarter)} = B' \Sigma \Delta p \times W_{eD} = 455 \times 948.4 = 431{,}500 \text{ bbl}$$

In calculating the water influx in Ex. 8.3 at the end of the third quarter, it should be carefully noted in Table 8.4 that since the first pressure drop, $\Delta p_1 = 2.5$ psi, had been operating for the full three quarters ($t_D = 45$), it was multiplied by $W_{eD} = 22.9$, which corresponds to $t_D = 45$. Similarly, for the fourth quarter calculation in Table 8.5, the 2.5 psi was multiplied by $W_{eD} = 28.7$, which is the value for $t_D = 60$. Thus the W_{eD} values are inverted so that the one corresponding to the longest time is multiplied by the first pressure drop, and vice versa. Also, in calculating each successive value of $\Sigma \Delta p \times W_{eD}$, it is not simply a matter of adding a new $\Delta p \times W_{eD}$ term to the former summation, but a complete recalculation, as shown in Tables 8.4 and 8.5.

You should show that the water influx values at the end of the fifth and sixth quarters are 773,100 and 1,201,600 bbl, respectively.

From the previous discussion it is evident that it is possible to calculate water influx independently of material balance calculations from a knowledge of the history of the reservoir, boundary pressure, and the dimensions and physical characteristics of the aquifer, as shown by Chatas.[7] Although strictly speaking, the van Everdingen and Hurst solutions to the diffusivity equation apply only to circular reservoirs surrounded concentrically by horizontal, circular (or infinite) aquifers of constant thickness, porosity, permeability, and

effective water compressibility, for many engineering purposes good results may be obtained when the situation is somewhat less than ideal, as it nearly always is. The radius of the reservoir may be approximated by using the radius of a circle equal in area to the area of the reservoir; and where the approximate size of the aquifer is known, the same approximation may be used for the aquifer radius. Where the aquifer is more than approximately 99 times the size (volume) of the reservoir ($r_e/r_R = 10$), the aquifer behaves essentially as if it were infinite for a considerable period so that the values of Table 8.1 may be used. There are to be sure, uncertainties in the permeability, porosity, and thickness of the aquifer which must be estimated from information obtained from wells drilled in the reservoir and whatever wells are drilled in the aquifer. The viscosity of the water can be estimated from the temperature and pressure (Chapter 1, Sect. 7.4) and the water and rock compressibilities from the data of Chapter 1, Sects. 7.3 and 4.2.

Because of the many uncertainties in the dimensions and properties of the aquifer, the calculation of water influx independently of material balance appears somewhat unreliable. For instance in Ex. 8.3 it was assumed that the fault against which the reservoir accumulated was of large (actually infinite) extent; and since the permeability of only the reservoir rock was known, it was assumed that the average permeability of the aquifer was also 275 md. There may be variations in the aquifer thickness and porosity, and the aquifer may contain faults, impermeable areas, and unknown hydrocarbon accumulations, all of which can introduce variations of greater or lesser importance.

As Ex. Probs. 8.1, 8.2, and 8.3 suggest, the calculations for water influx can become long and tedious. The use of the computer with these calculations requires large data files containing the values of W_{eD}, t_D, and r_e/r_R from Tables 8.1 and 8.2 as well as a table lookup routine. Several authors have attempted to develop equations to describe the dimensionless water influx as a function of the dimensionless time and radius ratio.[10,11,12] These equations reduce the data storage required when using the computer in calculations of water influx.

3.2. Bottom-Water Drive

The van Everdingen and Hurst model discussed in the previous section is based on the radial diffusivity equation written without a term describing vertical flow from the aquifer. In theory, this model should not be used when there is significant movement of water into the reservoir from a bottom-water drive. To account for the flow of water in a vertical direction, Coats and later Allard and Chen, added a term to Eq. (7.35) to yield the following:

$$\frac{\partial^2 p}{\partial r^2} + \frac{1}{r}\frac{\partial p}{\partial r} + F_k \frac{\partial^2 p}{\partial z^2} = \frac{\phi \mu c_t}{0.0002637k}\frac{\partial p}{\partial t} \tag{8.10}$$

where F_k is the ratio of vertical to horizontal permeability.[13,14]

3.2. Bottom-Water Drive

The van Everdingen and Hurst model discussed in the previous section is based on the radial diffusivity equation written without a term describing vertical flow from the aquifer. In theory, this model should not be used when there is significant movement of water into the reservoir from a bottom-water drive. To account for the flow of water in a vertical direction, Coats and later Allard and Chen, added a term to Eq. (7.35) to yield the following:

$$\frac{\partial^2 p}{\partial r^2}+\frac{1}{r}\frac{\partial p}{\partial r}+F_k\frac{\partial^2 p}{\partial z^2}=\frac{\phi\mu c_t}{0.0002637k}\frac{\partial p}{\partial t} \tag{8.10}$$

where F_k is the ratio of vertical to horizontal permeability.[13,14]

Using the definitions of dimensionless time, radius, and pressure and introducing a second dimensionless distance, z_D, Eq. (8.10) becomes Eq. (8.11):

$$z_D=\frac{z}{r_R F_k^{1/2}}$$

$$\frac{\partial^2 p_D}{\partial r_D^2}+\frac{1}{r_D}\frac{\partial p_D}{\partial r_D}+\frac{\partial^2 p_D}{\partial z_D^2}=\frac{\partial p_D}{\partial t_D} \tag{8.11}$$

Coats solved Eq. (8.11) for the terminal rate case for infinite aquifers.[13] Allard and Chen used a numerical simulator to solve the problem for the terminal pressure case.[14] They defined a water influx constant, B', and a dimensionless water influx, W_{eD} analogous to those defined by van Everdingen and Hurst except that B' does not include the angle θ:

$$B'=1.119\phi hc_t r_R^2 \tag{8.12}$$

The actual values of W_{eD} will be different from those of the van Everdingen and Hurst model because W_{eD} for the bottom-water drive is a function of the vertical permeability. Because of this functionality, the solutions presented by Allard and Chen, found in Tables 8.6 to 8.10, are functions of two dimensionless parameters, r_D' and z_D'.

$$r_D'=\frac{r_e}{r_R} \tag{8.13}$$

$$z_D'=\frac{h}{r_R F_k^{1/2}} \tag{8.14}$$

The method of calculating water influx from the dimensionless values obtained from these tables follows exactly the method illustrated in Exs. 8.1 to 8.3. The procedure is shown in Ex. 8.4, which is a problem taken from Allard and Chen.[14]

Using the definitions of dimensionless time, radius, and pressure and introducing a second dimensionless distance, z_D, Eq. (8.10) becomes Eq. (8.11):

$$z_D=\frac{z}{r_R F_k^{1/2}}$$

$$\frac{\partial^2 p_D}{\partial r_D^2}+\frac{1}{r_D}\frac{\partial p_D}{\partial r_D}+\frac{\partial^2 p_D}{\partial z_D^2}=\frac{\partial p_D}{\partial t_D} \tag{8.11}$$

Coats solved Eq. (8.11) for the terminal rate case for infinite aquifers.[13] Allard and Chen used a numerical simulator to solve the problem for the terminal pressure case.[14] They defined a water influx constant, B', and a dimensionless water influx, W_{eD} analogous to those defined by van Everdingen and Hurst except that B' does not include the angle θ:

$$B'=1.119\phi hc_t r_R^2 \tag{8.12}$$

The actual values of W_{eD} will be different from those of the van Everdingen and Hurst model because W_{eD} for the bottom-water drive is a function of the vertical permeability. Because of this functionality, the solutions presented by Allard and Chen, found in Tables 8.6 to 8.10, are functions of two dimensionless parameters, r_D' and z_D'.

$$r_D'=\frac{r_e}{r_R} \tag{8.13}$$

$$z_D'=\frac{h}{r_R F_k^{1/2}} \tag{8.14}$$

The method of calculating water influx from the dimensionless values obtained from these tables follows exactly the method illustrated in Exs. 8.1 to 8.3. The procedure is shown in Ex. 8.4, which is a problem taken from Allard and Chen.[14]

Example 8.4. Calculate the water influx as a function of time for the reservoir data and boundary pressure data that follow:

Given:

$r_R = 2000$ ft $\quad r_e = \infty$

$h = 200$ ft $\quad k = 50$ md

$F_c = 0.04$ $\quad \phi = 0.10$

$\mu = 0.395$ cp $\quad c_t = 8 \times 10^{-6}$ psi^{-1}

Time in Days (t)	Average Boundary Pressure, psia (p_B)
0	3000
30	2956
60	2917
90	2877
120	2844
150	2811
180	2791
210	2773
240	2755

Ex. 8.4 Advanced Reservoir.

① water influx at the end of the third Period.

t_D	Wed	ΔP	$\Delta P \times$ Wed	
22.5	11.414	22	251.1	$\Sigma = 798.2$
15.0	8.389	41.5	348.1	
7.5	5.038	39.5	199	

$We = B' \Sigma \Delta P Wed$

$= 716 \times 798.2 = 572{,}000$ bbl

② At the end of fourth Period

t_D	Wed	ΔP	$\Delta P \times$ Wed	
30	14.263	22	314	$\Sigma = 1303$
22.5	11.414	41.5	474	
15	8.389	39.5	331	
7.5	5.038	36.5	184	

$We = 716 \times 1303 = 933$ Mbbl

③ At the end of fifth Period

37.5	16.994	22	374	$= 1889$
30	14.263	41.5	592	
22.5	11.414	39.5	451	$We = 1889 \times 716$
15	8.389	36.5	306	
7.5	5.038	33	166	$= 1353$ Mbbl

end of Period 2

$W_e = B' \Sigma \Delta P_{wed}$

(41.5×5.038 + 22.0×8.389)

SOLUTION:

$r_D' = \infty$

$z_D' = \frac{200}{2000(0.040)^{1/2}} = 0.5$

$t_D = \frac{0.0002637(50)}{0.10(0.395)8(10)^{-6}2000^2} = 0.0104t$ (where t is in hours)

$B' = 1.119(0.10)(\text{illegible})^2 = 716$ bbl/psi

$\frac{3000 - 2956}{2}$

Time in Days (t)	Dimensionless Time (t_D)	W_{eD}	Average Boundary Pressure, psia (p_B)	Step Pressure (Δp)	Water Influx, M bbl (W_e)
0	0	0	3000 p_0	0	0
30	7.5	5.038	2956 p_1	22.0	79
60	15.0	8.389	2917 p_2	41.5	282
90	22.5	11.414	2877	39.5	572
120	30.0	14.263	2841	36.5	933
150	37.5	16.994	2811	33.0	1353
180	45.0	19.641	2791	26.5	1810
210	52.5	22.214	2773	19.0	2284
240	60.0	24.728	2755	18.0	2782

Using the definitions of dimensionless time, radius, and pressure and introducing a second dimensionless distance, z_D, Eq. (8.10) becomes Eq. (8.11):

$$z_D = \frac{z}{r_R F_k^{1/2}} \qquad F_k = \frac{K_v}{K_h}$$

$$\frac{\partial^2 p_D}{\partial r_D^2} + \frac{1}{r_D}\frac{\partial p_D}{\partial r_D} + \frac{\partial^2 p_D}{\partial z_D^2} = \frac{\partial p_D}{\partial t_D} \qquad (8.11)$$

Coats solved Eq. (8.11) for the terminal rate case for infinite aquifers.[13] Allard and Chen used a numerical simulator to solve the problem for the terminal pressure case.[14] They defined a water influx constant, B', and a dimensionless water influx, W_D, analogous to those defined by van Everdingen and Hurst except that B' does not include the angle θ:

$$B' = 1.119\phi hc r_R^2 \qquad (8.12)$$

The actual values of W_D will be different from those of the van Everdingen and Hurst model because W_D for the bottom-water drive is a function of the vertical permeability. Because of this functionality, the solutions presented by Allard and Chen, found in Tables 8.6 to 8.10, are functions of two dimensionless parameters, r_D' and z_D'.

$W_e = B' \Sigma \Delta P_{wed}$

$$r_D' = \frac{r_e}{r_R} \qquad (8.13)$$

$$z_D' = \frac{h}{r_R F_k^{1/2}} \qquad F_k = \frac{K_v}{K_h} \qquad (8.14)$$

The method of calculating water influx from the dimensionless values obtained from these tables follows exactly the method illustrated in Exs. 8.1 to 8.3. The procedure is shown in Ex. 8.4, which is a problem taken from Allard and Chen.[14]

end of Period 2

$W_e = B' \Sigma \Delta P_{wed}$

(41.5×5.038 + 22.0×8.389)

SOLUTION:

$r_D' = \infty$

$z_D' = \frac{200}{2000(0.040)^{1/2}} = 0.5$

$t_D = \frac{0.0002637(50)}{0.10(0.395)8(10)^{-6}2000^2} = 0.0104t$ (where t is in hours)

$B' = 1.119(0.10)(\text{illegible})^2 = 716$ bbl/psi

$\frac{3000 - 2956}{2}$

we= 1809831

Time in Days (t)	Dimensionless Time (t_D)	W_{eD}	Average Boundary Pressure, psia (p_B)	Step Pressure (Δp)	Water Influx, M bbl (W_e)
0	0	0	3000 p_0	0	0
30	7.5	5.038	2956 p_1	22.0	79
60	15.0	8.389	2917 p_2	41.5	282
90	22.5	11.414	2877	39.5	572
120	30.0	14.263	2841	36.5	933
150	37.5	16.994	2811	33.0	1353
180	45.0	19.641	2791	26.5	1810
210	52.5	22.214	2773	19.0	2284
240	60.0	24.728	2755	18.0	2782

TABLE 8.6.
Dimensionless influx, W_{eD}, for infinite aquifer for bottom-water drive

t_D	z_D = 0.05	0.1	0.3	0.5	0.7
0.1	0.700	0.677	0.508	0.349	0.251
0.2	0.793	0.766	0.696	0.547	0.436
0.3	0.936	0.926	0.834	0.692	0.548
0.4	1.051	1.041	0.952	0.812	0.662
0.5	1.156	1.155	1.059	0.918	0.764
0.6	1.270	1.268	1.167	1.021	0.862
0.7	1.384	1.383	1.270	1.126	0.953
0.8	1.505	1.499	1.373	1.205	1.039
0.9	1.628	1.612	1.477	1.296	1.117
1	1.745	1.726	1.581	1.347	1.193
2	2.402	2.393	2.208	2.034	1.827
3	3.031	3.018	2.895	2.650	2.408
4	3.629	3.615	3.477	3.225	2.949
5	4.217	4.201	4.046	3.766	3.462
6	4.784	4.766	4.601	4.288	3.956
7	5.323	5.303	5.128	4.792	4.434
8	5.797	5.777	5.603	5.263	5.000
9	6.306	6.283	6.094	5.762	5.335
10	6.837	6.836	6.583	6.214	5.792
11	7.263	7.242	7.040	6.664	6.217
12	7.742	7.716	7.495	7.104	6.636
13	8.196	8.172	7.943	7.539	7.052
14	8.648	8.623	8.385	7.967	7.494
15	9.094	9.068	8.823	8.389	8.38
16	9.534	9.507	9.253	8.806	8.795
17	9.969	9.942	9.679	9.208	9.196
18	10.399	10.371	10.100	9.626	9.606
19	10.823	10.794	10.516	10.029	9.982
20	11.241	11.211	10.929	10.430	9.815
21	11.664	11.633	11.339	10.826	10.194
22	12.075	12.045	11.744	11.219	10.571
23	12.486	12.454	12.147	11.609	10.944
24	12.893	12.863	12.546	11.996	11.315
25	13.297	13.264	12.942	12.380	11.683
26	13.698	13.665	13.336	12.761	12.048
27	14.097	14.062	13.726	13.140	12.411
28	14.493	14.458	14.115	13.517	12.772
29	14.886	14.850	14.501	13.890	13.132
30	15.277	15.241	14.884	14.263	14.19
31	15.666	15.628	15.266	14.634	13.845
32	16.053	16.015	15.645	15.002	14.196
33	16.437	16.398	16.023	15.366	14.546
34	16.819	16.780	16.398	15.732	14.897
35	17.200	17.160	16.772	16.095	15.245
36	17.579	17.536	17.143	16.456	15.592
37	17.956	17.915	17.515	16.815	15.937
38	18.331	18.289	17.882	17.173	16.280
39	18.704	18.662	18.249	17.529	16.622
40	19.076	19.045	18.620	17.885	16.964
41	19.450	19.407	18.982	18.240	17.305
42	19.823	19.777	19.344	18.592	17.644
43	20.196	20.144	19.706	18.943	17.981
44	20.555	20.530	20.065	19.293	18.317
45	20.920	20.874	20.424	19.641	18.651
46	21.263	21.237	20.781	19.986	18.985
47	21.645	21.598	21.137	20.335	19.317

500	49.65	49.64	49.58	49.45	49.26	48.98	48.82
600	49.84	49.84	49.81	49.74	49.65	49.50	49.41
700	49.91	49.91	49.90	49.87	49.82	49.74	49.69
800	49.94	49.94	49.93	49.92	49.90	49.85	49.83
900	49.96	49.96	49.94	49.94	49.93	49.91	49.90
1,000	49.96	49.96	49.96	49.96	49.94	49.93	49.93
1,200	49.96	49.96	49.96	49.96	49.96	49.96	49.96

4. PSEUDOSTEADY-STATE MODELS ของ Fetkovich

The edge-water and bottom-water, unsteady-state methods discussed in Sect. 3 provide correct procedures for calculating water influx in nearly any reservoir application. However, the calculations tend to be somewhat cumbersome, and therefore there have been various attempts to simplify the calculations. The most popular and seemingly accurate method is one developed by Fetkovich using an aquifer material balance and an equation that describes the flow rate from the aquifer.[15] The equations for flow rate used by Fetkovich are similar to the productivity index equation defined in Chapter 7. The productivity index required pseudosteady-state flow conditions. Thus, this method neglects the effects of the transient period in the calculations of water influx, which will obviously introduce errors into the calculations. However, the method has been found to give results similar to those of the van Everdingen and Hurst model in many applications.

Fetkovich first wrote a material balance equation on the aquifer for constant water and rock compressibilities as

$$\bar{p} = -\left(\frac{p_i}{W_a}\right) W_e + p_i \qquad (8.15)$$

where $\bar{p}$ is the average pressure in the aquifer after the removal of W_e bbl of water, p_i is the initial pressure of the aquifer, and W_a is the initial encroachable water in place at the initial pressure. Fetkovich next defined a generalized rate equation as

$$q_w B_w = J(\bar{p} - p_R)^n \qquad (8.16)$$

where $q_w B_w$ is the flow rate of water from the aquifer, J is the productivity index of the aquifer and is a function of the aquifer geometry, p_R is the

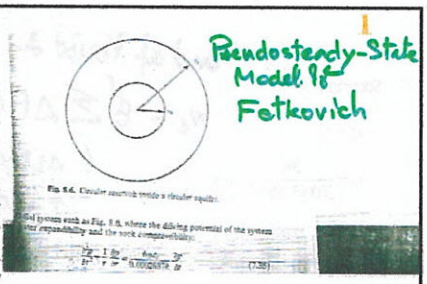

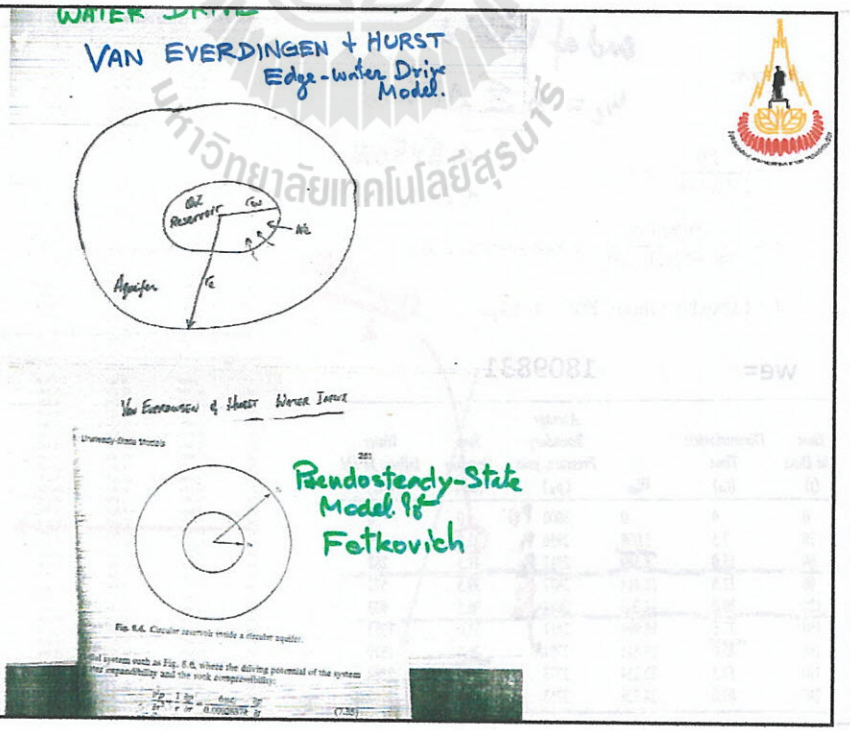

Fetkovich Pseudosteady-State Model.

เมื่อ Compressibility

$We \propto \Delta P$ or $P_i - \bar{P}$

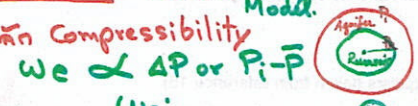

$$We = \frac{We_i}{P_i}(P_i - \bar{P}) \quad -(1)$$

Definition of Productivity

$$q_w B_w = J(\bar{P} - P_R) = \frac{dWe}{dt} \quad -(2)$$

diff. Integrate eq (1)

$$\frac{dWe}{dt} = \frac{We_i}{P_i}\left(-\frac{d\bar{P}}{dt}\right) \text{ แทนค่าใน (2)}$$

$$\frac{dWe}{dt} = -\frac{We_i}{P_i}\cdot\frac{d\bar{P}}{dt} = J(\bar{P} - P_R) \quad -(3)$$

Integrate Eq.(3)

$$-\frac{We_i}{P_i}\int_{P_i}^{\bar{P}}\frac{d\bar{P}}{(\bar{P} - P_R)} = J\int_0^t dt$$

$$-\frac{We_i}{P_i}\ln\frac{(\bar{P} - P_R)}{(P_i - P_R)} = Jt$$

WATER DRIVE : Unsteady-State

VAN EVERDINGEN + HURST
Edge-water Drive Model.

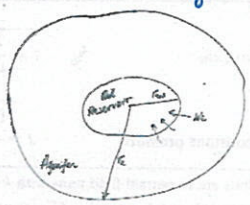

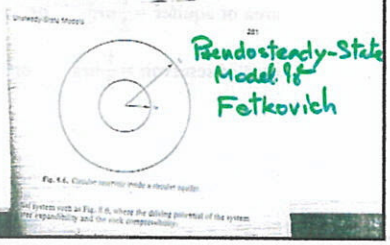

$$\ln\frac{\bar{P} - P_R}{P_i - P_R} = -\frac{Jt P_i}{We_i}$$

$$\frac{(\bar{P} - P_R)}{(P_i - P_R)} = e^{-\frac{Jt P_i}{We_i}}$$

$$\bar{P} - P_R = (P_i - P_R)e^{-\frac{Jt P_i}{We_i}}$$

$$-\left(\frac{P_i}{We_i}\right)We + P_i - P_R = (P_i - P_R)e^{-\frac{Jt P_i}{We_i}}$$

$$\frac{P_i}{We_i}We = (P_i - P_R) - (P_i - P_R)e^{-\frac{Jt P_i}{We_i}}$$

$$We = \frac{We_i}{P_i}(P_i - P_R)\left(1 - e^{-\frac{Jt P_i}{We_i}}\right)$$

Compressibility

$$c_t = -\frac{1}{V}\frac{dV}{dP} = +\frac{1}{Vb\times\phi}\cdot\frac{We_i}{P_i}$$

$$\therefore We_i = c_t P_i \cdot Vb \cdot \phi\left(\frac{\theta}{360}\right)$$

$$\ln\frac{\bar{P} - P_R}{P_i - P_R} = -\frac{Jt P_i}{We_i}$$

pressure at the reservoir-aquifer boundary, and n, is equal to 1 for Darcy flow during the pseudosteady-state flow region. Equations (8.15) and (8.16) can be combined to yield the following equation (see References 15 and 16 for the complete derivation):

$$W_e = \frac{W_e}{p_i}(p_i - p_R)\left(1 - e^{-\frac{Jp_i\Delta t}{W_e}}\right) \tag{8.17}$$

This equation was derived for constant pressures at both the reservoir-aquifer boundary, p_R, and the average pressure in the aquifer, $\bar{p}$. At this point, to apply the equation to a typical reservoir application where both of these pressures are changing with time, it would normally be required to use the principle of superposition. Fetkovich showed that by calculating the water influx for a short time period, Δt, with a corresponding average aquifer pressure, $\bar{p}$, and an average boundary pressure, $\bar{p}_R$, and then starting the calculation over again for a new period and new pressures, superposition was not needed. The following equations are used in the calculation for water influx with this method

$$\Delta W_{en} = \frac{W_e}{p_i}(\bar{p}_{n-1} - \bar{p}_{Rn})\left(1 - e^{-\frac{Jp_i\Delta t_n}{W_e}}\right) \tag{8.18}$$

$$\bar{p}_{n-1} = p_i\left(1 - \frac{W_e}{W_{ei}}\right) \text{ แทน Eq 8.15} \tag{8.19}$$

$$\bar{p}_{Rn} = \frac{p_{Rn-1} + p_{Rn}}{2} \tag{8.20}$$

$We_i = c_t\left(\frac{\theta}{360}\right) Vb\times\phi\times P_i$ $c_t = \frac{1}{V}\frac{dV}{dP}$

where n represents a particular interval, $\bar{p}_{n-1}$ is the average aquifer pressure at the end of the $n-1$ time interval, $\bar{p}_{Rn}$ is the average reservoir-aquifer boundary pressure during interval n, and W_e is the total, or cumulative, water influx and is given by

$$W_e = \Sigma\Delta W_{en} \tag{8.21}$$

The productivity index, J, used in the calculation procedure is a function of the geometry of the aquifer. Table 8.11 contains several aquifer productivity indexes as presented by Fetkovich.[15] When you use the equations for the condition of a constant pressure outer aquifer boundary, the average aquifer pressure in Eq. (8.18) will always be equal to the initial outer boundary pressure, which is usually p_i. Example 8.5 illustrates the use of the Fetkovich method.

Example 8.5. Repeat the water influx calculations for the reservoir in Ex. 8.3 using the Fetkovich approach.

TABLE 8.11.
Productivity indices for radial and linear aquifers (taken from reference 15)
Fetkovich

Type of Outer Aquifer Boundary	*Radial Flow*[a]	*Linear Flow*[b]
Finite—no flow	$J=\dfrac{0.00708kh\left(\frac{\theta}{360}\right)}{\mu[\ln(r_e/r_R)-0.75]}$	$J=\dfrac{0.003381kwh}{\mu L}$
Finite—constant pressure	$J=\dfrac{0.00708kh\left(\frac{\theta}{360}\right)}{\mu[\ln(r_e/r_R)]}$	$J=\dfrac{0.001127kwh}{\mu L}$

[a] Units are in normal field units with k in millidarcies.

[b] w is width and L is length of linear aquifer.

SOLUTION:

$$\text{area of aquifer}=\frac{1}{2}\pi r_e^2 \quad \text{or} \quad r_e=\left[\frac{250{,}000(43560)}{0.5\pi}\right]^{1/2}=83{,}263 \text{ ft}$$

$$\text{area of reservoir}=\frac{1}{2}\pi r_R^2 \quad \text{or} \quad r_R=\left[\frac{1216(43560)}{0.5\pi}\right]^{1/2}=5807 \text{ ft}$$

$$W_{ei}=\frac{c_t\left(\frac{\theta}{360}\right)\pi(r_e^2-r_R^2)h\phi p_i}{5.615}$$

$$W_{ei}=\frac{6(10)^{-6}\left(\frac{180}{360}\right)\pi(83{,}263^2-5807^2)19.2(0.209)3793}{5.615}=176.3(10)^6 \text{ bbl}$$

$$J=\frac{0.00708kh\left(\frac{\theta}{360}\right)}{\mu[\ln(r_e/r_R-0.75]}=\frac{0.00708(275)(19.2)\left(\frac{180}{360}\right)}{0.25\left[\ln\left(\frac{83{,}263}{5807}\right)-0.75\right]}=39.08$$

$$\Delta W_{en}=\frac{W_{ei}}{p_i}(\bar{p}_{n-1}-\bar{p}_{Rn})\left(1-e^{-\frac{Jp_i\Delta t_n}{W_{ei}}}\right)$$

$$=\frac{176.3\ (10)^6}{3793}(\bar{p}_{n-1}-\bar{p}_{Rn})\left(1-e^{-\frac{39.08(3793)(91.3)}{176.3(10)^6}}\right)$$

$$\Delta W_{en}=3435(\bar{p}_{n-1}-\bar{p}_{Rn}) \qquad (8.22)$$

$$\bar{p}_{n-1}=p_i\left(1-\frac{\Sigma\Delta W_{en}}{W_{ei}}\right)$$

$$\bar{p}_{n-1}=3793\left(1-\frac{\Sigma\Delta W_{en}}{176.3(10)^6}\right) \qquad (8.23)$$

Solving Eqs. (8.22) and (8.23), we get Table 8.12.

TABLE 8.12.

Time	p_R	$\bar{p}_{Rn}$	$\bar{p}_{n-1} - \bar{p}_{Rn}$	ΔW_e	W_e	$\bar{p}_n$
0	3793	3793	0	0	0	3793
1	3788	3790.5	2.5	8,600	8,600	3792.8
2	3774	3781	11.8	40,500	49,100	3791.9
3	3748	3761	30.9	106,100	155,200	3789.7
4	3709	3728.5	61.2	210,000	365,300	3785.1
5	3680	3694.5	90.6	311,200	676,500	3778.4
6	3643	3661.5	116.9	401,600	1,078,100	3769.8

The water influx values calculated by the Fetkovich method agree fairly closely with those calculated by the van Everdingen and Hurst method used in Ex. 8.3. The Fetkovich method consistently gives water influx values smaller than the values calculated by the van Everdingen and Hurst method for this problem (Fig. 8.14). This result could be because the Fetkovich method does not apply to an aquifer that remains in the transient time flow. It is apparent from observing the values of p_{n-1}, which are the average pressure values in the aquifer, that the pressure in the aquifer is not dropping very fast, which would indicate that the aquifer is very large and that the water flow from it to the reservoir could be transient in nature.

indicate that the aquifer is very large and that the water flow from it to the reservoir could be transient in nature.

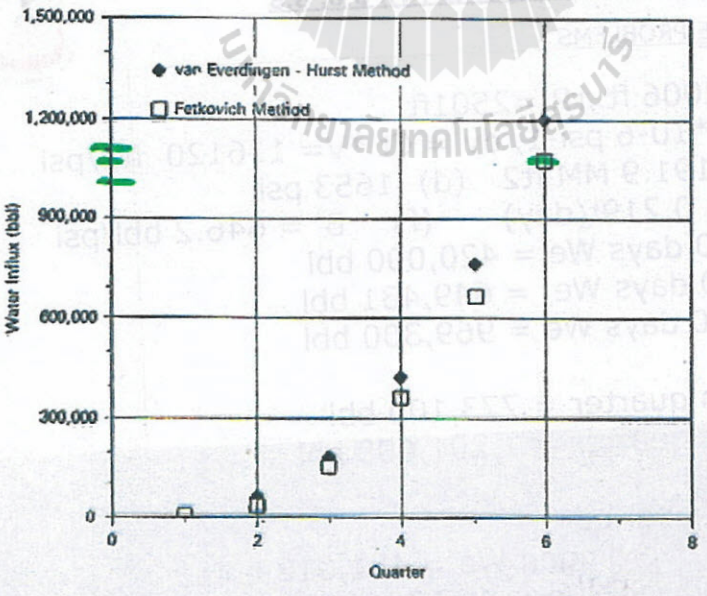

Fig. 8.14 Results of water influx calculations from Ex. 8.5.

Material Balance Equation:

The various forms of the Water Influx equation can be used to determine the term W_e which is part of the MBE. This additional information is incorporated into one form of MBE equation as follows:

$$N = N_{p_o} + G_{p_g} + W_{p_w} - W_e + \phi_w$$

$$= " \quad " \quad " - k\int(P_i - P)dt\ \phi_w \quad \text{steady}$$

$$= " \quad " \quad " - \frac{c\int(P_i - P)dt}{\log at}\ \phi_w$$

$$= " \quad " \quad " - [B]\Delta PQ(t)]\phi_w \quad \text{Unsteady}$$

$$\frac{F}{E_o} = N + \frac{We}{E_o} \quad \text{oil No gas Cap}$$

$$\frac{F}{E_g} = N + \frac{We}{E_g} \quad \text{Gas Reservoir.}$$

Wed

$$\frac{F}{E_o + m\frac{B_{ti}}{B_{gi}}E_g} = N + C\frac{\Sigma\Delta PQ(\Delta t_D)}{E_o + m\frac{B_{ti}}{B_{gi}}E_g}$$

Reservoir Engineering I, 2012

HW NO 8 Due date: Friday, August 24, 2012

Chapter 8: 8.5(a) to (g), 8.6, 8.8

ANSWERS TO THE PROBLEMS

8.5;(a) re= 2006 ft.,rR =2501ft.
(b) Ct=7*10-6 psi-1, dv = Ct *V= 116120 ft3/psi
(c) N= 191.9 MM ft2 (d) 1653 psi
(e) td = 0.219t(day) (f) B' = 646.2 bbl/psi
(g) @ 100 days We = 420,000 bbl
@ 200 days We = 649,431 bbl
@ 800 days We = 969,300 bbl

8.6; We at 5th quarter = 773,100 bbl
We at 6th quarter = 1,201,600 bbl

8.8; for the last period
(a) Van Everdingen We = 451,018 bbl
(b) Fetkovich We = 457,096 bbl

13. CHAPTER 9

Chapter 9

DISPLACEMENT OF

The Displacement of Oil and Gas

OIL AND GAS

1. INTRODUCTION

This chapter includes a discussion of the displacement of oil and gas both by external flooding processes and by internal displacement processes. It is not meant to be an exhaustive treatise but only an introduction. Several good books cover the material in this chapter more extensively.*[1-5] The reservoir engineer should be exposed to these concepts because they form the basis for understanding secondary and tertiary flooding techniques as well as some primary recovery mechanisms.

2. RECOVERY EFFICIENCY

The overall recovery efficiency E of any fluid displacement process is given by the product of the macroscopic, or volumetric displacement, efficiency, E_v, and the microscopic displacement efficiency, E_d:

$$E = E_v E_d \qquad (9.1)$$

*References throughout the text are given at the end of each chapter.

Chapter 9

$E = E_v \cdot E_d$

Macro Micro

The Displacement of Oil and Gas

1. INTRODUCTION

This chapter includes a discussion of the displacement of oil and gas both by external flooding processes and by internal displacement processes. It is not meant to be an exhaustive treatise but only an introduction. Several good books cover the material in this chapter more extensively.*[1-5] The reservoir engineer should be exposed to these concepts because they form the basis for understanding secondary and tertiary flooding techniques as well as some primary recovery mechanisms.

2. RECOVERY EFFICIENCY

The overall recovery efficiency E of any fluid displacement process is given by the product of the macroscopic, or volumetric displacement, efficiency, E_v, and the microscopic displacement efficiency, E_d:

$$E = E_v E_d \qquad (9.1)$$

* References throughout the text are given at the end of each chapter.

8.3.1 Injection Efficiency and Definition

The total efficiency is the recovery factor (for the zone subjected to flooding) in reservoir conditions:

$$E = \frac{N_p B_o}{V_p S_{oi}}$$

with S_{oi} at the start of flooding.

The total efficiency E of flooding can be defined as the product of the following three efficiencies (Fig. 8.8a):

$$E = E_A \cdot E_V \cdot E_D$$

with

E_A = areal sweep efficiency (in the same phase as the bed),
E_V = vertical or invasion efficiency (in vertical cross-section),
E_D = displacement efficiency, at the scale of the pores (microscopic efficiency).

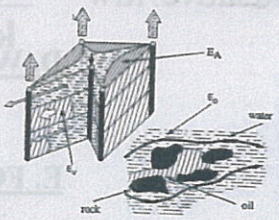

Fig. 8.8a

8.3.2 Areal Sweep Efficiency E_A

$$E_A \text{ (areal sweep efficiency)} = \frac{\text{Area swept by the front}}{\text{Total area}}$$

8. SECONDARY AND ENHANCED OIL RECOVERY

The surfaces are viewed in a horizontal plane (or bedding plane).

For a five-spot pattern, for example, the diagrams in Fig. 8.8b show the "front" at three times, for a homogeneous medium and draw off at four equal wells.

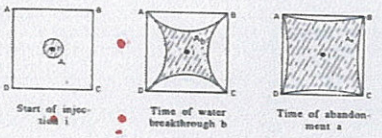

Start of injection i | Time of water breakthrough b | Time of abandonment a

Fig. 8.8b

The area sweep efficiency is written:

$$E_{Ai} = \frac{A_i}{\text{Area ABCD}} \qquad E_{Ab} = \frac{A_b}{\text{Area ABCD}} \qquad E_{Aa} = \frac{A_a}{\text{Area ABCD}}$$

E_A depends on the time (volume injected), the well pattern, and also on the **mobility ratio M**. Let us consider the direct streamline between an injection and a production well, and assume that the flood fluid is more mobile than the displaced fluid (M > 1).

Since the total pressure drop over the streamlines is constant, the pressure gradient is higher (shorter distance), and the speed of the front is greater on the direct line. Hence, if a bulge is formed in the front, it tends to lengthen and the flood fluid is produced before the zone between the injection and production wells is thoroughly swept.

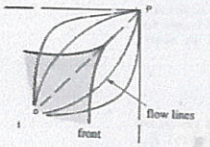

Fig. 8.8c

R. COSSE

273

RECOVERY Efficiency

$E = E_A \cdot E_h \cdot E_d$

$= E_v \cdot E_d$

= Macroscopic D. × Microscopic

Microscopic Displacement Ef

ขึ้นอยู่กับ 1. PORE SIZE
2. PERMEABILITY.
3. Interfacial Tension
4. Wettability
5. Capillary Pressure

MICROSCOPIC

PERMEABILITY $K = \dfrac{Q\mu\Delta L}{A\Delta P}$

- Absolute : one fluid phase in pore = k = 413 md ; k_w @ S_w = 1.0 or k_o @ S_o = 1.0
- Effective 2-3 phases in pore; k_{ew} @ S_w = 0.7, k_{ew} = 248 md, k_{eo} =50 md.
- Relative: $Krw = \dfrac{k_{ew}}{k}$.$Kro = \dfrac{k_{eo}}{k}$

D. WETTABILITY

- Water wet
- Oil wet

E. FORMATION COMPRESSIBILITY

$Cf = 1.87 \times 10^{-6} \times \phi^{-0.415}$ by Hall Humble

$= -\left(\frac{1}{V}\right)\left(\frac{dV}{dp}\right)$

F. FORMATION FACTORS

$F = Ro/Rw = a/\phi^m$

MICROSCOPIC ABSOLUTE PERMEABILITY

a single fluid is called the *absolute permeability* of the rock. If a core sample 0.00215 ft² in cross section and 0.1 ft long flows a 1.0 cp brine with a formation volume factor of 1.0 bbl/STB at the rate of 0.30 STB/day under a 30 psi pressure differential, it has an absolute permeability of Absolute K.

K_w

$$k = \frac{q_w B_w \mu_w L}{0.001127 A_c \Delta p} = \frac{0.30(1.0)(0.1)}{0.001127(0.00215)(30)} = 413 \text{ md}$$

If the water is replaced by an oil of 3.0 cp viscosity and 1.2 bbl/STB formation volume factor, under the same pressure differential the flow rate will be 0.0834 STB/day, and again the absolute permeability is

K_o

$$k = \frac{q_o B_o \mu_o L}{0.001127 A_c \Delta p} = \frac{0.0834(1.2)(3.0)(0.1)}{0.001127(0.00215)(30)} = 413 \text{ md}$$

If the same core is maintained at 70% water saturation ($S_w = 70\%$) and 30% oil saturation ($S_o = 30\%$), and at these and only these saturations and

under the same pressure drop it flows 0.18 STB/day of the brine and 0.01 STB/day of the oil, then the effective permeability to water is

Ed

$$k_w = \frac{q_w B_w \mu_w L}{0.001127 A_c \Delta p} = \frac{0.18(1.0)(1.0)(0.1)}{0.001127(0.00215)(30)} = 248 \text{ md}$$

and the effective permeability to oil is

$$k_o = \frac{q_o B_o \mu_o L}{0.001127 A_c \Delta p} = \frac{0.01(1.2)(3.0)(0.1)}{0.001127(0.00215)(30)} = 50 \text{ md}$$

The effective permeability, then, is the permeability of a rock to a particular fluid when that fluid has a pore saturation of less than 100%. As noted in the foregoing example, the sum of the effective permeabilities (i.e., 298 md) is always less than the absolute permeability, 413 md.

When two fluids, such as oil and water, are present, their relative rates of flow are determined by their relative viscosities, their relative formation volume factors, and their relative permeabilities. Relative permeability is the ratio of effective permeability to the absolute permeability. For the previous example, the relative permeabilities to water and to oil are

$$k_{rw} = \frac{k_w}{k} = \frac{248}{413} = 0.60$$

$$k_{ro} = \frac{k_o}{k} = \frac{50}{413} = 0.12$$

The flowing water-oil ratio at reservoir conditions depends on the viscosity ratio and the effective permeability ratio (i.e., on the mobility ratio), or

ratio, k_{rw}/k_{ro}, equals the effective permeability ratio, k_w/k_o. The term *relative permeability ratio* is more commonly used. For the previous example:

$$\frac{k_{rw}}{k_{ro}} = \frac{k_w/k}{k_o/k} = \frac{k_w}{k_o} = \frac{248}{50} = \frac{0.60}{0.12} = 5$$

Water flows at 14.9 times the oil rate because of a viscosity ratio of 3 and a relative permeability ratio of 5, both of which favor the water flow. Although the relative permeability ratio varies with the water-oil saturation ratio, in this example 70/30, or 2.33, the relationship is unfortunately far from one of simple proportionality.

Figure 9.1 shows a typical plot of oil and water relative permeability curves for a particular rock as a function of water saturation. Starting at 100% water saturation, the curves show that a decrease in water saturation to 85% (a 15% increase in oil saturation) sharply reduces the relative permeability to water from 100% down to 60%, and at 15% oil saturation the relative permeability to oil is essentially zero. This value of oil saturation, 15% in this case, is called the *critical saturation*, the saturation at which oil first begins to flow as the oil saturation increases. It is also called the *residual saturation*, the value below which the oil saturation cannot be reduced in an oil-water system. This explains why oil recovery by water drive is not 100% efficient. If the initial

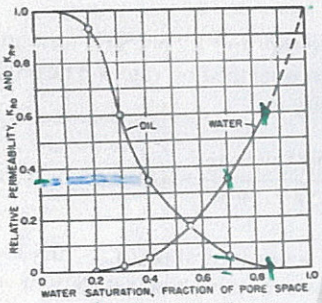

Fig. 9.1. Water-oil relative permeability curves.

connate water saturation is 20% for this particular rock, then the recovery from the portion of the reservoir invaded by high-pressure water influx is

$$\text{Recovery} = \frac{\text{initial-final}}{\text{initial}} = \frac{0.80 - 0.15}{0.80} = 81\%$$

Experiments show that essentially the same relative permeability curves are obtained for a gas-water system as for the oil-water system, which also means that the critical, or residual, gas saturation will be the same. Furthermore, it has been found that if both oil and free gas are present, the residual *hydrocarbon* saturation (oil and gas) will be about the same, in this case 15%. Suppose, then, that the rock is invaded by water at a pressure below saturation pressure so that free gas is present. If, for example, the residual free gas saturation behind the flood front is 10%, then the oil saturation is 5%, and neglecting small changes in the formation volume factors of the oil, the recovery is increased to:

$$\text{Recovery} = \frac{0.80 - 0.05}{0.80} = 94\%$$

Returning to Fig. 9.1, as the water saturation decreases further, the relative permeability to water continues to decrease and the relative permeability to oil increases. At 20% water saturation, the (connate) water is immobile, and the relative permeability to oil is quite high. This explains why some rocks may contain as much as 50% connate water and yet produce water-free oil. Most reservoir rocks are preferentially water wet—that is, the water phase and not the oil phase is next to the walls of the pore spaces. Because of this, at 20% water saturation the *water* occupies the *least favorable* portions of the pore spaces—that is, as thin layers about the sand grains, as thin layers on the walls of the pore cavities, and in the smaller crevices and capillaries. The oil, which occupies 80% of the pore space, is in the *most favorable* portions of the pore spaces, which is indicated by a relative permeability of 93%. The curves further indicate that about 10% of the pore spaces contribute nothing to the permeability, for at 10% water saturation, the relative permeability to oil is essentially 100%. Conversely, on the other end of the curves, 15% of the pore spaces contribute 40% of the permeability, for an increase in oil saturation from zero to 15% reduces the relative permeability to water from 100% to 60%.

In describing two-phase flow mathematically, it is always the relative permeability ratio that enters the equations. Figure 9.2 is a plot of the relative permeability ratio, k_o/k_w, versus water saturation for the same data of Fig. 9.1. Because of the wide range of k_o/k_w values, the relative permeability ratio is usually plotted on the log scale of semilog paper. Like many relative permeability ratio curves, the central or main portion of the curve is quite linear. As

a straight line or semilog paper, the relative permeability ratio may be expressed as a function of the water saturation by:

$$\frac{k_o}{k_w} = ae^{-bS_w} \tag{9.3}$$

The constants a and b may be determined from the graph shown in Fig. 9.2, or they may be determined from simultaneous equations. At $S_w = 0.30$, $k_o/k_w = 25$, and at $S_w = 0.70$, $k_o/k_w = 0.14$. Then

$$25 = ae^{-0.30b} \qquad \text{and} \qquad 0.14 = ae^{-0.70b}$$

Solving simultaneously, the intercept $a = 1220$, and the slope $b = 13.0$. Equation (9.3) indicates that the relative permeability ratio for a rock is a function of only the relative saturations of the fluids present. Although it is true that the viscosities, the interfacial tensions, and other factors have some effect on

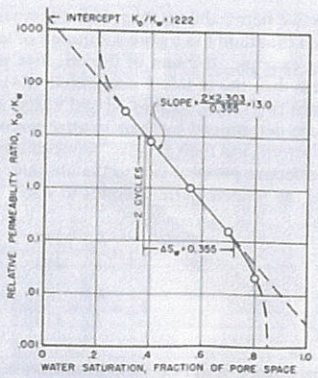

Fig. 9.2. Semilog plot of relative permeability ratio versus saturation.

tase permeability only to a limited extent. Since the nonwetting phase ccupies the central or larger pore openings which contribute materially to aid flow through the reservoir, however, a small nonwetting phase satution will drastically reduce the wetting phase permeability.

Figure 5-1 presents a typical set of relative permeability curves for a ater-oil system with the water being considered the wetting phase. Fige 5-1 shows the following four distinct and significant points:

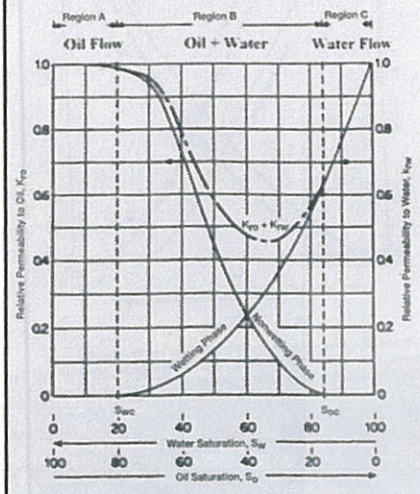

Figure 5-1. Typical two-phase flow behavior.

• Point 1

Point 1 on the wetting phase relative permeability shows that a saturation of the nonwetting phase will drastically reduce the r permeability of the wetting phase. The reason for this is that th wetting phase occupies the larger pore spaces, and it is in these pore spaces that flow occurs with the least difficulty.

• Point 2

Point 2 on the nonwetting phase relative permeability curve that the nonwetting phase begins to flow at the relatively low satu of the nonwetting phase. The saturation of the oil at this point is *critical oil saturation* S_{oc}.

• Point 3

Point 3 on the wetting phase relative permeability curve show the wetting phase will cease to flow at a relatively large saturatio is because the wetting phase preferentially occupies the smalle spaces, where capillary forces are the greatest. The saturation water at this point is referred to as the *irreducible water saturati* or *connate water saturation* S_{wi}—both terms are used interchange

• Point 4

Point 4 on the nonwetting phase relative permeability curve that, at the lower saturations of the wetting phase, changes in th ting phase saturation have only a small effect on the magnitude nonwetting phase relative permeability curve. The reason for th nomenon at Point 4 is that at the low saturations the wetting phas occupies the small pore spaces which do not contribute materia flow, and therefore changing the saturation in these small pore s has a relatively small effect on the flow of the nonwetting phase.

This process could have been visualized in reverse just as w should be noted that this example portrays oil as nonwetting and as wetting. The curve shapes shown are typical for wetting and no ting phases and may be mentally reversed to visualize the behav an oil-wet system. Note also that the total permeability to both p $k_{rw} + k_{ro}$, is less than 1, in regions B and C.

The above discussion may be also applied to gas-oil relative p ability data, as can be seen for a typical set of data in Figure 5-2. Lat this might be termed gas-liquid relative permeability since it i ted versus the liquid saturation. This is typical of gas-oil relative p ability data in the presence of connate water. Since the connate ducible) water normally occupies the smallest pores in the presence

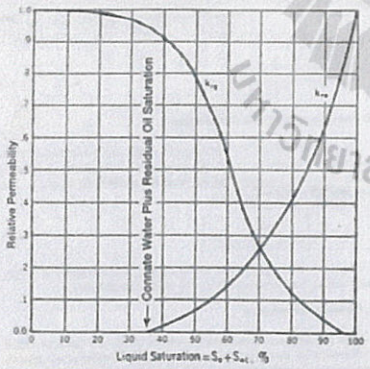

Figure 5-2. Gas-oil relative permeability curves.

and gas, it appears to make little difference whether water or oil that would also be immobile in these small pores occupies these pores. Consequently, in applying the gas-oil relative permeability data to a reservoir, the total liquid saturation is normally used as a basis for evaluating the relative permeability to the gas and oil.

Note that the relative permeability curve representing oil changes completely from the shape of the relative permeability curve for oil in the water-oil system. In the water-oil system, as noted previously, oil is normally the nonwetting phase, whereas in the presence of gas the oil is the wetting phase. Consequently, in the presence of water only, the oil relative permeability curve takes on an S shape whereas in the presence of gas the oil relative-permeability curve takes on the shape of the wetting phase, or is concave upward. Note further that the critical gas saturation S_{gc} is generally very small.

Another important phenomenon associated with fluid flow throug porous media is the concept of residual saturations. As when one immis cible fluid is displacing another, it is impossible to reduce the saturatio of the displaced fluid to zero. At some small saturation, which is pre sumed to be the saturation at which the displaced phase ceases to be con tinuous, flow of the displaced phase will cease. This saturation is ofte referred to as the *residual* saturation. This is an important concept as determines the maximum recovery from the reservoir. Conversely, a flui must develop a certain minimum saturation before the phase will begi to flow. This is evident from an examination of the relative permeabilit curves shown in Figure 5-1. The saturation at which a fluid will jus begin to flow is called the *critical* saturation.

Theoretically, the critical saturation and the residual saturation shoul be exactly equal for any fluid; however, they are not identical. **Critica saturation is measured in the direction of increasing saturation, whil irreducible saturation is measured in the direction of reducing satura tion.** Thus, the saturation histories of the two measurements are different.

As was discussed for capillary-pressure data, there is also a saturatio history effect for relative permeability. The effect of saturation history o relative permeability is illustrated in Figure 5-3. If the rock sample is ini tially saturated with the wetting phase (e.g., water) and relative-perme ability data are obtained by decreasing the wetting-phase saturation whil flowing nonwetting fluid (e.g., oil) in the core, the process is classified a *drainage* or *desaturation.*

If the data are obtained by increasing the saturation of the wettin phase, the process is termed *imbibition* or *resaturation.* The nomencla ture is consistent with that used in connection with capillary pressure. This difference in permeability when changing the saturation history i called *hysteresis.* Since relative permeability measurements are subject t hysteresis, it is important to duplicate, in the laboratory, the saturatio history of the reservoir.

Drainage Process

It is generally agreed that the pore spaces of reservoir rocks were orig inally filled with water, after which oil moved into the reservoir, displac ing some of the water, and reducing the water to some residual satura tion. When discovered, the reservoir pore spaces are filled with a connate water saturation and an oil saturation. If gas is the displacing agent, then gas moves into the reservoir, displacing the oil.

This same history must be duplicated in the laboratory to eliminate the effects of hysteresis. The laboratory procedure is to first saturate the core with water, then displace the water to a residual, or connate, water saturation with oil after which the oil in the core is displaced by gas. This flow process is called the gas drive, or drainage, depletion process. In the gas drive depletion process, the nonwetting phase fluid is continuously increased, and the wetting phase fluid is continuously decreased.

Imbibition Process

The *imbibition process* is performed in the laboratory by first saturating the core with the water (wetting phase), then displacing the water to its irreducible (connate) saturation by injection oil. This "drainage" procedure is designed to establish the original fluid saturations that are found when the reservoir is discovered. The wetting phase (water) is reintroduced into the core and the water (wetting phase) is continuously increased. This is the imbibition process and is intended to produce the relative permeability data needed for water drive or water flooding calculations.

Figure 5-3 schematically illustrates the difference in the drainage and imbibition processes of measuring relative permeability. It is noted that the imbibition technique causes the nonwetting phase (oil) to lose its mobility at higher values of water saturation than does the drainage process. The two processes have similar effects on the wetting phase (water) curve. The drainage method causes the wetting phase to lose its mobility at higher values of wetting-phase saturation than does the imbibition method.

Two-phase Relative Permeability Correlations

In many cases, relative permeability data on actual samples from the reservoir under study may not be available, in which case it is necessary to obtain the desired relative permeability data in some other manner. Field relative permeability data can usually be calculated, and the procedure will be discussed more fully in Chapter 6. The field data are unavailable for future production, however, and some substitute must be devised. Several methods have been developed for calculating relative permeability relationships. Various parameters have been used to calculate the relative permeability relationships, including:

- Residual and initial saturations
- Capillary pressure data

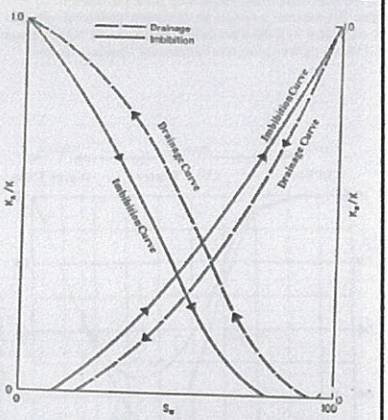

Figure 5-3. Hysteresis effects in relative permeability.

In addition, most of the proposed correlations use the effective phase saturation as a correlating parameter. The effective phase saturation is defined by the following set of relationships:

$$S_o^* = \frac{S_o}{1-S_{wc}} \tag{5-1}$$

$$S_w^* = \frac{S_w - S_{wc}}{1-S_{wc}} \tag{5-2}$$

$$S_g^* = \frac{S_g}{1-S_{wc}} \tag{5-3}$$

where S_o^*, S_w^*, S_g^* = effective oil, water, and gas saturation, respectively
S_o, S_w, S_g = oil, water and gas saturation, respectively
S_{wc} = connate (irreducible) water saturation

1. Wyllie and Gardner Correlation

Wyllie and Gardner (1958) observed that, in some rocks, the relationship between the reciprocal capillary pressure squared ($1/P_c^2$) and the effective water saturation S_w^* is linear over a wide range of saturation. Honapour et al. (1988) conveniently tabulated Wyllie and Gardner correlations as shown below:

Drainage Oil-Water Relative Permeabilities

Type of formation	k_{ro}	k_{rw}	Equation
Unconsolidated sand, well sorted	$(1-S_w^*)$	$(S_w^*)^3$	(5-4)
Unconsolidated sand, poorly sorted	$(1-S_w^*)^2(1-S_w^{*1.5})$	$(S_w^*)^{3.5}$	(5-5)
Cemented sandstone, oolitic limestone	$(1-S_w^*)^2(1-S_w^{*2})$	$(S_w^*)^4$	(5-6)

Drainage Gas-Oil Relative Permeabilities

Type of formation	k_{rw}	k_{rg}	Equation
Unconsolidated sand, well sorted	$(S_w^*)^3$	$(1-S_w^*)^3$	(5-7)
Unconsolidated sand, poorly sorted	$(S_w^*)^{3.5}$	$(1-S_w^*)^2(1-S_w^{*1.5})$	(5-8)
Cemented sandstone, oolitic limestone, rocks with vugular porosity	$(S_w^*)^4$	$(1-S_w^*)^2(1-S_w^{*2})$	(5-9)

Wyllie and Gardner have also suggested the following two expressions that can be used when one relative permeability is available:

- **Oil-water system**

$$k_{rw} = (S_w^*)^2 - k_{ro}\left[\frac{S_w^*}{1-S_w^*}\right] \tag{5-10}$$

- **Gas-oil system**

$$k_{ro} = (S_o^*) - k_{rg}\left[\frac{S_o^*}{1-S_o^*}\right] \tag{5-11}$$

2. Torcaso and Wyllie Correlation

Torcaso and Wyllie (1958) developed a simple expression to determine the relative permeability of the oil phase in a gas-oil system. The expression permits the calculation of k_{ro} from the measurements of k_{rg}. The equation has the following form:

$$k_{ro} = k_{rg}\left[\frac{(S_o^*)^4}{(1-S_o^*)^2(1-(S_o^*)^2)}\right] \tag{5-12}$$

The above expression is very useful since k_{rg} measurements are easily made and k_{ro} measurements are usually made with difficulty.

3. Pirson's Correlation

From petrophysical considerations, Pirson (1958) derived generalized relationships for determining the wetting and nonwetting phase relative permeability for both imbibition and drainage processes. The generalized expressions are applied for water-wet rocks.

For the water (wetting) phase

$$k_{rw} = \sqrt{S_w^*}\,S_w^3 \tag{5-13}$$

The above expression is valid for both the imbibition and drainage processes.

For the nonwetting phase

- **Imbibition**

$$(k_r)_{\text{nonwetting}} = \left[1-\left(\frac{S_w - S_{wc}}{1-S_{wc}-S_{orw}}\right)\right]^2 \tag{5-14}$$

• **Drainage**

$$(k_r)_{nonwetting} = (1 - S_w^*)\left[1 - (S_w^*)^{0.25}\sqrt{S_w^*}\right]^{0.5} \quad (5\text{-}15)$$

where S_{nw} = saturation of the nonwetting phase
S_w = water saturation
S_w^* = effective water saturation as defined by Equation 5-2

Example 5-1

Generate the drainage relative permeability data for an unconsolidated well-sorted sand by using the Wyllie and Gardner method. Assume the following critical saturation values:

$S_{iw} = 0.3, \quad S_{wc} = 0.25, \quad S_{gc} = 0.05$

Solution

Generate the oil-water relative permeability data by applying Equation 5-4 in conjunction with Equation 5-2, to give:

S_w	$S_w^* = \frac{S_w - S_{wc}}{1 - S_{wc}}$	$k_{rw} = (S_w^*)^3$	$k_{ro} = (S_o^*)^3$
0.25	0.0000	1.000	0.0000
0.30	0.0667	0.813	0.0003
0.35	0.1333	0.651	0.0024
0.40	0.2000	0.512	0.0080
0.45	0.2667	0.394	0.0190
0.50	0.3333	0.296	0.0370
0.60	0.4667	0.152	0.1017
0.70	0.6000	0.064	0.2160

Apply Equation 5-7 in conjunction with Equation 5-1 to generate relative permeability data for the gas-oil system.

S_g	$S_o = 1 - S_g - S_{wc}$	$S_o^* = \frac{S_o}{1 - S_{wc}}$	$k_{ro} = (S_o^*)^3$	$k_{rg} = (1 - S_g^*)^3$
0.05	0.70	0.933	0.813	—
0.10	0.65	0.867	0.651	0.002
0.20	0.55	0.733	0.394	0.019
0.30	0.45	0.600	0.216	0.064
0.40	0.35	0.467	0.102	0.152
0.50	0.25	0.333	0.037	0.296
0.60	0.15	0.200	0.008	0.512
0.70	0.05	0.067	0.000	0.813

Example 5-2

Resolve Example 5-1 by using Pirson's correlation for the water-oil system.

Solution

S_w	$k_{rw} = \frac{k_w}{k}$	$k_{ro} = \sqrt{S_w^*}\,S_o^2$	$k_{rw} = (1 - S_w^*)^2\left[1 - (S_w^*)^{1.25}\sqrt{S_w^*}\right]^{0.5}$
0.25	0.0000	0.000	1.000
0.30	0.0667	0.007	0.793
0.35	0.1333	0.016	0.695
0.40	0.2000	0.029	0.608
0.45	0.2667	0.047	0.528
0.50	0.3333	0.072	0.454
0.60	0.4667	0.148	0.320
0.70	0.6000	0.266	0.205

4. Corey's Method

Corey (1954) proposed a simple mathematical expression for generating the relative permeability data of the gas-oil system. The approximation is good for drainage processes, i.e., gas-displacing oil.

$$k_{ro} = (1 - S_g^*)^4 \quad (5\text{-}16)$$

$$k_{rg} = (S_g^*)(2 - S_g^*) \quad (5\text{-}17)$$

where the effective gas saturation S_g^* is defined in Equation 5-3.

Example 5-3

Use Corey's approximation to generate the gas-oil relative permeability for a formation with a connate water saturation of 0.25.

Solution

S_g	$S_g^* = \frac{S_g}{1 - S_{wc}}$	$k_{ro} = (1 - S_g^*)^4$	$k_{rg} = (S_g^*)^2(2 - S_g^*)$
0.05	0.0667	0.759	0.001
0.10	0.1333	0.564	0.004
0.20	0.2667	0.289	0.033
0.30	0.4000	0.130	0.102
0.40	0.5333	0.047	0.222
0.50	0.6667	0.012	0.395
0.60	0.8000	0.002	0.614
0.70	0.9333	0.000	0.867

5. Relative Permeability from Capillary Pressure Data

Rose and Bruce (1949) showed that capillary pressure p_c is a measure of the fundamental characteristics of the formation and could also be used to predict the relative permeabilities. Based on the concepts of tortuosity, Wyllie and Gardner (1958) developed the following mathematical expression for determining the drainage water-oil relative permeability from capillary pressure data:

$$k_{rw} = \left(\frac{S_w - S_{wc}}{1 - S_{wc}}\right)^2 \frac{\int_{S_{wc}}^{S_w} dS_w / p_c^2}{\int_{S_{wc}}^{1} dS_w / p_c^2} \quad (5\text{-}18)$$

$$k_{ro} = \left(\frac{1 - S_w}{1 - S_{wc}}\right)^2 \frac{\int_{S_w}^{1} dS_w / p_c^2}{\int_{S_{wc}}^{1} dS_w / (p_c)^2} \quad (5\text{-}19)$$

Wyllie and Gardner also presented two expressions for generating the oil and gas relative permeabilities in the presence of the connate water saturation. The authors considered the connate water as part of the rock matrix to give:

$$k_{ro} = \left(\frac{S_o - S_{or}}{1 - S_{wc}}\right)^2 \frac{\int_0^{S_o} dS_w / p_c^2}{\int_0^{1} dS_w / p_c^2} \quad (5\text{-}20)$$

$$k_{rg} = \left(1 - \frac{S_o - S_{or}}{S_g - S_{gc}}\right)^2 \frac{\int_{S_{or}}^{1} dS_w / p_c^2}{\int_0^{1} dS_w / p_c^2} \quad (5\text{-}21)$$

where S_{gc} = critical gas saturation
S_{wc} = connate water saturation
S_{or} = residual oil saturation

Example 5-4

The laboratory capillary pressure curve for a water-oil system, between the connate water saturation and a water saturation of 100% is represented by the following linear equation:

$$P_c = 22 - 20\,S_w$$

The connate water saturation is 30%. Using Wyllie and Gardner methods, generate the relative permeability data for the oil-water system.

Solution

Step 1. Integrate the capillary pressure equation, to give:

$$I = \int_a^b \frac{dS_w}{(22 - 20S_w)^2} = \left[\frac{1}{440 - 400b}\right] - \left[\frac{1}{440 - 400a}\right]$$

MACROSCOPIC

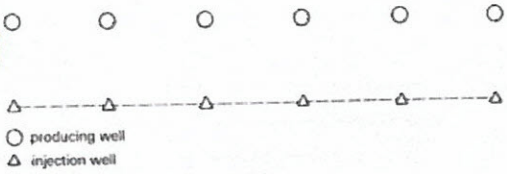

Fig. 9.5(a). Direct-line-drive flooding network.

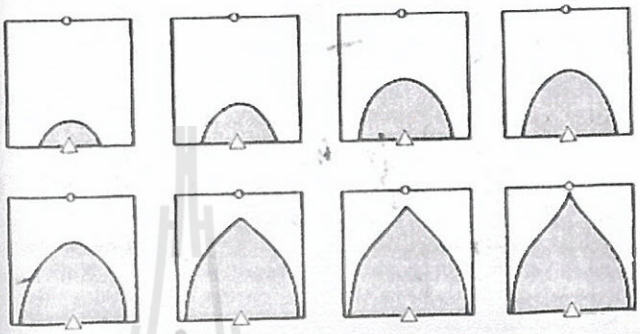

Fig. 9.5(b). The photographic history of a direct-line-drive fluid-injection system under steady-state conditions, as obtained with a blotting-paper electrolytic model (*After* Wyckoff, Botset, and Muskat.[6])

MACROSCOPIC

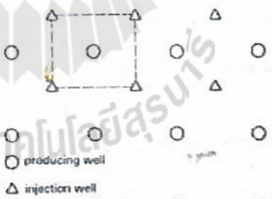

Fig. 9.6(a). Five-spot flooding network.

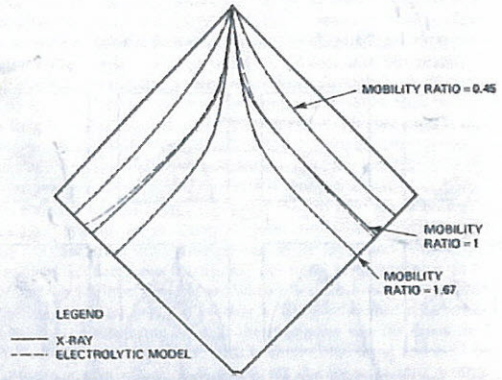

Fig. 9.6(b). X-ray shadowgraph studies showing the effect of mobility ratio on areal sweep efficiency at breakthrough. (*After* Slobod and Caudle.[7])

3. IMMISCIBLE DISPLACEMENT PROCESSES

3.1. The Buckley-Leverett Displacement Mechanism

Oil is displaced from a rock by water somewhat as fluid is displaced from a cylinder by a leaky piston. Buckley and Leverett developed a theory of displacement based on the relative permeability concept.[8] Their theory is presented here.

Consider a linear bed containing oil and water (Fig. 9.7). Let the total throughput, $q_t' = q_w B_w + q_o B_o$ in reservoir barrels be the same at all cross

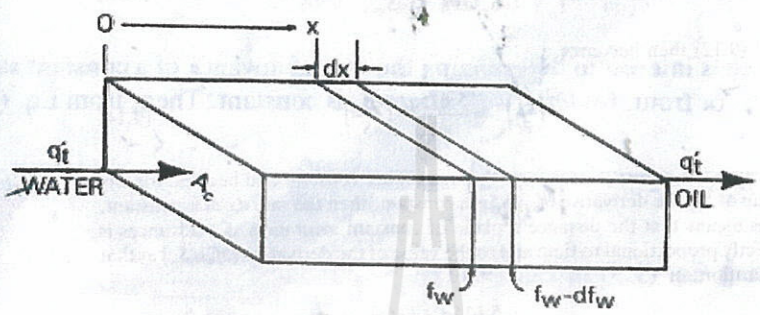

Fig. 9.7.

$$\frac{dW}{dt} = \frac{\phi A_c\, dx}{5.615}\left(\frac{\partial S_w}{\partial t}\right)_x \tag{9.7}$$

The subscript x on the derivative indicates that this derivative is different for each element. If f_w is the fraction of water in the total flow of q_t' barrels per day, then $f_w q_t'$ is the rate of water entering the left-hand face of the element dx. The oil saturation will be slightly higher at the right-hand face, so the fraction of water flowing there will be slightly less, or $f_w - df_w$. Then the rate of water leaving the element is $(f_w - df_w)q_t'$. The net rate of gain of water in the element at any time then is

$$\frac{dW}{dt} = (f_w - df_w)q_t' - f_w q_t' = -q_t' df_w$$

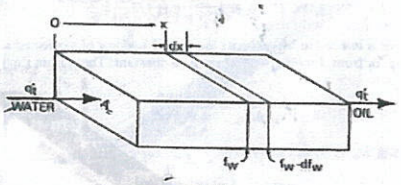

Fig. 9.7.

Equating (9.7) and (9.8),

$$\left(\frac{\partial S_w}{\partial t}\right)_x = -\frac{5.615 q_t'}{\phi A_c}\left(\frac{\partial f_w}{\partial x}\right)_t$$

Now for a given rock, the fraction of water f_w is a function only of the water saturation S_w, as indicated by Eq. (9.5), assuming constant oil and water viscosities. The water saturation, however, is a function of both time and position, x, which may be expressed as $f_w = F(S_w)$ and $S_w = G(t, x)$. Then

$$dS_w = \left(\frac{\partial S_w}{\partial t}\right)_x dt + \left(\frac{\partial S_w}{\partial x}\right)_t dx$$

at front dSw=0

Now, there is interest in determining the rate of advance of a constant saturation plane, or front, $(\partial x/\partial t)_{S_w}$ i.e., where S_w is constant. Then, from Eq. (9.10)

$$\left(\frac{\partial x}{\partial t}\right)_{S_w} = -\frac{(\partial S_w/\partial t)_x}{(\partial S_w/\partial x)_t} \tag{9.11}$$

Substituting Eq. (9.9) in Eq. (9.11),

$$\left(\frac{\partial x}{\partial t}\right)_{S_w} = \frac{5.615 q_t'}{\phi A_c} \frac{(\partial f_w/\partial x)_t}{(\partial S_w/\partial x)_t} \tag{9.12}$$

But

$$\frac{(\partial f_w/\partial x)_t}{(\partial S_w/\partial x)_t} = \left(\frac{\partial f_w}{\partial S_w}\right)_t \tag{9.13}$$

Eq. (9.12) then becomes

$$\left(\frac{\partial x}{\partial t}\right)_{S_w} = \frac{5.615 q_t'}{\phi A_c} \left(\frac{\partial f_w}{\partial S_w}\right)_t \tag{9.14}$$

Because the porosity, area, and throughput are constant and because for any value of S_w, the derivative $\partial f_w/\partial S_w$ is a constant, then the rate dx/dt is constant. This means that the distance a plane of constant saturation, S_w, advances is directly proportional to time and to the value of the derivative $(\partial f_w/\partial S_w)$ at that saturation, or

$$x = \frac{5.615 q_t' t}{\phi A_c} \left(\frac{\partial f_w}{\partial S_w}\right)_{S_w} \tag{9.15}$$

$$x = \frac{5.615 q_t' t}{\phi A_c} \left(\frac{\partial f_w}{\partial S_w}\right)_{S_w} \tag{9.15}$$

We now apply Eq. (9.15) to a reservoir under active water drive where the wells are located in uniform rows along the strike on 40 ac spacing, as shown in Fig. 9.8. This gives rise to approximate linear flow, and if the daily production of each of the three wells located along the dip is 200 STB of oil per day, then for an active water drive and an oil volume factor of 1.50 bbl/STB, the total reservoir throughput, q_t', will be 900 bbl/day.

The cross-sectional area is the product of the width, 1320 ft, and the true formation thickness, 20 ft, so that for a porosity of 25%, Eq. (9.15) becomes

$$x = \frac{5.615 \times 900 \times t}{0.25 \times 1320 \times 20} \left(\frac{\partial f_w}{\partial S_w}\right)_{S_w}$$

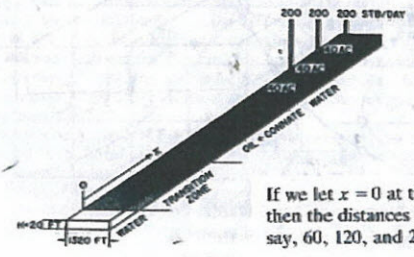

Fig. 9.8.

If we let $x = 0$ at the bottom of the transition zone, as indicated in Fig. 9.8, then the distances the various constant water saturation planes will travel in, say, 60, 120, and 240 days are given by:

$$x_{60} = 46\,(\partial f_w/\partial S_w)_{S_w}$$
$$x_{120} = 92\,(\partial f_w/\partial S_w)_{S_w}$$
$$x_{240} = 184\,(\partial f_w/\partial S_w)_{S_w} \tag{9.16}$$

The value of the derivative $(\partial f_w/\partial S_w)$ may be obtained for any value of water saturation, S_w, by plotting f_w from Eq. (9.5) versus S_w and graphically taking the slopes at values of S_w. This is shown in Fig. 9.9 at 40% water saturation using the relative permeability ratio data of Table 9.1 and a water-oil viscosity ratio of 0.50. For example, at $S_w = 0.40$, where $k_o/k_w = 5.50$ (Table 9.1),

$$f_w = \frac{1}{1 + 0.50 \times 5.50} = 0.267$$

The slope taken graphically at $S_w = 0.40$ and $f_w = 0.267$ is 2.25, as shown in Fig. 9.9.

The derivative $(\partial f_w/\partial S_w)$ may also be obtained mathematically using

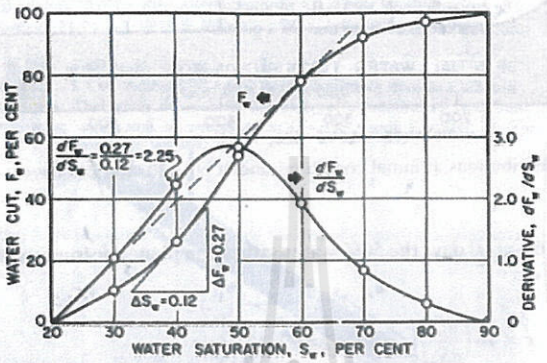

Fig. 9.9.

TABLE 9.1.
Buckley-Leverett frontal advance calculations

(1) S_w	(2) $\frac{k_o}{k_w}$	(3) $\frac{\mu_w}{\mu_o} = 0.50$ f_w Eq. (9.5)	(4) $\frac{\partial f_w}{\partial S_w}$ Eq. (9.17)	(5) $46\frac{\partial f_w}{\partial S_w}$ (60 days) Eq. (9.16)	(6) $92\frac{\partial f_w}{\partial S_w}$ (120 days) Eq. (9.16)	(7) $184\frac{\partial f_w}{\partial S_w}$ (240 days) Eq. (9.16)
0.20	inf.	0.000	0.00	0	0	0
0.30	17.0	0.105	1.08	50	100	200
0.40	5.50	0.267	2.25	104	208	416
0.50	1.70	0.541	2.86	131	262	524
0.60	0.55	0.784	1.95	89	179	358
0.70	0.17	0.922	0.83	38	76	153
0.80	0.0055	0.973	0.30	14	28	55
0.90	0.000	1.000	0.00	0	0	0

Eq. (9.3) to represent the relationship between the relative permeability ratio and the water saturation. Differentiating Eq. (9.16), we obtain

$$\frac{\partial f_w}{\partial S_w} = \frac{(\mu_w/\mu_o)bae^{-bS_w}}{[1 + (\mu_w/\mu_o)ae^{-bS_w}]^2} = \frac{(\mu_w/\mu_o)b(k_o/k_w)}{[1 + (\mu_w/\mu_o)(k_o/k_w)]^2} \qquad (9.17)$$

For the k_o/k_w data of Table 9.1, $a = 540$ and $b = 11.5$. Then, at $S_w = 0.40$, for example, by Eq. (9.17).

$$\frac{\partial f_w}{\partial S_w} = \frac{0.50 \times 11.5 \times 5.50}{[1 + 0.50 \times 5.50]^2} = 2.25$$

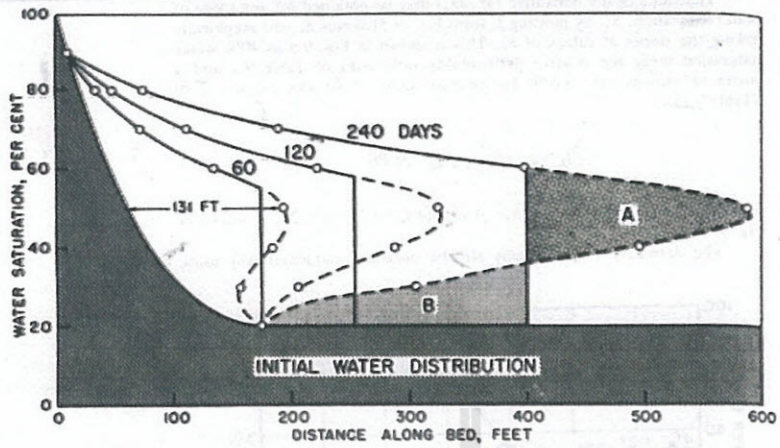

Fig. 9.10. Fluid distributions at initial conditions and at 60, 120, and 240 days.

2.86; so by Eq. (9.16), at 60 days the 50% water saturation plane, or front, will advance a distance of:

$$x = 46\left(\frac{\partial f_w}{\partial S_w}\right)_{S_w} = 46 \times 2.86 = 131 \text{ feet}$$

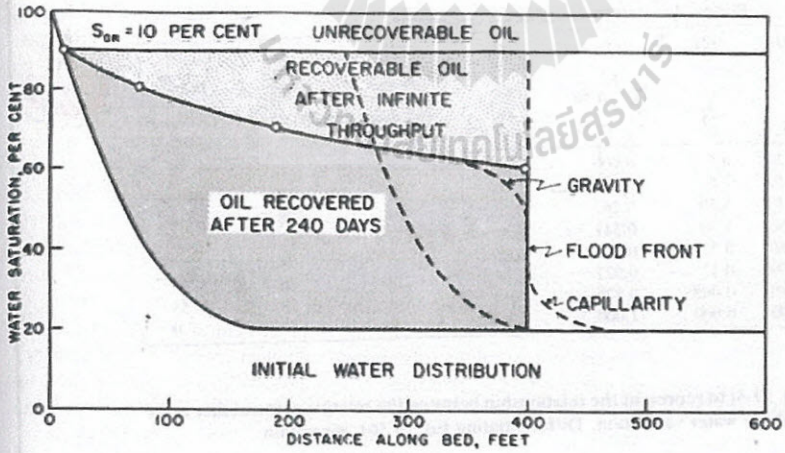

Fig. 9.11.

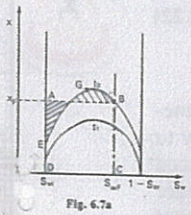

Fig. 6.7a

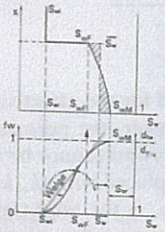

S_{wi} = Pore water saturation (oil zone).
S_{wF} = Water saturation at front.
S_{wM} = Maximum water saturation = $1 - S_{or}$.
S_{wm} = Average water saturation behind the front.

Fig. 6.7b

speed of the front is thus obtained by calculating df_w/dS_w from f_w (Fig. 6.7b). The calculation of the slope of the Welge tangent gives:

$$\left(\frac{df_w}{dS_w}\right)_{S_{wF}} = \frac{1}{S_{wm} - S_{wi}}$$

It can be shown that S_{wm} is the value of the average saturation behind the front.

This leads to the second application of the Welge tangent: the value of the average saturation behind the front S_{wm} is obtained from the intersection of the tangent with $f_w = 1$. Hence the equation:

$$V_F = \frac{Q_T}{A\,\phi\,(S_{wm} - S_{wi})}$$

where V_F = speed at the front.

$[df_w/dS_w]_{S_{we}}$

Welge demonstrated that

$$[df_w/dS_w]_{S_{we}} = \frac{1 - f_{we}}{\bar{S}_w - S_{we}}$$

This relationship at some time after breakthrough can be seen in Fig. 7.10. Since

$$\frac{q_T - qS_{wi}}{LA\phi} = \frac{1}{df_w/dS_w}$$

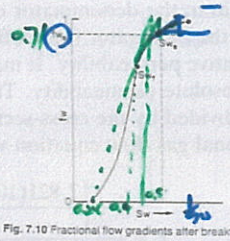

Fig. 7.10 Fractional flow gradients after breakthrough.

then the relationship between time and the attainment of a given outlet end face saturation is readily obtained, i.e.

$$t_{(S_w=c)} = \frac{LA\phi}{q_T}\left[\frac{1}{df_w/dS_w}\right]_{S_w}$$

$$\bar{S}_w = S_{we} + \left[\frac{1 - f_{we}}{df_w/dS_w}\right]_{S_{we}}$$

$$f_g = \frac{v_g}{v_t} = -\frac{0.001127k_g}{\mu_g v_t}\left[\left(\frac{dp}{dx}\right)_g - 0.00694\,\rho_g\cos\alpha\right] \qquad (9.18)$$

The total velocity is v_t, which is the total throughput rate q_t' divided by the cross-sectional area A_c. The reservoir gas density, ρ_g, is in lb_m/ft^3. When capillary forces are neglected, as they are in this application, the pressure gradients in the oil and gas phases are equal. Equation (7.1) may be solved for the pressure gradient by applying it to the oil phase, or

$$\left(\frac{dp}{dx}\right)_o = \left(\frac{dp}{dx}\right)_g = -\frac{\mu_o v_o}{0.001127k_o} + 0.00694\,\rho_o\cos\alpha \qquad (9.19)$$

Substituting the pressure gradient of Eq. (9.19) in Eq. (9.18),

$$f_g = -\frac{0.001127k_g}{\mu_g v_t}\left[-\frac{\mu_o v_o}{0.001127k_o} + 0.00694\,(\rho_o - \rho_g)\cos\alpha\right] \qquad (9.20)$$

Expanding and multiplying through by $(k_o/k_g)(\mu_g/\mu_o)$,

$$f_g\left[\frac{k_o\mu_g}{k_g\mu_o}\right] = \frac{v_o}{v_t} - \frac{7.821(10^{-6})k_o(\rho_o - \rho_g)\cos\alpha}{\mu_o v_t} \qquad (9.21)$$

But v_o/v_t is the fraction of oil flowing, which equals 1 minus the gas flowing, $(1 - f_g)$. Then, finally,

$$f_g = \frac{1 - \left[\dfrac{7.821(10^{-6})k_o(\rho_o - \rho_g)\cos\alpha}{\mu_o v_t}\right]}{1 + \dfrac{k_o\mu_g}{k_g\mu_o}} \tag{9.22}$$

The relative permeability ratio (k_{ro}/k_{rg}) may be used for the effective permeability ratio in the denominator of Eq. (9.22); however, the permeability to oil, k_o, in the numerator is the effective permeability and cannot be replaced by the relative permeability. It may, however, be replaced with ($k_{ro}k$), where k is the absolute permeability. The total velocity, v_t, is the total throughput rate, q_t', divided by the cross-sectional area, A_c. Inserting these equivalents, the fractional gas flow equation with gravitational segregation becomes

$$f_g = \frac{1 - \left[\dfrac{7.821(10^{-6})kA_c(\rho_o - \rho_g)\cos\alpha}{\mu_o}\right]\left(\dfrac{k_{ro}}{q_t'}\right)}{1 + \dfrac{k_o\mu_g}{k_g\mu_o}} \tag{9.23}$$

If the gravitational forces are small, Eq. (9.23) reduces to the same type of fractional flow equation as Eq. (9.5), or

$$f_g = \frac{1}{1 + \dfrac{k_o\mu_g}{k_g\mu_o}} \tag{9.24}$$

$$f_g = \frac{1 - \left[\dfrac{7.821(10^{-6})(300)(1.237(10)^{\circ})(48.7 - 5.)\cos 72.5^{\circ}}{1.32}\right]\left(\dfrac{k_{ro}}{11,600}\right)}{1 + \dfrac{k_o(0.0134)}{k_g(1.32)}}$$

$$f_g = \frac{1 - 2.50k_{ro}}{1 + 0.0102\left(\dfrac{k_{ro}}{k_g}\right)} \tag{9.25}$$

The values of f_g have been calculated in Table 9.2 for three conditions: (a) assuming negligible gravitational segregation by using Eq. (9.24); (b) using the gravitational term equal to 2.50 k_{ro} for the Mile Six Pool, Eq. (9.25); and (c) assuming the gravitational term equals 1.25 k_{ro}, or half the value at Mile Six Pool. The values of f_g for these three conditions are shown plotted in Fig. 9.13. The negative values of f_g for the conditions that existed in the Mile Six Pool indicate counter-current gas flow (i.e., gas updip and oil downdip) in the range of gas saturations between an assumed critical gas saturation of 5% and about 17%.

The distance of advance of any gas saturation plane may be calculated

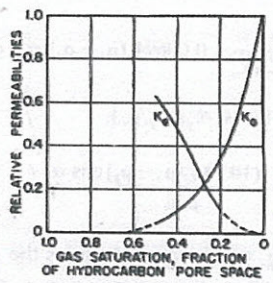

Fig. 9.12. Relative permeabilities for the Mile Six Pool, Peru.

TABLE 9.2.
Mile Six Pool Reservoir data and calculations

Avg. Absolute permeability = 300 md
Avg. hydrocarbon porosity = 0.1625
Avg. connate water = 0.35
Avg. dip angle = 17° 30′ ($\alpha = 90° - 17°30'$)
Ave. cross-sectional area = 1,237,000 sq ft
Reservoir oil viscosity = 1.32 cp
Reservoir gas viscosity = 0.0134 cp

Reservoir oil sp. gr. = 0.78 (water = 1)
Reservoir gas sp. gr. = 0.08 (water = 1)
Reservoir temperature = 114°F
Average reservoir pressure = 850 psia
Average throughput = 11,600 reservoir bbl per day
Oil volume factor = 1.25 bbl/STB
Solution gas at 850 psia = 400 SCF/STB
Gas deviation factor = 0.74

S_g	0.05	0.10	0.15	0.20	0.25	0.30	0.35	0.40	0.45	0.50	0.55	0.60
k_o/k_g	inf.	38	8.80	3.10	1.40	0.72	0.364	0.210	0.118	0.072	0.024	0.00
Gravity term = 0												
f_g	0	0.720	0.918	0.969	0.986	0.993	0.996	0.998	0.990	1.00	1.00	1.00
$\partial f_g/\partial S_g$		7.40	1.20	0.60	0.30							
$x = 32\ \partial f_g/\partial S_g$		237	38	19	10							
Gravity term = 2.50 × k_{ro}												
k_{ro}	0.77	0.59	0.44	0.34	0.26	0.19	0.14	0.10	0.065	0.040	0.018	0.00
2.50 × k_{ro}	1.92	1.48	1.10	0.85	0.65	0.48	0.35	0.25	0.160	0.10	0.045	0.00
1-2.5 k_{ro}	−0.92	−0.48	−0.10	0.15	0.35	0.52	0.65	0.75	0.84	0.90	0.955	1.00
f_g	0	−0.29	−0.092	0.145	0.345	0.516	0.647	0.749	0.840	0.900	0.955	1.00
$\partial f_g/\partial S_g$		3.30	4.40	4.30	3.60	3.00	2.50	1.95	1.60	1.20	0.80	
32 $\partial f_g/\partial S_g$		106	141	138	115	96	80	62	51	38	26	
Gravity term = 1.25 × k_{ro}												
1.25 k_{ro}	0.96	0.74	0.55	0.425	0.325	0.240	0.175	0.125	0.080	0.050	0.023	0.00
1-1.25 k_{ro}	0.04	0.26	0.45	0.575	0.675	0.760	0.825	0.875	0.920	0.950	0.977	1.00
f_g		0.190	0.413	0.557	0.666	0.755	0.822	0.873	0.920	0.950	0.977	1.00
$\partial f_g/\partial S_g$		4.00	3.60	2.40	1.90	1.50	1.20	1.00	0.80	0.60		
32 $\partial f_g/\partial S_g$		128	115	77	61	48	38	32	26	19		

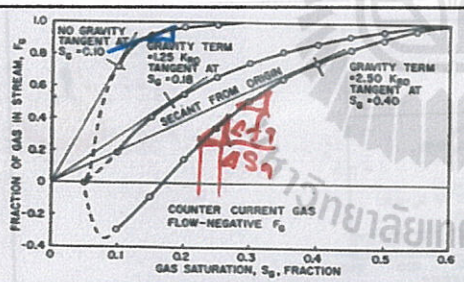

Fig. 9.13. Fraction of gas in reservoir stream for the Mile Six Pool, Peru.

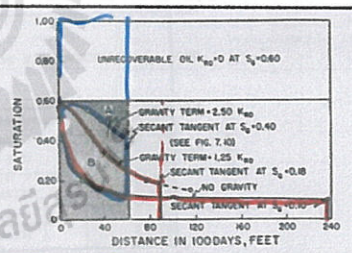

Fig. 9.14. Fluid distributions in the Mile Six Pool after 100 days injection.

for the Mile Six Pool, using Eq. (9.15), replacing water as the displacing fluid by gas, or

$$x = \frac{5.615\, q_t' t}{\phi A_c}\left(\frac{\partial f_g}{\partial S_g}\right)_{S_g}$$

In 100 days, then,

$$x = \frac{5.615(11{,}600)(100)}{0.1625(1{,}237{,}000)}\left(\frac{\partial f_g}{\partial S_g}\right)_{S_g}$$

$$x = 32.4\left(\frac{\partial f_g}{\partial S_g}\right)_{S_g} \qquad (9.26)$$

The values of the derivatives $(\partial f_g/\partial S_g)$ given in Table 9.2 have been determined graphically from Fig. 9.13. Figure 9.14 shows the plots of Eq. (9.26) to obtain the gas-oil distributions and the positions of the gas front after 100 days. The shape of the curves will not be altered for any other time. The distribution and fronts at 1000 days, for example, may be obtained by simply changing the scale on the distance axis by a factor of 10.

Welge showed that the position of the front may be obtained by drawing a secant from the origin as shown in Fig. 9.13.[9] For example, the secant is tangent to the lower curve at 40% gas saturation. Then in Fig. 9.14 the front

connate water saturation, as indicated by the dashed line in Fig. 9.9. This is tangent at a water saturation of 60%. Referring to Fig. 9.10, the 240-day front is seen to occur at 60% water saturation. Owing to the presence of an initial transition zone, the fronts at 60 and 120 days occur at slightly lower values of water saturation.

The much greater displacement efficiency with gravity segregation than without is apparent from Fig. 9.14. Since the permeability to oil is *essentially* zero at 60% gas saturation, the maximum recovery by gas displacement and gravity drainage is 60% of the initial oil in place. Actually some small permeability to oil exists at even very low oil saturations, which explains why some fields may continue to produce at low rates for quite long periods after the pressure has been depleted. The displacement efficiency may be calculated from Fig. 9.14 by the measurement of areas. For example, the displacement efficiency at Mile Six Pool with full gravity segregation is in excess of

$$\text{Recovery} = \frac{\text{Area } B}{\text{Area } A + \text{Area } B} = \frac{32.5}{4.7 + 32.5} = 0.874, \text{ or } 87.4\%$$

If the gravity segregation had been half as effective, the recovery would have been about 60%; without gravity segregation, the recovery would have been only 24%. These recoveries are expressed as percentages of the *recoverable oil*. In terms of the *initial oil* in place, the recoveries are only 60% as large, or 52.4, 36.0, and 14.4%, respectively. Welge, Shreve and Welch, Kern, and others have extended the concepts presented here to the prediction of gas-oil ratios, production rates, and cumulative recoveries, including the treatment of

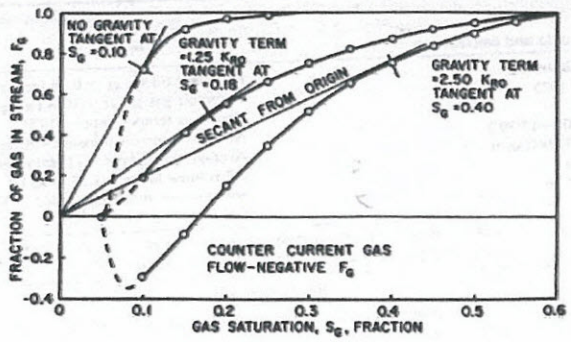

Fig. 9.13. Fraction of gas in reservoir stream for the Mile Six Pool, Peru.

for the Mile Six Pool, using Eq. (9.15), replacing water as the displacing fluid by gas, or

$$x = \frac{5.615\, q_t' t}{\phi A_c}\left(\frac{\partial f_g}{\partial S_g}\right)_{S_g}$$

In 100 days, then,

$$x = \frac{5.615(11{,}600)(100)}{0.1625(1{,}237{,}000)}\left(\frac{\partial f_g}{\partial S_g}\right)_{S_g}$$

$$x = 32.4\left(\frac{\partial f_g}{\partial S_g}\right)_{S_g} \qquad (9.26)$$

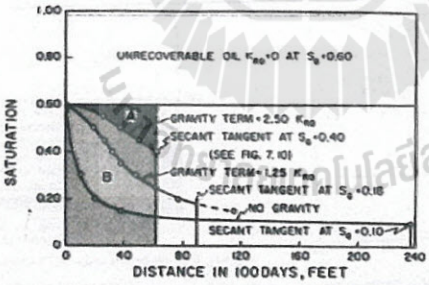

Fig. 9.14. Fluid distributions in the Mile Six Pool after 100 days injection.

connate water saturation, as indicated by the dashed line in Fig. 9.9. This is tangent at a water saturation of 60%. Referring to Fig. 9.10, the 240-day front is seen to occur at 60% water saturation. Owing to the presence of an initial transition zone, the fronts at 60 and 120 days occur at slightly lower values of water saturation.

The much greater displacement efficiency with gravity segregation than without is apparent from Fig. 9.14. Since the permeability to oil is *essentially* zero at 60% gas saturation, the maximum recovery by gas displacement and gravity drainage is 60% of the initial oil in place. Actually some small permeability to oil exists at even very low oil saturations, which explains why some fields may continue to produce at low rates for quite long periods after the pressure has been depleted. The displacement efficiency may be calculated from Fig. 9.14 by the measurement of areas. For example, the displacement efficiency at Mile Six Pool with full gravity segregation is in excess of

$$\text{Recovery} = \frac{\text{Area } B}{\text{Area } A + \text{Area } B} = \frac{32.5}{4.7 + 32.5} = 0.874, \text{ or } 87.4\%$$

Lecture Note and Document

of

RESERVOIR ENGINEERING

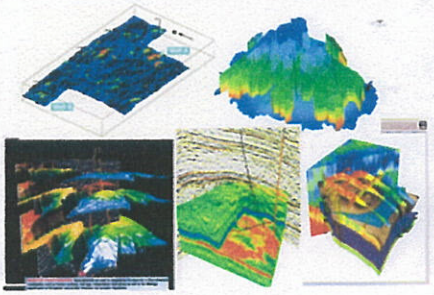

Prepared by

Kriangkrai Trisarn

Petroleum Engineering

School of Geotechnology

Institute of Engineering

END OF THE COURSE.
THANK YOU.

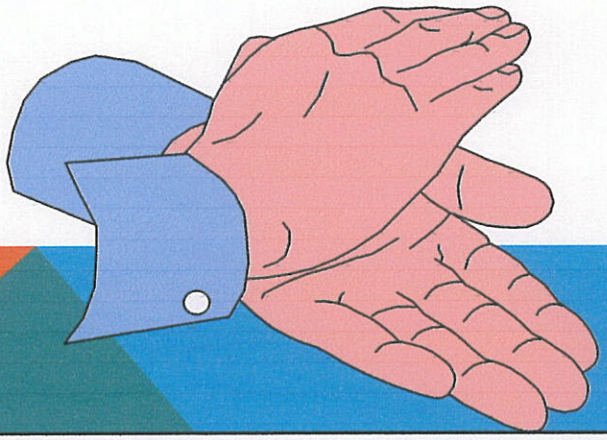

SCF(standard cubic feet). Sometimes the letter *M* will appear in the units, e.g *MCF* or *MSCF*, this refers to *1,000* standard cubic feet.

Example 1.1. Calculating the contents of a tank of ethane in moles, pounds, molecules, and SCF.

Given: A 500 cu ft tank of ethane at 100 psia and 100°F.

SOLUTION: Assuming ideal gas behavior:

$$\text{Moles} = \frac{100 \times 500}{10.73 \times 560} = 8.32$$

$$\text{Pounds} = 8.32 \times 30.07 = 250.2$$

$$\text{Molecules} = 8.32 \times 2.733 \times 10^{26} = 22.75 \times 10^{26}$$

At 14.7 psia and 60°F:

$$\text{SCF} = 8.32 \times 379.4 = 3157$$

Alternate solution using Eq. (1.4):

$$\text{SCF} = \frac{nR'T}{p} = \frac{8.32 \times 10.73 \times 520}{14.7} = 3158$$

Example 2–5. A gas reservoir has an area of 4 sq mi and a net pay thickness of 10 ft. The porosity is 10%, connate water is 25%, reservoir temperature of 85°F, and reservoir pressure is 700 psia. Calculate the volume of gas in place at 14.65 psia and 60°F and the gas remaining in place when the reservoir pressure has been reduced to 50 psia. The gas composition is given as mass fractions in the following table:

1 Component	2 Mass Fraction	3 Molecular Weight	4 Moles/lb	Mole Fraction = Vol Fraction
Methane (C_1)	0.94	16.043	0.05859	0.973
Ethane (C_2)	0.03	30.070	0.00100	0.017
Propane (C_3)	0.02	44.097	0.00045	0.007
n-Butane (n-C_4)	0.01	58.123	0.00017	0.003
Total	1.00		0.06021	1.000

$$\text{Molecular weight} = \frac{\text{mass}}{\text{moles}} = \frac{1.000}{0.06021} = 16.61$$

$\frac{0.94\ \text{lb}}{16.043\ \text{M.W}} = \text{lb-mole}$

④ = ② / ③ ; ⑤ = ④ / 0.06021 = 0.05859 / 0.06021 = 0.973

Gas Density

- Density = $\frac{\text{Mass}}{\text{Volume}}$

$= nM_W/V$

$= PM_w/zRT$

- Gravity(γ_g) = M_W/M_{Wair}

$= M_W/28.97$

Example 21

Find the volume of three pounds n-butane at 120 F and 60 psia

PV = n.R.T, V = n.R.T/P

$$V_g = \frac{(m/M.W)RT}{P}$$

$$V_g = \frac{(3/58.123)\,(10.73)(12\ 0+460)}{60} = 5.35 cu.ft$$

Example 22

Find the density of three pounds n-butane at 120 F and 60 psia

$$\text{Density} = m/V = \frac{(P*M.W)}{RT}$$

$$\text{Density} = \frac{(60)58.123)}{(10.73)(580)} = 0.56 lb/cu.ft.$$

Standard Volume

PV = n.R.T, V = n.R.T/P

$$V_g = \frac{(m/M.W)RT_{sc}}{P_{sc}} = \frac{(1\text{lb-mole})(10.73)(520)}{60}$$

$$= 379.4 scf/lb-mol$$

Specific Volume

is the volume per one unit mass

$$v = V/m = \frac{(RT)}{P*MW} = \frac{1}{\text{density}}$$

$$v = \frac{1}{(0.56)} = 1.79 cu.ft/lb.$$

Gas Deviation Factor

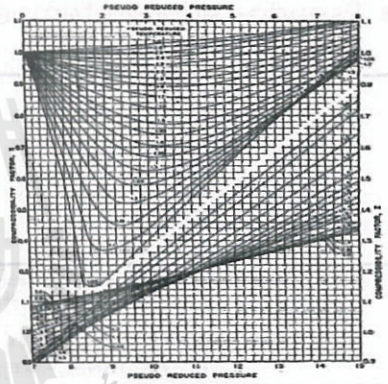

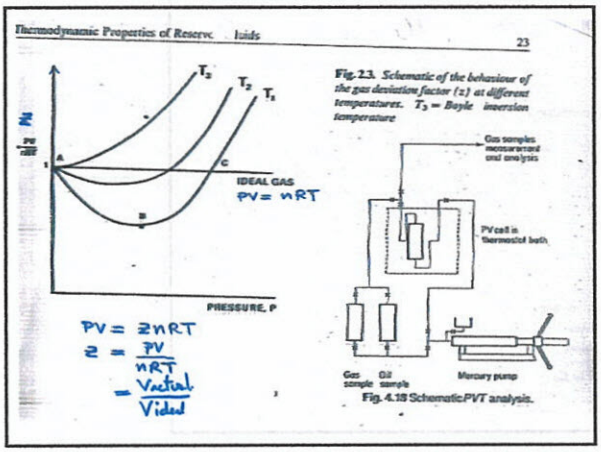

Gas Compressibility Factor

$$\frac{V_{actual}}{V_{ideal}}$$

Gas Compressibility Factor

Since the volume of a gas will be less than what the ideal gas volume would be, the gas is said to be **supercompressible.** The number, **z**, which is a measure of the amount the gas deviates from perfect behavior, is sometimes called the ***Supercompessibility Factor***, usually shortened to the ***Compessibility Factor***, or Gas ***Deviation Factor.*** The ***z – factor*** must be introduced into Equation 2-1 to account for the departure of gases from ideality. The equation has the following form:

$$pV = znRT = mRT \qquad (2\text{-}11)$$

Where the gas compressibility factor z is a dimensionless quantity and is defined as the ratio of the actual volume of n-moles of gas at T and p to the ideal volume of the same number of moles at the same T and p:

$$z = = \frac{V_{actual}}{V_{ideal}} = \frac{V}{(nRT)/p}$$

Studies of the gas compressibility factors for natural gases of various compositions, for most engineering purposes, the two dimensionless properties have to be applied.

- Pseudo-reduced pressure $p_{pr} = \frac{P}{P_{pc}}$

(2-12)

- Pseudo-reduced temperature $T_{pr} = \frac{T}{T_{pc}}$

analysis on the raw data and obtained the following equations over the range of specific gas gravities with which he worked—$0.57 < \gamma_g < 1.68$:

$$p_{pc} = 756.8 - 131.0\gamma_g - 3.6\gamma_g^2 \qquad (1.8)$$

$$T_{pc} = 169.2 + 349.5\gamma_g - 74.0\gamma_g^2 \qquad (1.9)$$

Having obtained the pseudocritical values, the pseudoreduced pressure and temperature are calculated. The gas deviation factor is then found by using the correlation chart of Fig. 1.5.

Example 1.2. Calculating the gas deviation factor of the Bell Field gas from its specific gravity.

Given:

Specific gravity = 0.665
Reservoir temperature = 213°F
Reservoir pressure = 3250 psia

SOLUTION: From Fig. 1.4 the pseudocritical pressure and temperature are

$$p_{pc} = 668 \text{ psia} \quad \text{and} \quad T_{pc} = 369°R$$

Using Eq. (1.8) and (1.9), the pseudocritical values are

$$p_{pc} = 756.8 - 131.0(.665) - 3.6(.665)^2 = 668 \text{ psia}$$

$$T_{pc} = 169.2 + 349.5(.665) - 74.0(.665)^2 = 369°R.$$

For 3250 psia and 213°F, the pseudoreduced pressure and temperature are

$$\frac{P}{P_{pc}} = p_{pr} = \frac{3250}{668} = 4.87. \qquad T_{pr} = \frac{460 + 213}{369} = 1.82 = \frac{T}{T_{pc}}$$

Enter Fig. 1.5 with these values. Find $z = 0.918$.

Gas Compressibility Factor

Since the volume of a gas will be less than what the ideal gas volume would be, the gas is said to be **supercompressible.** The number, ***z***, which is a measure of the amount the gas deviates from perfect behavior, is sometimes called the ***Supercompressibility Factor***, usually shortened to the ***Compressibility Factor***, or Gas ***Deviation Factor.*** The ***z*** – *factor* must be introduced into Equation 2-1 to account for the departure of gases from ideality. The equation has the following form:

$$pV = znRT = mRT \qquad (2\text{-}11)$$

Where the gas compressibility factor z is a dimensionless quantity and is defined as the ratio of the actual volume of n-moles of gas at T and p to the ideal volume of the same number of moles at the same T and p:

$$z = = \frac{V_{actual}}{V_{ideal}} = \frac{V}{(nRT)/p}$$

Studies of the gas compressibility factors for natural gases of various compositions, for most engineering purposes, the two dimensionless properties have to be applied.

- Pseudo-reduced pressure p_{pr} $\frac{P}{P_{pc}}$ =

(2-12)

- Pseudo-reduced temperature $T_{pr} = \frac{T}{T_{pc}}$

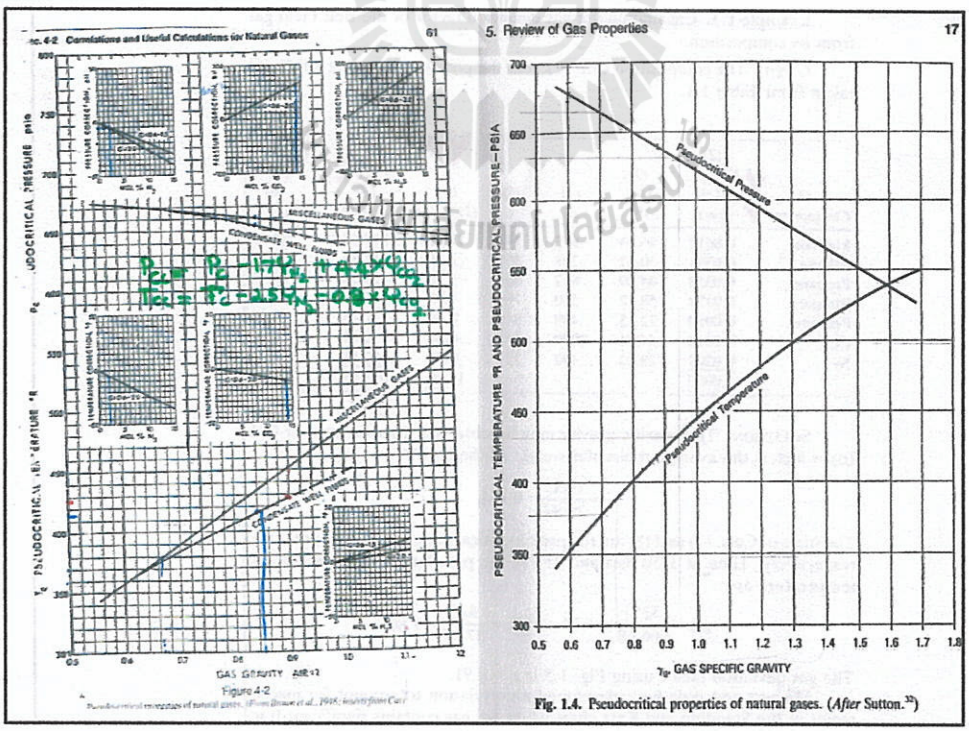

Fig. 1.4. Pseudocritical properties of natural gases. (*After* Sutton.[33])

Gas Properties from Gas Composition

$$\gamma_g = \sum_{i=1}^{n} \gamma_{gi}(y_i)$$

$$T_{pc} = \sum_{i=1}^{n} T_{ci}(y_i)$$

$$p_{pc} = \sum_{i=1}^{n} p_{ci}(y_i)$$

$$\text{NHV} = \sum_{i=1}^{n} \text{NHV}_i(y_i)$$

$$\text{GHVD} = \sum_{i=1}^{n} \text{GHVD}_i(y_i)$$

Example 1.3. Calculating the gas deviation factor of the Bell Field gas from its composition.

Given: The composition Col. (2), and the physical data Cols. (3) to (5) taken from Table 1.1.

(1) Component	(2) Comp., Mole Fract.	(3) Mol. Wt.	(4) p_c	(5) T_c	(6) (2) × (3)	(7) (2) × (4)	(8) (2) × (5)
Methane	0.8612	16.04	673	343	13.81	579.59	295.39
Ethane	0.0591	30.07	708	550	1.78	41.84	32.51
Propane	0.0358	44.09	617	666	1.58	22.09	23.84
Butane	0.0172	58.12	550	766	1.00	9.46	13.18
Pentanes	0.0050	72.15	490	846	0.36	2.45	4.23
CO_2	0.0010	44.01	1070	548	0.04	1.07	0.55
N_2	0.0207	28.02	492	227	0.58	10.18	4.70
	1.0000				19.15	666.68	374.40

SOLUTION: The specific gravity may be obtained from the sum of Col. (6), which is the average molecular weight of the gas,

$$\gamma_g = \frac{19.15}{28.97} = 0.661$$

The sums of Cols. (7) and (8) are the pseudocritical pressure and temperature, respectively. Then at 3250 psia and 213°F, the pseudoreduced pressure and temperature are

$$p_{pr} = \frac{3250}{666.68} = 4.87 \qquad T_{pr} = \frac{673}{374.4} = 1.80$$

The gas deviation factor using Fig. 1.5 is $z = 0.91$.

Wichert and Aziz have developed a correlation to account for inaccuracies in the Standing and Katz chart when the gas contains significant frac-

The sums of Cols. (7) and (8) are the pseudocritical pressure and temperature, respectively. Then at 3250 psia and 213°F, the pseudoreduced pressure and temperature are

$$p_{pr} = \frac{3250}{666.68} = 4.87 \qquad T_{pr} = \frac{673}{374.4} = 1.80$$

The gas deviation factor using Fig. 1.5 is $z = 0.91$.

Wichert and Aziz have developed a correlation to account for inaccuracies in the Standing and Katz chart when the gas contains significant fractions of carbon dioxide (CO_2) and hydrogen sulfide (H_2S).[37] The Wichert and Aziz correlation modifies the values of the pseudocritical constants of the natural gas. Once the modified constants are obtained, they are used to calculate pseudoreduced properties as described in Ex. 1.2 and the z-factor is determined from Fig. 1.5 or Eq. (1.10). The Wichert and Aziz correlation equation is as follows:

$$\varepsilon = 120(A^{0.9} - A^{1.6}) + 15(B^{0.5} - B^4) \tag{1.15}$$

where,

A = sum of the mole fractions of CO_2 and H_2S in the gas mixture

B = mole fraction of H_2S in the gas mixture

The modified pseudocritical properties are given by:

$$T'_{pc} = T_{pc} - \varepsilon \tag{1.15a}$$

$$p'_{pc} = \frac{p_{pc} T'_{pc}}{(T_{pc} + B(1-B)\varepsilon)} \tag{1.15b}$$

5.5 Isothermal Compressibility

The change in volume with pressure for gases under *isothermal* cond which is closely realized in reservoir gas flow, is expressed by the real g

$$V = \frac{znR'T}{p} \text{ or } V = \text{constant} \times \frac{z}{p}$$

Sometimes it is useful to introduce the concept of *gas compressibility* must not be confused with the gas deviation factor, which is also refer as the gas *compressibility factor*. The above equation may be differen with respect to pressure at constant temperature to give

$$\frac{dV}{dp} = \frac{nR'T}{p}\frac{dz}{dp} - \frac{znR'T}{p^2}$$

$$= \left(\frac{znR'T}{p}\right)\frac{1}{z}\frac{dz}{dp} - \left(\frac{znR'T}{p}\right)\times\frac{1}{p}$$

$$c_g = \frac{1}{V}\times\frac{dV}{dp} = \frac{1}{z}\frac{dz}{dp} - \frac{1}{p}$$

Finally, because

$$c = -\frac{1}{V}\frac{dV}{dp}$$

$$c_g = \frac{1}{p} - \frac{1}{z}\frac{dz}{dp}$$

For an ideal gas $z = 1.00$ and $dz/dp = 0$ and the compressibility is simply reciprocal of the pressure. An ideal gas at 1000 psia, then, has a co pressibility of 1/1000 or 1000×10^{-6} psi^{-1}. Example 1.4 shows the calculat of the compressibility of a gas from the gas deviation factor curve of Fig. using Eq. (1.19).

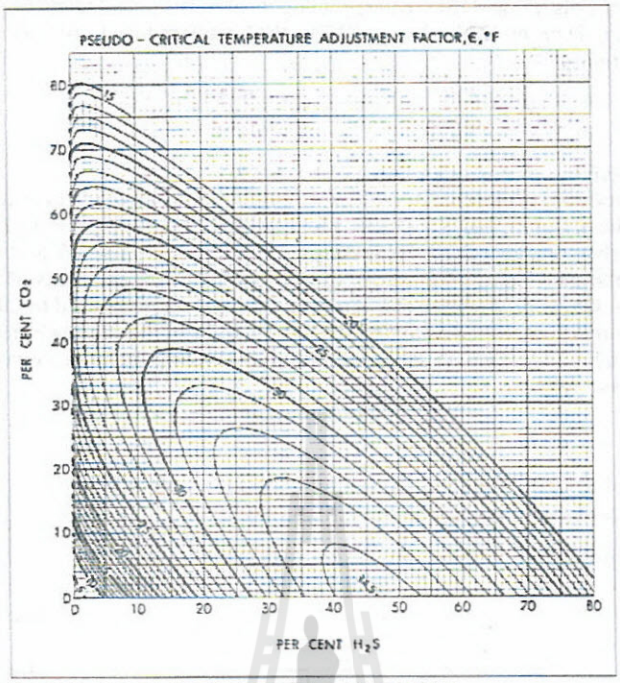

Figure 2–2. Correction factor chart for sour gases (courtesy of GPSA).[1]

Example 4.2. Given the composition of mixture 18 shown on Table 4.6, find the compressibility factor at 1623 psia (11.2MPa) and 100°F (37.8°C). The measured Z is 0.8211. Use the Wichert and Aziz adjustment factor method [4-76] and the *Standing* and Katz chart.

Solution. Find the usual critical temperature and pressure data in Table 4.4. Then, calculate the pseudocritical properties for the mixture as shown in Table 4.6.

From Fig. 4-19, read the critical temperature adjustment factor, using CO_2 and H_2S percentages. In this case, $\epsilon_3 = 20$. The adjusted pseudocritical temperature and pressure are

$$T_c' = T_c - \epsilon_3 = 384.5 - 20 = 364.5°R$$

$$P_c' = \frac{P_c T_c'}{T_c + B(1 - B)\epsilon_3} = \frac{748.3 \times 364.5}{384.5 + 0.0735(1 - 0.0735) \times 20} = 678.7 \text{ psia}$$

Thus, the reduced temperature T_r and pressure P_r are

$$T_r = \frac{T}{T_c'} = \frac{560}{364.5} = 1.54 \qquad P_r = \frac{P}{P_c'} = \frac{1623}{678.7} = 2.39$$

$A = 0.0744 + 0.0735 = 0.1479$

$B = 0.0735$

TABLE 4.6
Mole fractions and critical properties for mixture 18

Component	y	T_c, °R	yT_c	P_c, psia	yP_c
N_2	.0081	226.9	1.8	492	4.0
C_1	.8303	343.3	285.0	673.1	558.9
CO_2	.0744	547.7	40.7	1073	79.8
C_2	.0130	549.8	7.1	708.3	9.2
H_2S	.0735	672.4	49.4	1306	96.0
C_3	.0007	666.0	0.5	617.4	0.4
		T_c	384.5°R	P_c	748.3 psia

$\epsilon_3 = 120(.1479^{0.9} - .1479) + 15(.0735^{0.5} - .0735^4)$

$= 20$

$T_r = 1.54$, $P_r = 2.39$

Fig. 1.3 $\Rightarrow Z = 0.82$

6..GAS FORMATION VOLUME FACTOR

$$B_g = \frac{V_{Reservoir}}{V_{Std.Cond.}} = \frac{(znRT/P)_{Reservoir}}{(znRT/p)_{Std.Cond.}} = \frac{P_{sc}zT}{T_{sc}p}$$

$= 0.02829\ z*T/P$ cu.ft./SCF

$= 0.00504\ z*T/P$ bbl./SCF

$= 35.35\ P/(z*T)$ SCF/cu.ft.

$= 198.4\ P/(z*T)$ SCF/bbl.

TABLE 2–2. Properties of different natural gas constituents

Constituent, i	γ_{gi}	T_{ci}	p_{ci}	NHV_i	GHV_i
Nitrogen, N_2	0.9672	227.30	493.00	0	0
Carbon dioxide, CO_2	1.5195	547.60	1,071.0	0	0
Hydrogen sulfide, H_2S	1.1765	672.40	1,306.0	588.0	637.0
Methane, C_1	0.5539	343.04	667.8	909.1	1,009.7
Ethane, C_2	1.0382	549.76	707.8	1,617.8	1,768.8
Propane, C_3	1.5225	665.68	616.3	2,316.1	2,517.4
Isobutane, i-C_4	2.0068	734.65	529.1	3,001.1	3,252.7
N-Butane, n-C_4	2.0068	765.32	550.7	3,010.4	3,262.1
Isopentane, i-C_5	2.4911	828.77	490.4	3,698.3	4,000.3
N-Pentane, n-C_5	2.4911	845.40	486.6	3,707.5	4,009.5
N-Hexane, n-C_6	2.9753	913.40	436.9	4,403.7	4,756.1
N-Heptane, n-C_7	3.4596	972.50	396.8	5,100.2	5,502.9
N-Octane, n-C_8	3.9439	1,023.89	360.6	5,796.7	6,249.7
N-Nonane, n-C_9	4.4282	1,070.35	332.0	6,493.3	6,996.6
N-Decane, n-C_{10}	4.9125	1,111.80	304.0	7,186.6	7,742.3
Oxygen, O_2	1.1048	278.60	736.9	0	0
Hydrogen, H_2	0.0696	59.90	188.1	274	324
Helium, He	0.1380	9.50	33.2	0	0
Water Vapor, H_2O	0.6220	1,165.30	3,208.0	0	0

$$GHVW = 0.9826(GHVD) \quad (2.22)$$

where y_i is the mole fraction of the ith component in the mixture, γ_{gi} is the gravity of the ith component, T_{ci} is the critical temperature of the ith component, p_{ci} is the critical pressure of the ith component, NHV_i is the net heating value of the ith component in BTU/SCF, and GHVD is the gross

The reciprocal of the gas formation volume factor is called the gas expansion factor and is designated by the symbol E_g, or:

$$E_g = 35.37 \frac{p}{zT}, \text{ scf/ft}^3 \qquad (2\text{-}55)$$

GAS EXPANSION

In other units:

$$E_g = 198.6 \frac{p}{zT}, \text{ scf/bbl} \qquad (2\text{-}56)$$

Example 2-12

A gas well is producing at a rate of 15,000 ft³/day from a gas reservoir at an average pressure of 2,000 psia and a temperature of 120°F. The specific gravity is 0.72. Calculate the gas flow rate in scf/day.

Solution

Step 1. Calculate the pseudo-critical properties from Equations 2-17 and 2-18, to give:

$$T_{pc} = 395.5 \text{ °R} \qquad p_{pc} = 668.4 \text{ psia}$$

Step 2. Calculate the p_{pr} and T_{pr}:

$$p_{pr} = \frac{2000}{668.4} = 2.99$$

$$T_{pr} = \frac{600}{395.5} = 1.52$$

Step 3. Determine the z-factor from Figure 2.6:

$$z = 0.78$$

Step 4. Calculate the gas expansion factor from Equation 2-55:

$$E_g = 35.37 \frac{2000}{(0.78)\,(600)} = 151.15 \text{ scf/ft}^3$$

GAS EXPANSION

Step 5. Calculate the gas flow rate in scf/day by multiplying the gas flow rate (in ft³/day) by the gas expansion factor E_g as expressed in scf/ft³:

Gas flow rate = (151.15) (15,000) = 2.267 MMscf/day

5.5 Isothermal Compressibility

Gas Isothermal Compressibility

The change in volume with pressure for gases under *isothermal* cond
which is closely realized in reservoir gas flow, is expressed by the real g

$$V = \frac{znR'T}{p} \quad \text{or} \quad V = \text{constant} \times \frac{z}{p}$$

Sometimes it is useful to introduce the concept of *gas compressibility* must not be confused with the gas deviation factor, which is also refer as the gas *compressibility factor*. The above equation may be differen with respect to pressure at constant temperature to give

$$\frac{dV}{dp} = \frac{nR'T}{p}\frac{dz}{dp} - \frac{znR'T}{p^2}$$

$$= \left(\frac{znR'T}{p}\right)\frac{1}{z}\frac{dz}{dp} - \left(\frac{znR'T}{p}\right)\times\frac{1}{p}$$

$$C_g = \frac{1}{V}\times\frac{dV}{dp} = \frac{1}{z}\frac{dz}{dp} - \frac{1}{p}$$

$$C_g = \frac{1}{P} - \frac{1}{z}\frac{dz}{dP}$$

Isothermal Compressibility

Finally, because

$$c = -\frac{1}{V}\frac{dV}{dp}$$

$$c_g = -\frac{1}{p} - \frac{1}{z}\frac{dz}{dp}$$

$$= \frac{C_{pr}}{P_{pc}}$$

For an ideal gas $z = 1.00$ and $dz/dp = 0$ and the compressibility is simply reciprocal of the pressure. An ideal gas at 1000 psia, then, has a co pressibility of 1/1000 or 1000×10^{-6} psi^{-1}. Example 1.4 shows the calculat of the compressibility of a gas from the gas deviation factor curve of Fig. using Eq. (1.19).

Example 1.4. To find the compressibility of a gas from the gas deviation factor curve.

Given: The gas deviation factor curve for a gas at 150°F, Fig. 1.6.

SOLUTION: At 1000 psia, the slope dz/dp is shown graphically in Fig. 1.6 as -127×10^{-6}. Note that this is a negative slope. Then, because $z = 0.83$:

$$c_g = \frac{1}{1000} - \frac{1}{0.83}(-127 \times 10^{-6})$$

$$= 1000 \times 10^{-6} + 153 \times 10^{-6} = 1153 \times 10^{-6}\text{psi}^{-1}$$

At 2500 psia the slope dz/dp is zero, so the compressibility is simply:

$$c_g = \frac{1}{2500} = 400 \times 10^{-6}\text{psi}^{-1}$$

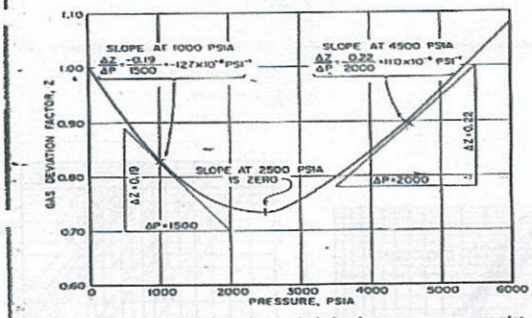

Fig. 1.6. Gas compressibility from the gas deviation factor versus pressure plot. (See Example 1.4)

At 4500 psia the slope dz/dp is positive and as shown in Fig. 1.6 is equal t 110×10^{-6}psi^{-1}. Since $z = 0.90$ at 4500 psia:

$$c_g = \frac{1}{4500} - \frac{1}{0.90}(110 \times 10^{-6})$$

$$= 222 \times 10^{-6} - 122 \times 10^{-6} = 100 \times 10^{-6}\text{psi}^{-1}$$

Gas Isothermal Compressibility

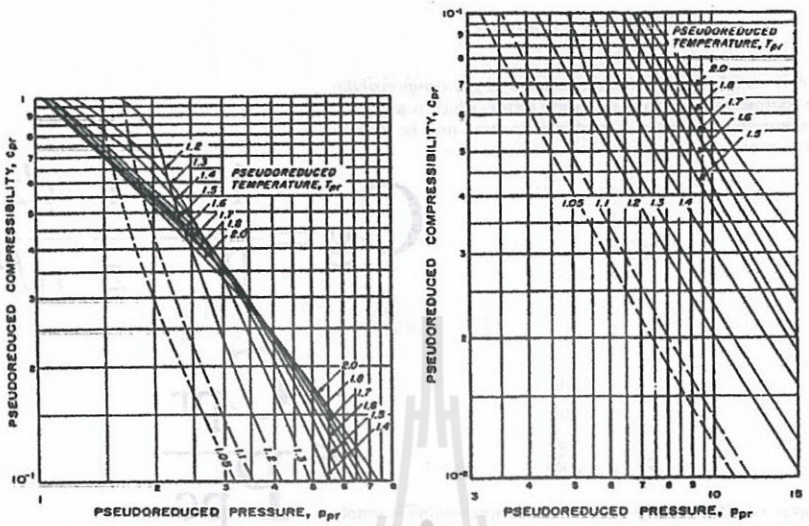

Figure 2–6. Correlation of pseudoreduced compressibility for natural gases (© SPE, Trans. AIME, 1957).[7]

Isothermal Compressibility

$$c_r = \frac{c_r}{p_{pc}} = \frac{\text{Pseudoreduced } c_{pr}}{\text{Critical Pressure}} \quad (2.16)$$

where c_r = the isothermal gas compressibility in 1/psia and c_{pr} is the pseudoreduced gas compressibility in 1/psia.

Example 2–6. Determine the gas isothermal compressibility for a 0.65 gravity dry gas. The reservoir pressure and temperature are 1,800 psia and 170°F, respectively.

Solution:

T_{pc} = 374°R (from Fig. 2–1) Tc

p_{pc} = 671 psia (from Fig. 2–1) Pc

$$T_{pr} = \frac{170 + 460}{374} = 1.68$$

$$p_{pr} = \frac{1{,}800}{671} = 2.68$$

Determine pseudoreduced compressibility from Figure 2–6, and using Equation (2.16), cal

c_{pr} = 0.41 (from Fig. 2–6)

$$c_r = \frac{c_{pr}}{p_{pc}} = 0.41/671$$

$$= 6.11 \times 10^{-4} \text{ 1/psia}$$

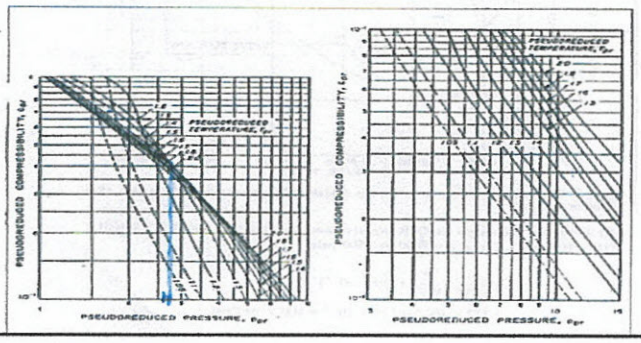

GAS VISCOSITY

GAS VISCOSITY

Viscosity of natural gases, symbol μ_g, at reservoir pressure and temperature can be estimated from correlations developed by Carr et al. and presented in Figures 2–4 and 2–5.* The correlations require gas gravity or molecular weight, pseudoreduced pressure and temperature, and reservoir pressure and temperature. If the gas contains any contaminant gases, the viscosity read from Figure 2–4 must be corrected using the correction factors from the insets. The correction factors may be calculated using Equations (2.15a) through (2.15c). The gas viscosity is reported in centipoise (cp). The following steps are required to obtain gas viscosity:

1.Find μ_1 @ atm P, reservoir Temp.

Step 1. Using gas gravity or molecular weight ($MW = \gamma_g \times 28.97$) and Figure 2–4, determine gas viscosity (μ_1) at atmospheric pressure and reservoir temperature.

Step 2. Correct (μ_1) for contaminant gas, if any, using insets in Figure 2–4 or Equations (2.15a) through (2.15c). Corrected μ_1 = μ_1 (uncorrected) + N_2 correction + H_2S correction + CO_2 correction.

2.Correct μ_1 for sour gas

Step 3. Read viscosity ratio (μ/μ_1) from Figure 2–5 and convert gas viscosity at atmospheric pressure (from Step 1 or 2) to reservoir pressure using the following equation.

$$\mu_g = (\mu/\mu_1) \times \mu_1 \qquad \textbf{(2.15)}$$

3.Read μ_1/μ and cal $\mu = \mu_1 * (\mu_1/\mu)$

where μ_g is the gas viscosity at reservoir conditions in centipoise, and μ_1 is the gas viscosity at one atmosphere in centipoise. Equations used to compute correction factors are:

$$N_2 \text{ correction} = y_{N_2}\, 8.48 \times 10^{-3} \log(\gamma_g) + 9.59 \times 10^{-3} \qquad \textbf{(2.15a)}$$

$$CO_2 \text{ correction} = y_{CO_2}\, 9.08 \times 10^{-3} \log(\gamma_g) + 6.24 \times 10^{-3} \qquad \textbf{(2.15b)}$$

$$H_2S \text{ correction} = y_{H_2S}\, 8.49 \times 10^{-3} \log(\gamma_g) + 3.73 \times 10^{-3} \qquad \textbf{(2.15c)}$$

Example 2–5. Estimate gas viscosity μ_g for the gas in Example 2–3.

Solution:

$$T_{pr} = 1.65$$
$$p_{pr} = 3.74$$
$$\gamma_g = 0.7$$
$$p_R = 2{,}500 \text{ psia}$$
$$T_R = 180^\circ\text{F}$$

Step 1. Read μ_1 from Figure 2–4, using $\gamma_g = 0.70$ and $T_R = 180$ °F.

$$\mu_1 = 0.012 \text{ cp}$$

Step 2. No contaminants are present, so proceed to Step 3.

Step 3. Read the ratio (μ/μ_1) from Figure 2–5, using T_{pr} and p_{pr}. Compute μ_g using Equation (2.15) as

$$\mu/\mu_1 = 1.48 \quad \text{(from Fig. 2–5)}$$
$$\mu_g = 1.48 \times 0.012$$
$$= 0.01776 \text{ cp}$$

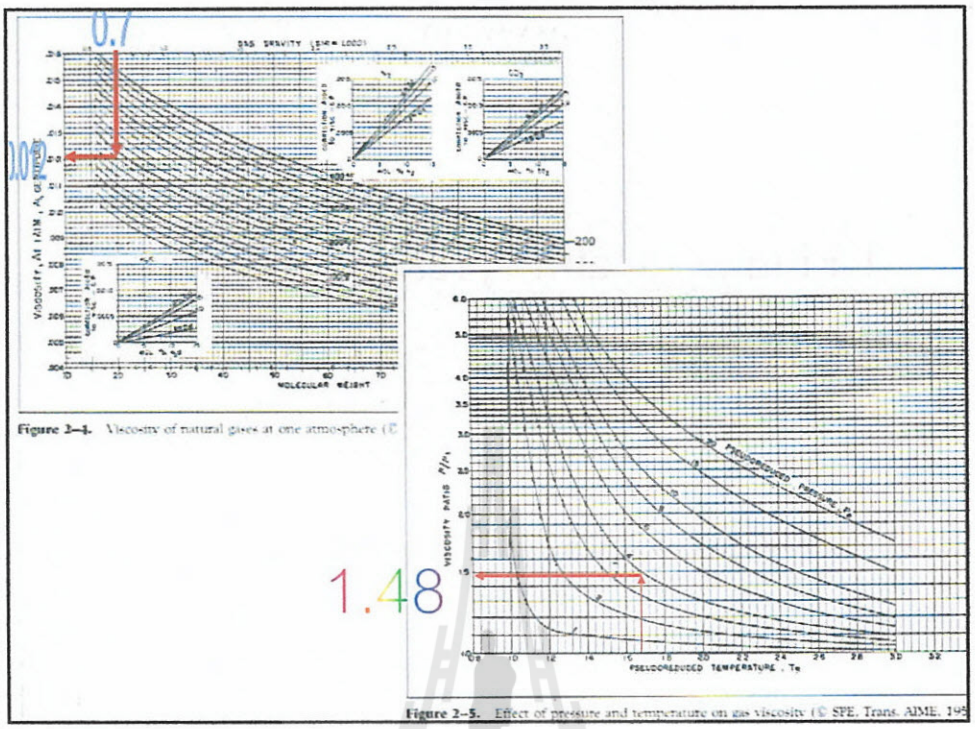

Figure 2–4. Viscosity of natural gases at one atmosphere (© SPE, Trans. AIME, 195

Figure 2–5. Effect of pressure and temperature on gas viscosity (© SPE, Trans. AIME, 195

Example 2.6. Use of correlation charts to estimate reservoir gas viscosity.

Given:

Reservoir pressure = 2680 psia
Reservoir temperature = 212°F
Well fluid specific gravity = 0.90 (Air = 1.00)
Pseudocritical temperature = 420°R
Pseudocritical pressure = 670 psia
Carbon dioxide content = 5 mole %

1.Find μ_1 @ atm P, reservoir Temp.

Step 1
Read μ_1 at ATM Fig 1.9

Step 2
correction for CO_2, N_2, H_2S
$\mu_{1c} = \mu_1 + \text{correction}$

2.Correct μ_1 for sour gas

Step 3
Read $(\mu/\mu_1)_{atm}$ Fig 1.10
Then Cal. μ
$\mu = \mu_{1c} \times \text{Reading}$
$= \mu_{1c} * (\mu/\mu_1)$

3.Read μ_1/μ and cal $\mu = \mu_1 * (\mu/\mu_1)$

Fig 1.9

Fig 1.10

$\mu_1 = 0.0117$ cp at one atmosphere (Fig. 1.9)
Correction for $CO_2 = 0.0003$ cp (Fig. 1.9, insert)
$\mu_1 = 0.0117 + 0.0003 = 0.0120$ cp (corrected for CO_2)
$T_{pr} = \frac{672}{420} = 1.60$ $P_{pr} = \frac{2680}{670} = 4.00$
$\mu/\mu_1 = 1.60$ (Fig. 1.10)
$\mu = 1.60 \times 0.0120 = 0.0192$ cp at 212°F and 2608 psia

The Lee-Gonzalez-Eakin Method

Lee, Gonzalez, and Eakin (1966) presented a semi-empirical relationship for calculating the viscosity of natural gases. The authors expressed the gas viscosity in terms of the reservoir temperature, gas density, and the molecular weight of the gas. Their proposed equation is given by:

$$\mu_g = 10^{-4} K \exp\left[X\left(\frac{\rho_g}{62.4}\right)^Y\right] \quad (2-63)$$

where

$$K = \frac{(9.4 + 0.02 M_a) T^{1.5}}{209 + 19 M_a + T} \quad (2-64)$$

$$X = 3.5 + \frac{986}{T} + 0.01 M_a \quad (2-65)$$

$$Y = 2.4 - 0.2 X \quad (2-66)$$

Example 1.6. Use of correlation chart
cosity.

Given:

Reservoir pressure = 2680 psia
Reservoir temperature = 212°F
Well fluid specific gravity = 0.90 (Air = 1.00)
Pseudocritical temperature = 420°R
Pseudocritical pressure = 670 psia
Carbon dioxide content = 5 mole

P=2680 psia T =672°R

M_a=29*0.9=26.1

z =0.82

Step 1. Calculate the gas density from Equation 2-16:

$$\rho_g = \frac{(2680)(26.1)}{(10.73)(672)(0.82)} = 11.83 \text{ lb/ft}^3$$

Step 2. Solve for the parameters K, X, and Y by using Equations 2-64, 2-65, and 2-66, respectively:

$$\mu_g = 10^{-4} K \exp\left[X\left(\frac{\rho_g}{62.4}\right)^Y\right]$$

where

$$K = \frac{(9.4 + 0.02 M_a) T^{1.5}}{209 + 19 M_a + T}$$

$$X = 3.5 + \frac{986}{T} + 0.01 M_a$$

$$Y = 2.4 - 0.2 X$$

$$K = \frac{[9.4 + 0.02 (26.1)] (672)^{1.5}}{209 + 19 (26.1) + 672} = 125.5$$

$$X = 3.5 + \frac{986}{672} + 0.01 (26.1) = 5.23$$

$$Y = 2.4 - 0.2 (5.23) = 1.354$$

Step 3. Calculate the viscosity from Equation 2-63:

$$\mu_g = 10^{-4} (125.5) \exp\left[5.23\left(\frac{11.83}{62.4}\right)^{1.354}\right] = 0.022 \text{ cp}$$

ρ_g = gas density at reservoir pressure and temperature, lb/ft^3
T = reservoir temperature, °R
M_a = apparent molecular weight of the gas mixture

The proposed correlation can predict viscosity values with a standard deviation of 2.7% and a maximum deviation of 8.99%. The correlation is less accurate for gases with higher specific gravities. The authors pointed out that the method cannot be used for sour gases.

Example 2-14

Rework Example 2-13 and calculate the gas viscosity by using the Lee-Gonzalez-Eakin method.

Step 1. Calculate the gas density from Equation 2-16:

$$\rho_g = \frac{(2000)(20.85)}{(10.73)(600)(0.78)} = 8.3 \text{ lb/ft}^3$$

Step 2. Solve for the parameters K, X, and Y by using Equations 2-64, 2-65, and 2-66, respectively:

$$K = \frac{[9.4 + 0.02(20.85)](600)^{1.5}}{209 + 19(20.85) + 600} = 119.72$$

$$X = 3.5 + \frac{986}{600} + 0.01(20.85) = 5.35$$

$$Y = 2.4 - 0.2(5.35) = 1.33$$

Step 3. Calculate the viscosity from Equation 2-63:

$$\mu_g = 10^{-4}(119.72)\exp\left[5.35\left(\frac{8.3}{62.4}\right)^{1.33}\right] = 0.0173 \text{ cp}$$

P=2000 psia
M_a=20.85

T =600°R
M_a=20.85

ρ_g = gas density at reservoir pressure and temperature, lb/ft^3
T = reservoir temperature, °R
M_a = apparent molecular weight of the gas mixture

The proposed correlation can predict viscosity values with a standard deviation of 2.7% and a maximum deviation of 8.99%. The correlation is less accurate for gases with higher specific gravities. The authors pointed out that the method cannot be used for sour gases.

Example 2-14

Rework Example 2-13 and calculate the gas viscosity by using the Lee-Gonzalez-Eakin method.

Step 1. Calculate the gas density from Equation 2-16:

$$\rho_g = \frac{(2000)(20.85)}{(10.73)(600)(0.78)} = 8.3 \text{ lb/ft}^3$$

Step 2. Solve for the parameters K, X, and Y by using Equations 2-64, 2-65, and 2-66, respectively:

$$K = \frac{[9.4 + 0.02(20.85)](600)^{1.5}}{209 + 19(20.85) + 600} = 119.72$$

$$X = 3.5 + \frac{986}{600} + 0.01(20.85) = 5.35$$

$$Y = 2.4 - 0.2(5.35) = 1.33$$

Step 3. Calculate the viscosity from Equation 2-63:

$$\mu_g = 10^{-4}(119.72)\exp\left[5.35\left(\frac{8.3}{62.4}\right)^{1.33}\right] = 0.0173 \text{ cp}$$

1.Find μ_1 @ atm P, reservoir Temp

1.μ_1 = 0.0114 cp.

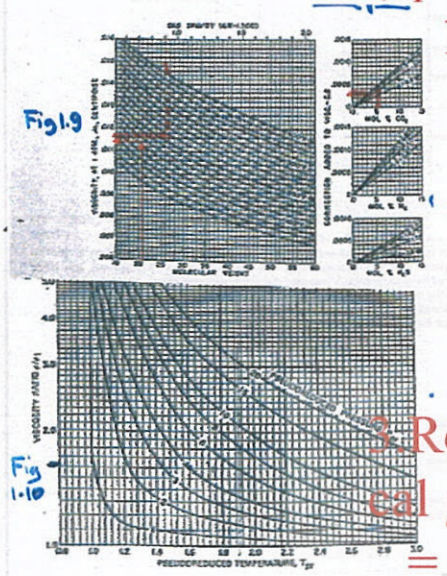

2.Correct μ_1 for sour gas

T_{pr} =600/395=1.54

P_{pr} =2000/670=3

3. Read μ_1/μ = 1.47 and cal $\mu = \mu_1 * (\mu/\mu_1)$

= 1.47*0.0114= 0.017 cp

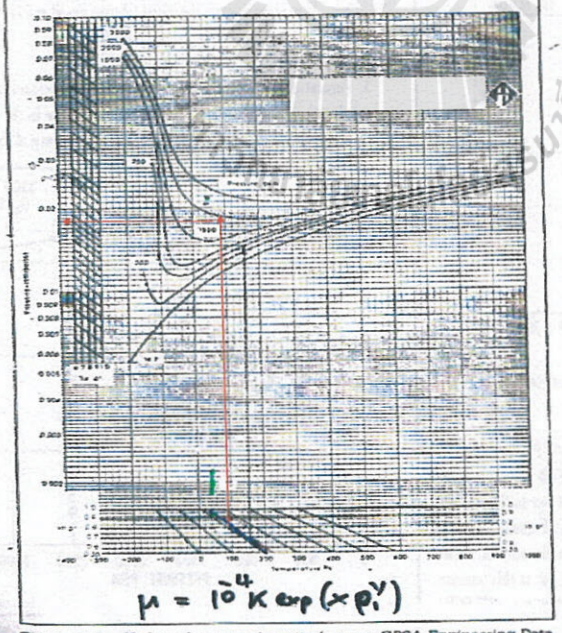

Figure 2–3 *Hydrocarbon gas viscosity* (source: GPSA Engineering Data Book).

by Lee et al. (Lee A.L.)

LIQUID PROPERTIES

1.COMPOSITION

- Water
- Hydrocarbon

2.SG & API Gravity

- $SG = \frac{\text{Wt.in.gram}}{\text{Volume.in.cc.}}$
- $API = \frac{141.5}{SG} - 131.5$

3. PHASE BEHAVIOUR

- PVT Diagram

4. COMPRESSIBILITY(Isothermal)

- $c = -\frac{1}{V}\left(\frac{\partial V}{\partial P}\right)_T$

5. VISCOSITY

6. FORMATION VOLUME FACTOR

7.THERMODYNAMIC PROPERTIES

6.1. Solution Gas-Oil Ratio, R_s 33

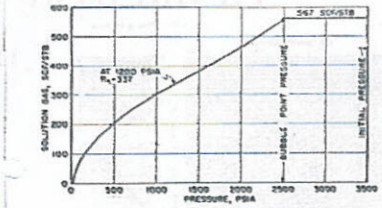

Fig. 1.11. Solution gas-oil ratio of the Big Sandy Field reservoir oil, by flash liberation at reservoir temperature of 160°F.

When laboratory analyses of the reservoir fluids are not available, it is often possible to estimate with reasonable accuracy the solution gas-oil ratio. Standing gives a correlation method from which the solution gas-oil ratio may be estimated from the reservoir pressure, the reservoir temperature, the API gravity of the tank oil, and the specific gravity of the produced gas.[9] Beggs presents Standing's correlation in equation form for pressures less than or equal to the bubble point pressure.[4] That equation is:

$$R_s = \gamma_g \left(\frac{p}{18(10)^{Y_g}}\right)^{1.205} \qquad (1.26)$$

where,

$Y_g = 0.00091T - 0.0125p_{o,API}$

T = temperature, °F

p = pressure, psia

For 105 samples tested, the absolute error found in this correlation was 4.8%. The database contained the following ranges of parameters:

$130 < p_b$ (psia) < 7000

$100 < T$ (°F) < 258

$20 <$ gas-oil ratio (SCF/STB) < 1425

$16.5 < p_{o,API}$ (API) < 63.8

$0.59 < \gamma_g < 0.95$

$1.024 <$ oil formation volume factor (bbl/STB) < 2.05

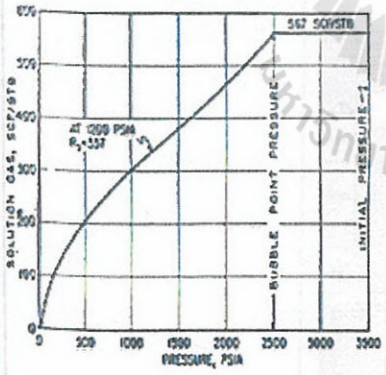

Fig. 3.1. Solution gas-oil ratio of the Big Sandy Field reservoir oil, by flash liberation, at reservoir temperature of 160°F.

...ndy reservoir fluid at reservoir temperature of 160°F. At the initial ...ervoir pressure of 3500 psia there is 567 SCF/STB of solution gas. ...e graph indicates that no gas is evolved from solution as the pressure ...ops from the initial pressure to 2500 psia. Thus the oil is undersaturated ...this region, and there is no free gas phase (cap) in the reservoir. The ...ssure 2500 psia is called the *bubble-point pressure*, for at this pressure ...bbles of free gas first appear. At 1200 psia the solution gas is 337 SCF/

ture, the API gravity of the tank oil, and the specific gravity of the produced gas. Also, in many cases the initial solution gas-oil ratio is close to the producing gas-oil ratio of the initial production.

3. Formation Volume Factors. In the preceding section it was observed that the solution gas causes a considerable increase in the volume of the crude oil. Figure 3.2 shows the variation in the volume of the reser-

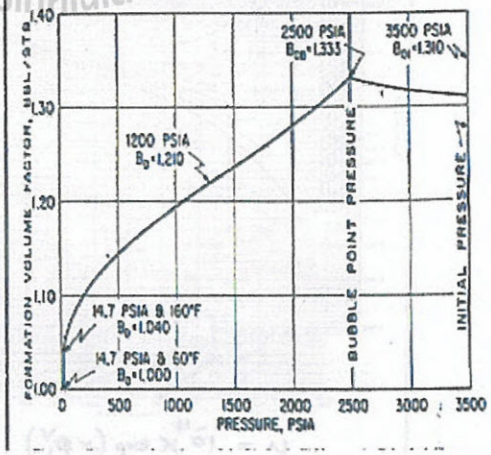

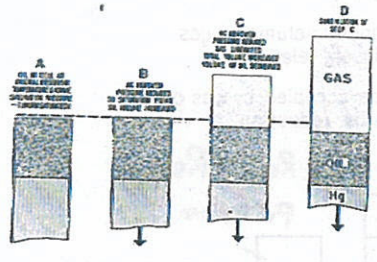

Fig. 45—*Laboratory equilibrium liberation (P-V-T) of gas from oil.*
(Courtesy World Oil*—April, 1953.)*

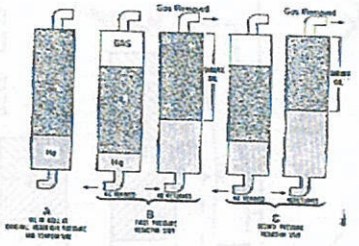

Fig. 46—*Laboratory differential liberation of gas from oil.*
(Courtesy World Oil*—April, 1953.)*

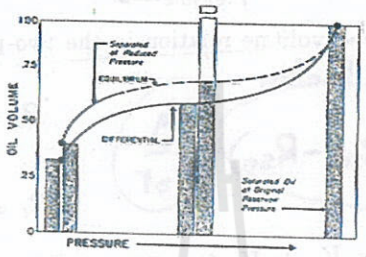

Fig. 48—*Differential and equilibrium shrinkage of high shrinkage oil.*
(Courtesy World Oil*—April, 1953.)*

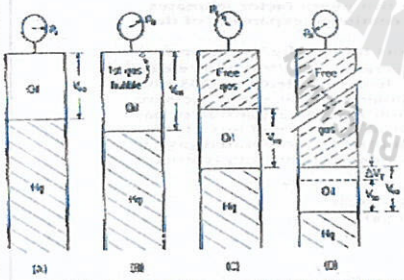

Fig. 1.2. Behavior of typical reservoir oil sample on isothermal pressure reduction. **(A)** Oil sample at original reservoir conditions. All gas is in solution and oil is undersaturated since $p_r > p_b$. **(B)** Pressure is reduced to p_b by removing mercury from the cell. First bubble of gas escapes from solution, hence p_b = bubble point or saturation pressure of the oil. Liquid volume has expanded slightly. **(C)** Pressure is reduced to p_1 and considerable free gas has evolved. Liquid volume has shrunk due to loss of volatile fractions. **(D)** Pressure is now atmospheric. Liquid volume has shrunk to V_{sc}, the oil volume at the reservoir temperature and 14.7 psia. Cooling this oil to standard temperature (60°F) results in its shrinking by an amount ΔV_T to the tank oil volume, V_o.

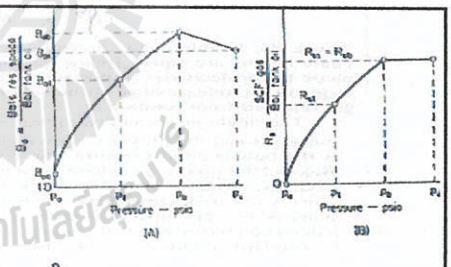

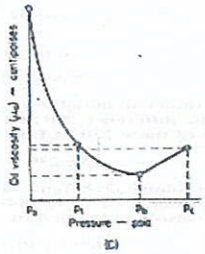

Fig. 1.3. Graphical representation of fluid properties depicted in Fig. 1.2. **(A)** Formation volume factor for oil as a function of pressure

$$B_o = \frac{V_o \text{ (at each pressure)}}{V_{sc}}$$

(B) Solution gas-oil ratio as a function of pressure. **(C)** Oil viscosity as a function of pressure.

API Gravity (degree)
$= \frac{141.5}{\text{Sp.gr.}} - 131.5$

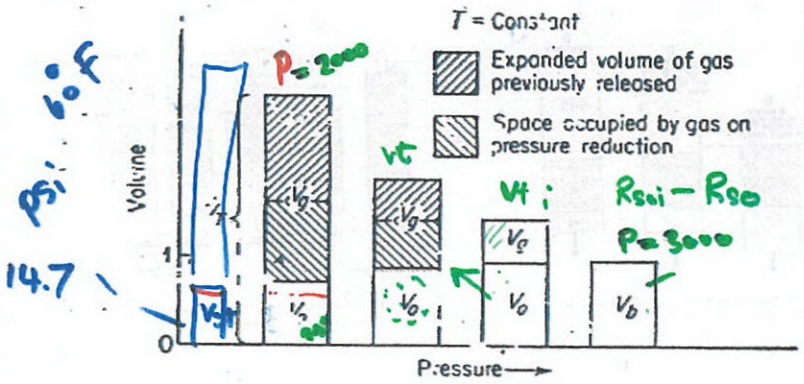

FIG. 4-61—Idealized volume relation in the two-phase region

Two Phase Volume Factor

$$B_t = B_o + B_g(R_{soi} - R_{so})\frac{V_g}{V_{st}}$$

$$B_o = \frac{V_o}{V_{st}}$$

$$B_t = \frac{V_t}{V_{st}} = \frac{V_o}{V_{st}} + \frac{V_g}{V_{st}}$$

and $\frac{V_t}{V_{st}} = \frac{V_o}{V_{st}} + \frac{V_g}{V_{st}}$ (see Fig. 4-61).

$$B_t = B_o + B_g(R_{soi} - R_{so}) \tag{1.28}$$

Above the bubble-point pressure $R_{soi} = R_s$ and the single-phase and two-phase factors are equal. Below the bubble point, however, while the single-phase factor decreases as pressure decreases, the two-phase factor increases owing to the release of gas from solution and the continued expansion of the gas released from solution.

The single-phase and two-phase volume factors for the Big Sandy reser- increases and the pressure consequently must decrease. At 2500 psia, which is the bubble-point pressure, the liquid volume has expanded to 1.333 bbl. Below 2500 psia, a gas phase appears and continues to grow as the pressure declines, owing to the release of gas from solution and the expansion of gas already released; conversely, the liquid phase shrinks because of loss of solution gas, to 1.210 bbl at 1200 psia. At 1200 psia and 160°F the liberated gas has a deviation factor of 0.890, and therefore the gas volume factor with reference to standard conditions of 14.7 psia and 60°F is

$$B_g = \frac{znR'T}{p} = \frac{0.890 \times 10.73 \times 620}{379.4 \times 1200}$$

$$= 0.01300 \text{ cu ft/SCF}$$

$$= 0.002316 \text{ bbl/SCF}$$

Figure 1.11 shows an initial solution gas of 567 SCF/STB and at 1200 psia 337 SCF/STB, the difference 230 SCF being the gas liberated down to 1200 psia. The volume of these 230 SCF is

$$V_g = 230 \times 0.01300 = 2.990 \text{ cu ft}$$

This free gas volume, 2.990 cu ft or 0.533 bbl, plus the liquid volume, 1.210 bbl, is the total volume, or 1.743 bbl/STB—the two-phase volume factor at 1200 psia. It may also be obtained by Eq. (1.28) as:

$$B_t = 1.210 + 0.002316\,(567 - 337)$$

$$= 1.210 + 0.533 = 1.743 \text{ bbl/STB}$$

$$B_t = B_t + B_g(R_{si} - R_s) \qquad (1.28)$$

Above the bubble-point, pressure $R_{si} = R_s$; and the single-phase and two-phase factors are equal. Below the bubble point, however, while the single-phase factor decreases as pressure decreases, the two-phase factor increases owing to the release of gas from solution and the continued expansion of the gas released from solution.

The single-phase and two-phase volume factors for the Big Sandy reser- increases and the pressure consequently must decrease. At 2500 psia, which is the bubble-point pressure, the liquid volume has expanded to 1.333 bbl. Below 2500 psia, a gas phase appears and continues to grow as the pressure declines, owing to the release of gas from solution and the expansion of gas already released; conversely, the liquid phase shrinks because of loss of solution gas, to 1.210 bbl at 1200 psia. At 1200 psia and 160°F the liberated gas has a deviation factor of 0.890, and therefore the gas volume factor with reference to standard conditions of 14.7 psia and 60°F is

$$B_g = \frac{znR'T}{p} = \frac{0.890 \times 10.73 \times 620}{379.4 \times 1200}$$
$$= 0.01300 \text{ cu ft/SCF}$$
$$= 0.002316 \text{ bbl/SCF}$$

Figure 1.11 shows an initial solution gas of 567 SCF/STB and at 1200 psia 337 SCF/STB, the difference 230 SCF being the gas liberated down to 1200 psia. The volume of these 230 SCF is

$$V_g = 230 \times 0.01300 = 2.990 \text{ cu-ft}$$

This free gas volume, 2.990 cu ft or 0.533 bbl, plus the liquid volume, 1.210 bbl, is the total volume, or 1.743 bbl/STB—the two-phase volume factor at 1200 psia. It may also be obtained by Eq. (1.28) as:

$$B_t = 1.210 + 0.002316\ (567 - 337)$$
$$= 1.210 + 0.533 = 1.743 \text{ bbl/STB}$$

Fig. 1.11. Visual conception of the change in single-phase and in two-phase formation

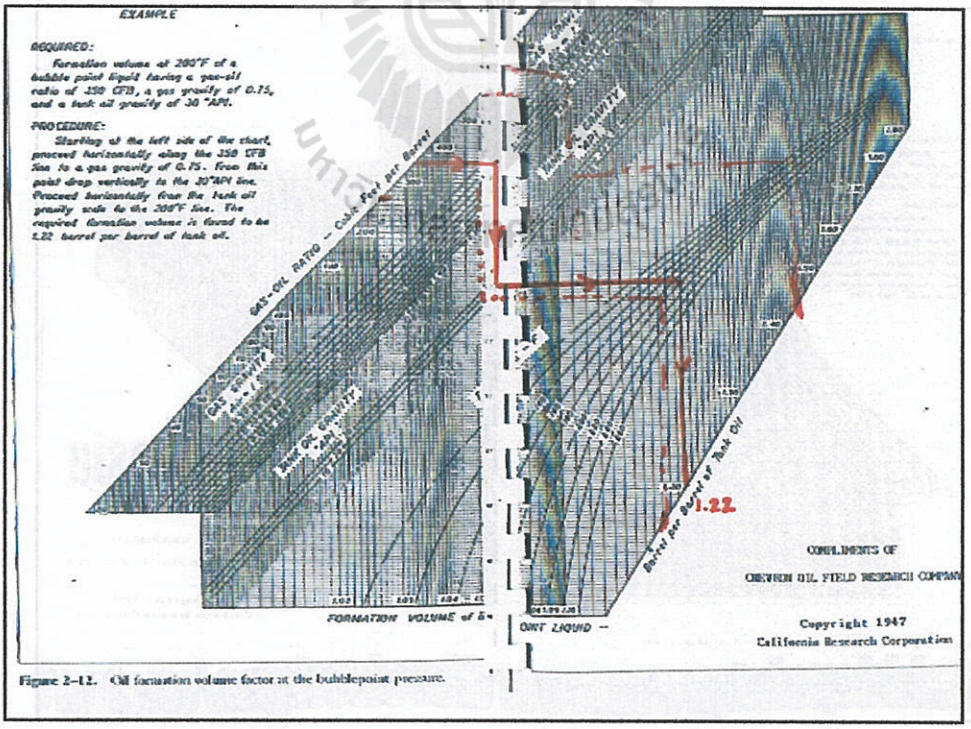

Figure 2–12. Oil formation volume factor at the bubblepoint pressure.

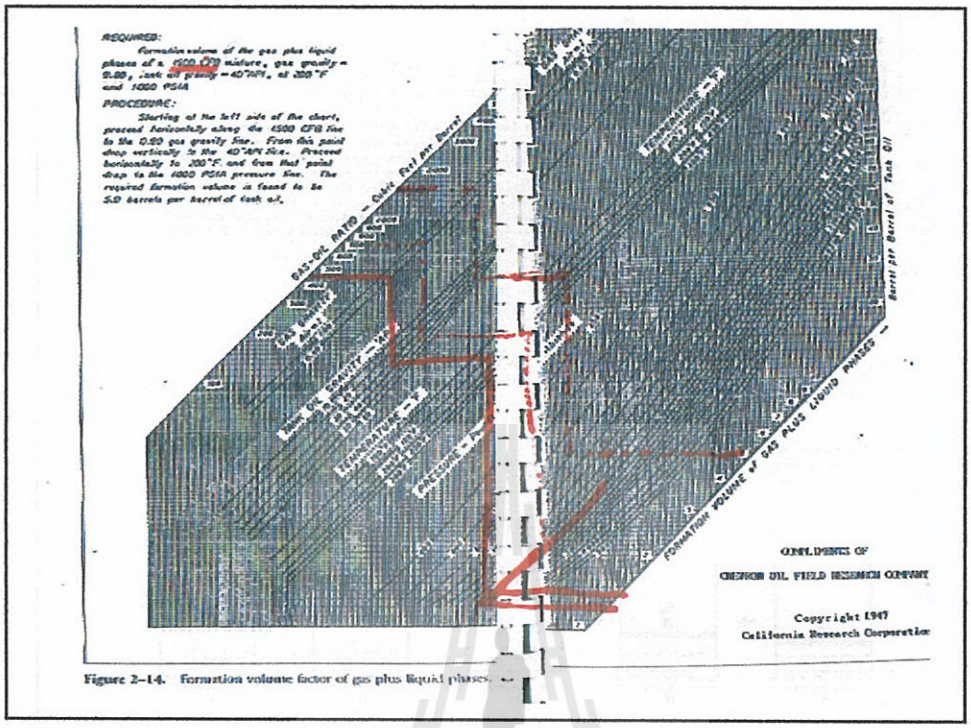

Figure 2–14. Formation volume factor of gas plus liquid phases.

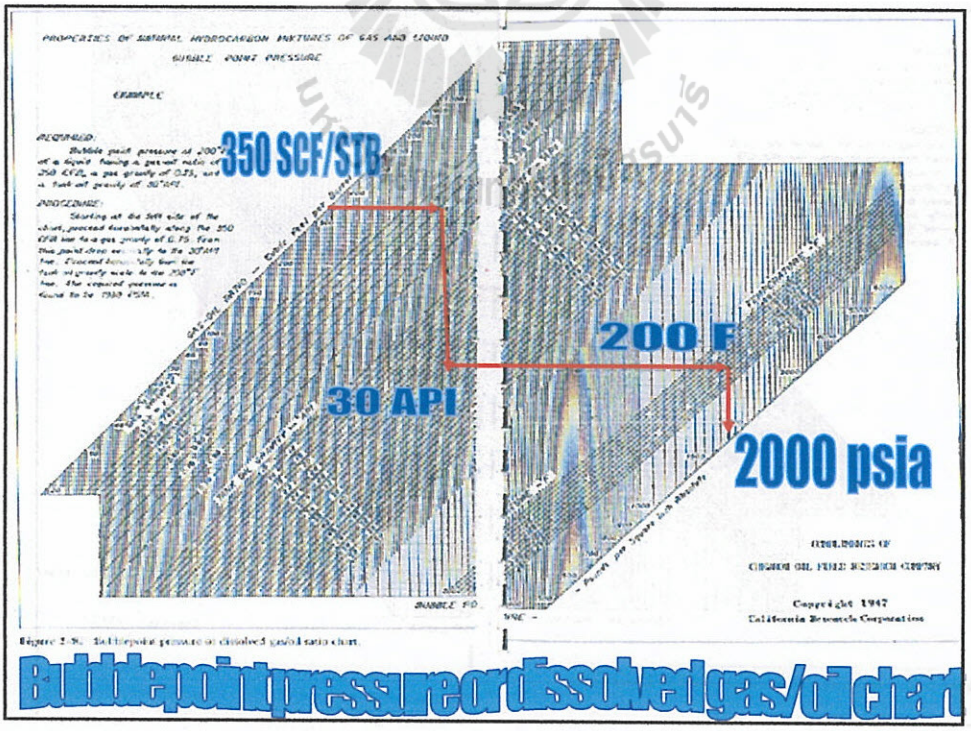

Bubblepoint pressure or dissolved gas/oil chart

Oil formation volume factor, symbol B_o, is defined as the ratio of the liquid volume at reservoir conditions to the liquid volume at stock-tank (standard) conditions. This factor is used to convert reservoir barrels to stock-tank barrels. Figure 2–12 or Equation (2.36) developed by Standing is used to estimate B_o at or below the bubblepoint pressure.

...ure.

Standing

$$B_{ob} = 0.972 + \frac{1.47}{10^4}\left[(R_s)\sqrt{\frac{\gamma_g}{\gamma_o}} + 1.25(T_R)\right]^{1.175} \quad \text{(2.36)}$$

BELOW B.P

where B_{ob} is the formation volume factor at the bubblepoint pressure (p_b) in RB/bbl and T_R is reservoir temperature in °F. If the reservoir pressure is above the bubblepoint pressure, then Equation (2.37) is used to compute B_o. This equation requires oil isothermal compressibility to be discussed in the next section.

$$B_o = B_{ob}e^{c_o(p_b - p)} \quad \text{(2.37)}$$

ABOVE B.P

where B_o is the oil formation volume factor at $p_R > p_b$ in RB/bbl and c_o is the oil isothermal compressibility in 1/psia.

Figure 1.13 (C) shows these separate and total volumes at 1200 psia. At 14.7 psia and 160°F (D), the gas volume has increased to 676 cu ft and the oil volume has decreased to 1.040 bbl. The total liberated gas volume, 676 cu ft, at 160°F and 14.7 psia, is converted to standard cubic feet at 60°F and 14.7 psia using the ideal gas law to give 567 SCF/STB as shown in (E). Correspondingly, 1.040 bbl at 160°F is converted to stock tank conditions of 60°F as shown by Eq. (1.27) to give 1.000 STB, also shown in (E).

The single-phase formation volume factor may be estimated from the solution gas, the gravity of the solution gas, the API gravity of the tank oil, and reservoir temperature using a correlation prepared by Standing.[43] Beggs[44] presents Standing's correlation for the oil formation volume factor in equation form as:

For $p \le p_b$:

Standing

$$B_o = 0.972 + 0.000147F^{1.175} \quad (1.29)$$

where,

$$F = R_{sb}\left(\frac{\gamma_g}{\gamma_o}\right)^{.5} + 1.25T$$

γ_o = oil specific gravity $= \dfrac{141.5}{131.5 + ^\circ API}$

T = temperature, °F

The average error determined from this correlation with the same database used by Standing and Beggs in the solution gas-ratio correlation was 1.17%.

For $p > p_b$:

$$B_o = B_{ob}\exp\left[c_o(p_b - p)\right] \quad (1.30)$$

where,

B_{ob} = oil formation volume factor at the bubble-point pressure

c_o = oil compressibility, psi^{-1}

Col (2) of Table 1.2 shows the variation in the volume of a reservoir fluid relative to the volume at the bubble point of 2695 psig, as measured in the laboratory. These relative volume factors (RVF) may be converted to formation volume factors if the formation volume factor at the bubble point is

the API gravity, the lighter the crude, and vice versa. The API gravity and crude c
vater = 1) are related by the following equations:

SPECIFIC GRAVITY

$$\gamma_o = \frac{141.5}{131.5 + °API}$$

API GRAVITY

$$°API = \frac{141.5}{\gamma_o} - 131.5$$

OIL DENSITY DETERMINATION

The knowledge of oil density at various reservoir pressures and a reservoir temperature is quired for most reservoir engineering calculations. An equation for oil density is

$$\rho_o = \frac{350\gamma_o + 0.0764\gamma_g R_s}{5.615 B_o}$$

here 350 = density of water at standard conditions (lb/STB), ρ_o = oil density (lb/ft^3), R_s = solution dissolved gas (SCF/STB), and 0.0764 = density of air at standard conditions (lb/SCF).

r the case when $p_R > p_b$, the ρ_o is given by

$$\rho_o = \rho_{ob} \exp [c_o(p_R - p_b)]$$

DISSOLVED GAS/OIL RATIO

To estimate oil viscosity and formation volume factor at reservoir pressure below the bub-epoint pressure ($p_R < p_b$), the free gas must be considered. The gas/oil ratio below the bubblepoint

OIL VOLUME CHANGE FROM STANDARD TEMPERATUE

$$V_T = V_{60}[1 + \beta(T - 60)[$$

$$V_{160} = V_{60}[1 + 0.0004(160 - 60)] = 1.04V_{60}$$

SPECIFIC GRAVITY

$$= \frac{MASS.in.gm.}{VOLUME.in.cc} = \frac{141.5}{131.5 + °API}$$

The correlation gives good results for the following ranges of data:

$$126 < p \text{ (psig)} < 9500$$
$$1.006 < B_o \text{ (bbl/STB)} < 2.226$$
$$9.3 < \text{GOR, gas-oil ratio (SCF/STB)} < 2199$$
$$15.3 < \rho_{o,API} \text{ (°API)} < 59.5$$
$$0.511 < \gamma_g < 1.351$$

6.4. Viscosity

The viscosity of oil under reservoir conditions is commonly measured in the laboratory. Fig. 1.14 shows the viscosities of four oils at reservoir temperature, above and below bubble-point pressure. Below the bubble point, the viscosity decreases with increasing pressure owing to the thinning effect of gas entering solution, but above the bubble point, the viscosity increases with increasing pressure.

When it is necessary to estimate the viscosity of reservoir oils, correlations have been developed for both above and below the bubble-point pressure. Egbogah presented a correlation which is accurate to an average error of 6.6% for 394 different oils.[47] The correlation is for what is referred to as "dead" oil, which simply means it does not contain solution gas. A second correlation is used in conjuction with the Egbogah correlation to include the effect of solution gas. Egbogah's correlation for dead oil at pressures less than or equal to the bubble-point pressure is

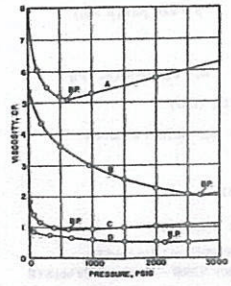

Fig. 1.14. The viscosity of four crude oil samples under reservoir conditions.

$$\log_{10}[\log_{10}(\mu_{od} + 1)] = 1.8653 - 0.025086\rho_{o,API} - 0.5644\log(T) \quad (1.34)$$

where,

μ_{od} = dead oil viscosity, *cp*
T = temperature, °F

The correlation was developed from a database containing the following ranges:

$$59 < T \text{ (°F)} < 176$$
$$-58 < T_{pour} \text{ (°F)} < 59$$
$$5.0 < \rho_{o,API} \text{ (°API)} < 58.0$$

Beggs and Robinson[44,45] developed the live oil viscosity correlation that is used in conjunction with the dead oil correlation given in Eq. (1.34)

$$\mu_o = A\mu_{od}^B \quad (1.35)$$

where,

$A = 10.715\,(R_{so} + 100)^{-0.515}$
$B = 5.44\,(R_{so} + 150)^{-0.338}$

The average absolute error found by Beggs and Robinson while working with 2073 oil samples was 1.83%. The oil samples contained the following ranges:

$$0 < p \text{ (psig)} < 5250$$
$$70 < T \text{ (°F)} < 295$$
$$20 < \text{GOR, gas-oil ratio (SCF/STB)} < 2070$$
$$16 < \rho_{o,API} \text{ (°API)} < 58$$

For pressures above the bubble point, the oil viscosity can be estimated by the following correlation developed by Vasquez and Beggs:

$$\mu_o = \mu_{ob}\,(p/p_b)^m \quad (1.36)$$

where,

$m = 2.6\,p^{1.187} \exp[-11.513 - 8.98(10)^{-5}\,p]$
μ_{ob} = oil viscosity at the bubble point-pressure, *cp*

effect of solution gas. Egbogah's correlation for dead oil at pressures less than or equal to the bubble-point pressure is

$$\log_{10}[\log_{10}(\mu_{od} + 1)] = 1.8653 - 0.025086\rho_{o,API} - 0.5644\log(T) \quad (1.34)$$

where,

μ_{od} = dead oil viscosity, *cp*
T = temperature, °F

The correlation was developed from a database containing the following ranges:

$$59 < T \text{ (°F)} < 176$$
$$-58 < T_{pour} \text{ (°F)} < 59$$
$$5.0 < \rho_{o,API} \text{ (°API)} < 58.0$$

Beggs and Robinson[44,45] developed the live oil viscosity correlation that is used in conjunction with the dead oil correlation given in Eq. (1.34)

$$\mu_o = A\mu_{od}^B \quad (1.35)$$

where,

$A = 10.715\,(R_{so} + 100)^{-0.515}$
$B = 5.44\,(R_{so} + 150)^{-0.338}$

The average absolute error found by Beggs and Robinson while working with 2073 oil samples was 1.83%. The oil samples contained the following ranges:

$$0 < p \text{ (psig)} < 5250$$
$$70 < T \text{ (°F)} < 295$$
$$20 < \text{GOR, gas-oil ratio (SCF/STB)} < 2070$$
$$16 < \rho_{o,API} \text{ (°API)} < 58$$

For pressures above the bubble point, the oil viscosity can be estimated by the following correlation developed by Vasquez and Beggs:

$$\mu_o = \mu_{ob}\,(p/p_b)^m \quad (1.36)$$

where,

$m = 2.6\,p^{1.187} \exp[-11.513 - 8.98(10)^{-5}\,p]$
μ_{ob} = oil viscosity at the bubble point-pressure, *cp*

Vasquez and Beggs found an average absolute error for this correlation of 7.54% for 3143 oil samples that involved the following ranges:

$$126 < p \text{ (psig)} < 9500$$
$$0.117 < \mu_o \text{ (cp)} < 148.0$$
$$9.3 < \text{GOR, gas-oil ratio (SCF/STB)} < 2199$$
$$15.3 < \rho_{o,API} \text{ (°API)} < 59.5$$
$$0.511 < \gamma_g < 1.351$$

The following example problem illustrates the use of the correlations that have been presented for the various oil properties.

Example 1.7. Use of correlations to estimate values for liquid properties at pressures of 2000 and 4000 psia.

Given:

$$T = 180°F$$
$$p_b = 2500 \text{ psia}$$
$$\gamma_g = 0.80$$
$$\rho_{o,API} = 40°API$$
$$\gamma_o = 0.85$$

SOLUTION: Solution gas-oil ratio, R_{so}:

$$p = 4000 \text{ psia } (p > p_b)$$

For pressures greater than the bubble-point pressure, $R_{so} = R_{sob}$, therefore from Eq. (1.26):

$$R_{sob} = R_{so} = \gamma_g \left[\frac{p}{18(10)^{Y_g}}\right]^{1.204}$$

$$Y_g = 0.00091T - 0.0125\rho_{o,API} = 0.00091(180) - 0.0125(40) = -0.336$$

$$R_{sob} = R_{so} = 0.80\left[\frac{2500}{18(10)^{-0.336}}\right]^{1.204} = 772 \text{ SCF/STB}$$

$$p = 2000 \text{ psia } (p < p_b)$$

$$R_{so} = \gamma_g \left[\frac{p}{18(10)^{Y_g}}\right]^{1.204} = 0.80\left[\frac{2000}{18(10)^{-0.336}}\right]^{1.204} = 590 \text{ SCF/STB}$$

Isothermal compressibility, c_o:

$$p = 4000 \text{ psia } (p > p_b)$$

From Eq. (1.33):

$$c_o = (5R_{sob} + 17.2T - 1180\gamma_g + 12.61\,\rho_{o,API} - 1433)/(p(10)^5)$$

$$c_o = (5(772) + 17.2(180) - 1180(0.80) + 12.61(40) - 1433)/(4000(10)^5)$$

$$= 12.7(10)^{-6} \text{ psi}^{-1}$$

$$p = 2000 \text{ psia } (p < p_b)$$

From Eq. (1.32):

$$\ln c_o = -0.664 - 1.430 \ln(p) - 0.395 \ln(p_b) + 0.390 \ln(T) + 0.455 \ln(R_{sob}) + 0.262 \ln(\rho_{o,API})$$

$$\ln c_o = -0.664 - 1.430 \ln(2000) - 0.395 \ln(2500) + 0.390 \ln(180) + 0.455 \ln(772) + 0.262 \ln(40)$$

$$c_o = 183\,(10)^{-6} \text{ psi}^{-1}$$

Formation volume factor, B_o:

$$p = 4000 \text{ psia } (p > p_b)$$

From Eq. (1.30):

$$B_o = B_{ob} \exp[c_o(p_b - p)]$$

B_{ob} is calculated from Eq. (1.29)

$$B_{ob} = 0.972 + 0.000147F^{1.175}$$

where,

$$F = R_{sob}\left(\frac{\gamma_g}{\gamma_o}\right)^{0.5} + 1.25T$$

$$F = 772\left(\frac{0.80}{0.825}\right)^{0.5} + 1.25(180) = 985$$

$$B_{ob} = 0.972 + 0.000147(985)^{1.175} = 1.456 \text{ bbl/STB}$$

$$B_o = 1.456 \exp[12.7(10)^{-6}(2500 - 4000)] = 1.429 \text{ bbl/STB}$$

$$p = 2000 \text{ psia } (p < p_b)$$

Vasquez and Beggs found an average absolute error for this correlation o 7.54% for 3143 oil samples that involved the following ranges:

$$126 < p \text{ (psig)} < 9500$$
$$0.117 < \mu_o \text{ (cp)} < 148.0$$
$$9.3 < \text{GOR, gas-oil ratio (SCF/STB)} < 2199$$
$$15.3 < \rho_{o,API} \text{ (°API)} < 59.5$$
$$0.511 < \gamma_g < 1.351$$

The following example problem illustrates the use of the correlations that hav been presented for the various oil properties.

Example 1.7. Use of correlations to estimate values for liquid properties at pressures of 2000 and 4000 psia.

Given:

$$T = 180°F$$
$$p_b = 2500 \text{ psia}$$
$$\gamma_g = 0.80$$
$$\rho_{o,API} = 40°API$$
$$\gamma_o = 0.85$$

SOLUTION: Solution gas-oil ratio, R_{so}:

$$p = 4000 \text{ psia } (p > p_b)$$

For pressures greater than the bubble-point pressure, $R_{so} = R_{sob}$, therefor from Eq. (1.26):

$$R_{sob} = R_{so} = \gamma_g \left[\frac{p}{18(10)^{Y_g}}\right]^{1.204}$$

$$Y_g = 0.00091T - 0.0125\rho_{o,API} = 0.00091(180) - 0.0125(40) = -0.336$$

$$R_{sob} = R_{so} = 0.80\left[\frac{2500}{18(10)^{-0.336}}\right]^{1.204} = 772 \text{ SCF/STB}$$

$$p = 2000 \text{ psia } (p < p_b)$$

$$R_{so} = \gamma_g \left[\frac{p}{18(10)^{Y_g}}\right]^{1.204} = 0.80\left[\frac{2000}{18(10)^{-0.336}}\right]^{1.204} = 590 \text{ SCF/STB}$$

fluid may be visualized by referring to Fig. 1.13, which is based on data n Figs. 1.11 and 1.12. Fig. 1.13 (A) shows a cylinder fitted with a piston initially contains 1.310 bbl of the initial reservoir fluid (liquid) at the initial ssure of 3500 psia and 160°F. As the piston is withdrawn, the volume eases and the pressure consequently must decrease. At 2500 psia, which he bubble-point pressure, the liquid volume has expanded to 1.333 bbl. ow 2500 psia, a gas phase appears and continues to grow as the pressure lines, owing to the release of gas from solution and the expansion of gas eady released; conversely, the liquid phase shrinks because of loss of solu- n gas, to 1.210 bbl at 1200 psia. At 1200 psia and 160°F the liberated gas has eviation factor of 0.890, and therefore the gas volume factor with reference standard conditions of 14.7 psia and 60°F is

$$B_g = \frac{znR'T}{p} = \frac{0.890 \times 10.73 \times 620}{379.4 \times 1200}$$

$$= 0.01300 \text{ cu ft/SCF}$$

$$= 0.002316 \text{ bbl/SCF}$$

gure 1.11 shows an initial solution gas of 567 SCF/STB and at 1200 psia 337 CF/STB, the difference 230 SCF being the gas liberated down to 1200 psia. he volume of these 230 SCF is

$$V_g = 230 \times 0.01300 = 2.990 \text{ cu ft}$$

his free gas volume, 2.990 cu ft or 0.533 bbl, plus the liquid volume, 1.210 bbl, the total volume, or 1.743 bbl/STB—the two-phase volume factor at 1200 sia. It may also be obtained by Eq. (1.28) as:

$$B_t = 1.210 + 0.002316\ (567 - 337)$$

$$= 1.210 + 0.533 = 1.743 \text{ bbl/STB}$$

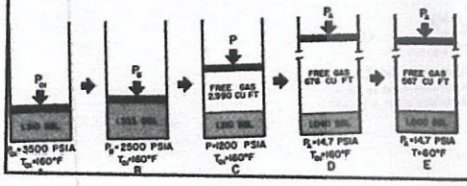

Figure 1.13 (C) shows these separate and total volumes at 1200 psia. At 1 psia and 160°F (D), the gas volume has increased to 676 cu ft and the volume has decreased to 1.040 bbl. The total liberated gas volume, 676 cu at 160°F and 14.7 psia, is converted to standard cubic feet at 60°F and 14.7 using the ideal gas law to give 567 SCF/STB as shown in (E). Correspondin 1.040 bbl at 160°F is converted to stock tank conditions of 60°F as shown Eq. (1.27) to give 1.000 STB, also shown in (E).

The single-phase formation volume factor may be estimated from solution gas, the gravity of the solution gas, the API gravity of the tank and reservoir temperature using a correlation prepared by Standing.[43] Beg presents Standing's correlation for the oil formation volume factor in equa form as:

For $p \leq p_b$:

$$B_o = 0.972 + 0.000147F^{1.175} \quad (1$$

where,

$$F = R_{so}\left(\frac{\gamma_g}{\gamma_o}\right)^{.5} + 1.25T$$

γ_o = oil specific gravity = $\dfrac{141.5}{131.5 + \rho_{o,API}}$

T = temperature, °F

The average error determined from this correlation with the same datal used by Standing and Beggs in the solution gas-ratio correlation was 1.1

For $p > p_b$:

$$B_o = B_{ob} \exp\left[c_o(p_b - p)\right] \quad (1$$

where,

B_{ob} = oil formation volume factor at the bubble-point pressure

c_o = oil compressibility, psi^{-1}

Col (2) of Table 1.2 shows the variation in the volume of a reservoir relative to the volume at the bubble point of 2695 psig, as measured in laboratory. These relative volume factors (RVF) may be converted to mation volume factors if the formation volume factor at the bubble poi known. For example, if $B_{ob} = 1.391$ bbl/STB, then the formation volume tor at 4100 psig is

TABLE 1.2.
Relative volume data

(1) Pressure, psig	(2) RVF* V_r
5000	0.9739
4700	0.9768
4400	0.9799
4100	0.9829
3800	0.9862
3600	0.9886
3400	0.9909
3200	0.9934
3000	0.9960
2900	0.9972
2800	0.9985
2695	1.0000

*V_r = volume relative to the volume at the bubble-point pressure V_b, laboratory data.

6.3. Isothermal Compressibility

Sometimes it is desirable to work with values of the liquid compressibility rather than the formation or relative volume factors. The compressibility, or the bulk modulus of elasticity of a liquid, is defined by:

$$c_o = -\frac{1}{V}\frac{dV}{dp} \quad (1.1)$$

Because dV/dp is a negative slope, the negative sign converts the compressibility c_o into a positive number. Because the values of the volume V and the slope of dV/dp are different at each pressure, the compressibility is different at each pressure, being higher at the lower pressure. Average compressibilities may be used by writing Eq. (1.1) in the difference form as:

$$c_o = -\frac{1}{V} \times \frac{(V_1 - V_2)}{(p_1 - p_2)} \quad (1.31)$$

The reference volume V in Eq. (1.31) may be V_1, V_2, or an average of V_1 and V_2. It is commonly reported for reference to the smaller volume—that is, the volume at the higher pressure. Then the average compressibility of the fluid of Table 1.2 between 5000 psig and 4100 psig is

$$c_o = \frac{0.9829 - 0.9739}{0.9739\ (5000 - 4100)} = 10.27 \times 10^{-6}\ \text{psi}^{-1}$$

Between 4100 psig and 3400 psig,

$$c_o = \frac{0.9909 - 0.9829}{0.9829\ (4100 - 3400)} = 11.63 \times 10^{-6}\ \text{psi}^{-1}$$

And between 3400 psig and 2695 psig,

$$c_o = \frac{1.0000 - 0.9909}{0.9909\ (3400 - 2695)} = 13.03 \times 10^{-6}\ \text{psi}^{-1}$$

A compressibility of $13.03 \times 10^{-6}\ \text{psi}^{-1}$ means that the volume of 1 million barrels of *reservoir* fluid will increase by 13.03 bbls for a reduction of 1 psi in pressure. The compressibility of undersaturated oils ranges from 5 to $100 \times 10^{-6}\ \text{psi}^{-1}$, being higher for the higher API gravities, for the greater quantity of solution gas, and for higher temperatures.

Villena-Lanzi developed a correlation to estimate c_o for black oils.[47] The correlation is good for pressures below the bubble-point pressure and is given by:

$$\ln(c_o) = -0.664 - 1.430\ \ln(p) - 0.395\ \ln(p_b) + 0.390\ \ln(T) + 0.455\ \ln(R_{sob}) + 0.262\ \ln(\rho_{o,API}) \quad (1.32)$$

where,

T = °F

The correlation was developed from a database containing the following ranges:

$31.0(10)^{-6} < c_o$ (psia) $< 6600(10)^{-6}$

$500 < p$ (psig) < 5300

$763 < p_b$ (psig) < 5300

$78 < T$ (°F) < 330

$1.5 \leq$ GOR, gas-oil ratio (SCF/STB) < 1947

$6.0 < \rho_{o,API}$ (°API) < 52.0

$0.58 < \gamma_g < 1.20$

Vasquez and Beggs presented a correlation for estimating the compressibility for pressures above the bubble point pressure.[45,46] This correlation is

$$c_o = (5\ R_{sob} + 17.2T - 1180\gamma_g + 12.61\rho_{o,API} - 1433)/(p \times 10^6) \quad (1.33)$$

TABLE 1.2.
Relative volume data

(1) Pressure, psig	(2) RVF* V_r
5000	0.9739
4700	0.9768
4400	0.9799
4100	0.9829
3900	0.9862
3600	0.9886
3400	0.9909
3200	0.9934
3000	0.9960
2900	0.9972
2800	0.9985
2695	1.0000

*V_r = volume relative to the volume at the bubble-point pressure V_b, laboratory data.

6.3. Isothermal Compressibility

Sometimes it is desirable to work with values of the liquid compressibility rather than the formation or relative volume factors. The compressibility, or the bulk modulus of elasticity of a liquid, is defined by:

$$c_o = -\frac{1}{V}\frac{dV}{dp} \tag{1.1}$$

Because dV/dp is a negative slope, the negative sign converts the compressibility c_o into a positive number. Because the values of the volume V and the slope of dV/dp are different at each pressure, the compressibility is different at each pressure, being higher at the lower pressure. Average compressibilities may be used by writing Eq. (1.1) in the difference form as:

$$c_o = -\frac{1}{V}\times\frac{(V_1 - V_2)}{(p_1 - p_2)} \tag{1.31}$$

The reference volume V in Eq. (1.31) may be V_1, V_2, or an average of V_1 and V_2. It is commonly reported for reference to the smaller volume—that is, the volume at the higher pressure. Then the average compressibility of the fluid of Table 1.2 between 5000 psig and 4100 psig is

$$c_o = \frac{0.9829 - 0.9739}{0.9739\,(5000 - 4100)} = 10.27\times10^{-6}\ \text{psi}^{-1}$$

Between 4100 psig and 3400 psig,

$$c_o = \frac{0.9909 - 0.9829}{0.9829\,(4100 - 3400)} = 11.63\times10^{-6}\ \text{psi}^{-1}$$

And between 3400 psig and 2695 psig,

$$c_o = \frac{1.0000 - 0.9909}{0.9909\,(3400 - 2695)} = 13.03\times10^{-6}\ \text{psi}^{-1}$$

A compressibility of 13.03×10^{-6} psi^{-1} means that the volume of 1 million barrels of *reservoir* fluid will increase by 13.03 bbls for a reduction of 1 psi in pressure. The compressibility of undersaturated oils ranges from 5 to 100×10^{-6} psi^{-1}, being higher for the higher API gravities, for the greater quantity of solution gas, and for higher temperatures.

Villena-Lanzi developed a correlation to estimate c_o for black oils.[45] The correlation is good for pressures below the bubble-point pressure and is given by:

$$\ln(c_o) = -0.664 - 1.430\ln(p) - 0.395\ln(p_b) + 0.390\ln(T) + 0.455\ln(R_{sob}) + 0.262\ln(\rho_{o,API}) \tag{1.32}$$

where,

T = °F

The correlation was developed from a database containing the following ranges:

$$31.0(10)^{-6} < c_o\ (\text{psia}) < 6600(10)^{-6}$$
$$500 < p\ (\text{psig}) < 5300$$
$$763 < p_b\ (\text{psig}) < 5300$$
$$78 < T\ (°\text{F}) < 330$$
$$1.5 < \text{GOR, gas-oil ratio (SCF/STB)} < 1947$$
$$6.0 < \rho_{o,API}\ (°\text{API}) < 52.0$$
$$0.58 < \gamma_g < 1.20$$

Vasquez and Beggs presented a correlation for estimating the compressibility for pressures above the bubble point pressure.[55,46] This correlation is

$$c_o = (5R_{sob} + 17.2T - 1180\gamma_g + 12.61\rho_{o,API} - 1433)/(p\times10^5) \tag{1.33}$$

From Eq. (1.29):

$$B_o = 0.972 + 0.000147F^{1.175}$$

$$F = R_{so}\left(\frac{\gamma_g}{\gamma_o}\right)1.25T = 590\left(\frac{0.80}{0.825}\right)^{0.5} + 1.25(180) = 806$$

$$B_o = 0.972 + 0.000147(806)^{1.175} = 1.354 \text{ bbl/STB}$$

Viscosity, μ_o:

$$p = 4000 \text{ psia } (p > p_b)$$

From Eq. (1.36):

$$\mu_o = \mu_{ob}\,(p/p_b)^m$$

$$m = 2.6p^{1.187}\exp[-11.513 - 8.98(10)^{-5}p]$$

$$m = 2.6(4000)^{1.187}\exp[-11.513 - 8.98(10)^{-5}(4000)] = 0.342$$

From Eq. (1.34):

$$\log_{10}[\log_{10}(\mu_{obd} + 1)] = 1.8653 - 0.025086\rho_{o,API} - 0.5644\log(T)$$

$$\log_{10}[\log_{10}(\mu_{obd} + 1)] = 1.8653 - 0.025086(40) - 0.5644\log(180)$$

$$\mu_{obd} = 1.444 \text{ cp}$$

From Eq. (1.35):

$$\mu_{ob} = A\,\mu_{obd}^B$$

$$A = 10.715\,(R_{sob} + 100)^{-0.515} = 10.715\,(772 + 100)^{-0.515} = 0.328$$

$$B = 5.44\,(R_{sob} + 150)^{-0.338} = 5.44\,(772 + 150)^{-0.338} = 0.541$$

$$\mu_{ob} = 0.328(1.444)^{0.541} = 0.400 \text{ cp}$$

$$\mu_o = 0.400(4000/2500)^{0.342} = 0.470 \text{ cp}$$

$p = 2000$ psia $(p < p_b)$

From Eq. (1.34), μ_{od} will be the same as μ_{obd}:

$$\mu_{od} = 1.444 \text{ cp}$$

$$\mu_o = A\,\mu_{od}^B$$

$$A = 10.715\,(R_{so} + 100)^{-0.515} = 10.715(590 + 100)^{-0.515} = 0.370$$

$$B = 5.44\,(R_{so} + 150)^{-0.338} = 5.44(590 + 150)^{-0.338} = 0.583$$

$$\mu_o = 0.370(1.444)^{0.583} = 0.458 \text{ cp}$$

7. REVIEW OF RESERVOIR WATER PROPERTIES

The properties of formation waters, like crude oils but to a much smaller degree, are affected by temperature, pressure, and the quantity of solution gas and dissolved solids. The compressibility of the formation, or connate, water contributes materially in some cases to the production of volumetric reservoirs above the bubble point and accounts for much of the water influx in water-drive reservoirs. When the accuracy of other data warrants it, the properties of the connate water should be entered into the material-balance calculations on reservoirs. The following sections contain a number of correlations adequate for use in engineering applications.

7.1. Formation Volume Factor

McCain[49,50] developed the following correlation for the water formation volume factor, B_w (bbl/STB):

$$B_w = (1 + \Delta V_{wt})(1 + \Delta V_{wp}) \tag{1.37}$$

where,

$$\Delta V_{wt} = -1.00010 \times 10^{-2} + 1.33391 \times 10^{-4}\, T + 5.50654 \times 10^{-7}\, T^2$$

$$\Delta V_{wp} = -1.95301 \times 10^{-9}\, pT - 1.72834 \times 10^{-13}\, p^2 T - 3.58922 \times 10^{-7}\, p - 2.25341 \times 10^{-10}\, p^2$$

T = temperature, °F

p = pressure, psia

For the data used in the development of the correlation, the correlation was found to be accurate to within 2%. The correlation does not account for the salinity of normal reservoir brines explicitly, but McCain observed that variations in salinity caused offsetting errors in the terms ΔV_{wt} and ΔV_{wp}. The offsetting errors cause the correlation to be within engineering accuracy for the estimation of the B_w of reservoir brines.

7.2. Solution Gas-Water Ratio

McCain has also developed a correlation for the solution gas-water ratio, R_{sw} (SCF/STB).[49,50] The correlation is:

$$\frac{R_{sw}}{R_{swp}} = 10^{(-0.0840655\, S\, T^{-0.285854})} \tag{1.38}$$

where

S = salinity, % by weight solids

T = temperature, °F

R_{swp} = solution gas to pure water ratio, SCF/STB

R_{swp} is given by another correlation developed by McCain as:

$$R_{swp} = A + Bp + Cp^2 \tag{1.39}$$

where,

$$A = 8.15839 - 6.12265 \times 10^{-2}\, T + 1.91663 \times 10^{-4}\, T^2 - 2.1654 \times 10^{-7}\, T^3$$

$$B = 1.01021 \times 10^{-2} - 7.44241 \times 10^{-5}\, T + 3.05553 \times 10^{-7}\, T^2 - 2.94883 \times 10^{-10}\, T^3$$

$$C = -10^{-7}\,(9.02505 - 0.130237\, T + 8.53425 \times 10^{-4}\, T^2 - 2.34122 \times 10^{-6}\, T^3 + 2.37049 \times 10^{-9}\, T^4)$$

T = temperature, °F

The correlation of Eq. (1.39) was developed for the following range of data and found to be within 5% of the published data:

$$1000 < p \text{ (psia)} < 10{,}000$$

$$100 < T \text{ (°F)} < 340$$

Eq. (1.38) was developed for the following range of data and found to be accurate to within 3% of published data:

$$0 < S \text{ (\%)} < 30$$

$$70 < T \text{ (°F)} < 250$$

7.3. Isothermal Compressibility

Osif developed a correlation for the water isothermal compressibility, c_w, for pressures greater than the bubble point pressure.[51] The equation is

$$c_w = -\frac{1}{B_w}\left(\frac{\partial B_w}{\partial p}\right)_T = \frac{1}{[7.033p + 541.5C_{NaCl} - 537.0T + 403{,}300]} \tag{1.40}$$

where,

C_{NaCl} = salinity, g NaCl/liter

T = temperature, °F

where

S = salinity, % by weight solids

T = temperature, °F

R_{swp} = solution gas to pure water ratio, SCF/STB

R_{swp} is given by another correlation developed by McCain as:

$$R_{swp} = A + Bp + Cp^2 \tag{1.39}$$

where,

$$A = 8.15839 - 6.12265 \times 10^{-2}\, T + 1.91663 \times 10^{-4}\, T^2 - 2.1654 \times 10^{-7}\, T^3$$

$$B = 1.01021 \times 10^{-2} - 7.44241 \times 10^{-5}\, T + 3.05553 \times 10^{-7}\, T^2 - 2.94883 \times 10^{-10}\, T^3$$

$$C = -10^{-7}\,(9.02505 - 0.130237\, T + 8.53425 \times 10^{-4}\, T^2 - 2.34122 \times 10^{-6}\, T^3 + 2.37049 \times 10^{-9}\, T^4)$$

T = temperature, °F

The correlation of Eq. (1.39) was developed for the following range of data and found to be within 5% of the published data:

$$1000 < p \text{ (psia)} < 10{,}000$$

$$100 < T \text{ (°F)} < 340$$

Eq. (1.38) was developed for the following range of data and found to be accurate to within 3% of published data:

$$0 < S \text{ (\%)} < 30$$

$$70 < T \text{ (°F)} < 250$$

7.3. Isothermal Compressibility

Osif developed a correlation for the water isothermal compressibility, c_w, for pressures greater than the bubble point pressure.[51] The equation is

$$c_w = -\frac{1}{B_w}\left(\frac{\partial B_w}{\partial p}\right)_T = \frac{1}{[7.033p + 541.5C_{NaCl} - 537.0T + 403{,}300]} \tag{1.40}$$

where,

C_{NaCl} = salinity, g NaCl/liter

T = temperature, °F

The correlation was developed for the following range of data:

$$1000 < p \text{ (psig)} < 20{,}000$$

$$0 < C_{NaCl} \text{ (g NaCl/liter)} < 200$$

$$200 < T \text{ (°F)} < 270$$

The water isothermal compressibility has been found to be strongly affected by the presence of free gas. Therefore, McCain proposed using the following expression for estimating c_w for pressures below or equal to the bubble-point pressure:

$$c_w = -\frac{1}{B_w}\left(\frac{\partial B_w}{\partial p}\right)_T + \frac{B_g}{B_w}\left(\frac{\partial R_{swp}}{\partial p}\right)_T \tag{1.41}$$

The first term on the right-hand side of Eq. (1.41) is simply the expression for c_w in Eq. (1.40). The second term on the right-hand side is found by differentiating Eq. (1.39) with respect to pressure, or:

$$\left(\frac{\partial R_{swp}}{\partial p}\right)_T = B + 2Cp$$

where

B and C are defined in Eq. (1.39).

In proposing Eq. (1.41), McCain suggested that B_g should be estimated using a gas with a gas gravity of 0.63, which represents a gas composed mostly of methane and a small amount of ethane. McCain could not verify this expression by comparing calculated values of c_w with published data, so there is no guarantee of accuracy. This suggests that Eq. (1.41) should be used only for gross estimations of c_w.

7.4. Viscosity

The viscosity of water increases with decreasing temperature and in general with increasing pressure and salinity. Pressure below about 70°F causes a reduction in viscosity, and some salts (e.g., KCl) reduce the viscosity at some concentrations and within some temperature ranges. The effect of dissolved gases is believed to cause a minor reduction in viscosity. McCain developed the following correlation for water viscosity at atmospheric pressure and reservoir temperature:

$$\mu_{w1} = AT^B \tag{1.42}$$

The correlation was developed for the following range of data:

$$1000 < p \text{ (psig)} < 20{,}000$$
$$0 < C_{NaCl} \text{ (g NaCl/liter)} < 200$$
$$200 < T \text{ (°F)} < 270$$

The water isothermal compressibility has been found to be strongly affected by the presence of free gas. Therefore, McCain proposed using the following expression for estimating c_w for pressures below or equal to the bubble-point pressure:

$$c_w = -\frac{1}{B_w}\left(\frac{\partial B_w}{\partial p}\right)_T + \frac{B_g}{B_w}\left(\frac{\partial R_{sw}}{\partial p}\right)_T \quad (1.41)$$

The first term on the right-hand side of Eq. (1.41) is simply the expression for c_w in Eq. (1.40). The second term on the right-hand side is found by differentiating Eq. (1.39) with respect to pressure, or:

$$\left(\frac{\partial R_{sw}}{\partial p}\right)_T = B + 2Cp$$

where

B and C are defined in Eq. (1.39).

In proposing Eq. (1.41), McCain suggested that B_g should be estimated using a gas with a gas gravity of 0.63, which represents a gas composed mostly of methane and a small amount of ethane. McCain could not verify this expression by comparing calculated values of c_w with published data, so there is no guarantee of accuracy. This suggests that Eq. (1.41) should be used only for gross estimations of c_w.

7.4. Viscosity

The viscosity of water increases with decreasing temperature and in general with increasing pressure and salinity. Pressure below about 70°F causes a reduction in viscosity, and some salts (e.g., KCl) reduce the viscosity at some concentrations and within some temperature ranges. The effect of dissolved gases is believed to cause a minor reduction in viscosity. McCain developed the following correlation for water viscosity at atmospheric pressure and reservoir temperature:

$$\mu_{wt} = AT^B \quad (1.42)$$

where

$$A = 109.574 - 8.40564\,S + 0.313314\,S^2 + 8.72213 \times 10^{-3}\,S^3$$

$$B = -1.12166 + 2.63951 \times 10^{-2}\,S - 6.79461 \times 10^{-4}\,S^2 - 5.47119 \times 10^{-5}\,S^3 + 1.55586 \times 10^{-6}\,S^4$$

T = temperature, °F

S = salinity, % by weight solids

Eq. (1.42) was found to be accurate to within 5% over the following range of data:

$$100 < T \text{ (°F)} < 400$$
$$0 < S \text{ (\%)} < 26$$

The water viscosity can be adjusted to reservoir pressure by the following correlation, again developed by McCain:

$$\frac{\mu_w}{\mu_{wt}} = 0.9994 + 4.0295(10)^{-5}p + 3.1062(10)^{-9}p^2 \quad (1.43)$$

This correlation was found to be accurate to within 4% for pressures below 10,000 psia and within 7% for pressures between 10,000 and 15,000 psia. The temperature range for which the correlation was developed was between 86 and 167 °F.

8. SUMMARY

The correlations presented in this chapter are valid for estimating properties providing the parameters fall within the specified ranges for the particular property in question. The correlations were presented in the form of equations to facilitate their implementation into computer programs.

PROBLEMS

1.1 Calculate the volume 1 lb-mole of ideal gas will occupy at:
- (a) 14.7 psia and 60°F
- (b) 14.7 psia and 32°F
- (c) 14.7 plus 10 oz and 80°F
- (d) 15.025 psia and 60°F

Reservoir Engineering I
HW NO 1; Due date: Friday, June 22, 2012

A.CHAPTER 1; 1.3, 1.5, 1.6, 1.10, 1.21 and 1.27

B.C.CRAFT and M.F. HAWKINS; "*Applied Petroleum Reservoir Engineering*", 1991.

HW NO.1 Chapter 1
Due Date: Friday 22 June 2012

ANSWERS to the problems

1; 1.3 Molecular weight = 30, specific gravity= 1.034
2; 1.5. $3.14, and $15.4 (Hint; 16 oz = 1 lb)
3; 1.6 (a) 3.9 min, (b) 64,147 lb, (c) explain(Hint; 16 oz = 1 lb)
4; 1.10. P(psia) = 300, 750, 1500, 2500, 4000, 5000, 6000
Z = 0.96 0.914 0.86 0.84 0.91 0.99 1.08
B_g(cu.ft/SCF)= 0.05613, 0.0214, 0.0098, 0.0059, 0.004, 0.0035,0.0032
5; 1.21 ANS= $B_t(B_o)$=1.515 bbl/STB
6; 1.27; (a) dw=4.77 cc (b)dw 4.67cc (c) dw=16.3 cc (d) μ_w= 0.36072 cp

AND HANDOUT

7; The Satun Gas consists of mole % as follows

	Mole %	MW	P_C (psia)	T_C (°R)	NHV (BTU/SCF)
Methane(CH_4)	69.0	16	668	343	909
Ethane C_2H_6	10.0	30	778	550	1618
Propane C_3H_8	6.0	44	616	666	2316
Iso-Butane iC_4	1.3	58	529	735	3001
n-Butane nC_4	1.1	58	550	766	3010
n-Pentane nC_5	0.4	72	490	846	3708
n-Hexane nC_6	0.2	86	440	914	4404
Carbon dioxide	12.0	44	1071	548	0

Determine; γ_g, ρ_g ,μ_g@ 3000 psia, 340° F, and NHV

8. Use of correlations to estimate values for oil properties; R_{sb}, C_o, B_o, and μ_o at pressure of 2100 and 3800 psia: Given
T = 200° F , Pb = 2500 psia, γ_g = 0.8, ρ_o = 40 °API, γ_w = 0.83

3-4th WEEK (June 18-29, 2012)
Outline

- 3. Reserve Calculation
- 4. Gas Reservoir

Reserve Calculation Methods

1.VOLUMETRIC METHOD 2.MATERIAL BALANCE METHOD

1 Volumetric METHOD

2 Material Balance METHOD

3 Monte Carlo Simulations

4 Stochatic(Statistic) & Deterministic

5 Reservoir Performances

5.1 Decline Curves

5.2 Reservoir Simulations

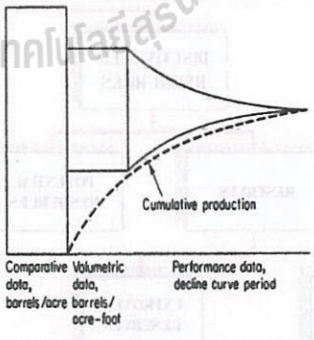

Figure 11.1. Schematic presentation of ranges of recovery estimates made during the life of a producing property. (After Arps[3])

3.DECLINE CURVE METHOD

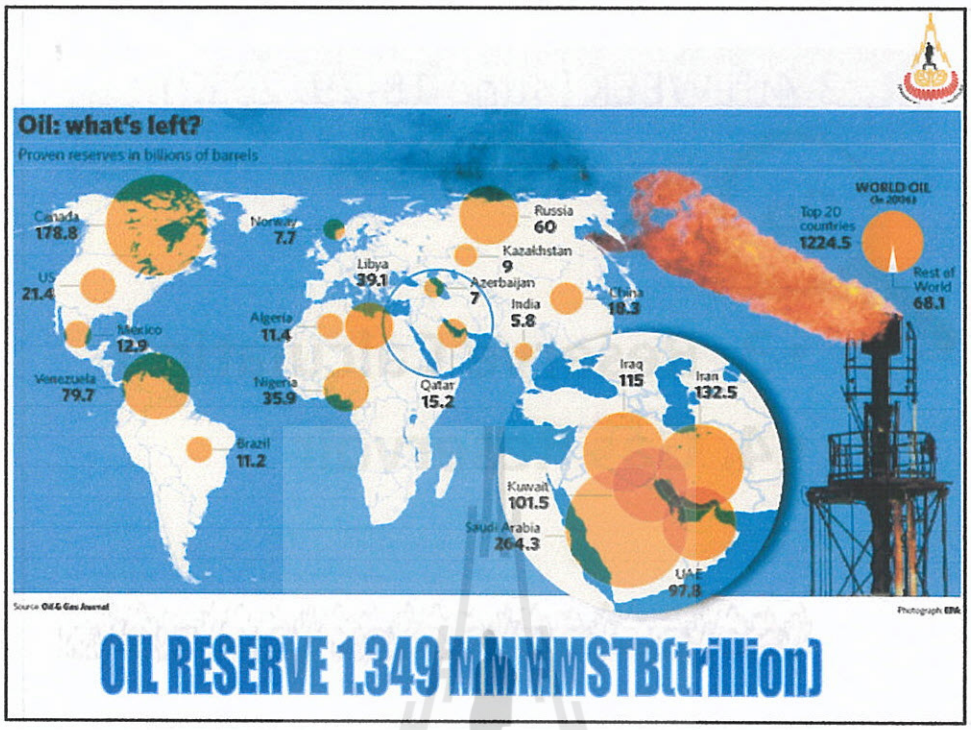

Figure : CCOP Petroleum Resource Classification Chart of Recoverable Resources

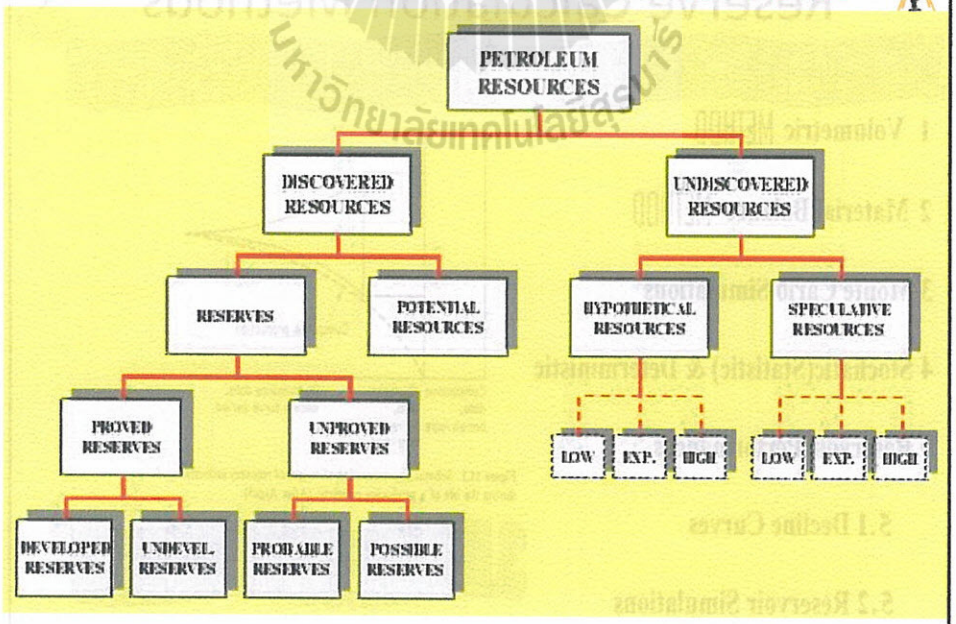

PROVED RESERVE

- Commercially Recoverable
  - Geological, Engineering And Economic Data, Rule & Regulation
  - Operating Methods
  - Developed/ Undeveloped
  - Price, Cost, Time Span Of Development
  - Deterministic (High Degree Of Confidence)
  - Probabilistic (90% Probability >= The Estimate)

PROBABLE RESERVE

- More Likely Than Not To Be Recoverable
- Step-Out Drilling/ Inadequate Subsurface Control
- Well Log/No Core Test/No Analogous To Proved Or Producing Area
- In Fill Which Can Be Proved If Approved
- Improved Recovery/Adjacent to Proved Area/Workover/Incremental From Volumetric Estimation
- 50-90% Confidence

PROBABLE RESERVE

- **Separated From Proved Area By Faults And In The Higher Structure**

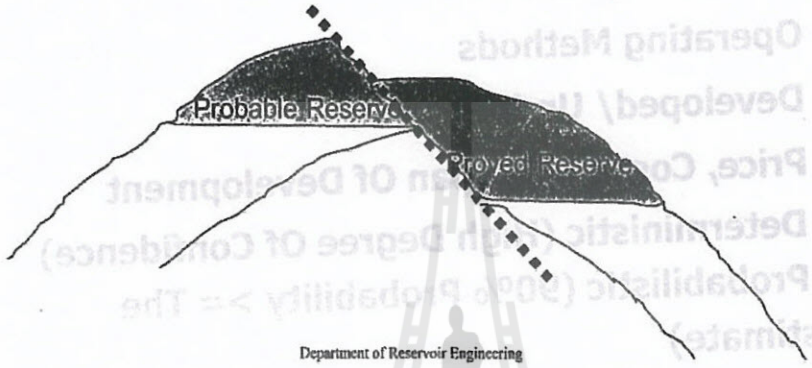

POSSIBLE RESERVE

- **Less Likely To Be Recoverable**
- **10-50% Confidence**
- **Supported By Geo/ Eng/ Eco Data But Beyond Probable Areas**
- **Log /Core Not Productive @ Commercial Rate**
- **Infill Drilling Subject To Uncertainty**
- **Improved Recovery**

POSSIBLE RESERVE

- **Adjacent To Proved Areas, Separated By Faults But In Lower Structure**

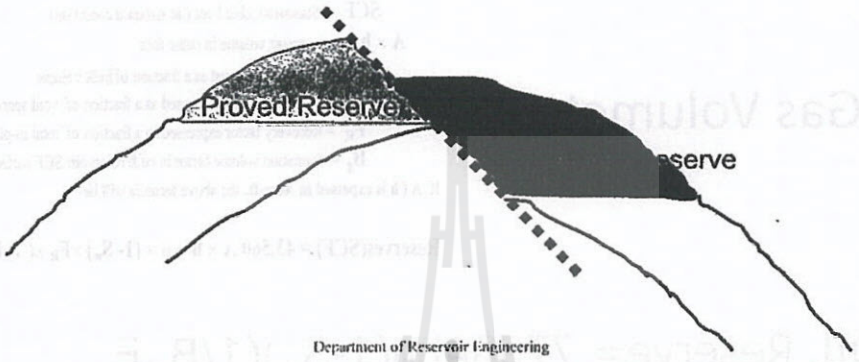

Department of Reservoir Engineering

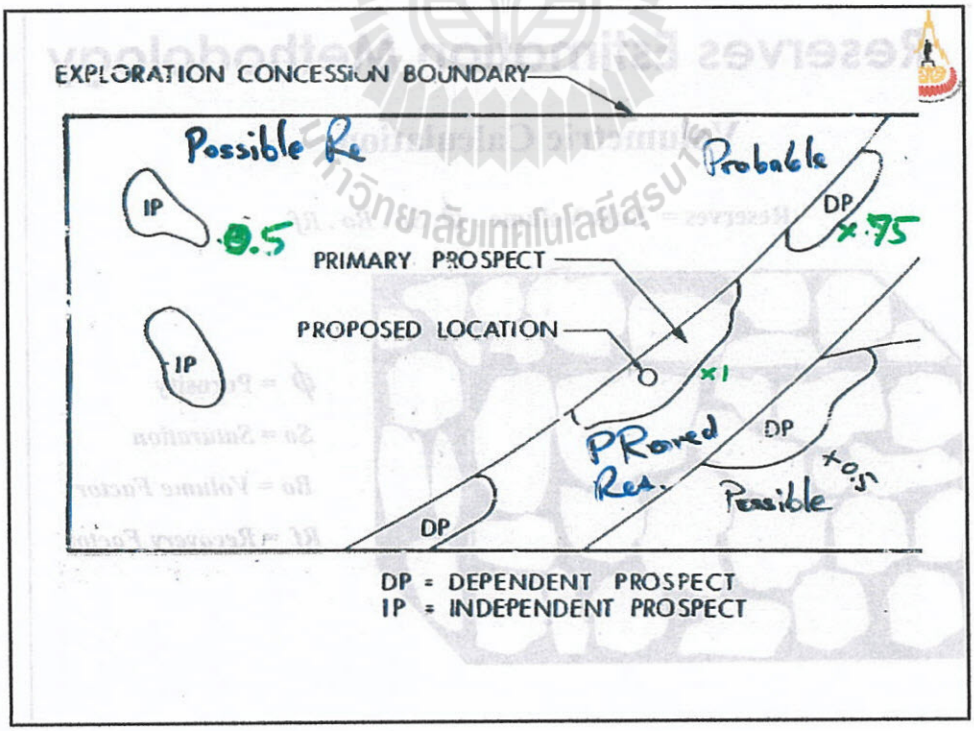

The gas volumetric calculation can be performed as follows:

(a) Determine volume of rock containing gas(or hydrocarbons) from the structural and isopach maps.
(b) Determine void space in rock; average effective ((porosity)
(c) Determine volume percentage containing gas(or hydrocarbons)
. fluid saturation $S_g = 1-S_w$
(d) Determine recoverable gas (or hydrocarbons) by multipling with recovery factor (F_R)
(e) Determine reserve volume in standard condition by dividing with gas formation volume factor (B_g).

$$\text{Reserves (SCF)} = A \times h \times \phi \times (1- S_w) \times F_R \times (1/ B_g)$$

- $A \times h$: Bulk Reservoir Volume
- ϕ : Pore Volume
- $(1- S_w)$: Gas Volume in Reservoir
- F_R : Recoverable Gas Volume
- $(1/ B_g)$: Recoverable Gas Volume in SCF

Gas Volumetric

SCF = Standard Cubic Foot (at standard condition)
$A \times h$ = reservoir volume in cubic foot
ϕ = porosity expressed as a fraction of bulk volume
S_w = water saturation expressed as a fraction of void space
F_R = Recovery factor expressed as a fraction of total in-place
B_g = formation volume factor in cu.ft reservoir/ SCF surface

If A (h is expessed in Acre-ft. the above formula will be

$$\text{Reserves(SCF)} = 43{,}560\, A \times h \times \phi \times (1- S_w) \times F_R \times (1/ B_g)$$

$$\text{OIL Reserve} = 7758 A h \phi (1-S_w)(1/B_o) F_r$$

Reserves Estimation Methodology

Volumetric Calculation

$$\text{Reserves} = \text{Bulk Volume} \cdot \phi \cdot So \cdot Bo \cdot Rf$$

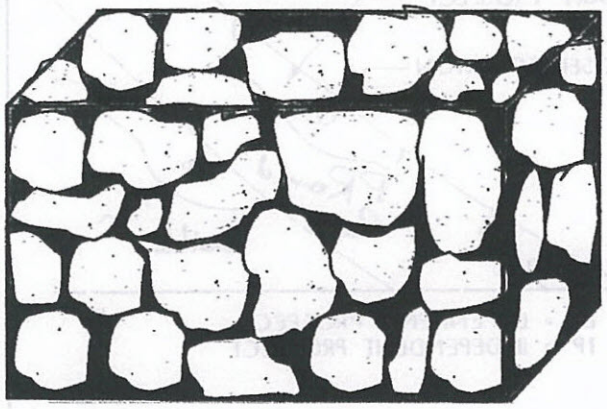

ϕ = Porosity
So = Saturation
Bo = Volume Factor
Rf = Recovery Factor

Gas Volumetric

The gas volumetric calculation can be performed as follows:

(a) Determine volume of rock containing gas(or hydrocarbons) from the structural and isopach maps.
(b) Determine void space in rock; average effective ((porosity)
(c) Determine volume percentage containing gas(or hydrocarbons) . fluid saturation $S_g = 1-S_w$
(d) Determine recoverable gas (or hydrocarbons) by multipling with recovery factor (F_R)
(e) Determine reserve volume in standard condition by dividing with gas formation volume factor (B_g).

$$\text{Reserves (SCF)} = \underbrace{A \times h}_{\text{Bulk Reservoir Volume}} \times \underbrace{\phi}_{\text{Pore Volume}} \times \underbrace{(1-S_w)}_{\text{Gas Volume in Reservoir}} \times \underbrace{F_R}_{\text{Recoverable Gas Volume}} \times \underbrace{(1/B_g)}_{\text{Recoverable Gas Volume in SCF}}$$

SCF = Standard Cubic Foot (at standard condition)
$A \times h$ = reservoir volume in cubic foot
ϕ = porosity expressed as a fraction of bulk volume
S_w = water saturation expressed as a fraction of void space
F_R = Recovery factor expressed as a fraction of total in-place
B_g = formation volume factor in cu.ft reservoir/ SCF surface

If A (h is expessed in Acre-ft. the above formula will be

$$\text{Reserves(SCF)} = 43{,}560\, A \times h \times \phi \times (1-S_w) \times F_R \times (1/B_g)$$

$$\text{OIL Reserve} = 7758Ah\phi(1-S_w)B_oF_r$$

Volumetric Estimates

- Reserves = Reservoir Volume x Porosity x Oil Saturation x Recovery Factor x Shrinkage to Surface Conditions
- In oilfield units:

Reserves = [7758 x A x h x ø x (1-S_w) x R]/Bo

where Or 43560 for gas or Bg

7757 = bbls/acre-ft
A = area (sq. ft) or Acre
h = net thickness (ft)
ø = porosity (fraction)
S_w = water saturation (fraction)
R = recovery factor (fraction)
Bo = formation volume factor
Bg = Gas formatiom volume factor

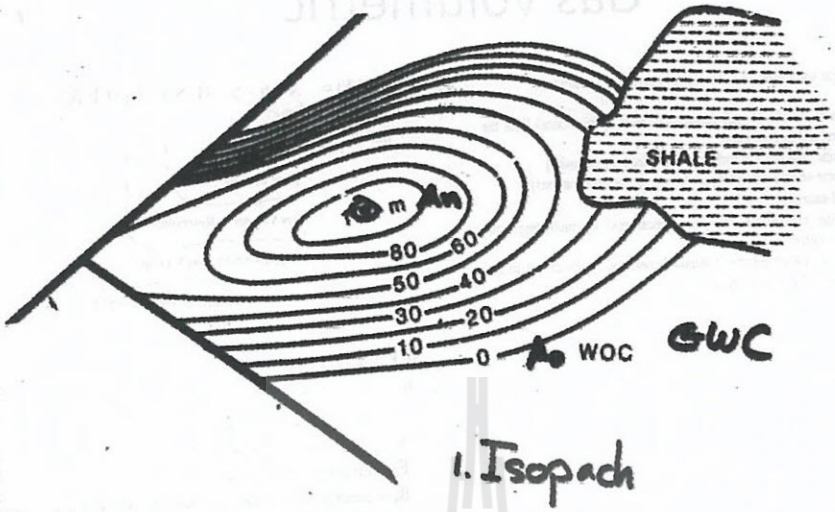

Fig. 4.3. *Isopay map for a hydrocarbon-bearing pool*

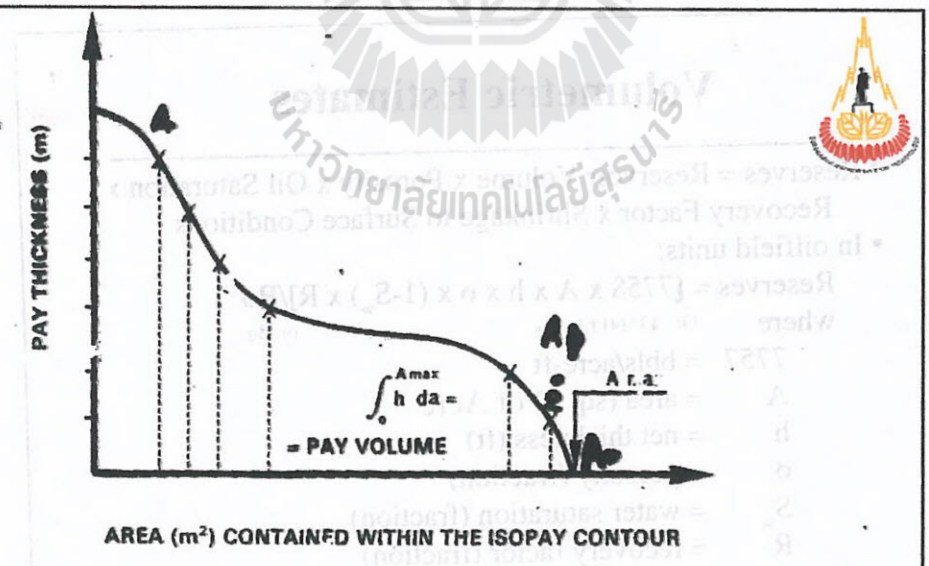

Fig. 4.4. *Graphical method for the calculation of the net pay volume. From Ref permission of Kluwer Academic Publishers and of Professors Archer and Wall*

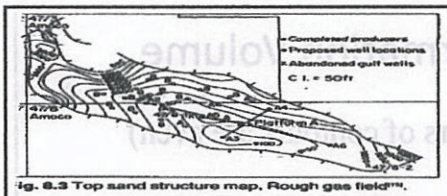

Fig. 8.3 Top sand structure map, Rough gas field[15].

tructure contour maps are used to connect points qual elevation. It is customary to map structure he top and base of porosity and the map indicates external geometry of the reservoir. The map in Fig. 8.1 shows the boundaries as a fluid porosity limit to reservoir quality rock and boundaries. The contour intervals are regular represent subsea depths. The map would be lled *top sand*, *base sand* or refer to a geological boundary. The difference in elevation between hydrocarbon–water contact and the top of the ucture is known as the closure or height of the rocarbon column. Structure maps of the top ds of Thistle oil reservoir[14] and the Rough gas d[15] are shown in Figs 8.2 and 8.3. A schematic ss-section of the Rough field is illustrated in Fig. [8].

he area contained within each structural contour be measured by various mathematical techni-

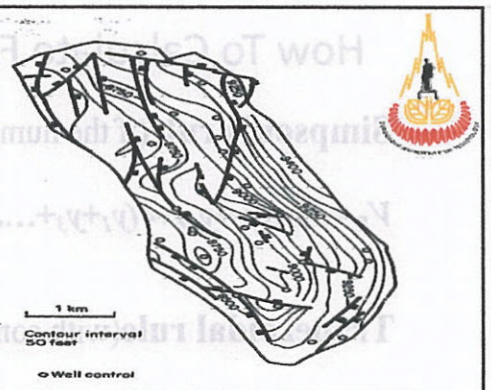

Fig. 8.2 Top sand structure map, Thistle oil reservoir. (after [14])

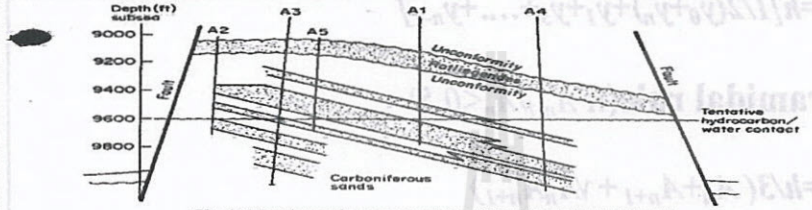

Fig. 8.4 A schematic cross-section of the Rough field. (after[15])

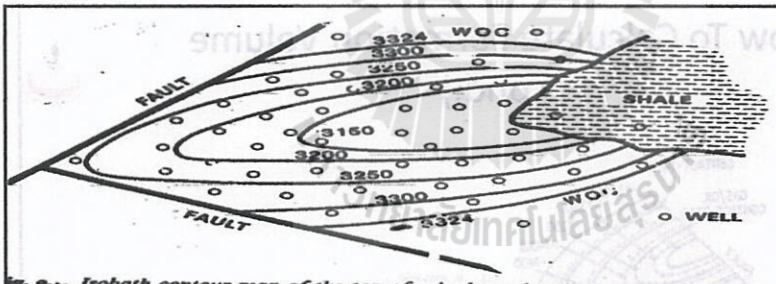

Isobath contour map of the top of a hydrocarbon-bearing pool

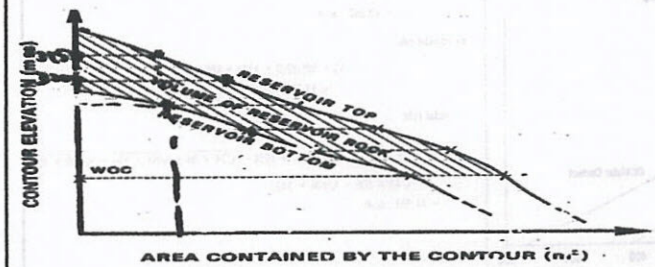

Fig. 4.2. *The hydrocarbon-bearing volume plotted against depth. From Ref. 4, reprinted with pern of Kluwer Academic Publishers and of Professors Archer and Wall*

How To Calculate Formation Volume

Simpson's rule(if the numbers of contours are even)

$$V_B = h/3[(y_0+y_n)+4(y_1+y_3+....+y_{n-1}) +2(y_2+y_4+....+y_{n-2})]$$

Trapezoidal rule(with some what less accuracy)

$$V_B = h[1/2(y_0+y_n)+y_1+y_3+....+y_{n-1}]$$

Pyramidal rule(if $A_{n-1}/A_n<0.5$)

$$V_B = h/3(A_n+A_{n+1}+\sqrt{A_nA_{n+1}})$$

How To Calculate Formation Volume (Cond.)

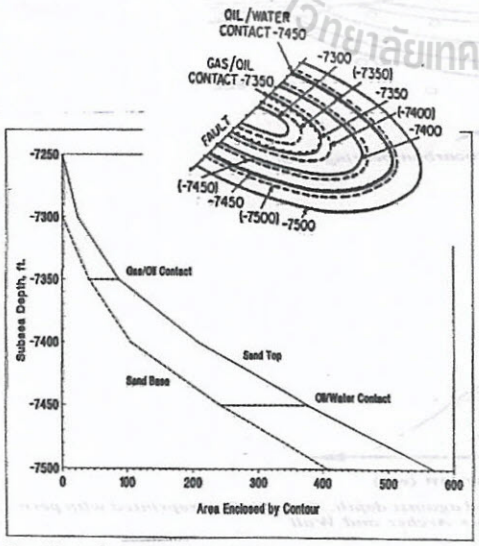

Figure 4–2. Acre-feet diagram for the map in Fig. 4–1.

...rson's rule:

$$V_B = \frac{50}{3}[0 + (578 - 242) + 4(24 - 0 + 209 - 106) + 2(88 - 42)]$$

$$= \frac{50}{3}[(136) + 4(24 + 103) + (2 \times 46)]$$

$$= 12{,}267 \text{ ac-ft}$$

...zoidal rule:

$$V_B = 50[1/2(0 + 136) + (24 + 46 + 103)]$$

$$= 12{,}050 \text{ ac-ft}$$

...idal rule:

$$V_B = \frac{50}{3}[(0 + 136) + 2(24 + 46 + 103) + \sqrt{24 \times 88} + \sqrt{88 \times 209} + \sqrt{209 \times 378} - \sqrt{42 \times 106} - \sqrt{106 \times 242}]$$

$$= 11{,}963 \text{ ac-ft}$$

Reserves Estimation Methodology

Material Balance

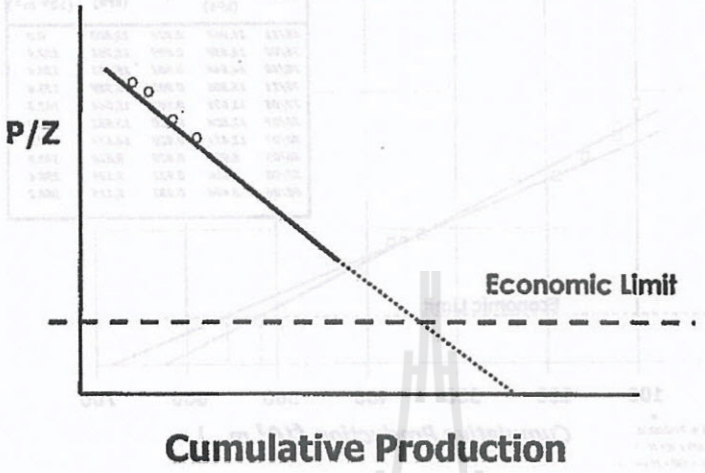

Material Balance for Gas Reservoirs

Material Balance Equations

$$GB_{gi} = (G - G_p)B_g \qquad (5\text{-}145)$$

$$GB_{gi} = (G - G_p)B_g + (W_e - W_p) \qquad (5\text{-}146)$$

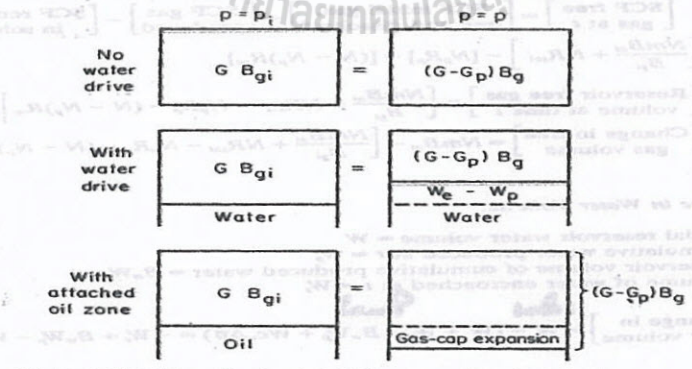

Figure 5-141. Schematic of material balance equations for a dry-gas reservoir [197].

PRODUCTION FORCEAST TECHNIQUES

Material Balance

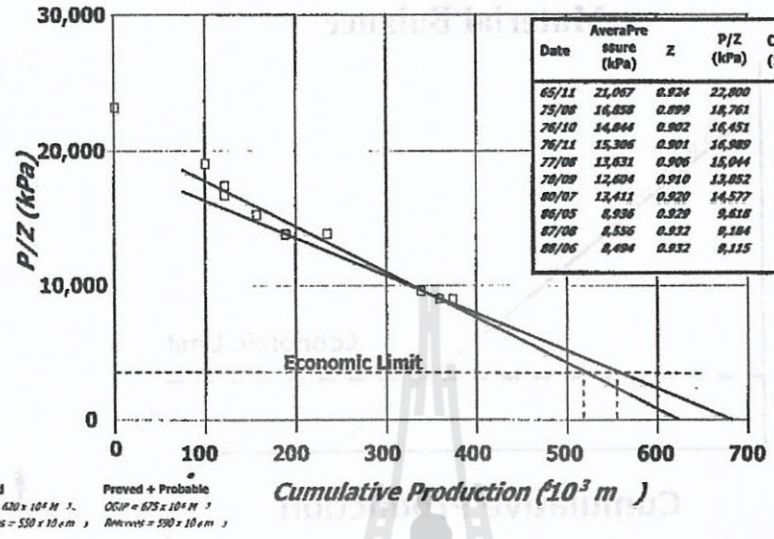

Date	AveraPressure (kPa)	Z	P/Z (kPa)	Cum.Prod. (10^6 m^3)
65/11	21,067	0.924	22,800	0.0
75/08	16,858	0.899	18,761	102.9
76/10	14,844	0.902	16,451	138.4
76/11	15,306	0.901	16,989	138.4
77/08	13,631	0.906	15,044	162.3
78/09	12,604	0.910	13,852	190.5
80/07	13,411	0.920	14,577	237.1
86/05	8,936	0.929	9,618	340.6
87/08	8,556	0.932	9,184	358.4
88/06	8,494	0.932	9,115	368.2

Proved
OGIP = 620 x 10^4 M ^{3}
Reserves = 530 x 10 e m ^{3}

Proved + Probable
OGIP = 675 x 10^4 M ^{3}
Reserves = 590 x 10 e m ^{3}

Initial reservoir oil volume $= NB_{oi}$

Oil volume at time t and pressure $p = (N - N_p)B_o$

① Change in oil volume $= NB_{oi} - (N - N_p)B_o$ (2.1)

Change in Oil Volume

Change in Free Gas Volume:

$$\left[\begin{matrix}\text{Ratio of initial free gas}\\ \text{to initial oil volume}\end{matrix}\right] = m = \frac{GB_{gi}}{NB_{oi}} = \frac{V_g}{V_o}$$

Initial free gas volume $= GB_{gi} = NmB_{oi}$

$$\left[\begin{matrix}\text{SCF free}\\ \text{gas at } t\end{matrix}\right] = \left[\begin{matrix}\text{SCF initial gas,}\\ \text{free and dissolved}\end{matrix}\right] - \left[\begin{matrix}\text{SCF gas}\\ \text{produced}\end{matrix}\right] - \left[\begin{matrix}\text{SCF remaining}\\ \text{in solution}\end{matrix}\right]$$

$$G_f = \left[\frac{NmB_{oi}}{B_{gi}} + NR_{soi}\right] - [N_pR_p] - [(N - N_p)R_{so}]$$

$$\left[\begin{matrix}\text{Reservoir free gas}\\ \text{volume at time } t\end{matrix}\right] = \left[\frac{NmB_{oi}}{B_{gi}} + NR_{soi} - N_pR_p - (N - N_p)R_{so}\right]B_g$$

② $$\left[\begin{matrix}\text{Change in free}\\ \text{gas volume}\end{matrix}\right] = NmB_{oi} - \left[\frac{NmB_{oi}}{B_{gi}} + NR_{soi} - N_pR_p - (N - N_p)R_{so}\right]B_g$$ (2.2)

Change in Water Volume:

Initial reservoir water volume $= W$
Cumulative water produced at $t = W_p$
Reservoir volume of cumulative produced water $= B_wW_p$
Volume of water encroached at $t = W_e$

③ $$\left[\begin{matrix}\text{Change in}\\ \text{water volume}\end{matrix}\right] = W - (W + W_e - B_wW_p + Wc_w\Delta p) = -W_e + B_wW_p - Wc_w\Delta p)$$ (2.3)

Change in the Void Space Volume:

Initial void space volume $= V_f$ V_p

④ $$\left[\begin{matrix}\text{Change in void}\\ \text{space volume}\end{matrix}\right] = V_f - [V_f - V_fc_f\Delta p] = V_fc_f\Delta p$$

..., because the change in void space volume is the negative of the change in rock volume:

$$\begin{bmatrix}\text{Change in}\\ \text{rock volume}\end{bmatrix} = -V_f c_f \Delta\bar{p} \qquad (2.4)$$

Combining the changes in water and rock volumes into a single term, yields the following:

$$= -W_e + B_w W_p - W c_w \Delta\bar{p} - V_f c_f \Delta\bar{p}$$

Recognizing that $W = V_f S_{wi}$ and that $V_f = \frac{NB_{oi} + NmB_{oi}}{1 - S_{wi}}$ and substituting, the following is obtained:

$$= -W_e + B_w W_p - \left[\frac{NB_{oi} + NmB_{oi}}{1 - S_{wi}}\right](c_w S_{wi} + c_f)\ \Delta\bar{p}$$

or

$$= -W_e + B_w W_p - (1 + m)\ NB_{oi}\left[\frac{c_w S_{wi} + c_f}{1 - S_{wi}}\right]\Delta\bar{p} \qquad (2.5)$$

Equating the changes in the oil and free gas volumes to the negative of the changes in the water and rock volumes and expanding all terms

$$N B_{oi} - N B_o + N_p B_o + NmB_{oi} - \left[\frac{NmB_{oi}B_g}{B_{gi}}\right] - N R_{soi}B_g + N_p R_p B_g$$

$$+ NB_g R_{so} - N_p B_g R_{so} = W_e - B_w W_p + (1 + m) N B_{oi}\left[\frac{c_w S_{wi} + c_f}{1 - S_{wi}}\right]\Delta\bar{p}$$

Now adding and subtracting the term $N_p B_g R_{soi}$

$$N B_{oi} - N B_o + N_p B_o + NmB_{oi} - \left[\frac{NmB_{oi}B_g}{B_{gi}}\right] - N R_{soi}B_g + N_p R_p B_g + NB_g R_{so}$$

$$- N_p B_g R_{so} + N_p B_g R_{soi} - N_p B_g R_{soi} = W_e - B_w W_p + (1 + m)\ N B_{oi}\left[\frac{c_w S_{wi} + c_f}{1 - S_{wi}}\right]\Delta\bar{p}$$

Then grouping terms:

$$NB_{oi} + NmB_{oi} - N[B_o + (R_{soi} - R_{so})B_g] + N_p[B_o + (R_{soi} - R_{so})B_g]$$

$$+ (R_p - R_{soi})B_g N_p - \left[\frac{NmB_{oi}B_g}{B_{gi}}\right] = W_e - B_w W_p + (1 + m)\ N B_{oi}\left[\frac{c_w S_{wi} + c_f}{1 - S_{wi}}\right]\Delta\bar{p}$$

Monte Carlo Simulations

FIGURE 8.1
MONTE CARLO SIMULATION SCHEMATIC

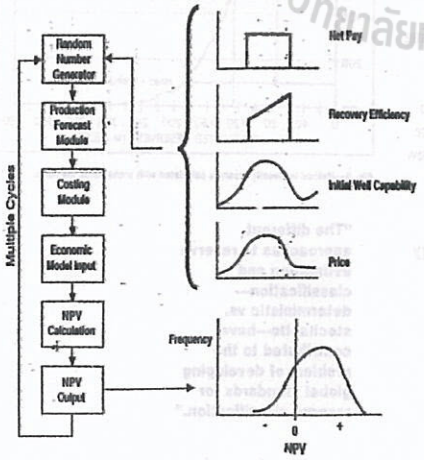

Reserves Estimation Methodology

Probabilistic Evaluation

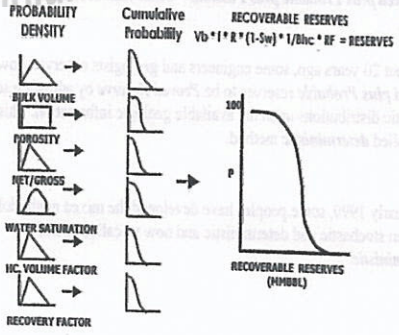

Department of Reservoir Engineering

Monte Carlo ชื่อเมืองใน Monaco

- Von Neumann & Ulam ใช้การทดลองหาค่า Random Numbers
- ระเบิดนิวเคลียร์ที่ Los Alamos ต้องการใช้ ระเบิดปรมาณู
- Solve Probabilitic Problem

1. Direct Simulation
   - Operation Research
   - Reserve Calculation
2. Monte Carlo Integration
3. Conditional Simulation

Random number generator
- middle-square - von Neuman
- Congruential method

$x_{i+1} = (ax_i + c) \bmod m$ ได้ค่าที่มากที่สุดเท่ากับ m

3.6 Stochastic(Statistic) & Deterministic

Regarding the probabilistic method, ***Monte Carlo type*** simulation may or may not be uses, but most schemes ***Stochastic Method*** for probabilistic reserve classification specify the following.

Proved – better than ***90%*** chance of being recovered.

Proved plus Probable – better than ***50%*** chance of being recovered.

Proved plus Probable plus Possible – better than ***10%*** chance of being recovered.

About 20 years ago, some engineers and geologists observed how to get ***Proved plus Probable*** reserves to be ***Proved Reserve*** by adjusting some probabilistic distributions upon the available geologic information. This new method called ***deterministic*** method.

Since early 1990, some peoples have developed the mixed methodology between stochastic and deterministic and now so-called "***Semi-Deterministic***".

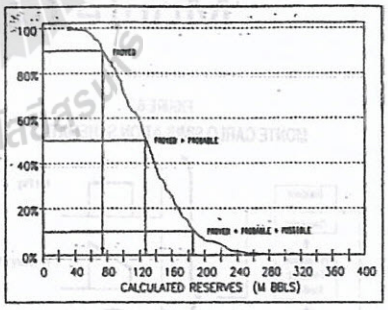

Fig. 2—Method to classify reserves calculated with probabilistic methods.

"The different approaches to reserve estimation and classification—deterministic vs. stochastic—have contributed to the problem of developing global standards for reserve classification."

Stochastic & Deterministic

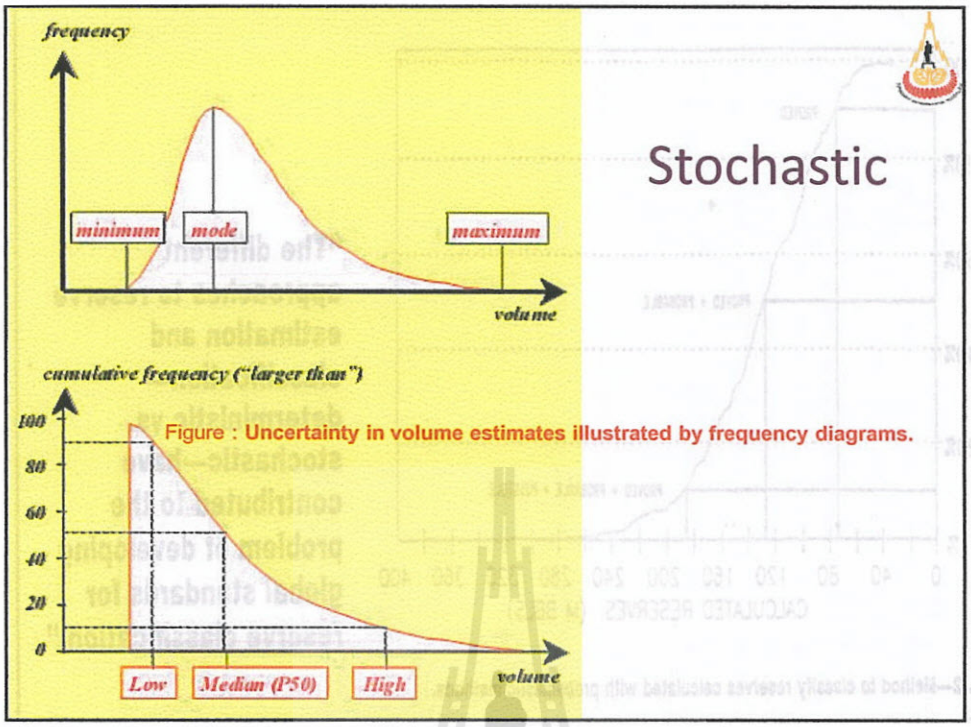

Stochastic

Figure : **Uncertainty in volume estimates illustrated by frequency diagrams.**

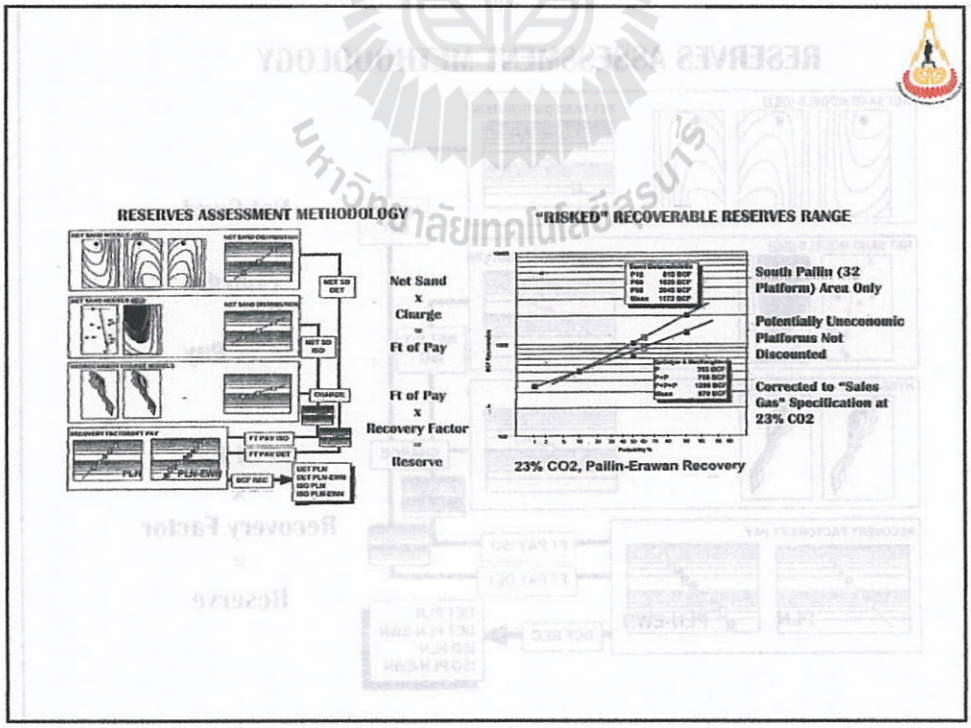

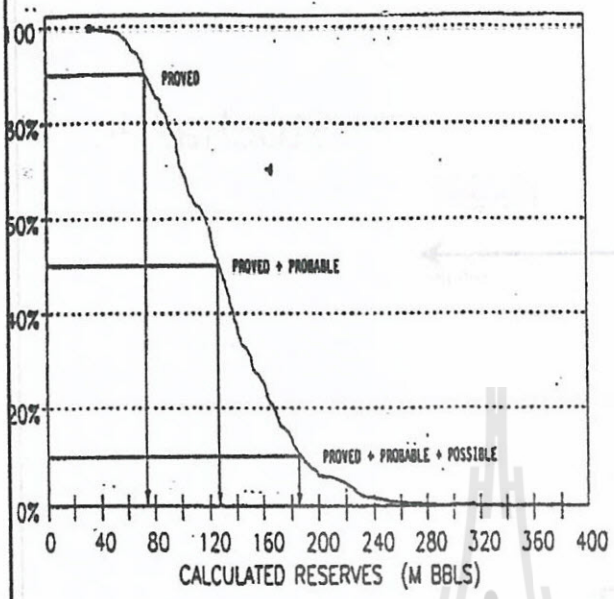

"The different approaches to reserve estimation and classification—deterministic vs. stochastic—have contributed to the problem of developing global standards for reserve classification."

. 2—Method to classify reserves calculated with probabilistic methods.

RESERVES ASSESSMENT METHODOLOGY

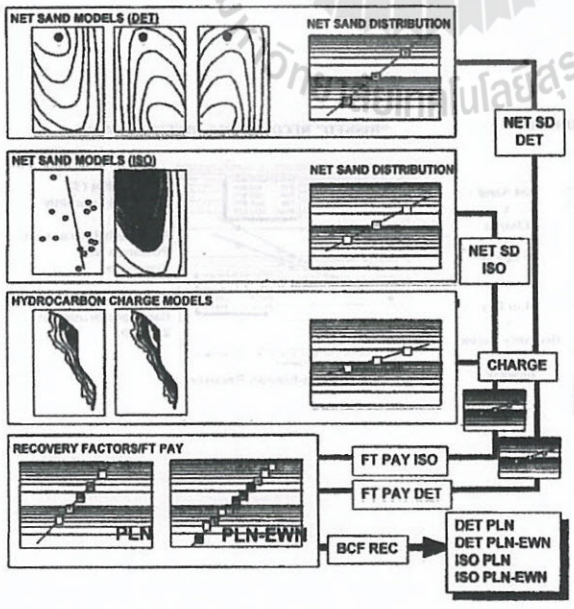

Net Sand
x
Charge
=
Ft of Pay

Ft of Pay
x
Recovery Factor
=
Reserve

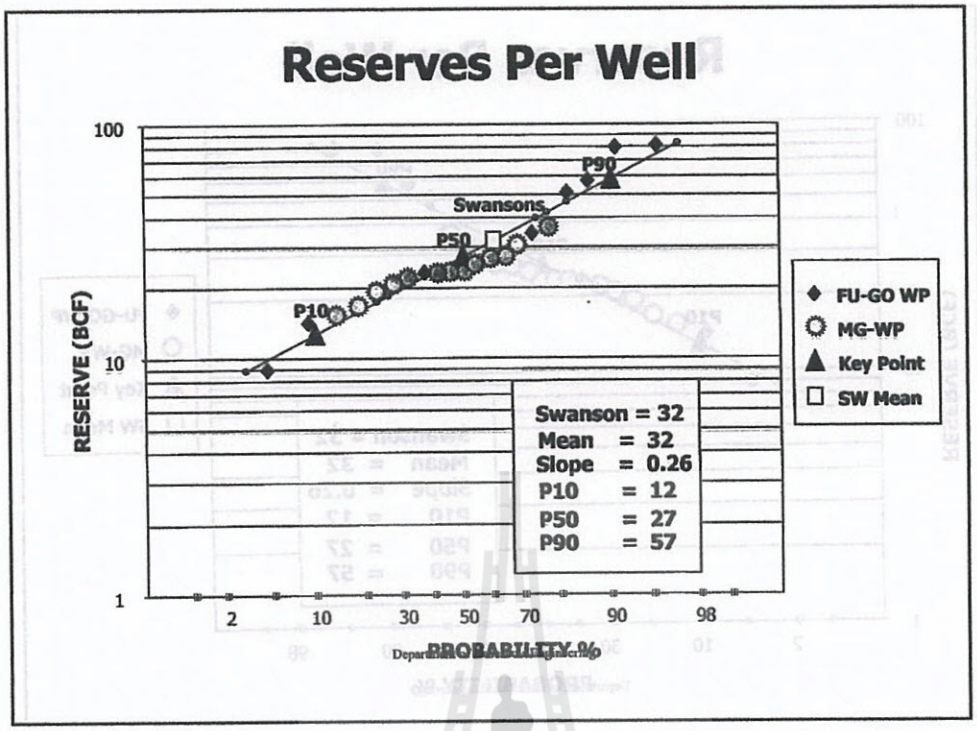

DEFINITIONS

Swanson's Mean (SM) - a quick approximate method to estimate the mean value of a log-normal distribution which can be used instead of the statistical mean if the ratio of the reserve at the P90 level over the reserve at the P50 level is less than five.

$$SM = (0.30 \times P10) + (0.4 \times P50) + (0.3 \times P90)$$

where,

P10 = the level for which there is a 10% probability of occurrence.
P50 = the level for which there is a 50% probability of occurrence.
P90 = the level for which there is a 90% probability of occurrence.

Probability of Success (POS) - the possibility of getting onto the reserves distribution or range of outcomes being used in the evaluation, and is a function of the risks (geologic, mechanical, etc.) of the project.

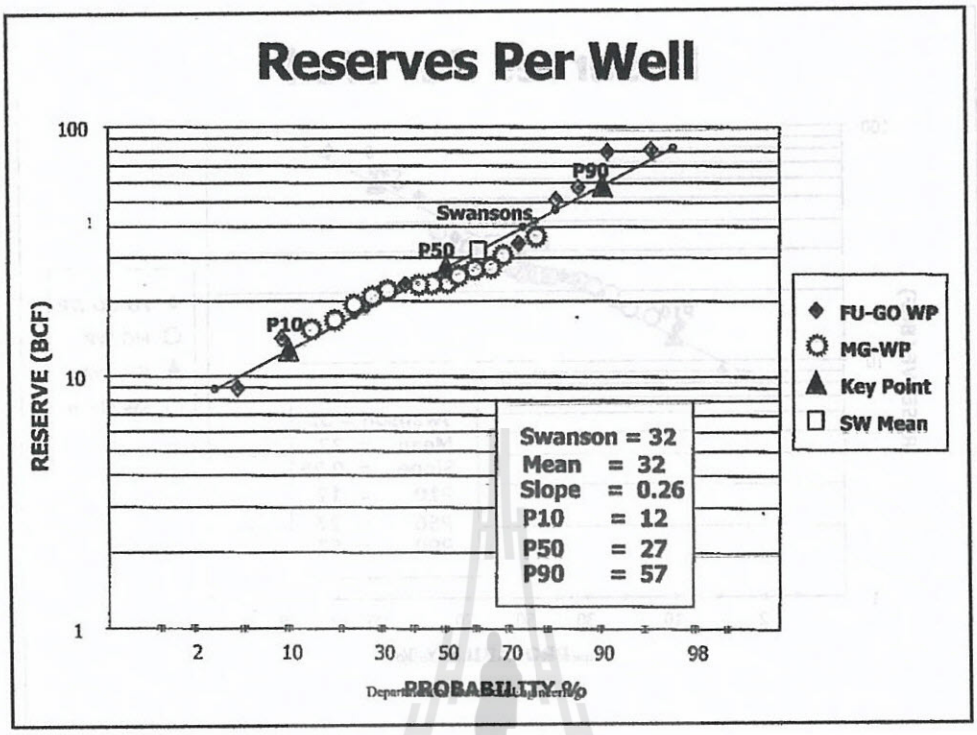
Reserves Per Well
100
10
1
RESERVE (BCF)
P90
Swansons
P50
P10
Swanson = 32
Mean = 32
Slope = 0.26
P10 = 12
P50 = 27
P90 = 57
FU-GO WP
MG-WP
Key Point
SW Mean
2
10
30
50
70
90
98
PROBABILITY %

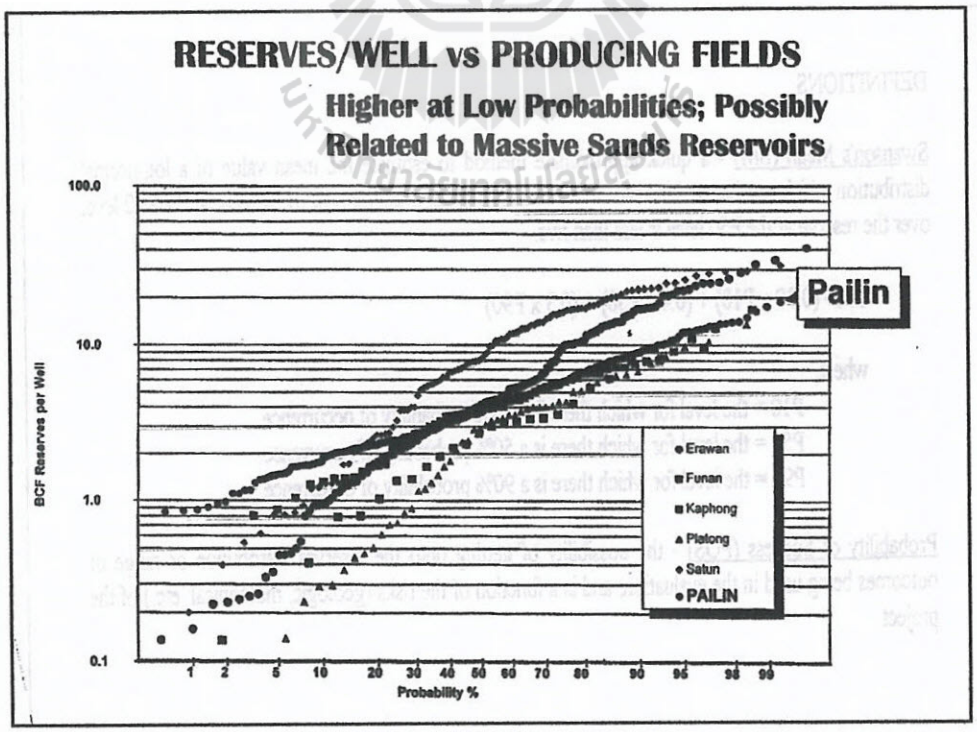
RESERVES/WELL vs PRODUCING FIELDS
Higher at Low Probabilities; Possibly
Related to Massive Sands Reservoirs
100.0
10.0
1.0
0.1
BCF Reserves per Well
Pailin
Erawan
Funan
Kaphong
Platong
Satun
PAILIN
1
2
5
10
20
30
40
50
60
70
80
90
95
98
99
Probability %

Reserves Estimation Methodology

Probabilistic Evaluation

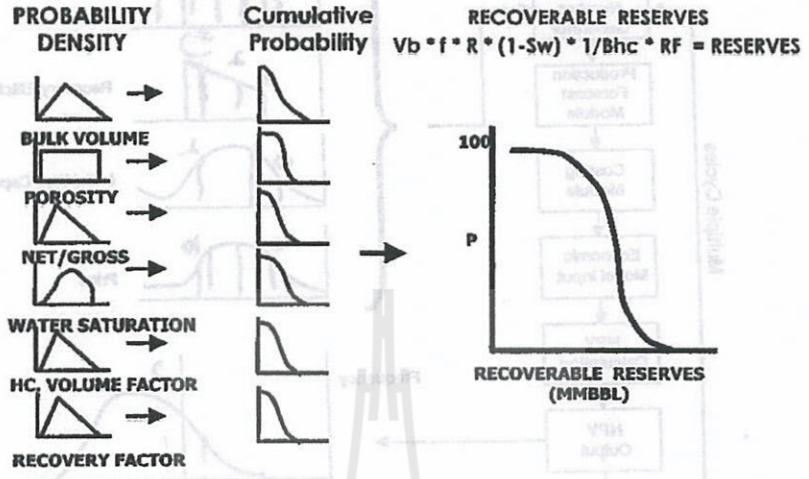

Department of Reservoir Engineering

"RISKED" RECOVERABLE RESERVES RANGE

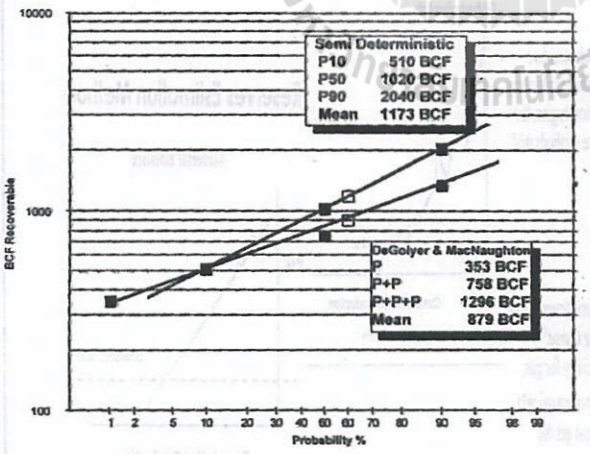

South Pailin (32 Platform) Area Only

Potentially Uneconomic Platforms Not Discounted

Corrected to "Sales Gas" Specification at 23% CO2

23% CO2, Pailin-Erawan Recovery

D and M "Sales Gas" Category

FIGURE 8.1

MONTE CARLO SIMULATION SCHEMATIC

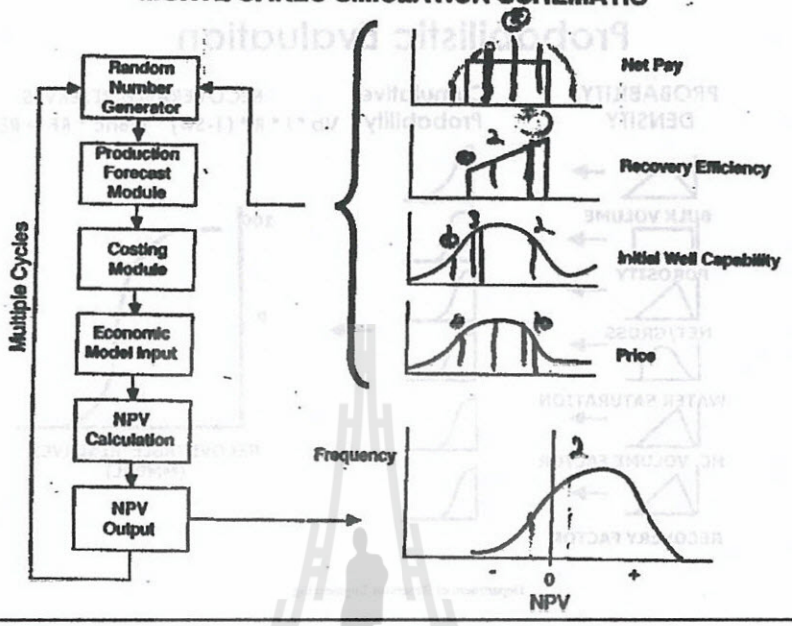

3.7 Reservoir Performances

Prior to drilling, the reserve may be estimated by reservoir structure size comparison with the previous discovered reservoir, but after exploratory drilling the volumetric method will be applied. After production begins, the reservoir performance will be collected and the more accurate methods will be applied to determine gas(or petroleum) reserve.

3.7.1 Decline Curves

When the production data has been collected for some time (cumulative production about 5-10% of the gas in place) then the "*Decline Curve*" method can be applied to give the more accurate results. Specially for gas, P/Z V.S. G_p (cumulative production from material balance equation)) plot can be projected as a straight line to the economic limit and get the reserve.

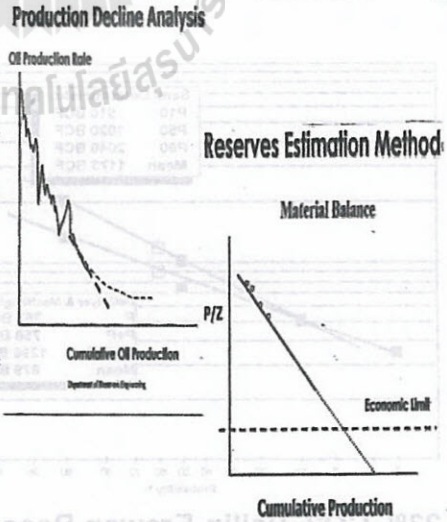

Table B1 - Gas-in-Place Estimates

Δp (psi)	c_f (1/psi)	GIP (Gscf)	Comments
7.70	6×10^{-6}	433	No communication wit Nam Phong 2
4.47	6×10^{-6}	744	90% confidence interval
10.93	6×10^{-6}	304	90% confidence interval
7.70	6×10^{-5}	249	High formation compressibilit
6.00	6×10^{-6}	565	Communication with Nam Phong 2 Includes gas volume of both wells

Values for other variables used in the equation:

G_p	: 0.3267 Gscf
z	: 1.140082
$\Delta z/\Delta p$	: 0.0000707/psi
S_w	: 0.25
c_w	: 0.0000034/psi

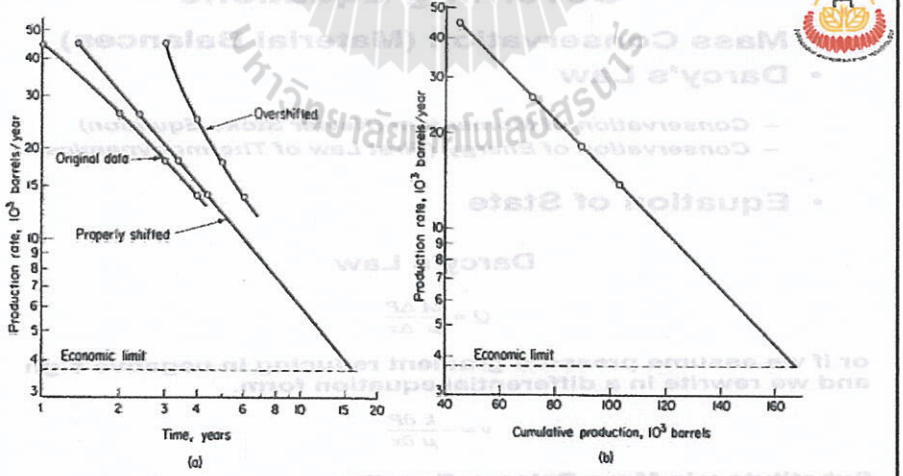

Figure 11.7. Harmonic decline example. (a) Rate versus time on log-log plot. (b) Rate versus cumulative on semilog plot.

3.7.2 Reservoir Simulations

What Simulation is

- ***Simulate*** = to give the appearance of m a reservoir
- ***Simulation*** involves the utilization of a model to obtain some insight into the behavior of a physical process.
- ***Simulation*** has long been recognized in many applied science disciplines as the final resort; as Wagner aptly says: " When all else fails,... simulate.
- In operations research, extensive use has been made of simulation studies; some examples are:
  1. Transportation model networks
  2. Stock market performance
  3. Telephone system design
  4. Supermarket checkout counter
  5. Engine Simulation
  6. Other Simulations

What Reservoir Simulation is

- A ***RESERVOIR Simulation*** is a mathematical model that represents the physical phenomena of a reservoir

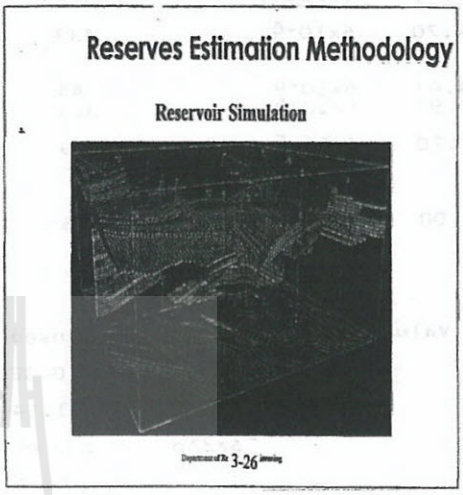

Reservoir Simulation

Fluid Flow Equations

Governing Equations

- **Mass Conservation (Material Balances)**
- **Darcy's Law**
  - ***Conservation of Momentum (Navier Stoke Equation)***
  - ***Conservation of Energy (First Law of Thermodynamics)***
- **Equation of State**

Darcy's Law

$$Q = \frac{kA}{\mu}\frac{\Delta P}{\Delta x}$$

or if we assume pressure gradient reducing in negative sign and we rewrite in a differential equation form.

$$v = -\frac{k}{\mu}\frac{\partial P}{\partial x}$$

Substitute *v* in Mass Balance Equation (consider only x-direction)

$$\frac{\partial\left(-\frac{k}{\mu}\frac{\partial P}{\partial x}\rho\right)}{\partial x} = -\phi\frac{\partial \rho}{\partial t}$$

What is reservoir simulation?

- A reservoir simulation is a mathematical model that represent the physical phenomena of a reservoir.

Why do we need a Reservoir Simulator?

- Because a reservoir simulator is a powerful tool and not expensive . We can predict what is going in the reservoir and a amount of production from alternative operations.

Types of Reservoir Simulation

- Black Oil Simulation
- Compositional Black Oil Simulation
- Coupled Fluid Flow /Geomechanic Simulation

GOMIN 'A' PLATFORM

Well	Unrisked Reserves(BCF)	POS (%)	Risked Reserves(BCF)	
Gomin-3	4.89	1.00	4.89	
Gomin A-10	3.73	0.71	2.66	omit from economics
Gomin A-5	3.73	0.81	3.02	
Gomin A-2	3.73	0.90	3.36	
Gomin A-9	3.73	0.77	2.85	
Gomin A-6	3.73	0.81	3.01	
Gomin A-12	3.73	0.70	2.61	
Gomin A-4	2.80	0.90	2.52	
Gomin A-13	2.80	0.80	2.24	
Gomin A-8	1.87	0.80	1.49	
Gomin A-7	3.43	0.81	2.77	omit from economics
Gomin A-3	3.43	0.81	2.77	omit from economics
Gomin A-11	3.43	0.72	2.48	omit from economics
total	45.03		36.67	

GOMIN 'B' PLATFORM

Well	Unrisked Reserves(BCF)	POS (%)	Risked Reserves(BCF)	
Gomin-5	4.10	1.00	4.10	
G875A S.	4.36	0.70	3.05	omit from economics
G875A M.	4.36	0.60	2.62	omit from economics
G875A N.	4.36	0.60	2.62	omit from economics
G860A N.	2.18	0.90	1.96	
G865A S.	4.36	0.90	3.92	
G865A S.M.	4.36	0.90	3.92	
G865A N.M	4.36	0.85	3.71	
G865A N.	4.36	0.85	3.71	
G855A N.	4.36	0.86	3.73	
G855A M.	4.36	0.81	3.52	
G855A S.	4.36	0.81	3.52	
total	49.89		40.38	

Why do we need a Reservoir Simulator?

- Because a reservoir simulator is a powerful tool and not expensive . We can predict what is going in the reservoir and a amount of production from alternative operations.

Fluid Flow Equations

Governing Equations

- Mass Conservation (Material Balances)
- Darcy's Law
  - *Conservation of Momentum (Navier Stoke Equation)*
  - *Conservation of Energy (First Law of Thermodynamics)*
- Equation of State

Types of Reservoir Simulation

- Black Oil Simulation
- Compositional Black Oil Simulation
- Coupled Fluid Flow /Geomechanic Simulation

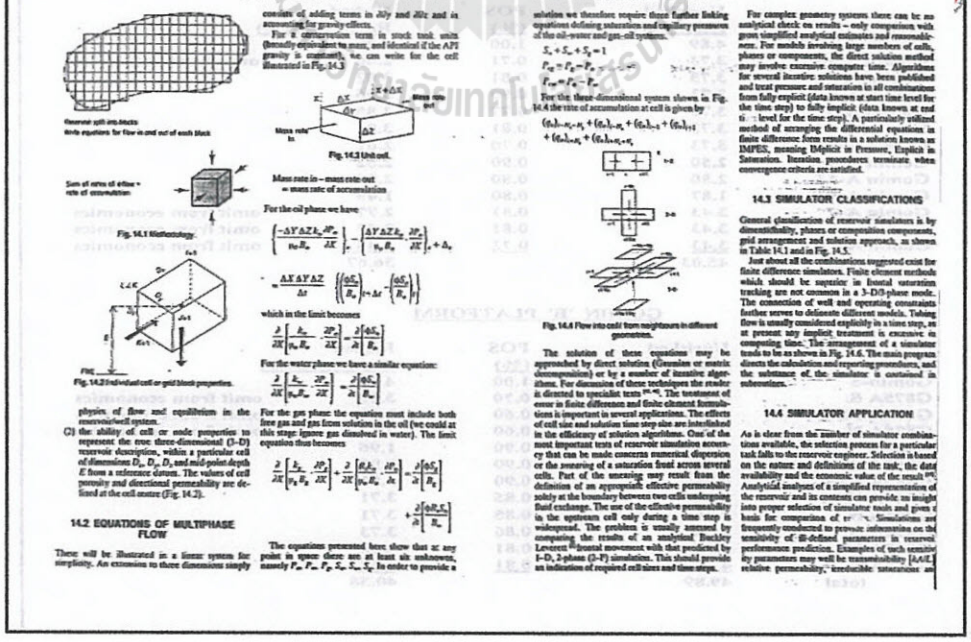

PETROLEUM ENGINEERING: PRINCIPLES AND PRACTICE

Fig. 14.1 Methodology.

Fig. 14.2 Typical cell or grid block properties.

physics of flow and equilibrium in the reservoir/well system.

(2) the ability of cell or node properties to represent the true three-dimensional (3-D) reservoir description, within a particular cell of dimensions D_x, D_y, D_z and mid-point depth E from a reference datum. The values of cell porosity and directional permeability are defined at the cell centre (Fig. 14.2).

14.2 EQUATIONS OF MULTIPHASE FLOW

There will be illustrated in a linear system for simplicity. An extension to three dimensions simply consists of adding terms in ∂y and ∂z and in accounting for gravity effects.

For a conservation term in stock tank units (density equivalent to mass, and identical if the API gravity is constant), we can write for the cell illustrated in Fig. 14.3

Fig. 14.3 Unit cell.

Mass rate in − mass rate out = mass rate of accumulation

For the oil phase we have

$$\left(\frac{-\Delta Y \Delta Z k_x}{\mu_o B_o}\frac{\partial P_o}{\partial x}\right)_x - \left(\frac{\Delta Y \Delta Z k_x}{\mu_o B_o}\frac{\partial P_o}{\partial x}\right)_{x+\Delta x} + Q_o$$

$$= \frac{\Delta X \Delta Y \Delta Z}{\Delta t}\left[\left(\frac{\phi S_o}{B_o}\right)_{t+\Delta t} - \left(\frac{\phi S_o}{B_o}\right)_t\right]$$

which in the limit becomes

$$\frac{\partial}{\partial x}\left[\frac{k_x}{\mu_o B_o}\frac{\partial P_o}{\partial x}\right] - \frac{\partial}{\partial t}\left[\frac{\phi S_o}{B_o}\right]$$

For the water phase we have a similar equation:

$$\frac{\partial}{\partial x}\left[\frac{k_x}{\mu_w B_w}\frac{\partial P_w}{\partial x}\right] = \frac{\partial}{\partial t}\left[\frac{\phi S_w}{B_w}\right]$$

For the gas phase the equation must include both free gas and gas from solution in the oil (we could at this stage ignore gas dissolved in water). The limit equation thus becomes

$$\frac{\partial}{\partial x}\left[\frac{k_x}{\mu_g B_g}\frac{\partial P_g}{\partial x}\right] + \frac{\partial}{\partial x}\left[\frac{R_s k_x}{\mu_o B_o}\frac{\partial P_o}{\partial x}\right] = \frac{\partial}{\partial t}\left[\frac{\phi S_g}{B_g}\right] + \frac{\partial}{\partial t}\left[\frac{\phi R_s S_o}{B_o}\right]$$

The equations presented here show that at any point in space there are at least six unknowns, namely P_o, P_w, P_g, S_o, S_w, S_g. In order to provide a solution we therefore require three further linking equations defining saturation and capillary pressure of the oil–water and gas–oil systems.

$$S_o + S_w + S_g = 1$$

$$P_{cw} = P_o - P_w \quad \ldots$$

$$P_{cw} = P_o - P_w$$

For the three-dimensional system shown in Fig. 14.4 the rate of accumulation at cell is given by

$$(q_x)_{i-\frac{1}{2},j,k} + (q_y)_{i,j-\frac{1}{2},k} + (q_z)_{i,j,k-\frac{1}{2}} + (q_x)_{i+\frac{1}{2},j,k} + (q_y)_{i,j+\frac{1}{2},k} + (q_z)_{i,j,k+\frac{1}{2}}$$

Fig. 14.4 Flow into cell from neighbours in different geometries.

The solution of these equations may be approached by direct solution (Gaussian or matrix decomposition) or by a number of iterative algorithms. For discussion of these techniques the reader is directed to specialist texts[14.4–6]. The treatment of error in finite difference and finite element formulations is important in several applications. The effects of cell size and solution time step size are interlinked in the efficiency of solution algorithms. One of the most important tests of reservoir simulation accuracy that can be made concerns numerical dispersion or the smearing of a saturation front across several cells. Part of the smearing may result from the definition of an appropriate effective permeability solely at the boundary between two cells undergoing fluid exchange. The use of the effective permeability in the upstream cell only during a time step is widespread. The problem is usually assessed by comparing the results of an analytical Buckley Leverett frontal movement with that predicted by 1-D, 2-phase (2-P) simulations. This should provide an indication of required cell sizes and time steps.

For complex geometry systems there can be no analytical check on results – only comparison with gross simplified analytical estimates and reasonableness. For models involving large numbers of cells, phases or components, the direct solution method may involve excessive computer time. Algorithms for several iterative solutions have been published and treat pressure and saturation in all combinations from fully explicit (data known at start time level for the time step) to fully implicit (data known at end time level for the time step). A particularly utilized method of arranging the differential equations in finite difference form results in a solution known as IMPES, meaning IMplicit in Pressure, Explicit in Saturation. Iteration procedures terminate when convergence criteria are satisfied.

14.3 SIMULATOR CLASSIFICATIONS

General classification of reservoir simulators is by dimensionality, phases or composition components, grid arrangement and solution approach, as shown in Table 14.1 and in Fig. 14.5.

Just about all the combinations suggested exist for finite difference simulators. Finite element methods which should be superior in frontal saturation tracking are not common in a 3-D/3-phase mode. The connection of well and operating constraints further serves to delineate different models. Tubing flow is usually considered explicitly in a time step, as at present any implicit treatment is excessive in computing time. The arrangement of a simulator tends to be as shown in Fig. 14.6. The main program directs the calculation and reporting procedures, and the substance of the simulator is contained in subroutines.

14.4 SIMULATOR APPLICATION

As is clear from the number of simulator combinations available, the selection process for a particular task falls to the reservoir engineer. Selection is based on the nature and definitions of the task, the data availability and the economic value of the result[14.7]. Analytical analyses of a simplified representation of the reservoir and its contents can provide an insight into proper selection of simulator tools and given a basis for comparison of results. Simulations are frequently conducted to provide information on the sensitivity of ill-defined parameters in reservoir performance prediction. Examples of such sensitivity parameters may well be transmissibility [k/μB], relative permeability, irreducible saturations an

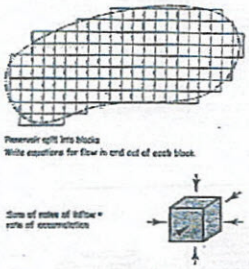

Figure 3.23 Methodology

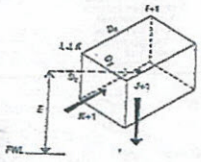

Figure 3.24 Individual cell or grid block properties

EQUATION OF MULTIPHASE FLOW

These will be illustrated in a linear system for simplicity. An extension to three dimensions simply consists of adding terms in $\partial/\partial y$ and $\partial/\partial z$ and account for gravity effects.

For a conservation term in stock tank units (broadly equivalent to mass, and identical if the API gravity is constant), we can write for the cell illustrated in Fig. 2.25

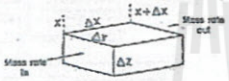

Figure 3.25 Unit Cell.

Mass rate in – Mass rate out = Mass rate of accumulation

For the oil phase we have

The equations presented here show that at any point in space there are at least six unknowns, namely P_o, P_w, P_g, S_o, S_w, S_g. In order to provide a solution we therefore require three further linking equations defining saturation and capillary pressures of the oil-water and gas-oil system

$$S_o + S_w + S_g = 1 \quad , \quad P_{cg} = P_g - P_o \quad , \quad P_{cw} = P_o - P_w$$

For three-dimensional system shown in Fig.3.26

$$(q_o)_{i-N_x-N_y} + (q_o)_{i-N_x} + (q_o)_{i-1} + (q_o)_{i+1} + (q_o)_{i+N_x} + (q_o)_{i+N_x+N_y}$$

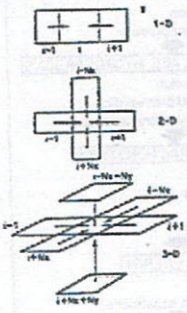

Figure 3.26 Flow in the cell *i* from neighbors in different geometries.

TABLE Classification of simulators

Dimensions	Phases/ composition	Grid mode arrangement	Options for solution
0-D (material balance) 1-D linear 1-D vertical	1-P gas 1-P water 2-P black oil-w 2-P black oil-g	Cartesian (regular) Cartesian (irregular) Radial (vertical wells) Radial (horizontal wells)	Finite element Finite difference – direct soln – implicit – IMPES
2-D cross-section 2-D areal 2-D sector 3-D full field	3-P bo-w-g N component N pseudo-components N comp-chem-oil flood – thermal process – miscible process – inert gas process – volatile oil – gas condensate	Local	Semi implicit – explicit Conformal mapping

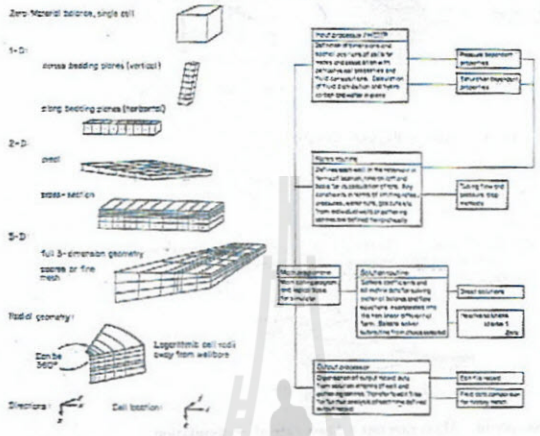

Figure 3.27 Simulator types

Figure 3.28 Arrangement of simulator routines

RESERVOIR DESCRIPTION IN MODELLING

Whether a complex of simple reservoir model is being applied, a number of steps in analysis and data requirements are common, and illustrated in Fig. 3.29. The validity of the initialization reservoir model is largely dependent on geological model and the flow performance is linked to reservoir and production engineering description.

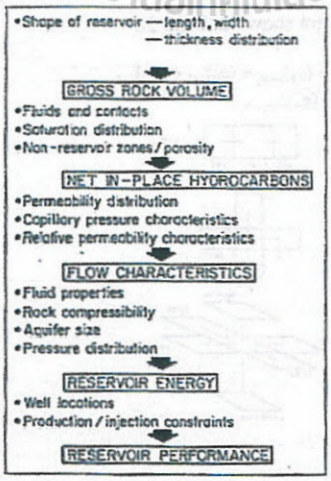

Figure 3.29 Steps needed to build a reservoir model.

Comprehensive Reservoir Management Model

- Reservoir Model
- Well Model
- Wellbore Model
- Surface Model

Classification of Reservoir Simulation

- Single phase reservoir simulator (liquid or gas)
- Multiphase reservoir simulator
  - black-oil simulator
  - compositional simulator

Other classification

- type of reservoir
  - gas reservoir simulator
  - black-oil reservoir simulator
  - compositional reservoir simulator
- fluid representation
  - compositional
  - non-compositional

- recovery process
  - primary recovery
    - solution gas drive
    - gas cap expansion
    - gravity drainage
    - water influx
  - secondary recovery
    - gas injection
    - water injection
  - enhanced oil recovery
    - chemical flood
    - miscible displacement
    - thermal recovery

Reservoir Model

- Represent fluid flow within reservoir.
- Subdivide the reservoir volume into an array or grid of smaller volume elements.

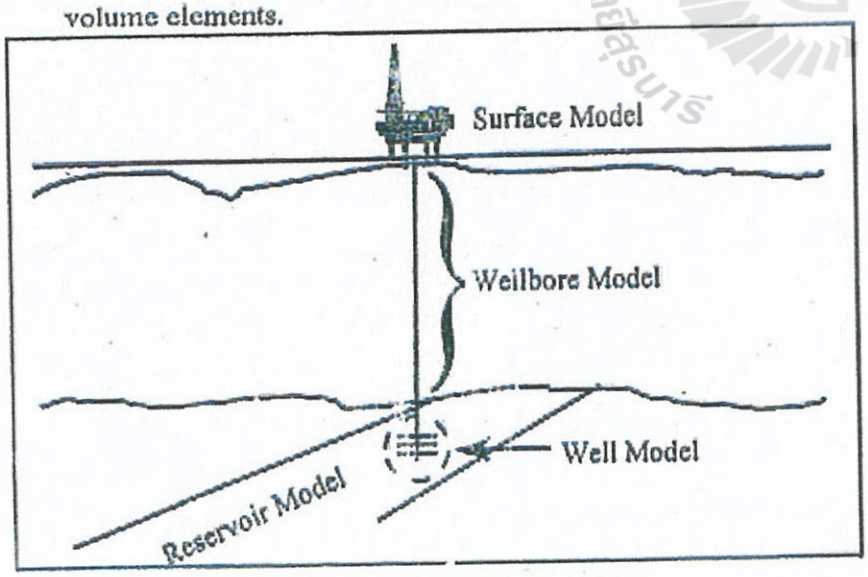

Reservoir management system.

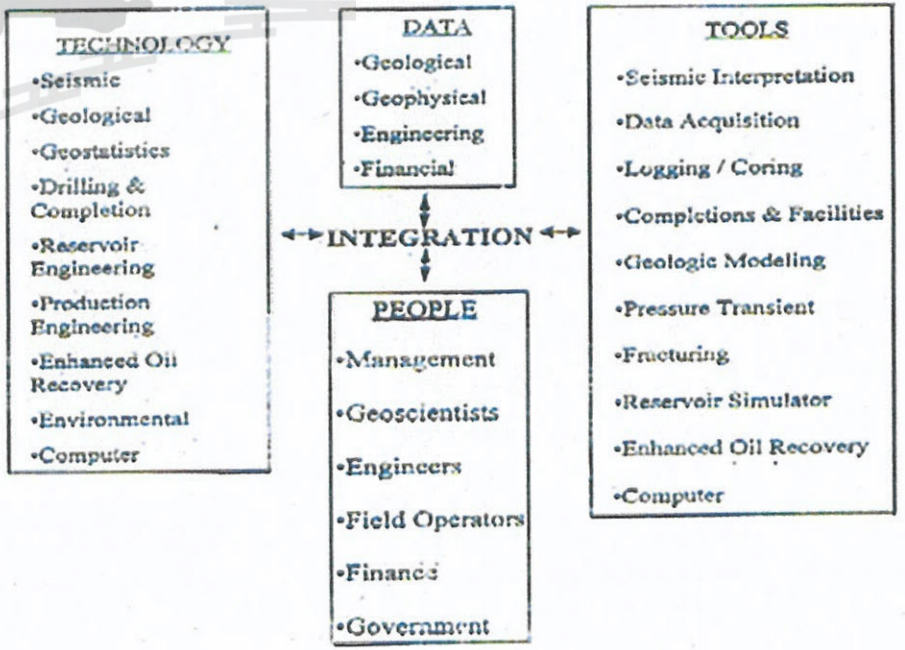

3-4th WEEK (June 6-17, 2012)
Outline

- Reserve Calculation

•Volumetric

Gas Volumetric

The gas volumetric calculation can be performed as follows:

(a) Determine volume of rock containing gas(or hydrocarbons) from the structural and isopach maps.
(b) Determine void space in rock; average effective ((porosity)
(c) Determine volume percentage containing gas(or hydrocarbons) . fluid saturation $S_g = 1-S_w$
(d) Determine recoverable gas (or hydrocarbons) by multipling with recovery factor (F_R)
(e) Determine reserve volume in standard condition by dividing with gas formation volume factor (B_g).

$$\text{Reserves (SCF)} = \underbrace{A \times h}_{\text{Bulk Reservoir Volume}} \times \underbrace{\phi}_{\text{Pore Volume}} \times \underbrace{(1-S_w)}_{\text{Gas Volume in Reservoir}} \times \underbrace{F_R}_{\text{Recoverable Gas Volume}} \times \underbrace{(1/B_g)}_{\text{Recoverable Gas Volume in SCF}}$$

SCF = Standard Cubic Foot (at standard condition)
$A \times h$ = reservoir volume in cubic foot
ϕ = porosity expressed as a fraction of bulk volume
S_w = water saturation expressed as a fraction of void space
F_R = Recovery factor expressed as a fraction of total in-place
B_g = formation volume factor in cu.ft reservoir/ SCF surface

If A (h is expessed in Acre-ft. the above formula will be

$$\text{Reserves(SCF)} = 43{,}560\, A \times h \times \phi \times (1-S_w) \times F_R \times (1/B_g)$$

$$\text{OIL Reserve} = 7758Ah\phi(1-S_w)B_oF_r$$

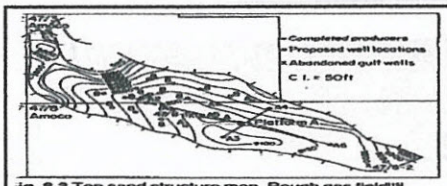

ig. 8.3 Top sand structure map, Rough gas field[116].

tructure contour maps are used to connect points qual elevation. It is customary to map structure he top and base of porosity and the map indicates external geometry of the reservoir. The map wn in Fig. 8.1 shows the boundaries as a fluid porosity limit to reservoir quality rock and r boundaries. The contour intervals are regular represent subsea depths. The map would be lled *top sand*, *base sand* or refer to a geological boundary. The difference in elevation between hydrocarbon–water contact and the top of the cture is known as the closure or height of the rocarbon column. Structure maps of the top ds of Thistle oil reservoir[116] and the Rough gas d[116] are shown in Figs 8.2 and 8.3. A schematic ss-section of the Rough field is illustrated in Fig. [116].

he area contained within each structural contour be measured by various mathematical techni-

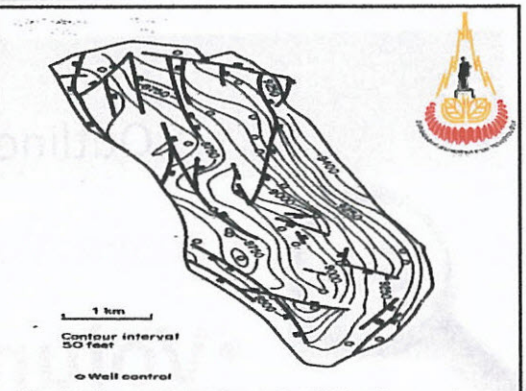

Fig. 8.2 Top sand structure map, Thistle oil reservoir. (after [116])

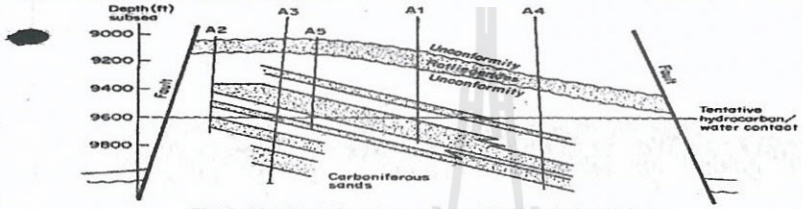

Fig. 8.4 A schematic cross-section of the Rough field. (after[116])

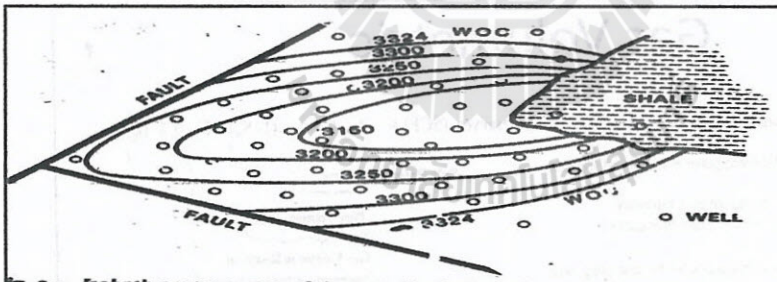

Isobath contour map of the top of a hydrocarbon-bearing pool

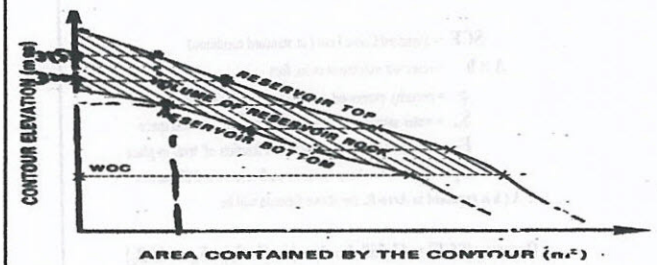

Fig. 4.2. *The hydrocarbon-bearing volume plotted against depth. From Ref. 4, reprinted with pern of Kluwer Academic Publishers and of Professors Archer and Wall*

Reserves Estimation Methodology

Volumetric Calculation

Reserves = Bulk Volume . ϕ. *So* . *Bo* . *Rf*

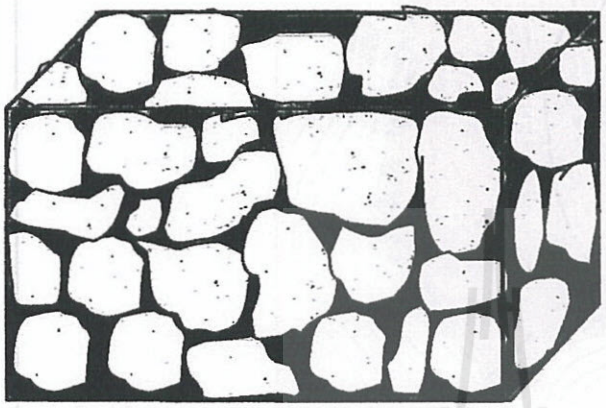

ϕ = **Porosity**

So* = *Saturation

Bo* = *Volume Factor

Rf* = *Recovery Factor

Volumetric Estimates

- Reserves = Reservoir Volume x Porosity x Oil Saturation x Recovery Factor x Shrinkage to Surface Conditions
- In oilfield units:

  Reserves = [7758 x A x h x ø x (1-S_w) x R]/Bo

  where Or 43560 for gas or Bg

  7757 = bbls/acre-ft

  A = area (sq. ft) or Acre

  h = net thickness (ft)

  ø = porosity (fraction)

  S_w = water saturation (fraction)

  R = recovery factor (fraction)

  Bo = formation volume factor

  Bg = Gas formatiom volume factor

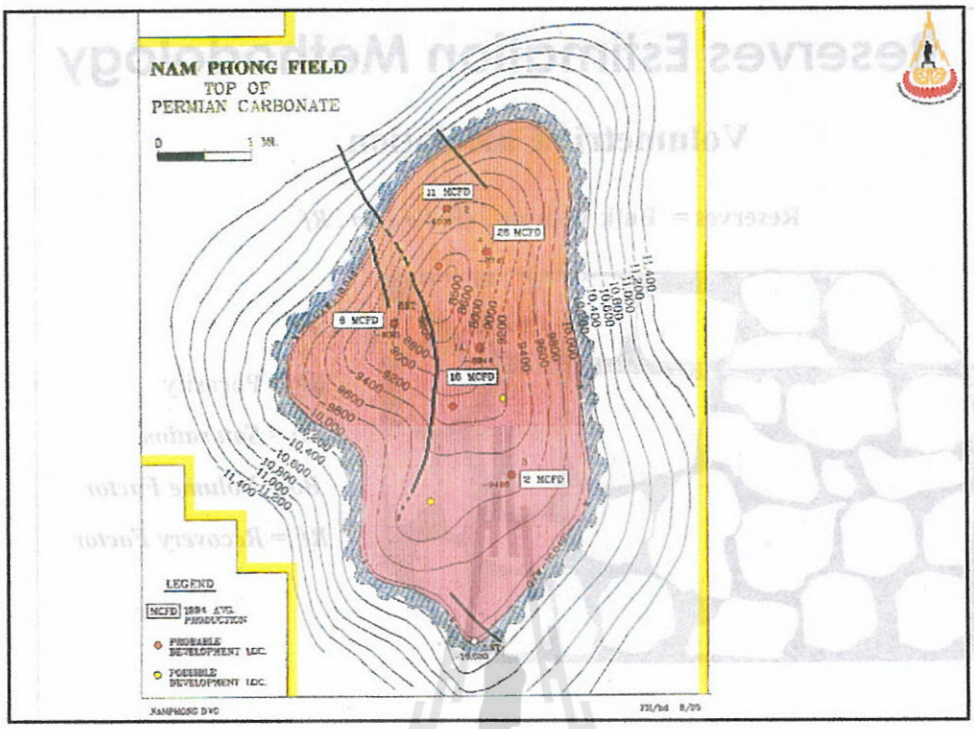

4.3 Basic Data for the Volumetric Calculation of Reserves

4.3.1 Equations Used

The following equations are used in the volumetric calculation of reserves:

For oil reservoirs:

$$N_{pa} = \iint_A \frac{h_n \phi (1 - S_w)}{B_o} E_{R,o}\, dx\, dy = \frac{A \bar{h}_n \bar{\phi} (1 - \bar{S}_w)}{\bar{B}_o} \bar{E}_{R,o}\,, \tag{4.1a}$$

For gas reservoirs:

$$G_{pa} = \iint_A \frac{h_n \phi (1 - S_w)}{B_g} E_{R,g}\, dx\, dy = \frac{A \bar{h}_n \bar{\phi} (1 - \bar{S}_w)}{\bar{B}_g} \bar{E}_{R,g}\,, \tag{4.1b}$$

where N_{pa} and G_{pa} are the oil or gas reserves (the estimated cumulative produced hydrocarbons at the time of abandonment of the reservoir, when the reserves are exhausted), measured at stock tank (i.e. standard) conditions of 288 K and 0.1013 MPa.

h_n, ϕ and S_w are, respectively, the *net* thickness of the hydrocarbon-bearing formation (pay), the effective porosity and the water saturation: all these parameters may vary spatially, and are therefore functions of the coordinates (x, y) within the area A of the reservoir.

B_o and B_g are the volume factors of the oil ($B_o \equiv B_{of}$, Sect. 2.3.2.1) and gas (Sect. 2.3.1.1) and E_R is the recovery factor. These too are a function of position. The bar over each term in the equations indicates the *average* value.

A is the area of the reservoir. It will correspond to the proven, probable or possible area depending on the category of reserves to be evaluated.

4.3.3 Net Pay Thickness

Within the reservoir interval, there are almost always intercalations of shale or other rock, which, owing to their low ϕ and k or high S_w, do not contain recoverable reserves.

We should therefore subtract the cumulative thickness of these non-productive strata from the gross thickness h_t of the reservoir to obtain the net pay thickness h_n.

The estimation of h_n, and the *net to gross ratio* h_n/h_t, is a critical stage in the evaluation, as it will have major implications for the volume of reserves.

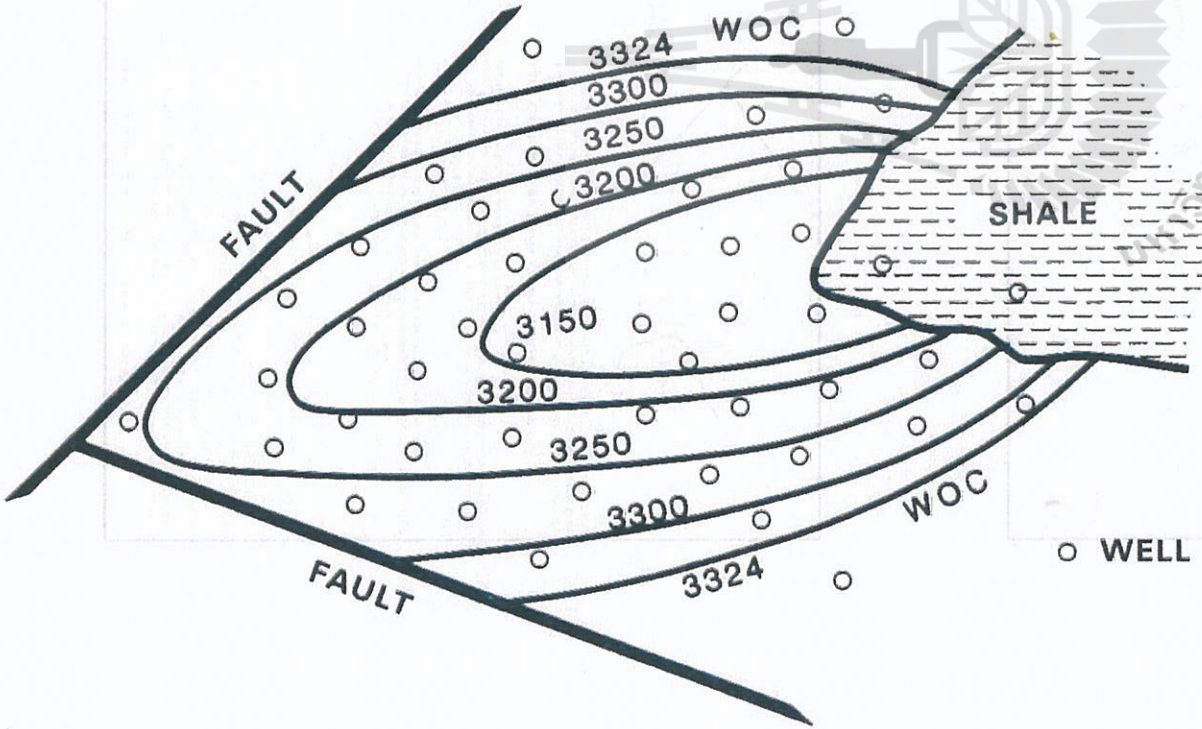

Fig. 4.1. *Isobath contour map of the top of a hydrocarbon-bearing pool*

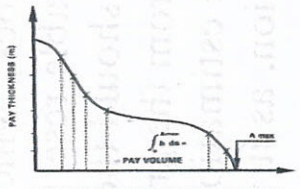

Fig. 4.4. Graphical method for the calculation of the net pay volume. From Ref. 4, reprinted with permission of Kluwer Academic Publishers and of Professors Archer and Wall

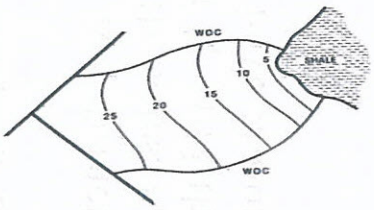

Fig. 4.5. Isoporosity map for a hydrocarbon-bearing pool

ϕ_a being the log-derived porosity over a small section, of thickness $h_{a,k}$, within the net pay, thickness h_a.

The values of ϕ_a are plotted well by well to produce the isoporosity map shown in Fig. 4.5.

The average porosity of the reservoir, $\bar{\phi}$, is then computed as the volume weighted mean of the well porosities ϕ_a:

$$\bar{\phi} = \frac{\iint_A \phi_a h_a \, dx \, dy}{V_R} \qquad (4.5)$$

This requires preparation of a contour map of constant $\phi_a h_a$ (iso-porosity thickness). The numerical integration over the field can then be performed in a similar way to the calculation of V_R described earlier.

4.3.5 Calculation of the Water Saturation, S_w, and Mean $\bar{S}_w$

As we have seen, in a given lithology the water saturation S_w is dependent on the height above the free water level. This fact must be taken into account in the large proportion of reservoirs which have water in contact with oil or gas.

Firstly, the average reservoir saturation curve $S_w = S_w(h)$ must be established versus height h. This can be obtained by interpolation of log (CPI)-derived values of S_w noted at various depths in each well; or, where cores are available, by the normalisation process (Leverett *J*-function) described in Sects. 3.4.4.5 and 3.4.4.7.

The average curve is then used to correct or eliminate any values present on the CPI of each well which may be anomalous with respect to their height above the free water level.

The next step is to calculate the average water saturation $S_{w,a}$ in each well taking the volume-weighted mean *across only those intervals classed as pay*:

$$S_{w,a} = \frac{\sum_{k=1}^{m} S_{w,k} \phi_k h_{a,k}}{\phi_a h_a} \qquad (4.6$$

These values of $S_{w,a}$ can now be plotted on the reservoir map and contours of constant S_w ("isosaturation") constructed (Fig. 4.6).

The average reservoir saturation $\bar{S}_w$ is computed as the mean of these saturations weighted by total pore volume, over the area of the reservoir:

$$\bar{S}_w = \frac{\iint_A S_{w,a} \phi_a h_a \, dx \, dy}{\bar{\phi} V_R} \qquad (4.7$$

This requires preparation of a contour map of constant "water thickness" $h_a \phi_a S_{w,a}$, before the integral can be evaluated. The numerical integration follows the same procedure as described in Sect. 4.3.3.

4.3.6 Calculation of the Volume Factors of Oil (B_o) and Gas (B_g)

The volume factor of oil, B_o, and especially gas, B_g, do not in general vary much within a reservoir. An experimental value is therefore usually adequate, failing which one of the correlations described in Sect. 2.3.2.2 (B_o) or 2.3.1 (B_g) can be used.

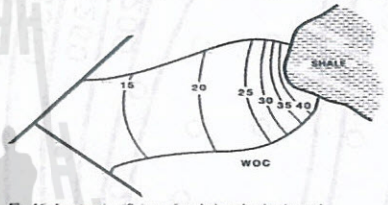

Fig. 4.6. Isosaturation (S_w) map for a hydrocarbon-bearing pool

$$RF = 0.114 + 0.272 \log k + 0.256 S_w - 0.136 \log \mu_o$$
$$- 1.538\phi - 0.00035 h \qquad (5.5$$

For $k = 1000$ md, $S_w = 0.25$, $\mu_o = 2.0$ cp, $\phi = 0.20$, and $h = 10$ ft,

$$RF = 0.114 + 0.272 \times \log 1000 + 0.256 \times 0.25 - 0.136 \times$$
$$\log 2 - 1.538 \times 0.20 - 0.00035 \times 10$$
$$0.642 \text{ or } 64.2\% \text{ (of initial stock tank oil)}$$

where,

RF = recovery factor

For Sandstone

For sandstone and carbonate reservoirs with solution gas drive:

$$\bar{E}_{R,o} = 0.41815 \left[\frac{\bar{\phi}(1 - \bar{S}_w)}{B_{ob}} \right]^{0.1611} \left(\frac{\bar{k}}{\mu_{ob}} \right)^{0.0979} (\bar{S}_w)^{0.3722} \left(\frac{p_b}{p_a} \right)^{0.1741} . \qquad (4.8a)$$

For sandstone reservoirs with water drive:

$$\bar{E}_{R,o} = 0.54898 \left[\frac{\bar{\phi}(1 - \bar{S}_w)}{B_{oi}} \right]^{0.0422} \left(\frac{\bar{k}\mu_{wi}}{\mu_{oi}} \right)^{0.0770} (\bar{S}_w)^{-0.1903} \left(\frac{p_i}{p_a} \right)^{-0.2159} . \qquad (4.8b)$$

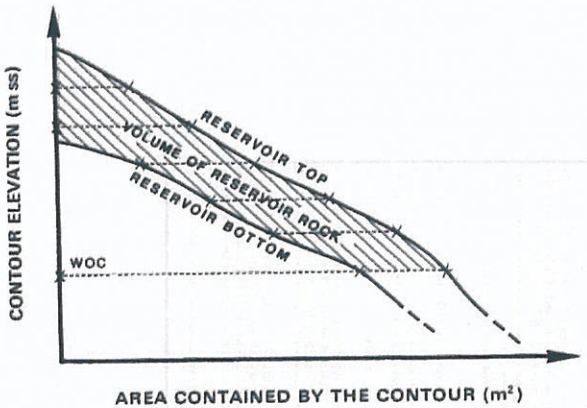

Fig. 4.2. *The hydrocarbon-bearing volume plotted against depth. From Ref. 4, reprinted with permission of Kluwer Academic Publishers and of Professors Archer and Wall*

If a cluster analysis is available (Sect. 3.6.3), it is a straightforward matter to distinguish pay and non-pay zones, and their distribution through the reservoir interval.

Otherwise, the non-pay footage will have to be identified from cores, using porosity (usually very low), and from log characteristics (for example, the SP, GR, ML, PL and MLL to pick out the shales).

A logical criterion for the definition of non-producing intervals would be to fix a lower limit to the permeability – the *permeability cut-off*, k_f. Wherever $k < k_f$, the rock would be non-pay. However, we have seen, logs cannot provide reliable quantitative estimates of permeability. Some form of correlation $k = f(\phi)$ is therefore needed (Sect. 3.5.1.8), so that from k_f a porosity cut-off ϕ_f can be defined.

Using the computed porosity curve from a Computer Processed Interpretation (CPI) of the well logs, the net pay thickness h_n can then be calculated immediately by summing the intervals where $\phi > \phi_f$.

This method, however, does discriminate against certain rocks which, although of very low k, contain movable hydrocarbons.

Although this type of interval does not produce freely under normal drawdown conditions because of its low permeability, it can contribute to the producible reserves through imbibition processes which occur in the reservoir at large, as described in Sect. 3.4.4.3

Use of a cut-off based on log data may therefore underestimate h_n.

The isopay map shown in Fig. 4.3 can now be drawn by plotting the values of h_n from each well onto a map of the reservoir. The net volume of hydrocarbon-bearing rock will be

$$V_R = \iint_A h_n \, dx \, dy \, . \tag{4.2}$$

Several methods are employed to perform this calculation.

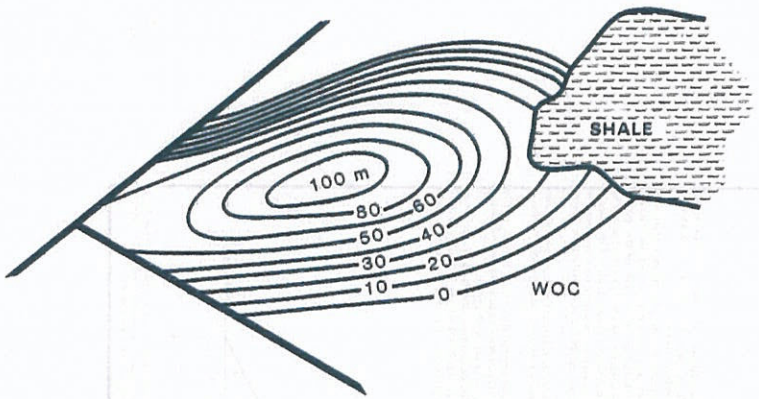

Fig. 4.3. *Isopay map for a hydrocarbon-bearing pool*

The most rigorous approach is a by-product of the initialisation phase of numerical simulators used in reservoir modelling. The hydrocarbon-bearing volume is subdivided into parallelepiped blocks using a fine grid in orthogonal coordinates (x, y). The volume of each block (base area $\times \bar{h}_n$) is calculated, then summed over all blocks.

A second procedure is to planimeter the area contained within each isopay contour, and to plot each area against the corresponding pay thickness (Fig. 4.4). The total net pay volume V_R is then obtained by integrating the resulting curve.

Yet another approach involves dividing the isopay map into a number of overlying trapezoids. The volume of the trapezoid between the isopay contours $h_{n,i}$ and $h_{n,i+1}$ is

$$V_{i,i+1} = \frac{A_{i+1} + A_i}{2} (h_{n,i+1} - h_{n,i}) \, , \tag{4.3a}$$

i.e. the average area multiplied by the incremental thickness.

The topmost trapezoid represents a special case and is treated as a pyramid:

$$V_{top} = A_{min} \frac{h_{max} - h_{i,max}}{3} \, , \tag{4.3b}$$

A_{min}, its base area, being of course the smallest isopay area on the map.

4.3.4 Porosity ϕ, and Average Porosity $\bar{\phi}$

Using the (CPI) log interpretations calibrated against cores, the values of ϕ are read off *across the intervals which constitute net pay* in each well in the field. The average porosity, ϕ_w, in each well is calculated as the thickness-weighted mean of the log porosities:

$$\phi_w = \frac{\sum_{k=1}^{m} \phi_k h_{n,k}}{h_n} \, . \tag{4.4}$$

4.4.1 Deterministic Method

4.4.1.1 *Method of Mean Values*

The mean values $\bar{h}_n$, $\bar{\phi}$, $\bar{S}_w$, $\bar{B}_o$ (or $\bar{B}_g$), and $\bar{E}_{R,A}$ (or $\bar{E}_{R,g}$) are calculated for each area A by the methods described in Sects. 4.3.2–4.3.7. The following two equations then give the volume of reserves – proven, probable or possible – for oil and gas respectively:

$$N_{pa} = \frac{Ah_n\bar{\phi}(1-\bar{S}_w)}{\bar{B}_o}\bar{E}_{R,o}. \tag{4.10a}$$

$$G_{pa} = \frac{Ah_n\bar{\phi}(1-\bar{S}_w)}{\bar{B}_g}\bar{E}_{R,g}. \tag{4.10b}$$

4.4.1.2 *Equivalent Hydrocarbon Column*

Starting from the values of h_n, ϕ_e and $S_{w,e}$ determined in each well (Sects. 4.3.3–4.3.5), we calculate the hypothetical thickness of the column of hydrocarbon that would result from removing the rock matrix and pore water (the local equivalent hydrocarbon column, or EHC):

$$\text{EHC} = h_n\phi_e(1-S_{w,e}). \tag{4.11}$$

The EHC of each well is plotted on the reservoir map, and the iso-EHC contours are constructed (Fig. 4.9).

The total volume of hydrocarbons V_R *at reservoir p and T* is calculated from

$$V_R = \iint_A \text{EHC}\,dx\,dy. \tag{4.12}$$

This integration must be performed separately for the proven, probable and possible reserves areas, following the procedure outlined in Sect. 4.3.3 for V_R.

We then have:

$$N_{ps} = \frac{V_R}{\bar{B}_o}\bar{E}_{R,o}, \tag{4.13a}$$

$$G_{ps} = \frac{V_R}{\bar{B}_g}\bar{E}_{R,g}. \tag{4.13b}$$

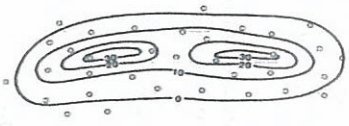

Fig. 4.9. *Iso-EHC contour map*

Being the quicker of the two methods, the EHC is a preferable approach from a practical point of view.

4.4.2 Probabilistic, or Monte Carlo, Method

The probabilistic, or Monte Carlo,[4,9,9] method replaces the need for the rigid definitions of "proven", "probable" and "possible", described in Sect. 4.2, with the concept of the *probability* of reserves having a certain value.

The distribution curve shown in Fig. 4.10 expresses the probability that the reserves will have a volume equal to or greater than any chosen value on the x-axis.

This curve itself is based on the probability distribution of each of the parameters appearing in Eq. (4.10). The likely range of values that each parameter could assume must be decided, and a probability assigned to the values within this range. The *probability density* curve, f, in Fig. 4.11 has been normalised so that there is unit area beneath it. F, the integral of f, is the actual probability distribution of the parameter in question.

Note that it is possible for certain parameters to be related: for example, within a given reservoir unit it is quite common to find an inverse correlation between S_{wi} and ϕ.

When this is the case, we need only consider the probability curve for *one* of the interrelated parameters (ϕ in this example); the dependent variable is represented by the appropriate correlating equation (e.g. $S_{wi} = a/\phi$) or diagram.

In applying the Monte Carlo technique, a table of random numbers is drawn up for each *independent* parameter in Eq. (4.10). In each table, the maximum and minimum values of the numbers, and their probability distribution, correspond

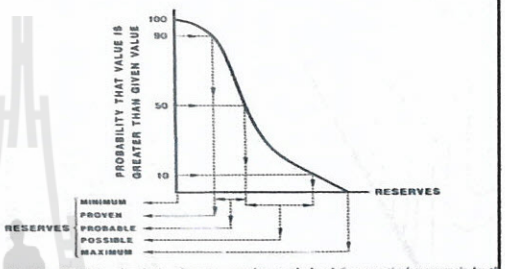

Fig. 4.10. *Probability distribution for reserves volume, calculated for a particular reservoir by the Monte Carlo method. Classifications according to probability are also shown. From Ref. 4, reprinted with permission of Kluwer Academic Publishers and of Professors Archer and Wall*

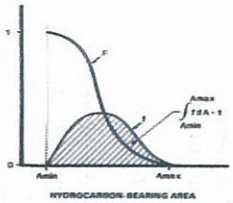

Fig. 4.11. *An example of the probability distribution for reservoir area, as input to the Monte Carlo reserves calculation*

with those assumed for the parameter itself. Random number generation can be handled rapidly by readily available computer programs.

A number is then extracted at random from each table, the corresponding values for any dependent (correlated) variables are calculated, and N_{ps} (or G_{ps}) are computed for that case.

This is repeated many times (at least 5000), each case being calculated for a randomly selected set of values from the tables.

At the conclusion of the analysis, we have a large number of reserves estimates, each corresponding to a random combination of parameter values. The results are arranged in ascending order and the probability density determined. The probability distribution for the reserves can then be computed from this, as in Fig. 4.10.

The reserves categories are conventionally defined as follows:

proven reserves: reserves volume corresponding to 90% probability on the distribution curve,

probable reserves: reserves volume corresponding to the difference between 50 and 90% probability on the distribution curve,

possible reserves: reserves volume corresponding to the difference between 10 and 50% probability on the distribution curve.

The probabilistic method has the advantage of reducing the degree of subjectivity in the criteria employed in evaluating the reservoir area. However, the assessment of the probability densities specified for each of the input parameters remains a highly subjective process.

4.5 Classification of Fields in Terms of Hydrocarbon Volume

Two sets of standards are in current use for the classification of fields according to the volume of reserves they contain. The first, proposed by the API, is applied to fields of small to medium size. The second, which has been in common use for many years although it has never been recognised officially by any regulatory body, applies to "giant" fields.

The different field types are summarised below:

API Classification[2]

Major field: oilfield with reserves in excess of 16×10^6 sm³ (100 Mbbl, or 14 Mt); gas field with reserves in excess of 17×10^9 sm³ (600 Gcuft).

Class A field: oilfield with reserves between 8 and 16×10^6 sm³ (50–100 Mbbl, or 7–14 Mt);
gas field with reserves between 8.5 and 17×10^9 sm³ (300–600 Gcuft).

Class B field: oilfield with reserves between 4 and 8×10^6 sm³ (25–50 Mbbl, or 3.5–7 Mt);
gas field with reserves between 4.2 and 8.5×10^9 sm³ (150–300 Gcuft).

Class C field: oilfield with reserves between 1.6 and 4×10^6 sm³ (10–25 Mbbl, or 1.4–3.5 Mt);
gas field with reserves between 1.7 and 4.2×10^9 sm³ (60–150 Gcuft).

Class D field: oilfield with reserves between 0.16 and 1.6×10^6 sm³ (1–10 Mbbl, or 0.14–1.4 Mt);
gas field with reserves between 0.17 and 1.7×10^9 sm³ (6–60 Gcuft).

Class E field: oilfield with reserves less than 0.16×10^6 sm³ (1 Mbbl, or 0.14 Mt);
gas field with reserves less than 0.17×10^9 sm³ (6 Gcuft).

Class F field: any field abandoned during the year of its discovery, even if it had been completed for production.

Fields in category D and above are referred to as "significant".

Classification[6] *of "Giant Fields"*

Super-giant field: oilfield with reserves in excess of 800×10^6 sm³ (5 Gbbl, or 700 Mt);
gas field with reserves in excess of 850×10^9 sm³ (30 000 Gcuft).

Giant field: oilfield with reserves between 80 and 800×10^6 sm³ (0.5–5 Gbbl, or 70–700 Mt);
gas field with reserves between 85 and 850×10^9 sm³ (3000–30 000 Gcuft).

Potentially giant field: an oilfield which could be made into a giant field by means of further development or improved recovery. Potential giants can be either "probable giants" or "possible giants", depending on the degree of uncertainty associated with the assessment of their potential.

"Combination" giant oilfield: a field containing at least 40×10^6 sm³ (250 Mbbl, or 35 Mt) of oil reserves, plus at least 80×10^6 sm³ (500 Mbbl, or 70 Mt) of hydrocarbon recoverable as condensate, or its calculated liquid equivalent. This would be an oil reservoir with an overlying gas cap.

Figure 4.12 provides a qualitative idea of the worldwide occurrence of oilfields of different sizes.

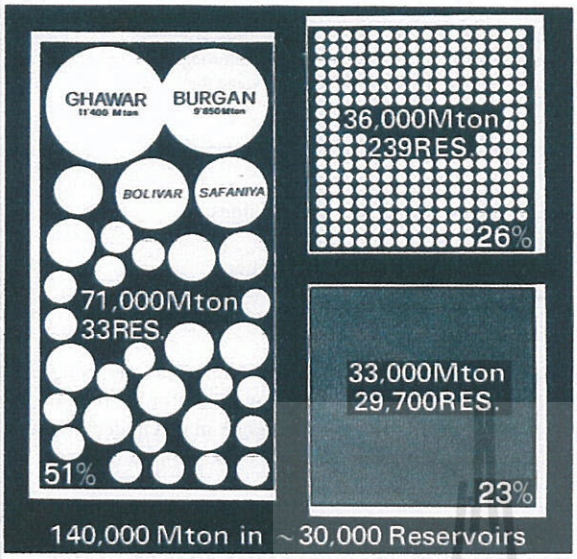

Fig. 4.12. *Distribution of the world's approximately 30 000 known oilfields in terms of the size of their reserves. More than half the world's reserves are contained in only 33 oilfields (0.1% of the 30 000 total); a further 26% of the reserves are found in roughly 0.8% of the total. Overall, 0.91% of the world's oilfields hold 76.4% of the total oil reserves*

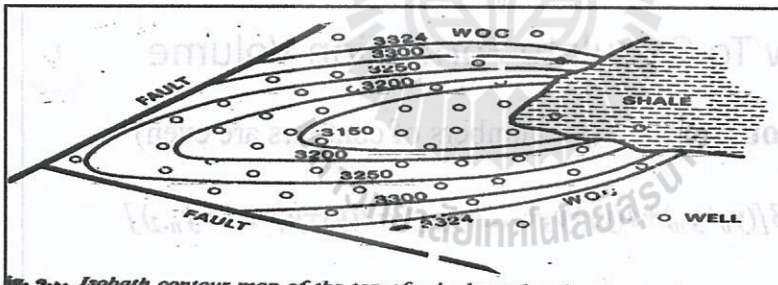

Fig. 4... Isobath contour map of the top of a hydrocarbon-bearing pool

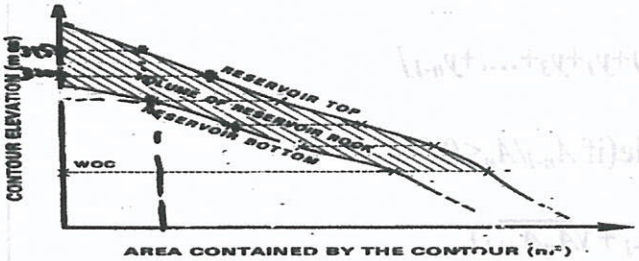

Fig. 4.2. *The hydrocarbon-bearing volume plotted against depth. From Ref. 4, reprinted with permission of Kluwer Academic Publishers and of Professors Archer and Wall*

Vertical Slice Method

VERTICAL SLICE

The vertical slice method sums the volumes of *vertical* slices through the depicted reservoir volume (Fig. 14-41). The method is sometimes referred to as the donut method because the individual areas used to determine the reservoir volume fall between successive contour lines and commonly appear to be donut-shaped. Many people consider this method to be less confusing than the horizontal slice method, particularly if isochore maps have a number of thick and thin areas. The equation for the vertical slice method is

$$\text{Volume} = h(A_0 - A_1) + h(A_1 - A_2) + \ldots h(A_{n-1} - A_n) + h_{avg}(A_n) \qquad (14\text{-}3)$$

where

h = Average thickness between successive contour lines
A_0 = Zero contour line
A_1 = Next higher value, or next successive, contour line
A_n = Highest value contour line
h_{avg} = Average thickness within A_n

Figure 14-41 and Table 14-2 illustrate the procedure for volume determinations using the vertical slice method. The reservoir used for this example is the same one used for the horizontal slice method (Fig. 14-40), so the results can be compared. The difference in calculated volume between the horizontal and vertical slice methods, for the example in Figs. 14-40 and 14-41, is less than 1 percent.

How To Calculate Formation Volume

Simpson's rule(if the numbers of contours are even)

$$V_B = h/3[(y_0+y_n)+4(y_1+y_3+\ldots+y_{n-1}) +2(y_2+y_4+\ldots+y_{n-2})]$$

Trapezoidal rule(with some what less accuracy)

$$V_B = h[1/2(y_0+y_n)+y_1+y_3+\ldots+y_{n-1}]$$

Pyramidal rule(if $A_{n-1}/A_n<0.5$)

$$V_B = h/3(A_n+A_{n+1}+\sqrt{A_nA_{n+1}})$$

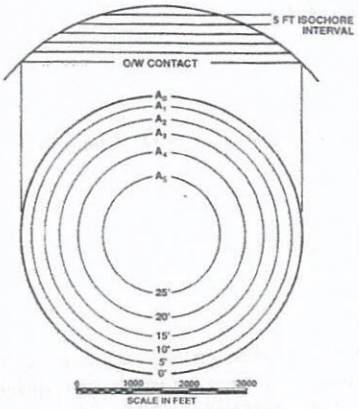

Figure 14-40 Cross section and net pay isochore map of an idealized reservoir. The cross section shows the depicted solid divided into 5-ft-thick horizontal slices. (Craft and Hawkins 1959. Reprinted by permission of Prentice-Hall, Inc.)

Table 14-1

Area	Planimeter Area Sq. In.	Area Acres	Ratio of Areas	Interval H Feet	Equation	ΔV Ac. Ft.
A_0	19.64	450	–	–	–	–
A_1	16.34	375	0.83	5	Trapezoid	2063
A_2	13.19	303	0.80	5	Trapezoid	1695
A_3	10.05	231	0.76	5	Trapezoid	1335
A_4	6.69	154	0.67	5	Trapezoid	963
A_5	3.22	74	0.48	5	Pyramid	558
A_6	0.00	0	0.00	4	Pyramid	99
					Total ac. ft.	**6713***

*The percentage difference in acre-feet between the horizontal and vertical slice methods is less than 1%.

Horizontal Slice Method

One way to determine volume of a reservoir is to *horizontally* slice the depicted reservoir solid, and sum the volumes of the layers to calculate total volume of the reservoir. For the horizontal slice method, two equations are generally used to determine the volume from a net pay isochore map that has been planimetered (Craft and Hawkins 1959). The first determines the volume of the frustum of a pyramid.

$$\text{Volume} = \frac{1}{3}h(A_n + A_{n+1} + \sqrt{A_n A_{n+1}}) \tag{14-1}$$

where

h = Interval thickness between isochore lines
A_n = Area enclosed by lower value isochore line
A_{n+1} = Area enclosed by higher value isochore line

This equation is used to determine the volume of a layer between successive slices, which are based on vertical thickness and represented on the map by net pay contour lines (Fig. 14-40). The total volume of the reservoir is the sum of these separate volumes.

The second equation used in the horizontal slice method determines the volume of a trapezoid.

$$\text{Volume} = \frac{1}{2}h(A_n + A_{n+1})$$

$$\text{Volume} = \frac{1}{2}h(A_n + A_{n+1})$$

or, for a series of successive trapezoids,

$$\textbf{Volume} = \frac{1}{2}h(A_0 + 2A_1 + 2A_2 \ldots 2A_{n-1} + A_n) + t_{avg}A_n \qquad (14\text{-}2)$$

where

A_0 = Area enclosed by the zero isochore line

$A_1, A_2 \ldots A_n$ = Areas enclosed by successive contour lines

t_{avg} = Average thickness within the maximum thickness contour line

The pyramidal equation usually provides the most accurate results; however, because of its simplicity, the trapezoidal equation is commonly used. Since the trapezoidal equation introduces an error of about 2 percent where the ratio of successive areas is 0.5, a common convention is used to employ both equations. Wherever the ratio of the areas within any two successive isochore lines is smaller than 0.5, the pyramidal equation is applied. Wherever the ratio of the areas within any two successive isochore lines is larger than 0.5, the trapezoidal equation is used. Computer programs, for calculating reservoir volumes from net pay maps, are capable of combining the pyramidal and trapezoidal equations in the manner described. However, the programs may vary in the cutoff ratio that is used, so that ratio for a given program should be determined by the user.

Figure 14-40 and Table 14-1 outline the volume determination using the horizontal slice method. Take a few minutes and review this example to obtain a good understanding of the procedure.

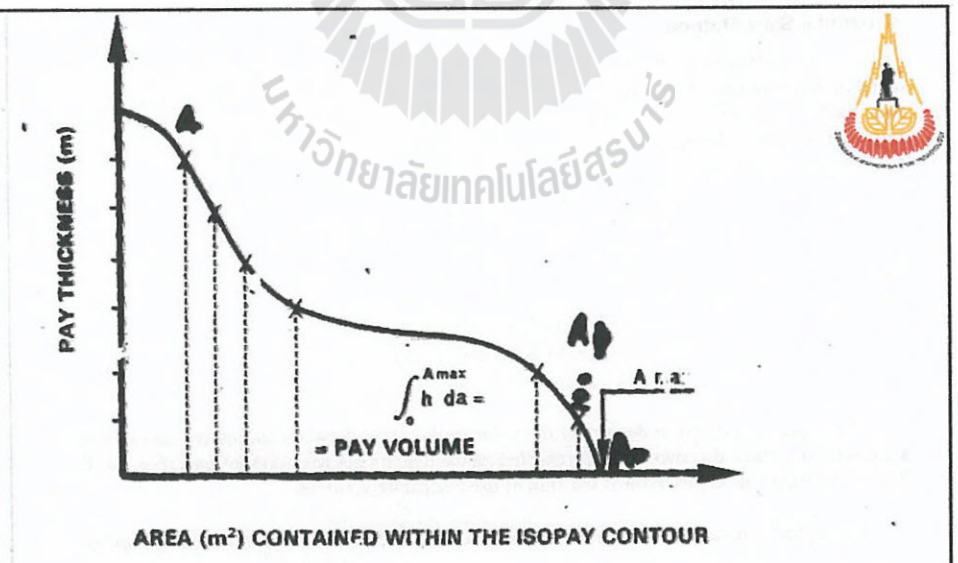

Fig. 4.4. *Graphical method for the calculation of the net pay volume. From Ref permission of Kluwer Academic Publishers and of Professors Archer and Wall*

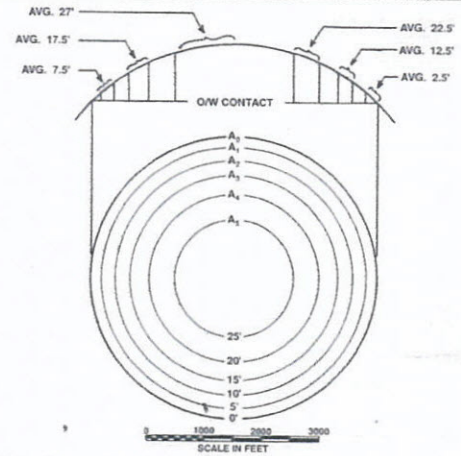

Figure 14-41 Cross section and net pay isochore of an idealized reservoir. The cross section shows the reservoir divided into vertical slices. (Craft and Hawkins 1959. Reprinted by permission of Prentice-Hall, Inc.)

Table 14-2

Area	Planimeter Area Sq. In.	Area Acres	Difference in Areas $A_{n-1} - A_n$	Average Thickness Feet	V Ac. Ft.
A_0	19.64	450	–	–	–
A_1	16.34	375	75	2.5	187
A_2	13.19	303	72	7.5	540
A_3	10.05	231	72	12.5	900
A_4	6.69	154	77	17.5	1347
A_5	3.22	74	80	22.5	1800
A_6	0.00	0	74	27.0	1998
				Total ac. ft.	6772*

*The percentage difference in acre-feet between the horizontal and vertical slice methods is less than 1%.

Example 10.2 [Katz et al., I-1]. Compute the gas reserve for sand No. 44 at Deep Lake, Louisiana. The isopachous map is given in Fig. 10-14, and reservoir conditions are given in Table 10.1.

Solution. Find the acre-feet of sand by planimetering area between contours and multiplying by average thickness between contours.

Contour interval	Area, acres	Average thickness, ft	Volume, acre · ft
0–5	153.37	2.5	383.4
5–10	142.75	7.5	1,070.6
10–15	136.78	12.5	1,709.8
15–20	128.38	17.5	2,246.7
20–25	183.55	22.5	4,129.6
25–30	506.10	27.5	13,917.6
30–30	23.77	30.0	713.1
30–35	560.79	32.5	18,518.2
35–40	281.41	37.5	10,552.9
40–44	132.69	42.0	5,573.0
44–44	27.77	44.0	1,045.9
Total	2286.36		59,861

Gas reserve:

$$Q_{sc} = 43,560 A h \phi (1 - S_w) \frac{P T_{sc}}{P_{sc} T Z}$$

$$= 43,560(59,861)(0.28)(1 - 0.25) \frac{(5164)(520)}{(14.73)(657)} \frac{1}{(0.987)} = 153$$

$$= 153.9 \text{ Bcf}$$

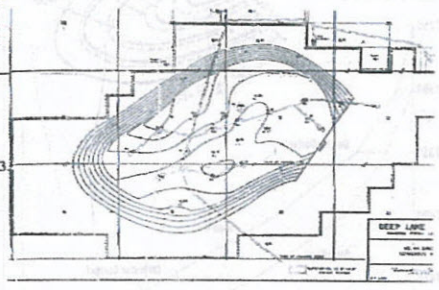

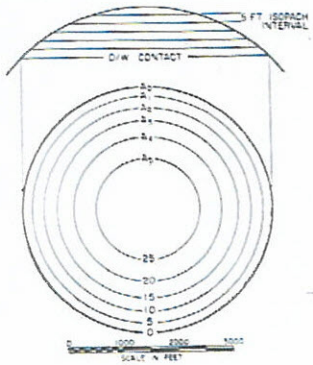

Fig. 3.1. Cross section and isopachous map of an idealized reservoir.

SOLUTION:

Productive Area	Planimeter Area* sq in.	Area Acres*	Ratio of Areas	Interval ft, feet	Equation	ΔV ac-ft
A_0	19.64	450				
A_1	16.34	375	0.83	5	Trap.	2063
A_2	13.19	303	0.80	5	Trap.	1695
A_3	10.05	231	0.76	5	Trap.	1335
A_4	6.69	154	0.67	5	Trap.	963†
A_5	3.22	74	0.48	5	Pyr.	558‡
A_6	0.00	0	0.00	4	Pyr.	99§
						6713 ac-ft

* For a map scale of 1 in. = 1000 ft; 1 sq in. = 22.96 acres.

† $\Delta V = \frac{5}{2}(231 + 154) = 963$ ac-ft

‡ $\Delta V = \frac{5}{3}(154 + 74 + \sqrt{154 \times 74}) = 558$ ac-ft

§ $\Delta V = \frac{4}{3}(74) = 99$ ac-ft

How To Calculate Formation Volume (Cond.)

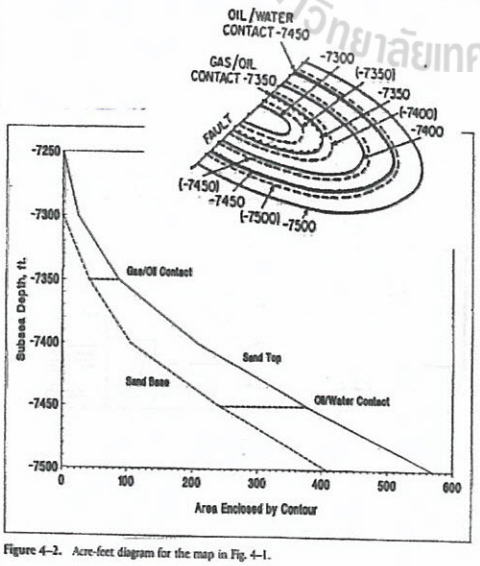

Figure 4–2. Acre-feet diagram for the map in Fig. 4–1.

rc son's rule:

$$V_R = \frac{50}{3}[0 + (378 - 242) + 4(24 - 0 + 209 - 106) + 2(88 - 42)]$$

$$= \frac{50}{3}[(136) + 4(24 + 103) + (2 \times 46)]$$

$$= 12{,}267 \text{ ac-ft}$$

r: zoidal rule:

$$V_R = 50[1/2(0 + 136) + (24 + 46 + 103)]$$

$$= 12{,}050 \text{ ac-ft}$$

nidal rule:

$$V_R = \frac{50}{3}[(0 + 136) + 2(24 + 46 + 103) + \sqrt{24 \times 88} + \sqrt{88 \times 209} + \sqrt{209 \times 378} - \sqrt{42 \times 106} - \sqrt{106 \times 242}]$$

$$= 11{,}963 \text{ ac-ft}$$

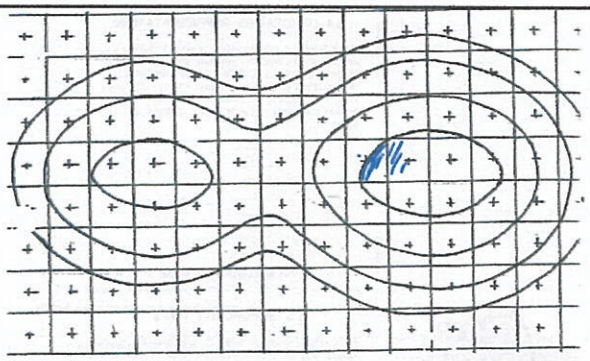

Figure 5. Example grid for hand integration of contour maps.

The equations to be used are: $7758 \times A \times h \; \phi(1-$ B_o

$$\text{Oil, Bbls} = 7758 \sum_{j=1}^{n} \frac{(A_j)(h_{nj})(N/G_j)(\phi_j)(1-S_{wj})}{B_{oj}} \quad (8$$

$$\text{Gas, MCF} = 43.56 \sum_{j=1}^{n} \frac{(A_j)(h_{nj})(N/G_j)(\phi_j)(1-S_{wj})}{B_{gj}} \quad (9$$

43560 B_g

where
- j = subscript indicating value from the jth element,
- A = area, acres,
- h_n = gross pay thickness, feet,
- N/G = net-to-gross ratio, fraction,
- ϕ = porosity, fraction,
- S_w = average water saturation, fraction,
- B_o = oil formation volume factor, res. barrels / STB, and
- B_g = gas formation volume factor, res. cubic feet / SCF.

Equations (8) and (9) are better approximations than are equations (1)

(2) to the actual volume of hydrocarbons in place. The reasons come from th

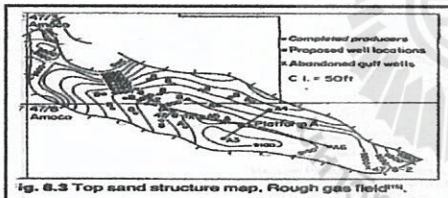

ig. 8.3 Top sand structure map, Rough gas field[14].

tructure contour maps are used to connect points qual elevation. It is customary to map structure he top and base of porosity and the map indicates external geometry of the reservoir. The map wn in Fig. 8.1 shows the boundaries as a fluid porosity limit to reservoir quality rock and t boundaries. The contour intervals are regular represent subsea depths. The map would be lled *top sand*, *base sand* or refer to a geological boundary. The difference in elevation between hydrocarbon–water contact and the top of the ucture is known as the closure or height of the rocarbon column. Structure maps of the top ds of Thistle oil reservoir[15] and the Rough gas d[14] are shown in Figs 8.2 and 8.3. A schematic ss-section of the Rough field is illustrated in Fig. 1].

he area contained within each structural contour be measured by various mathematical techni-

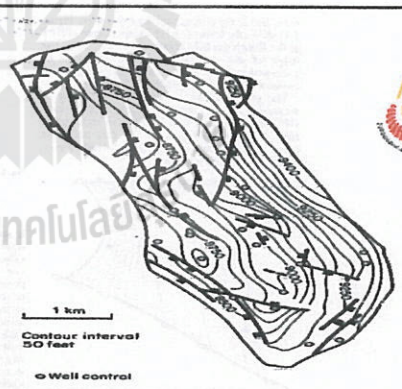

Fig. 8.2 Top sand structure map, Thistle oil reservoir. (after [15])

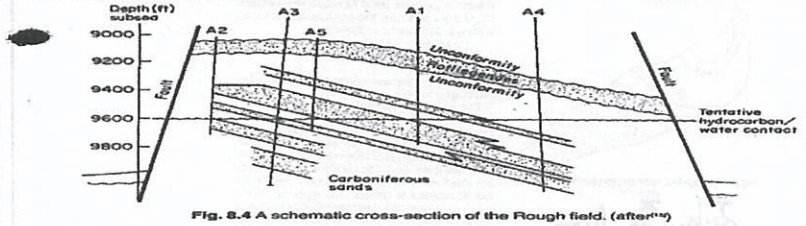

Fig. 8.4 A schematic cross-section of the Rough field. (after[14])

8.4 LITHOFACIES REPRESENTATION

Rock lithology can provide a guide in contouring, and lithofacies maps are generally presented as ratio maps, typically sand:shale or limestone:anhydrite (Fig. 8.10). The ratios follow geometric progressions (1:1, 1:2, 1:4, 1:8 etc.) and equal contour spacings do not therefore represent equal changes in lithology.

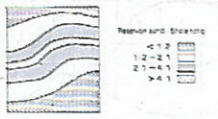

Fig. 8.10 Lithofacies mapping.

8.5 ISOPOROSITY MAPS

In a given reservoir zone or subzone, the areal variation in mean porosity may be represented. The porosity control values are thickness weighted average porosities for the zone at each well.

The shape of the isoporosity map shown in Fig. 8.11 may be obtained by application of geological modelling, by statistical techniques such as Kriging mapping [8.10] or by computer controlled contour mapping. An example of an isoporosity map of the Rough gas field is shown in Fig. 8.12.

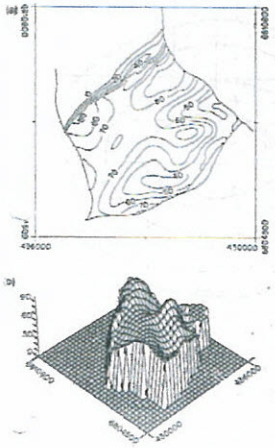

Fig. 8.8 Isopach map (a) and mesh perspective diagram (b) of Brent Sands, Murchison reservoir.

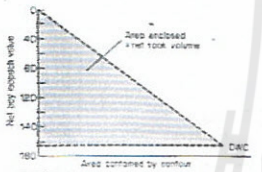

Fig. 8.9 Hydrocarbon volume from net pay isopach.

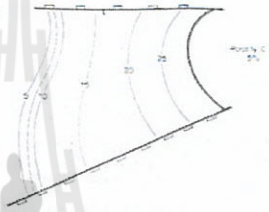

Fig. 8.11 Isoporosity map.

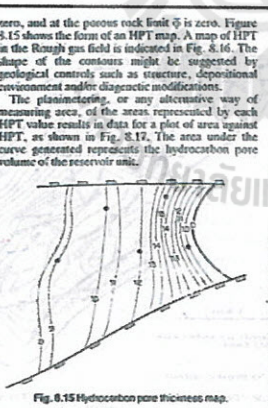

Fig. 8.16 Rough field hydrocarbon pore thickness map (after [8.9]).

$\phi \cdot h_N \cdot \bar{S}_h$ Map
(HPT)

zero, and at the porous rock limit $\bar{\phi}$ is zero. Figure 8.15 shows the form of an HPT map. A map of HPT in the Rough gas field is indicated in Fig. 8.16. The shape of the contours might be suggested by geological controls such as structure, depositional environment and/or diagenetic modifications.

The *planimetering*, or any alternative way of measuring area, of the areas represented by each HPT value results in data for a plot of area against HPT, as shown in Fig. 8.17. The area under the curve generated represents the hydrocarbon pore volume of the reservoir unit.

Fig. 8.15 Hydrocarbon pore thickness map.

Fig. 8.17 Hydrocarbon pore volume from HPT maps (area under curve = net hydrocarbon pore volume).

8.8 PROBABILISTIC ESTIMATION

It should be apparent that there are a number of ways to map any given set of data. A numerical value of hydrocarbon pore volume thus represents one outcome of a given map architecture. The presentation of hydrocarbon in place as a probabilistic estimate rather than as a deterministic value seeks to show the uncertainty of the estimate. The association of ranges and distribution shape with each of the components $A_r(\phi S_h)$, h, N/G of the volumetric equation is a subjective technical exercise. One method, which has found widespread use in arriving at a probabilistic estimate, is the Monte Carlo approach [8.11]. Since standard condition (V_w) volumes are usually needed, the reservoir volume of hydrocarbon in place is converted to a standard volume by use of an initial formation volume factor (B_{hi}) for the particular hydrocarbon, and its uncertainty is included in the estimation:

$$V_w = \frac{HCPV}{B_{hi}}$$

where *HCPV* represents reservoir condition hydrocarbon pore volume.

The shape of distributions and maximum and minimum values are generally agreed in specialist group committees, and rectangular and triangular distributions (Fig. 8.18 (a) and (b)) based on subjective assessment of reservoir characteristics are most frequently used. The distribution can easily be converted into a cumulative frequency curve which can be sampled at random. The repeated random selection of values and their probabilities from each independent variable set leads to the calculation of a large number of volumetric estimates (Fig. 8.19). The cumulative frequency of these estimates is used to show the likelihood that a given value will be at least as great as that shown, as indicated in Fig. 8.18 (c). The independent variables considered in

ORIGINAL-GAS-IN-PLACE ESTIMATE

NAM PHONG TECHNICAL REVIEW
NOVEMBER 1994

VOLUMETRIC ESTIMATE

STANDARD CALCULATION:

RESERVOIR ROCK VOLUME	4.79 M acre-feet
AVERAGE NET/GROSS	41%
AVERAGE POROSITY	3.1%
AVERAGE WATER SATURATION	25%
RESERVOIR GAS VOLUME FACTOR	304 SCF/ft³
CALCULATED OGIP =	610 GCF
ORIGINAL RESERVOIR MODEL CALCULATION: OGIP =	602 GCF

MATERIAL BALANCE ADJUSTMENT

RESERVOIR MODEL ADJUSTMENT FOR HISTORY MATCH: OGIP = 639 GCF

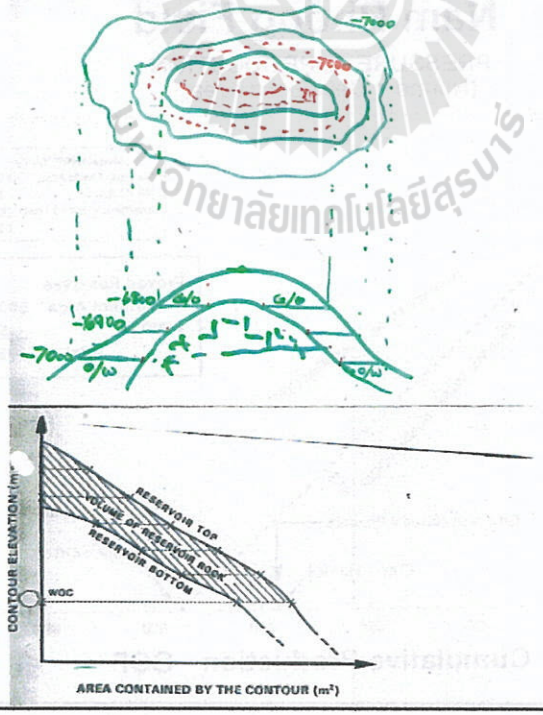

2. Better Way

This method assumes that there have been enough wells drilled to be able to repare each of the following types of maps for this reservoir:

(a) structure top map,

(b) gross isopach map,

(c) net-to-gross ratio map,

(d) iso-porosity map,

(e) iso-water saturation map,

(f) water-oil contact map (if WOC is not constant), and

(g) gas-oil contact map (if the GOC is not constant).

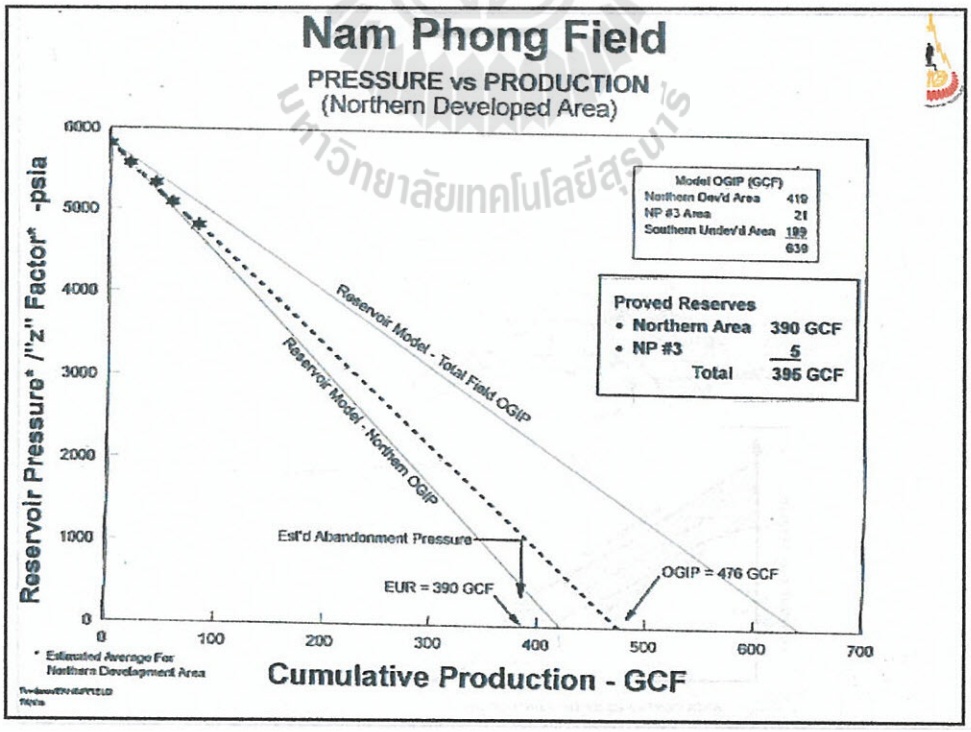

Reservoir Engineering I
HW NO 1; Due date: Friday, June 11, 2010.

A.CHAPTER 1; 1.3, 1.5, 1.6, 1.10, 1.21 and 1.27

B.C.CRAFT and M.F. HAWKINS; "***Applied Petroleum Reservoir Engineering'***, 1991.

HW NO.1 Chapter 1
Due Date: Friday 15 June 2012

ANSWERS to the problems

1; 1.3 Molecular weight = 30, specific gravity= 1.034
2; 1.5. $3.14, and $15.4 (Hint; 16 oz = 1 lb)
3; 1.6 (a) 3.9 min, (b) 64,147 lb, (c) explain(Hint; 16 oz = 1 lb)
4; 1.10. P(psia) = 300, 750, 1500, 2500, 4000, 5000, 6000
Z = 0.96 0.914 0.86 0.84 0.91 0.99 1.08
B_g(cu.ft/SCF)= 0.05613, 0.0214, 0.0098, 0.0059, 0.004, 0.0035,0.0032
5; 1.21 ANS= $B_L(B_O)$=1.515 bbl/STB
6; 1.27; (a) dw=4.77 cc (b)dw 4.67cc (c) dw=16.3 cc (d) μ_w= 0.36072 cp

AND HANDOUT

7; The Satun Gas consists of mole % as follows

	Mole %	MW	P_C (psia)	T_C (°R)	NHV (BTU/SCF)
Methane(CH_4)	69.0	16	668	343	909
Ethane C_2H_6	10.0	30	778	550	1618
Propane C_3H_8	6.0	44	616	666	2316
Iso-Butane iC_4	1.3	58	529	735	3001
n-Butane nC_4	1.1	58	550	766	3010
n-Pentane nC_5	0.4	72	490	846	3708
n-Hexane nC_6	0.2	86	440	914	4404
Carbon dioxide	12.0	44	1071	548	0

Determine; γ_g, ρ_g ,μ_g@ 3000 psia, 340° F, and NHV

8. Use of correlations to estimate values for oil properties; R_{so}, C_o, B_o, and μ_o at pressure of 2100 and 3800 psia: Given
T = 200° F , Pb = 2500 psia, γ_g = 0.8, ρ_o = 40 °API, γ_o = 0.83

Reservoir Engineering I
HW NO 2; Due date: June 22, 2012.
1.Determine the gas in place in the given net gas isochore map;

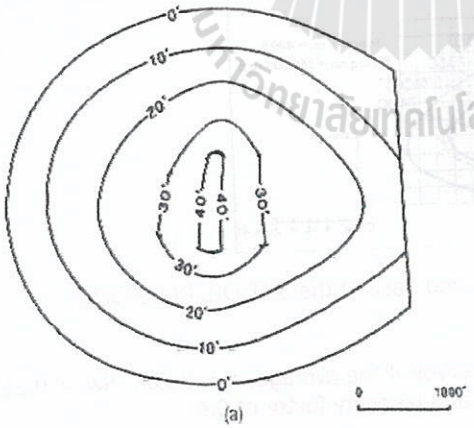

(a)

Figure 14-13 (a) Net gas isochore map based on equally and proportionally spaced contours. (b) Net gas isochore map with the contour spacing based on walking Wells No. 2 and 3 through the wedge. Compare this map to that shown in Fig. 14-13a. (From Tearpock and Harris 1987. Published by permission of Tenneco Oil Company.)

$\phi = 0.20$, $S_{wi} = 0.25$, $B_{gi} =$ 300 SCF/ res cu.ft

1. Determine the gas in place in the given net gas isochore map;

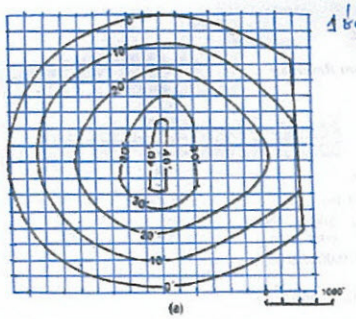

1 block = 250 × 250
= 62500 ft²

Figure 14-19 (a) Net gas isochore map based on equally and proportionally spaced contours. (b) Net gas isochore map with the contour spacing based on walking wells No. 2 and 3 through the wedge. Compare this map to that shown in Fig. 14-19a. (From Tearpock and Harris 1987. Published by permission of Tenneco Oil Company.)

$\phi = 0.20$, $S_{wi} = 0.25$, $B_{gi} =$ 300 SCF/ res cu.ft

ค่า Isochore (Thickness)	จำนวน NO. block	Area (ft^2)
40	4.5	281,250
30	4.5+18.5=23	1,437,500
20	23+59=82	5,125,000
10	82+72=154	9,625,000
0	154+81=235	14,687,500

2. 2.1 Find the rock volume of the SUT OIL RESERVOIR IN FIG.2.

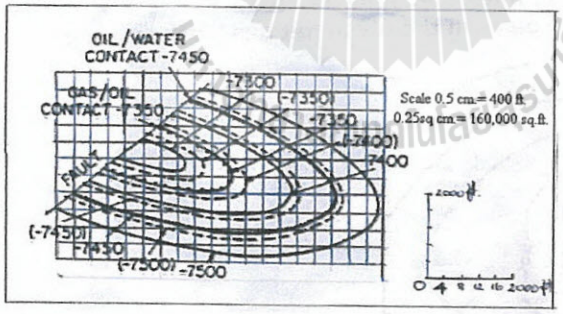

FIGURE 2. Geological map on top and base of the SUT OIL RESERVOIR

2.2 Find oil inplace in the SUT OIL reservoir if the average; ø = 0.20 , Swi = 0.25 , Bo = 1.3 res bbl/ STB, and recovery factor of 0.4.

3th WEEK (June 12-15, 2012)

Outline

Reserve Calculation

- **Material Balance**

Material Balance for Gas Reservoirs

Material Balance Equations

$$GB_{gi} = (G - G_p)B_g \qquad (5\text{-}145)$$

$$GB_{gi} = (G - G_p)B_g + (W_e - W_p) \qquad (5\text{-}146)$$

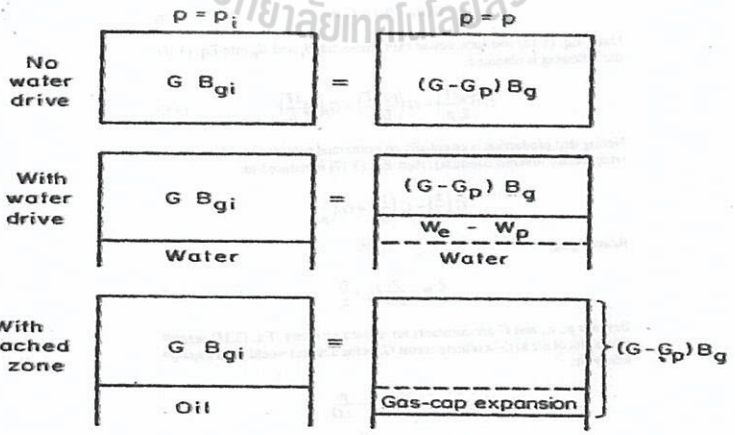

Figure 5-141. Schematic of material balance equations for a dry-gas reservoir [197].

MATERIAL BALANCES IN GAS RESERVOIRS

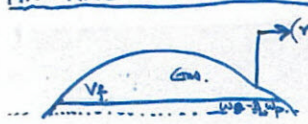

$$V_f = V_i - W_e + B_w W_p$$

Conservation of Mass.

$$\left[\begin{matrix}\text{Wt. of Gas}\\ \text{Produced}\end{matrix}\right] = \left[\begin{matrix}\text{Initial wt.}\\ \text{in the Reservoir}\end{matrix}\right] - \left[\begin{matrix}\text{Remaining}\\ \text{wt.}\end{matrix}\right]$$

$$n_p = n_i - n_f$$

$$\frac{P_{sc} G_p}{T_{sc}} = \frac{P_i V_i}{z_i T} - \frac{P_f V_f}{z_f T}$$

$$= \frac{P_i V_i}{z_i T} - \frac{P_f (V_i - W_e + B_w W_p)}{z_f T}$$

Volumetric Reservoir $V_i = V_f$

$$\frac{P_{sc} G_p}{T_{sc}} = \frac{P_i V_i}{z_i T} - \frac{P_f V_i}{z_f T}$$

$$G_p = b - m\left(\frac{P_f}{z_f}\right) \qquad b = \frac{P_i V_i T_{sc}}{z_i P_{sc} T}, \quad m = \frac{V_i T_{sc}}{z_i T}$$

$$\frac{P_{sc} G_p}{T_{sc}} = \frac{P_i V_i}{z_i T} - \frac{P_f V_i}{z_f T}$$

$$\frac{P_{sc} z_f T}{T_{sc} P_f} G_p = \frac{P_i}{z_i T} \cdot \frac{z_f T}{P_f} \cdot V_i - V_i$$

$$B_{gf} = \frac{P_{sc} z_f T}{T_{sc} P_f} \quad \text{Eq. 1.16}, \quad V_i \Rightarrow B_{gi} G$$

$$\frac{B_{gf}}{B_{gi}} = \frac{\frac{P_{sc} z_f T}{T_{sc} P_f}}{\frac{P_{sc} z_i T}{T_{sc} P_i}} = \frac{P_i}{z_i T} \cdot \frac{z_f T}{P_f}$$

and Eq.(1) becomes

$$B_{gf} G_p = \frac{B_{gf}}{B_{gi}} \cdot B_{gi} G - G_{gi} \cdot G$$

$$B_{gf} G_p = B_{gf} G - B_{gi} G$$

$$G B_{gi} = (G - G_p) B_{gf}$$

$$= (G - G_p) B_g$$

$$G(B_g - B_{gi}) = G_p B_g$$

For most gas reservoirs, the gas compressibility term is much greater than the formation and water compressibilities, and the second term on the left-hand side of Eq. (2.10) becomes negligible

$$G B_{gi}\left[\frac{c_w S_{wi} + c_f}{1 - S_{wi}}\right] \Delta p + G(B_g - B_{gi}) + W_e = G_p B_g + B_w W_p \qquad (3.15)$$

When reservoir pressures are abnormally high, this term is not negligible and should not be ignored. This situation is discussed in a later section of this chapter.

When there is neither water encroachment into nor water production from a reservoir of interest, the reservoir is said to be *volumetric*. For a volumetric gas reservoir, Eq. (3.15) reduces to:

$$G(B_g - B_{gi}) = G_p B_g \qquad (3.16)$$

Using Eq. (1.16) and substituting expressions for B_g and B_{gi} into Eq. (3.16), the following is obtained:

$$G\left(\frac{p_{sc} z T}{T_{sc} p}\right) - G\left(\frac{p_{sc} z_i T_i}{T_{sc} p_i}\right) = G_p\left(\frac{p_{sc} z T}{T_{sc} p}\right) \qquad (3.17)$$

Noting that production is essentially an isothermal process (i.e., the reservoir temperature remains constant), then Eq. (3.17) is reduced to:

$$G\left(\frac{z}{p}\right) - G\left(\frac{z_i}{p_i}\right) = G_p\left(\frac{z}{p}\right)$$

Rearranging:

$$\frac{p}{z} = -\frac{p_i}{z_i G} G_p + \frac{p_i}{z_i} \qquad (3.18)$$

Because p_i, z_i, and G are constants for a given reservoir, Eq. (3.18) suggests that a plot of p/z as the ordinate versus G_p as the abscissa would yield a straight line with:

$$\text{slope} = -\frac{p_i}{z_i G}$$

$$y \text{ intercept} = \frac{p_i}{z_i}$$

This plot is shown in Fig. 3.6.

Table B1 - Gas-in-Place Estimates

Δp (psi)	cf (1/psi)	GIP (Gscf)	Comments
7.70	6x10-6	433	No communication wit Nam Phong 2
4.47	6x10-6	744	90% confidence interval
10.93	6x10-6	304	90% confidence interval
7.70	6x10-5	249	High formation compressibilit
6.00	6x10-6	565	Communication with Nam Phong 2 Includes gas volume of both wells

Values for other variables used in the equation:

Gp	: 0.3267 Gscf
z	: 1.140082
Δz/Δp	: 0.0000707/psi
S_w	: 0.25
c_w	: 0.0000034/psi

time *t*. The change in the rock volume is expressed as a char
space volume, which is simply the negative of the change in th
In the development of the general material balance equation
terms are used:

N	Initial reservoir oil, STB @ P_i
B_{oi}	Initial oil formation volume factor, bbl/STB >1.4
N_p	Cumulative produced oil, STB
B_o	oil formation volume factor, bbl/STB @ P
G_i	Initial reservoir gas, SCF Free Gas @ P_i
B_{gi}	Initial gas formation volume factor, bbl/SCF @ P_i
G_f	Amount of free gas in the reservoir, SCF @ P
R_{soi}	Initial solution gas-oil ratio, SCF/STB @ P_i
R_p	Cumulative produced gas-oil ratio, SCF/STB G_p/N_p
R_{so}	Solution gas-oil ratio, SCF/STB @ P
B_g	Gas formation volume factor, bbl/SCF @ P
W	Initial reservoir water, bbl
W_p	Cumulative produced water, STB
B_w	Water formation volume factor, bbl/STB >1.03
W_e	Water influx into reservoir, bbl
c_w	Water isothermal compressibility, psi^{-1}
$\Delta\bar{p}$	Change in average reservoir pressure, psia $P_i - P$
S_{wc}	Initial water saturation
V_f	Initial void space, bbl
c_f	Formation isothermal compressibility, psi^{-1}

c_o
c_g

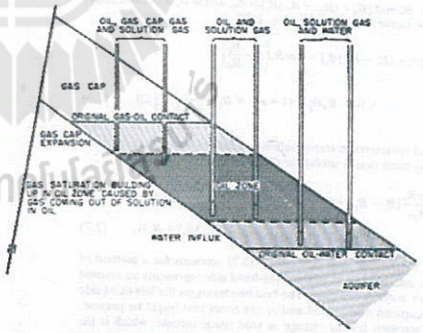

2.1. Cross section of a combination drive reservoir. (*After* Woody and Moscrip.[1] *ms.* AIME.)

Reservoirs under Simultaneous Drives

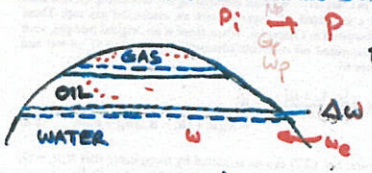

① Change in Oil Volume

Change in the Oil Volume:

Initial reservoir oil volume = NB_{oi}

Oil volume at time t and pressure $p = (N - N_p)B_o$

Change in oil volume = $NB_{oi} - (N - N_p)B_o$ (2.1)

Change in Free Gas Volume:

$$\begin{bmatrix}\text{Ratio of initial free gas}\\ \text{to initial oil volume}\end{bmatrix} = m = \frac{GB_{gi}}{NB_{oi}}$$

Initial free gas volume = $GB_{gi} = NmB_{oi}$

$$\begin{bmatrix}\text{SCF free}\\ \text{gas at } t\end{bmatrix} = \begin{bmatrix}\text{SCF initial gas,}\\ \text{free and dissolved}\end{bmatrix} - \begin{bmatrix}\text{SCF gas}\\ \text{produced}\end{bmatrix} - \begin{bmatrix}\text{SCF remaining}\\ \text{in solution}\end{bmatrix}$$

$$G_f = \left[\frac{NmB_{oi}}{B_{gi}} + NR_{soi}\right] - [N_pR_p] - [(N - N_p)R_{so}]$$

$$\begin{bmatrix}\text{Reservoir free gas}\\ \text{volume at time } t\end{bmatrix} = \left[\frac{NmB_{oi}}{B_{gi}} + NR_{soi} - N_pR_p - (N - N_p)R_{so}\right] B_g$$

$$\begin{bmatrix}\text{Change in free}\\ \text{gas volume}\end{bmatrix} = NmB_{oi} - \left[\frac{NmB_{oi}}{B_{gi}} + NR_{soi} - N_pR_p - (N - N_p)R_{so}\right]B_g \quad (2.2)$$

Change in Water Volume:

Initial reservoir water volume = W
Cumulative water produced at $t = W_p$
Reservoir volume of cumulative produced water = B_wW_p
Volume of water encroached at $t = W_e$

$$\begin{bmatrix}\text{Change in}\\ \text{water volume}\end{bmatrix} = W - (W + W_e - B_wW_p + Wc_w\Delta\bar{p}) = -W_e + B_wW_p - Wc_w\Delta\bar{p}) \quad (2.3)$$

Change in the Void Space Volume:

Initial void space volume = V_f

$$\begin{bmatrix}\text{Change in void}\\ \text{space volume}\end{bmatrix} = V_f - [V_f - V_fc_f\Delta\bar{p}] = V_fc_f\Delta\bar{p}$$

Or, because the change in void space volume is the negative of the change in rock volume:

$$\begin{bmatrix}\text{Change in}\\ \text{rock volume}\end{bmatrix} = -V_fc_f\Delta\bar{p} \quad (2.4)$$

Combining the changes in water and rock volumes into a single term, yields the following:

$$= -W_e + B_wW_p - Wc_w\Delta\bar{p} - V_fc_f\Delta\bar{p}$$

Recognizing that $W = V_fS_{wi}$ and that $V_f = \frac{NB_{oi} + NmB_{oi}}{1 - S_{wi}}$ and substituting, the following is obtained:

$$= -W_e + B_wW_p - \left[\frac{NB_{oi} + NmB_{oi}}{1 - S_{wi}}\right](c_wS_{wi} + c_f)\Delta\bar{p}$$

or

$$= -W_e + B_wW_p - (1 + m)\,NB_{oi}\left[\frac{c_wS_{wi} + c_f}{1 - S_{wi}}\right]\Delta\bar{p} \quad (2.5)$$

Equating the changes in the oil and free gas volumes to the negative of the changes in the water and rock volumes and expanding all terms

$$N B_{oi} - N B_o + N_pB_o + NmB_{oi} - \left[\frac{NmB_{oi}B_g}{B_{gi}}\right] - N R_{soi}B_g + N_pR_pB_g$$

$$+ NB_gR_{so} - N_pB_gR_{so} = W_e - B_wW_p + (1 + m)N B_{oi}\left[\frac{c_wS_{wi} + c_f}{1 - S_{wi}}\right]\Delta\bar{p}$$

Now adding and subtracting the term $N_pB_gR_{soi}$

$$N B_{oi} - N B_o + N_pB_o + NmB_{oi} - \left[\frac{NmB_{oi}B_g}{B_{gi}}\right] - N R_{soi}B_g + N_pR_pB_g + NB_gR_{so}$$

$$- N_pB_gR_{so} + N_pB_gR_{soi} - N_pB_gR_{soi} = W_e - B_wW_p + (1 + m)\,N B_{oi}\left[\frac{c_wS_{wi} + c_f}{1 - S_{wi}}\right]\Delta\bar{p}$$

Then grouping terms:

$$NB_{oi} + NmB_{oi} - N[B_o + (R_{soi} - R_{so})B_g] + N_p[B_o + (R_{soi} - R_{so})B_g]$$

$$+ (R_p - R_{soi})B_gN_p - \left[\frac{NmB_{oi}B_g}{B_{gi}}\right] = W_e - B_wW_p + (1 + m)\,N B_{oi}\left[\frac{c_wS_{wi} + c_f}{1 - S_{wi}}\right]\Delta\bar{p}$$

Now writing $B_{oi} = B_{ti}$ and $[B_o + (R_{soi} - R_{so})B_g] = B_t$, where B_t is the two phase formation volume factor, as defined by Eq. 1.28:

$$N(B_{ti} - B_{ti}) + N_p[B_t + (R_p - R_{so})B_g] + NmB_{oi}\left(1 - \frac{B_g}{B_{gi}}\right)$$

$$= W_e - B_wW_p + (1 + m)\,N B_{oi}\left[\frac{c_wS_{wi} + c_f}{1 - S_{wi}}\right]\Delta\bar{p} \quad (2.6)$$

This is the general volumetric material balance equation. It can be rearranged into the following form that is useful for discussion purposes.

$$N(B_t - B_{ti}) + \frac{NmB_{gi}}{B_{gi}}(B_g - B_{gi}) + (1 + m)\,N B_{oi}\left[\frac{c_wS_{wi} + c_f}{1 - S_{wi}}\right]\Delta\bar{p} + W_e$$

$$= N_p[B_t + (R_p - R_{so})B_g] + B_wW_p \quad (2.7)$$

Each term on the left-hand side of Eq. (2.7) accounts for a method of fluid production, and each term on the right-hand side represents an amount of hydrocarbon or water production. The first two terms on the left-hand side account for the expansion of any oil and/or gas zones that might be present. The third term accounts for the change in void space volume, which is the expansion of the formation and connate water. The fourth term is the amount of water influx that has occurred into the reservoir. On the right-hand side, the first term represents the production of oil and gas and the second term represents the water production.

Equation (2.7) can be arranged to apply to any of the different reservoir types discussed in Chapter 1. Without eliminating any terms, Eq. (2.7) is used for the case of a saturated oil reservoir with an associated gas cap. These reservoirs are discussed in Chapter 6. When there is no original free gas, such as in an undersaturated oil reservoir (discussed in Chapter 5), $m = 0$ and Eq. (2.7) reduces to:

$$N(B_t - B_{ti}) + N B_{oi}\left[\frac{c_wS_{wi} + c_f}{1 - S_{wi}}\right]\Delta\bar{p} + W_e$$

$$= N_p[B_t + (R_p - R_{so})B_g] + B_wW_p \quad (2.8)$$

For gas reservoirs, Eq. (2.7) can be modified by recognizing that $N_pR_p = G_p$ and that $NmB_{gi} = GB_{gi}$ and substituting these terms into Eq. (2.7):

$$N(B_t - B_{ti}) + G(B_g - B_{gi}) + (N B_{ti} + GB_{gi})\left[\frac{c_wS_{wi} + c_f}{1 - S_{wi}}\right]\Delta\bar{p} + W_e$$

$$= N_pB_t + (G_p - NR_{so})\,B_g + B_wW_p \quad (2.9)$$

When working with gas reservoirs, there is no initial oil amount; therefore, N and N_p are equal to zero. The general material balance equation for a gas reservoir can then be obtained

$$G(B_g - B_{gi}) + GB_{gi}\left[\frac{c_wS_{wi} + c_f}{1 - S_{wi}}\right]\Delta\bar{p} + W_e = G_pB_g + B_wW_p \quad (2.10)$$

This equation is discussed in conjunction with gas and gas-condensate reservoirs in Chapters 3 and 4.

In the study of reservoirs that are produced simultaneously by the three major mechanisms of depletion drive, gas cap drive, and water drive, it is of practical interest to determine the relative magnitude of each of these mechanisms that contribute to the production. Pirson rearranged the material balance Equation (2.7) as follows to obtain three fractions, whose sum is one, which he called the depletion drive index (DDI), the segregation (gas cap) index (SDI), and the water-drive index (WDI).[6]

When all three drive mechanisms are contributing to the production of oil and gas from the reservoir, the compressibility term in Eq. (2.7) is negligible and can be ignored. Moving the water production term to the left-hand side of the equation, the following is obtained:

$$N(B_t - B_{ti}) + \frac{NmB_{gi}}{B_{gi}}(B_g - B_{gi}) + (W_e - B_wW_p) = N_p[B_t + (R_p - R_{so})B_g]$$

Dividing through by the term on the right hand side of the equation:

$$\frac{N(B_t - B_{ti})}{N_p[B_t + (R_p - R_{so})B_g]} + \frac{\frac{NmB_{gi}}{B_{gi}}(B_g - B_{gi})}{N_p[B_t + (R_p - R_{so})B_g]} + \frac{(W_e - B_wW_p)}{N_p[B_t + (R_p - R_{so})B_g]} = 1 \quad (2.11)$$

The numerators of these three fractions that result on the left-hand side of Eq. (2.11) are the expansion of the initial oil zone, the expansion of the initial gas zone, and the net water influx, respectively. The common denominator is the reservoir volume of the cumulative gas and oil production expressed at the lower pressure, which evidently equals the sum of the gas and oil zone expansions plus the net water influx. Then, using Pirson's abbreviations:

$$\text{DDI} + \text{SDI} + \text{WDI} = 1$$

Calculations are performed in Chapter 6 to illustrate how these drive indexes are used.

diminishes the initial free gas volume. Well tests are often useful in locating gas-oil and water-oil contacts in the determination of m. In some cases, these contacts are not horizontal planes but are tilted owing to water movement in the aquifer, or dish-shaped owing to the effect of capillarity in the less permeable boundary rocks of volumetric reservoirs.

Whereas the cumulative oil production is generally known quite precisely, the corresponding gas and water production is usually much less accurate, and therefore introduces additional sources of errors. This is particularly true when the gas and water production is not directly measured but must be inferred from periodic tests to determine the gas-oil ratios and water cuts of the individual wells. When two or more wells completed in different reservoirs are producing to common storage, unless there are individual meters on the wells, only the aggregate production is known and not the individual oil production from each reservoir. Under the circumstances that exist in many fields, it is doubtful that the cumulative gas and water production is known to within 10% and in some instances the errors may be larger. With the growing importance of natural gas and because more of the gas associated with the oil is being sold, better values of gas production are becoming available.

4. THE HAVLENA AND ODEH METHOD OF APPLYING THE MATERIAL BALANCE EQUATION

As early as 1953, van Everdingen, Timmerman, and McMahon recognized a method of applying the material balance equation as a straight line.[9] But it wasn't until Havlena and Odeh published their work that the method became fully exploited.[3,4] Normally, when using the material balance equation, an engineer considers each pressure and the corresponding production data as being separate points from other pressure values. From each separate point, a calculation for a dependent variable is made. The results of the calculations are sometimes averaged. The Havlena-Odeh method uses all the data points, with the further requirement that these points must yield solutions to the material balance equation that behave linearly to obtain values of the independent variable.

The straight-line method begins with the material balance equation written as:

$$N_p[B_t + (R_p - R_{si})B_g] + B_w W_p - W_i - G_i B_{ig} = N\left[(B_t - B_{ti}) + B_{ti}(1+m)\left(\frac{c_w S_{wi} + c_f}{1 - S_{wi}}\right)\Delta\bar{p} + \frac{mB_{ti}}{B_{gi}}(B_g - B_{gi})\right] + W_e \qquad (2.12)$$

The terms W_i, cumulative water injection, G_i, cumulative gas injection, and B_{ig}, formation volume factor of the injected gas have been added to Eq. (2.7). In Havlena and Odeh's original development, they chose to neglect the effect

of the compressibilities of the formation and connate water in the gas cap portion of the reservoir. That is, in their development the compressibility term is multiplied by N and not by $N(1+m)$. In Eq. (2.12), the compressibility term is multiplied by $N(1+m)$ for completeness. You may choose to ignore the $(1+m)$ multiplier in particular applications. Havlena and Odeh defined the following terms and rewrote Eq. (2.12) as:

$$F = N_p[B_t + (R_p - R_{si})B_g] + B_w W_p - W_i - G_i B_{ig}$$

$$E_o = B_t - B_{ti}$$

$$E_{f,w} = \left[\frac{c_w S_{wi} + c_f}{1 - S_{wi}}\right]\Delta\bar{p}$$

$$E_g = B_g - B_{gi}$$

$$F = NE_o + N(1+m)B_{ti}E_{f,w} + \left[\frac{NmB_{ti}}{B_{gi}}\right]E_g + W_e \qquad (2.13)$$

In Eq. (2.13) F represents the net production from the reservoir. E_o, $E_{f,w}$, and E_g represent the expansion of oil, formation and water, and gas, respectively. Havlena and Odeh examined several cases of varying reservoir types with this equation and found that the equation can be rearranged into the form of a straight line. For instance, consider the case of no original gas cap, no water influx, and negligible formation and water compressibilities. With these assumptions, Eq. (2.13) reduces to:

$$F = NE_o \qquad (2.14)$$

This would suggest that a plot of F as the y coordinate and E_o as the x coordinate would yield a straight line with slope N and intercept equal to zero. Additional cases can be derived as will be shown in Chapter 6.

Once a linear relationship has been obtained, the plot can be used as a predictive tool for estimating future production. Examples are shown in subsequent chapters to illustrate the application of the Havelena-Odeh method.

REFERENCES

[1] Ralph J. Schilthuis, "Active Oil and Reservoir Energy," *Trans.* AIME (1936), 118, 33.

[2] L. P. Dake, *Fundamentals of Reservoir Engineering*, 1st ed. Amsterdam: Elsevier, 1978, pp. 73–102.

[3] D. Havlena and A. S. Odeh, "The Material Balance as an Equation of a Straight Line," Part I. *Jour. of Petroleum Technology* (Aug. 1963), 896–900.

[4] D. Havlena and A. S. Odeh, "The Material Balance as an Equation of a Straight Line. Part II—Field Cases," *Jour. of Petroleum Technology* (July 1964), 815–822.

In field units where permeability is in mD, time in years, pressure in psi, length in feet, rate in reservoir barrels per day

$U = 1.119\phi\bar{c}r_e^2$ bbl/psi (radial system)

$U = 0.1781\, w\, L\, h\, \phi\bar{c}$ bbl/psi (linear system)

$t_D = 2.309kt/(\phi\mu\bar{c}r_e^2)$ (radial system, t in years)

$t_D = 2.309kt/(\phi\mu\bar{c}L^2)$ (linear system, t in years)

If water injection is employed in a reservoir then natural water influx may still occur if the pressure at the original water contact decreases from initial pressure. The combination drive material balance equation which represents a step change from equilibrium at pressure P_i to equilibrium at pressure P can be formulated to show all expansion, production and injection terms as shown below.

In this formulation the subscripts c and s refer to gas terms to conditions in the gas cap and in solution gas. W_{inj} and G_{inj} are cumulative injection volumes at stock tank conditions.

Setting $G(B_g)_i = mN(B_{ti})$; $R_p = G_p/N_p$ and $G_p = (G_{ps})_s + (G_{pc})_c$ we can write

$$F = N\left(E_o + mE_g + (1+m)E_{f,w}\right) + \left(W_e + W_{inj}B_w - G_{inj}B_g - W_pB_w\right)$$

or

$$F = NE_T + W_e'$$

where: $F = N_p(B_o + (R_p - R_s)B_g)$

$$E_o = (B_o - (B_{oi})) + ((R_{si}) - R_s)B_g$$

$$E_g = (B_{oi})\left[\frac{B_g}{(B_{gi})} - 1\right]$$

$$E_{f,w} = (1+m)(B_{oi})\Delta P\left(\frac{c_w S_{wi} + c_f}{1 - S_{wi}}\right)$$

$$E_T = E_o + mE_g + E_{f,w}$$

Present oil volume	Original oil volume	Freed solution gas	Gas cap expansion	Net water influx	Rock and connate water expansion	Injected volumes
$(N - N_p)B_o =$	$N(B_{oi}) -$	$(B_g)_i\left[N(R_{si}) - (N - N_p)R_s - (G_p)_s\right] -$	$\left[(G - (G_p)_c)(B_g)_c - G(B_g)_i\right] -$	$\left[W_e - W_pB_w\right] -$	$N(B_{oi})(1+m)\Delta P\left[\frac{c_f + S_{wi}c_w}{1 - S_{wi}}\right] -$	$\left[W_{inj}B_w + G_{inj}B_g\right]$

$$N = \frac{N_p(B_o - R_s(B_g)_s) + (G_p)_c(B_g)_c - \left[(G - (G_p)_c)(B_g)_c - G(B_g)_i\right] - \left[W_e - W_pB_w\right] - W_{inj}B_w - G_{inj}B_g}{(B_o - (B_{oi})) + ((R_{si}) - R_s)(B_g)_s + (B_{oi})\Delta P\left[\frac{c_f + S_{wi}c_w}{1 - S_{wi}}\right](1+m)}$$

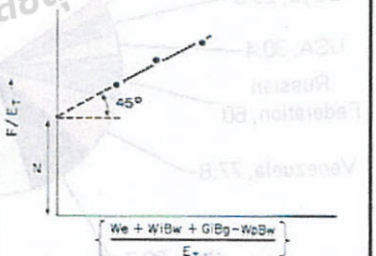

Fig. 10.10 Combination drive, Havlena-Odeh plot.

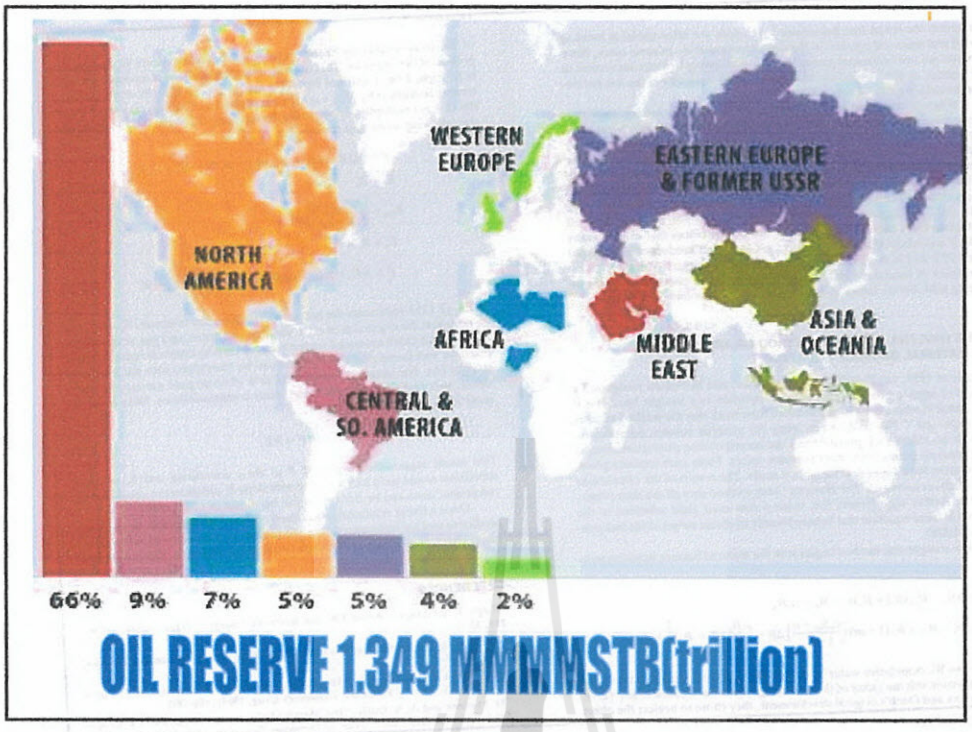

OIL RESERVE 1.349 MMMMSTB(trillion)

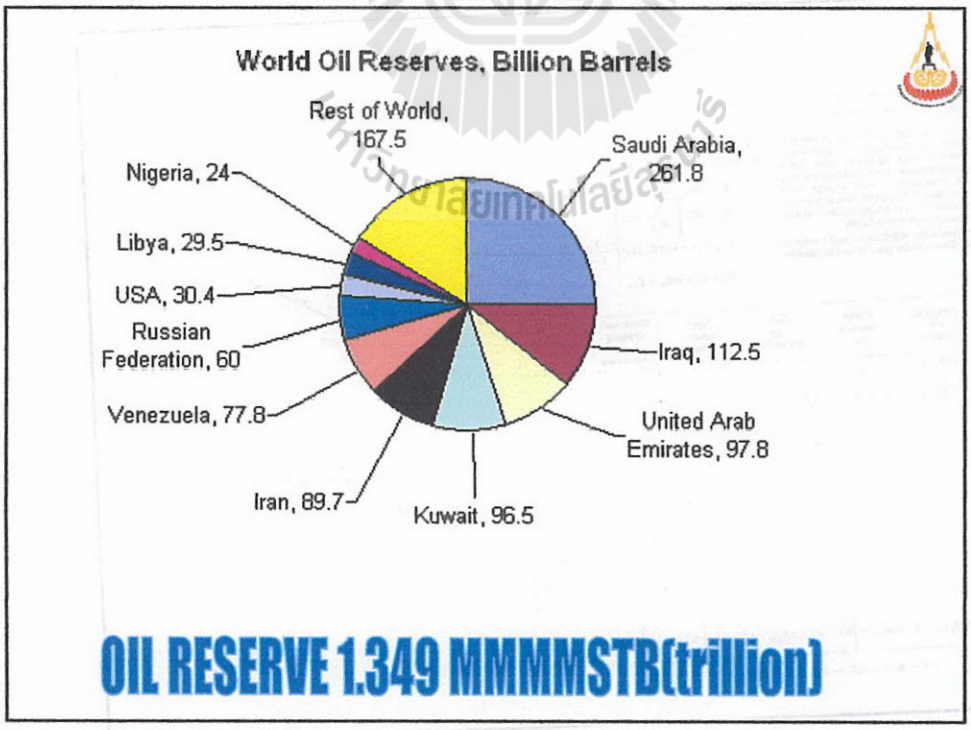

OIL RESERVE 1.349 MMMMSTB(trillion)

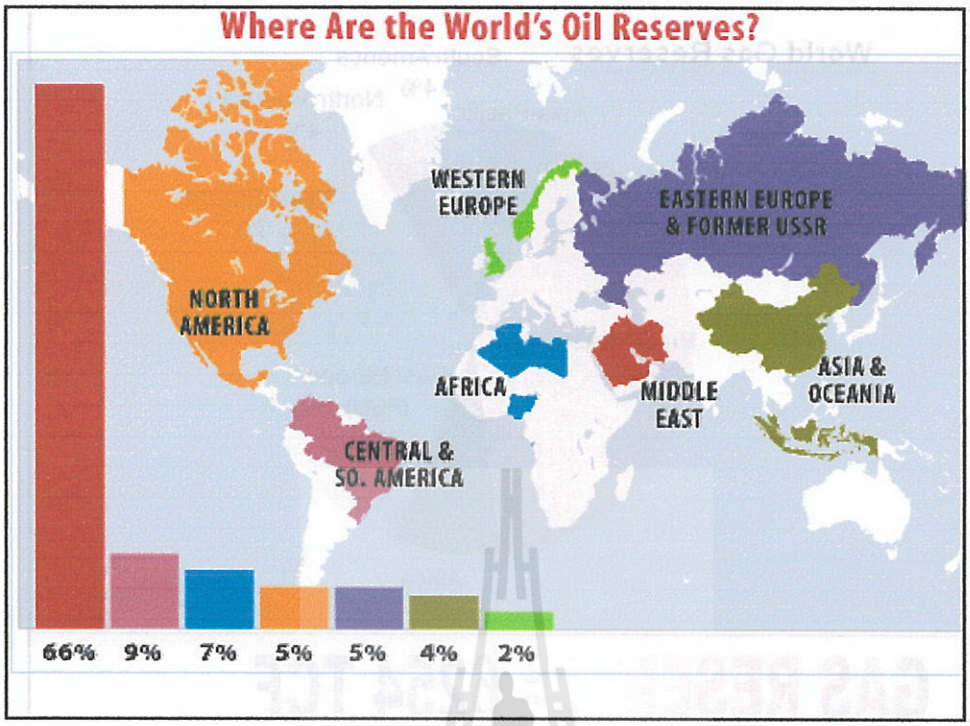
Where Are the World's Oil Reserves?
WESTERN EUROPE
EASTERN EUROPE & FORMER USSR
NORTH AMERICA
AFRICA
MIDDLE EAST
ASIA & OCEANIA
CENTRAL & SO. AMERICA
66%
9%
7%
5%
5%
4%
2%

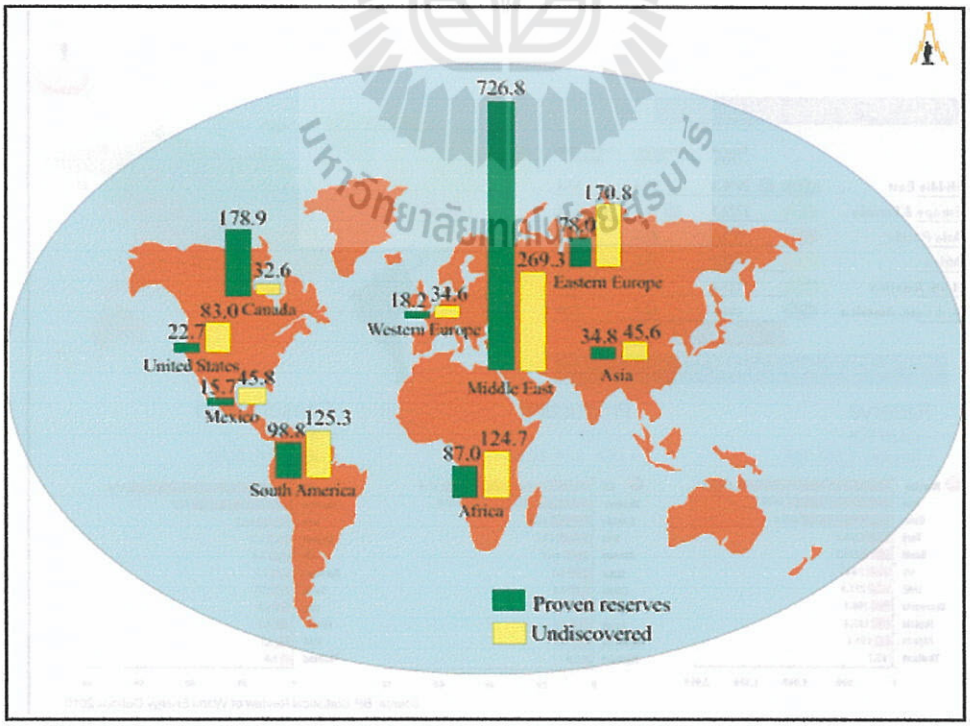
726.8
178.9
32.6
83.0 Canada
22.7
United States
15.7
45.8
Mexico
98.8
125.3
South America
18.2
34.6
Western Europe
78.0
170.8
269.3
Eastern Europe
34.8
45.6
Asia
Middle East
87.0
124.7
Africa
Proven reserves
Undiscovered

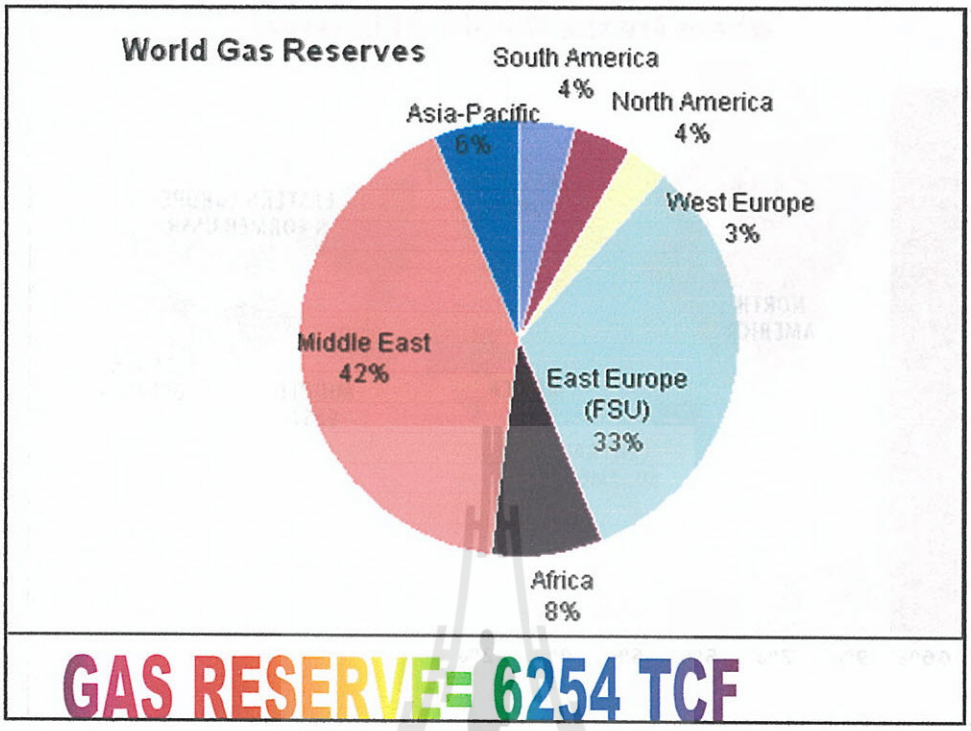
World Gas Reserves
South America 4%
North America 4%
Asia-Pacific 6%
West Europe 3%
Middle East 42%
East Europe (FSU) 33%
Africa 8%
GAS RESERVE= 6254 TCF

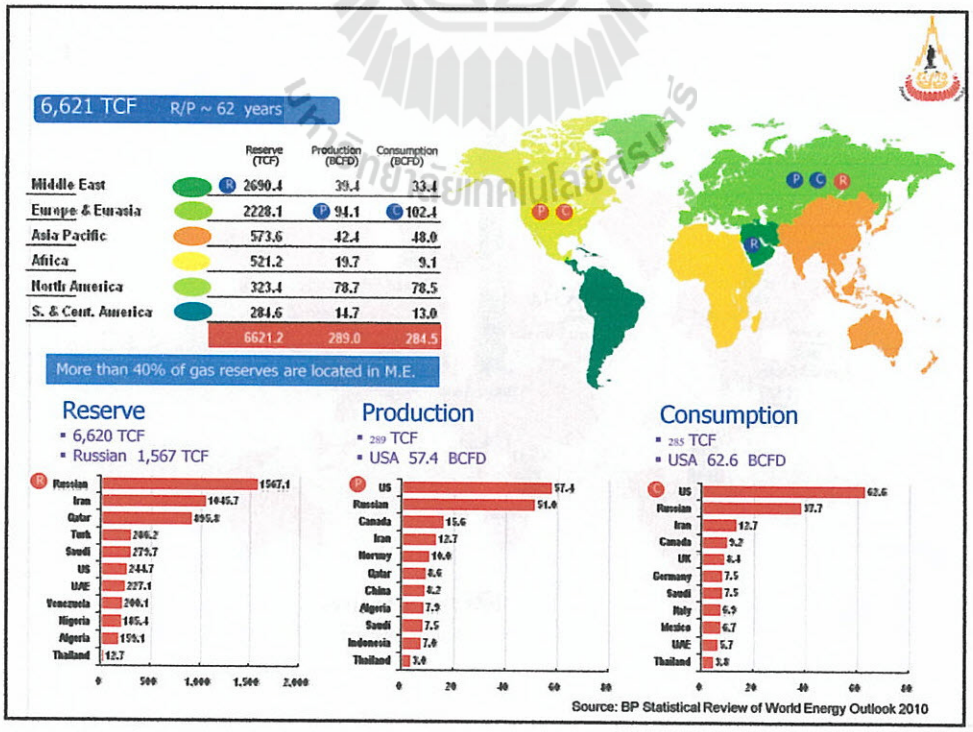
6,621 TCF R/P ~ 62 years
Reserve (TCF) Production (BCFD) Consumption (BCFD)
Middle East 2690.4 39.4 33.4
Europe & Eurasia 2228.1 94.1 102.4
Asia Pacific 573.6 42.4 48.0
Africa 521.2 19.7 9.1
North America 323.4 78.7 78.5
S. & Cent. America 284.6 14.7 13.0
6621.2 289.0 284.5
More than 40% of gas reserves are located in M.E.
Reserve
6,620 TCF
Russian 1,567 TCF
Production
289 TCF
USA 57.4 BCFD
Consumption
285 TCF
USA 62.6 BCFD
Source: BP Statistical Review of World Energy Outlook 2010

1,333 MMMBBL R/P ~ 45 years

	Reserve (MMMBBL)	Production (MBBLD)	Consumption (MBBLD)
Middle East	754	24,357	7,146
S. & Cent. America	199	6,760	5,653
Europe & Eurasia	137	17,702	19,372
Africa	128	9,705	3,082
North America	73	13,388	22,826
Asia Pacific	42	8,036	25,998
	1,333	79,948	84,077

More than 57% of oil reserves are located in M.E.

Reserve

- 1,333 MMMBBL
- Saudi Arabia 265 MMMBBL

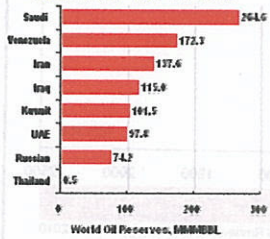

Production

- 80 MMBBLD
- Russian 10 MMBBLD

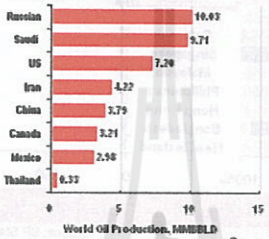

Consumption

- 84 MMBBLD
- USA 18.6 MMBBLD

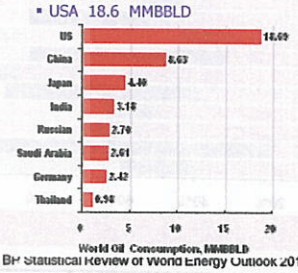

Source: BP Statistical Review of World Energy Outlook 2010

826,000 MMT R/P ~ 120 years

	Reserve (MM t)	Production (MM toe)	Consumption (MM toe)
Europe & Eurasia	272,246	1,153	456
Asia Pacific	259,253	4,403	2,152
North America	246,097	1,047	531
Africa	32,013	253	107
S. & Cent. America	15,006	83	22
Middle East	1,386	2	9
	826,001	6,941	3,278

*** It might be the best choice for Thailand ***

Reserve

- 826 MMM Tonnes
- USA 238 MMM Tonnes

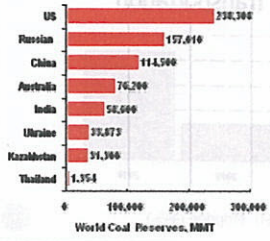

Production

- 6,941 MM toe
- China 1,553 MM toe

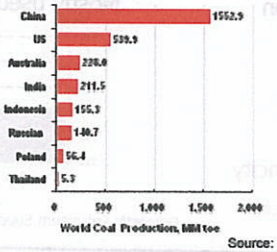

Consumption

- 3,278 MM toe
- China 1,538 MM toe

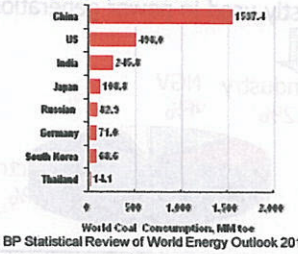

Source: BP Statistical Review of World Energy Outlook 2010

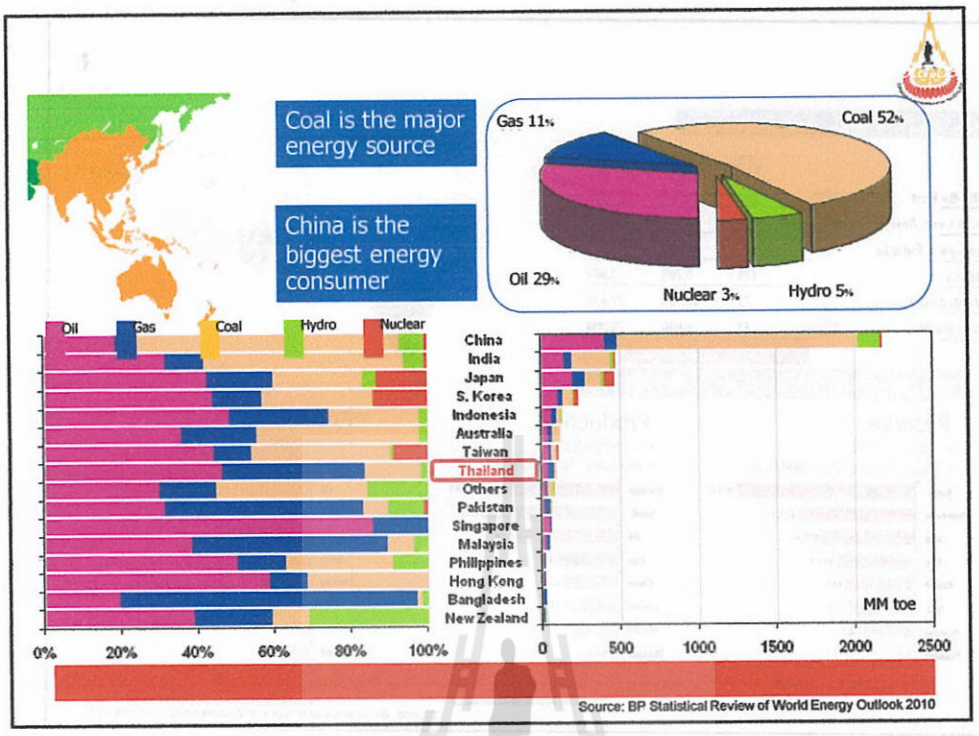
Coal is the major energy source
China is the biggest energy consumer
Gas 11%
Coal 52%
Oil 29%
Nuclear 3%
Hydro 5%
Oil
Gas
Coal
Hydro
Nuclear
China
India
Japan
S. Korea
Indonesia
Australia
Taiwan
Thailand
Others
Pakistan
Singapore
Malaysia
Philippines
Hong Kong
Bangladesh
New Zealand
0%
20%
40%
60%
80%
100%
0
500
1000
1500
2000
2500
MM toe
Source: BP Statistical Review of World Energy Outlook 2010

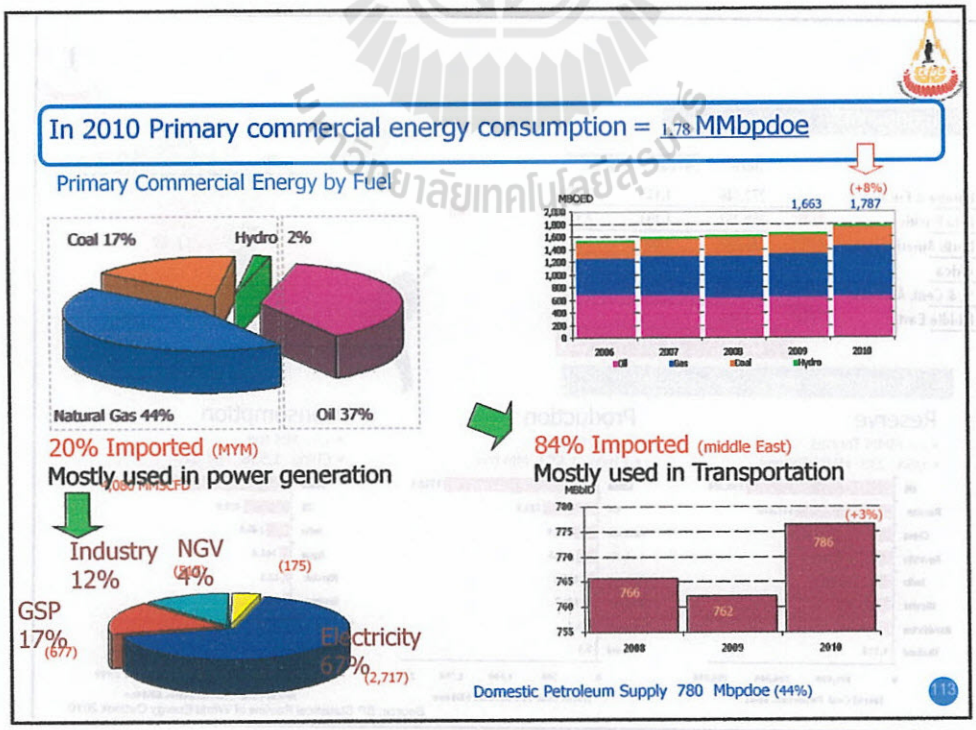
In 2010 Primary commercial energy consumption = 1,78 MMbpdoe
Primary Commercial Energy by Fuel
Coal 17%
Hydro 2%
Natural Gas 44%
Oil 37%
MBOED
1,663
1,787
(+8%)
2006
2007
2008
2009
2010
20% Imported (MYM)
Mostly used in power generation
84% Imported (middle East)
Mostly used in Transportation
Industry 12%
NGV 4%
(175)
GSP 17%
(677)
Electricity 67%
(2,717)
MBBD
780
775
770
765
760
755
766
762
786
(+3%)
2008
2009
2010
Domestic Petroleum Supply 780 Mbpdoe (44%)
113

3th WEEK (June 11-15, 2012)
Outline

•Gas Reservoir

2. CALCULATING GAS IN PLACE BY THE VOLUMETRIC METHOD

The standard cubic feet of gas in a reservoir with a gas pore volume of V_p cu ft is simply V_p/B_g, where B_g is expressed in units of cubic feet per standard cubic foot. As the gas volume factor B_g changes with pressure (see Eq. 1.17, the gas in place also changes as the pressure declines. The gas pore volume V_p may also be changing, owing to water influx into the reservoir. The gas pore volume is related to the bulk, or total, reservoir volume by the average porosity ϕ and the average connate water S_w. The bulk reservoir volume V_b is commonly expressed in acre-feet, and the standard cubic feet of gas in place, G, is given by:

$$G = \frac{43{,}560\, V_b \phi (1 - S_w)}{B_g} \tag{3.1}$$

The areal extent of the Bell Field gas reservoir was 1500 acres. The average thickness was 40 ft, so that the initial bulk volume was 60,000 ac-ft. Average porosity was 22%, and average connate water was 23%. B_g at the initial reservoir pressure of 3250 psia was calculated to be 0.00533 cu ft/SCF. Therefore,

Initial pressure=3250 psia

$$G = 43{,}560 \times 60{,}000 \times 0.22 \times (1 - 0.23) \div 0.00533$$
$$= 83.1\ MMM\ SCF$$

Because the gas volume factor was calculated using 14.7 psia and 60°F as standard conditions, the initial gas in place is also expressed at these conditions.

The volumetric method uses subsurface and isopachous maps based on the data from electric logs, cores, and drill-stem and production tests.*[1,2] A *subsurface contour* map shows lines connecting points of equal elevations on the top of a marker bed and therefore shows geologic structure. A net *isopachous* map shows lines connecting points of equal net formation thickness; and the individual lines connecting points of equal thickness are called *isopach* lines. The reservoir engineer uses these maps to determine the bulk productive volume of the reservoir. The contour map is used in preparing the isopachous maps when there is an oil-water, gas-water, or gas-oil contact. The contact line is the zero isopach line. The volume is obtained by planimetering the areas between the isopach lines of the entire reservoir or of the individual units under consideration. The principal problems in preparing a map of this type are the proper interpretation of net sand thickness from the well logs and the outlining of the productive area of the field as defined by the fluid contacts, faults, or permeability barriers on the subsurface contour map.

* References throughout the text are given at the end of each chapter.

Two equations are commonly used to determine the approximate volume of the productive zone from the planimeter readings. The volume of the frustum of a pyramid is given by:

$$\Delta V_b = \frac{h}{3}(A_n + A_{n+1} + \sqrt{A_n A_{n+1}}) \tag{3.2}$$

where ΔV_b is the bulk volume in acre-feet, A_n is the area enclosed by the lower isopach line in acres, A_{n+1} is the area enclosed by the upper isopach line in acres, and h is the interval between the isopach lines in feet. This equation is used to determine the volume between successive isopach lines, and the total volume is the sum of these separate volumes. The volume of a trapezoid is:

$$\Delta V_b = \frac{h}{2}(A_n + A_{n+1})$$

or for a series of successive trapezoids:

$$V_b = \frac{h}{2}(A_0 + 2A_1 + 2A_2 \ldots 2A_{n-1} + A_n) + t_{av} A_n \tag{3.3}$$

A_0 is the area enclosed by the zero isopach line in acres; $A_1, A_2 \ldots A_n$ are the areas enclosed by successive isopach lines in acres; t_{av} is the average thickness above the top or maximum thickness isopach line in feet; and h is the isopach interval.

For best accuracy the pyramidal formula should be used. Because of its simpler form, however, the trapezoidal formula is commonly used, but it introduces an error of 2% when the ratio of successive areas is 0.50. Therefore, a commonly adopted rule in unitization programs is that wherever the ratio of the areas of any two successive isopach lines is smaller than 0.5, the pyramidal formula is applied. Whenever the ratio of the areas of any two successive isopach lines is found to be larger than 0.5, the trapezoidal formula is applied. Example 3.1 shows the method of calculating the volume of a gas reservoir from an isopachous map, Fig. 3.1. The volume between areas A_4 and A_5 by the trapezoidal equation is 570 ac-ft, compared with the more accurate figure of 558 ac-ft by the pyramidal equation. When the formation is rather uniformly developed and there is good well control, the error in the net bulk reservoir volume should not exceed a few percentage points.

Example 3.1. Calculating the net volume of an idealized reservoir from the isopachous map.

Given: The planimetered areas in Fig. 3.1 within each isopach line, A_0, A_1, A_2, etc., and the planimeter constant.

Example 3.1. Calculating the net volume of an idealized reservoir from the isopachous map.

Given: The planimetered areas in Fig. 3.1 within each isopach line, A_0, A_1, A_2, etc. and the planimeter constant.

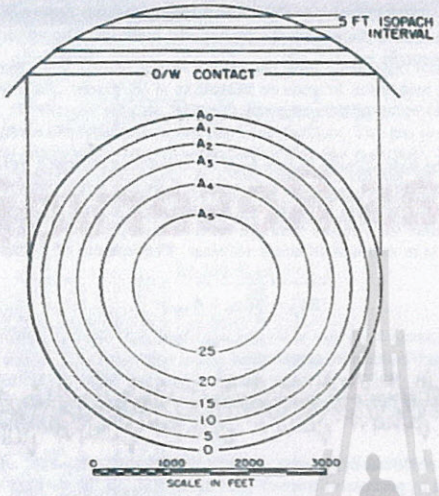

Fig. 3.1. Cross section and isopachous map of an idealized reservoir.

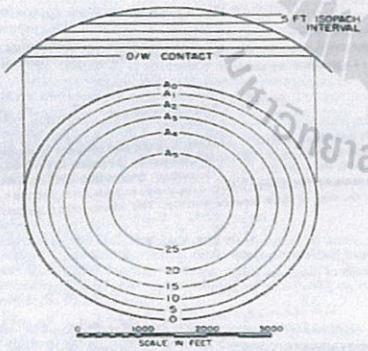

Fig. 3.1. Cross section and isopachous map of an idealized reservoir.

SOLUTION:

Productive Area	*Planimeter Area* sq in.*	*Area Acres**	*Ratio of Areas*	*Interval h, feet*	*Equation*	*ΔV ac-ft*
A_0	19.64	450				
A_1	16.34	375	0.83	5	Trap.	2063
A_2	13.19	303	0.80	5	Trap.	1695
A_3	10.05	231	0.76	5	Trap.	1335
A_4	6.69	154	0.67	5	Trap.	963[a]
A_5	3.22	74	0.48	5	Pyr.	558[b]
A_6	0.00	0	0.00	4	Pyr.	99[c]
						6713 ac-ft

* For a map scale of 1 in. = 1000 ft; 1 sq in. = 22.96 ac

[a] $\Delta V = \frac{5}{2}(231 + 154) = 963$ ac-ft

[b] $\Delta V = \frac{5}{3}(154 + 74 + \sqrt{154 \times 74}) = 558$ ac-ft

[c] $\Delta V = \frac{4}{3}(74) = 99$ ac-ft

The water in the oil- and gas-bearing parts of a petroleum reservoir above the transition zone is called *connate*, or *interstitial*, water. The two terms are used more or less interchangeably. Connate water is important primarily because it reduces the amount of pore space available to oil and gas and it also affects their recovery. It is generally not uniformly distributed throughout the reservoir but varies with the permeability and lithology as shown in Fig. 3.2 and with the height above the free water table as shown in Fig. 3.3.

Another problem in any volumetric or material balance calculation is that of obtaining the average reservoir pressure at any time after initial production. Figure 3.4 is a static reservoir pressure survey of the Jones sand in the Schuler Field.[4] Because of the large reservoir pressure gradient from east to west, some averaging technique must be used to obtain an average reservoir pressure. This can be calculated either as an average well pressure, average areal pressure, or average volumetric pressure as follows:

$$\text{Well average pressure} = \frac{\sum_{0}^{n} p_i}{n} \tag{3.4}$$

$$\text{Areal average pressure} = \frac{\sum_{0}^{n} p_i A_i}{\sum_{0}^{n} A_i} \tag{3.5}$$

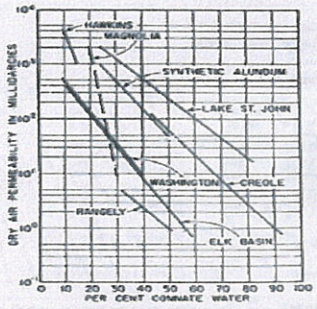

Fig. 3.2. Connate water versus permeability. (*After* Bruce and Welge,[3] Bruce Trans. AIME.)

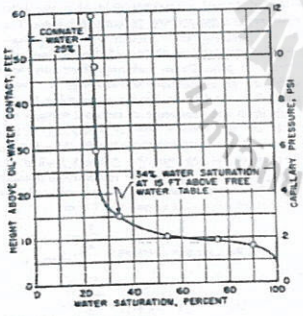

Fig. 3.3. Typical capillary pressure curve.

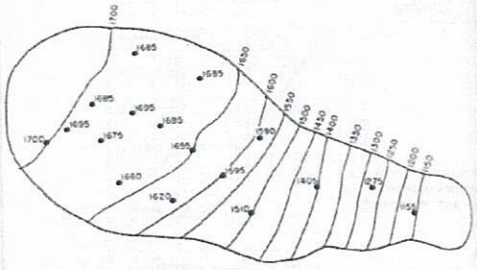

Fig. 3.4. Reservoir pressure survey showing isobaric lines drawn from the measured bottom-hole pressures. (*After* Kaveler,[4] *Trans.* AIME.)

$$\text{Well average pressure} = \frac{\sum_{0}^{n} p_i}{n} \qquad (1.16)$$

$$\text{Areal average pressure} = \frac{\sum_{0}^{n} p_i A_i}{\sum_{0}^{n} A_i} \qquad (1.17)$$

$$\text{Volumetric average pressure} = \frac{\sum_{0}^{n} p_i A_i h_i}{\sum_{0}^{n} A_i h_i} \qquad (1.18)$$

(3.6)

where n is the number of wells in Eq. (1.16) and the number of reservoir units in Eqs. (1.17) and (1.18). Because we are interested in obtaining the average pressure of the hydrocarbon contents, the volumetric average, Eq. (1.18), should be used in the volumetric and material-balance calculations. Where the pressure gradients in the reservoir are small, the average pressures obtained with Eqs. (1.16) and (1.17) will be very close to the volumetric average. Where the gradients are large there may be considerable differences. For example, the average volumetric pressure of the Jones sand survey in Fig. 1.7 is 1658 psia as compared with 1598 psia on an average well basis.

The calculations in Table 1.6 show how the average pressures are obtained. The figures in Col. (3) are the estimated drainage areas of the

3.1

Table 1.6. Calculation of Average Reservoir Pressure

Well No.	Pressure psia	Drainage Area Acres	$p \times A$	Est. Sd. Thick.	$p \times A \times h$	$A \times h$
1	2750	160	440,000	20	8,800,000	3200
2	2680	125	335,000	25	8,375,000	3125
3	2840	190	539,600	26	14,029,600	4940
4	2700	145	391,500	31	12,136,500	4495
	10,970	620	1,706,100		43,341,100	15,760

$$\text{Well average pressure} = \frac{10{,}970}{4} = 2743 \text{ psia}$$

$$\text{Areal average pressure} = \frac{1{,}706{,}100}{620} = 2752 \text{ psia}$$

$$\text{Vol metric average pressure} = \frac{43{,}341{,}100}{15{,}760} = 2750 \text{ psia}$$

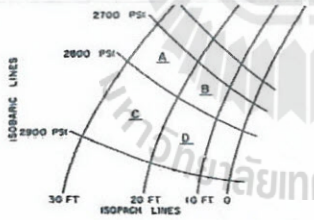

Fig. 3.5. Section of an isobaric and isopachous map.

TABLE 3.2.
Volumetric calculations of reservoir pressure

(1) Area	(2) Acres*	(3) Pressure psia	(4) h ft	(5) A × h	(6) p × A × h
A	25.5	2750	25	637.5	175,313,000
B	15.1	2750	15	226.5	62,288,000
C	50.5	2850	25	1262.5	359,813,000
D	30.2	2850	15	453.0	129,105,000
				2579.5	726,519,000

*Planimetered areas of Fig. 3.5

$$\text{Average pressure on a volume basis} = \frac{726{,}519{,}000}{2579.5}$$

$$= 2817 \text{ psia}$$

3. CALCULATION OF UNIT RECOVERY FROM VOLUMETRIC GAS RESERVOIRS

In many gas reservoirs, particularly during the development period, the bulk volume is not known. In this case it is better to place the reservoir calculations on a unit basis, usually 1 ac-ft of bulk reservoir rock. Then one unit, or 1 ac-ft, of bulk reservoir rock contains:

Connate water: $43{,}560 \times \phi \times S_w$ cu ft

Reservoir gas volume: $43{,}560 \times \phi\,(1 - S_w)$ cu ft

TABLE 3.2.
Volumetric calculations of reservoir pressure

(1) Area	(2) Acres*	(3) Pressure psia	(4) h ft	(5) A × h	(6) p × A × h
A	25.5	2750	25	637.5	175,313,000
D	15.1	2750	15	226.5	62,288,000
C	50.5	2850	25	1262.5	359,813,000
D	30.2	2850	15	453.0	129,105,000
				2579.5	726,519,000

*Planimetered areas of Fig. 3.5

$$\text{Average pressure on a volume basis} = \frac{726{,}519{,}000}{2579.5}$$

$$= 2817 \text{ psia}$$

3. CALCULATION OF UNIT RECOVERY FROM VOLUMETRIC GAS RESERVOIRS

In many gas reservoirs, particularly during the development period, the bulk volume is not known. In this case it is better to place the reservoir calculations on a unit basis, usually 1 ac-ft of bulk reservoir rock. Then one unit, or 1 ac-ft, of bulk reservoir rock contains:

Connate water: $43{,}560 \times \phi \times S_w$ cu ft

Reservoir gas volume: $43{,}560 \times \phi\,(1 - S_w)$ cu ft

Reservoir pore volume: $43{,}560 \times \phi$ cu ft

The initial standard cubic feet of gas in place in the unit is:

$$G = \frac{43{,}560\,(\phi)(1 - S_w)}{B_g} \text{ SCF/ac-ft} \qquad (3.7)$$

G is in standard cubic feet when the gas volume factor B_g is in cubic feet per standard cubic foot Eq. (1.17). The *standard* conditions are those used in the calculation of the gas volume factor, and they may be changed to any other standard by means of the ideal gas law. The porosity ϕ is expressed as a fraction of the bulk volume, and the initial connate water S_w as a fraction of the pore volume. For a reservoir under volumetric control, there is no change in the interstitial water, so the *reservoir* gas volume remains the same. If B_{gi} is the gas volume factor at the abandonment pressure, then the standard cubic feet of gas remaining at abandonment is:

$$G_a = \frac{43{,}560\,(\phi)(1 - S_w)}{B_{gi}} \text{ SCF/ac-ft} \qquad (3.8)$$

Unit recovery is the difference between the initial gas in place and that remaining at abandonment pressure (i.e., that produced at abandonment pressure), or:

$$\text{Unit recovery} = 43{,}560(\phi)(1 - S_w)\left[\frac{1}{B_g} - \frac{1}{B_{gi}}\right] \text{ SCF/ac-ft} \qquad (3.9)$$

The unit recovery is also called the *initial unit reserve*, which is generally lower than the initial unit in-place gas. The remaining reserve at any stage of depletion is the difference between this initial reserve and the unit production at that stage of depletion. The fractional recovery or recovery factor expressed as a percentage of the initial in-place gas is

$$\text{Recovery factor} = \frac{100(G - G_a)}{G} = \frac{100\left[\frac{1}{B_g} - \frac{1}{B_{gi}}\right]}{\frac{1}{B_g}}\% \qquad (3.10)$$

or

$$\text{Recovery factor} = 100\left[1 - \frac{B_g}{B_{gi}}\right]$$

Experience with volumetric gas reservoirs indicates that the recoveries will range from 80 to 90%. Some gas pipeline companies use an abandonment pressure of 100 psi per 1000 ft of depth.

The gas volume factor in the Bell Gas Field at initial reservoir pressure is 0.00533 cu ft/SCF and at 500 psia it is 0.03623. The initial unit reserve or unit recovery based on volumetric performance at an abandonment pressure of 500 psia is

$$\text{Unit recovery} = 43{,}560 \times 0.22 \times (1 - 0.23) \times \left[\frac{1}{0.00533} - \frac{1}{0.03623}\right]$$

$$= 1180\text{M SCF/ac-ft}$$

$$\text{Recovery factor} = 100\left[1 - \frac{0.00533}{0.03623}\right]$$

$$= 85\%$$

These recovery calculations are valid provided the unit neither drains nor is drained by adjacent units.

4. CALCULATION OF UNIT RECOVERY FROM GAS RESERVOIRS UNDER WATER DRIVE

Under initial conditions one unit (1 ac-ft) of bulk reservoir rock contains

Connate water: $43{,}560 \times \phi \times S_w$ cu ft

Reservoir gas volume: $43{,}560 \times \phi \times (1 - S_w)$ cu ft

Surface units of gas: $43{,}560 \times \phi \times (1 - S_w) \div B_{gi}$ SCF

In many reservoirs under water drive, the pressure suffers an initial decline, after which water enters the reservoir at a rate to equal the production, and the pressure stabilizes. In this case the stabilized pressure is the abandonment pressure. If B_{gi} is the gas volume factor at the abandonment pressure and S_{gr} is the *residual* gas saturation, expressed as a fraction of the pore volume, after water invades the unit, then under abandonment conditions a unit (1 ac-ft) of the reservoir rock contains

Water volume: $43{,}560 \times \phi \times (1 - S_{gr})$ cu ft

Reservoir gas volume: $43{,}560 \times \phi \times S_{gr}$ cu ft

Surface units of gas: $43{,}560 \times \phi \times S_{gr} \div B_{gi}$ SCF

Unit recovery is the difference between the initial and the residual surface units of gas, or:

$$\text{Unit recovery in SCF/ac-ft} = 43{,}560\,(\phi)\left[\frac{1 - S_{wi}}{B_{gi}} - \frac{S_{gr}}{B_{gi}}\right] \qquad (3.11)$$

The recovery factor expressed in a percentage of the initial gas in place is

$$\text{Recovery factor} = \frac{100\left[\frac{1-S_{wi}}{B_{gi}} - \frac{S_{gr}}{B_{gs}}\right]}{\left[\frac{1-S_{wi}}{B_{gi}}\right]} \qquad (3.12)$$

Suppose the Bell Gas Field is produced under a water drive such that the pressure stabilizes at 1500 psia. If the residual gas saturation is 24% and the gas volume factor at 1500 psia is 0.01122 cu ft/SCF, then the initial unit *reserve* or unit recovery is

Partial water drive

$$\text{Unit recovery} = 43{,}560 \times 0.22 \times \left[\frac{(1-0.23)}{0.00533} - \frac{0.24}{0.0112}\right]$$

$$= 1180 \text{ M SCF/ac-ft}$$

Initial pressure = 3250 psia
Abandonment pressure = 1500 psia

The recovery factor under these conditions is

$$\text{Recovery factor} = \frac{100\left[\frac{1-0.23}{0.00533} - \frac{0.24}{0.0112}\right]}{\left[\frac{1-0.23}{0.00533}\right]} = 85\%$$

Under these particular conditions, the recovery by water drive is the same as the recovery by volumetric depletion, illustrated in Sect. 3. If the water drive is very active so that there is essentially no decline in reservoir pressure, unit recovery and the recovery factor become

$$\text{Unit recovery} = 43{,}560 \times \phi \times (1 - S_{wi} - S_{gr}) \div B_g \text{ SCF/ac-ft} \qquad (3.13)$$

$$\text{Recovery factor} = \frac{100(1 - S_{wi} - S_{gr})}{(1 - S_{wi})} \epsilon_E \qquad (3.14)$$

vary active water drive

For the Bell Gas Field, assuming a residual gas saturation of 24%:

$$\text{Unit recovery} = 43{,}560 \times 0.22 \times (1 - 0.23 - 0.24) \div 0.00533$$

$$= 953 \text{ M SCF/ac-ft}$$

Abandonment pressure = 3250 psia

$$\text{Recovery factor} = \frac{100(1 - 0.23 - 0.24)}{(1 - 0.23)}$$

$$= 69\%$$

Because the residual gas saturation is independent of the pressure, the recov-

The residual gas saturation can be measured in the laboratory on representative core samples. Table 3.3 gives the residual gas saturations that were measured on core samples from a number of producing horizons and on some synthetic laboratory samples. The values, which range from 16 to 50% and average near 30%, help to explain the disappointing recoveries obtained in some water-drive reservoirs. For example, a gas reservoir with an initial water saturation of 30% and a residual gas saturation of 35% has a recovery factor of only 50% if produced under an active water drive (i.e., where the reservoir pressure stabilizes near the initial pressure). When the reservoir permeability is uniform, this recovery factor should be representative, except for a correction to allow for the efficiency of the drainage pattern and water coning or fingering. When there are well-defined continuous beds of higher and lower permeability, the water will advance more rapidly through the more permeable beds so that when a gas well is abandoned owing to excessive water production, considerable unrecovered gas remains in the less permeable beds. Because of these factors, it may be concluded that generally gas recoveries by water drive are lower than by volumetric depletion; however, the same conclusion does not apply to oil recovery, which is discussed separately. Water-drive gas reservoirs do have the advantage of maintaining higher flowing wellhead pressures and higher well rates compared with depletion gas reservoirs. This is due, of course, to the maintenance of higher reservoir pressure as a result of the water influx.

TABLE 3.3.
Residual gas saturation after water flood as measured on core plugs
(After Geffen, Parish, Haynes, and Morse.)*

Porous Material	*Formation*	*Residual Gas Saturation, Percentage of Pore Space*	*Remarks*
Unconsolidated sand		16	(13-ft Column)
Slightly consolidated sand (synthetic)		21	(1 Core)
Synthetic consolidated materials	Selas Porcelain	17	(1 Core)
	Norton Alundum	24	(1 Core)
Consolidated sandstones	Wilcox	25	(3 Cores)
	Frio	30	(1 Core)
	Nellie Bly	30–36	(12 Cores)
	Frontier	31–34	(3 Cores)
	Springer	33	(3 Cores)
	Frio	30–38	(14 Cores)
		(Average 34.6)	
	Torpedo	34–37	(6 Cores)
	Tensleep	40–50	(4 Cores)
Limestone	Canyon Reef	50	(2 Cores)

Average residual gas = 0.30 or 30%

In calculating the gas reserve of a particular lease or unit, the gas that can be recovered by the well(s) on the lease is important rather than the total recoverable gas *initially* underlying the lease, some of which may be recovered by adjacent wells. In volumetric reservoirs where the recoverable gas beneath each lease (well) is the same, the recoveries will be the same only if all wells are produced at the same rate. On the other hand, if wells are produced at equal rates when the gas beneath the leases (wells) varies, as from variable formation thickness, the initial gas reserve of the lease where the formation is thicker will be less than the initial recoverable gas underlying the lease.

In water-drive gas reservoirs, when the pressure stabilizes near the initial reservoir pressure, the lowest well on structure will divide its initial recoverable gas with all updip wells in line with it. For example, if three wells in line along the dip are drilled at the updip edge of their units, which are presumed equal, and if they all produce at the same rate, the lowest well on structure will recover approximately one-third of the gas initially underlying it. If the well is drilled further downstructure near the center of the unit, it will recover still less. If the pressure stabilizes at some pressure below the initial reservoir pressure, the recovery factor will be improved for the wells low on structure. Example 3.2 shows the calculation of the initial gas reserve of a 160-acre unit by volumetric depletion, partial water drive, and complete water drive.

Example 3.2. Calculating the initial gas reserve of a 160-acre unit of the Bell Gas Field by volumetric depletion and under partial and complete water drive.

Given:

Average porosity = 22%

Connate water = 23%

Residual gas saturation after water displacement = 34%

$B_{gi} = 0.00533$ cu ft/SCF at $p_i = 3250$ psia

$B_g = 0.00667$ cu ft/SCF at 2500 psia

$= 0.03623$ cu ft/SCF at 500 psia

Area = 160 acres

Net productive thickness = 40 ft

SOLUTION:

Pore volume $= 43{,}560 \times 0.22 \times 160 \times 40 = 61.33 \times 10^6$ cu ft

Initial gas in place:

$G_i = 61.33 \times 10^6 \times (1 - 0.23) \div 0.00533 = 8860$ MM SCF

Gas in place after volumetric depletion to 2500 psia:

$$G_2 = 61.33 \times 10^6 \times (1 - 0.23) \div 0.00667 = 7080 \text{ MM SCF}$$

Gas in place after volumetric depletion to 500 psia:

$$G_3 = 61.33 \times 10^6 \times (1 - 0.23) \div 0.03623 = 1303 \text{ MM SCF}$$

Gas in place after water invasion at 3250 psia:

$$G_4 = 61.33 \times 10^6 \times 0.34 \div 0.00533 = 3912 \text{ MM SCF}$$

Gas in place after water invasion at 2500 psia:

$$G_5 = 61.33 \times 10^6 \times 0.34 \div 0.00667 = 3126 \text{ MM SCF}$$

Initial reserve by depletion to 500 psia:

$$G_1 - G_3 = (8860 - 1303) \times 10^6 = 7557 \text{ MM SCF}$$

Initial reserve by water drive at 3250 psia:

$$G_1 - G_4 = (8860 - 3912) \times 10^6 = 4948 \text{ MM SCF}$$

Initial reserve by water drive at 2500 psia:

$$(G_1 - G_5) = (8860 - 3126) \times 10^6 = 5734 \text{ MM SCF}$$

If there is one undip well, the initial reserve by water drive at 3250 psia is

$$\tfrac{1}{2}(G_1 - G_4) = \tfrac{1}{2}(8860 - 3912) \times 10^6 = 2474 \text{ MM SCF}$$

The recovery factors calculate to be 85%, 65%, and 56% for the cases of no water drive, partial water drive, and full water drive, respectively. These recoveries are fairly typical and can be explained in the following way. As water invades the reservoir, the reservoir pressure is maintained at a higher level than if there were no water encroachment. This leads to higher abandonment pressures for water-drive reservoirs. Because the main mechanism of production in a gas reservoir is that of depletion, or gas expansion, recoveries are lower, as shown in Ex. 3.2.

Gas in place after volumetric depletion to 2500 psia:

$$G_2 = 61.33 \times 10^6 \times (1 - 0.23) \div 0.00667 = 7080 \text{ MM SCF}$$

Gas in place after volumetric depletion to 500 psia:

$$G_3 = 61.33 \times 10^6 \times (1 - 0.23) \div 0.03623 = 1303 \text{ MM SCF}$$

Gas in place after water invasion at 3250 psia:

$$G_4 = 61.33 \times 10^6 \times 0.34 \div 0.00533 = 3912 \text{ MM SCF}$$

Gas in place after water invasion at 2500 psia:

$$G_5 = 61.33 \times 10^6 \times 0.34 \div 0.00667 = 3126 \text{ MM SCF}$$

Initial reserve by depletion to 500 psia:

$$G_1 - G_3 = (8860 - 1303) \times 10^6 = 7557 \text{ MM SCF}$$

Initial reserve by water drive at 3250 psia:

$$G_1 - G_4 = (8860 - 3912) \times 10^6 = 4948 \text{ MM SCF}$$

Initial reserve by water drive at 2500 psia:

$$(G_1 - G_5) = (8860 - 3126) \times 10^6 = 5734 \text{ MM SCF}$$

If there is one undip well, the initial reserve by water drive at 3250 psia is

$$\tfrac{1}{2}(G_1 - G_4) = \tfrac{1}{2}(8860 - 3912) \times 10^6 = 2474 \text{ MM SCF}$$

The recovery factors calculate to be 85%, 65%, and 56% for the cases of no water drive, partial water drive, and full water drive, respectively. These recoveries are fairly typical and can be explained in the following way. As water invades the reservoir, the reservoir pressure is maintained at a higher level than if there were no water encroachment. This leads to higher abandonment pressures for water-drive reservoirs. Because the main mechanism of production in a gas reservoir is that of depletion, or gas expansion, recoveries are lower, as shown in Ex. 3.2.

In water-drive gas reservoirs, when the pressure stabilizes near the initial reservoir pressure, the lowest well on structure will divide its initial recoverable gas with all updip wells in line with it. For example, if three wells in line along the dip are drilled at the updip edge of their units, which are presumed equal, and if they all produce at the same rate, the lowest well on structure will recover approximately one-third of the gas initially underlying it. If the well is drilled farther downstructure near the center of the unit, it will recover still less. If the pressure stabilizes at some pressure below the initial reservoir pressure, the recovery factor will be improved for the wells low on structure. Example 3.2 shows the calculation of the initial gas reserve of a 160-acre unit by volumetric depletion, partial water drive, and complete water drive.

Gas in place after volumetric depletion to 2500 psia:

$$G_2 = 61.33 \times 10^6 \times (1 - 0.23) \div 0.00667 = 7080 \text{ MM SCF}$$

Gas in place after volumetric depletion to 500 psia:

$$G_3 = 61.33 \times 10^6 \times (1 - 0.23) \div 0.03623 = 1303 \text{ MM SCF}$$

Gas in place after water invasion at 3250 psia:

$$G_4 = 61.33 \times 10^6 \times 0.34 \div 0.00533 = 3912 \text{ MM SCF}$$

Gas in place after water invasion at 2500 psia:

$$G_5 = 61.33 \times 10^6 \times 0.34 \div 0.00667 = 3126 \text{ MM SCF}$$

Initial reserve by depletion to 500 psia:

$$G_1 - G_3 = (8860 - 1303) \times 10^6 = 7557 \text{ MM SCF}$$

Initial reserve by water drive at 3250 psia:

$$G_1 - G_4 = (8860 - 3912) \times 10^6 = 4948 \text{ MM SCF}$$

Initial reserve by water drive at 2500 psia:

$$(G_1 - G_5) = (8860 - 3126) \times 10^6 = 5734 \text{ MM SCF}$$

If there is one undip well, the initial reserve by water drive at 3250 psia is

$$\tfrac{1}{2}(G_1 - G_4) = \tfrac{1}{2}(8860 - 3912) \times 10^6 = 2474 \text{ MM SCF}$$

The recovery factors calculate to be 85%, 65%, and 56% for the cases of no water drive, partial water drive, and full water drive, respectively. These recoveries are fairly typical and can be explained in the following way. As water invades the reservoir, the reservoir pressure is maintained at a higher level than if there were no water encroachment. This leads to higher abandonment pressures for water-drive reservoirs. Because the main mechanism of production in a gas reservoir is that of depletion, or gas expansion, recoveries are lower, as shown in Ex. 3.2.

Agarwal, Al-Hussainy, and Ramey conducted a theoretical study and showed that gas recoveries increased with increasing production rates from [illegible] the water has been attempted in the field and has been found to be successful. Matthes, Jackson, Schuler, and Marudiak showed that ultimate recovery increased from 69 to 74% by increasing the field production rate from 50 to 75 MM SCF/D in the Bierwang Field in West Germany.[7] Lutes, Chiang, Brady, and Rossen reported an 8.5% increase in ultimate recovery with an increased production rate in a strong water-drive Gulf Coast gas reservoir.[8]

A second technique used in the field is the coproduction technique discussed by Arcaro and Bassiouni.[9] The coproduction technique is defined as the simultaneous production of gas and water. In the coproduction process, as downdip wells begin to be watered out, they are converted to high-rate water production wells, while the updip wells are maintained on gas production. This technique enhances the production of gas by several methods. First, the high-rate downdip water wells act as a pressure sink for the water because the water is drawn to these wells. This retards the invasion of water into productive gas zones in the reservoir, therefore prolonging the useful productive life to these zones. Second, the high-rate production of water lowers the average pressure in the reservoir, allowing for more gas expansion and therefore more gas production. Third, when the average reservoir pressure is lowered, immobile gas in the water-swept portion of the reservoir could become mobile. The coproduction technique performs best before the reservoir is totally invaded by water. Arcaro and Bassiouni reported the improvement of gas production from 62% to 83% from the Louisiana Gulf Coast Eugene Island Block 305 Reservoir by using the coproduction technique instead of the conventional production approach. Water-drive reservoirs are discussed in much more detail in Chapter 8.

5. MATERIAL BALANCE

In the previous sections, the initial gas in place was calculated on a unit basis of 1 ac-ft of bulk productive rock from a knowledge of the porosity and connate water. To calculate the initial gas in place on any particular portion of a reservoir, it is necessary to know, in addition, the bulk volume of that portion of the reservoir. If the porosity, connate water, and/or the bulk volumes are not known with any reasonable precision, the methods described cannot be used. In this case, the material balance method may be used to calculate the initial gas in place; however, this method is applicable only to the reservoir as a whole, because of the migration of gas from one portion of the reservoir to another in both volumetric and water-drive reservoirs.

The general material balance equation for a gas reservoir was derived in Chapter 2.

$$G(B_g - B_{gi}) + GB_{gi}\left[\frac{c_w S_{wi} + c_f}{1 - S_{wi}}\right]\Delta\bar{p} + W_e = G_p B_g + B_w W_p \qquad (2.10)$$

than the formation and water compressibilities, and the left-hand side of Eq. (2.10) becomes negligible

$$G(B_g - B_{gi}) + GB_{gi}\left[\frac{c_w S_{wi} + c_f}{1 - S_{wi}}\right]\Delta\bar{p} + W_e = G_p B_g + B_w W_p \qquad (2.10)$$

$$GB_{gi}\left[\frac{c_w S_{wi} + c_f}{1 - S_{wi}}\right] + G(B_g - B_{gi}) + W_e = G_p B_g + B_w W_p \qquad (3.15)$$

When reservoir pressures are abnormally high, this term is not negligible and should not be ignored. This situation is discussed in a later section of this chapter.

When there is neither water encroachment into nor water production from a reservoir of interest, the reservoir is said to be *volumetric*. For a volumetric gas reservoir, Eq. (3.15) reduces to:

$$G(B_g - B_{gi}) = G_p B_g \qquad (3.16)$$

Using Eq. (1.16) and substituting expressions for B_g and B_{gi} into Eq. (3.16), the following is obtained.

$$G\left(\frac{p_{sc} z T}{T_{sc} p}\right) - G\left(\frac{p_{sc} z_i T_i}{T_{sc} p_i}\right) = G_p\left(\frac{p_{sc} z T}{T_{sc} p}\right) \qquad (3.17)$$

Noting that production is essentially an isothermal process (i.e., the reservoir temperature remains constant), then Eq. (3.17) is reduced to:

$$G\left(\frac{z}{p}\right) - G\left(\frac{z_i}{p_i}\right) = G_p\left(\frac{z}{p}\right)$$

Rearranging:

$$\frac{p}{z} = -\frac{p_i}{z_i G} G_p + \frac{p_i}{z_i} \qquad (3.18)$$

Because p_i, z_i, and G are constants for a given reservoir, Eq. (3.18) suggests that a plot of p/z as the ordinate versus G_p as the abscissa would yield a straight line with:

$$\text{slope} = -\frac{p_i}{z_i G}$$

$$y \text{ intercept} = \frac{p_i}{z_i}$$

This plot is shown in Fig. 3.6.

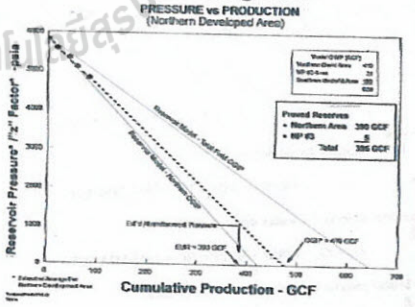

Rearranging:

$$\frac{p}{z} = -\frac{p_i}{z_i G} G_p + \frac{p_i}{z_i} \qquad (3.18)$$

Because p_i, z_i, and G are constants for a given reservoir, Eq. (3.18) suggests that a plot of p/z as the ordinate versus G_p as the abscissa would yield a straight line with:

$$\text{slope} = -\frac{p_i}{z_i G}$$

$$y \text{ interecept} = \frac{p_i}{z_i}$$

This plot is shown in Fig. 3.6.

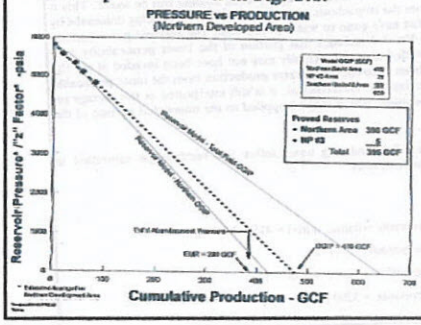

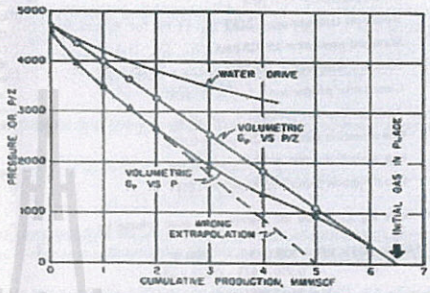

Fig. 3.6. Comparison of theoretical values of p and p/z plotted versus cumulative production from a volumetric gas reservoir.

Equation (2.10) could have been derived by applying the law of conservation of mass to the reservoir and associated production.

For most gas reservoirs, the gas compressibility term is much greater than the formation and water compressibilities, and the second term on the left-hand side of Eq. (2.10) becomes negligible

$$G(B_g - B_{gi}) + W_e = G_p B_g + B_w W_p \qquad (3.15)$$

When reservoir pressures are abnormally high, this term is not negligible and should not be ignored. This situation is discussed in a later section of this chapter.

When there is neither water encroachment into nor water production from a reservoir of interest, the reservoir is said to be *volumetric*. For a volumetric gas reservoir, Eq. (3.15) reduces to:

$$G(B_g - B_{gi}) = G_p B_g \qquad (3.16)$$

Using Eq. (1.16) and substituting expressions for B_g and B_{gi} into Eq. (3.16), the following is obtained:

$$G\left(\frac{p_{sc} z T}{T_{sc} p}\right) - G\left(\frac{p_{sc} z_i T_i}{T_{sc} p_i}\right) = G_p\left(\frac{p_{sc} z T}{T_{sc} p}\right) \qquad (3.17)$$

Noting that production is essentially an isothermal process (i.e., the reservoir temperature remains constant), then Eq. (3.17) is reduced to:

$$G\left(\frac{z}{p}\right) - G\left(\frac{z_i}{p_i}\right) = G_p\left(\frac{z}{p}\right)$$

Rearranging:

$$\frac{p}{z} = -\frac{p_i}{z_i G} G_p + \frac{p_i}{z_i} \qquad (3.18)$$

Because p_i, z_i, and G are constants for a given reservoir, Eq. (3.18) suggests that a plot of p/z as the ordinate versus G_p as the abscissa would yield a straight line with:

$$\text{slope} = -\frac{p_i}{z_i G}$$

$$y \text{ interecept} = \frac{p_i}{z_i}$$

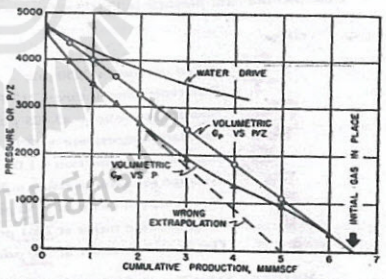

Fig. 3.6. Comparison of theoretical values of p and p/z plotted versus cumulati production from a volumetric gas reservoir.

If p/z is set equal to zero, which would represent the production of the gas from a reservoir, then the corresponding G_p equals G, the initial g in place. The plot could also be extrapolated to any abandonment p/z to fi the initial reserve. Usually this extrapolation requires at least three years accurate pressure depletion and gas production data.

Figure 3.6 also contains a plot of cumulative gas production G_p vers pressure. As indicated by Eq. (3.18), this is not linear, and extrapolatio from the pressure-production data may be in considerable error. Because t minimum value of the gas deviation factor generally occurs near 2500 psia, t extrapolations will be low for pressures above 2500 psia and high for pressur below 2500 psia. Equation (3.18) may be used graphically as shown in Fig. 3 to find the initial gas in place or the reserves at any pressure for any selecte abandonment pressure. For example, at 1000 psia (or p/z = 1220) abando ment pressure, the initial reserve is 4.85 MMM SCF. At 2500 psia (or p/z 3130), the (remaining) reserve is 4.85 less 2.20—that is, 2.65 MMM SCF.

In water-drive reservoirs, the relation between G_p and p/z is not linea as can be seen by an inspection of Eq. (3.15) and (3.18). Because of the wat influx, the pressure drops less rapidly with production than under volumetr control, as shown in the upper curve of Fig. 3.6. Consequently, the extrap lation technique described for volumetric reservoirs is not applicable. Als where there is water influx, the initial gas in place calculated at successiv stages of depletion, assuming no water influx, takes on successively high

Equation (3.15) may be expressed in terms of the initial pore volume, V_i, by recognizing that $V_i = GB_{gi}$ and using Eq. (1.16) for B_g and B_{gi}:

$$V_i\left[\frac{z_i T}{P_i}\frac{P V_i}{Z_i T} - 1\right] = \frac{Z_i T}{P_i}\frac{P_{sc} G_p}{T_{sc}} + B_w W_p - W_e \qquad (3.19)$$

For volumetric reservoirs, this equation can be reduced and rearranged to give:

$$\frac{P_{sc} G_p}{T_{sc}} = \frac{P V_i}{z_i T} - \frac{P V_i}{z_i T} \qquad (3.20)$$

The following three example problems illustrate the use of the various equations that we have described in gas reservoir calculations.

Example 3.3. Calculating the initial gas in place and the initial reserve of a gas reservoir from pressure-production data for a volumetric reservoir. Note that the base pressure is 15.025 psia.

Given:

Initial pressure = 3250 psia
Reservoir temperature = 213°F
Standard pressure = 15.025 psia
Standard temperature = 60°F
Cumulative production = 1.00×10^9 SCF
Average reservoir pressure = 2864 psia
Gas deviation factor at 3250 psia = 0.910
Gas deviation factor at 2864 psia = 0.888
Gas deviation factor at 500 psia = 0.951

SOLUTION: Solve Eq. (3.20) for the reservoir gas pore volume V_i:

$$\frac{15.025 \times 1.00 \times 10^9}{520} = \frac{3250 \times V_i}{0.910 \times 673} - \frac{2864\ V_i}{0.888 \times 673}$$

$$V_i = 56.17 \text{ MM cu ft}$$

The initial gas in place by the real gas law is:

$$G = \frac{p_i V_i}{z_i T} \times \frac{T_{sc}}{p_{sc}} = \frac{3250 \times 56.17 \times 10^6 \times 520}{0.910 \times 673 \times 15.025}$$

$$= 10.32 \text{ MMM SCF}$$

The gas remaining at 500 psia abandonment pressure is:

$$G_a = \frac{p_a V_i}{z_a T} \times \frac{T_{sc}}{p_{sc}} = \frac{500 \times 56.17 \times 10^6 \times 520}{0.951 \times 673 \times 15.025}$$

$$= 1.52 \text{ MMM SCF}$$

The initial gas reserve based on a 500 psia abandonment pressure is the difference between the initial gas in place and the gas remaining at 500 psia, or:

$$G_r = G - G_a = (10.32 - 1.52) \times 10^9$$

$$= 8.80 \text{ MMM SCF}$$

Example 3.4 illustrates the use of equations to calculate the water influx when the initial gas in place is known. It also shows the method of estimating the residual gas saturation of the portion of the reservoir invaded by water, at which time a reliable estimate of the invaded volume can be made. This is calculated from the isopachous map, the invaded volume being dilineated by those wells that have gone to water production. The residual gas saturation calculated in Ex. 3.4 includes that portion of the lower permeability rock within the invaded area that actually may not have been invaded at all, the wells having been "drowned" by water production from the more permeable beds of the formation. Nevertheless, it is still interpreted as the *average* residual gas saturation, which may be applied to the uninvaded portion of the reservoir.

Example 3.4 Calculating water influx and residual gas saturation in water-drive gas reservoirs.

Given:

Bulk reservoir volume, initial = 415.3 MM cu ft
Average porosity = 0.172
Average connate water = 0.25
Initial pressure = 3200 psia

Example 3.3. Calculating the initial gas in place and the initial reserve of a gas reservoir from pressure-production data for a volumetric reservoir. Note that the base pressure is 15.025 psia.

Given:

Initial pressure = 3250 psia
Reservoir temperature = 213°F
Standard pressure = 15.025 psia
Standard temperature = 60°F
Cumulative production = 1.00×10^9 SCF
Average reservoir pressure = 2864 psia
Gas deviation factor at 3250 psia = 0.910
Gas deviation factor at 2864 psia = 0.888
Gas deviation factor at 500 psia = 0.951

SOLUTION: Solve Eq. (3.20) for the reservoir gas pore volume V_i:

$$\frac{15.025 \times 1.00 \times 10^9}{520} = \frac{3250 \times V_i}{0.910 \times 673} - \frac{2864\ V_i}{0.888 \times 673}$$

$$V_i = 56.17 \text{ MM cu ft}$$

The initial gas in place by the real gas law is:

$$G = \frac{p_i V_i}{z_i T} \times \frac{T_{sc}}{p_{sc}} = \frac{3250 \times 56.17 \times 10^6 \times 520}{0.910 \times 673 \times 15.025}$$

$$= 10.32 \text{ MMM SCF}$$

The gas remaining at 500 psia abandonment pressure is:

$$G_a = \frac{p_a V_i}{z_a T} \times \frac{T_{sc}}{p_{sc}} = \frac{500 \times 56.17 \times 10^6 \times 520}{0.951 \times 673 \times 15.025}$$

$$= 1.52 \text{ MMM SCF}$$

The initial gas reserve based on a 500 psia abandonment pressure is the difference between the initial gas in place and the gas remaining at 500 psia, or:

$$G_r = G - G_a = (10.32 - 1.52) \times 10^9$$

$$= 8.80 \text{ MMM SCF}$$

Example 3.4 Calculating water influx and residual gas saturation in water-drive gas reservoirs.

Given:

Bulk reservoir volume, initial = 415.3 MM cu ft
Average porosity = 0.172
Average connate water = 0.25
Initial pressure = 3200 psia

B_{gi} = 0.005262 cu ft/SCF, 14.7 psia and 60°F
Final pressure = 2925 psia
B_g = 0.005700 cu ft/SCF, 14.7 psia and 60°F
Cumulative water production = 15,200 bbl (surface)
B_w = 1.03 bbl/surface bbl
G_p = 935.4 MM SCF at 14.7 psia and 60°F
Bulk volume invaded by water at 2925 psia = 13.04 MM cu ft

SOLUTION:

$$\text{Initial gas in place} = G = \frac{415.3 \times 10^6 \times 0.172 \times (1 - 0.25)}{0.005262}$$

$$= 10{,}180 \text{ MM SCF at 14.7 psia and 60°F}$$

Substitute in Eq. (3.15) to find W_e: $G(B_g - B_{gi}) + W_e = G_p B_g + B_w W_p$

$$W_e = 935.4 \times 10^6 \times 0.005700 - 10{,}180 \times 10^6 (0.005700 - 0.005262) + 15{,}200 \times 1.03 \times 5.615$$

$$= 960{,}400 \text{ cu ft}$$

This much water has invaded 13.04 MM cu ft of bulk rock that initially contained 25% connate water. Then the final water saturation of the flooded portion of the reservoir is

$$S_w = \frac{\text{Connate water} + \text{Water influx} - \text{Produced water}}{\text{Pore space}}$$

$$= \frac{(13.04 \times 10^6 \times 0.172 \times 0.25) + 960{,}400 - 15{,}200 \times 1.03}{13.04 \times 10^6 \times 0.172}$$

$$= 0.67 \text{ or } 67\%$$

Then the residual gas saturation S_{gr} is 33%.

B_{gi} = 0.005262 cu ft/SCF, 14.7 psia and 60°F
Final pressure = 2925 psia
B_g = 0.005700 cu ft/SCF, 14.7 psia and 60°F
Cumulative water production = 15,200 bbl (surface)
B_w = 1.03 bbl/surface bbl
G_p = 935.4 MM SCF at 14.7 psia and 60°F
Bulk volume invaded by water at 2925 psia = 13.04 MM cu ft

SOLUTION:

$$\text{Initial gas in place} = G = \frac{415.3 \times 10^6 \times 0.172 \times (1 - 0.25)}{0.005262}$$

$$= 10{,}180 \text{ MM SCF at 14.7 psia and 60°F}$$

Substitute in Eq. (3.15) to find W_e:

$$W_e = 935.4 \times 10^6 \times 0.005700 - 10{,}180 \times 10^6 (0.005700 - 0.005262) + 15{,}200 \times 1.03 \times 5.615$$

$$= 960{,}400 \text{ cu ft}$$

This much water has invaded 13.04 MM cu ft of bulk rock that initially contained 25% connate water. Then the final water saturation of the flooded portion of the reservoir is

$$S_w = \frac{\text{Connate water} + \text{Water influx} - \text{Produced water}}{\text{Pore space}}$$

$$= \frac{(13.04 \times 10^6 \times 0.172 \times 0.25) + 960{,}400 - 15{,}200 \times 1.03}{13.04 \times 10^6 \times 0.172}$$

$$= 0.67 \text{ or } 67\%$$

Then the residual gas saturation S_{gr} is 33%.

Example 3.5. Using the p/z plot to estimate cumulative gas production. A dry gas reservoir contains gas of the following composition:

	Mole Fraction
Methane	0.75
Ethane	0.20
n-Hexane	0.05

The initial reservoir pressure was 4200 psia, with a temperature of 180°F. The reservoir has been producing for some time. Two pressure surveys have been made at different times.

p/z (psia)	G_p (MMM SCF)
4600	0
3700	1
2800	2

(a) What will be the cumulative gas produced when the average reservoir pressure has dropped to 2000 psia?
(b) Assuming the reservoir rock has a porosity of 12%, the water saturation is 30%, and the reservoir thickness is 15 ft, how many acres does the reservoir cover?

SOLUTION:

		P_c	T_c	YP_c	YT_c
Methane	0.75	673.1	343.2	504.8	257.4
Ethane	0.20	708.3	504.8	141.7	110.0
n-Hexane	0.05	440.1	914.2	22.0	45.7
Totals				668.5	413.1

(a) To get G_p at 2000 psia, calculate z and the p/z. Use pseudocritical properties.

$$p_r = \frac{2000}{668.5} = 2.99$$

$$T_r = \frac{640}{413.1} = 1.55$$

$$z = 0.8$$

$$p/z = \frac{2000}{0.8} = 2500$$

A linear regression of the data plotted in Fig. 3.7 yields the following equation for the best straight line through the data:

$$p/z = -9(10)^{-7} G_p + 4600$$

Substituting a value of $p/z = 2500$ in this equation yields:

$$2500 = -9(10)^{-7} G_p + 4600$$

$$G_p = 2.33(10)^9 \text{ SCF} \quad \text{or} \quad 2.33 \text{ MMM SCF}$$

B_w = 0.005262 cu ft/SCF, 14.7 psia and 60°F

Final pressure = 2925 psia

B_g = 0.005700 cu ft/SCF, 14.7 psia and 60°F

Cumulative water production = 15,200 bbl (surface)

B_w = 1.03 bbl/surface bbl

G_p = 935.4 MM SCF at 14.7 psia and 60°F

Bulk volume invaded by water at 2925 psia = 13.04 MM cu ft

SOLUTION:

$$\text{Initial gas in place} = G = \frac{415.3 \times 10^6 \times 0.172 \times (1 - 0.25)}{0.005262}$$

$$= 10{,}180 \text{ MM SCF at 14.7 psia and 60°F}$$

Substitute in Eq. (3.15) to find W_e:

$$W_e = 935.4 \times 10^6 \times 0.005700 - 10{,}180 \times 10^6 (0.005700 - 0.005262) + 15{,}200 \times 1.03 \times 5.615$$

$$= 960{,}400 \text{ cu ft}$$

This much water has invaded 13.04 MM cu ft of bulk rock that initially contained 25% connate water. Then the final water saturation of the flooded portion of the reservoir is

$$S_w = \frac{\text{Connate water} + \text{Water influx} - \text{Produced water}}{\text{Pore space}}$$

$$= \frac{(13.04 \times 10^6 \times 0.172 \times 0.25) + 960{,}400 - 15{,}200 \times 1.03}{13.04 \times 10^6 \times 0.172}$$

$$= 0.67 \text{ or } 67\%$$

Then the residual gas saturation S_g is 33%.

Example 3.5. Using the *p/z* plot to estimate cumulative gas production. A dry gas reservoir contains gas of the following composition:

	Mole Fraction
Methane	0.75
Ethane	0.20
n-Hexane	0.05

Example 3.5. Using the *p/z* plot to estimate cumulative gas production. A dry gas reservoir contains gas of the following composition:

	Mole Fraction
Methane	0.75
Ethane	0.20
n-Hexane	0.05

The initial reservoir pressure was 4200 psia, with a temperature of 180°F. The reservoir has been producing for some time. Two pressure surveys have been made at different times.

p/z (psia)	G_p (MMM SCF)
4600	0
3700	1
2800	2

(a) What will be the cumulative gas produced when the average reservoir pressure has dropped to 2000 psia?

(b) Assuming the reservoir rock has a porosity of 12%, the water saturation is 30%, and the reservoir thickness is 15 ft, how many acres does the reservoir cover?

SOLUTION:

		P_c	T_c	YP_c	YT_c
Methane	0.75	673.1	343.2	504.8	257.4
Ethane	0.20	708.3	504.8	141.7	110.0
n-Hexane	0.05	440.1	914.2	22.0	45.7
Totals				668.5	413.1

(a) To get G_p at 2000 psia, calculate z and the p/z [illegible] pseudocritical

Example 3.5. Using the p/z plot to estimate cumulative gas production. A dry gas reservoir contains gas of the following composition:

	Mole Fraction
Methane	0.75
Ethane	0.20
n-Hexane	0.05

The initial reservoir pressure was 4200 psia, with a temperature of 180°F. The reservoir has been producing for some time. Two pressure surveys have been made at different times.

p/z (psia)	G_p (MMM SCF)
4600	0
3700	1
2800	2

(a) What will be the cumulative gas produced when the average reservoir pressure has dropped to 2000 psia?

(b) Assuming the reservoir rock has a porosity of 12%, the water saturation is 30%, and the reservoir thickness is 15 ft, how many acres does the reservoir cover?

SOLUTION:

		P_c	T_c	YP_c	YT_c
Methane	0.75	673.1	343.2	504.8	257.4
Ethane	0.20	708.3	504.8	141.7	110.0
n-Hexane	0.05	440.1	914.2	22.0	45.7
Totals				668.5	413.1

(a) To get G_p at 2000 psia, calculate z and the p/z. [illegible] pseudocritical properties.

$$p_r = \frac{2000}{668.5} = 2.99$$

$$T_r = \frac{640}{413.1} = 1.55$$

$$z = 0.8$$

$$p/z = \frac{2000}{0.8} = 2500$$

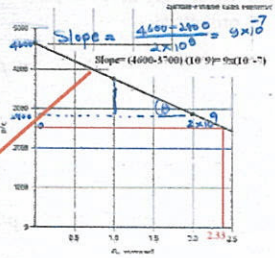

A linear regression of the data plotted in Fig. 3.7 yields the following equation for the best straight line through the data:

$$p/z = -9(10)^{-7}G_p + 4600$$

Substituting a value of $p/z = 2500$ in this equation yields:

$$2500 = -9(10)^{-7}G_p + 4600$$

$$G_p = 2.33(10)^9 \text{ SCF} \quad \text{or} \quad 2.33 \text{ MMM SCF}$$

Example 3.5. Using the p/z plot to estimate cumulative gas production. A dry gas reservoir contains gas of the following composition:

	Mole Fraction
Methane	0.75
Ethane	0.20
n-Hexane	0.05

The initial reservoir pressure was 4200 psia, with a temperature of 180°F. The reservoir has been producing for some time. Two pressure surveys have been made at different times.

p/z (psia)	G_p (MMM SCF)
4600	0
3700	1
2800	2

(a) What will be the cumulative gas produced when the average reservoir pressure has dropped to 2000 psia?

(b) Assuming the reservoir rock has a porosity of 12%, the water saturation is 30%, and the reservoir thickness is 15 ft, how many acres does the reservoir cover?

SOLUTION:

		P_c	T_c	YP_c	YT_c
Methane	0.75	673.1	343.2	504.8	257.4
Ethane	0.20	708.3	504.8	141.7	110.0
n-Hexane	0.05	440.1	914.2	22.0	45.7
Totals				668.5	413.1

(a) To get G_p at 2000 psia, calculate z and the p/z. [illegible] pseudocritical properties.

$$p_r = \frac{2000}{668.5} = 2.99$$

$$T_r = \frac{640}{413.1} = 1.55$$

$$z = 0.8$$

$$p/z = \frac{2000}{0.8} = 2500$$

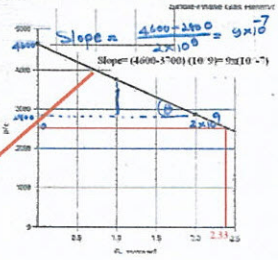

A linear regression of the data plotted in Fig. 3.7 yields the following equation for the best straight line through the data:

$$p/z = -9(10)^{-7}G_p + 4600$$

Substituting a value of $p/z = 2500$ in this equation yields:

$$2500 = -9(10)^{-7}G_p + 4600$$

$$G_p = 2.33(10)^9 \text{ SCF} \quad \text{or} \quad 2.33 \text{ MMM SCF}$$

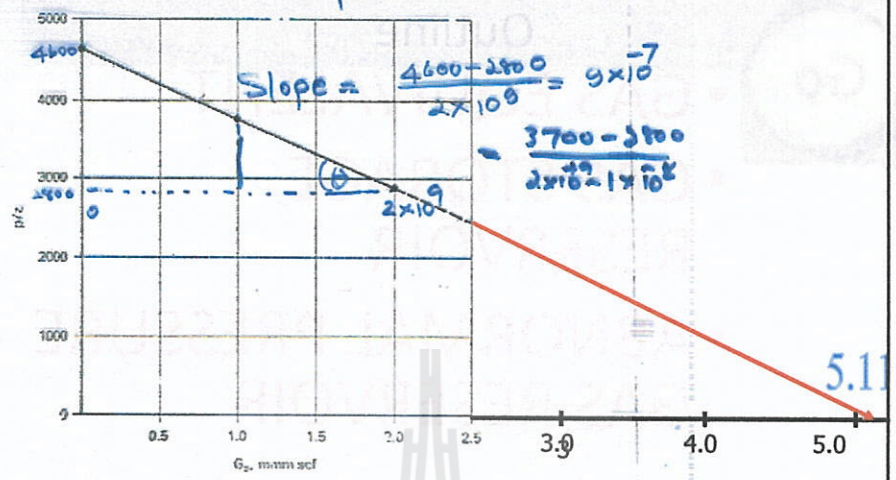

Fig. 3.7. p/z versus G_p for Ex. 3.5.

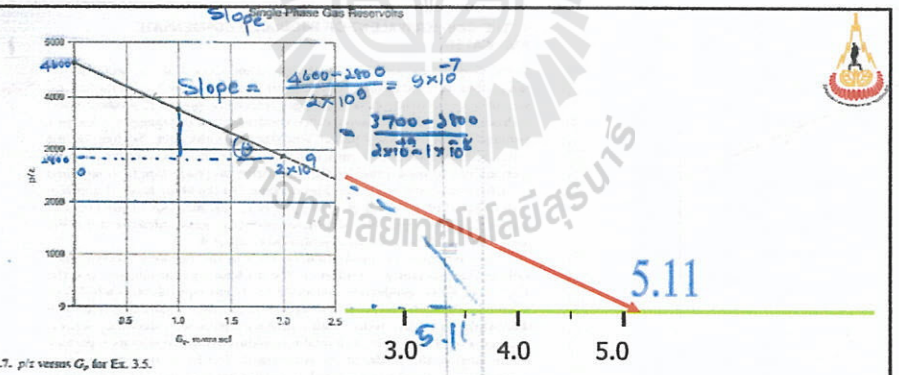

Fig. 3.7. p/z versus G_p for Ex. 3.5.

(b) Substituting a value of $p/z = 0$ into the straight-line equation, would yield the amount of produced gas if all of the initial gas were produced; therefore, the G_p at this p/z is equal to the initial gas in place.

$$0 = -9(10)^{-7}G_p + 4600$$

$$G_p\,(p/z = 0) = G = 5.11(10)^9 \text{ SCF} \quad \text{or} \quad 5.11 \text{ MMM SCF}$$

Recognizing that $V_i = GB_{gi}$ and that $B_g = 0.02829\ (z/p)T$:

$$V_i = GB_{gi} = 5.11(10)^9\left[\frac{0.02829(180+460)}{4600}\right] = 20.1(10)^6 \text{ cu ft}$$

also

$$V_i = Ah\phi(1 - S_w) = \text{Acre-ft}$$

$$A = \frac{20.1(10)^6}{15(0.12)(1-0.30)} = 15.55(10)^6 \text{ ft}^2 \quad \text{or} \quad 366 \text{ acres}$$

Outline

- GAS EQUIVALENT
- GAS STORAGE RESERVOIR
- ABNORMAL PRESSURE GAS RESERVOIR

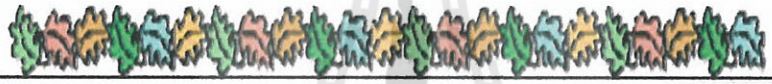

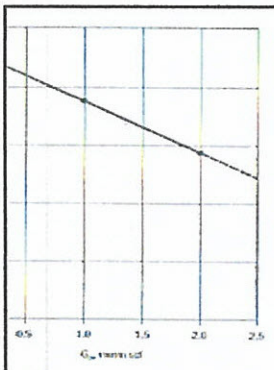

Eq. 3.5.

$p/z = 0$ into the straight-line equation, would yield
ood gas if all of the initial gas were produced; there-
/z is equal to the initial gas in place.

$$9(10)^7 G_{pi} + 4600$$

$$= 5.11(10)^9 \text{ SCF} \quad \text{or} \quad 5.11 \text{ MMM SCF}$$

T_{sc} and that $B_{gi} = 0.02829\,(z/p)T$:

$$(10)^9 \left[\frac{0.02829(180 + 460)}{4600}\right] = 20.1(10)^6 \text{ cu ft}$$

3

6. THE GAS EQUIVALENT OF PRODUCED CONDENSATE AND WATER

In the study of gas reservoirs in the preceding section, it was implicitly assumed that the fluid in the reservoir at all pressures as well as on the surface was in a *single* (gas) phase. Most gas reservoirs, however, produce some hydrocarbon liquid, commonly called condensate, in the range of a few to a hundred or more barrels per million standard cubic feet. So long as the reservoir fluid remains in a single (gas) phase, the calculations of the previous sections may be used, provided the cumulative gas production G_p is modified to include the condensate liquid production. On the other hand, if a hydrocarbon liquid phase develops in the reservoir, the methods of the previous sections are not applicable, and these *retrograde*, gas-condensate reservoirs must be treated specially, as described in Chapter 4.

The reservoir gas production G_p used in the previous sections must include the separator gas production, the stock tank gas production, and the stock tank liquid production converted to its gas equivalent, symbol GE. Figure 3.8 illustrates two common separation schemes. Figure 3.8(a) shows a three-stage separation system with a primary separator, a secondary separator, and a stock tank. The well fluid is introduced into the primary separator where most of the produced gas is obtained. The liquid from the primary separator is then sent to the secondary separator where an additional amount of gas is obtained. The liquid from the secondary separator is then flashed into the stock tank. The liquid from the stock tank is N_p and any gas from the stock tank is added to the primary and secondary gas to arrive at the total produced surface gas, $G_{p(sc)}$. Figure 3.8(b) shows a two-stage separation process similar to the one shown in Fig. 3.8(a) without the secondary separator.

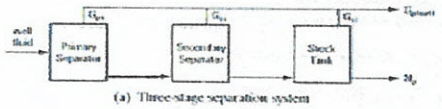

(a) Three-stage separation system

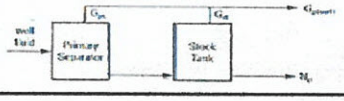

The produced hydrocarbon liquid is converted to its gas equivalent, assuming it behaves as an ideal gas when vaporized in the produced gas. Taking 14.7 psia and 60°F as standard conditions, the gas equivalent of one stock tank barrel of condensate liquid is:

$$GE = V = \frac{nR'T_{sc}}{p_{sc}} = \frac{350.5\gamma_o(10.73)(520)}{M_{wo}(14.7)} = 133{,}000\frac{\gamma_o}{M_{wo}} \qquad (3.21)$$

The gas equivalent of one barrel of condensate of specific gravity of 0.780 (water = 1.00) and molecular weight 138 is 752 SCF. The specific gravity may be calculated from the API gravity. If the molecular weight of the condensate is not measured, as by the freezing point depression method, it may be estimated using Eq. (3.22).

$$M_{wo} = \frac{5954}{^\circ API - 8.811} = \frac{42.43\gamma_o}{1.008 - \gamma_o} \qquad (3.22)$$

The total gas equivalent for N_p STB of condensate production is $GE(N_p)$. The total reservoir gas production, G_p, is given by Eq. (3.23) for a three-stage separation system and by Eq. (3.24) for a two-stage separation system:

$$G_p = G_{p(sep)} + GE(N_p) = G_{gs} + G_{gt} + G_{gr} + GE(N_p) \qquad (3.23)$$

$$G_p = G_{p(sep)} + GE(N_p) = G_{gs} + G_{gt} + GE(N_p) \qquad (3.24)$$

If the gas volumes from the low-pressure separators and the stock tank are not measured, then the correlations found in Figs. 3.9 and 3.10 can be used to estimate the vapor equivalent of these gas volumes plus the gas equivalent of the liquid condensate. Figure 3.9 is for a three-stage separator system, and Fig. 3.10 is for a two-stage separator system. The correlations are based on production parameters that are routinely measured (i.e., the primary separator pressure, temperature, and gas gravity), the secondary separator temperature, and the stock tank liquid gravity. The total reservoir gas production, G_p, is given by Eq. (3.25) when using the correlations of Figs. 3.9 and 3.10.

$$G_p = G_{gr} + V_{wp}(N_p) \qquad (3.25)$$

When water is produced on the surface as a condensate from the gas phase in the reservoir, it is fresh water and should be converted to a gas equivalent and added to the gas production. Since the specific gravity of water is 1.00 and its molecular weight is 18, its gas equivalent is

$$GE_w = \frac{nR'T_{sc}}{p_{sc}} = \frac{350.5 \times 1.00}{18} \times \frac{10.73 \times 520}{14.7}$$
$$= 7390 \text{ SCF/surface barrel}$$

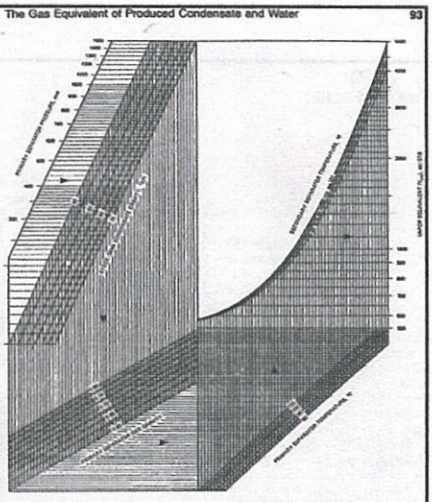

Fig. 3.9. Vapor-Equivalent Nomograph for Three-Stage Separation Systems. (*After* Gold, McCain, and Jennings.[20])

Studies by McCarthy, Boyd, and Reid indicate that the water vapor content of reservoir gases at usual reservoir temperatures and usual *initial* reservoir pressures is in the range of a fraction of one barrel per million standard cubic feet of gas.[18] Production data from a Gulf Coast gas reservoir show a production of 0.64 barrel of water per million standard cubic feet compared with a reservoir *content* of about 1.00 bbl/MM SCF using the data of McCarthy, Boyd, and Reid. The difference is presumably that water remaining in the vapor state at separator temperature and pressure, most of which must be removed by dehydration to a level of about six *pounds* per million standard

Gas reservoirs as storage reservoir

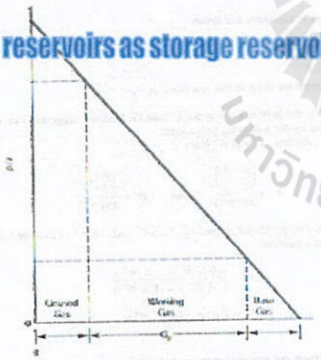

Fig. 3.11. p/z plot showing different types of gas in a gas storage reservoir.

and production simply run up and down the p/z versus G_p curve between the pressure limits just discussed.

In certain applications, the use of the delta pressure concept may be advantageous.[17] The *delta pressure* is defined as the pressure at maximum storage minus the initial reservoir pressure. Under the right conditions, an amount of gas larger than the initial gas in place can be achieved. This again is dictated by the economics of the given situation.

Hollis presented an interesting case history of the considerations involved in changing the Rough Gas Field in the North Sea over to a storage reservoir.[4] Considerations in the design of storage and deliverability rates included the probability of a severe winter occurring in the demand area. A severe winter was given a probability of 1 in 50 of happening. Hollis concluded that the differences between offshore and onshore storage facilities are owing mainly to economics and the integrated planning that must take place in offshore development.

Storage is a useful application of gas reservoirs. We encourage you to pursue the references for more detailed information if it becomes necessary.

9. ABNORMALLY PRESSURED GAS RESERVOIRS

Normal pressure gradients observed in gas reservoirs are in the range of 0 to 0.5 psia per foot of depth. Reservoirs with abnormal pressures may ha gradients as high as 0.7 to 1.0 psia per foot of depth.[15,16,17,18] Bernard h reported that over 300 gas reservoirs have been discovered in the offshore G Coast alone with initial gradients in excess of 0.65 psia per foot of depth formations over 10,000 feet deep.[15]

When the water and formation compressibility term in the mater balance equation can be ignored, the normal p/z behavior for a volumetric g reservoir plots a straight line versus cumulative gas produced (Fig. 3.6, Se 5). This is not the case for an abnormally pressured gas reservoir, as can b seen in Figure 3.12, which illustrates the p/z behavior for this type of reservoi

For an abnormally pressured volumetric reservoir, the p/z plot is straight line during the early life of production, but then it usually curv downward during the later stages of production. If the early data are used extrapolate for G or for an abandonment G_a, the extrapolation can yie significant errors.

To explain the curvature in the p/z plot for abnormally pressured reservoirs, Harville and Hawkins postulated a "rock collapse" theory that used high rock compressibility at abnormally high pressures and a reduced ro compressibility at normal reservoir pressures.[15] However, working with no

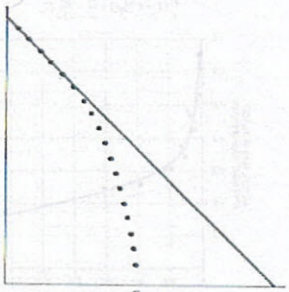

Fig. 3.12. p/z plot illustrating nonlinear behavior of abnormally pressured reservoi

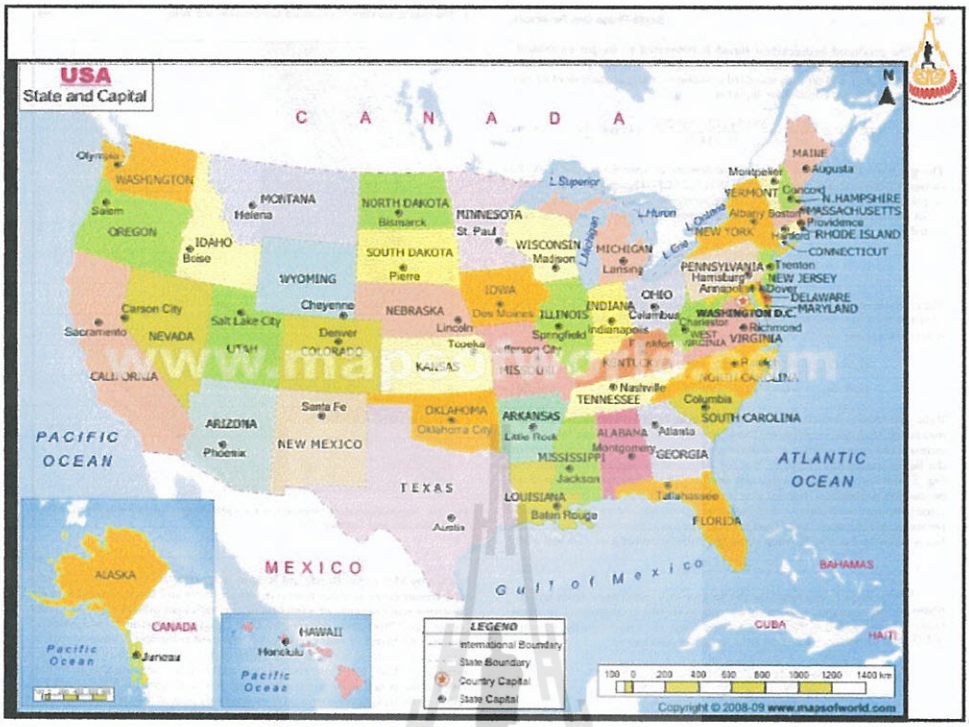

samples taken from abnormally pressured reservoirs, Jogi, Gray, Ashman, and Thompson and Sinha, Holland, Borsheel, and Schatz reported rock compressibilities measured at high pressures in the order of 2 to 5 (10) $^{-6}$ psi $^{-1}$.[19,20] These values are representative of typical values at low pressures and suggest that rock compressibilities do not change with pressure. Ramagost and Farshad showed that in some cases the p/z data could be adjusted to yield straight-line behavior by including the water and formation compressibility term.[21] Bourgoyne, Hawkins, Lavaquial, and Wickenhauser suggested that the nonlinear behavior could be due to water influx from shales.[22]

Bernard has proposed a method of analyzing the p/z curve for abnormally pressured reservoirs to determine initial gas in place and gas reserve as a function of abandonment p/z.[18] The method uses two approaches. The first involves the early production life when the p/z plot exhibits linear behavior. Bernard developed a correlation for actual gas in place as a function of apparent gas in place as shown in Fig. 3.13.

The apparent gas in place is obtained by extrapolating the early, linear p/z data. Then, by entering Figure 3.13 with the apparent value of the gas in place, the ratio of actual gas in place to apparent gas in place can be obtained. The correlation appears to be reasonably accurate for the reservoirs that Bernard studied. For later production times, when the p/z data exhibit nonlinear behavior, Bernard defined a constant C' according to Eq. (3.26)

$$\frac{p}{z}(1 - C'\Delta p) = \frac{p_i}{z_i} - \frac{p_i}{z_i G} G_p \tag{3.26}$$

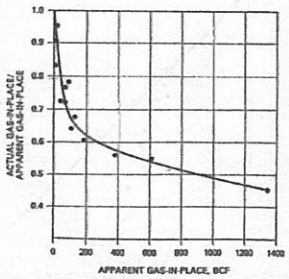

Fig. 3.13. Correction for initial gas in place. (*After* Bernard.[18])

where

C' = constant

Δp = total pressure drop in the reservoir, $p_i - p$

In Eq. (3.26), the only unknowns are C' and G. Bernard suggested that they can be found by the following procedure:

First, calculate A' and B' from:

$$A' = \frac{\left(\frac{p}{z} - \frac{p_i}{z_i}\right)}{\Delta p\left(p/z\right)} \quad \text{and} \quad B' = \frac{\left(\frac{p_i}{z_i}\right) G_p}{\Delta p\left(p/z\right)}$$

If there are n data points for p/z and G_p, then C' and G can be calculated from the following equations:

$$G = \frac{\Sigma B' \Sigma\, B' ln - \Sigma\,(B' ln)}{\Sigma\, A' B' - \Sigma\, A' \Sigma\, B' ln}$$

$$C' = \Sigma A' ln + \left(\frac{1}{G}\right) \Sigma\, B' ln$$

9. LIMITATIONS OF EQUATIONS AND ERRORS

The precision of the reserve calculations by the volumetric method depends on the accuracy of the data that enter the computations. The precision of the initial gas in place depends on the probable errors in the averages of the porosity, connate water, pressure, and gas deviation factor, and in the error in the determination of the bulk productive volume. With the best of core and log data in rather uniform reservoirs, it is doubtful that the initial gas in place can be calculated more accurately than about 5%, and the figure will range upward to 100% or higher depending on the uniformity of the reservoir and the quantity and quality of the data available.

The reserve is the product of the gas in place and the recovery factor. For volumetric reservoirs, the reserve of the reservoir as a whole, for any selected abandonment pressure, should be known to about the same precision as the initial gas in place. Water-drive reservoirs require, in addition, the estimate of the volume of the reservoir invaded at abandonment and the average residual gas saturation. When the reservoir exhibits permeability stratification, the difficulties are increased, and the accuracy is therefore reduced. In general, reserve calculations are more accurate for volumetric than for water-drive reservoirs. When the reserves are placed on a well or lease basis, the accuracy may be reduced further because of lease drainage, which occurs in both volumetric and water-drive reservoirs.

The use of the material balance equation to calculate gas in place involves the terms of the gas volume factor. The precision of the calculations is

MATERIAL BALANCE LIMITATIONS

1.METERINGACCURACY=1%

2.ΔP>.05G or 5%

Table B1 - Gas-in-Place Estimates

METERINGACCURACY=0.05%OR.0005

Δp (psi)	cf (1/psi)	GIP (Gscf)	Comments
7.70	6x10-6	433	No communication wit Nam Phong 2
4.47	6x10-6	744	90% confidence interval
10.93	6x10-6	304	90% confidence interval
7.70	6x10-5	249	High formation compressibility
6.00	6x10-6	565	Communication with Nam Phong 2 Includes gas volume of both wells

ΔP= 6460-6452.3=7.7

ΔP= 6460*0.9995-6452.3=4.47

ΔP= 6460*1.0005-6452.3=10.93

Values for other variables used in the equation:

Gp	: 0.3267 Gscf
z	: 1.140082
Δz/Δp	: 0.0000707/psi
S_w	: 0.25
c_w	: 0.0000034/psi

ΔP>=.0075G or 0.075%

Reservoir Engineering I, 2012
HW NO 3; Due date: Friday, June 29, 2012.

Chapter 3; 3.2, 3.4, 3.9, 3.12, 3.15

- ANSWERS TO THE PROBLEMS

- 3.2; (a) 4038 psia, (b) 0.9; 249 SCF/cu.ft., (.c) 33.8 MMM SCF

- 3.4; (a) 433 x 106 cu.ft., (b) 2.43 MMM lb., (.c) 48.9 MMM SCF (d) 29.3 MMM SCF, (e) 32 psi , (f) 24.8 MMM SCF@ 750 psia abandonment pressure.
- 3.9; (a) 289 MMM SCF , (b) 1000 Acres, (.c) 22.8 MM bbl

- 3.12; (a) 1.83 MMM SCF , (b) 17.1 yrs, (.c) 67.24% (d) 24.24%

- 3.15; 6.134 MM SCF (use Mo = 6084/(API-5.9) formula to get this number)

7. CHAPTER 4 GAS-CONDENSATE RESERVOIR
5-6th WEEK, 22 June -8 JULY 2012

Table 2. Classification of Reservoir Fluids: GOR, Oil and Gas Gravities

	GOR (scf/bbl)	API Gravity (°API)	Gas Gravity (air = 1)
Wet gas	15–100,000	50–70	0.65–0.85
Condensed gas	3–15,000	50–70	0.65–0.85
Volatile oil	3,000	40–50	0.65–0.85
Non-volatile oil	100–2,500	30–40	0.80–0.90
Heavy oil	0	10–30	
Tar/bitumen	0	<10	

Table 3. Classification of Reservoir Fluids: Composition (mol% C_n)

Hydrocarbon	C_1	C_2	C_3	C_4	C_5	C_{6+}
Dry gas	88	4	4	1	1	1
Condensate	71	8	5	5	4	7
Volatile oil	60	8	5	4	3	20
Nonvolatile oil	41	3	5	5	4	42
Heavy oil	11	3	1	1	4	80
Tar/bitumen						100

Table 4. C_7, Fraction, Oil FVF and Color of Typical Reservoir Fluids

	Nonvolatile Oil	Volatile Oil	Condensate Gas	Wet Gas	Dry Gas
Phase system	Bubblepoint	Bubblepoint	Dewpoint	Dewpoint	No change
C_{7+}	> 20%	20–12.5%	< 12.5%	< 4%	< 0.8%
B_o† at P_b‡	< 2	> 2	–	–	–
Color	Dark	Colored	Light color	Clear, white	No liquid

†B_o oil formation volume factor
‡P_b bubblepoint pressure

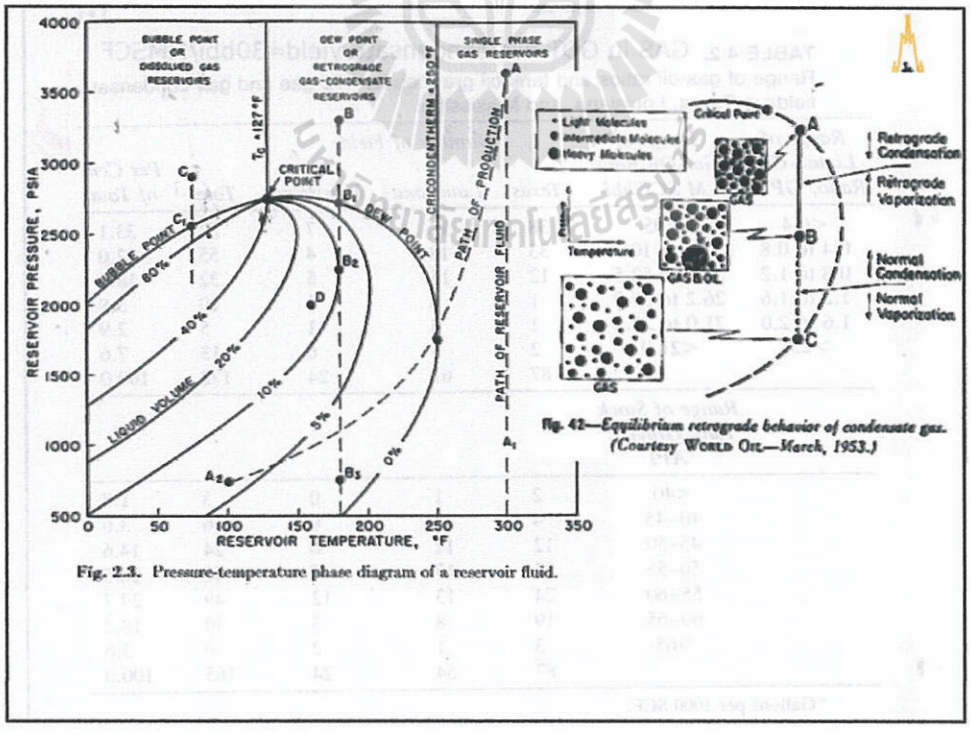

Fig. 42—Equilibrium retrograde behavior of condensate gas. (Courtesy World Oil.—March, 1953.)

Fig. 2.3. Pressure-temperature phase diagram of a reservoir fluid.

GAS-CONDENSATE RESERVOIR

TABLE 4.1.
Mole composition and other properties of typical single-phase reservoir fluids

Component	*Black Oil* LKU	*Volatile Oil*	*Gas-Condensate*	*Dry Gas* WET	*Gas* SATUN
C_1	48.83 **54**	64.36	87.07	95.85	86.67 **70**
C_2	2.75 **4**	7.52	4.39	2.67	7.77 **10**
C_3	1.93 **2**	4.74	2.29	0.34	2.95 **6**
C_4	1.60 **1**	4.12	1.74	0.52	1.73 **1.3**
C_5	1.15 **1**	2.97	0.83	0.08	0.88 **1.1**
C_6	1.59 **3**	1.38	0.60	0.12	**0.1**
C_7^+	42.15 **42**	14.91	3.80	0.42	**0.5**
	100.00	100.00	100.00	100.00	100.00
Mol. wt. C_7^+	225	181	112	157	
GOR, SCF/bbl	625	2000	18,200	105,000	Inf. **33000**
Tank gravity, °API	34.3	50.1	60.8	54.7	**50-54**
Liquid color	Greenish black	Medium orange	Light straw	Water white	

TABLE 4.2. GAS in GOT has condensate yield=30bbl/MMSCF
Range of gas-oil ratios and tank oil gravities for 172 gas and gas-condensate fields in Texas, Louisiana, and Mississippi

Range of Liquid-Gas Ratio, GPM[a]	*Range of Gas-Oil Ratio M SCF/bbl*	*Number of Fields* *Texas*	*Louisiana*	*Mississippi*	*Total*	*Per Cent of Total*
<0.4	>105	38	12	7	57	33.1
0.4 to 0.8	52.5 to 105	33	18	4	55	32.0
0.8 to 1.2	35.0 to 52.5	12	15	5	32	18.6
1.2 to 1.6	26.2 to 35.0	1	8	1	10	5.8
1.6 to 2.0	21.0 to 26.2	1	3	1	5	2.9
>2.0	<21.0	2	5	6	13	7.6
		87	61	24	172	100.0
	Range of Stock Tank Gravity, °API					
	<40	2	1	0	3	1.8
	40–45	4	2	0	6	3.6
	45–50	12	12	0	24	14.6
	50–55	23	17	7	47	28.5
	55–60	24	13	12	49	29.7
	60–65	19	8	3	30	18.2
	>65	3	1	2	6	3.6
		87	54	24	165	100.0

[a] Gallons per 1000 SCF.

average specific gravity (air = 1.00) of the total well fluid, which is presumably being produced initially from a one-phase reservoir. Consider the two-stage separation system shown in Fig. 3.8. The average specific gravity of the total well fluid is given by Eq. (4.1):

$$\gamma_w = \frac{R_1\gamma_1 + 4602.\gamma_o + R_3\gamma_3}{R_1 + \dfrac{133{,}316\gamma_o}{M_{wo}} + R_3} \qquad (4.1)$$

where,

R_1, R_3—producing gas-oil ratios from the separator (1) and stock tank (3)

γ_1, γ_3—specific gravities of separator and stock tank gases

γ_o—specific gravity of the stock tank oil (water = 1.00). This is given by:

$$\gamma_o = \frac{141.5}{\rho_{o,API} + 131.5} \qquad (4.2)$$

M_{wo}—molecular weight of the stock tank oil that is given by Eq. (3.22):

$$M_{wo} = \frac{5954}{\rho_{o,API} - 8.811} = \frac{42.43\gamma_o}{1.008 - \gamma_o} \qquad (3.22)$$

$$\gamma_o = \frac{141.5}{\rho_{o,API} + 131.5} \qquad (4.2)$$

M_{wo}—molecular weight of the stock tank oil that is given by Eq. (3.22):

$$M_{wo} = \frac{5954}{\rho_{o,API} - 8.811} = \frac{42.43\gamma_o}{1.008 - \gamma_o} \qquad (3.22)$$

Example 4.1 shows the use of Eq. (4.1) to calculate the initial gas and oil in place per acre-foot of a gas-condensate reservoir from the usual production data. The three example problems in this chapter represent the type of calculations that an engineer would perform on data generated from laboratory tests on reservoir fluid samples from gas-condensate systems. Sample reports containing additional example calculations may be obtained from commercial laboratories which conduct PVT studies. The engineer dealing with gas-condensate reservoirs should obtain these sample reports to supplement the material in this chapter. The gas deviation factor at initial reservoir temperature and pressure is estimated from the gas gravity of the recombined oil and gas as shown in Chapter 1. From the estimated gas deviation factor and the reservoir temperature, pressure, porosity, and connate water, the moles of hydrocarbons per acre-foot can be calculated, and from this the initial gas and oil in place.

Example 4.1. Calculate the initial oil and gas in place per acre-foot for a gas-condensate reservoir.

Given:

Initial pressure	2740 psia
Reservoir temperature	215°F
Average porosity	25%
Average connate water	30%
Daily tank oil	242 STB
Oil gravity, 60°F	48.0°API
Daily separator gas	3100 MCF
Separator gas gravity	0.650
Daily tank gas	120 MCF
Tank gas gravity	1.20

SOLUTION:

$$\gamma_o = \frac{141.5}{48.0 + 131.5} = 0.788$$

$$M_{wo} = \frac{5954}{\rho_{o,API} - 8.811} = \frac{5954}{48.0 - 8.811} = 151.9$$

$$R_1 = \frac{3{,}100{,}000}{242} = 12{,}810$$

$$R_3 = \frac{120{,}000}{242} = 496$$

$$\gamma_w = \frac{12{,}180(0.650) + 4602.(0.788) + 496(1.20)}{12{,}810 + \dfrac{133{,}316(0.788)}{151.9} + 496} = 0.896$$

From Fig. 1.4, $T_c = 423°R$ and $p_c = 637$ psia. Then $T_r = 1.60$ and $p_r = 4.30$, from which, using Fig. 1.5, the gas deviation factor is 0.825 at the initial conditions. Then the total initial gas in place per acre-foot of bulk reservoir is

$$G = \frac{379.4\,pV}{zR'T} = \frac{379.4(2740)(43560)(0.25)(1-0.30)}{0.825(10.73)(675)} = 1326\ MCFlac\text{-}ft$$

Because the volume fraction equals the mole fraction in the gas state, the fraction of the total produced on the surface as gas is

$$f_g = \frac{n_g}{n_g + n_o} = \frac{\dfrac{R_1}{379.4} + \dfrac{R_3}{379.4}}{\dfrac{R_1}{379.4} + \dfrac{R_3}{379.4} + \dfrac{350\gamma_o}{M_{wo}}} \qquad (4.3)$$

$$f_g = \frac{\dfrac{12{,}810}{379.4} + \dfrac{496}{379.4}}{\dfrac{12{,}810}{379.4} + \dfrac{496}{379.4} + \dfrac{350(0.788)}{151.9}} = 0.951$$

Example 4.1. Calculate the initial oil and gas in place per acre-foot for a gas-condensate reservoir.

Given:

Initial pressure	2740 psia
Reservoir temperature	215°F
Average porosity	25%
Average connate water	30%
Daily tank oil	242 STB
Oil gravity, 60°F	48.0°API
Daily separator gas	3100 MCF
Separator gas gravity	0.650
Daily tank gas	120 MCF
Tank gas gravity	1.20

SOLUTION:

$$\gamma_o = \frac{141.5}{48.0 + 131.5} = 0.788$$

$$M_{ao} = \frac{5954}{\rho_{o,API} - 8.811} = \frac{5954}{48.0 - 8.811} = 151.9$$

$$R_1 = \frac{3{,}100{,}000}{242} = 12{,}810$$

$$R_2 = \frac{120{,}000}{242} = 496$$

$$\gamma_a = \frac{12{,}180(0.650) + 4602.(0.788) + 496(1.20)}{12{,}810 + \dfrac{133{,}316(0.788)}{151.9} + 496} = 0.896$$

From Fig. 1.4, $T_r = 423°R$ and $p_r = 637$ psia. Then $T_r = 1.60$ and $p_r = 4.30$, from which, using Fig. 1.5, the gas deviation factor is 0.825 at the initial conditions. Then the total initial gas in place per acre-foot of bulk reservoir is

$$G = \frac{379.4\,pV}{zR'T} = \frac{379.4(2740)(43560)(0.25)(1 - 0.30)}{0.825(10.73)(675)} = 1326\ MCF/ac\text{-}ft$$

Because the volume fraction equals the mole fraction in the gas state, the fraction of the total produced on the surface as gas is

$$f_g = \frac{n_g}{n_g + n_o} = \frac{\dfrac{R_1}{379.4} + \dfrac{R_2}{379.4}}{\dfrac{R_1}{379.4} + \dfrac{R_2}{379.4} + \dfrac{350\gamma_o}{M_{ao}}} \qquad (4.3)$$

$$f_g = \frac{\dfrac{12{,}810}{379.4} + \dfrac{496}{379.4}}{\dfrac{12{,}810}{379.4} + \dfrac{496}{379.4} + \dfrac{350(0.788)}{151.9}} = 0.951$$

From Fig. 1.4, $T_r = 423°R$ and $p_r = 637$ psia. Then $T_r = 1.60$ and $p_r = 4.30$, from which, using Fig. 1.5, the gas deviation factor is 0.825 at the initial conditions. Then the total initial gas in place per acre-foot of bulk reservoir is

$$G = \frac{379.4\,pV}{zR'T} = \frac{379.4(2740)(43560)(0.25)(1 - 0.30)}{0.825(10.73)(675)} = 1326\ MCF/ac\text{-}ft$$

Because the volume fraction equals the mole fraction in the gas state, the fraction of the total produced on the surface as gas is

$$f_g = \frac{n_g}{n_g + n_o} = \frac{\dfrac{R_1}{379.4} + \dfrac{R_2}{379.4}}{\dfrac{R_1}{379.4} + \dfrac{R_2}{379.4} + \dfrac{350\gamma_o}{M_{ao}}} \qquad (4.3)$$

$$f_g = \frac{\dfrac{12{,}810}{379.4} + \dfrac{496}{379.4}}{\dfrac{12{,}810}{379.4} + \dfrac{496}{379.4} + \dfrac{350(0.788)}{151.9}} = 0.951$$

Then

$$\text{Initial gas in place} = 0.951(1326) = 1261\ MCF/ac\text{-}ft$$

$$\text{Initial oil in place} = \frac{1261(10^3)}{12{,}810 + 496} = 94.8\ STB/ac\text{-}ft$$

fo=1-fg
=1-0.951
=0.049

Because the gas production is 95.1% of the total moles produced, the total daily gas-condensate production in MCF is

$$\Delta G_p = \frac{\text{daily gas}}{0.951} = \frac{3100 + 120}{0.951} = 3386\ MCF/day$$

The total daily reservoir voidage by the gas law is

$$\Delta V = 3{,}386{,}000\left\{\frac{675(14.7)(0.825)}{520(2740)}\right\} = 19{,}450\ cu\ ft/day$$

Then

$$\text{Initial gas in place} = 0.951(1326) = 1261 \ MCF/ac\text{-}ft$$

$$\text{Initial oil in place} = \frac{1261(10^3)}{12{,}810 + 496} = 94.8 \ STB/ac\text{-}ft$$

Because the gas production is 95.1% of the total moles produced, the total daily gas-condensate production in MCF is

$$\Delta G_p = \frac{\text{daily gas}}{0.951} = \frac{3100 + 120}{0.951} = 3386 \ MCF/day$$

The total daily reservoir voidage by the gas law is

$$\Delta V = 3{,}386{,}000\left(\frac{675(14.7)(0.825)}{520(2740)}\right) = 19{,}450 \ cu\ ft/day$$

The gas deviation factor of the total well fluid at reservoir temperature and pressure can also be calculated from its composition. The composition of the total well fluid is calculated from the analyses of the produced gas(es) and liquid by recombining them in the ratio in which they are produced. When the composition of the stock tank liquid is known, a unit of this liquid must be combined with the proper amounts of gas(es) from the separator(s) and the stock tank, each of which has its own composition. When the compositions of the gas and liquid in the first or high-pressure separator are known, the shrinkage the separator liquid undergoes in passing to the stock tank must be measured or calculated in order to know the proper proportions in which the separator gas and liquid must be combined. For example, if the volume factor of the separator liquid is 1.20 separator bbl per stock tank barrel and the measured gas-oil ratio is 20,000 SCF of high-pressure gas per bbl of stock tank liquid, then the separator gas and liquid samples should be recombined in the proportions of 20,000 SCF of gas to 1.20 bbl of separator liquid, since 1.20 bbl of separator liquid shrinks to 1.00 bbl in the stock tank.

Example 4.2 shows the calculation of initial gas and oil in place for a gas-condensate reservoir from the analyses of the high pressure gas and liquid, assuming the well fluid to be the same as the reservoir fluid. The calculation is the same as that shown in Ex. 4.1 except that the gas deviation factor of the reservoir fluid is found from the pseudoreduced temperature and pressure,

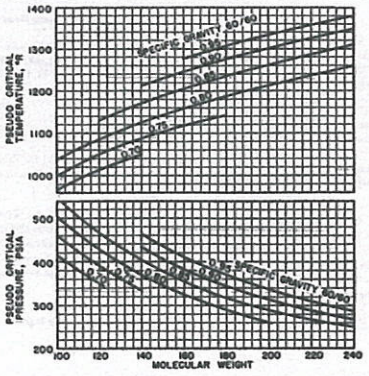

Fig. 4.3. Correlation charts for estimation of the pseudocritical temperature and pressure of heptanes plus fractions from molecular weight and specific gravity. (*After* Mathews, Roland, and Katz,[7] *Proc.* NGAA.)

which are determined from the composition of the total well fluid rather than from its specific gravity. Figure 4.3 presents charts for estimating the pseudocritical temperature and pressure of the heptanes-plus fraction from its molecular weight and specific gravity.

Example 4.2. To calculate the initial gas and oil in place from the compositions of the gas and liquid from the high-pressure separator.

Given:

Reservoir pressure	4350 psia
Reservoir temperature	217°F
Hydrocarbon porosity	17.4 per cent

Example 4.2. To calculate the initial gas and oil in place from the compositions of the gas and liquid from the high-pressure separator.

Given:

Reservoir pressure $P_i = 4350$ psia — 4350 psia
Reservoir temperature $T = 217°F$ — 217°F
Hydrocarbon porosity $\phi = 17.4\%$ — 17.4 per cent

Std. cond. $P_{st} = 15.025$ psia, $T_{st} = 60°F$	15.025 psia, 60°F
Separator gas	842,600 SCF/day
Stock tank oil	31.1 STB/day
Mol. wt. C_7^+ in separator liquid	185.0 *
Sp. gr. C_7^+ in separator liquid	0.8343
Sp. gr. separator liquid at 880 psig and 60°F	0.7675
Separator liquid volume factor B_o	1.235 bbl at 880 psia/STB, both at 60°F
Compositions of high-pressure gas and liquid	Cols. (2) and (3), Table 4.3
Molar volume at 15.025 psia and 60°F	371.2 cu ft/mole.

SOLUTION: (column numbers refer to Table 4.3):

Calculate the mole proportions to recombine the seperator Gas & liquid.

Std. cond.	15.025 psia, 60°F
Separator gas	842,600 SCF/day
Stock tank oil	31.1 STB/day
Mol. wt. C_7^+ in separator liquid	185.0
Sp. gr. C_7^+ in separator liquid	0.8343
Sp. gr. separator liquid at 880 psig and 60°F	0.7675
Separator liquid volume factor	1.235 bbl at 880 psia/STB, both at 60°F
Compositions of high-pressure gas and liquid	Cols. (2) and (3), Table 4.3
Molar volume at 15.025 psia and 60°F	371.2 cu ft/mole

SOLUTION: (column numbers refer to Table 4.3):

1. Calculate the mole proportions in which to recombine the separator gas and liquid. Multiply the mole fraction of each component in the liquid, Col. (3), by its molecular weight, Col. (4), and enter the products in Col. (5). The sum of Col. (5) is the molecular weight of the separator liquid, 127.48. Because the specific gravity of the separator liquid is 0.7675 at 880 psig and 60°F, the moles per barrel is

$$\frac{0.7675 \times 350 \text{ lb/bbl}}{127.48 \text{ lb/mole}} = 2.107 \text{ moles/bbl for the separator liquid}$$

TABLE 4.3.
Calculations for Example 4.2 on gas-condensate fluid

(1)	(2) Gas	(3) Liquid	(4) Mol. wt.	(5) (3) × (4) lb/mole	(6) Liquid bbl/mole for Each Component	(7) (3) × (6) bbl of Each Component per Mole of sep. liq.	(8) Moles of Each Component in 59.11 Moles of Gas (2) × 59.11
	Mole Composition of Separator Fluids						
CO_2	0.0120	0.0000					0.709
C_1	0.9404	0.2024	16.04	3.247	0.1317	0.02666	55.587
C_2	0.0305	0.0484	30.07	1.455	0.1771	0.00857	1.803
C_3	0.0095	0.0312	44.09	1.376	0.2480	0.00774	0.562
i-C_4	0.0024	0.0113	58.12	0.657	0.2948	0.00333	0.142
n-C_4	0.0023	0.0196	58.12	1.139	0.2840	0.00557	0.136
i-C_5	0.0006	0.0159	72.15	1.147	0.3298	0.00524	0.035
n-C_5	0.0003	0.0170	72.15	1.227	0.3264	0.00555	0.018
C_6	0.0013	0.0384	86.17	3.309	0.3706	0.01423	0.077
C_7^+	0.0007	0.6158	185.0	113.923	0.6336[a]	0.39017	0.041
	1.0000	1.0000		127.480		0.46706	59.110

[a] 185 lb/mole ÷ (0.8343 × 350 lb/bbl) = 0.6336 bbl/mole.

The separator liquid rate is 31.1 STB/day × 1.235 sep. bbl/STB so that the separator gas-oil ratio is

$$\frac{842{,}600}{31.1 \times 1.235} = 21{,}940 \text{ SCF sep. gas/bbl sep. liquid}$$

Because the 21,940 SCF is 21,940/371.2, or 59.11 moles, the separator gas and liquid must be recombined in the ratio of 59.11 moles of gas to 2.107 moles of liquid.

If the specific gravity of the separator liquid is not available, the mole per barrel figure may be calculated as follows. Multiply the mole fraction of each component in the liquid, Col. (3), by its barrel per mole figure, Col. (6), obtained from data in Table 1.1 and enter the product in Col. (7). The sum of Col. (7), 0.46706 is the number of barrels of separator liquid per mole of separator liquid, and the reciprocal is 2.141 moles/bbl (versus 2.107 measured).

2. Recombine 59.11 moles of gas and 2.107 moles of liquid. Multiply the mole fraction of each component in the gas, Col. (2), by 59.11 moles, and enter in Col. (8). Multiply the mole fraction of each component in the liquid, Col. (3), by 2.107 moles, and enter in Col. (9). Enter the sum of the moles of

(9) Moles of Each Component in 2.107 Moles of Liquid (3) × 2.107	(10) Moles of Each Component in 61.217 Moles of Gas and Liquid (8) + (9)	(11) Mole Composition of Total Well Fluid (10) ÷ 61.217	(12) Critical Pressure, psia	(13) Partial Critical Pressure, psia (11) × (12)	(14) Critical Temp. °R	(15) Partial Critical Temp. °R (11) × (14)
0.0000	0.7090	0.0116	1070	12.41	548	6.36
0.4265	56.0135	0.9150	673	615.89	343	313.85
0.1039	1.9059	0.0311	708	22.02	550	17.11
0.0657	0.6277	0.0102	987	6.29	666	6.79
0.0238	0.1658	0.0027	529	1.43	735	1.98
0.0413	0.1773	0.0029	550	1.60	766	2.22
0.0335	0.0685	0.0011	484	0.53	830	0.91
0.0358	0.0536	0.0009	490	0.44	846	0.76
0.0809	0.1579	0.0026	440	1.14	914	2.38
1.2975	1.3385	0.0219	300[a]	6.57	1227[a]	26.87
2.1070	61.2170	1.0000		668.23		379.23

[a] From Fig. 4.3, after Mathews, Roland, and Katz for Mol. wt. C_7^+ = 185 and sp. gr. = 0.8342.

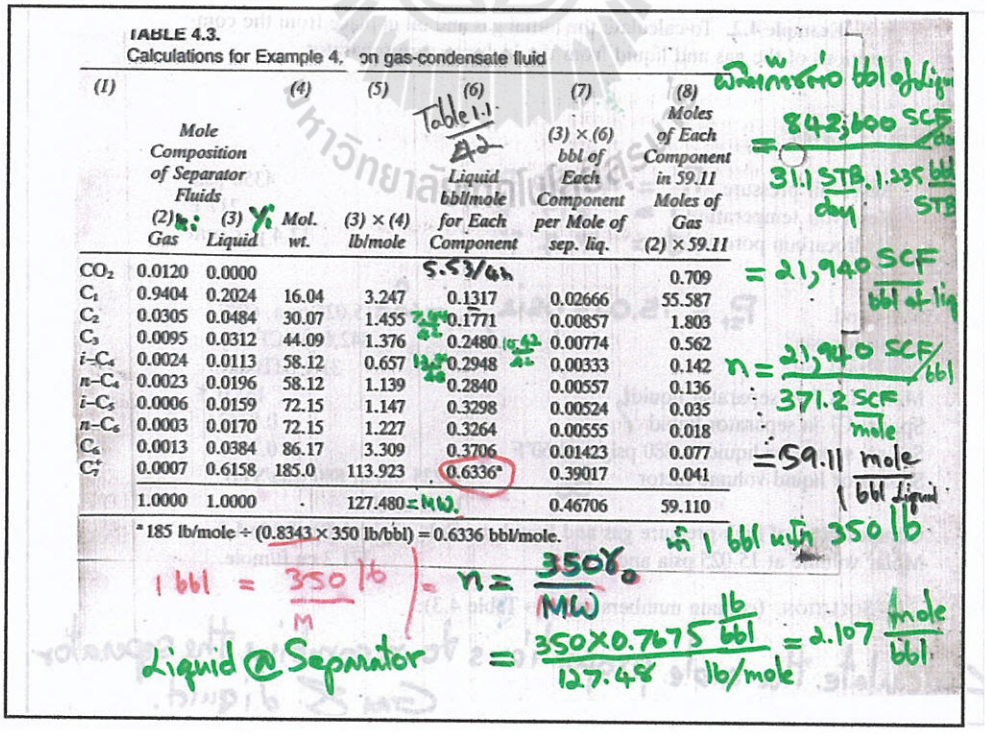

The separator liquid rate is 31.1 STB/day × 1.235 sep. bbl/STB so that the separator gas-oil ratio is

$$\frac{842{,}600}{31.1 \times 1.235} = 21{,}940 \text{ SCF sep. gas/bbl sep. liquid}$$

Because the 21,940 SCF is 21,940/371.2, or 59.11 moles, the separator gas and liquid must be recombined in the ratio of 59.11 moles of gas to 2.107 moles of liquid.

If the specific gravity of the separator liquid is not available, the mole per barrel figure may be calculated as follows. Multiply the mole fraction of each component in the liquid, Col. (3), by its barrel per mole figure, Col. (6), obtained from data in Table 1.1 and enter the product in Col. (7). The sum of Col. (7), 0.46706 is the number of barrels of separator liquid per mole of separator liquid, and the reciprocal is 2.141 moles/bbl (versus 2.107 measured).

2. Recombine 59.11 moles of gas and 2.107 moles of liquid. Multiply the mole fraction of each component in the gas, Col. (2), by 59.11 moles, and enter in Col. (8). Multiply the mole fraction of each component in the liquid, Col. (3), by 2.107 moles, and enter in Col. (9). Enter the sum of the moles of

(9) Moles of Each Component in 2.107 Moles of Liquid (3) × 2.107	*(10) Moles of Each Component in 61.217 Moles of Gas and Liquid (8) + (9)*	*(11) Mole Composition of Total Well Fluid (10) ÷ 61.217*	*(12) Critical Pressure, psia*	*(13) Partial Critical Pressure, psia (11) × (12)*	*(14) Critical Temp. °R*	*(15) Partial Critical Temp. °R (11) × (14)*
0.0000	0.7090	0.0116	1070	12.41	548	6.36
0.4265	56.0135	0.9150	673	615.80	343	313.85
0.1020	1.9050	0.0311	708	22.02	550	17.11
0.0657	0.6277	0.0102	617	6.29	666	6.79
0.0238	0.1658	0.0027	529	1.43	735	1.98
0.0413	0.1773	0.0029	550	1.60	766	2.22
0.0335	0.0685	0.0011	484	0.53	830	0.91
0.0358	0.0538	0.0009	490	0.44	846	0.76
0.0809	0.1579	0.0026	440	1.14	914	2.38
1.2975	1.3385	0.0219	300[a]	6.57	1227[b]	26.87
2.1070	61.2170	1.0000		P_c = 668.23		T_c = 379.23

[a] From Fig. 4.3, *after* Mathews, Roland, and Katz for Mol. wt. C_7^+ = 185 and sp. gr. = 0.8342.[7]

Reservoir gas volume: $43{,}560 \times \phi\,(1 - S_w)$ cu ft

3. Find the gas and oil (condensate) in place per acre-foot of net reservoir rock. From the gas law, the initial moles per acre-foot at 17.4% hydrocarbon porosity is:

$$\frac{pV}{zRT} = \frac{4350 \times (43{,}560 \times 0.174)}{0.963 \times 10.73 \times 677} = 4713 \text{ moles/ac-ft}$$

$$\text{Gas mole fraction} = \frac{59.11}{59.11 + 2.107} = 0.966$$

$$\text{Initial gas in place} = \frac{0.966 \times 4713 \times 371.2}{1000} = 1690 \text{ MCF/ac-ft}$$

$$\text{Initial oil in place} = \frac{(1 - 0.966) \times 4713}{2.107 \times 1.235} = 61.6 \text{ STB/ac-ft}$$

Because the high-pressure gas is 96.6% of the total mole production, the daily gas-condensate production expressed in standard cubic feet is

$$\Delta G_p = \frac{\text{Daily hp gas}}{0.966} = \frac{842{,}600}{0.966} = 872{,}200 \text{ SCF/day}$$

The daily reservoir voidage at 4350 psia is

$$\Delta V = 872{,}200 \times \frac{677}{520} \times \frac{15.025}{4350} \times 0.963 = 3777 \text{ cu ft/day}$$

3. THE PERFORMANCE OF VOLUMETRIC RESERVOIRS

The behavior of single-phase gas and gas-condensate reservoirs has been treated in Chapter 3. Since no liquid phase develops within the reservoir, where the temperature is above the cricondentherm, the calculations are simplified. When the reservoir temperature is below the cricondentherm, however, a liquid phase develops within the reservoir when pressure declines below the dew point owing to retrograde condensation, and the treatment is considerably more complex, even for volumetric reservoirs.

One solution is to duplicate closely the reservoir depletion by laboratory studies on a representative sample of the initial, single-phase reservoir fluid. The sample is placed in a high-pressure cell at reservoir temperature and

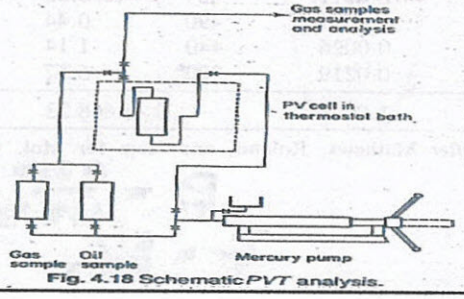

Fig. 4.18 Schematic *PVT* analysis.

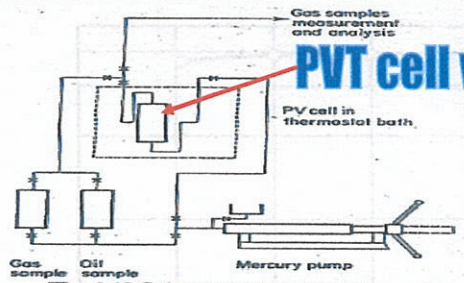

PVT cell volume=947.5 cc.

Fig. 4.18 Schematic *PVT* analysis.

TABLE 4.4.
Volume, composition, and gas deviation factors for a retrograde condensate fluid

(1)	(2)	(3)	(4)	(5)	(6)	(7)	(8)	(9)	(10)	(11)	(12)
	Composition of Produced Gas Increments, Mole Fraction							Produced Gas, cu cm at 195°F and Cell Pressure	Retrograde Liquid Volume, cu cm Cell Volume, 947.5 cu cm	Retrograde Volume, Per Cent of Hydrocarbon Volume	Gas Deviation Factor at 195°F and Cell Pressure
Pressure psia	C_1	C_2	C_3	C_4	C_5	C_6	C_7^+				
2960	0.752	0.077	0.044	0.031	0.022	0.022	0.052	0.0	0.0	0.0	0.771
2500	0.783	0.077	0.043	0.028	0.019	0.016	0.034	175.3	62.5	6.6	0.794
2000	0.795	0.078	0.042	0.027	0.017	0.014	0.027	227.0	77.7	8.2	0.805
1500	0.798	0.079	0.042	0.027	0.016	0.013	0.025	340.4	75.0	7.9	0.835
1000	0.793	0.080	0.043	0.028	0.017	0.013	0.026	544.7	67.2	7.1	0.875
500	0.768	0.082	0.048	0.033	0.021	0.015	0.033	1080.7	56.9	6.0	0.945

Volume, composition, and gas deviation factors for a retrograde condensate fluid

(1)	(2)	(3)	(4)	(5)	(6)	(7)	(8)	(9)	(10)	(11)	(12)
	Composition of Produced Gas Increments, Mole Fraction							Produced Gas, cu cm at 195°F and Cell Pressure	Retrograde Liquid Volume, cu cm Cell Volume, 947.5 cu cm	Retrograde Volume, Per Cent of Hydrocarbon Volume	Gas Deviation Factor at 195°F and Cell Pressure
Pressure psia	C_1	C_2	C_3	C_4	C_5	C_6	C_7^+				
2960	0.752	0.077	0.044	0.031	0.022	0.022	0.052	0.0	0.0	0.0	0.771
2500	0.783	0.077	0.043	0.028	0.019	0.016	0.034	175.3	62.5	6.6	0.794
2000	0.795	0.078	0.042	0.027	0.017	0.014	0.027	227.0	77.7	8.2	0.805
1500	0.798	0.079	0.042	0.027	0.016	0.013	0.025	340.4	75.0	7.9	0.835
1000	0.793	0.080	0.043	0.028	0.017	0.013	0.026	544.7	67.2	7.1	0.875
500	0.768	0.082	0.048	0.033	0.021	0.015	0.033	1080.7	56.9	6.0	0.945

TABLE 4.5.
Gas and liquid recoveries in percentage and per acre-foot for Example 4.3

(1)	(2)	(3)	(4)	(5)	(6)	(7)	(8)	(9)	(10)	(11)
Pressure, psia	Increments of Gross Gas Production, M SCF	Cumulative Gross Gas Production, M SCF, Σ(2)	Residue Gas in Each Increment, M SCF	Cumulative Residue Gas Production, M SCF Σ(4)	Liquid in Each Increment, bbl	Cumulative Liquid Production, bbl Σ(6)	Average Gas-Oil Ratio of Each Increment, SCF Residue Gas per bbl, (4) ÷ (6)	Cumulative Gross Gas Recovery, percentage (3) × 100/1580	Cumulative Residue Gas Recovery, percentage (5) × 100/1441	Cumulative Liquid Recovery, percentage (7) × 100/143.2
2960	0	0	0	0	0	0	10,600	0	0	0
2500	240.1	240.1	225.1	225.1	15.3	15.3	14,700	15.2	15.6	10.7
2000	245.2	485.3	232.3	457.4	13.1	28.4	17,730	30.7	31.7	19.8
1500	266.0	751.3	252.8	710.2	13.3	41.7	19,010	47.6	49.3	29.1
1000	270.8	1022.1	256.9	967.1	14.0	55.7	18,350	64.7	67.1	38.9
500	248.7	1270.8	233.0	1200.1	15.9	71.6	14,650	80.4	83.3	50.0

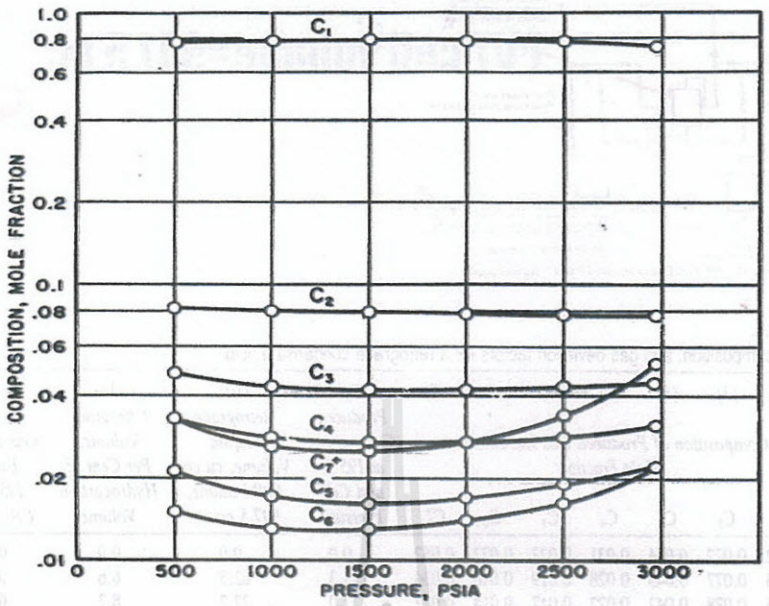

Fig. 4.4. Variations in the composition of the produced gas phase material of a retrograde gas-condensate fluid with pressure decline. (Data from Table 4.4.)

emoved from a PVT cell in each of five increments, as previously described. Table 4.4 also gives the volume of retrograde liquid in the cell at each pressure and the gas deviation factor and volume of the produced gas increments at cell pressure and temperature.

The liquid recovery from the gas increments produced from the cell may be measured by passing the gas through small-scale separators, or it may be calculated from the composition for usual field separation methods, or for gasoline plant methods.[8,9,10] Liquid recovery of the pentanes-plus is somewhat greater in gasoline plants than is obtained by field separation, and much greater for the propanes and butanes, commonly called liquified petroleum gas (LPG). For simplicity, the liquid recovery from the gas increments of Table 4.4 is calculated in Ex. 4.3 assuming 25% of the butanes, 50% of the pentanes, 75% of the hexane, and 100% of the heptanes-plus is recovered as liquid.

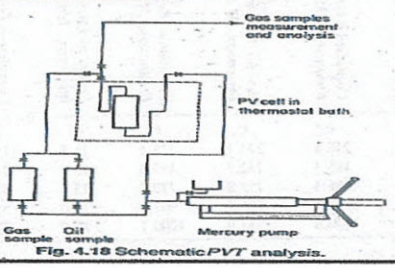

Fig. 4.18 Schematic *PVT* analysis.

SOLUTION: (column numbers refer to Table 4.5):

1. Calculate the increments of gross production in M SCF per ac-ft of net, bulk reservoir rock. Enter in Col. (2):

$$V_{HC} = 43{,}560 \times 0.25 \times (1 - 0.30) = 7623 \text{ cu ft/ac-ft}$$

For the increment produced from 2960 to 2500 psia, for example,

$$\Delta V = 7623 \times \frac{175.3 \text{ cu cm}}{947.5 \text{ cu cm}} = 1410 \text{ cu ft/ac-ft at 2500 psia and 195°F}$$

$$\Delta G_p = \frac{379.4\, p \Delta V}{1000\, zRT} = \frac{379.4 \times 2500 \times 1410}{1000 \times 0.794 \times 10.73 \times 655} = 240.1\text{M SCF}$$

Find the cumulative gross gas production, $G_p = \Sigma\, \Delta G_p$ and enter in Col. (3).

2. Calculate the M SCF of residue gas and the barrels of liquid obtained from each increment of gross gas production. Enter in Col. (4) and Col. (6). Assume that 0.25 C_4, 0.50 C_5, 0.75 C_6, and all C_7^+ is recovered as stock tank liquid. For example, in the 240.1 M SCF produced from 2960 to 2500 psia, the mole fraction recovered as liquid is

$$\Delta n_L = 0.25 \times 0.028 + 0.50 \times 0.019 + 0.75 \times 0.016 + 0.034$$
$$= 0.0070 + 0.0095 + 0.0120 + 0.034 = 0.0625 \text{ mole fraction}$$

As the mole fraction also equals the volume fraction in gas, the M SCF recovered as liquid from 240.1 M SCF is

$$\Delta G_L = 0.0070 \times 240.1 + 0.0095 \times 240.1 + 0.0120 \times 240.1 + 0.034 \times 240.1$$
$$= 1.681 + 2.281 + 2.881 + 8.163 = 15.006\text{M SCF}$$

The gas volume can be converted to gallons of liquid using the gal/M SCF figures of Table 1.1 for C_4, C_5 and C_6. The average of the iso and normal compounds is used for C_4 and C_5.

For C_7^+

$$\frac{114 \text{ lb/lb-mole}}{0.3794\text{M SCF/lb-mole} \times 8.337 \text{ lb/gal} \times 0.755} = 47.71 \text{ gal/M SCF}$$

0.3794 is the molar volume at standard conditions of 14.7 psia and 60°F. Then the total liquid recovered from 240.1M SCF is $1.681 \times 32.04 + 2.281 \times 36.32 + 2.881 \times 41.03 + 8.163 \times 47.71 = 53.9 + 82.8 + 118.2 + 389.5 = 644.4$ gal = 15.3 bbl. The residue gas recovered from the 240.1 M SCF is $240.1 \times (1 - 0.0625) = 225.1$ M SCF. Calculate the cumulative residue gas and stock tank liquid recoveries from Cols. (4) and (6) and enter in Cols. (5) and (7), respectively.

3. Calculate the gas-oil ratio for each increment of gross production in units of residue gas per barrel of liquid. Enter in Col. (8). For example, the gas-oil ratio of the increment produced from 2960 to 2500 psia is

$$\frac{225.1 \times 1000}{15.3} = 14{,}700 \text{ SCF/bbl}$$

4. Calculate the cumulative recovery percentages of gross gas, residue gas, and liquid. Enter in Cols. (9), (10), and (11). The initial gross gas in place is:

$$\frac{379.4\,pV}{1000\,zRT} = \frac{379.4 \times 2960 \times 7623}{1000 \times 0.771 \times 10.73 \times 655} = 1580 \text{ M SCF/ac-ft}$$

Of this, the liquid mole fraction is 0.088 and the total liquid recovery is 3.808 gal/M SCF of gross gas, which are calculated from the initial composition in the same manner as shown in Part 2. Then

$$G = (1 - 0.088) \times 1580 = 1441 \text{ M SCF residue gas/ac-ft}$$

$$N = \frac{3.808 \times 1580}{42} = 143.2 \text{ bbl/ac-ft}$$

$$\text{Gross gas recovery} = \frac{100 \times 240.1}{1580} = 15.2\%$$

$$\text{Residue gas recovery} = \frac{100 \times 225.1}{1441} = 15.6\%$$

$$\text{Liquid recovery} = \frac{100 \times 15.3}{143.2} = 10.7\%$$

TABLE 4.6.
Two-phase and single-phase gas deviation factors for the retrograde gas-condensate fluid of Example 4.3

(1)	(2)	(3)	(4)	(5)	(6)
			Gas Deviation Factors		
Pressure, psia	G_p[a] *M SCF/ac-ft*	$(G - G_p)$[a] *M SCF/ac-ft*	*Two-phase*[b]	*Initial Gas*[c]	*Produced Gas*[a]
2960	0.0	1580.0	0.771	0.780	0.771
2500	240.1	1339.9	0.768	0.755	0.794
2000	485.3	1094.7	0.752	0.755	0.805
1500	751.3	828.7	0.745	0.790	0.835
1000	1022.1	557.9	0.738	0.845	0.875
500	1270.8	309.2	0.666	0.920	0.945

[a] Data from Table 4.5 and Example 4.3.

[b] Calculated from the data of Table 4.5 and Example 4.3.

[c] Calculated from initial gas composition using correlation charts.

$$\text{Recovery} = \frac{V_i\phi(1 - S_{wi} - S_{gr})B_{gi}F}{V_i\phi(1 - S_{wi})B_{gi}} = \frac{(1 - S_{wi} - S_{gr})F}{(1 - S_{wi})} \qquad (4.4)$$

TABLE 4.8. ACTIVE WATER DRIVE F Function invaded by H_2O

Recovery factors for complete water-drive reservoirs based on Eq. (4.4)

S_{gr}	S_w	$F = 40$	$F = 60$	$F = 80$	$F = 90$	$F = 100$
20	10	31.1	46.7	62.2	70.0	77.8
	20	30.0	45.0	60.0	67.5	75.0
	30	28.6	42.8	57.1	64.3	71.4
	40	26.7	40.0	53.4	60.0	66.7
30	10	26.7	40.0	53.4	60.0	66.7
	20	25.0	37.5	50.0	56.3	62.5
	30	22.8	34.3	45.7	51.4	57.1
	40	20.0	30.0	40.0	45.0	50.0
40	10	22.2	33.3	44.4	50.0	55.6
	20	20.0	30.0	40.0	45.0	50.0
	30	17.1	25.7	34.2	38.5	42.8
	40	13.3	20.0	26.6	30.0	33.3
50	10	17.7	26.6	35.5	40.0	44.4
	20	15.0	22.5	30.0	33.8	37.5
	30	11.4	17.1	22.8	25.7	28.5
	40	6.7	10.0	13.6	15.0	16.7

TABLE 4.9.

Comparison of gas-condensate recovery by volumetric performance, complete water drive, and partial water drive (based on the data of Tables 4.4 and 4.5 for Ex. 4.3: $S_w = 30\%$; $S_{gr} = S_{or} + S_{gr} = 20\%$; $F = 80\%$)

strong F = 100%

Recovery Mechanism	Condensate Recovery bbl/ac-ft	Condensate Recovery Percentage	Gas Recovery MCF/ac-ft	Gas Recovery Percentage	Gross Recovery MCF/ac-ft	Gross Recovery Percentage
Initial in-place	143.2	100.0	1441	100.0	1580	100.0
Depletion to 500 psia	71.6	50.0	1200	83.3	1271	80.4
Water drive at 2960 psia	81.8	57.1	823	57.1	902	57.1
(a) Depletion to 2000 psia	28.4	19.8	457	31.7	485	30.7
(b) Water drive at 2000 psia	31.2	21.8	553	38.4	584	37.0
Total by partial water drive, (a) + (b)	59.6	41.6	1010	70.1	1069	67.7

Strong Patil

obtained from Ex. 4.3 and Tables 4.4 and 4.5. Under complete water drive, the recovery is 57.1% for a residual gas saturation of 20%, a connate water of 30%, and a fractional invasion of 80% at abandonment, as may be found by Eq. (4.4) or Table 4.8. Because there is no retrograde loss, this figure applies equally to the gross gas, gas, and condensate recovery.

When a partial water drive exists and the reservoir pressure stabilizes at some pressure, here 2000 psia, the recovery is approximately the sum of the recovery by pressure depletion down to the stabilization pressure, plus the

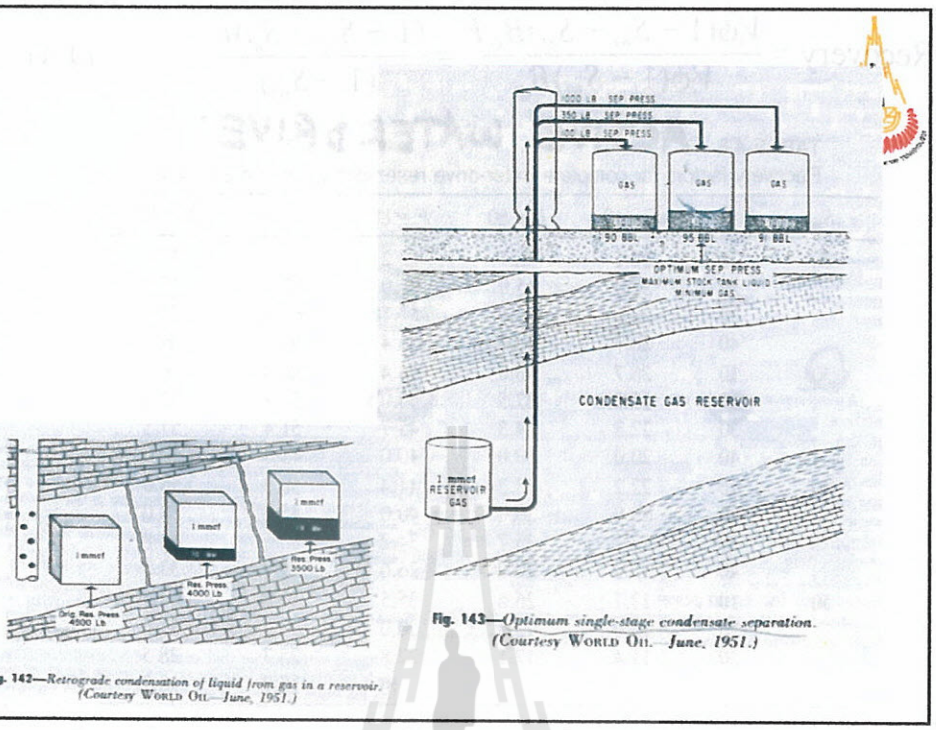

Fig. 142—*Retrograde condensation of liquid from gas in a reservoir.* (Courtesy World Oil—*June, 1951.*)

Fig. 143—*Optimum single-stage condensate separation.* (Courtesy World Oil—*June, 1951.*)

gas recycling in gas-condensate reservoirs

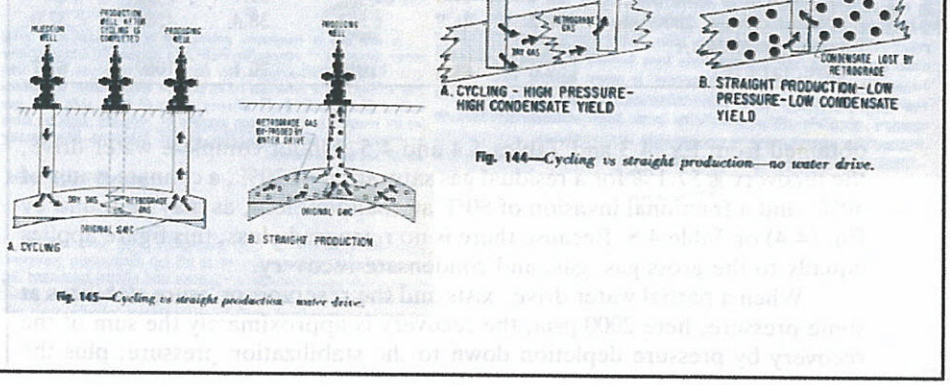

Fig. 144—*Cycling vs straight production—no water drive.*

Fig. 145—*Cycling vs straight production—water drive.*

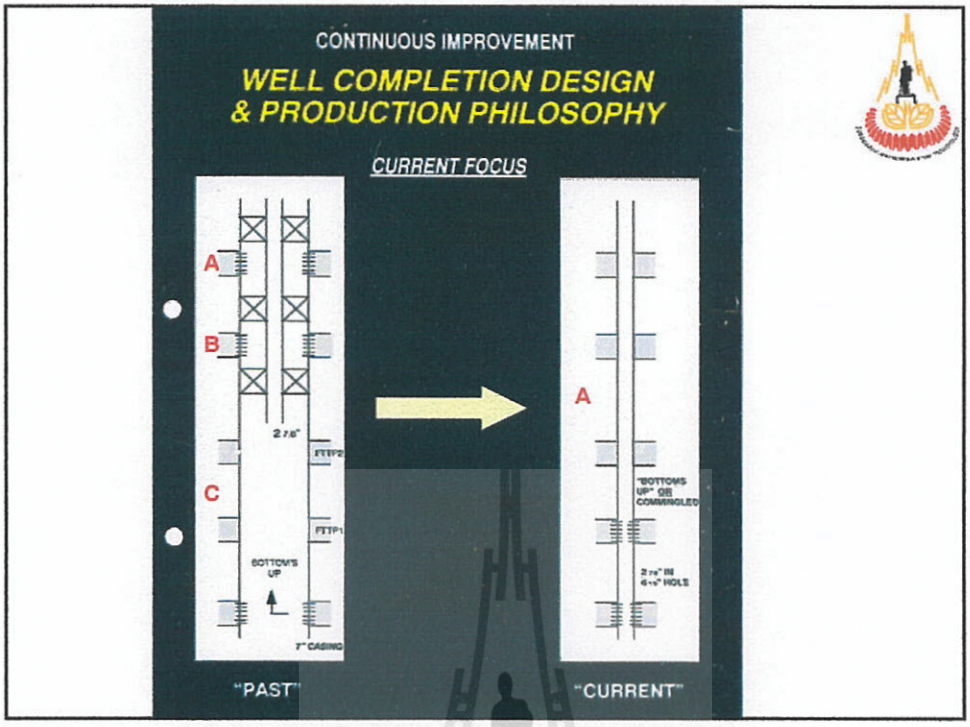

Reservoir Engineering I, 2012
HW NO 4; Due date: Friday, July 6, 2012.

Chapter 4; 4.1, 4.3, 4.8, 4.13, 4.15

ANSWERS TO THE PROBLEMS

1. 4.1; $2100, $1330
2. 4.3; (a) 0.727, (b) 20,700 SCF/STB, (.c) 140.5 (d) 0.868, (e) 0.865, (f) 3883 lb-mole/acre-ft, (g) 0.966, (h) 1,423 MSCF/acre-ft, 68.8 STB/acre-ft
3. 4.8; (a) 53.72 MSCF,48.5 MSCF, 5.86 STB@3500 psia
(b) 891.6 MSCF, 125.1 bbl
(.c)@605 psia 768 M SCF, 739.5 MSCF and 29.8 bbl
76.8%, 82.9%, and 23.8%
(d) 675 M SCF, 650 MSCF and 26.14 bbl
4. 4.13; Answer in Table 4.5
5. 4.15; 1968.5 MMSCF, 674 STB

OIL RESERVOIR 7-8th weeks 9-20 JULY 2012

Chapter 5 Undersaturated Oil Reservoir

Chapter6 Saturated Oil Reservoir

TABLE 4.1.

Mole composition and other properties of typical single-phase reservoir fluids

SATUN

Component	Black Oil LKU	Volatile Oil	Gas-Condensate	Dry Gas	WETGas	
C_1	48.83 **54**	64.36	87.07	95.85	86.67	**70**
C_2	2.75 **4**	7.52	4.39	2.67	7.77	**10**
C_3	1.93 **2**	4.74	2.29	0.34	2.95	**6**
C_4	1.60 **1**	4.12	1.74	0.52	1.73	**1.3**
C_5	1.15 **1**	2.97	0.83	0.08	0.88	**1.1**
C_6	1.59 **3**	1.38	0.60	0.12		**0.1**
C_7^+	42.15 **42**	14.91	3.80	0.42		**0.5**
	100.00	100.00	100.00	100.00	100.00	
Mol. wt. C_7^+	225	181	112	157		
GOR, SCF/bbl	625	2000	18,200	105,000		Inf.**33000**
Tank gravity, °API	34.3	50.1	60.8	54.7		**50-54**
Liquid color	Greenish black	Medium orange	Light straw	Water white		

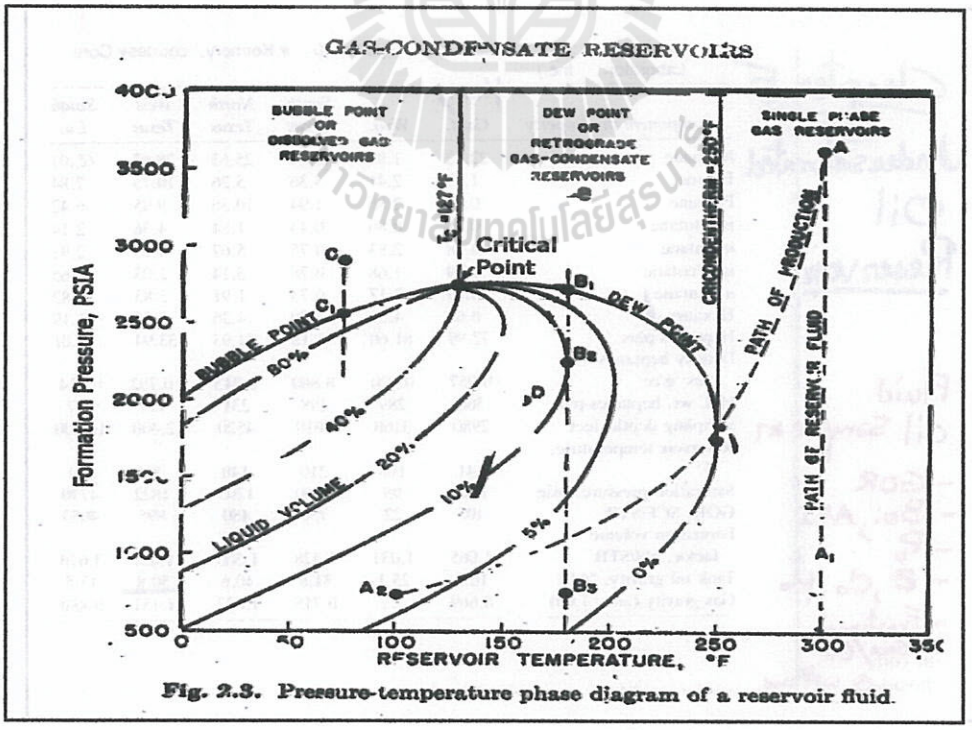

Fig. 2.3. Pressure-temperature phase diagram of a reservoir fluid.

TABLE 4.1.
Mole composition and other properties of typical single-phase reservoir fluids

Component	Black Oil	Volatile Oil	Gas-Condensate	Dry Gas	Gas
C_1	48.83	64.36	87.07	95.85	86.67
C_2	2.75	7.52	4.39	2.67	7.77
C_3	1.93	4.74	2.29	0.34	2.95
C_4	1.60	4.12	1.74	0.52	1.73
C_5	1.15	2.97	0.83	0.08	0.98
C_6	1.59	1.38	0.60	0.12	
C_7^+	42.15	14.91	1.80	0.42	
	100.00	100.00	100.00	100.00	100.00
Mol. wt. C_7^+	225	181	112	157	
GOR, SCF/bbl	625	2000	18,200	105,000	Inf.
Tank gravity, °API	34.3	50.1	60.8	54.7	
Liquid color	Greenish black	Medium orange	Light straw	Water white	

Light oil API > 31.1°
Medium 31.1 > API > 22.3
Heavy 22.3 > API > 10

API > 45°
GOR 500 - 100,000 SCF/STB

Chapter 5
Undersaturated Oil Reservoir

Fluid Oil Sample
- GOR
- Boi, API
- Pb
- Z, Co, μo
- Fractional Gas/Oil

Reservoir fluid compositions and properties (after Kennery,[1] courtesy Core Laboratories, Inc.)

Component or Property	Calif.	Wyo.	South Texas	North Texas	West Texas	South La.
Methane	22.62	1.08	48.04	25.63	28.63	65.01
Ethane	1.69	2.41	3.36	5.26	10.75	7.84
Propane	0.81	2.86	1.94	10.36	9.95	6.42
iso-Butane	0.51	0.86	0.43	1.84	4.36	2.14
n-Butane	0.38	2.83	0.75	5.67	4.16	2.91
iso-Pentane	0.19	1.68	0.78	3.14	2.03	1.65
n-Pentane	0.19	2.17	0.73	1.91	1.83	0.83
Hexanes	0.62	4.51	2.79	4.26	2.35	1.19
Heptanes-plus	72.99	81.60	41.18	41.93	33.94	12.01
Density heptanes-plus: g/cc	0.957	0.920	0.860	0.843	0.792	0.814
Mol. wt. heptanes-plus	360	289	198	231	177	177
Sampling depth, feet	2980	3160	8010	4520	12,400	10,600
Reservoir temperature, °F	141	108	210	140	202	241
Saturation pressure, psig	1217	95	3660	1205	1822	4730
GOR, SCF/STB	105	22	750	480	895	4053
Formation volume factor, bbl/STB	1.065	1.031	1.428	1.305	1.659	3.610
Tank oil gravity, °API	16.3	25.1	34.8	40.6	50.8	43.5
Gas gravity (air = 1.00)	0.669	...	0.715	1.032	1.151	0.880

on coming
thoxide @ wellhead.

surface and later recombined in appropriate

DISSOLVES GAS DRIVE

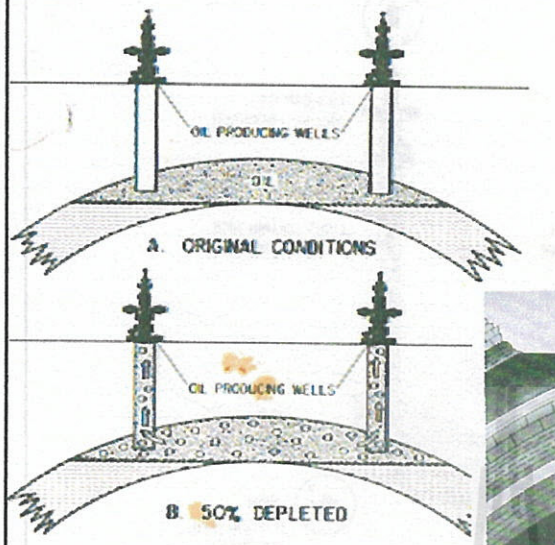

Fig. 61—*Dissolved gas drive reservoir.*

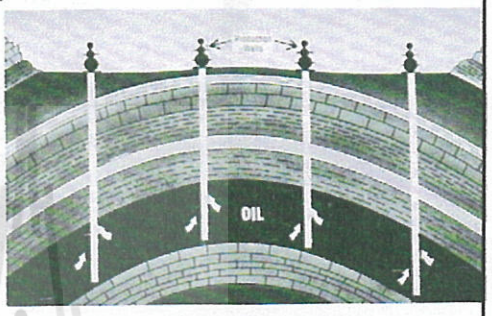

Fig. 1.3—Dissolved gas drive.

WATER DRIVE

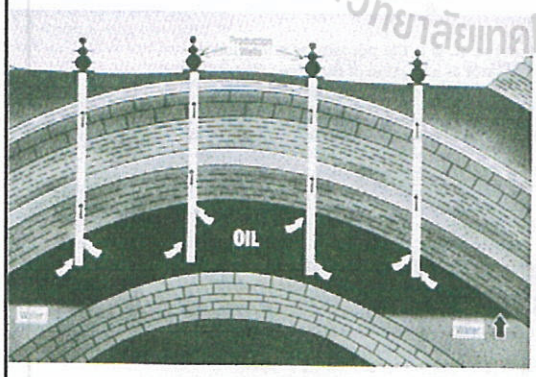

Fig. 1.2—Water-drive reservoir.

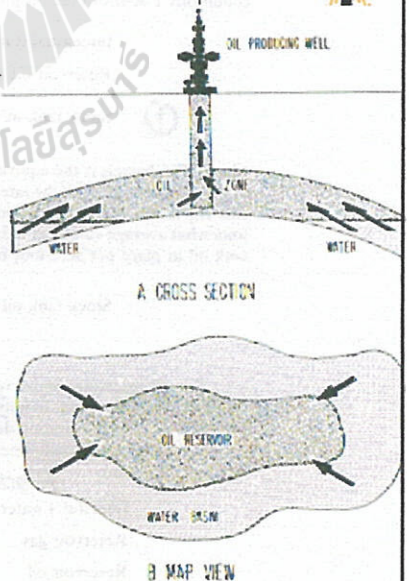

Fig. 65—*Water drive reservoir.*

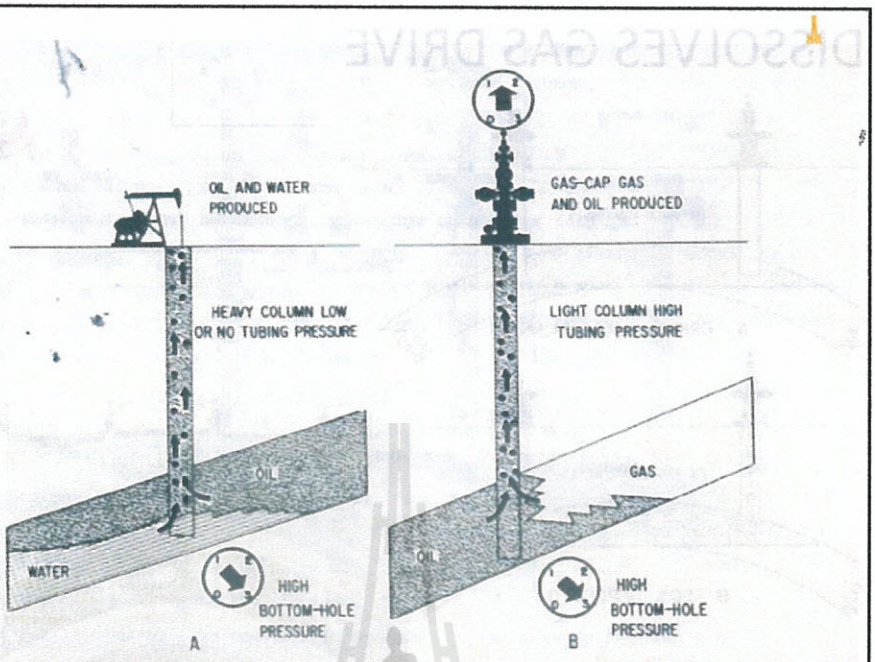

Fig. 80—*Effects of water and gas-cap production on tubing-head pressure.*

The *volumetric method* for estimating oil in place is based on log and core analysis data to determine the bulk volume, the porosity, and the fluid saturations, and on fluid analysis to determine the oil volume factor. Under initial conditions 1 ac-ft of bulk oil productive rock contains

Interstitial water	$7758 \times \phi \times S_w$
Reservoir oil	$7758 \times \phi \times (1 - S_w)$
Stock tank oil	$\dfrac{7758 \times \phi \times (1 - S_w)}{B_{oi}}$

where 7758 barrels is the equivalent of 1 ac-ft, ϕ is the porosity as a fraction of the bulk volume, S_w is the interstitial water as a fraction of the pore volume, and B_{oi} is the initial formation volume factor of the reservoir oil. Using somewhat average values, $\phi = 0.20$, $S_w = 0.20$, and $B_{oi} = 1.24$, the initial stock tank oil in place per acre-foot is on the order of 1000 STB/ac-ft, or

$$\text{Stock tank oil} = \frac{7758 \times 0.20 \times (1 - 0.20)}{1.24}$$

$$= 1000 \text{ STB/ac-ft}$$

For oil reservoirs under *volumetric control*, there is no water influx to replace the produced oil, so it must be replaced by gas the saturation of which increases as the oil saturation decreases. If S_g is the gas saturation and B_o the oil volume factor at abandonment, then at abandonment conditions 1 ac-ft of bulk rock contains

Abandonment Condition

Interstitial water	$7758 \times \phi \times S_w$
Reservoir gas	$7758 \times \phi \times S_g$
Reservoir oil	$7758 \times \phi \times (1 - S_w - S_g)$
Stock tank oil	$\dfrac{7758 \times \phi \times (1 - S_w - S_g)}{B_o}$

$$\text{Recovery} = 7758 \times \phi \left[\frac{(1 - S_{wc})}{B_{oi}} - \frac{(1 - S_{wc} - S_{or})}{B_o} \right] \quad (5.1)$$

d the fractional recovery in terms of stock tank barrels is

$$\text{Recovery} = 1 - \frac{(1 - S_{wc} - S_{or})}{(1 - S_{wc})} \times \frac{B_{oi}}{B_o} \quad (5.2)$$

e total free gas saturation to be expected at abandonment can be estimated m the oil and water saturations as reported in core analysis.[7] This expecta- n is based on the assumption that, while being removed from the well, the e is subjected to fluid removal by the expansion of the gas liberated from residual oil, and that this process is somewhat similar to the depletion ocess in the reservoir. In a study of the well spacing problem, Craze and ic collected a large amount of statistical data on 103 oil reservoirs, 27 of ich were considered to be producing under volumetric control.[8] The final s saturation in most of these reservoirs ranged from 20 to 40% of the pore ce, with an average saturation of 30.4%. Recoveries may also be calculated depletion performance from a knowledge of the properties of the reservoir ck and fluids.

In the case of reservoirs under *hydraulic control*, where there is no ap- eciable decline in reservoir pressure, water influx is either inward and par- el to the bedding planes as found in thin, relatively steep dipping beds dge-water drive), or upward where the producing oil zone (column) is un- rlain by water (bottom-water drive). The oil remaining at abandonment in ose portions of the reservoir invaded by water, in barrels per acre-foot, is:

Reservoir oil	$7758 \times \phi \times S_{or}$	
Stock tank oil	$\frac{7758 \times \phi \times S_{or}}{B_{oi}}$	

here S_{or} is the residual oil saturation remaining after water displacement. nce it was assumed that the reservoir pressure was maintained at its initial lue by the water influx, no free gas saturation develops in the oil zone and e oil volume factor at abandonment remains B_{oi}. The recovery by active ater drive then is

$$\text{Recovery} = \frac{7758 \times \phi (1 - S_{wc} - S_{or})}{B_{oi}} \text{ STB/ac-ft} \quad (5.3)$$

nd the recovery factor is

$$\text{Recovery factor} = \frac{(1 - S_{wc} - S_{or})}{(1 - S_{wc})} \quad (5.4)$$

TABLE 5.2.
Correlation between reservoir oil viscosity, average reservoir permeability, and residual oil saturation (*After* Craze and Buckley[8] and Arps[7])

Reservoir Oil Viscosity (in cp)	*Residual Oil Saturation (percentage of pore space)*
0.2	30
0.5	32
1.0	34.5
2.0	37
5.0	40.5
10.0	43.5
20.0	64.5

Average Reservoir Permeability (in md)	*Deviation of Residual Oil Saturation from Viscosity Trend (percentage of pore space)*
50	+12
100	+ 9
200	+ 6
500	+ 2
1000	− 1
2000	− 4.5
5000	− 8.5

$$RF = 0.114 + 0.272 \log k + 0.256 S_w - 0.136 \log \mu_o - 1.538\phi - 0.00035 h \quad (5.5$$

For k = 1000 md, $S_w = 0.25$, $\mu_o = 2.0$ cp, $\phi = 0.20$, and $h = 10$ ft,

$$RF = 0.114 + 0.272 \times \log 1000 + 0.256 \times 0.25 - 0.136 \log 2 - 1.538 \times 0.20 - 0.00035 \times 10$$

$$0.642 \text{ or } 64.2\% \text{ (of initial stock tank oil)}$$

where,

For Sandstone

RF = recovery factor

For sandstone and carbonate reservoirs with solution gas drive:

$$\bar{E}_{R,o} = 0.41815\left[\frac{\bar{\phi}(1-\bar{S}_w)}{B_{ob}}\right]^{0.1611}\left(\frac{\bar{k}}{\mu_{ob}}\right)^{0.0979}(\bar{S}_w)^{0.3722}\left(\frac{p_b}{p_a}\right)^{0.1741} . \quad (4.8a)$$

For sandstone reservoirs with water drive:

$$\bar{E}_{R,o} = 0.54898\left[\frac{\bar{\phi}(1-\bar{S}_w)}{B_{oi}}\right]^{0.0422}\left(\frac{\bar{k}\mu_{wi}}{\mu_{oi}}\right)^{0.0770}(\bar{S}_w)^{-0.1903}\left(\frac{p_i}{p_a}\right)^{-0.2159} . \quad (4.8b)$$

In very thick oil reservoirs, where gravity segregation can be significant, the oil will tend to be heavier towards the bottom.

In this case it would be advantageous to have B_o measured or calculated at different depths. The average $\bar{B}_o$ can then be estimated as the mean weighted by the hydrocarbon volume $[\phi(1 - S_w)V_R]$ at each depth.

4.3.7 Recovery Factor E_R

The calculation of the oil recovery factor $E_{R,o}$ is perhaps the most delicate, and controversial, part of reserves evaluation by the volumetric method.

$E_{R,o}$ depends on a number of interrelated factors: reservoir drive mechanism (water drive, gas cap, solution gas, etc.), mobility ratio [displacing fluid/oil – Eq. (3.52)], heterogeneity of reservoir rock, number of wells and their distribution, production schedule of each well, possible implementation of improved recovery).

An accurate prediction of the recovery factor is only accessible through the use of a numerical simulator to model the reservoir behaviour. This is rarely feasible at such an early stage because of the scarcity of data during the discovery phase.

Evaluation of $E_{R,o}$ therefore usually has to depend on final recovery figures achieved elsewhere in a comparable reservoir rock – preferably in the same sedimentary basin – where the oil, and the drive mechanism, are of the same type.

Using final recoveries achieved in reservoirs in which the oil properties and petrophysical characteristics are well known, a number of correlations have been published. The most commonly used of these are supplied by the American Petroleum Institute:[4]

For sandstone and carbonate reservoirs with solution gas drive:

$$\bar{E}_{R,o} = 0.41815\left[\frac{\bar{\phi}(1-\bar{S}_w)}{B_{ob}}\right]^{0.1611}\left(\frac{\bar{k}}{\mu_{ob}}\right)^{0.0979}(\bar{S}_w)^{0.3722}\left(\frac{p_b}{p_a}\right)^{0.1741} . \quad (4.8a)$$

For sandstone reservoirs with water drive:

$$\bar{E}_{R,o} = 0.54898\left[\frac{\bar{\phi}(1-\bar{S}_w)}{B_{oi}}\right]^{0.0422}\left(\frac{\bar{k}\mu_{wi}}{\mu_{oi}}\right)^{0.0770}(\bar{S}_w)^{-0.1903}\left(\frac{p_i}{p_a}\right)^{-0.2159} . \quad (4.8b)$$

In both these equations, ϕ and S_w are decimal fractions, k is in Darcy, and μ in cP. The subscript b indicates "value at bubble point", i is "initial value", and p_a is the abandonment pressure (depleted reservoir). The two formulae are derived from a statistical analysis of data from, respectively, 80 and 70 reservoirs.

The *distribution* of E_R, S_w (for water drive) and S_g (for solution gas drive) are shown in Figs. 4.7 and 4.8 for the reservoirs in the survey.

It should be mentioned that in a subsequent publication,[5] the API expressed doubts about the accuracy of these correlations, and recommended they be used with caution!

The recovery factor for gas production, $E_{R,g}$, is a far simpler quantity to predict.

For expansion drive reservoirs (without water drive), recovery is controlled essentially by the level set for the abandonment pressure p_a. This in turn depends on the minimum acceptable wellhead pressure.

$$\bar{E}_{R,g} = 1 - \frac{p_a/z_a}{p_i/z_i} \quad (4.9a)$$

In a statistical study of Craze and Buckley's *water-drive* recovery data, Guthrie and Greenberger, using multiple correlation analysis methods, found the following correlation between water-drive recovery and five variables that affect recovery in *sandstone* reservoirs.[11]

$$RF = 0.114 + 0.272 \log k + 0.256 S_w - 0.136 \log \mu_o - 1.538\phi - 0.00035 h \quad (5.5)$$

For k = 1000 md, $S_w = 0.25$, $\mu_o = 2.0$ cp, $\phi = 0.20$, and $h = 10$ ft,

$$RF = 0.114 + 0.272 \times \log 1000 + 0.256 \times 0.25 - 0.136 \log 2 - 1.538 \times 0.20 - 0.00035 \times 10$$

$$0.642 \text{ or } 64.2\% \text{ (of initial stock tank oil)}$$

where,

RF = recovery factor

$$N(B_t - B_{ti}) + \frac{NmB_{ti}}{B_{gi}}(B_g - B_{gi}) + (1+m)\,N\,B_{ti}\left[\frac{c_w S_{wi} + c_f}{1 - S_{wi}}\right]\Delta\bar{p} + W_e$$
$$= N_p[B_t + (R_p - R_{soi})B_g] + B_w W_p \qquad (2.7)$$

3. MATERIAL BALANCE IN UNDERSATURATED RESERVOIRS

The material balance equation for undersaturated reservoirs was developed in Chapter 2 and is

$$N(B_t - B_{ti}) + NB_{ti}\left[\frac{c_w S_{wi} + c_f}{1 - S_{wi}}\right]\Delta\bar{p} + W_e = N_p[B_t + (R_p - R_{soi})B_g] + B_w W_p \qquad (2.8)$$

Neglecting the change in porosity of rocks with the change of internal fluid pressure, which is treated later, reservoirs with zero or negligible water influx are constant volume or volumetric reservoirs. If the reservoir oil is initially undersaturated, then initially it contains only connate water and oil, with their solution gas. The solubility of gas in reservoir waters is generally quite low and is considered negligible for the present discussion. Because the water production from volumetric reservoirs is generally small or negligible, it will be considered as zero. From initial reservoir pressure down to the bubble point, then, the reservoir oil volume remains a constant, and oil, is produced by liquid expansion. Incorporating these assumptions into Eq. (2.8), we get

$$N(B_t - B_{ti}) = N_p[B_t + (R_p - R_{soi})B_g] \qquad (5.6)$$

comes

$$N(B_t - B_{ti}) = N_p B_t \qquad (5.7)$$

his can be rearranged to yield fractional recovery, RF, as

$$RF = \frac{N_p}{N} = \frac{B_t - B_{ti}}{B_t} \qquad (5.8)$$

he fractional recovery is generally expressed as a fraction of the initial stock nk oil in place. The PVT data for the 3–A–2 reservoir of a field is given in g. 5.2.

The formation volume factor plotted in Fig. 5.2 is the single-phase ormation volume factor, B_o. The material balance equation has been derived sing the two-phase formation volume factor, B_t. B_o and B_t are related by q. (1.28)

$$B_t = B_o + B_g(R_{soi} - R_{so}) \qquad (1.28)$$

should be appareat that $B_t = B_o$ above the bubble-point pressure because R_{so} constant and equal to R_{soi}.

The reservoir fluid has an oil volume factor of 1.572 bbl/STB at the initial ressure 4400 psia and 1.600 bbl/STB at the bubble-point pressure of 3550 sia. Then by volumetric depletion, the fractional recovery of the stock tank il at 3550 psia by Eq. (5.8) is

$$RF = \frac{1.600 - 1.572}{1.600} = 0.0175 \text{ or } 1.75\%$$

f the reservoir produced 680,000 STB when the pressure dropped at 3550 sia, then the initial oil in place by Eq. (5.7) is

$$N = \frac{1.600 \times 680{,}000}{1.600 - 1.572} = 38.8\text{MM STB}$$

Below 3550 psia a *free gas* phase develops; and for a volumetric, under-

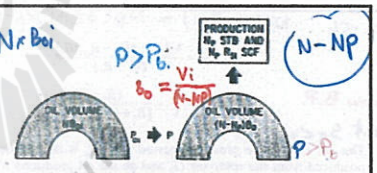

Fig. 3.6. Diagram showing that the oil saturation remains constant in a volumetric reservoir producing by liquid expansion above the bubble point.

pressure down to the bubble point, then, the reservoir oil volume remains a constant and oil is produced by liquid expansion as indicated in the diagrams of Fig. 3.6. Equating the initial volume to the final volume,

$$NB_{oi} = (N - N_p)B_o$$

$$N = \frac{B_o N_p}{B_o - B_{oi}} \qquad (3.8)$$

Figure 5.3 shows schematically the changes that occur between initial reserv
pressure and some pressure below the bubble point. The free-gas phase d
not necessarily rise to form an *artificial* gas cap, and the equations are the sa

$P_i = 4400$; $B_o = 1.572$ @ $P_b = 3550$ $B_o = 1.600$

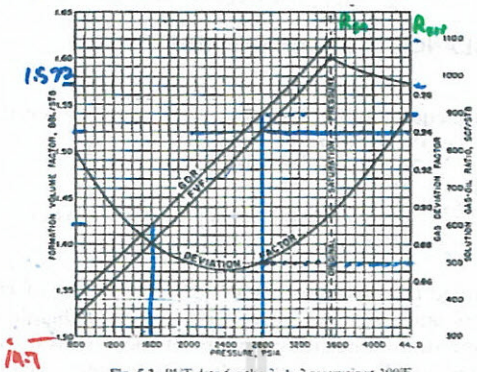

Fig. 5.2. PVT data for the 3–A–2 reservoir at 190°F.

$$N = \frac{B_o N_P}{B_o - B_{oi}} = \frac{1.6 \times 650{,}000}{1.6 - 1.572} = 38.5 \text{ MMSTB}$$

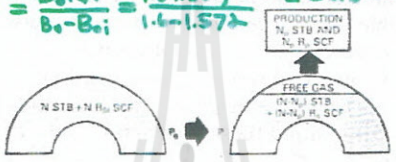

Fig. 5.3. Diagram showing the formation of a free-gas phase in a volumetric rese
below the bubble point.

$V_{oi} = V_o + V_g$

P-156 $N(B_t - B_{ti}) = N_p(B_t + (R_p - R_{oi})B_g)$ -(5.6

$$N = \frac{N_p[B_t + (R_p - R_{soi})B_g]}{(B_t - B_{ti})} \quad (5.10)$$

Below B.P. but $S_g < 10\%$

$$RF = \frac{N_p}{N} = \frac{(B_t - B_{ti})}{[B_t + (R_p - R_{soi})B_g]} \quad (5.11)$$

The *net cumulative produced gas-oil ratio* R_p is the quotient of all the gas produced from the reservoir G_p and all the oil produced N_p. In some reservoirs, some of the produced gas is returned to the *same* reservoir, so that the *net* produced gas is only that which is not returned to the reservoir. When all the produced gas is returned to the reservoir, R_p is zero.

An inspection of Eq. (5.11) indicates that all the terms except the produced gas-oil ratio, R_p, are functions of pressure only and are the properties of the reservoir fluid. Because the nature of the fluid is fixed, it follows that the fractional recovery RF is fixed by the PVT properties of the reservoir fluid and the produced gas-oil ratio. Since the produced gas-oil ratio occurs in the denominator of Eq. (5.11), large gas-oil ratios give low recoveries and vice versa.

Example 5.1. Calculations to show the effect of the produced gas-oil ratio R_p on fractional recovery in volumetric, undersaturated reservoirs.

Given:

The PVT data for the 3–A–2 reservoir, Fig. 5.2.
Cumulative GOR at 2800 psia = 3300 SCF/STB.
Reservoir temperature = 190°F = 650°R.
Standard conditions = 14.7 psia and 60°F.

$R_p = \frac{\text{Cum Gas}}{\text{Cum Oil}}$

SOLUTION: $R_{si} = 1100$ SCF/STB; $B_o = 1.572$ bbl/STB; R_{soi} at 2800 psia = 900 SCF/STB; B_o at 2800 psia = 1.520 bbl/STB; $R_p = 3300$ SCF/STB; and B_g at 2800 psia calculated as

$$B_g = \frac{znR'T}{5.615\,p} = \frac{0.870 \times 10.73 \times 650}{5.615 \times 379.4 \times 2800} = 0.00102 \text{ bbl/SCF} \times \frac{\text{SCF}}{\text{STB}}$$

$$B_t = B_o + B_g(R_{soi} - R_{si})$$

$$B_t = 1.520 + 0.00102(1100 - 900) = 1.724 \text{ bbl/STB}$$

Figure 5.3 shows schematically the changes that occur between initial reserv
pressure and some pressure below the bubble point. The free-gas phase d
not necessarily rise to form an *artificial* gas cap, and the equations are the sa
$P_i = 4400$; $B_o = 1.572$ @ $P_b = 3550$ $B_o = 1.600$

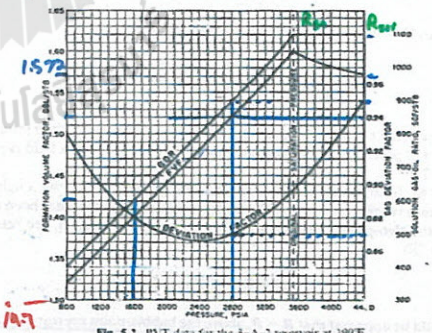

Fig. 5.2. PVT data for the 3–A–2 reservoir at 190°F.

$$N = \frac{B_o N_P}{B_o - B_{oi}} = \frac{1.6 \times 650{,}000}{1.6 - 1.572} = 38.5 \text{ MMSTB}$$

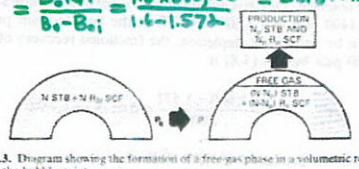

Fig. 5.3. Diagram showing the formation of a free-gas phase in a volumetric rese
below the bubble point.

$V_{oi} = V_o + V_g$

P-156 $N(B_t - B_{ti}) = N_p(B_t + (R_p - R_{si})B_g)$ -(5.6)

$$N = \frac{N_p[B_t + (R_p - R_{si})B_g]}{(B_t - B_{ti})} \quad (5.10)$$

Below B.P. but $S_g < 10\%$

$$RF = \frac{N_p}{N} = \frac{(B_t - B_{ti})}{[B_t + (R_p - R_{si})B_g]} \quad (5.11)$$

The *net cumulative produced gas-oil ratio* R_p is the quotient of all the gas produced from the reservoir G_p and all the oil produced N_p. In some reservoirs, some of the produced gas is returned to the *same* reservoir, so that the *net* produced gas is only that which is not returned to the reservoir. When all the produced gas is returned to the reservoir, R_p is zero.

An inspection of Eq. (5.11) indicates that all the terms except the produced gas-oil ratio, R_p, are functions of pressure only and are the properties of the reservoir fluid. Because the nature of the fluid is fixed, it follows that the fractional recovery RF is fixed by the PVT properties of the reservoir fluid and the produced gas-oil ratio. Since the produced gas-oil ratio occurs in the denominator of Eq. (5.11), large gas-oil ratios give low recoveries and vice versa.

Example 5.1. Calculations to show the effect of the produced gas-oil ratio R_p on fractional recovery in volumetric, undersaturated reservoirs.

Given:

The PVT data for the 3–A–2 reservoir, Fig. 5.2.
Cumulative GOR at 2800 psia = 3300 SCF/STB. $R_p = \frac{\text{Cum Gas}}{\text{Cum Oil}}$
Reservoir temperature = 190°F = 650°R.
Standard conditions = 14.7 psia and 60°F.

SOLUTION: R_{si} = 1100 SCF/STB; B_{oi} = 1.572 bbl/STB; R_{si} at 2800 psia = 900 SCF/STB; B_o at 2800 psia = 1.520 bbl/STB; R_p = 3300 SCF/STB; and B_g at 2800 psia calculated as

$$B_g = \frac{znR'T}{5.615\,p} = \frac{0.870 \times 10.73 \times 650}{5.615 \times 379.4 \times 2800} = 0.00102 \text{ bbl/SCF} \times \frac{\text{SCF}}{\text{STB}}$$

$$B_t = B_o + B_g(R_{si} - R_{so})$$

$$B_t = 1.520 + 0.00102(1100 - 900) = 1.724 \text{ bbl/STB}$$

Figure 5.3 shows schematically the changes that occur between initial reservoir pressure and some pressure below the bubble point. The free-gas phase does not necessarily rise to form an *artificial* gas cap, and the equations are the same.

P_i = 4,800 ; B_o = 1.572 @ P_i ; 3650 B_o = 1.600

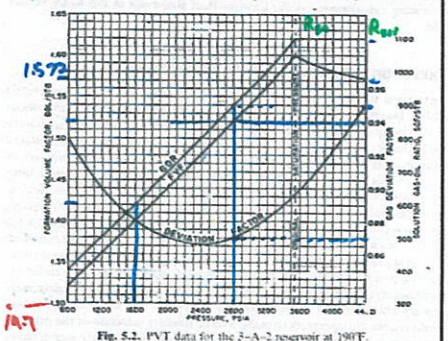

Fig. 5.2. PVT data for the 3–A–2 reservoir at 190°F.

$$N = \frac{B_o N_P}{B_o - B_{oi}} = \frac{1.6 \times 1{,}480{,}000}{1.6 - 1.572} = 38.8 \text{ MM STB}$$

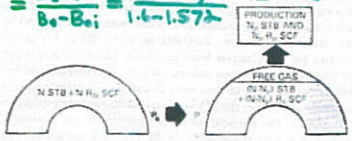

Fig. 5.3. Diagram showing the formation of a free-gas phase in a volumetric reservoir below the bubble point.

$V_{oi} = V_o + V_g$

Then at 2800 psia

P-157 $B_t - B_{ti}$

$$\frac{N_p}{N} = RF = \frac{1.724 - 1.572}{1.724 + 0.00102(3300 - 1100)} = 0.0383, \text{ or } 3.83\%$$

$B_t + B_g(R_p - R_{si})$

If two-thirds of the produced gas had been returned to the reservoir, at the same pressure (i.e., 2800 psia), the fractional recovery would have been

$$RF = \frac{1.724 - 1.572}{1.724 + 0.00102(1100 - 1100)} = 0.088, \text{ or } 8.8\%$$

$\frac{2}{3}$ Return to Reservoir

$R_p = 1100 \frac{\text{SCF}}{\text{STB}}$

uation (5.10) may be used to find the initial oil in place. For example, if 1.486 MM STB had been produced down to 2800 psia, for R_p = 3300 SCF/STB, the initial oil in place is

N_p $(B_t + B_g(R_p - R_{si})$ if N_p = 1.486

$$N = \frac{1.486 \times 10^6[1.724 + 0.00102(3300 - 1100)]}{1.724 - 1.572} = 38.8 \text{ MM STB}$$

$B_t - B_{ti}$

The calculations of Ex. 5.1 for the 3–A–2 reservoir show that for R_p = 3300 SCF/STB the recovery at 2800 psia is 3.83%, and that if R_p had been only 1100 SCF/STB, the recovery would have been 8.80%. Neglecting in each case the ~ 75% recovery by liquid expansion down to the bubble-point pressure, the effect of reducing the gas-oil ratio by one-third is approximately to triple the recovery. The produced gas-oil ratio can be controlled by working over

gravity drainage, and there may be a considerable period in which the oil drains downward to the wells from which it is pumped to the surface.

In the next section, we present a method that allows the material balance equation to be used as a predictive tool. The method was used by engineers performing calculations on the Canyon Reef Reservoir in the Kelly-Snyder Field.

5. KELLY-SNYDER FIELD, CANYON REEF RESERVOIR

The Canyon Reef reservoir of the Kelly-Snyder Field, Texas, was discovered in 1948. During the early years of production, there was much concern about the very rapid decline in reservoir pressure; however, reservoir engineers were able to show that this was to be expected of a volumetric undersaturated reservoir with an initial pressure of 3112 psig and a bubble-point pressure of only 1725 psig, both at a datum of 4300 ft subsea.[15] Their calculations further showed that when the bubble-point pressure is reached, the pressure decline should be much less rapid, and that the reservoir could be produced without pressure maintenance for many years thereafter without prejudice to the pressure maintenance program eventually adopted. In the meantime, with additional pressure drop and production, further reservoir studies could evaluate the potentialities of water influx, gravity drainage, and intrareservoir communication. These, together with laboratory studies on cores to determine recovery efficiencies of oil by depletion and by gas and water displacement, should enable the operators to make a more prudent selection of the pressure maintenance program to be used, or demonstrate that a pressure maintenance program would not be successful.

Although additional and revised data have become available in subsequent years, the following calculations, which were made in 1950 by reservoir engineers, are based on data available in 1950. Table 5.3 gives the basic reservoir data for the Canyon Reef reservoir. Geologic and other evidence indicated that the reservoir was volumetric (i.e., that there would be negligible water influx), so the calculations were based on volumetric behavior. If any water entry should occur, the effect would be to make the calculations more optimistic, that is, there would be more recovery at any reservoir pressure. The reservoir was undersaturated, so the recovery from initial pressure to bubble-point pressure is by liquid expansion, and the fractional recovery at the bubble point is

$$RF = \frac{B_t - B_{ti}}{B_t} = \frac{1.4509 - 1.4235}{1.4509} = 0.0189 \text{ or } 1.89\%$$

Based on an initial content of 1.4235 reservoir barrels or 1.00 STB, this is recovery of 0.0189 STB. Because the solution gas remains at 885 SCF/STB

Kelly-Snyder Field, Texas (Courtesy, The Oil and Gas Journal[14])

Initial reservoir pressure	3112 psig (at 4300 ft subsea)
Bubble-point pressure	1725 psig (at 4300 ft subsea)
Average reservoir temperature	125°F
Average porosity	7.7%
Average connate water	20%
Critical gas saturation (estimated)	10%

Differential Liberation Analyses of a Bottom-hole Sample from the Standard Oil Company of Texas No. 2-1, J. W. Brown, at 125°F

Pressure psig	B_o bbl/STB	B_g bbl/SCF	Solution GOR SCF/STB	B_t bbl/STB
3112	1.4235	...	885	1.4235
2800	1.4290	...	885	1.4290
2400	1.4370	...	885	1.4370
2000	1.4446	...	885	1.4446
1725	1.4509	...	885	1.4509
1700	1.4468	0.00141	876	1.4595
1600	1.4303	0.00151	842	1.4952
1500	1.4139	0.00162	807	1.5403
1400	1.3978	0.00174	772	1.5944

down to 1725 psig, the producing gas-oil ratio and the cumulative produced gas-oil ratio should remain near 885 SCF/STB during this pressure decline.

Below 1725 psig, a free gas phase develops in the reservoir. As long as this gas phase remains immobile, it can neither flow to the well bores nor migrate upward to develop a gas cap but must remain distributed throughout the reservoir, increasing in size as the pressure declines. Because pressure changes much less rapidly with reservoir voidage for gases than for liquids, the reservoir pressure declines at a much lower rate below the bubble point. It was estimated that the gas in the Canyon Reef reservoir would remain immobile until the gas saturation reached a value near 10% of the pore volume. When the free gas begins to flow, the calculations become quite complex (see Chapter 9); but as long as the free gas is immobile, calculations may be made assuming that the producing gas-oil ratio R at any pressure will equal the solution gas-oil ratio R_s at the pressure, since the only gas that reaches the well bore is that in solution, the free gas being immobile. Then the average producing (daily) gas-oil ratio between any two pressures p_1 and p_2 is approximately

$$R_{avg} = \frac{R_{s1} + R_{s2}}{2} \qquad (5.12)$$

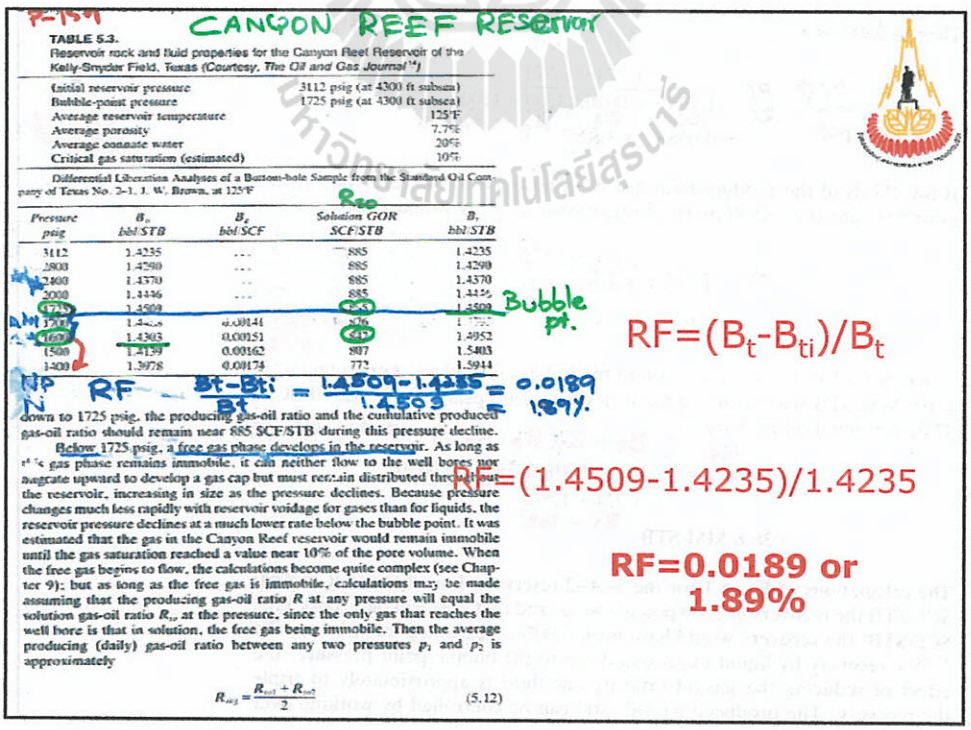

and the cumulative gas-oil ratio at any pressure is

$$R_p = \frac{\Sigma \Delta N_p \times R}{N_p} = \frac{N_{pb} \times R_{ave} + (N_{p1} - N_{pb})R_{ave1} + (N_{p2} - N_{p1})R_{ave2} + \text{etc.}}{N_{pb} + (N_{p1} - N_{pb}) + (N_{p2} - N_{p1}) + \text{etc.}} \quad (5.13)$$

On the basis of 1.00 STB of initial oil, the production at bubble-point pressure N_{pb} is 0.0189 STB. The average producing gas-oil ratio between 1725 and 1600 psig will be

$$R_{ave1} = \frac{885 + 842}{2} = 864 \text{ SCF/STB}$$

The cumulative recovery at 1600 psig N_{p1} is unknown; however the cumulative gas-oil ratio R_p may be expressed by Eq. (5.13) as

$$R_{p1} = \frac{0.0189 \times 885 + (N_{p1} - 0.0189)864}{N_{p1}}$$

This value of R_{p1} may be placed in Eq. (5.11) together with the PVT values at 1600 psig as,

$$N_{p1} = \frac{1.4952 - 1.4235}{1.4952 - 0.00151\left[\dfrac{0.0189 \times 885 + (N_{p1} - 0.0189)864}{N_{p1}} - 885\right]}$$

$$= 0.0486 \text{ STB at 1600 psig}$$

In a similar manner the recovery at 1400 psig may be calculated, the results being valid only if the gas saturation remains below the critical gas saturation, assumed to be 10% for the present calculations.

When N_p stock tank barrels of oil have been produced from a *volumetric undersaturated reservoir*, and the average reservoir pressure is p, the volume of the remaining oil is $(N - N_p)B_o$. Since the initial pore volume of the reservoir V_p is

$$V_p = \frac{NB_{oi}}{(1 - S_{wc})} \quad (5.14)$$

and since the oil saturation is the oil volume divided by the pore volume,

$$S_o = \frac{(N - N_p)B_o(1 - S_{wc})}{NB_{oi}} = \frac{(1 - N_p)B_o(1 - S_{wc})}{N B_{oi}} \quad (5.15)$$

$$R_{avg2} = \frac{842 + 807}{2} = 824.5$$

$$R_{p2} = \frac{N_{pb} * R_{ave1} + (N_{p1} - N_{pb}) * R_{avg2} + (N_{p2} - N_{p1}) * R_{avg3}}{N_{pb} + (N_{p1} - N_{pb}) + (N_{p2} - N_{p1})}$$

$$R_{p2} = \frac{0.0189 * 885 + (0.0486 - 0.0189) * 864 + (N_{p2} - 0.048) * 8245}{0.0189 + (0.0486 - 0.0189) + (N_{p2} - 0.0486)}$$

$$R_{p2} = \frac{2.8113 + 824.5 N_{p2}}{N_{p2}}$$

$$N_{p2} = \frac{B_t - B_{ti}}{B_t + (R_p - R_{soi})B_g}$$

$$N_{p2} = \frac{1.5403 - 1.4235}{1.5403 + \left(\dfrac{2.8113 - 824.5 N_{p2}}{N_{p2}} - 885\right)0.00162}$$

$$N_{p2} = \frac{1.5403 - 1.4235}{\left(\dfrac{1.44229 N_{p2} + 0.004554}{N_{p2}}\right)}$$

$$1.44229 N_{p2} = 1.5403 - 1.4235 - 0.004554 = 0.112246$$

$$N_{p2} = \frac{0.112246}{1.44229} = 0.077825$$

So=(1-Np/N)B$_0$(1-Sw)/B$_{oi}$

On the basis of $N = 1.00$ STB initially, N_p is the fractional recovery RF, or N_p/N, and Eq. (5.15) may be written as

$$S_o = (1 - RF)(1 - S_{wc})\left(\frac{B_o}{B_{oi}}\right) \quad (5.16)$$

where S_{wc} is the connate volumetric reservoirs. The

$$S_o = (1 - 0.0486)(1 - 0.20)\left(\frac{1.4303}{1.4235}\right)$$

$$= 0.765$$

The gas saturation is $(1 - S_o - S_{wc})$, or

$$S_g = 1 - 0.765 - 0.200 = 0.035$$

Figure 5.4 shows the calculated performance of the Kelly-Snyder Field down to a pressure of 1400 psig. Calculations were not continued beyond this point because the free gas saturation had reached approximately 10%, the estimated critical gas saturation for the reservoir. The graph shows the rapid pressure decline above the bubble point and the predicted flattening below the

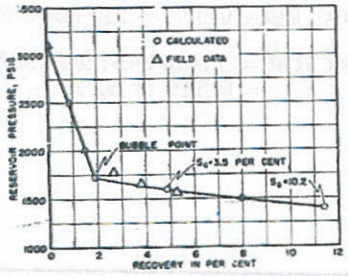

Fig. 5.4. Material balance calculations and performance, Canyon Reef reservoir, Kelly-Snyder Field.

$$R_{avg3} = \frac{807 + 772}{2} = 784.5$$

$$R_{p3} = \frac{0.0189 * 885 + (0.0486 - 0.0189 * 864 + (0.08414 - 0.0486) * 8245 + (N_{p3} - 0.077825) * 7845}{0.0189 + (0.0486 - 0.0189) + (0.077825 - 0.0486) + (N_{p3} - 0.077825} = \frac{5.4296 + 7845 N_{p3}}{N_{p3}}$$

$$N_{p3} = \frac{1.5944 - 1.4235}{1.5944 + \left(\dfrac{5.4296 + 784.5 N_{p3}}{N_{p2}} - 885\right)0.00174}$$

$$N_{p3} = \frac{0.1709}{\left(\dfrac{1.41953\ N_{p3} + 0.009448}{N_{p3}}\right)}$$

$$N_{p3} = \frac{0.1709 - 0.009448}{1.41953} = 0.113737$$

On the basis of $N = 1.00$ STB initially, N_p is the fractional recovery RF, or N_p/N, and Eq. (5.15) may be written as

$$S_o = (1 - RF)(1 - S_{wi})\left(\frac{B_o}{B_{oi}}\right) \quad (5.16)$$

So=(1-Np/N)B_0(1-Sw)/B_{oi}

So=(1-RF)(1-Sw)(B_0/B_{oi})

where S_{wi} is the connate water, which is assumed to remain constant in volumetric reservoirs. Then at 1600 psig the oil saturation is

$$S_o = (1 - 0.0486)(1 - 0.20)\left(\frac{1.4303}{1.4235}\right) = 0.765$$

The gas saturation is $(1 - S_o - S_{wi})$, or

$$S_g = 1 - 0.765 - 0.200 = 0.035$$

$$at P = 1500\ psia;\ S_o = (1 - 0.1137)(1 - 0.2)\left(\frac{1.3978}{1.4235}\right) = 0.698$$

Figure 5.4 shows the calculated performance of the Kelly-Snyder Field down to a pressure of 1400 psig. Calculations were not continued beyond this point because the free gas saturation had reached approximately 10%, the estimated critical gas saturation for the reservoir. The graph shows the rapid pressure decline above the bubble point and the predicted flattening below the

$$S_g = 1 - S_{wi} - S_o = 1 - 0.2 - 0.698 = 0.102$$

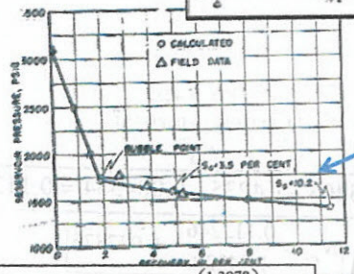

$at P = 1500\ psia;\ S_o = (1 - 0.1137)(1 - 0.2)\left(\frac{1.3978}{1.4235}\right) = 0.698$ Reef reservoir.

N = 2.25MMMSTB → M.B

bubble point. The predictions are in good agreement with the field performance, which is calculated in Table 5.4 using field pressures and production data, and a value of 2.25 MMM STB for the initial oil in place. The producing gas-oil ratio, Col. (2), increases instead of decreasing, as predicted by the previous theory. This is due to the more rapid depletion of some portions of the reservoir—for example, those drilled first, those of low net productive thickness, and those in the vicinity of the well bores. For the present predictions, it is pointed out that the previous calculations would not be altered greatly if a constant producing gas-oil ratio of 885 SCF/STB (i.e., the initial dissolved ratio) had been assumed throughout the entire calculation.

The initial oil under a 40 acre unit of the Canyon Reef reservoir for a net formation thickness of 200 feet is

A x h x ϕ

$$N = \frac{7758 \times 40 \times 200 \times 0.077 \times (1 - 0.20)}{1.4235} = 2.66\text{MM STB}$$

Kelly-Snyder Canyon Reef Reservoir

Then at the average daily well rate of 92 BOPD in 1950, the time to produce 11.35% of the initial oil (i.e., at 1400 psig when the gas saturation is calculated to be near 10%) is

0.1133 x 2.25 = 255 MMSTB

$$t = \frac{0.1135 \times 2.69 \times 10^6}{92 \times 365} = 9.1 \text{ years}$$

Primary Recovery 25% = 560 MMSTB (Planned)

By means of this calculation, the reservoir engineers were able to show that there was no immediate need for a curtailment of production and that there was plenty of time in which to make further reservoir studies and carefully

water injection D.N. 1954 Recovery 600 MMSTB 1961 50%

TOTAL RECOVERY = 560+600 MMSTB

RECOVERY FACTOR = 1160MMSTB/2250MMSTB

= 0.516 or 52%

TABLE 5.4.
Recovery from Kelly-Snyder Canyon Reef Reservoir based on production data and measured average reservoir pressures, and assuming an initial oil content of 2.25 MMM STB

1.2MMMSTB

(1) Pressure Interval, psig	(2) Ave. Producing Gas-Oil Ratio, SCF/STB	(3) Incremental Oil Production, MM STB	(4) Cumulative Oil Production, MM STB	(5) Percentage Recovery (N = 2.25 MMM STB)
3512 to 1771	896	60.421	60.421	2.69
1771 to 1713	934	11.958	72.379	3.22
1713 to 1662	971	13.320	85.699	3.81
1662 to 1570	1023	20.009	105.708	4.70
1570 to 1461	1045	11.864	117.572	5.23

255 MM 10.35

RODESSA FIELD, Louisiana.

Average monthly production de Gloyd-Mitchell Zone of the . ndess Field

(1) Months after Start of Production	(2) No. Wells	(3) Average Daily Oil, Barrels	(4) Average Daily GOR, SCF/STB	(5) Average Pressure, psig	(6) Daily Oil per Well, (3) ÷ (2)	(7) Monthly Oil, Barrels, 30.4 × (3)	(8) Cumulative Oil, Barrels, Sum (7)	(9) Monthly Gas, M SCF, (4) × (7)	(10) Cumulative Gas, M SCF, Sum (9)	(11) Cumulative GOR, SCF/STB, 10 ÷ (8)
1	2	400	625	2700*	200	12,160	12,160	7,600	7,600	625
2	1	500	750		500	15,200	27,360	11,400	19,000	694
3	3	700	875		233	21,280	48,640	18,620	37,620	773
4	4	1,300	1,000	2490	325	39,520	88,160	39,520	77,140	875
5	4	1,200	950		300	36,480	124,640	34,656	111,796	897
6	6	1,900	1,000		316	57,760	182,400	57,760	169,556	930
7	12	3,600	1,200	2280	300	109,440	291,840	131,328	300,884	1031
8	16	4,900	1,200		306	148,960	440,800	178,752	479,636	1088
9	21	6,100	1,450		290	185,440	626,240	259,616	739,252	1181
10	28	7,500	1,700	2070	268	228,000	854,240	387,600	1,127M	1319
11	48	9,800	1,800		204	297,920	1,152,160	536,256	1,663M	1443
12	55	11,700	1,900		213	355,680	1,507,840	675,792	2,339M	1551
13	59	9,900	2,100	1860	168	300,960	1,808,800	632,016	2,971M	1643
14	65	10,000	2,400		154	304,000	2,112,800	729,600	3,701M	1752
15	74	11,200	2,750		138	310,080	2,422,880	852,720	4,554M	1880
16	79	11,400	3,200	1650*	144	346,560	2,769,440	1,108,992	5,662M	2045
17	87	10,800	4,100		124	328,320	3,097,760	1,346,112	7,008M	2262
18	91	9,200	4,800		101	279,680	3,377,440	1,342,464	8,351M	2473
19	93	9,000	5,300	1250	97	273,600	3,651,040	1,450,080	9,801M	2684

*Linear decline assumed from original to first measured BHP.

†First measured reservoir pressure. All subsequent pressures are measured.

TABLE 5.5. (Continued)

RODESSA FIELD, Louisiana.

(1) Months after Start of Production	(2) No. Wells	(3) Average Daily Oil, Barrels	(4) Average Daily GOR, SCF/STB	(5) Average Pressure, psig	(6) Daily Oil per Well, (3) ÷ (2)	(7) Monthly Oil, Barrels, 30.4 × (3)	(8) Cumulative Oil, Barrels, Sum (7)	(9) Monthly Gas, M SCF, (4) × (7)	(10) Cumulative Gas, M SCF, Sum (9)	(11) Cumulative GOR, SCF/STB, 10 ÷ (8)
20	96	8,300	5,900	1115	86	252,320	3,903,360	1,488,688	11,290M	2892
21	93	7,200	6,800	1000	77	218,880	4,122,240	1,488,384	12,778M	3100
22	93	6,400	7,500	900	69	194,560	4,316,800	1,459,200	14,237M	3298
23	95	5,800	7,600	8[illegible]5	61	176,320	4,493,120	1,340,032	15,577M	3467
24	94	5,400	7,700	7[illegible]0	57	164,160	4,657,280	1,264,032	16,841M	3616
25	95	5,000	7,800	7[illegible]5	53	152,000	4,809,280	1,185,600	18,027M	3748
26	92	4,400	7,500	5[illegible]5	48	133,760	4,943,040	1,003,200	19,030M	3850
27	94	4,200	7,300	5[illegible]0	45	127,680	5,070,720	932,064	19,962M	3937
28	94	4,000	7,300	5[illegible]0	43	121,600	5,192,320	887,680	20,850M	4016
29	93	3,400	6,800	4[illegible]0	37	103,360	5,295,680	702,848	21,553M	4070
30	95	3,200	6,300	4[illegible]5	34	97,280	5,392,960	612,864	22,165M	4110
31	91	3,100	6,100	3[illegible]0	34	94,240	5,487,200	574,864	22,740M	4144
32	93	2,900	5,700	310	31	88,160	5,575,360	502,512	23,243M	4169
33	92	3,000	5,300	390	33	91,200	5,666,560	483,360	23,726M	4187
34	88	2,900	5,100	300	33	88,160	5,754,720	449,616	24,176M	4201
35	87	2,000	4,900	280	23	60,800	5,815,520	297,920	24,474M	4208
36	90	2,400	4,800	310	27	72,960	5,888,480	350,208	24,824M	4216
37	88	2,100	4,500	300	24	63,840	5,952,320	287,280	25,111M	4219
38	88	2,200	4,500	2[illegible]5	25	66,880	6,019,200	300,960	25,412M	4222
39	87	2,100	4,300	300	24	63,840	6,083,040	274,512	25,687M	4223
40	82	2,000	4,000	275	24	60,800	6,143,840	243,200	25,930M	4220
41	85	2,100	3,600	225	25	63,840	6,207,680	229,824	26,160M	4214

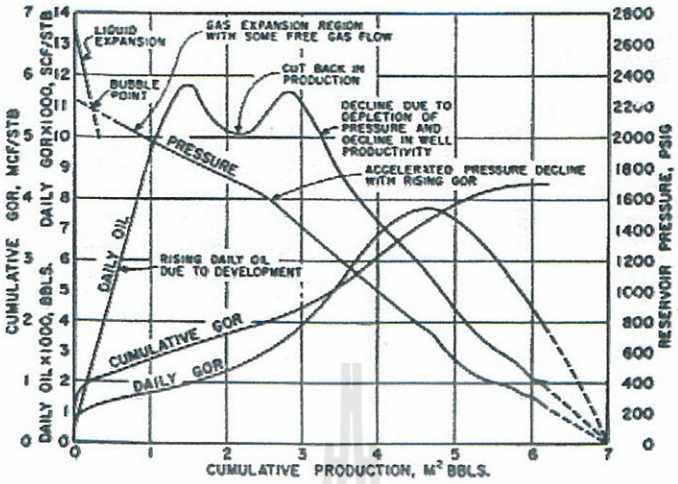

Fig. 5.6. History of the Gloyd-Mitchell Zone of the Rodessa Field plotted versus cumulative recovery.

P-109

The rapid increase in gas-oil ratios in the Rodessa Field led to the enactment of a gas-conservation order. In this order, oil and gas production were allocated partly on a volumetric basis to restrict production from wells with high gas-oil ratios. The basic ratio for oil wells was set at 2000 SCF/bbl. For leases on which the wells produced more than 2000 SCF/STB, the allowable in barrels per day per well, based on acreage and pressure, was multiplied by 2000 and divided by the gas-oil ratio of the well. This cut in production produced a double hump in the daily production curve.

In addition to a graph showing the production history versus *time*, it is usually desirable to have a graph that shows the production history plotted versus the *cumulative produced oil*. Figure 5.6 is such a plot for the Gloyd-Mitchell zone data and is also obtained from Table 5.5. This graph shows some features that do not appear in the time graph. For example, a study of the reservoir pressure curve shows the Gloyd-Mitchell zone was producing by liquid expansion until approximately 200,000 bbl were produced. This was followed by a period of production by gas expansion with a limited amount of free gas flow. When approximately 3 million bbl had been produced, the gas began to flow much more rapidly than the oil, resulting in a rapid increase in the gas-oil ratio. In the course of this trend, the gas-oil ratio curve reached a maximum, then declined as the gas was depleted and the reservoir pressure approached zero. The decline in gas-oil ratio beginning after approximately 4.5 million bbl were produced was due mainly to the expansion of the flowing reservoir gas as pressure declined. Thus the same gas-oil ratio in standard cubic feet per day gives approximately twice the reservoir flow rate at 400 psig

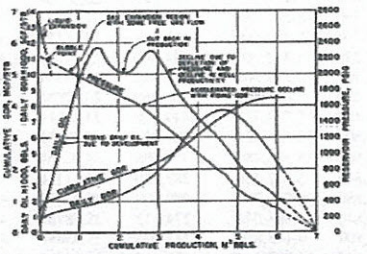

Fig. 5.6. History of the Gloyd-Mitchell Zone of the Rodessa Field plotted versus cumulative recovery.

as at 800 psig; hence, the surface gas-oil ratio may decline and yet the ratio of the rate of flow of gas to the rate of flow of oil *under reservoir conditions* continues to increase. It may also be reduced by the occurrence of some gravitational segregation, and also, from a quite practical point of view, by the failure of operators to measure or report gas production on wells producing fairly low volumes of low-pressure gas.

The results of a differential gas-liberation test on a bottom-hole sample from the Gloyd zone show that the solution gas-oil ratio was 624 SCF/STB which is in excellent agreement with the initial producing gas-oil ratio of 625 SCF/STB.[9] In the absence of gas-liberation tests on a bottom-hole sample, the initial gas-oil ratio of a properly completed well in either a dissolved gas drive, gas cap drive, or water-drive reservoir, is usually a reliable value to use for the initial solution gas-oil ratio of the reservoir. The extrapolations of the pressure, oil rate, and producing gas-oil ratio curves on the cumulative oil plot all indicate an ultimate recovery of about 7 million bbl. However, no such extrapolation can be made on the time plot. It is also of interest that whereas the daily producing rate is exponential on the time plot, it is close to a straight line on the cumulative oil plot.

The average gas-oil ratio during any production interval and the cumulative gas-oil ratio may be indicated by integrals and shaded areas on a typical daily gas-oil ratio versus cumulative stock tank oil production curve as shown in Fig. 5.7. If R represents the daily gas-oil ratio at any time, and N_p the cumulative stock tank production at the same time, then the production during a short interval of time is dN_p and the total volume of gas produced during that production interval is $R\,dN_p$. The gas produced over a longer period when the gas-oil ratio is changing is given by

$$\Delta G_p = \int_{N_{p1}}^{N_{p2}} R\,dN_p \tag{5.18}$$

The shaded area between N_{p1} and N_{p2} is proportional to the gas produced during the interval. The average daily gas-oil ratio during the production

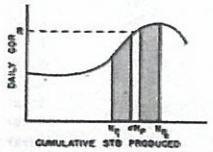

Fig. 5.7. Typical daily gas-oil ratio curve for a dissolved gas drive reservoir.

in Fig. 5.7. If R represents the daily gas-oil ratio at any time, and N_p the cumulative stock tank production at the same time, then the production during a short interval of time is dN_p and the total volume of gas produced during that production interval is $R\,dN_p$. The gas produced over a longer period when the gas-oil ratio is changing is given by

$$\Delta G_p = \int_{N_{p1}}^{N_{p2}} R\,dN_p \qquad (5.18)$$

The shaded area between N_{p1} and N_{p2} is proportional to the gas produced during the interval. The average daily gas-oil ratio during the production

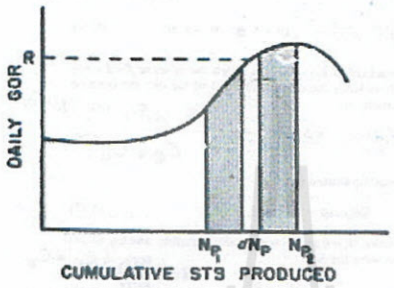

Fig. 5.7. Typical daily gas-oil ratio curve for a dissolved gas drive reservoir.

interval equals the area under the gas-oil ratio curve between N_{p1} and N_{p2} in units given by the coordinate scales, divided by the oil produced in the interval $(N_{p2} - N_{p1})$, and

$$R_{av} = \frac{\int_{N_{p1}}^{N_{p2}} R\,dN_p}{(N_{p2} - N_{p1})} \qquad (5.19)$$

The cumulative gas-oil ratio, R_p, is the total net gas produced up to any period divided by the total oil produced up to that period, or

$$R_p = \frac{\int_0^{N_p} R\,dN_p}{N_p} \qquad (5.20)$$

The cumulative produced gas-oil ratio was calculated in this manner in Col. (11) of Table 5.5. For example, at the end of the third period,

$$R_p = \frac{625 \times 12{,}160 + 750 \times 15{,}200 + 875 \times 21{,}280}{12{,}160 + 15{,}200 + 21{,}280} = 773 \text{ SCF/STB}$$

6. CALCULATIONS INCLUDING FORMATION AND WATER COMPRESSIBILITIES

In Chapter 1, it was shown that both formation and water compressibilities are functions of pressure. This suggests that there are in fact no volumetric reservoirs—that is, those in which the hydrocarbon pore volume of the reservoir remains constant. Hall showed the magnitude of the effect of formation compressibility on volumetric reservoir calculations.[16] The term *volumetric*, however, is retained to indicate those reservoirs in which there is no water influx but in which volumes change slightly with pressure due to the effects just mentioned.

The effect of compressibilities above the bubble point on calculations for N are examined first. Equation (2.8), with $R_p = R_{si}$ above the bubble point becomes

$$N(B_t - B_{ti}) + N B_{ti}\left[\frac{c_w S_{wi} + c_f}{1 - S_{wi}}\right]\Delta\bar{p} + W_e = N_p B_t + B_w W_p \qquad (5.21)$$

This equation may be rearranged to solve for N

$$N = \frac{N_p B_t - W_e + B_w W_p}{B_t - B_{ti} + B_{ti}\left[\frac{c_w S_{wi} + c_f}{1 - S_{wi}}\right]\Delta\bar{p}} \qquad (5.22)$$

Although this equation is entirely satisfactory, often an oil compressibility, c_o, is introduced with the following defining relationship

$$c_o = \frac{v_o - v_{oi}}{v_{oi}(p_i - \bar{p})} = \frac{B_o - B_{oi}}{B_{oi}\Delta\bar{p}}$$

and

$$B_o = B_{oi} + B_{oi}c_o\Delta\bar{p} \quad (5.23)$$

The definition of c_o uses the single-phase formation volume factor, but it should be apparent that as long as the calculations are being conducted above the bubble point, $B_o = B_t$. If Eq. (5.23) is substituted into the first term in Eq. (5.21), the result is

$$N(B_o - B_{oi}) + NB_{oi}c_o\Delta\bar{p} + NB_{oi}\left[\frac{c_w S_{wi} + c_f}{1 - S_{wi}}\right]\Delta\bar{p} = N_pB_t - W_e + B_wW_p \quad (5.24)$$

Multiplying both the numerator and the denominator of the term containing c_o by S_{oi} and realizing that above the bubble point there is no gas saturation, $S_{oi} = 1 - S_{wi}$, Eq. (5.24) becomes

$$NB_{oi}\left[\frac{c_oS_{oi}\Delta\bar{p}}{1 - S_{wi}}\right] + NB_{oi}\left[\frac{c_w S_{wi} + c_f}{1 - S_{wi}}\right]\Delta\bar{p} = N_pB_t - W_e + B_wW_p$$

or

$$NB_{oi}\left[\frac{c_oS_{oi} + c_wS_{wi} + c_f}{1 - S_{wi}}\right]\Delta\bar{p} = N_pB_t - W_e + B_wW_p \quad (5.25)$$

The expression in brackets of Eq. (5.25) is called the *effective fluid compressibility*, c_f, which includes the compressibilities of the oil, the connate water, and the formation, or

$$c_f = \frac{c_oS_{oi} + c_wS_{wi} + c_f}{1 - S_{wi}} \quad (5.26)$$

Finally, Eq. (5.26) may be written as

$$NB_{oi}c_f\Delta\bar{p} = N_pB_t - W_e + B_wW_p \quad (5.27)$$

For volumetric reservoirs, $W_e = 0$ and W_p is generally negligible, and Eq. (5.27) can be rearranged to solve for N.

$$N = \frac{N_p}{c_f\Delta\bar{p}}\left(\frac{B_t}{B_{oi}}\right) \quad (5.28)$$

then c_f is simply c_o, and Eq. (5.28) reduces to Eq. (5.8) derived in Sect. 5.1 for production above the bubble point.

$$\frac{N_p}{N} = \frac{B_t - B_{ti}}{B_t}$$

Example 5.3 shows the use of Eq. (5.22) and (5.28) to find the initial oil in place from the pressure-production data of a reservoir that all geologic evidence indicates is volumetric (i.e., it is bounded on all sides by impermeable rocks). Because the equations are basically identical, they give the same calculation of initial oil, 51.73 MM STB. A calculation is also included to show that an error of 61% is introduced by neglecting the formation and water compressibilities.

Example 5.3. Calculation of initial oil in place in a volumetric, undersaturated reservoir.

Given:

B_{oi} = 1.35469 bbl/STB
B_t at 3600 psig = 1.37500 bbl/STB
Connate water = 0.20
$c_w = 3.6\ (10)^{-6}$ psi^{-1}
B_w at 3600 psig = 1.04 bbl/STB
$c_f = 5.0\ (10)^{-6}$ psi^{-1}
p_i = 5000 psig
N_p = 1.25 MM STB
$\Delta\bar{p}$ at 3600 psig = 1400 psi
W_p = 32,000 STB
$W_e = 0$

SOLUTION: Substituting into Eq. (5.28)

$$N = \frac{1.250{,}000(1.37500) + 32{,}000(1.04)}{1.37500 - 1.35469 + 1.35469\left[\frac{3.6(10^{-6})(0.20) + 5.0(10^{-6})}{1 - 0.20}\right](1400)}$$

$$= 51.73 \text{ MM STB}$$

The average compressibility of the reservoir oil is

$$c_o = \frac{B_o - B_{oi}}{B_{oi}\Delta\bar{p}} = \frac{1.375 - 1.35469}{1.35469\ (5000 - 3600)} = 10.71\ (10)^{-6}\ \text{psi}^{-1}$$

$$c_e = \frac{c_o S_o + c_w S_{wi} + c_f}{1 - S_{wi}} \qquad (5.26)$$

and the effective fluid compressibility by Eq. (5.26) is

$$c_e = \frac{[0.8(10.71) + 0.2(3.6) + 5.0]10^{-6}}{0.8} = 17.86\ (10)^{-6}\ \text{psi}^{-1}$$

Then the initial oil in place by Eq. (5.28) is

$$N = \frac{1{,}250{,}000(1.37500) + 32{,}000(1.04)}{17.86(10)^{-6}(1400)1.35469} = 51.73\ \text{MM STB}$$

If the water and formation compressibilities are neglected, $c_e = c_o$, and the initial oil in place is calculated to be

$$N = \frac{1{,}250{,}000(1.37500) + 32{,}000(1.04)}{10.71(10)^{-6}(1400)1.35469} = 86.25\ \text{MM STB}$$

As can be seen from the example calculations, the inclusion of the compressibility terms significantly affects the value of N. This is true above the bubble point where the oil-producing mechanism is depletion, or the swelling of reservoir fluids. After the bubble point is reached, the compressibilities have a much smaller effect on the calculations.

When Eq. (2.8) is rearranged and solved for N, we get the following:

$$N = \frac{N_p[B_t + (R_p - R_{soi})B_g] - W_e + B_w W_p}{B_t - B_{ti} + B_{ti}\left[\frac{c_w S_{wi} + c_f}{1 - S_{wi}}\right]\Delta\bar{p}} \qquad (5.29)$$

This is the general material balance equation written for an undersaturated reservoir below the bubble point. The effect of water and formation compressibilities are accounted for in this equation. Example Problem 5.4 compares the calculations for recovery factor, N_p/N, for an undersaturated reservoir

and the effective fluid compressibility by Eq. (5.26) is

$$c_e = \frac{[0.8(10.71) + 0.2(3.6) + 5.0]10^{-6}}{0.8} = 17.86\ (10)^{-6}\ \text{psi}^{-1}$$

Then the initial oil in place by Eq. (5.28) is

$$N = \frac{1{,}250{,}000(1.37500) + 32{,}000(1.04)}{17.86(10)^{-6}(1400)1.35469} = 51.73\ \text{MM STB}$$

If the water and formation compressibilities are neglected, $c_e = c_o$, and the initial oil in place is calculated to be

$$N = \frac{1{,}250{,}000(1.37500) + 32{,}000(1.04)}{10.71(10)^{-6}(1400)1.35469} = 86.25\ \text{MM STB}$$

As can be seen from the example calculations, the inclusion of the compressibility terms significantly affects the value of N. This is true above the bubble point where the oil-producing mechanism is depletion, or the swelling of reservoir fluids. After the bubble point is reached, the compressibilities have a much smaller effect on the calculations.

When Eq. (2.8) is rearranged and solved for N, we get the following:

$$N = \frac{N_p[B_t + (R_p - R_{soi})B_g] - W_e + B_w W_p}{B_t - B_{ti} + B_{ti}\left[\frac{c_w S_{wi} + c_f}{1 - S_{wi}}\right]\Delta\bar{p}} \qquad (5.29)$$

This is the general material balance equation written for an undersaturated reservoir below the bubble point. The effect of water and formation compressibilities are accounted for in this equation. Example Problem 5.4 compares

ample 5.4 Calculation of N_p/N for an undersaturated reservoir with
r production and negligible water influx. The calculation is performed
3 without including the effect of compressibilities. Assume that the
gas saturation is not reached until after the reservoir pressure drops
200 psia.

P 173
174

$S_w = 30\%$

Given:

$p_i = 4000$ psia
$p_b = 2500$ psia
$S_w = 30\%$

$c_w = 3 \times 10^{-6}$ psi^{-1}
$c_f = 5 \times 10^{-6}$ psi^{-1}
$\phi = 10\%$

$\Phi = 10\%$

Pressure psia	R_s SCF STB	B_g bbl/SCF	B_t bbl/SCF
4000	1000	0.00083	1.3000
2500	1000	0.00133	1.3200
2300	920	0.00144	1.3952
2250	900	0.00148	1.4180
2200	880	0.00151	1.4412

bbl/STB

SOLUTION: The calculations are performed first by including the effect of compressibilities. Equation (5.22) is used to calculate the recovery at the bubble point.

Above B.P.

$$\frac{N_p}{N} = \frac{B_t - B_{ti} + B_{ti}\left[\frac{c_w S_{wi} + c_f}{1 - S_{wi}}\right]\Delta\bar{p}}{B_t}$$

$$\frac{N_p}{N} = \frac{1.32 - 1.30 + 1.30\left[\frac{3(10^{-6})0.3 + 5(10^{-6})}{1 - 0.3}\right]1500}{1.32} = 0.0276$$

ow the bubble point. Eqs. (5.29) and (5.13) are used to calculate the very.

Below B.P

$$\frac{N_p}{N} = \frac{B_t - B_{ti} + B_{ti}\left[\frac{c_w S_{wi} + c_f}{1 - S_{wi}}\right]\Delta\bar{p}}{B_t + (R_p - R_{si})B_g}$$

recovery.

$$\frac{N_p}{N} = \frac{B_t - B_{ti} + B_{ti}\left[\frac{c_w S_{wi} + c_f}{1 - S_{wi}}\right]\Delta\bar{p}}{B_t + (R_p - R_{si})B_g}$$

Below B.P.

$$2500 - 2300 \text{ psia: } R_p = \frac{0.0276(1000) + \left(\frac{N_p}{N} - 0.0276\right)960}{\frac{N_p}{N}} = \frac{1.104 - \frac{960N_p}{N}}{\frac{N_p}{N}}$$

$$R_p = \frac{\Sigma(\Delta N_p)R}{N_p} = \frac{\Sigma(\Delta N_p/N)R}{N_p/N}$$

During the pressure increment 2500 – 2300 psia, the calculations yield

$$\frac{N_p}{N} = \frac{1.3952 - 1.30 + 1.30\left[\frac{3(10^{-6})0.3 + 5(10^{-6})}{1 - 0.3}\right]1700}{1.3952 + (R_p - 1000)0.00144}$$

$$R_p = \frac{0.0276(1000) + (N_p/N - 0.0276)R_{avg}}{N_p/N}$$

$N_p = R_{si}$ 0.0276

$$\frac{N_p}{N} = \frac{1.3952 - 1.3 + 1.3\left[\frac{3(10^{-5})0.3 + 5(10^{-5})}{1 - 0.3}\right]1700}{1.3952 + \left(\frac{1.104 + \frac{960N_p}{N}}{\frac{N_p}{N}} - 1000\right)0.00144} = \frac{0.113827\frac{N_p}{N}}{1.3376\frac{N_p}{N} + 0.00159}$$

where R_{avg} equals the average value of the solution GOR dur
increment.

From 2,500-2,300 psia

$$R_{avg} = \frac{1000 + 920}{2} = 960$$

900+880 = 890

$$\frac{N_p}{N} = \frac{0.113827 - 0.00159}{1.3376} = 0.08391$$

Solving these three equations for N_p/N yields

P-175

From 2,300-2,250 psia $\frac{N_p}{N} = 0.08391$

Repeating the calculations for the pressure increment 2300 – 2250 psia, the N_p/N is found to be

From 2,250-2,200 psia $\frac{N_p}{N} = 0.11754$

recovery.

$$\frac{N_p}{N}=\frac{B_t-B_{ti}+B_{ti}\left[\frac{c_w S_{wi}+c_f}{1-S_{wi}}\right]\Delta\bar{p}}{B_t+(R_p-R_{soi})B_g}$$

Below B.P.

$$R_p=\frac{\Sigma(\Delta N_p)R}{N_p}=\frac{\Sigma(\Delta N_p/N)R}{N_p/N}$$

During the pressure increment 2500 – 2300 psia, the calculations yield

$$\frac{N_p}{N}=\frac{1.3952-1.30+1.30\left[\frac{3(10^{-6})0.3+5(10^{-6})}{1-0.3}\right]1700}{1.3952+(R_p-1000)0.00144}$$

$$R_p=\frac{0.0276(1000)+(N_p/N-0.0276)R_{avei}}{N_p/N}$$

$$2300-2250\,psia;\ R_p=\frac{0.0276*1000+(0.08391-0.0276)960+\left(\frac{N_p}{N}-0.08391\right)910}{\frac{N_p}{N}}=\frac{5.2995+\frac{910N_p}{N}}{\frac{N_p}{N}}$$

where R_{avei} equals the average value of the solution GOR during the pressure increment.

$$R_{avei}=\frac{1000+920}{2}=960$$

$$\frac{N_p}{N}=\frac{1.418-1.3+1.3\left[\frac{3(10^{-6})0.3+5(10^{-6})}{1-0.3}\right]1750}{1.418+\left(\frac{5.2995+\frac{910N_p}{N}}{\frac{N_p}{N}}-1000\right)0.00148}=\frac{0.137175\frac{N_p}{N}}{1.2848\frac{N_p}{N}+0.007843}$$

From 2,500-2,300 psia

Solving these three equations for N_p/N yields

$$\frac{N_p}{N}=0.08391$$

From 2,300-2,250 psia

Repeating the calculations for the pressure increment 2300 – 2250 psia, the N_p/N is found to be

From 2,250-2,200 psia

$$\frac{N_p}{N}=0.11754$$

$$\frac{N_p}{N}=\frac{0.13827-0.007843}{1.2848}=0.100663$$

recovery.

$$\frac{N_p}{N}=\frac{B_t-B_{ti}+B_{ti}\left[\frac{c_w S_{wi}+c_f}{1-S_{wi}}\right]\Delta\bar{p}}{B_t+(R_p-R_{soi})B_g}$$

Below B.P.

$$R_p=\frac{\Sigma(\Delta N_p)R}{N_p}=\frac{\Sigma(\Delta N_p/N)R}{N_p/N}$$

During the pressure increment 2500 – 2300 psia, the calculations yield

$$\frac{N_p}{N}=\frac{1.3952-1.30+1.30\left[\frac{3(10^{-6})0.3+5(10^{-6})}{1-0.3}\right]1700}{1.3952+(R_p-1000)0.00144}$$

$$R_p=\frac{0.0276(1000)+(N_p/N-0.0276)R_{avei}}{N_p/N}$$

$$\frac{N_p}{N}=\frac{1.4412-1.3+1.3\left[\frac{3(10^{-6})0.3+5(10^{-6})}{1-0.3}\right]1800}{1.4412+\left(\frac{7.31276+\frac{890N_p}{N}}{\frac{N_p}{N}}-1000\right)0.00151}=\frac{0.160923\frac{N_p}{N}}{1.2751\frac{N_p}{N}+0.011042}$$

where R_{avei} equals the average value of the solution GOR during the pressure increment.

From 2250-2,200 psia

$$R_{avei}=\frac{1000+920}{2}=960$$

900+880 = 890

$$2250-2200psia;R_p=\frac{0.0276*1000-(0.08391-0.0276)960-(0.100663-0.08391)910-\left(\frac{N_p}{N}-0.100663\right)890}{\frac{N_p}{N}}=\frac{7.31276-\frac{890N_p}{N}}{\frac{N_p}{N}}$$

Repeating the calculations for the pressure increment 2300 – 2250 psia, the N_p/N is found to be

From 2,250-2,200 psia

$$\frac{N_p}{N}=0.11754$$

$$\frac{N_p}{N}=\frac{0.160923-0.011042}{1.2751}=0.117544$$

Below the bubble point, Eq. (5.11) and (5.13) are used to calculate N_p/N

$$\frac{N_p}{N} = \frac{B_t - B_g}{B_t + (R_p - R_{sol})B_t}$$

No compressibility Term. Below B.P.

and

$$R_p = \frac{\Sigma(\Delta N_p)R}{N_p} = \frac{\Sigma(\Delta N_p/N)R}{N_p/N}$$

For the pressure increment 2500 – 2300 psia

$$\frac{N_p}{N} = \frac{1.3952 - 1.30}{1.3952 + (R_p - 1000)0.00144}$$

$$R_p = \frac{0.01515(1000) + (N_p/N - 0.01515)R_{ave}}{N_p/N}$$

where R_{ave} is given by

$$R_{ave} = \frac{1000 + 920}{2} = 960$$

Solving these three equations yields

From 2,300-2,250 psia

$$\frac{N_p}{N} = 0.07051$$

Repeating the calculations for the pressure increment 2300 – 2250 psia:

From 2,300-2,500 psia

$$\frac{N_p}{N} = 0.08707$$

For the pressure increment 2250 – 2200 psia

From 2,250-2,000 psia

$$\frac{N_p}{N} = 0.10377$$

Now, the calculations are performed by assuming that the effect of including the compressibility terms is negligible. For this case, at the bubble point, the recovery can be calculated by using Eq. (5.8)

No compressibility term

$$\frac{N_p}{N} = \frac{B_t - B_g}{B_t} = \frac{1.32 - 1.30}{1.32} = 0.01515$$

Below the bubble point, Eq. (5.11) and (5.13) are used to calculate N_p/N

$$\frac{N_p}{N} = \frac{B_t - B_g}{B_t + (R_p - R_{sol})B_t}$$

and

$$R_p = \frac{\Sigma(\Delta N_p)R}{N_p} = \frac{\Sigma(\Delta N_p/N)R}{N_p/N}$$

For the pressure increment 2500 – 2300 psia

Bt - Bti

$$\frac{N_p}{N} = \frac{1.3952 - 1.30}{1.3952 + (R_p - 1000)0.00144}$$

$$R_p = \frac{0.01515(1000) + (N_p/N - 0.01515)R_{ave}}{N_p/N}$$

where R_{ave} is given by

$$R_{ave} = \frac{1000 + 920}{2} = 960$$

Solving these three equations yields

From 2,500-2,300 psia

$$\frac{N_p}{N} = 0.07051$$

The calculations suggest that there is a very significant difference in the results of the two cases down to the bubble point. The difference is the result he fact that the rock and water compressibilities are on the same order of magnitude as the oil compressibility. By including them, the fractional recovery has been significantly affected. The case that used the rock and water compressibilities comes closer to simulating real production above the bubble point from this type of reservoir. This is because the actual mechanism of oil

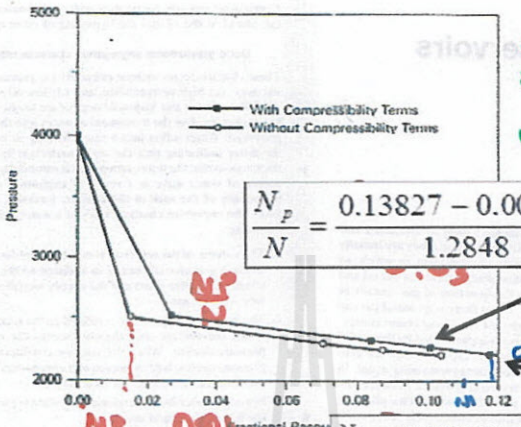

$$\frac{N_p}{N} = \frac{0.13827 - 0.007843}{1.2848} = 0.100663$$

$$\frac{N_p}{N} = \frac{0.160923 - 0.011042}{1.2751} = 0.117544$$

Fig. 5.8. Pressure versus fractional recovery for the
5.4.

Reservoir Engineering I, 2012
HW NO 5; Due date: Friday, August 9, 2012.
Chapter 5; 5.2, 5.6, 5.9, 5.13and 3.21

ANSWERS TO THE PROBLEMS

5.2; (a) %Recovery at 3550 psia = 1.75%,
at 2800 psia = 8.8%, at 2000 psia = 21.7%,
at 1200 psia = 44.6%, at 800 psia = 61%
(b) %Recovery at 3550 psia
at 2800 psia = 3.83%, at 2000 psia = 8.5%
at 1200 psia = 15.4%, at 800 psia = 19.5%
1/3 times
(a) N = 246 MMSTB, (b) Gf = 31.8 x 109 SCF
(c) So = 0.69 (d) Np = 89.8 MMSTB
(a) N = 10.75 MMSTB, (b) N = 10.8 MMSTB
(c) We = 46,000 bbl
5.13 Recovery Factor at 1700 psia = 0.0097
at 1500 psia = 0.0505, at 1300 psia = 0.1071
at 1100 psia = 0.197, at 900 psia = 0.33
at 700 psia = 0.55, at 500 psia = 0.89

Chapter 6

Saturated Oil Reservoirs

1. INTRODUCTION

The material balance equations discussed in Chapter 5 apply to volumetric and water-drive reservoirs in which there is no initial gas cap (i.e., they are initially undersaturated). However, the equations apply to reservoirs in which an artificial gas cap forms owing either to gravitational segregation of the oil and free gas phases below the bubble point, or to the injection of gas, usually in the higher structural portions of the reservoir. When there is an initial gas cap (i.e., the oil is initially saturated), there is negligible liquid expansion energy. However, the energy stored in the dissolved gas is supplemented by that in the cap, and it is not surprising that recoveries from gas cap reservoirs are generally higher than from those without caps, other things remaining equal. In gas cap drives, as production proceeds and reservoir pressure declines, the expansion of the gas displaces oil downward toward the wells. This phenomenon is observed in the increase of the gas-oil ratios in successively lower wells. At the same time, by virtue of its expansion, the gas cap retards pressure decline and therefore the liberation of solution gas within the oil zone, thus improving recovery by reducing the producing gas-oil ratios of the wells. This mechanism is most effective in those reservoirs of marked structural relief, which introduces a vertical component of fluid flow whereby gravitational

segregation of the oil and free gas in the sand may occur.*[1] The recoveries from volumetric gas cap reservoirs could range from the recoveries for undersaturated reservoirs up to 70 to 80% of the initial stock tank oil in place and will be higher for large gas caps, continuous uniform formations, and good gravitational segregation characteristics.

Large gas caps

The size of the gas cap is usually expressed relative to the size of the oil zone by the ratio m, as defined in Chapter 2.

Continuous uniform formations

Continuous uniform formations reduce the channeling of the expanding gas cap ahead of the oil and the bypassing of oil in the less permeable portions.

Good gravitational segregation characteristics

These characteristics include primarily (a) pronounced structure, (b) low oil viscosity, (c) high permeability, and (d) low oil velocities.

Water drive and *hydraulic control* are terms used in designating a mechanism that involves the movement of water into the reservoir as gas and oil are produced. Water influx into a reservoir may be edge water or bottom water, the latter indicating that the oil is underlain by a water zone of sufficient thickness so that the water movement is essentially vertical. The most common source of water drive is a result of expansion of the water and the compressibility of the rock in the aquifer; however, it may result from artesian flow. The important characteristics of a water-drive recovery process are the following:

1. The volume of the reservoir is constantly reduced by the water influx. This influx is a source of energy in addition to the energy of liquid expansion above the bubble point and the energy stored in the solution gas and in the free, or cap, gas.
2. The bottom-hole pressure is related to the ratio of water influx to voidage. When the voidage only slightly exceeds the influx, there is only a slight pressure decline. When the voidage considerably exceeds the influx, the pressure decline is pronounced and approaches that for gas cap or dissolved gas-drive reservoirs, as the case may be.
3. For edge-water drives, regional migration is pronounced in the direction of the higher structural areas.
4. As the water encroaches in both edge-water and bottom-water drives, there is an increasing volume of water produced, and eventually water is produced by all wells.

*References throughout the text are given at the end of each chapter.

GAS CAP DRIVE

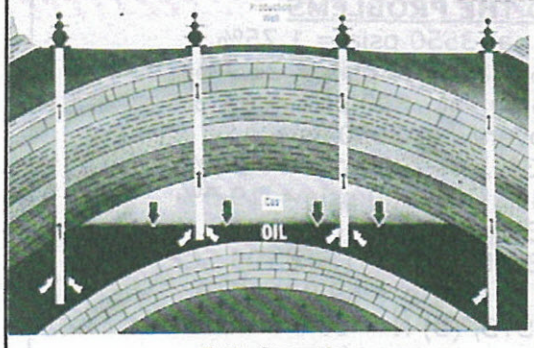

Fig. 1.6—Gas-cap drive.

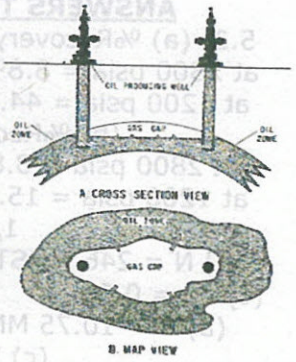

Fig. 53—*Gas cap drive reservoir.*

COMBINATION DRIVE

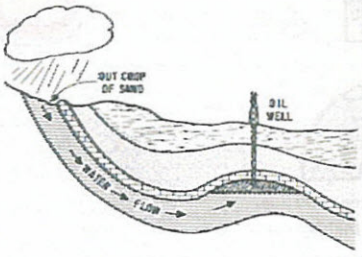

Fig. 68—*Reservoir having uniform water drive.*

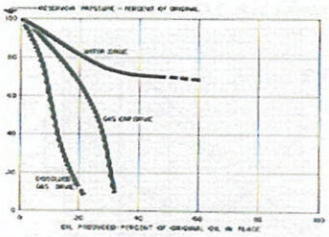

Fig. 69—*Reservoir pressure trends for reservoirs under various drives. (Courtesy API, Drilling and Production Practices—1943.)*

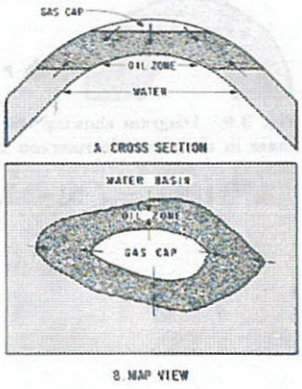

Fig. 71—*Combination drive reservoir.*

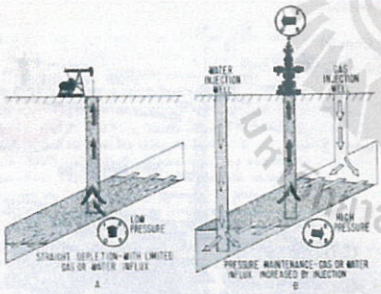

Fig. 83—*Effects of gas or water pressure maintenance on the producing ability of wells.*

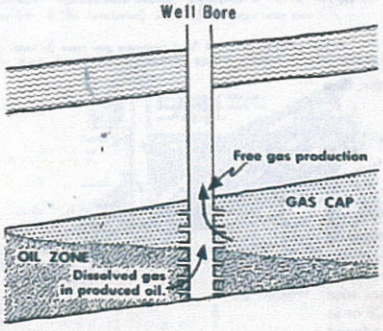

Fig. 84—*Gas produced with oil from associated gas cap and solution in the oil. (Courtesy* The Petroleum Engineer—*Sept., 1956.)*

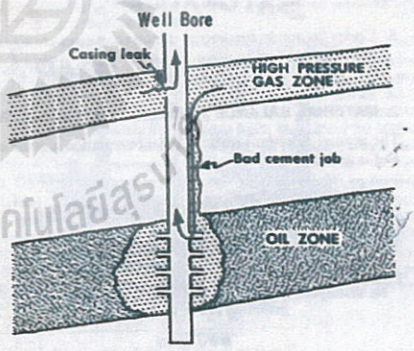

Fig. 85—*Free gas production from high pressure gas zone through casing oak and channel leak. (Courtesy* The Petroleum Engineer—*Sept., 1956.)*

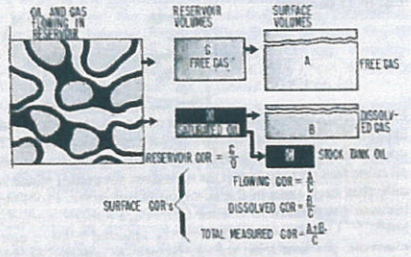

Fig. 86—*Gas-oil ratios under reservoir and surface measurements.*

$$V_{oi} = V_o + V_g \qquad (3$$

Figure 3.8 shows schematically the changes which occur between in

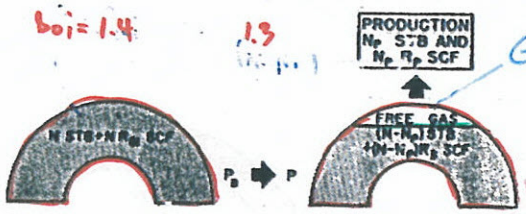

Fig. 3.8. Diagram showing the formation of a free gas phase in a volumetric reservoir below the bubble point.

$$V_i = NB_{oi} = (N-N_p)B_o + G_f B_g$$

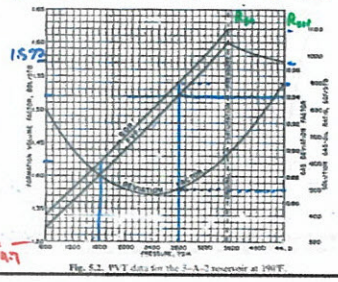

Fig. 5.2. PVT data for the 3-A-2 reservoir at 180°F.

SATURATED

5. Under favorable conditions, the oil recoveries are high and range from 60 to 80% of the oil in place.

2. MATERIAL BALANCE IN SATURATED RESERVOIRS

The general Schilthuis material balance equation was developed in Chapter 2 and is as follows:

$$N(B_t - B_{ti}) + \frac{NmB_{ti}}{B_{gi}}(B_g - B_{gi}) + (1+m)\,N\,B_{ti}\left[\frac{c_w S_{wi} + c_f}{1 - S_{wi}}\right]\Delta\bar{p} + W_e = N_p[B_t + (R_p - R_{si})B_g] + B_w W_p \qquad (2.7)$$

Equation (2.7) can be rearranged and solved for N, the initial oil in place:

$$N = \frac{N_p[B_t + (R_p - R_{si})B_g] - W_e + B_w W_p}{E_o - B_{ti} + \frac{mB_{ti}}{B_{gi}}(B_g - B_{gi}) + (1+m)B_{ti}\left[\frac{c_w S_{wi} + c_f}{1 - S_{wi}}\right]\Delta\bar{p}} \qquad (6.1)$$

If the expansion term due to the compressibilities of the formation and connate water can be neglected, as they usually are in a saturated reservoir, then Eq. (6.1) becomes

$$N = \frac{N_p[B_t + (R_p - R_{si})B_g] - W_e + B_w W_p}{B_t - B_{ti} + \frac{mB_{ti}}{B_{gi}}(B_g - B_{gi})} \qquad (6.2)$$

Example 6.1 shows the application of Eq. (6.2) to the calculation of initial oil in place for a water-drive reservoir with an initial gas cap. The calculations are done once by converting all barrel units to cubic feet units and then converting all cubic feet units to barrel units. It does not matter which set of units is used, only that each term in the equation is consistent. Problems sometimes arise because gas formation volume factors are either reported in cu ft/SCF or in bbl/SCF. Usually when applying the material balance equation for a liquid reservoir, gas formation volume factors are reported in bbl/SCF. Use care in making sure that the units are correct.

Example 6.1 To calculate the stock tank barrels of oil initially in place in a combination drive reservoir.

Given:

Volume of bulk oil zone = 112,000 ac-ft
Volume of bulk gas zone = 19,600 ac-ft

Initial reservoir pressure 2710 psia
Initial FVF = 1.340 bbl/STB
Initial gas volume factor = 0.006266 cu ft/SCF
Initial dissolved GOR = 562 SCF/STB
Oil produced during the interval = 20 MM STB
Reservoir pressure at the end of the interval = 2000 psia
Average produced GOR = 700 SCF/STB
Two-phase FVF at 2000 psia = 1.4954 bbl/STB
Volume of water encroached = 11.58MM bbl
Volume of water produced = 1.05MM STB
FVF of the water = 1.028 bbl/STB
Gas volume factor at 2000 psia = 0.008479 cu ft/SCF

SOLUTION: In the use of Eq. (6.2):

$B_{ti} = 1.3400 \times 5.615 = 7.5241$ cu ft/STB
$B_t = 1.4954 \times 5.615 = 8.3967$ cu ft/STB
$W_e = 11.58 \times 5.615 = 65.02$ MM cu ft
$W_p = 1.05 \times 1.028 \times 5.615 = 6.06$ MM res cu ft

Assuming the same porosity and connate water for the oil and gas zones:

Assuming the same porosity and connate water for the oil and gas zones:

$$m = \frac{19{,}600}{112{,}000} = 0.175$$

Substituting in Eq. (6.2):

$$N = \frac{20 \times 10^6[8.3967 + (700 - 562)0.008489] - (65.02 - 6.06) \times 10^6}{8.3967 - 7.5241 + 0.175\left(\frac{7.5241}{0.006266}\right)(0.008489 - 0.006266)}$$

$$= 98.97 \text{ MM STB}$$

If B_t is in barrels per stock tank barrel, then B_g must be in barrels per standard cubic foot and W_e and W_p in barrles, and the substitution is as follows:

$$N = \frac{20 \times 10^6[1.4954 + (700 - 562)0.001510] - (11.58 - 1.05 \times 1.028) \times 10^6}{1.4954 - 1.3400 + 0.175\left(\frac{1.3400}{0.001116}\right)(0.001510 - 0.001116)}$$

$$= 98.97 \text{ MM STB}$$

Eq. (6.1) becomes

$$N = \frac{N_p[B_t + (R_p - R_{si})B_g] - W_e + B_w W_p}{B_t - B_{ti} + \frac{mB_{ti}}{B_{gi}}(B_g - B_{gi})} \qquad (6.2)$$

Example 6.1 shows the application of Eq. (6.2) to the calculation of initial oil

Figure 6.1 shows the pressure and production history of the Conroe Field, and Fig. 6.2 gives the gas and two-phase oil formation volume factor for the reservoir fluids. Table 6.1 contains other reservoir and production data and summarizes the calculations in column form for three different periods.

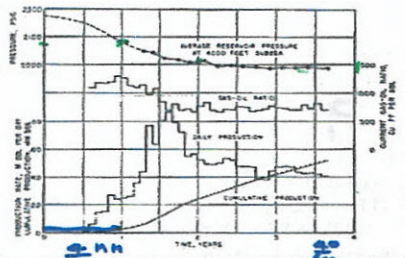

Fig. 6.1. Reservoir pressure and production data, Conroe Field. (*After* Schilthuis[3], *Trans.* AIME.)

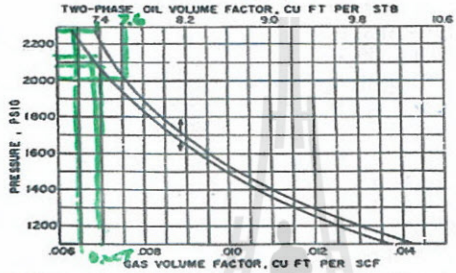

Fig. 6.2. Pressure volume relations for Conroe Field oil and original complement of dissolved gas. (*After* Schilthuis.[3] *Trans.* AIME.)

TABLE 6.1.
Material balance calculation of water influx or oil in place for oil reservoirs below the bubble-point pressure

For Conroe Field: $B_{oi} = 7.37$ cu ft/STB $\quad mB_{oi}/B_{gi} = 259$ SCF/STB
$B_{gi} = 0.00637$ cu ft/SCF (14.4 psia and 60°F) $\quad R_{soi} = 600$ SCF/STB

Example 6.2

$$m = \frac{181{,}225 \text{ ac-ft}}{810{,}000 \text{ ac-ft}} = 0.224$$

Line No.	Quantity	Units	Months after Start of Production				
			12	18	24	30	36
1	N_p	MM STB	9.070	22.34	32.03	40.18	48.24
2	R_p	SCF/STB	1630	1180	1070	1025	995
3	p	psig	2143	2108	2098	2087	2091
4	B_g	cu ft/SCF	0.00676	0.00687	0.00691	0.00694	0.00693
5	B_t	cu ft/STB	7.46	7.51	7.51	7.53	7.52
6	N_pR_p	MM SCF	14,800		34,400		48,100
7	$R_p - R_{soi}$	SCF/STB	10.0		470		395
8	$(R_p - R_{soi})B_g$	cu ft/STB	6.95		3.24		2.74
9	(5) + (8)	cu ft/STB	14.41		10.75		10.26
10	$B_g - B_{gi}$	cu ft/SCF	0.00039		0.00054		0.00056
11	(10) × (mB_{oi}/B_{gi})	cu ft/STB	0.101		0.137		0.145
12	$B_t - B_{oi}$	cu ft/STB	0.09		0.14		0.15
13	(11) + (12)	cu ft/STB	0.191		0.277		0.295
14	(1) × (9)	MM cu ft	131		345		495
15	$W_e - W_p$	MM cu ft	51.5		178		320
16	(14) − (15)	MM cu ft	79.5		167		175
17	N = (16)/(13)	MM STB	415		602		594
18	DDI	Fraction	0.285		0.244		0.180
19	SDI	Fraction	0.320		0.239		0.174
20	WDI	Fraction	0.395		0.516		0.646

oil in place is 415 MM STB, and the value of $N_p[B_t + (R_p - R_{soi})B_g]$ given in line 14 is 131 MM cu ft. Then

$$\text{DDI} = \frac{415 \times 10^6 (7.46 - 7.37)}{131 \times {}^6} = 0.285$$

$$\text{SDI} = \frac{\dfrac{415 \times 10^6 \times 0.224 \times 7.37}{0.00637}(0.00676 - 0.00637)}{131 \times 10^6} = 0.320$$

$$\text{WDI} = \frac{51.5 \times 10^6}{131 \times 10^6} = 0.395$$

These figures indicate that during the first 12 months 39.5% of the production was by water drive, 32.0% by gas cap expansion, and 28.5% by depletion drive. At the end of 36 months, as the pressure stabilized, the *current* mechanism was essentially 100% water drive and the *cumulative* mechanism increased to 64.6% by water drive. If figures for recovery by each of the three mechanisms could be obtained, the overall recovery could be estimated using the drive indexes. An increase in the depletion drive and gas-drive indexes would be reflected by declining pressures and increasing gas-oil ratios, and might indicate the need for water injection to supplement the natural water influx and to turn the recovery mechanism more toward water drive.

2. MATERIAL BALANCE AS A STRAIGHT LINE

In Chapter 2 Sect. 4, the method developed by Havlena and Odeh of applying the genereal material balance equation was presented.[4,5] This approach defines several new variables (see Chapter 2) and rewrites the material balance equation as Eq. (2.13):

$$F = NE_o + N(1+m)B_{ti}E_{f,w} + \left[\frac{NmB_{ti}}{B_{gi}}\right]E_g + W_e \qquad (2.13)$$

This equation is then reduced for a particular application and arranged into a form of a straight line. When this is done, the slope and intercept often yield valuable assistance in determining such parameters as N and m. The usefulness of this approach is illustrated by applying the method to the data from the Conroe Field example discussed in the last section.

For the case of a saturated reservoir with an initial gas cap, such as the Conroe Field, and neglecting the compressibility term, $E_{f,w}$, Eq. (2.13) becomes

$$F = NE_o + \frac{NmB_{ti}}{B_{gi}}E_g + W_e \qquad (6.3)$$

If N is factored out of the first two terms on the right-hand side and both sides of the equation are divided by the expression remaining after factoring, we get

$$\frac{F}{E_o + \frac{mB_{ti}}{B_{gi}}E_g} = N + \frac{W_e}{E_o + \frac{mB_{ti}}{B_{gi}}E_g} \qquad (6.4)$$

For the example of the Conroe Field in the previous section, the water production values were not known. For this reason, two dummy parameters are defined as $F' = F - W_p B_w$ and $W'_e = W_e - W_p B_w$. Equation (6.4) then becomes

$$\frac{F'}{E_o + \frac{mB_{ti}}{B_{gi}}E_g} = N + \frac{W'_e}{E_o + \frac{mB_{ti}}{B_{gi}}E_g} \qquad (6.5)$$

Equation (6.5) is now in the desired form. If a plot of $F'/[E_o + mB_{ti}E_g/B_{gi}]$ as the ordinate and $W'_e/[E_o + mB_{ti}E_g/B_{gi}]$ as the abscissa is constructed, a straight line with slope equal to 1 and intercept equal to N is obtained. Table 6.2 contains the calculated values of the ordinate, line 5, and abscissa, line 7, using the Conroe Field data from Table 6.1. Figure 6.4 is a plot of these values.

If a least squares regression analysis is done on all three data points calculated in Table 6.2, the result is the solid line shown in Fig. 6.4. The line has a slope of 1.21 and an intercept, of N, of 396 MM STB. This slope is significantly larger than 1, which is what we should have obtained from the Havlena-Odeh method. If we now ignore the first data point, which represents the earliest production, and determine the slope and intercept of a line drawn through the remaining two points (the dashed line in Fig. 6.4), we get 1.00 for

TABLE 6.2.
Tabulated values from the Conroe Field for use in the Havlena-Odeh method

Line No.	Quantity	Units	Months after Start of Production		
			12	24	36
1	F'	MM cu ft	131	345	495
2	E_o	cu ft/STB	0.09	0.14	0.15
3	E_g	cu ft/SCF	0.00039	0.00054	0.00056
4	$E_o + m\frac{B_{ti}}{B_{gi}}E_g$	cu ft/STB	0.191	0.283	0.295
5	(1)/(4)	MM STB	686	1232	1678
6	W'_e	MM cu ft	51.5	178	320
7	(6)/(4)	MM STB	270	636	1085

If a least squares regression analysis is done on all three data points calculated in Table 6.2, the result is the solid line shown in Fig. 6.4. The line has a slope of 1.21 and an intercept, of N, of 396 MM STB. This slope is significantly larger than 1, which is what we should have obtained from the Havlena-Odeh method. If we now ignore the first data point, which represents the earliest production, and determine the slope and intercept of a line drawn through the remaining two points (the dashed line in Fig. 6.4), we get 1.00 for

TABLE 6.2.
Tabulated values from the Conroe Field for use in the Havlena-Odeh method

Line No.	Quantity	Units	Months after Start of Production		
			12	24	36
1	F'	MM cu ft	131	345	495
2	E_o	cu ft/STB	0.09	0.14	0.15
3	E_g	cu ft/SCF	0.00039	0.00054	0.00056
4	$E_o+m\frac{B_{oi}}{B_{gi}}E_g$	cu ft/STB	0.121	0.283	0.295
5	(1)/(4)	MM STB	686	1232	1678
6	W_e	MM cu ft	51.5	178	320
7	(6)/(4)	MM STB	270	636	1085

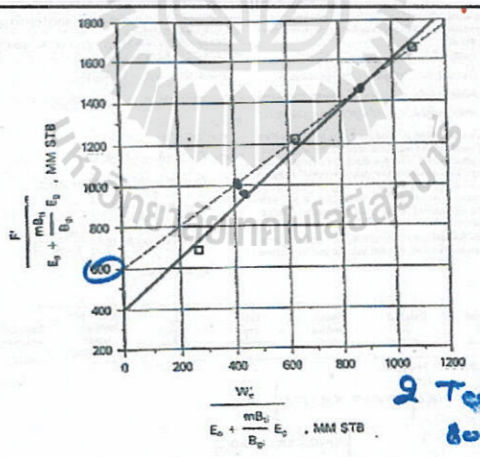

Fig. 6.4. Havlena-Odeh plot for the Conroe Field. Solid line represents line drawn through all the data points. Dashed line represents line drawn through data points from the later production periods.

a slope and 600 MM STB for N, the intercept. This value of the slope meets the requirement for the Havlena-Odeh method for this case. We should now raise the question: Can we justify ignoring the first point? If we realize that the production represents less than 5% of the initial oil in place and the fact that we have met the requirement for the slope of 1 for this case, then there is justification for not including the first point in our analysis. We conclude from our analysis that the initial oil in place is 600 MM STB for the Conroe Field.

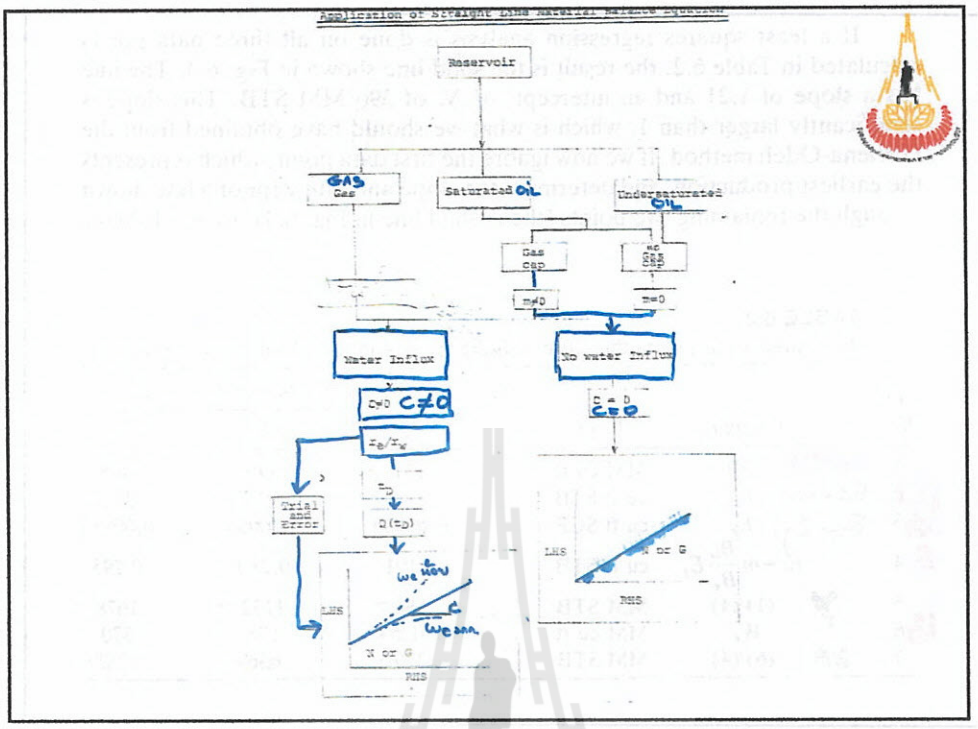

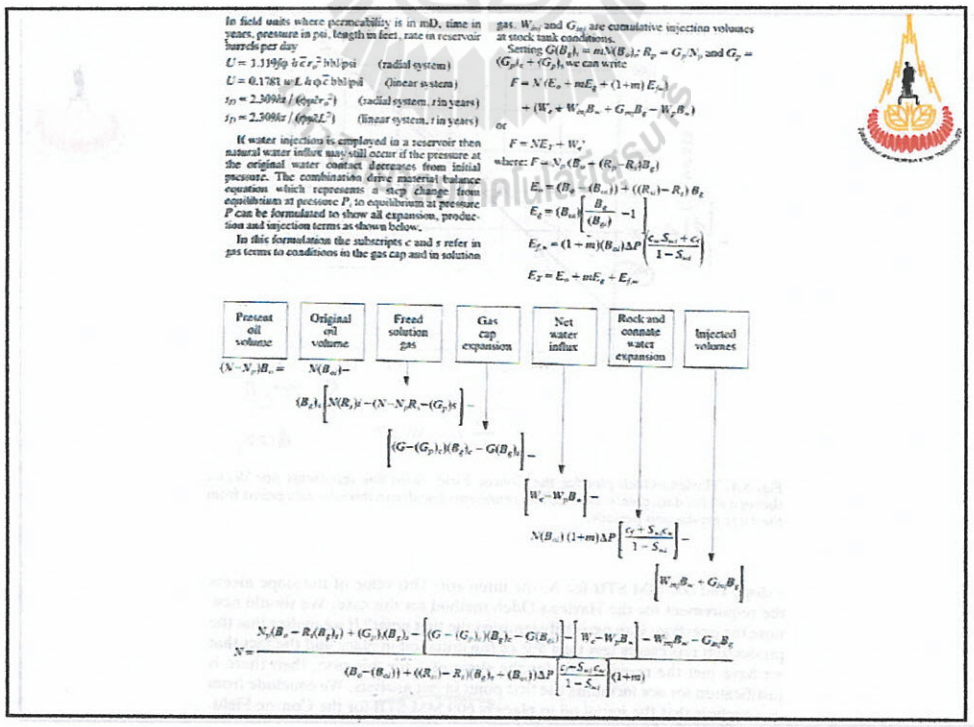

In field units where permeability is in mD, time in years, pressure in psi, length in feet, rate in reservoir barrels per day

$U = 1.119\phi c_t r_e^2 h$ bbl/psi (radial system)

$U = 0.1781\, wL\, h\, \phi c_t$ bbl/psi (linear system)

$t_D = 2.309kt / (\phi\mu c_t r_e^2)$ (radial system, t in years)

$t_D = 2.309kt / (\phi\mu c_t L^2)$ (linear system, t in years)

If water injection is employed in a reservoir then natural water influx may still occur if the pressure at the original water contact decreases from initial pressure. The combination drive material balance equation which represents a step change from equilibrium at pressure P_i to equilibrium at pressure P can be formulated to show all expansion, production and injection terms as shown below.

In this formulation the subscripts c and s refer in gas terms to conditions in the gas cap and in solution gas. W_{inj} and G_{inj} are cumulative injection volumes at stock tank conditions.

Setting $G(B_g)_i = mN(B_{gi})$; $R_p = G_p/N_p$ and $G_p = (G_p)_c + (G_p)_s$ we can write

$$F = N\left(E_o + mE_g + (1+m)E_{fw}\right) + \left(W_e + W_{inj}B_w + G_{inj}B_g - W_pB_w\right)$$

or

$$F = NE_T + W_e'$$

where: $F = N_p\left(B_o + (R_p - R_s)B_g\right)$

$$E_o = (B_o - (B_{oi})) + ((R_{si}) - R_s)\,B_g$$

$$E_g = (B_{oi})\left[\frac{B_g}{(B_g)_i} - 1\right]$$

$$E_{fw} = (1+m)(B_{oi})\Delta P\left[\frac{c_w S_{wi} + c_f}{1 - S_{wi}}\right]$$

$$E_T = E_o + mE_g + E_{fw}$$

Present oil volume	Original oil volume	Freed solution gas	Gas cap expansion	Net water influx	Rock and connate water expansion	Injected volumes
$(N-N_p)B_o +$	$N(B_{oi}) -$					
		$(B_g)_i\left[N(R_s)_i - (N-N_p)R_s - (G_p)_s\right] -$				
			$\left[(G-(G_p)_c)(B_g)_c - G(B_g)_i\right] -$			
				$\left[W_e - W_pB_w\right] -$		
					$N(B_{oi})(1+m)\Delta P\left[\frac{c_f + S_{wi}c_w}{1 - S_{wi}}\right] -$	
						$\left[W_{inj}B_w + G_{inj}B_g\right]$

$$N = \frac{N_p\left(B_o - R_s(B_g)_i\right) + (G_p)_s(B_g)_i - \left[(G-(G_p)_c)(B_g)_c - G(B_{gi})\right] - \left[W_e - W_pB_w\right] - W_{inj}B_w - G_{inj}B_g}{(B_o - (B_{oi})) + ((R_{si}) - R_s)(B_g)_i + (B_{oi})\Delta P\left[\frac{c_f + S_{wi}c_w}{1 - S_{wi}}\right](1+m)}$$

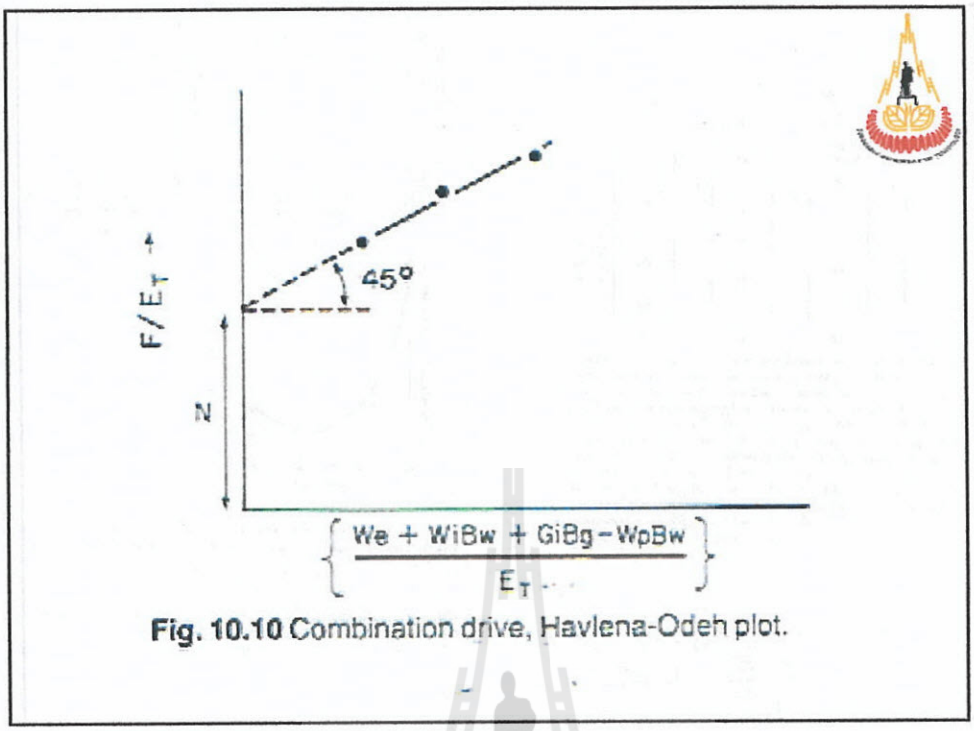

Fig. 10.10 Combination drive, Havlena-Odeh plot.

FLASH OR equilibrium gas liberation

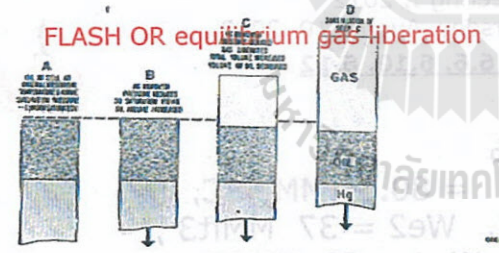

Fig. 45—Laboratory equilibrium liberation (P-V-T) of gas from oil. (Courtesy World Oil.—April, 1953.)

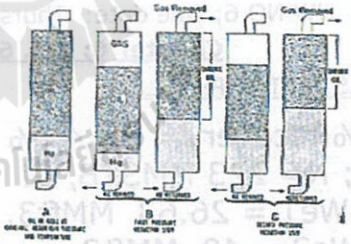

Fig. 46—Laboratory differential liberation of gas from oil. (Courtesy World Oil.—April, 1953.)

Differential gas liberation

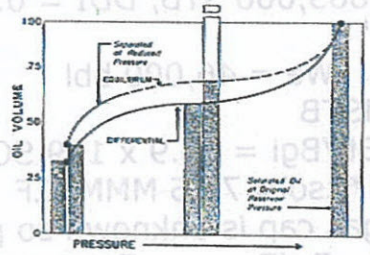

Fig. 48—Differential and equilibrium shrinkage of high shrinkage oil. (Courtesy World Oil.—April, 1953.)

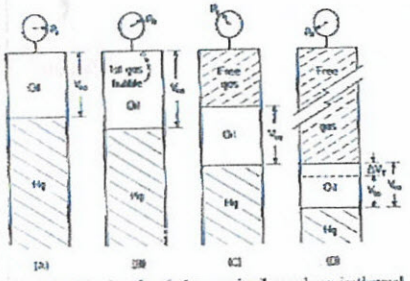

Fig. 1.2. Behavior of typical reservoir oil sample on isothermal pressure reduction. (A) Hit sample at original reservoir conditions. All gas is in solution and oil is undersaturated since $p_i > p_b$. (B) Pressure is reduced to p_b by removing mercury from the cell. First bubble of gas escapes from solution, hence p_b = bubble point or saturation pressure of the oil. Liquid volume has expanded slightly. (C) Pressure is reduced to p_1 and considerable free gas has evolved. Liquid volume has shrunk due to loss of volatile fractions. (D) Pressure is now atmospheric. Liquid volume has shrunk to V_{sc}, the oil volume at the reservoir temperature and 14.7 psia. Cooling this oil to standard temperature (60°F) results in its shrinking by an amount ΔV_T to the tank oil volume, V_o.

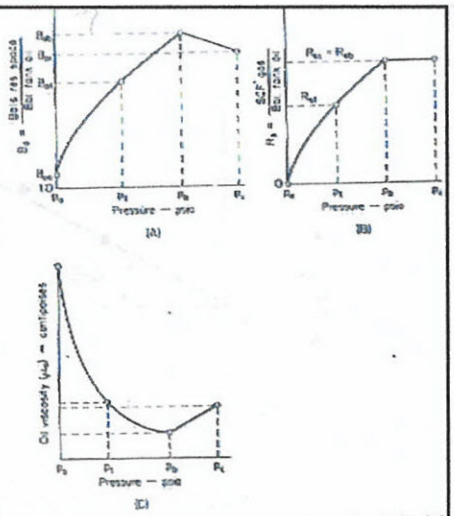

Fig. 1.3. Graphical representation of fluid properties depicted in Fig. 1.2. (A) Formation volume factor for oil as a function of pressure

$$B_o = \frac{V_o \text{ (at each pressure)}}{V_{sc}}$$

(B) Solution gas-oil ratio as a function of pressure. (C) Oil viscosity as a function of pressure.

API Gravity (degree)

$$= \frac{141.5}{\text{Sp.gr.}} - 131.5$$

Reservoir Engineering I, 2012

HW NO 6; Due date: Thursday, August 10, 2012.

Chapter 6; 6.3, 6.6, 6.10, 6.12

ANSWERS TO THE PROBLEMS

6.3; %Recovery= 58.42%

6.6; N= 223 MMSTB, Gi = 80.61 MMMSC,
We1 = 26.63 MMft3, We2 = 37 MMft3 ,
We3 = 49 MMft3, We4 = 63 MMft3

6.10; (a) We = 863,000 STB, DDI = 0.39, SDI = 0.42
WDI = 0.19, We = 46,000 bbl

6.12; N=150 MMSTB
Gi= slope = NmBti/Bgi = 66.9 x 109 SCF
Solution gas = N*Rsoi= 76.5 MMMSCF
(Hint: Since gas cap is unknown so plot
F/Eo VS Eg/Eo, From equation
F/Eo = N+ NmBti/Bgi (Eg/Eo)

10. Chapter7 Single Phase Fluid Flow in Reservoir

Chapter 7

9-10th week; 23 JULY-11 August 2012

Single-Phase Fluid Flow in Reservoirs

1. INTRODUCTION

In the previous four chapters, the material balance equations for each of the four reservoir types defined in Chapter 1 were developed. These material balance equations may be used to calculate the production of oil and/or gas as a function of reservoir pressure. The reservoir engineer, however, would like to know the production as a function of time. To learn this, it is necessary to develop a model containing time or some related property such as flow rate. This chapter discusses the flow of fluids in reservoirs and the models that are used to relate reservoir pressure to flow rate. The discussion in this chapter is limited to single-phase flow. Some multiphase flow considerations are presented in Chapters 9 and 10.

2. DARCY'S LAW AND PERMEABILITY

In 1856, as a result of experimental studies on the flow of water through unconsolidated sand filter beds, Henry Darcy formulated the law that bears his name. This law has been extended to describe, with some limitations, the movement of other fluids, including two or more immiscible fluids, in consol-

idated rocks and other porous media. Darcy's law states that the velocity a homogeneous fluid in a porous medium is proportional to the driving for and inversely proportional to the fluid viscosity, or

$$v = -0.001127\frac{k}{\mu}\left[\frac{dp}{ds} - 0.433\,\gamma' cos\,\alpha\right] \quad (7.$$

where,

v = the apparent velocity, bbls/day-ft²
k = permeability, millidarcies (md)
μ = fluid viscosity, cp
p = pressure, psia
s = distance along flow path in ft
γ' = fluid specific gravity (always relative to water)
α = the angle measured counterclockwise from the downward vertical to t positive s direction

and the term

$$\left[\frac{dp}{ds} - 0.433\,\gamma' cos\,\alpha\right]$$

represents the driving force. The driving force may be caused by fluid pressu gradients (dp/ds) and/or hydraulic (gravitational) gradients ($0.433\,\gamma' \cos\alpha$). many cases of practical interest, the hydraulic gradients, although alwa present, are small compared with the fluid pressure gradients, and are f quently neglected. In other cases, notably production by pumping from res voirs whose pressures have been depleted, and gas cap expansion reserv with good gravity drainage characteristics, the hydraulic gradients are i portant, and must be considered.

The apparent velocity, v, is equal to qB/A, where q is the volumetric fl rate in STB/day, B is the formation volume factor, and A is the apparent total cross-sectional area of the rock in square feet. In other words, A inclu the area of the rock material as well as the area of the pore channels. The fl pressure gradient, dp/ds, is taken in the same direction as v and q. T negative sign in front of the constant 0.001127 indicates that if the flow is tak as positive in the positive s-direction, then the pressure decreases in t direction so that the slope dp/ds is negative.

Darcy's law applies only in the region of laminar flow; in turbulent flo which occurs at higher velocities, the pressure gradient increases at a grea rate than does the flow rate. Fortunately, except for some instances of qu large production or injection rates in the vicinity of the well bore, flow in t reservoir and in most laboratory tests is by design, streamlined and Darc law is valid. Darcy's law does not apply to flow within individual pore chann

Q = Rate of Flow, cc/sec.
ΔP = Pressure Differential, Atmospheres
A = Area, cm²
μ = Fluid Viscosity, Centipoise
L = Length, cm
K = Permeability, Darcies

$$Q = \frac{K\cdot\Delta P\cdot A}{\mu\cdot L}$$

v = the apparent velocity

$$v = \frac{q}{A} = \frac{Q}{A} = \frac{K\cdot\Delta P}{\mu\cdot L}$$

The following conversion factors are needed:

1 darcy = 1000 millidarcys

1 barrel = 159,000 cc
1 ft = 30.48 cm
1 atm = 14.7 psi

$$q\ bbl/d \times \frac{159{,}000\ cc/bbl}{24\times 3600\ sec/d}$$

$$= \frac{2\pi\left(h\,ft\times 3048\frac{cm}{ft}\right)r ft\times 3048\frac{cm}{ft}\,k.md\times\frac{0.001d}{md}\left[psi\times\frac{1\ atm}{147\ psi}\right]dp}{\mu\ dr.ft\times 3048\frac{cm}{ft}}$$

v = the apparent velocity, bbls/day-ft²
k = permeability, millidarcies (md)
μ = fluid viscosity, cp
ρ = pressure, psia
s = distance along flow path in ft

$$q_{gs} = \frac{0.001127(2.\pi.rh)k}{\mu}\times\frac{dp}{dr_s}$$

Then:

$$\frac{q\ bbl/d\times\frac{159{,}000\ cc/bbl}{24\times 3600\ sec/d}}{A\cdot ft^2\left(.30.48\frac{cm}{ft}\right)^2} = \frac{k\ darcy}{\mu\ \frac{1000\ md}{darcys}}\frac{dp}{ds}\left[psi\times\frac{1\ atm}{14.7\ psi}\right]\Big/\left(30.48\frac{cm}{ft}\right)$$

$$v = -0.001127\frac{k}{\mu}\left[\frac{dp}{ds}\right]$$

$$v = -0.001127\frac{k}{\mu}\left[\frac{dp}{ds}\right]$$

The Classification of Reservoir Flow System

The fluids flow in reservoir may be categorized upon the characteristics as follows.

- **TYPES OF FLUID**

1. .Incompressible Fluids (Water).
2. . Slightly Compressible Fluids (Oil).
3. . Compressible Fluids(Gas).

FLOW REGIMES (TIME DEPENDENCE)

1. .Stead-State Flow
2. .Unstead-State (Transient) Flow.
3. .Pseudostead-State Flow

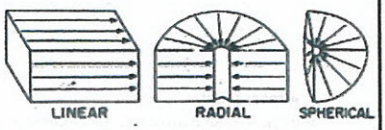

Fig. 7.1. Common flow geometries:

- **RESERVOIR GEOMETRY**

1. Linear Flow
2. Radial Flow
3. Spherical and Hemispherical Flow

- **NUMBER OF FLUIDS IN RESERVOIR**

1. Single-phase Flow(oil, water, or gas)
2. Two-phase Flow(oil-water, oil-gas, or gas-water).
3. Three-phase Flow(oil-water-gas).

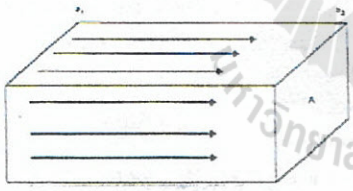

Figure.4.3 Linear flow

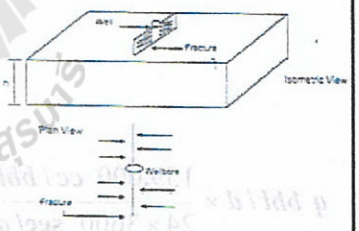

Figure.4.4 Ideal linear flow into vertical fracture

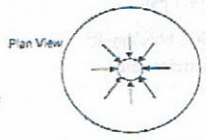

Figure.4.6 Spherical flow

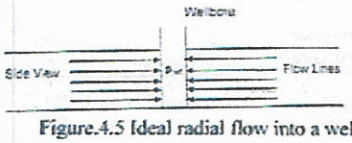

Figure.4.5 Ideal radial flow into a wellbore

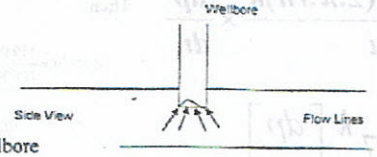

Figure.4.7Hemispherical flow

$$\eta = \frac{k}{\phi \mu c_t} \tag{7.4}$$

where k is the effective permeability of the flowing phase, ϕ is the total effective porosity, μ is the fluid viscosity of the flowing phase, and c_t is the total compressibility. The total compressibility is obtained by weighting the compressibility of each phase by its saturation and adding the formation compressibility, or:

$$c_t = c_g S_g + c_o S_o + c_w S_w + c_f \tag{7.5}$$

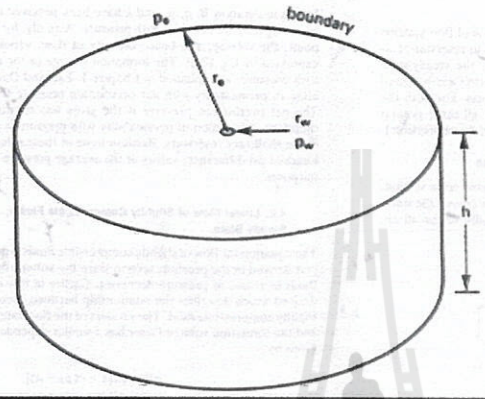

An estimation for the time when a flow system of the type shown in Figure 7.2 reaches pseudosteady-state can be made from the following equation

$$t_{pss} = \frac{1200 r_e^2}{\eta} = \frac{1200 \phi \mu c_t r_e^2}{k} \tag{7.6}$$

where t_{pss} is the time to reach pseudosteady-state expressed in hours.[3] For a well producing an oil with a reservoir viscosity of 1.5 cp and a total compressibility of 15×10^{-6} psi^{-1}, from a circular reservoir of 1000-ft radius with a permeability of 100 md and a total effective porosity of 20%:

$$t_{pss} = \frac{1200(0.2)(1.5)(15(10)^{-6})(1000^2)}{100} = 54 \text{ hr}$$

This means that approximately 54 hours, or 2.25 days, is required for the flow in this reservoir to reach pseudosteady-state conditions after a well located in its center is opened to flow, or following a change in the well flow rate. It also means that if the well is shut in, it will take approximately this time for the pressure to equalize throughout the drainage area of the well, so that the measured subsurface pressure equals the average drainage area pressure of the well.

This same criterion may be applied approximately to gas reservoirs but with less certainty because the gas is more compressible. For a gas viscosity of 0.015 cp and a compressibility of 400×10^{-6} psi^{-1},

$$t_{pss} = \frac{1200(0.2)(0.015)(400(10)^{-6})(1000^2)}{100} = 14.4 \text{ hr}$$

Thus, under somewhat comparable conditions (i.e., the same r_e and k), gas reservoirs reach pseudosteady-state conditions more rapidly than do oil reser-

$$t_{pss} = \frac{1200(0.2)(0.015)(400(10)^{-6})(2500^2)}{1} = 9000 \text{ hr}$$

the increase in fluid compressibility. On the other hand, gas wells are usually drilled on wider spacings so that the value of r_e generally is larger for gas wells than for oil wells, thus increasing the time required to reach pseudosteady-state. Many gas reservoirs, such as those found in the overthrust belt, are associated with sands of low permeability. If we consider an r_e value of 2500 ft and a permeability of 1 md, which would represent a tight gas sand, then we calculate the following value for t_{ps}:

$$t_{ps} = \frac{1200(0.2)(0.015)(400(10)^{-6})(2500^2)}{1} = 9000 \text{ hr}$$

The calculations suggest that reaching pseudosteady-state conditions in a typical tight gas reservoir takes a very long time compared to a typical oil reservoir. In general, pseudosteady-state mechanics suffice when the time required to reach pseudosteady-state is small compared with the time between substantial changes in the flow rate, or, in the case of reservoirs, small compared with the total producing life (time) of the reservoir.

4. STEADY-STATE FLOW SYSTEMS

Now that Darcy's law has been reviewed and the classification of flow systems has been discussed, the actual models that relate flow rate to reservoir pressure can be developed. The next several sections discuss the steady-state models. In this discussion, both linear and radial flow geometries are discussed since there are many applications for these types of systems. For both the linear and radial geometries, equations are developed for all three general types of fluids (i.e., incompressible, slightly compressible, and compressible).

4.1. Linear Flow of Incompressible Fluids, Steady State

Figure 7.3 represents linear flow through a body of constant cross section, where both ends are entirely open to flow, and where no flow crosses the sides, top, or bottom. If the fluid is incompressible, or essentially so for all engineering purposes, then the velocity is the same at all points, as is the total flow rate across any cross section, so that,

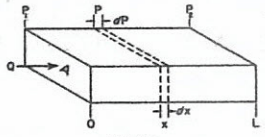

Fig. 7.3.

$$v = \frac{qB}{A_c} = -0.001127 \frac{k}{\mu} \frac{dp}{dx}$$

Separating variables and integrating over the length of the porous body;

$$\frac{qB}{A_c} \int_0^L dx = -0.001127 \frac{k}{\mu} \int_{p_1}^{p_2} dp$$

$$q = 0.001127 \frac{kA_c(p_1 - p_2)}{B\mu L} \tag{7.7}$$

For example, under a pressure differential of 100 psi for a permeability of 250 md, a fluid viscosity of 2.5 cp, a formation volume factor of 1.127 bbl/STB, a length of 450 ft, and a cross-sectional area of 45 sq ft, the flow rate is

$$q = 0.001127 \frac{(250)(45)(100)}{(1.127)(2.5)(450)} = 1.0 \text{ STB/day}$$

In this integration B, q, μ, and k have been removed from the integral sign, assuming they are invariant with pressure. Actually, for flow above the bubble point, the volume, and hence the rate of flow, varies with the pressure as expressed by Eq. (7.2). The formation volume factor and viscosity also vary with pressure, as explained in Chapter 1. Fatt and Davis have shown a variation in permeability with net overburden pressure for several sandstones. The net overburden pressure is the gross less the internal fluid pressure; therefore, a variation of permeability with pressure is indicated, particularly in the shallower reservoirs. Because none of these effects is serious for a few hundred psi difference, values at the average pressure may be used for most purposes.

4.2. Linear Flow of Slightly Compressible Fluids, Steady State

The equation for flow of slightly compressible fluids is modified from what was just derived in the previous section since the volume of slightly compressible fluids increases as pressure decreases. Earlier in this chapter, Eq. (7.3) was derived which describes the relationship between pressure and volume for a slightly compressible fluid. The product of the flow rate, defined in STB units, and the formation volume factor has a similar dependence on pressure and is given by

$$qB = q_R[1 + c(p_R - p)] \tag{7.8}$$

4. STEADY-STATE FLOW SYSTEMS

Now that Darcy's law has been reviewed and the classification of flow system has been discussed, the actual models that relate flow rate to reservoir pres

4.1. Linear Flow of Incompressible Fluids, Steady State

Figure 7.3 represents linear flow through a body of constant cross section where both ends are entirely open to flow, and where no flow crosses the sides top, or bottom. If the fluid is incompressible, or essentially so for all en

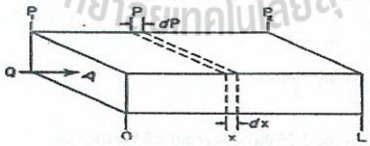

ering purposes, then the velocity is the same at all points, as is the total rate across any cross section, so that,

$$v = \frac{qB}{A_c} = -0.001127 \frac{k}{\mu} \frac{dp}{dx}$$

rating variables and integrating over the length of the porous body;

$$\frac{qB}{A_c} \int_0^L dx = -0.001127 \frac{k}{\mu} \int_{p_1}^{p_2} dp$$

$$q = 0.001127 \frac{kA_c(p_1 - p_2)}{B\mu L} \tag{7.7}$$

example, under a pressure differential of 100 psi for a permeability of 250 a fluid viscosity of 2.5 cp, a formation volume factor of 1.127 bbl/STB, a th of 450 ft, and a cross-sectional area of 45 sq ft, the flow rate is

$$q = 0.001127 \frac{(250)(45)(100)}{(1.127)(2.5)(450)} = 1.0 \text{ STB/day}$$

his integration B, q, μ, and k have been removed from the integral sign,

4.2. Linear Flow of Slightly Compressible Fluids, Steady State

$q_B = q_R[1+c(p_R-p)]$

equation for flow of slightly compressible fluids is modified from what was derived in the previous section since the volume of slightly compressible ~~[illegible]~~. Earlier in this chapter, Eq. (7.3) was written for this case, variables separated, and the resulting equation integrated over the length of the porous body, the following is obtained:

$$\frac{q_R}{A_c}\int_0^L dx = -0.001127\,\frac{k}{\mu}\int_{p_1}^{p_2}\frac{dp}{1+c(p_R-p)}$$

$$q_R = \frac{0.001127kA_c}{\mu Lc}\ln\left[\frac{1+c(p_R-p_2)}{1+c(p_R-p_1)}\right] \qquad (7.9)$$

This integration assumes a constant compressibility over the entire pressure [illegible]. For example, under a pressure differential of 100 psi for a permeability of 250 md, a fluid viscosity of 2.5 cp, a length of 450 ft, a cross-sectional area of 45 sq ft, a constant compressibility of $65(10^{-6})$ psi^{-1}, and choosing p_1 as the reference pressure, the flow rate is

$$q_1 = \frac{(0.001127)(250)(45)}{(2.5)(450)(65\times10^{-6})}\ln\left[\frac{1+65\times10^{-6}(100)}{1}\right] = 1.123 \text{ bbl/day}$$

When compared with the flow rate calculation in the preceding section, q_1 is found to be different due to the assumption of a slightly compressible fluid in the calculation rather than an incompressible fluid. Note also, that the flow rate is not in STB units because the calculation is being done at a reference [illegible]ure that is not the standard pressure. If p_2 is chosen to be the reference pressure, then the result of the calculation will be q_2, and the value of the calculated flow rate will be different still because of the volume dependence on the reference pressure:

$$q_2 = \frac{(0.001127)(250)(45)}{(2.5)(450)(65\times10^{-6})}\ln\left[\frac{1}{1+65\times10^{-6}(-100)}\right] = 1.131 \text{ bbl/day}$$

The calculations show that q_1 and q_2 are not largely different, which confirms what was discussed earlier: the fact that volume is not a strong function of pressure for slightly compressible fluids.

4.3. Linear Flow of Compressible Fluids, Steady State

(Stead State)

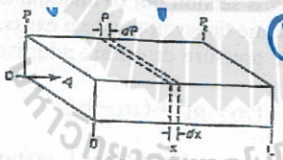

Fig. 7.3.

Substituting in Darcy's law: $v = \frac{qB}{A_c} = -0.001127\frac{k}{\mu}\frac{dp}{dx}$

$$\frac{qp_{sc}Tz}{5.615T_{sc}pA_c} = -0.001127\,\frac{k}{\mu}\frac{dp}{dx}$$

Separating variables and integrating;

$$\frac{qp_{sc}Tz\mu}{(5.615)(0.001127)kT_{sc}A_c}\int_0^L dx = -\int_{p_1}^{p_2} p\,dp = \frac{1}{2}(p_1^2-p_2^2)$$

Finally

$$q = \frac{0.003164T_{sc}A_ck\,(p_1^2-p_2^2)}{p_{sc}TzL\mu} \qquad (7.10)$$

For example, where $T_{sc} = 60°F$, $A_c = 45$ sq ft, $k = 125$ md, $p_1 = 1000$ psia, $p_2 = 500$ psia, $p_{sc} = 14.7$ psia, $T = 140°F$, $z = 0.92$, $L = 450$ ft, and $\mu = 0.015$ cp

126700

$$q = \frac{0.003164(520)(45)(125)\,(1000^2-500^2)}{14.7(600)(0.92)(450)(0.015)} = 126.7 \text{ M SCF/day}$$

psia, depending on the properties of the flowing gas. Above this pressure range, it would be more accurate to assume that the product $\mu z/p$ is constant. For the case of $\mu z/p$ constant, the following is obtained:

$$\frac{qp_{sc}T(z\mu/p)}{(5.615)(0.001127)kT_{sc}A_c}\int_0^L dx = -\int_{p_1}^{p_2} dp = p_1 - p_2$$

$$q = \frac{0.006328kT_{sc}A_c(p_1 - p_2)}{p_{sc}T(z\mu/p)L} \qquad (7.11)$$

In [illegible]

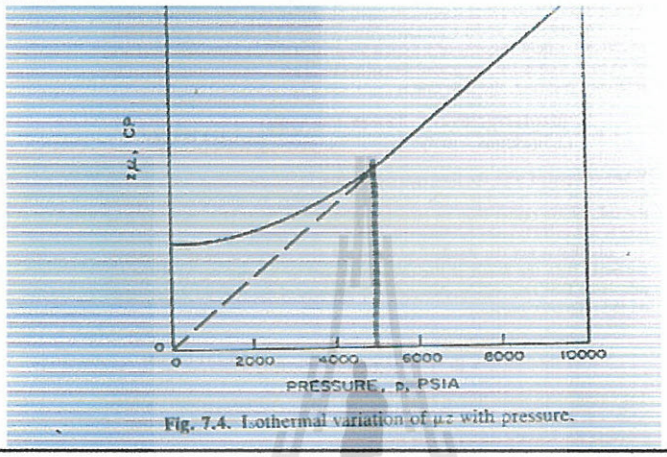

Fig. 7.4. Isothermal variation of μz with pressure.

4.4. Permeability Variations in Linear Systems

Consider two or more beds of equal cross section but of unequal lengths and permeabilities (Fig. 7.5) in which the same linear flow rate q exists, assuming an incompressible fluid. Obviously the pressure drops are additive, and

$$(p_1 - p_4) = (p_1 - p_2) + (p_2 - p_3) + (p_3 - p_4)$$

Substituting the equivalents of these pressure drops from Equation (7.7),

$$\frac{q_t B\mu L_t}{0.001127k_{avg}A_c} = \frac{q_1 B\mu L_1}{0.001127k_1 A_{c1}} + \frac{q_2 B\mu L_2}{0.001127k_2 A_{c2}} + \frac{q_3 B\mu L_3}{0.001127k_3 A_{c3}}$$

$$\frac{L_t}{K_{avg}} = \frac{L_1}{k_1} + \frac{L_2}{k_2} + \frac{L_3}{k_3}$$

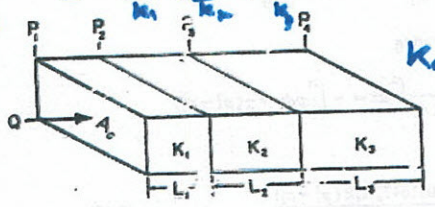

$$K_{avg} = \frac{\Sigma L_i}{\Sigma L_i/k_i}$$

Fig. 7.5. Series flow in linear beds.

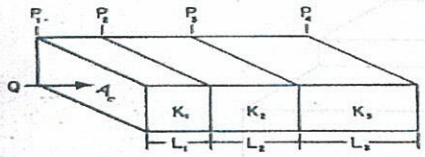

Fig. 7.5. Series flow in linear beds.

$$(p_1^2 - p_4^2) = (p_1^2 - p_2^2) + (p_2^2 - p_3^2) + (p_3^2 - p_4^2)$$

$$\frac{q_g B_{gc} T_{sc} L \mu}{0.003164 T_{sc} A_c k} = \frac{q_g B_{gc} T_{sc} \mu}{0} \frac{L_1}{K_1} + \frac{q_g B_{gc} T_{sc} \mu}{0} \frac{L_2}{K_2} + \frac{q_g B_{gc} T_{sc} \mu}{0} \frac{L_3}{K_3}$$

$$\frac{L_t}{k_{avg}} = \frac{L_1}{k_1} + \frac{L_2}{k_2} + \frac{L_3}{k_3}$$

$$k_{avg} = \frac{L_t}{\frac{L_1}{k_1} + \frac{L_2}{k_2} + \frac{L_3}{k_3}} = \frac{\Sigma L_i}{\Sigma L_i/k_i} \qquad (7.12)$$

The average permeability of 10 md, 50 md, and 1000 md beds, which a
t, 18 ft, and 40 ft in length, respectively, but of equal cross section, wh
aced in series is

$$k_{avg} = \frac{\Sigma L_i}{\Sigma L_i/k_i} = \frac{6 + 18 + 40}{6/10 + 18/50 + 40/1000} = 64 \text{ md}$$

$$\frac{L_t}{k_{avg}} = \frac{L_1}{k_1} + \frac{L_2}{k_2} + \frac{L_3}{k_3}$$

$$k_{avg} = \frac{L_t}{\frac{L_1}{k_1} + \frac{L_2}{k_2} + \frac{L_3}{k_3}} = \frac{\Sigma L_i}{\Sigma L_i/k_i} \qquad (7.12)$$

average permeability as defined by Eq. (7.12) is that permeability to
ch a number of beds of various geometries and permeabilities could be
nged, and yet the same total flow rate under the same applied pressure
p could be obtained.

Equation (7.12) was derived using the incompressible fluid equation.
ae... the permeability is a property of the rock and not of the fluids flowing
ough it, except for gases at low pressure, the average permeability must be
ally applicable to gases. This requirement may be demonstrated by observ-
that for pressures below 1500 to 2000 psia:

use Eq 7

$$(p_1^2 - p_4^2) = (p_1^2 - p_2^2) + (p_2^2 - p_3^2) + (p_3^2 - p_4^2)$$

stituting the equivalents from Eq. (7.10), the same Eq. (7.12) is obtained.

The average permeability of 10 md, 50 md, and 1000 md beds, which are
, 18 ft, and 40 ft in length, respectively, but of equal cross section, when
ced in series is

$$k_{avg} = \frac{\Sigma L_i}{\Sigma L_i/k_i} = \frac{6 + 18 + 40}{6/10 + 18/50 + 40/1000} = 64 \text{ md}$$

Consider two or more beds of equal length but unequal cross sections
d permeabilities flowing the same fluid in linear flow under the same pres-
re drop (p_1 to p_2) as shown in Fig. 7.6.
viously the total flow is the sum of the individual flows, or

$$q_t = q_1 + q_2 + q_3$$

rd

$$\frac{k_{avg} A_{ct} (p_1 - p_2)}{B \mu L} = \frac{k_1 A_{c1} (p_1 - p_2)}{B \mu L} + \frac{k_2 A_{c2} (p_1 - p_2)}{B \mu L} + \frac{k_3 A_{c3} (p_1 - p_2)}{B \mu L}$$

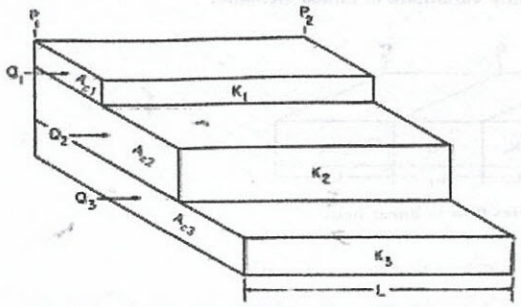

Fig. 7.6. Parallel flow in linear beds.

Cancelling

$$k_{avg}A_{ct} = k_1A_{c1} + k_2A_{c2} + k_3A_{c3}$$

$$k_{avg} = \frac{\Sigma\, k_iA_{ci}}{\Sigma\, A_{ci}} \qquad (7.13)$$

And where all beds are of the same width, so that their areas are proportional to their thicknesses,

$$k_{avg} = \frac{\Sigma\, k_ih_i}{\Sigma\, h_i} \qquad (7.14)$$

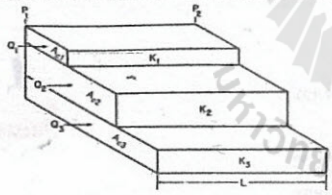

Fig. 7.6. Parallel flow in linear beds.

Cancelling

$$k_{avg}A_{ct} = k_1A_{c1} + k_2A_{c2} + k_3A_{c3}$$

$$k_{avg} = \frac{\Sigma\, k_iA_{ci}}{\Sigma\, A_{ci}} \qquad (7.13)$$

And where all beds are of the same width, so that their areas are proportional to their thicknesses,

$$k_{avg} = \frac{\Sigma\, k_ih_i}{\Sigma\, h_i} \qquad (7.14)$$

Where the parallel beds are homogeneous in permeability and fluid content, the pressure and the pressure gradient are the same in all beds at equal distances. Thus there will be no cross-flow between beds, owing to fluid pressure differences. However, when water displaces oil—for example from a set of parallel beds—the rates of advance of the flood fronts will be greater in the more permeable beds. Because the mobility of the oil (k_o/μ_o) ahead of the flood front is different from the mobility of water (k_w/μ_w) behind the flood front, the pressure gradients will be different. In this instance, there will be pressure differences between two points at the same distance through the rock, and cross flow will take place between the beds if they are not separated by impermeable barriers. Under these circumstances, Eqs. (7.13) and (7.14) are not strictly applicable, and the average permeability changes with the stage of displacement. Water may also move from the more permeable to the less permeable beds by capillary action, which further complicates the study of parallel flow.

The average permeability of three beds of 10 md, 50 md, and 1000 md and 6 ft, 18 ft, and 36 ft respectively in thickness but of equal width, when placed in parallel is

$$k_{avg} = \frac{\Sigma k_ih_i}{\Sigma h_i} = \frac{10\times 6 + 18\times 50 + 36\times 1000}{6+18+36} = 616 \text{ md}$$

4.5. Flow Through Capillaries and Fractures

Although the pore spaces within rocks seldom resemble straight, smooth-walled capillary tubes of constant diameter, it is often convenient and instructive to treat these pore spaces as if they were composed of bundles of parallel capillary tubes of various diameters. Consider a capillary tube of length L and inside radius r_o which is flowing an incompressible fluid of μ viscosity in laminar or viscous flow under a pressure difference of $(p_1 - p_2)$. From fluid dynamics, Poiseuille's law, which describes the total flow rate through the capillary, can be written as:

$$q = 1.30(10)^{10}\frac{\pi r_o^4(p_1 - p_2)}{B\mu L} \qquad (7.15)$$

Darcy's law for the linear flow of incompressible fluids in permeable beds, Eq. (7.7), and Poiseuille's law for incompressible fluid capillary flow, Eq. (7.15), are quite similar:

$$q = 0.001127\frac{kA_c(p_1 - p_2)}{B\mu L} \qquad (7.7)$$

Writing $A_c = \pi r_o^2$ for area in Eq. (7.7), and equating it to Eq. (7.15);

$$k = 1.15(10)^{13}r_o^2 \qquad (7.16)$$

Thus the permeability of a rock composed of closely packed capillaries, each having a radius of $4.17(10)^{-6}$ foot (0.00005 in.), is about 200 md. And if only 25% of the rock consists of pore channels (i.e., it has 25% porosity), the permeability is about one-quarter as large, or about 50 md.

An equation for the viscous flow of incompressible wetting fluids through smooth fractures of constant width may be obtained as:

$$q = 8.7(10)^9\frac{W^2A_c(p_1 - p_2)}{B\mu L} \qquad (7.17)$$

In Eq. (7.17), W is the width of the fracture, A_c is the cross-sectional area of the fracture, which equals the product of the width W and lateral extent of the fracture, and the pressure difference is that which exists between the ends of

4.5. Flow Through Capillaries and Fractures

Although the pore spaces within rocks seldom resemble straight, smooth-walled capillary tubes of constant diameter, it is often convenient and instructive to treat these pore spaces as if they were composed of bundles of parallel capillary tubes of various diameters. Consider a capillary tube of length L and inside radius r_o which is flowing an incompressible fluid of μ viscosity in laminar or viscous flow under a pressure difference of $(p_1 - p_2)$. From fluid dynamics, Poiseuille's law, which describes the total flow rate through the capillary, can be written as:

$$q = 1.30(10)^{10}\frac{\pi r_o^4(p_1 - p_2)}{B\mu L} \quad (7.15)$$

Darcy's law for the linear flow of incompressible fluids in permeable beds, Eq. (7.7), and Poiseuille's law for incompressible fluid capillary flow, Eq. (7.15), are quite similar:

$$q = 0.001127\frac{kA_c(p_1 - p_2)}{B\mu L} \quad (7.7)$$

Writing $A_c = \pi r_0^2$ for area in Eq. (7.7), and equating it to Eq. (7.15);

$$k = 1.15(10)^{13} r_0^2 \quad (7.16)$$

Thus the permeability of a rock composed of closely packed capillaries, each having a radius of $4.17(10)^{-6}$ foot (0.00005 in.), is about 200 md. And if only 25% of the rock consists of pore channels (i.e., it has 25% porosity), the permeability is about one-quarter as large, or about 50 md.

An equation for the viscous flow of incompressible wetting fluids through smooth fractures of constant width may be obtained as:

$$q = 8.7(10)^9\frac{w^2A_c(p_1 - p_2)}{B\mu L} \quad (7.17)$$

4.5. Flow Through Capillaries and Fractures

Although the pore spaces within rocks seldom resemble straight, smooth-walled capillary tubes of constant diameter, it is often convenient and instructive to treat these pore spaces as if they were composed of bundles of parallel capillary tubes of various diameters. Consider a capillary tube of length L and inside radius r_o which is flowing an incompressible fluid of μ viscosity in laminar or viscous flow under a pressure difference of $(p_1 - p_2)$. From fluid dynamics, Poiseuille's law, which describes the total flow rate through the capillary, can be written as:

$$q = 1.30(10)^{10}\frac{\pi r_o^4(p_1 - p_2)}{B\mu L} \quad (7.15)$$

Darcy's law for the linear flow of incompressible fluids in permeable beds, Eq. (7.7), and Poiseuille's law for incompressible fluid capillary flow, Eq. (7.15), are quite similar:

$$q = 0.001127\frac{kA_c(p_1 - p_2)}{B\mu L} \quad (7.7)$$

Writing $A_c = \pi r_0^2$ for area in Eq. (7.7), and equating it to Eq. (7.15);

$$k = 1.15(10)^{13} r_0^2 \quad (7.16)$$

Thus the permeability of a rock composed of closely packed capillaries, each having a radius of $4.17(10)^{-6}$ foot (0.00005 in.), is about 200 md. And if only 25% of the rock consists of pore channels (i.e., it has 25% porosity), the permeability is about one-quarter as large, or about 50 md.

An equation for the viscous flow of incompressible wetting fluids through smooth fractures of constant width may be obtained as:

$$q = 8.7(10)^9 \frac{W^2 A_c (p_1 - p_2)}{B\mu L} \tag{7.17}$$

In Eq. (7.17), W is the width of the fracture, A_c is the cross-sectional area of the fracture, which equals the product of the width W and lateral extent of the fracture, and the pressure difference is that which exists between the ends of the fracture of length L. Equation (7.17) may be combined with Eq. (7.7) to obtain an expression for the permeability of a fracture as:

$$k = 7.7(10)^{12} W^2 \tag{7.18}$$

The permeability of a fracture only $8.33(10)^{-5}$ ft wide (0.001 in.) is 53,500 md.

Fractures and solution channels account for economic production rates in many dolomite, limestone, and sandstone rocks, which could not be produced economically if such openings did not exist. Consider, for example, a rock of very low primary or matrix permeability, say 0.01 md, but which contains on the average a fracture $4.17(10)^{-4}$ ft wide and 1 ft in lateral extent per square foot of rock. Assuming the fracture is in the direction in which flow is desired, the law of parallel flow, Eq. (7.13) will apply, and

$$k_{avg} = \frac{0.01[1 - (1)(4.17(10)^{-4})] + (7.7(10)^{12})(4.17(10)^{-4})^3[1(4.17(10)^{-4})]}{1}$$

$$k_{avg} = 558 \text{ md}$$

4.6. Radial Flow of Incompressible Fluid, Steady State

Consider radial flow toward a vertical wellbore of radius r_w in a horizontal stratum of uniform thickness and permeability, as shown in Fig. 7.7. If the fluid is incompressible, the flow across any circumference is a const... be the pressure maintained in the wellbore when the well is flowing and a pressure p_e is maintained at the external radius r_e. Let the p... any radius r be p. Then at this radius r

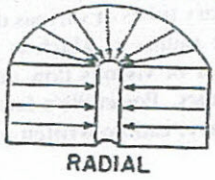

$$v = \frac{qB}{A_c} = \frac{qB}{2\pi rh} = -0.001127 \frac{k\,dp}{\mu\,dr}$$

where positive q is in the positive r direction. Separ... grating between any two radii, r_1 and r_2, where the ... respectively

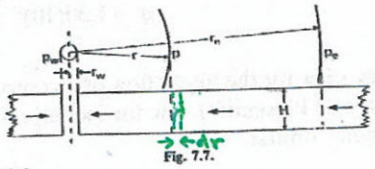

Fig. 7.7.

$$\int_{r_1}^{r_2} \frac{qB\,dr}{2\pi rh} = -0.001127 \int_{p_1}^{p_2} \frac{k}{\mu}\,dp$$

$$q = -\frac{0.00708\,kh\,(p_2 - p_1)}{\mu B \ln (r_2/r_1)}$$

The minus sign is usually dispensed with, for where p_2 is greater than p_1, the flow is known to be negative—that is, in the negative r direction, or toward ...e wellbore:

$$q = \frac{0.00708\,kh\,(p_2 - p_1)}{\mu B \ln (r_2/r_1)}$$

the fracture of length L. Equation (7.17) may be combined with Eq. (7.7) to obtain an expression for the permeability of a fracture as:

$$k = 7.7(10)^{12}w^2 \tag{7.18}$$

The permeability of a fracture only $8.33(10)^{-5}$ ft wide (0.001 in.) is 53,500 md.

Fractures and solution channels account for economic production rates in many dolomite, limestone, and sandstone rocks, which could not be produced economically if such openings did not exist. Consider, for example, a rock of very low primary or matrix permeability, say 0.01 md, but which contains on the average a fracture $4.17(10)^{-4}$ ft wide and 1 ft in lateral extent per square foot of rock. Assuming the fracture is in the direction in which flow is desired, the law of parallel flow, Eq. (7.13) will apply, and

$$k_{eq} = \frac{0.01[1-(1)(4.17(10)^{-4})]+(7.7(10)^{12}(4.17(10)^{-4})^2)[1(4.17(10)^{-4})]}{1}$$

$$k_{eq} = 558 \text{ md}$$

4.6. Radial Flow of Incompressible Fluid, Steady State

Consider radial flow toward a vertical wellbore of radius r_w in a horizontal stratum of uniform thickness and permeability, as shown in Fig. 7.7. If the fluid is incompressible, the flow across any circumference is a constant. Let p_w be the pressure maintained in the wellbore when the well is flowing q STB/day and a pressure p_e is maintained at the external radius r_e. Let the pressure at any radius r be p. Then at this radius r

$$v = \frac{qB}{A_c} = \frac{qB}{2\pi rh} = -0.001127\frac{k}{\mu}\frac{dp}{dr}$$

where positive q is in the positive r direction. Separating variables and integrating between any two radii, r_1 and r_2, where the pressures are p_1 and p_2, respectively

$$\int_{r_1}^{r_2}\frac{qB\,dr}{2\pi rh} = -0.001127\int_{p_1}^{p_2}\frac{k}{\mu}\,dp$$

$$q = -\frac{0.00708\,kh\,(p_2-p_1)}{\mu B\,\ln(r_2/r_1)}$$

The minus sign is usually dispensed with, for where p_2 is greater than p_1, the flow is known to be negative—that is, in the negative r direction, or toward the wellbore:

$$q = \frac{0.00708\,kh\,(p_2-p_1)}{\mu B\,\ln(r_2/r_1)}$$

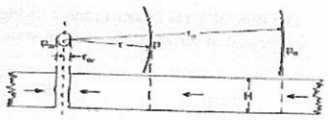

Fig. 7.7.

Frequently the two radii of interest are the wellbore radius r_w and the external or drainage radius r_e. Then

$$q = \frac{0.00708\,kh\,(p_e-p_w)}{\mu B\,\ln(r_e/r_w)} \tag{7.19}$$

The external radius is usually inferred from the well spacing. For example, a circle of 660 ft radius can be inscribed within a square 40 ac unit; so 660 ft is commonly used for r_e with 40 ac spacing. Sometimes a radius of 745 ft is used, this being the radius of a circle 40 ac in area. The wellbore radius is usually assigned from the bit diameter, the casing diameter, or a caliper survey. In practice, neither the external radius nor the wellbore radius is generally known with precision. Fortunately, they enter the equation as a logarithm, so that the error in the equation will be much less than the errors in the radii. Since wellbore radii are about 1/3 ft and 40 ac spacing ($r_e = 660$ ft) is quite common, a ratio 2000 is quite commonly used for r_e/r_w. Since ln 2000 is 7.60 and ln 3000 is 8.00, a 50% increase in the value of r_e/r_w gives only a 5.3% increase in the value of the logarithm.

The external pressure p_e used in Eq. (7.19) is generally taken as the static well pressure corrected to the middle of the producing interval, and the flowing well pressure p_w is the flowing well pressure also corrected to the middle of the producing interval during a period of stabilized flow at rate q. When reservoir pressure stabilizes as under natural water drive or pressure maintenance, Eq. (7.19) is quite applicable because the pressure is maintained at the external boundary, and the fluid produced at the well is replaced by fluid crossing the external boundary. The flow, however, may not be strictly radial.

4.7. Radial Flow of Slightly Compressible Fluids, Steady State

Equation (7.3) is again used to express the volume dependence on pressure for slightly compressible fluids. If this equation is substituted into the radial form of Darcy's law, the following is obtained:

4.7. Radial Flow of Slightly Compressible Fluids, Steady State

Equation (7.3) is again used to express the volume dependence on pressure for slightly compressible fluids. If this equation is substituted into the radial form of Darcy's law, the following is obtained:

$$qB = \frac{q_R[1+c(p_R-\bar{p})]}{2\pi rh} = -0.001127\frac{k}{\mu}\frac{dp}{dr}$$

Separating the variables, assuming a constant compressibility over the entire pressure drop, and integrating over the length of the porous medium,

$$q_R = \frac{0.00708\,kh}{\mu c\,\ln(r_2/r_1)}\ln\left[\frac{1+c(p_R-p_2)}{1+c(p_R-p_1)}\right] \tag{7.20}$$

4.8. Radial Flow of Compressible Fluids, Steady State

The flow of a gas at any radius r of Fig. 7.7, where the pressure is p, may be expressed in terms of the flow in standard cubic feet per day by:

$$qB_g = \frac{qp_{sc}Tz}{5.615T_{sc}p}$$

Substituting in the radial form of Darcy's law

$$\frac{qp_{sc}Tz}{5.615T_{sc}p(2\pi rh)} = -0.001127\frac{k}{\mu}\frac{dp}{dr}$$

Separating variables and integrating

$$\frac{qp_{sc}Tz\mu}{5.615(0.001127)(2\pi)T_{sc}kh}\int_{r_1}^{r_2}\frac{dr}{r} = -\int_{p_1}^{p_2}pdp = \frac{1}{2}(p_1^2 - p_2^2)$$

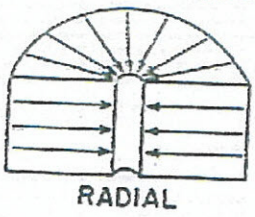

or

$$\frac{qp_{sc}Tz\mu}{0.01988T_{sc}kh}\ln(r_2/r_1) = p_1^2 - p_2^2$$

Finally

$$q = \frac{0.01988T_{sc}kh\,(p_1^2 - p_2^2)}{p_{sc}T(z\mu)\ln(r_2/r_1)} \qquad (7.21)$$

$$q = \frac{0.703\,kh\,(p_e^2 - p_w^2)}{\bar{\mu}\bar{z}\,T_f\,\ell n\,r_e/r_w} \qquad Q_g = \frac{kh\,(p_e^2 - p_{wf}^2)}{1422\,T\,(\mu_g z)_{avg}\ln\left(\frac{r_e}{r_w}\right)}$$

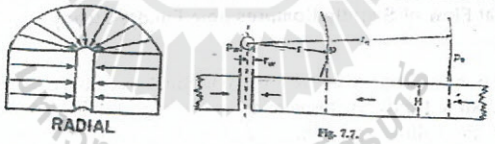

Fig. 7.7.

0.7032

$$q = \frac{707.8\,kh\,(p_e^2 - p_w^2)}{\bar{\mu}\bar{z}\,T_f\,\ell n\,r_e/r_w} \qquad Q_g = \frac{kh\,(p_e^2 - p_{wf}^2)}{1422\,T\,(\mu_g z)_{avg}\ln\left(\frac{r_e}{r_w}\right)}$$

$$q = 307.4\frac{kh\,(p_e^2 - p_w^2)}{\bar{\mu}\bar{z}\,T_f\log r_e/r_w}$$

where Q_g = gas flow rate, Mscf/day
k = permeability, md

here:
q = cu ft/day at 14.65 psia and 60°F
k = permeability, darcies
h = thickness, ft
p_e = pressure at external radius, r_e, psia
p_w = pressure at inner radius, r_w, psia
$\bar{\mu}$ = average viscosity, cp
$\bar{z}$ = average compressibility factor, ratio
T_f = flowing temperature, °F + 460
r = radius, ft

14.7

k = 0.01 darcy = 10 md
h = 20 ft
$\bar{\mu}$ = 0.02 cp
$\bar{z}$ = 0.90
T_f = 580°R abs
r_e = 2,640 ft
r_w = 0.25 ft
p_e = 3,000 psia
p_w = 1,000 psia
(q_g is calculated to be 11,708 Mcfd)

11,633 Mscf/day

$$q = \frac{0.7032 \times 10 \times 20 \times (3000^2 - 1000^2)}{0.02 \times 0.9 \times 580 \times \ln\frac{2640}{0.25}}$$

$$= 11{,}633{,}000 \text{ SCF/day}$$

Radial Flow of Gas in Pseudopressure Form

For more accuracy, the radial gas flow equation may be expressed in pseudopressure form. Gas pseudopressure, $\psi(p)$, is defined by the integral

$$\psi(p) = 2\int_{p_b}^{p} \frac{p}{\mu z} dp$$

Where p_b is some arbitrary low base pressure.

Rearrange Eq.(4.25)

$$\left(\frac{p_{sc}}{5.615 T_{sc}}\right)\left(\frac{zT}{p}\right) Q_g = -0.0011279(2\pi rh)\frac{k}{\mu}\frac{dp}{dr}$$

Assuming that T_{sc} = 520°R and p_{sc} = 14.7 psia

$$\left(\frac{TQ_g}{kh}\right)\frac{dr}{r} = 0.703\left(\frac{2p}{\mu_g z}\right)dp \qquad (4.28)$$

Integrating Eq.(4.28) from the wellbore conditions (r_w and p_{wf}) to any point in the reservoir (r and p)

$$\int_{r_w}^{r}\left(\frac{TQ_g}{kh}\right)\frac{dr}{r} = 0.703\int_{p_{wf}}^{p}\left(\frac{2p}{\mu_g z}\right)dp \qquad (4.29)$$

The term $\int_{p_{wf}}^{p}\left(\frac{2p}{\mu_g z}\right)dp$ can be expanded to give:

$$\int_{p_{wf}}^{p}\left(\frac{2p}{\mu_g z}\right)dp = \int_{0}^{p}\left(\frac{2p}{\mu_g z}\right)dp - \int_{0}^{p_{wf}}\left(\frac{2p}{\mu_g z}\right)dp$$

Combine the above relationships Eq.(4.29) yields:

$$\left(\frac{TQ_g}{kh}\right)\ln\left(\frac{r}{r_w}\right) = 0.703\left[\int_{0}^{p}\left(\frac{2p}{\mu_g z}\right)dp - \int_{0}^{p_{wf}}\left(\frac{2p}{\mu_g z}\right)dp\right] \qquad (4.30)$$

The integral $\int_{0}^{p}\left(\frac{2p}{\mu_g z}\right)dp$ is called the real gas potential or real gas pseudopressure and it is usually represented by m(p) or $\psi = \int_{0}^{p}\left(\frac{2p}{\mu_g z}\right)dp$

Equation (4.30) can be written in terms of the real gas potential to give:

$$\left(\frac{TQ_g}{kh}\right)\ln\left(\frac{r}{r_w}\right) = 0.703\,(\psi - \psi_w)$$

or $$\psi = \psi_w + \left(\frac{TQ_g}{0.703kh}\right)\ln\left(\frac{r}{r_w}\right)$$

or $$Q_g = \frac{0.703kh(\Psi - \Psi_w)}{T\ln\frac{r}{r_w}} \qquad (4.31)$$

The gas flow rate is commonly expressed in MSCF/D and r = r_e then

$$Q_g = \frac{kh(\Psi - \Psi_w)}{1422T \ln \frac{r_e}{r_w}} \qquad (4.32)$$

Example 4.1 The following PVT data from a gas well in the Anaconda Gas Field is given below:

p (psi)	μ_g (cp)	z
0	0.01270	1.000
400	0.01286	0.937
800	0.01390	0.882
1200	0.01530	0.832
1600	0.01680	0.794
2000	0.01840	0.770
2400	0.02010	0.763
2800	0.02170	0.775
3200	0.02340	0.797
3600	0.02500	0.827
4000	0.02660	0.860
4400	0.02831	0.896

The well is producing at a stabilized bottom-hole flowing pressure of 3600 psi. The wellbore radius is 0.3 ft. The following additional data is available:

k = md h = 15 ft T = 600°R
p_e = 4400 psi r_e = 1000 ft

Calculate the gas flow rate in Mscf/day

Solution.

Step1. Calculate the term $\left(\frac{2p}{\mu_g z}\right)$ for each pressure as shown below:

p (psi)	μ_g (cp)	z	$\left(\frac{2p}{\mu_g z}\right)\left(\frac{psia}{cp}\right)$
0	0.01270	1.000	00
400	0.01286	0.937	66391
800	0.01390	0.882	130508
1200	0.01530	0.832	188537
1600	0.01680	0.794	239894
2000	0.01840	0.770	282326
2400	0.02010	0.763	312983
2800	0.02170	0.775	332986
3200	0.02340	0.797	343167
3600	0.02500	0.827	348247
4000	0.02660	0.860	349711
4400	0.02831	0.896	346924

for each pressure as show below:

$$m(p) = \left(\frac{2p}{\mu_g z}\right) * dp$$

$$m(p) = ((0 + 66391) * 400/2) = 13278200$$

$$m(p) = 13278200 + ((66391 + 130508) * 400/2) = 52658000$$

$$m(p) = 52658000 + ((130508 + 138537) * 400/2) = 116467000$$

p (psi)	μ_g (cp)	z	$\frac{2p}{\mu_g z}\left(\frac{psia}{cp}\right)$
0	0.01270	1.000	0
400	0.01286	0.937	66391
800	0.01390	0.882	130508
1200	0.01530	0.832	188537
1600	0.01680	0.794	239894
2000	0.01840	0.770	282326
2400	0.02010	0.763	312983
2800	0.02170	0.775	332986
3200	0.02340	0.797	343167
3600	0.02500	0.827	348247
4000	0.02660	0.860	349711
4400	0.02831	0.896	346924

202153200
306597200
425659000
554852800
690083400
828366200
967957800
1107284800

Step 2. Plot the term $\left(\frac{2p}{\mu_g z}\right)$ versus pressure as shown in Figure 6-16.

Step 3. Calculate numerically the area under the curve for each value of p. These areas correspond to the real gas potential ψ at each pressure. These ψ values are tabulated below

ψ versus p is also plotted in the figure

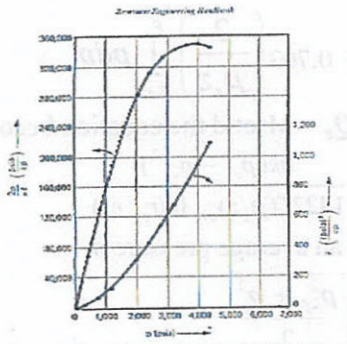

Figure 6-16. Real gas pseudopressure data for Example 6-7 [After Donohue and Farshad, 1982]

P=400psia, M(P)= 13278200
P=800psia, M(P)= 52658000
P=1200psia, M(P)= 116467000
P=1600psia, M(P)= 202153200
306597200
425659000
554852800
690083400
828366200
967957800
P=4400psia, M(P)= 1107284800

Step 4 Calculate the flow rate by applying Equation

$$Q = \frac{0.703kh(\psi - \psi_w}{T \ln \frac{r}{r_w}}$$

$$p_w = 816 \times 10^6 \qquad p_e = 1089 \times 10^6$$

$$Q_g = \frac{(65)(15)(1089-816)10^6}{(1422)(600)\ln(1000/0.25)}$$

$$= 37{,}614 \text{ Mscf/day}$$

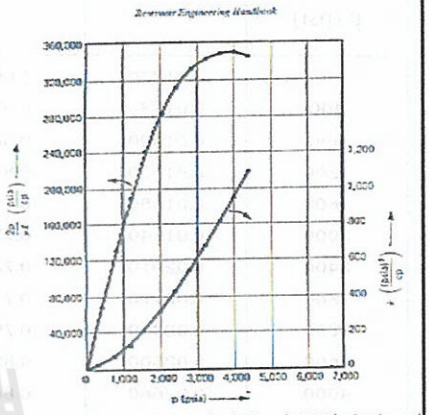

Figure 6-16. Real gas pseudopressure data for Example 6-7 (After Donohue and Stein, 1982)

Approximation of the Gas Flow Rate

The Eq.4.29 can be approximated by removing the term $\left(\frac{2}{\mu_g z}\right)$ outside the integral as a constant. It should be pointed out that the z is considered constant only under a pressure range of <2000psia.

$$\left(\frac{TQ_g}{kh}\right)\ln\left(\frac{r}{r_w}\right) = 0.703\left(\frac{2}{\mu_g z}\right)\int_{p_{wf}}^{p} pdp \qquad (4.33)$$

Perform the integration and let Q_g = Mscf/d the equation becomes

$$Q_g = \frac{hk(p_e^2 - p_{wf}^2)}{1422T(\mu_g z)_{avg}\ln(r_e/r_w)} \qquad (4.34)$$

The term $(\mu_g z)_{avg}$ is evaluated at an average pressure $\bar{p}$

$$\bar{p} = \sqrt{\frac{p_{wf}^2 + p_e^2}{2}}$$

Example 4.2 Using the data given in Ex.4.1, resolve for the gas flow rate by using the pressure-square method. Compare with the exact method(i.e. real gas potential ψ solution)

Solution.

Step1. Calculate the arithmetic average pressure.

$$\bar{p} = \left[\frac{4400^2 + 3600^2}{2}\right]^{.5} = 4020$$

Step2. Determine gas viscosity and gas compressibility factor at 4020 psi.

$\mu_g = 0.0267$

$z = 0.862$

Step3. Apply Equation 4.34

$$Q_g = \frac{(65)(15)(4400^2 - 3600^2)}{(1422)(600)(0.0267)(0.862)\ln(1000/0.25)}$$

$= 38.314$ Mscf/day

Step4. Results show that the pressure-squared method approximates the exact solution of 37,614 with an absolute error of 1.86%. This error is due to the limited applicability of the pressure-squared method to a pressure rang of <2000 psi.

4.9. Permeability Variations in Radial Flow

Many producing formations are composed of strata or stringers that may vary widely in permeability and thickness, as illustrated in Fig. 7.8. If these strata are producing fluid to a common wellbore under the same drawdown and from the same drainage radius, then

$$q_t = q_1 + q_2 + q_3 \cdots + q_n$$

$$\frac{0.00708\ k_{avg}h_t(p_e - p_w)}{\mu B\ \ln(r_e/r_w)} = \frac{0.00708\ k_1h_1(p_e - p_w)}{\mu B\ \ln(r_e/r_w)} + \frac{0.00708\ k_2h_2(p_e - p_w)}{\mu B\ \ln(r_e/r_w)} + \text{etc.}$$

Then cancelling

$$k_{avg}h_t = k_1h_1 + k_2h_2 + \cdots + k_nh_n$$

$$k_{avg} = \frac{\Sigma k_ih_i}{\Sigma h_i} \qquad (7.23)$$

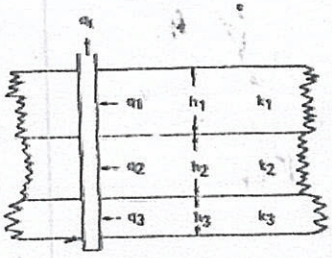

Fig. 7.8. Radial flow in parallel beds.

4.9 Permeability Variations

Radial flow in parallal beds

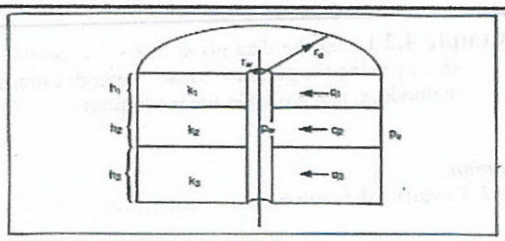

Figure 6–4 *Radial flow in parallel beds.*

Then:

$$q_1 + q_2 + q_3 = \frac{707.8\,(p_e^2 - p_w^2)}{\mu z\, T_f \ell n\, r_e/r_w}\left[k_1h_1 + k_2h_2 + k_3h_3\right] \qquad (6\text{–}9)$$

or:

$$\bar{k} = \frac{(k_1h_1 + k_2h_2 + k_3h_3)}{(h_1 + h_2 + h_3)} \qquad (6\text{–}10)$$

where the bar over the symbol indicates an average value. In a more-general form, the result is:

$$\bar{k} = \frac{\sum_1^n k_i h_i}{\sum_1^n h_i} \qquad (6\text{–}11)$$

We now consider a radial flow system of constant thickness with a permeability of k_e between the drainage radius r_e and some lesser radius r_a, and an *altered* permeability k_a between the radius r_a and the wellbore radius r_w as shown in Fig. 7.9. The pressure drops are additive, and

$$(p_e - p_w) = (p_e - p_a) + (p_a - p_w)$$

Then from Eq. (7.19)

$$\frac{q_2 \mu B \ln (r_e/r_w)}{0.00708\, k_{avg} h} = \frac{q \mu B \ln (r_e/r_a)}{0.00708\, k_e h} + \frac{q \mu B \ln (r_a/r_w)}{0.00708\, k_a h}$$

Cancelling and solving for k_{avg}

$$k_{avg} = \frac{k_a k_e \ln (r_e/r_w)}{k_a \ln (r_e/r_a) + k_e \ln (r_a/r_w)} \qquad (7.24)$$

Equation (7.24) may be extended to include three or more zones in series. The equation is important in studying the effect of a decrease or increase of permeability in the zone about the wellbore on the well productivity.

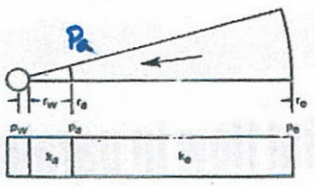

Fig. 7.9 Radial flow in beds in series

RADIAL FLOW OF GAS IN PARALLEL BEDS

If one considers radial flow in parallel beds as illustrated in Figure 4.11, the flow through each of the separate beds is as follows:

$$q_1 = \frac{0.703hk(p_e^2 - p_w^2)}{\overline{\mu z} T_f \ln(r_e / r_w)}$$

$$q_2 = \frac{0.703hk(p_e^2 - p_w^2)}{\overline{\mu z} T_f \ln(r_e / r_w)}$$

$$q_3 = \frac{0.703hk(p_e^2 - p_w^2)}{\overline{\mu z} T_f \ln(r_e / r_w)}$$

Then

$$Q_T = q_1 + q_2 + q_3 = \frac{0.703(p_e^2 - p_w^2)}{\overline{\mu z} T_f \ln(r_e / r_w)}\left[k_1h_1 + k_2h_2 + k_3h_3\right] \quad (4.35)$$

or

$$\overline{k} = \frac{k_1h_1 + k_2h_2 + k_3h_3}{(h_1 + h_2 + h_3)}$$

or

$$\overline{k} = \frac{\sum_1^n k_i h_i}{\sum_1^n h_i}$$

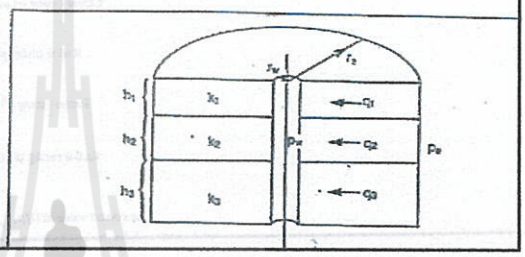

RADIAL FLOW OF GAS IN SERIES BEDS

If one considers radial flow in series beds as illustrated in Figure 4.12, the flow through each bed is as follows:

$$Q_1 = q_1 = \frac{0.703hk_1(p_e^2 - p_1^2)}{\overline{\mu}_2\overline{z}_2 T_f \ln(r_e / r_1)} = q_2 = \frac{0.703hk_2(p_1^2 - p_w^2)}{\overline{\mu}_1\overline{z}_1 T_f \ln(r_1 / r_w)}$$

$$= q = \frac{0.703hk(p_e^2 - p_w^2)}{\overline{\mu z} T_f \ln(r_e / r_w)}$$

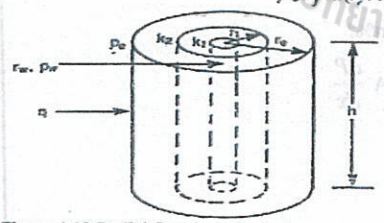

Figure 4.12 Radial flow in series beds

But

$$(p_e^2 - p_1^2) + (p_1^2 - p_w^2) = (p_e^2 - p_w^2) \quad (4.37)$$

Then

$$\frac{q\overline{\mu}_2\overline{z}_2 T_f \ln(r_e / r_1)}{0.703hk_2} + \frac{q\overline{\mu}_1\overline{z}_1 T_f \ln(r_1 / r_w)}{0.703hk_1} = \frac{q\overline{\mu}\,\overline{z}\, T_f \ln(r_e / r_w)}{0.703h\overline{k}}$$

and

$$\overline{k} = \frac{\overline{\mu}\,\overline{z}\,\ln(r_e / r_w)}{\frac{\overline{\mu}_2\overline{z}_2}{k_2}\ln(r_e / r_1) + \frac{\overline{\mu}_1\overline{z}_1}{k_1}\ln(r_1 / r_w)}$$

In more general form the result is:

$$\overline{k} = \frac{\overline{\mu}\,\overline{z}\,\ln(r_e / r_w)}{\sum_1^n \frac{\overline{\mu}_i\overline{z}_i}{k_i}\ln(r_i / r_{i-1})}$$

The steady-state flow equations—Darcy's equations accounting for specific geometries—are presented here.

Steady State Flow

For linear geometry: $$q_o = \frac{0.001127kA(p_1 - p_2)}{\mu L} \quad (6.1)$$

For radial geometry: $$q_o = \frac{0.00708kh(p_e - p_w)}{\mu \ln(r_e/r_w)} \quad (6.2)$$

For hemispherical geometry: $$q_o = \frac{0.00708k(p_e - p_w)}{\mu(1/r_1 - 1/r_2)} \quad (6.3)$$

5-spot waterflood: $$q_o = \frac{0.00354kh(p_{av} - p_{wf})}{\mu(\ln d/r_w - 0.619)} \quad (6.4)$$

7-spot waterflood: $$q_o = \frac{0.00472kh(p_{av} - p_{wf})}{\mu(\ln d/r_w - 0.569)} \quad (6.5)$$

For gas reservoirs:

Linear (using p): $$q_g = \frac{0.003164T_{sc}kA(2p/\mu z)_{avg}(p_1 - p_2)}{p_{sc}T_f L} \quad (6.6)$$

Linear (using p^2): $$q_g = \frac{0.003164T_{sc}kA(p_1^2 - p_2^2)}{p_{sc}(\mu z)_{avg}T_f L} \quad (6.7)$$

Linear (using $\psi(p)$): $$q_g = \frac{0.003164T_{sc}kA[\psi(p_1) - \psi(p_2)]}{p_{sc}T_f L} \quad (6.8)$$

Radial (using p): $$q_g = \frac{0.019881T_{sc}kh(2p/\mu z)_{avg}(p_e - p_w)}{p_{sc}T_f \ln(r_e/r_w)} \quad (6.9)$$

Radial (using p^2): $$q_g = \frac{0.019881T_{sc}kh(p_e^2 - p_w^2)}{p_{sc}(\mu z)_{avg}T_f \ln(r_e/r_w)} \quad (6.10)$$

Radial (using $\psi(p)$): $$q_g = \frac{0.019881T_{sc}kh[\psi(p_e) - \psi(p_w)]}{p_{sc}T_f \ln(r_e/r_w)} \quad (6.11)$$

The correct value of $(1/\mu z)_{avg}$ to use in the equations for gas is $\left(2\int_{p_w}^{p_e} p/\mu z\right)/(p_e^2 - p_w^2)$. It has

---

Reservoir Engineering I, 2012

HW NO 7 no.1, Due date: Thursday, August 16, 2012

Steady State Flow

Chapter 7; 7.2, 7.5, 7.7, 7.10, 7.16

7.2; (a) 343 psi, 686 psi (b) 0.156 ft/day
(c) 0.587 ft/day (d) 2555 days
(e) 0.229 psi/ft (f) What will be the effect%?
(g) $q=q_R(1+c(P_R-P)$, 2.23 BPD
(h) Derive $q=q_1(1+c(P_R-P) = -0.001127 \frac{k}{\mu} A \frac{dP}{dx}$
, ΔP=347 psi
(i) q = 102.26 bbl/day

7.5; (a) 3271 psia. (b) 2.01 psi/ft
(c) 2.27 psi/ft (d) 368 ft.

7.7; (a) 125 md. (b) 16:1:3
(c) Your ans. (d) 100 and 100 psi., 76 and 124 psi
(Hint; K must be in Darcies in eq. $P_1^2 - P_2^2 = 900L/K$)
(e) 29 md.

7.10; (a) 973 STB/D (b) 962 psia

7.16; $$q_{sc} = \frac{7.08kr_e r_w(P_e - P_w)}{\mu B_O(r_e - r_w)}$$

Hint: Surface area of semispherical flow = $2\pi r^2$)

5. DEVELOPMENT OF THE RADIAL DIFFERENTIAL EQUATION

The radial differential equation, which is the general differential equation used to model time-dependent flow systems, is now developed. Consider the volume element shown in Fig. 7.10. The element has a thickness Δr and is located r distance from the center of the well. Mass is allowed to flow into and out of the volume element during a period Δt. The volume element is in a reservoir of constant thickness and constant properties. Flow is allowed in only the radial direction. The following nomenclature, which is the same nomenclature defined previously, is used:

q = volume flow rate, STB/day for incompressible and slightly compressible fluids and SCF/day for compressible fluids

ρ = density of flowing fluid at reservoir conditions, lb/ft³

r = distance from wellbore, ft

h = formation thickness, ft

v = velocity of flowing fluid, bbl/day-ft²

t = hours

ϕ = porosity, fraction

k = permeability, md

μ = flowing fluid viscosity, cp

Unsteady State Flow

With these assumptions and definitions, a mass balance can be written around the volume element over the time interval Δt. In word form, the mass balance is written as:

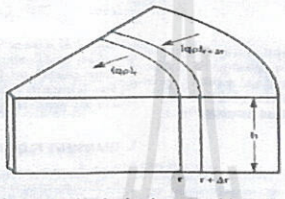

Fig. 7.10. Volume element used in the development of the radial differential equation.

The mass entering the volume element during Δt is given by:

Mass Entering

$$(qB\rho)_{r+\Delta r} = 2\pi(r+\Delta r)h(\rho v(5.615/24))_{r+\Delta r} \qquad (7.25)$$

The mass leaving the volume element during Δt is given by:

Mass Leaving

$$(qB\rho)_r = 2\pi rh(\rho v(5.615/24))_r \qquad (7.26)$$

The rate at which mass accumulates during the interval Δt is given by:

Mass Acc.

$$\frac{2\pi r\Delta rh[(\phi\rho)_{t+\Delta t}-(\phi\rho)_t]}{\Delta t} \qquad (7.27)$$

Combining Eqs. (7.25), (7.26), and (7.27), as suggested by the word "equation" written above,

MASS ENTER − MASS LEAVING = MASS ACC.

$$2\pi(r+\Delta r)h(\rho v(5.615/24))_{r+\Delta r} - 2\pi rh(\rho v(5.615/24))_r = \frac{2\pi r\Delta rh[(\phi\rho)_{t+\Delta t}-(\phi\rho)_t]}{\Delta t}$$

If both sides of this equation are divided by $2\pi r\Delta rh$ and the limit is taken in each term as Δr and Δt approach zero, the following is obtained:

$$\frac{\partial}{\partial r}(0.234\rho v) + \frac{1}{r}(0.234\rho v) = \frac{\partial}{\partial t}(\phi\rho)$$

or

$$\frac{0.234}{r}\frac{\partial}{\partial r}(r\rho v) = \frac{\partial}{\partial t}(\phi\rho) \qquad (7.28)$$

Equation (7.28) is the continuity equation and is valid for any flow system of

Mass entering volume element during interval Δt − Mass leaving volume element during interval Δt = Rate at which mass accumulates during interval Δt

The mass entering the volume element during Δt is given by:

$$(qB\rho)_{r+\Delta r} = 2\pi(r+\Delta)rh(\rho v(5.615/24))_{r+\Delta r} \tag{7.25}$$

The mass leaving the volume element during Δt is given by:

$$(qB\rho)_r = 2\pi rh(\rho v(5.615/24))_r \tag{7.26}$$

The rate at which mass accumulates during the interval Δt is given by:

$$\frac{2\pi r\Delta rh[(\phi\rho)_{t+\Delta t} - (\phi\rho)_t]}{\Delta t} \tag{7.27}$$

Combining Eqs. (7.25), (7.26), and (7.27), as suggested by the word "equation" written above,

$$2\pi(r+\Delta r)h(\rho v(5.615/24))_{r+\Delta r} - 2\pi rh(\rho v(5.615/24))_r = \frac{2\pi r\Delta rh[(\phi\rho)_{t+\Delta t} - (\phi\rho)_t]}{\Delta t}$$

If both sides of this equation are divided by $2\pi r\Delta rh$ and the limit is taken in each term as Δr and Δt approach zero, the following is obtained:

$$\frac{\partial}{\partial r}(0.234\rho v) + \frac{1}{r}(0.234\rho v) = \frac{\partial}{\partial t}(\phi\rho)$$

or

$$\frac{0.234}{r}\frac{\partial}{\partial r}(r\rho v) = \frac{\partial}{\partial t}(\phi\rho) \tag{7.28}$$

Equation (7.28) is the continuity equation and is valid for any flow system of radial geometry. To obtain the radial differential equation that will be the basis for time-dependent models, pressure must be introduced and ϕ eliminated from the partial derivative term on the right-hand side of Eq. (7.28). To do this, Darcy's equation must be introduced to relate the fluid flow rate to reservoir pressure:

$$v = -0.001127\frac{k}{\mu}\frac{\partial p}{\partial r}$$

Realizing that the minus sign can be dropped from Darcy's equation because

of the sign convention for fluid flow in porous media and substituting Darcy's equation into Eq. (7.28):

$$\frac{0.234}{r}\frac{\partial}{\partial r}\left(0.001127\frac{k}{\mu}\rho r\frac{\partial p}{\partial r}\right) = \frac{\partial}{\partial t}(\phi\rho) \tag{7.29}$$

The porosity from the partial derivative term on the right-hand side is eliminated by expanding the right-hand side by taking the indicated derivatives:

$$\frac{\partial}{\partial t}(\phi\rho) = \phi\frac{\partial\rho}{\partial t} + \rho\frac{\partial\phi}{\partial t} \tag{7.30}$$

It can be shown that porosity is related to the formation compressibility by the following:

$$c_f = \frac{1}{\phi}\frac{\partial\phi}{\partial p} \tag{7.31}$$

Applying the chain rule of differentiation to $\partial\phi/\partial t$,

$$\frac{\partial\phi}{\partial t} = \frac{\partial\phi}{\partial p}\frac{\partial p}{\partial t}$$

Substituting Eq. (7.31) into this equation,

$$\frac{\partial\phi}{\partial t} = \phi c_f\frac{\partial p}{\partial t}$$

Finally, substituting this equation into Eq. (7.30) and the result into Eq. (7.29),

$$\frac{0.234}{r}\frac{\partial}{\partial r}\left(0.001127\frac{k}{\mu}\rho r\frac{\partial p}{\partial r}\right) = \rho\phi c_f\frac{\partial p}{\partial t} + \phi\frac{\partial\rho}{\partial t} \tag{7.32}$$

Equation 7.32 is the general partial differential equation used to describe the flow of any fluid flowing in a radial direction in porous media. In addition to the initial assumptions, Darcy's equation has been added, which implies that the flow is laminar. Otherwise, the equation is not restricted to any type of fluid or any particular time region.

6. TRANSIENT FLOW SYSTEMS

By applying appropriate boundary and initial conditions, particular solutions to the differential equation derived in the preceding section can be discussed. The solutions obtained pertain to the transient and pseudosteady-state flow

reservoir pressure:

$$v = -0.001127\frac{k}{\mu}\frac{\partial p}{\partial r}$$

Realizing that the minus sign can be dropped from Darcy's equation because of the sign convention for fluid flow in porous media and substituting Darcy's equation into Eq. (7.28):

$$\frac{0.234}{r}\frac{\partial}{\partial r}\left(0.001127\frac{k}{\mu}\rho r\frac{\partial p}{\partial r}\right) = \frac{\partial}{\partial t}(\phi\rho) \tag{7.29}$$

The porosity from the partial derivative term on the right-hand side is eliminated by expanding the right-hand side by taking the indicated derivatives:

$$\frac{\partial}{\partial t}(\phi\rho) = \phi\frac{\partial\rho}{\partial t} + \rho\frac{\partial\phi}{\partial t} \tag{7.30}$$

It can be shown that porosity is related to the formation compressibility by the following:

$$c_f = \frac{1}{\phi}\frac{\partial\phi}{\partial p} \tag{7.31}$$

Applying the chain rule of differentiation to $\partial\phi/\partial t$,

$$\frac{\partial\phi}{\partial t} = \frac{\partial\phi}{\partial p}\frac{\partial p}{\partial t}$$

Substituting Eq. (7.31) into this equation,

$$\frac{\partial\phi}{\partial t} = \phi c_f\frac{\partial p}{\partial t}$$

Finally, substituting this equation into Eq. (7.30) and the result into Eq. (7.29),

$$\frac{0.234}{r}\frac{\partial}{\partial r}\left(0.001127\frac{k}{\mu}\rho r\frac{\partial p}{\partial r}\right) = \rho\phi c_f\frac{\partial p}{\partial t} + \phi\frac{\partial\rho}{\partial t} \tag{7.32}$$

6. TRANSIENT FLOW SYSTEM

6.1. Radial Flow of Slightly Compressible Fluids, Transient Flow

If Eq. (7.2) is expressed in terms of density, ρ, which is the inverse of specific volume, then the following is obtained:

$$\rho = \rho_R e^{c(p-p_R)} \tag{7.33}$$

where p_R is some reference pressure and ρ_R is the density at that reference pressure. Inherent in this equation is the assumption that the compressibility of the fluid is constant. This is nearly always a good assumption over the pressure range of a given application. Substituting Eq. (7.33) into Eq. (7.32),

$$\frac{0.234}{r}\frac{\partial}{\partial r}\left(0.001127\frac{k}{\mu}[\rho_R e^{c(p-p_R)}]r\frac{\partial p}{\partial r}\right) = [\rho_R e^{c(p-p_R)}]\phi c_f\frac{\partial p}{\partial t} + \phi\frac{\partial}{\partial t}[\rho_R e^{c(p-p_R)}]$$

To simplify this equation, one must make the assumption that k and μ are constant over the pressure, time, and distance ranges in our applications. This is rarely true about k. However, if k is assumed to be a volumetric average permeability over these ranges, then the assumption is good. In addition, it has been found that viscosities of liquids do not change significantly over typical pressure ranges of interest. Making this assumption allows k/μ to be brought outside the derivative. Taking the necessary derivatives and simplifying,

$$\frac{\partial^2 p}{\partial r^2} + \frac{1}{r}\frac{\partial p}{\partial r} + c\left[\frac{\partial p}{\partial r}\right]^2 = \frac{\phi\mu}{0.0002637k}(c_f + c)\frac{\partial p}{\partial t}$$

or

$$\frac{\partial^2 p}{\partial r^2} + \frac{1}{r}\frac{\partial p}{\partial r} + c\left[\frac{\partial p}{\partial r}\right]^2 = \frac{\phi\mu c_t}{0.0002637k}\frac{\partial p}{\partial t} \tag{7.34}$$

$$V = V_R e^{c(p_R - p)} \tag{7.2}$$

where

R = reference conditions.

Equation (7.2) may be derived by integrating Eq. (1.1), which defines compressibility between limits, assuming an average compressibility c, as

$$\int_{p_R}^{p} -c\,dp = \int_{V_R}^{V}\frac{dV}{V}$$

$$c(p_R - p) = \ln\left(\frac{V}{V_R}\right)$$

$$e^{c(p_R - p)} = \frac{V}{V_R}$$

$$V = V_R(e^{c(p_R - p)})$$

But e^x may be represented by a series expansion as

$$e^x = 1 + x + \frac{x^2}{2!} + \frac{x^3}{3!} + \cdots \frac{x^n}{n!}$$

Where x is small, the first two terms, $1 + x$, suffice, and where the exponent x is $c(p_R - p)$. the equation may be written as

$$V = V_R[1 + c(p_R - p)] \tag{7.3}$$

becomes negligible for the case of liquid flow, Eq. (7.34) reduces to:

$$\frac{\partial^2 p}{\partial r^2} + \frac{1}{r}\frac{\partial p}{\partial r} = \frac{\phi \mu c_t}{0.0002637k}\frac{\partial p}{\partial t} \qquad (7.35)$$

Continuity Eq.

equation is the diffusivity equation in radial form. The name comes from plication to the radial flow of the diffusion of heat. Basically, the flow of the flow of electricity, and the flow of fluids in permeable rocks can be ibed by the same mathematical forms. The group of terms $\phi\mu c_t/k$ was ously defined to be equal to $1/\eta$, where η is called the diffusivity constant Sect. 3). This same constant was encountered in Eq. (7.6) for the read- ient time.

To obtain a solution to Eq. (7.35), it is necessary first to specify one a two boundary conditions. The initial condition is simply that at time , the reservoir pressure is equal to the initial reservoir pressure, p_i. The boundary condition is given by Darcy's equation if it is required that there constant rate at the wellbore:

initial cond. $t = 0$, $P = P_i$

$$q = -0.001127\frac{kh}{B\mu}(2\pi r)\left(\frac{\partial p}{\partial r}\right)_{r=r_w}$$

First boundary Con. q = constant

second boundary condition is given by the fact that the desired solution transient period. For this period, the reservoir behaves as if it were nite in size. This suggests that at $r = \infty$, the reservoir pressure will remain al to the initial reservoir pressure, p_i. With these conditions, Matthews and sse the following solution:

Second boundary Con. $r = \infty$, $P = P_i$

$$p(r,t) = p_i - \frac{70.6q\mu B}{kh}\left[-E_i\left(-\frac{\phi\mu c_t r^2}{0.00105\,kt}\right)\right] \qquad (7.36)$$

ere all variables are consistent with units that have been defined previ- sly—that is, $p(r,t)$ and p_i are in psia, q is in STB/day, μ is in cp, B (formation lume factor) is in bbl/STB, k is in md, h is in ft, ϕ is in psi^{-1}, r is in ft, and is in hr.[6] Equation (7.36) is called the *line source solution* to the diffusivity uation and is used to predict the reservoir pressure as a function of time and sition. The mathematical function, E_i, is the exponential integral and is fined by:

$$E_i(-x) = -\int_x^\infty \frac{e^{-u}\,du}{u} = \left[\ln x - \frac{x}{1!} + \frac{x^2}{2(2!)} - \frac{x^3}{3(3!)} + \text{etc.}\right]$$

+ 0.57722

Theory

Ei = Exponential Integral Function Solution

x	$-E_i(-x)$	x	$-E_i(-x)$	x	$-E_i(-x)$
0.1	1.82292	4.3	0.00263	8.5	0.00002
0.2	1.22265	4.4	0.00234	8.6	0.00002
0.3	0.90568	4.5	0.00207	8.7	0.00002
0.4	0.70238	4.6	0.00184	8.8	0.00002
0.5	0.55977	4.7	0.00164	8.9	0.00001
0.6	0.45438	4.8	0.00145	9.0	0.00001
0.7	0.37377	4.9	0.00129	9.1	0.00001
0.8	0.31060	5.0	0.00115	9.2	0.00001
0.9	0.26018	5.1	0.00102	9.3	0.00001
1.0	0.21938	5.2	0.00091	9.4	0.00001
1.1	0.18599	5.3	0.00081	9.5	0.00001
1.2	0.15841	5.4	0.00072	9.6	0.00001
1.3	0.13545	5.5	0.00064	9.7	0.00001
1.4	0.11622	5.6	0.00057	9.8	0.00001
1.5	0.10002	5.7	0.00051	9.9	0.00000
1.6	0.08631	5.8	0.00045	10.0	0.00000
1.7	0.07465	5.9	0.00040		
1.8	0.06471	6.0	0.00036		
1.9	0.05620	6.1	0.00032		
2.0	0.04890	6.2	0.00029		
2.1	0.04261	6.3	0.00026		
2.2	0.03719	6.4	0.00023		
2.3	0.03250	6.5	0.00020		
2.4	0.02844	6.6	0.00018		
2.5	0.02491	6.7	0.00016		
2.6	0.02185	6.8	0.00014		
2.7	0.01918	6.9	0.00013		
2.8	0.01686	7.0	0.00012		
2.9	0.01482	7.1	0.00010		
3.0	0.01305	7.2	0.00009		
3.1	0.01149	7.3	0.00008		
3.2	0.01013	7.4	0.00007		
3.3	0.00894	7.5	0.00007		
3.4	0.00789	7.6	0.00006		
3.5	0.00697	7.7	0.00005		
3.6	0.00616	7.8	0.00005		
3.7	0.00545	7.9	0.00005		
3.8	0.00482	8.0	0.00004		
3.9	0.00427	8.1	0.00003		
4.0	0.00378	8.2	0.00003		
4.1	0.00335	8.3	0.00003		
4.2	0.00297	8.4	0.00002		

Ei

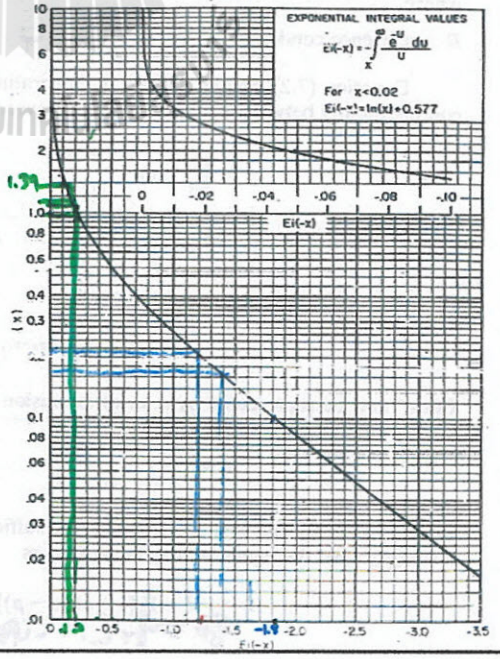

Values of $-E_i(-x)$ as a function of x

x	$-E_i(-x)$	x	$-E_i(-x)$	x	$-E_i(-x)$
0.1	1.82292	4.3	0.00263	8.5	0.00002
0.2	1.22265	4.4	0.00234	8.6	0.00002
0.3	0.90568	4.5	0.00207	8.7	0.00002
0.4	0.70238	4.6	0.00184	8.8	0.00002
0.5	0.55977	4.7	0.00164	8.9	0.00001
0.6	0.45438	4.8	0.00145	9.0	0.00001
0.7	0.37377	4.9	0.00129	9.1	0.00001
0.8	0.31060	5.0	0.00115	9.2	0.00001
0.9	0.26018	5.1	0.00102	9.3	0.00001
1.0	0.21938	5.2	0.00091	9.4	0.00001
1.1	0.18599	5.3	0.00081	9.5	0.00001
1.2	0.15841	5.4	0.00072	9.6	0.00001
1.3	0.13545	5.5	0.00064	9.7	0.00001
1.4	0.11622	5.6	0.00057	9.8	0.00001
1.5	0.10002	5.7	0.00051	9.9	0.00000
1.6	0.08631	5.8	0.00045	10.0	0.00000
1.7	0.07465	5.9	0.00040		
1.8	0.06471	6.0	0.00036		
1.9	0.05620	6.1	0.00032		
2.0	0.04890	6.2	0.00029		
2.1	0.04261	6.3	0.00026		
2.2	0.03719	6.4	0.00023		
2.3	0.03250	6.5	0.00020		
2.4	0.02844	6.6	0.00018		
2.5	0.02491	6.7	0.00016		
2.6	0.02185	6.8	0.00014		
2.7	0.01918	6.9	0.00013		
2.8	0.01686	7.0	0.00012		
2.9	0.01482	7.1	0.00010		
3.0	0.01305	7.2	0.00009		
3.1	0.01149	7.3	0.00008		
3.2	0.01013	7.4	0.00007		
3.3	0.00894	7.5	0.00007		
3.4	0.00789	7.6	0.00006		
3.5	0.00697	7.7	0.00005		
3.6	0.00616	7.8	0.00005		
3.7	0.00545	7.9	0.00004		
3.8	0.00482	8.0	0.00004		
3.9	0.00427	8.1	0.00003		
4.0	0.00378	8.2	0.00003		
4.1	0.00335	8.3	0.00003		
4.2	0.00297	8.4	0.00002		

5 Radial Flow Through Porous Media: Slightly Compressible Fluids

5.1 Introduction

The flow pattern in the strata in the vicinity of a well producing oil or gas can be considered as essentially horizontal radial (if we limit the discussion initially to near vertical wells and non-dipping formations). An understanding of horizontal radial flow is therefore important if we are to explain or predict the productive performance of a well.

The behaviour of *slightly* compressible fluids (undersaturated oil, water), whose properties are little affected by changes in pressure; and *highly* compressible fluids (dry and wet gas, condensates), which are very sensitive to the pressure, will be treated separately.

In this chapter, we will examine the bottom-hole pressure behaviour observed during the flow of the fluid through the formation towards the well, or vice versa, (production or injection tests); and during the period following the shutting in of the well – i.e. the termination of flow (buildup or fall off tests).

5.2 Equation for Single Phase Radial Flow

The basic assumptions made in the theory of single phase horizontal radial flow are:

- the porous medium is homogeneous in ϕ and k, and is horizontal and of uniform thickness; the permeability is isotropic ($k_r = k_\theta$),
- there are no saturation gradients: in the case of the flow of oil, its saturation is constant and equal to $(1 - S_{wi})$ everywhere, the water phase being immobile; in the case of the flow of water, its saturation is everywhere $\geq (1 - S_{or})$, and the oil phase (if present) is immobile,
- the pressure throughout the reservoir is above the bubble point of the fluid,
- the fluid properties are uniform over the thickness of the reservoir, so that gravitational effects can be ignored,
- the well has been perforated over the entire reservoir thickness, so that inflow is horizontal radial.

Consider the segment of a cylindrical reservoir shown in Fig. 5.1. An incremental volume (shaded) is defined by an arc at a distance r from the axis of the well, and is of thickness dr, with fluid flowing across it as indicated. Applying the principle of the conservation of mass to this volume:

(mass flow rate in) – (mass flow rate out) = (rate of change of mass in the incremental volume).

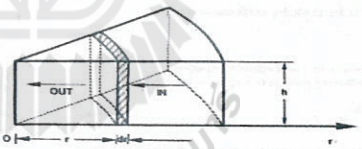

Fig. 5.1. *Diagram showing the conservation of mass in radial flow*

Therefore,

$$(q\rho)_{r+dr} - (q\rho)_r = 2\pi rh\,dr\frac{\partial}{\partial t}(\phi\rho)\,, \tag{5.1}$$

where $(2\pi rh\,dr)$ is the volume of the increment, ρ is the density of the mobile fluid, ϕ is the porosity. As was explained in Sect. 3.4.3, ϕ is pressure-dependent, given that the geostatic stress $\bar{\sigma}$ remains constant.

Recalling that:

$$(q\rho)_{r+dr} = (q\rho)_r + \frac{\partial(q\rho)}{\partial r}dr\,.$$

equation (5.1) becomes:

$$\frac{\partial(q\rho)}{\partial r} = 2\pi rh\frac{\partial(\phi\rho)}{\partial t}\,. \tag{5.2}$$

For a cross-sectional area to flow of $2\pi rh$, and a pressure gradient of $\partial p/\partial r$, Darcy's law can be written as:

$$q = \frac{2\pi rhk}{\mu}\frac{\partial p}{\partial r}\,. \tag{5.3}$$

Furthermore, we have:

$$\frac{\partial}{\partial t}(\phi\rho) = \frac{\mathrm{d}(\phi\rho)}{\mathrm{d}p}\frac{\partial p}{\partial t} \tag{5.4a}$$

with:

$$\frac{\mathrm{d}(\phi\rho)}{\mathrm{d}p} = \phi\frac{\mathrm{d}\rho}{\mathrm{d}p} + \rho\frac{\mathrm{d}\phi}{\mathrm{d}p} = \rho\phi\left[\frac{1}{\rho}\frac{\mathrm{d}\rho}{\mathrm{d}p} + \frac{1}{\phi}\frac{\mathrm{d}\phi}{\mathrm{d}p}\right]. \tag{5.4b}$$

If we define the compressibility of the pore fluid as:

$$c = \frac{1}{\rho}\frac{\mathrm{d}\rho}{\mathrm{d}p}\,, \tag{5.4c}$$

we have, by substituting from Eq. (3.8c):

$$\frac{\mathrm{d}(\rho\phi)}{\mathrm{d}p} = \rho\phi(c + c_f) = c_t\rho\phi\,. \tag{5.5a}$$

Here, c_t represents the *total system compressibility* (rock + pore fluid). If the pores contain only water ($S_w = 1$), $c = c_w$, and we have:

$$c_t = c_w + c_f \quad (S_w = 1)\,. \tag{5.5b}$$

If, on the other hand, there is oil in the presence of irreducible (and non-mobile) water, we can write the following reasonable approximation:

$$c = c_o S_o + c_w S_{iw} = c_o + (c_w - c_o)S_{iw}\,.$$

From these two cases we can derive a more general form for c_t:

$$c_t = c_o S_o + c_w S_w + c_f\,. \tag{5.5c}$$

From Eqs. (5.2), (5.3), (5.4a) and (5.5a) it follows that:

$$\frac{\partial}{\partial r}\left(\rho\frac{2\pi rhk}{\mu}\frac{\partial p}{\partial r}\right) = 2\pi rh\rho\phi c_t\frac{\partial p}{\partial t}\,,$$

which simplifies to:

$$\frac{1}{r}\frac{\partial}{\partial r}\left(\frac{k}{\mu}\rho r\frac{\partial p}{\partial r}\right) = \rho\phi c_t\frac{\partial p}{\partial t}\,, \tag{5.6}$$

where ρ and μ are the density and viscosity of the mobile single phase fluid.

Equation (5.6) describes the pressure at any time and at any point in the porous medium for a single phase fluid in horizontal radial flow. It is called the *general diffusivity equation.*

This is a *non-linear* partial differential equation – non-linear because ϕ, k, c_t, ρ and μ are all pressure-dependent. As a consequence, no analytical solution is possible without "linearising" the diffusivity equation so as to remove the pressure dependence of the parameters.

5.3 Linearisation of the Diffusivity Equation for Horizontal Radial Flow – Case Where the Rock-Fluid Diffusivity is Independent of the Pressure

Equation (5.6) can be expanded as:

$$\frac{1}{r}\left[\rho r\frac{\mathrm{d}}{\mathrm{d}p}\left(\frac{k}{\mu}\right)\left(\frac{\partial p}{\partial r}\right)^2 + \frac{k}{\mu}r\frac{\mathrm{d}\rho}{\mathrm{d}p}\left(\frac{\partial p}{\partial r}\right)^2 + \frac{k}{\mu}\rho r\frac{\partial^2 p}{\partial r^2}\right] = \rho\phi c_t\frac{\partial p}{\partial t}\,. \tag{5.7}$$

Since $\partial p/\partial r$ is small,* we can assume its square term to be negligible:

$$\left(\frac{\partial p}{\partial r}\right)^2 \ll \frac{\partial p}{\partial r}, \frac{\partial^2 p}{\partial r^2}\,. \tag{5.8}$$

Equation (5.7) then reduces to:

$$\frac{k}{\mu}\left[\frac{\partial^2 p}{\partial r^2} + \frac{1}{r}\frac{\partial p}{\partial r}\right] = \phi c_t\frac{\partial p}{\partial t}\,. \tag{5.9}$$

* This assumption is not necessarily valid close to the wellbore, where neglecting the term $\partial p/\partial r^2$ may cause errors in the local estimate of $p(r,t)$.

Rearranging:

$$\frac{1}{r}\frac{\partial}{\partial r}\left(r\frac{\partial p}{\partial r}\right) = \frac{\phi\mu c_t}{k}\frac{\partial p}{\partial t}\,, \tag{5.10}$$

where:

$$\frac{k}{\phi\mu c_t} = \eta = \text{hydraulic diffusivity} \tag{5.11}$$

is assumed to be constant for small changes of pressure, since k, ϕ and μ increase with pressure, while c_t decreases. The dimensions of η are $[L^2t^{-1}]$.

Equation (5.10) has now been linearised (provided the hydraulic diffusivity can be considered constant), and is referred to in this form as the *radial diffusivity equation.*

This can now be solved analytically. One approach is to take advantage of the similarity between it and the thermal diffusivity equation:

$$\frac{1}{r}\frac{\partial}{\partial r}\left(r\frac{\partial T}{\partial r}\right) = \frac{1}{K}\frac{\partial T}{\partial t}\,, \tag{5.12}$$

where K = thermal diffusivity (m^2/s),
T = temperature (K).

Solutions to Eq. (5.12) for a wide variety of initial and boundary conditions have been published in the definitive work by Carslaw and Jäger, *Conduction of Heat in Solids.*[2]

Dranchuk and Quon[7] have shown that the linearisation process just described is only valid when:

$$c_t p \ll 1\,. \tag{5.13}$$

5.4 Dimensionless Form of the Radial Diffusivity Equation

The usefulness of a dimensionless version of the radial diffusivity equation will become apparent in Chaps. 6 and 7.

In fact, any dimensionless analytical solution for a particular set of initial and boundary conditions can be converted immediately into practical units to suit the real case in question.

The dimensionless variables are defined as follows:

Dimensionless radius: $$r_D = \frac{r}{r_w}\,. \tag{5.14a}$$

Dimensionless time: $$t_D = \frac{k}{\phi\mu c_t r_w^2}t = \frac{\eta}{r_w^2}t\,. \tag{5.14b}$$

Dimensionless pressure: $$p_D(r_D, t_D) = \frac{2\pi kh}{q\mu}(p_i - p_{r,t})\,. \tag{5.14c}$$

where p_i is the initial static reservoir pressure; $p_{r,t}$ is the pressure at time t and radius r; q is the flow rate *at reservoir conditions*; and r_w is the wellbore radius.

Using the terms defined in Eq. (5.14), Eq. (5.10) can be rewritten:

$$\frac{1}{r_D}\frac{\partial}{\partial r_D}\left(r_D\frac{\partial p_D}{\partial r_D}\right) = \frac{\partial p_D}{\partial t_D}\,, \tag{5.15}$$

which is the *dimensionless form of the radial diffusivity equation.*

If p_{wf} is the bottom hole flowing pressure ($r = r_w$, $r_D = 1$), we have:

$$p_D(1, t_D) = p_{D,w}(t_D) = \frac{2\pi kh}{q\mu}(p_i - p_{wf}) \tag{5.16a}$$

and, in the absence of any additional pressure drop due to skin effect (to be covered later):

$$p_{wf} = p_i - \frac{q\mu}{2\pi kh}p_{D,w}(t_D)\,. \tag{5.16b}$$

This equation shows clearly the importance of having available $p_D(t_D)$ solutions for the flow of undersaturated oil towards the wellbore, with various initial and boundary conditions.

5.5 Behaviour with Time Under Flowing Conditions

Equations such as (5.10) or (5.15) are always associated with a set of initial and boundary conditions.

We will first consider qualitatively the idealised case of a cylindrical reservoir of uniform thickness h, with a sealing ("no-flow") external boundary of radius r_e. It is initially in a static condition, with a uniform pressure $p = p_i$ throughout.

There is a well of radius r_w at its centre. From time $t = 0$, oil is flowed from the well at a constant rate q (at reservoir conditions).

The assumptions listed in Sect. 5.2 regarding the nature of the well and reservoir are applied here.

The conclusions we shall draw about this single well will also be valid for the case where there are *other* wells present in the reservoir, provided their production rates – which may be different – do not change with time. In this situation, there is an area around each well within which the fluid movement is towards that well. This is referred to as the *drainage area*, A. Its shape and size depend on a number of factors, and the radius of the *equivalent circular area* is the *drainage radius* r_e of the well.

If the production rates from any of the wells change with time, their drainage areas (and consequently those of neighbouring wells) will expand or contract, and the pressure behaviour will differ from that predicted for a constant rate case.

We will use the dimensionless form of the radial diffusivity equation for convenience.

Consider a circular drainage area, with production starting at time $t_D = 0$, and continuing until:

$$t_{D,w} \cong 0.06\left(\frac{r_e}{r_w}\right)^2\,. \tag{5.17a}$$

From the definition of t_D, this corresponds to a real time of:

$$t_w \cong 0.06\frac{\phi\mu c_t}{k}r_e^2\,. \tag{5.17b}$$

Up to this time, the pressure disturbance invoked by flowing the well is contained within the drainage area of radius r_e (Fig. 5.2).

During this period, since $p_D(r_D, t_D)$ has not yet been affected by the non-permeable outer boundary at $r = r_e$, the reservoir is effectively infinite in size as far as the pressure is concerned. This is referred to as *infinite acting.*

For t_D between zero and $t_{D,w}$, the flow regime is said to be *transient* or *infinite acting.*

Still in the same circular geometry, let us now look at the period:

$$0.06\left(\frac{r_e}{r_w}\right)^2 \leq t_D \leq 0.1\left(\frac{r_e}{r_w}\right)^2\,. \tag{5.17c}$$

This is a transition period between early transient and the next mode, and the flow regime is referred to as *late transient.*

Note that the t_D period during which late transient flow occurs is different – in both start time and duration – for different drainage area geometries; Fig. 5.7 lists the relevant values for non-circular shapes.

In a circular geometry, when $t_D > 0.1\,(r_e/r_w)^2$, the pressure decreases at a constant rate at all points in the drainage area:

$$\frac{\partial p_D}{\partial t_D} = \text{constant for any } r_D \text{ or } t_D\,. \tag{5.18a}$$

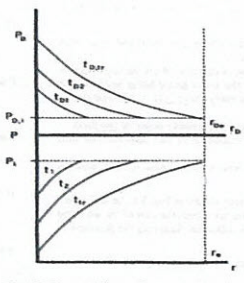

Fig. 5.2. *Outward diffusion of a pressure disturbance around a well: early transient period*

At the outer boundary of the drainage area (no-flow condition) for any r_D we have:

$$\left(\frac{\partial p_D}{\partial r_D}\right)_{r_{eD}} = 0 \,. \tag{5.18b}$$

In other words, the pressure profile $p_D(r_D)$ keeps the same *shape*, and the whole profile declines at a steady rate with increasing time. Figure 5.3 shows a series of these parallel profiles corresponding to different times, in both real and dimensionless terms. The flow regime is now *pseudo-steady state* (also called *semi-steady state*).

In order for mass to be conserved at any radius r:

$$\frac{dp}{dt} = -\frac{q}{\pi r_e^2 h \phi c_t} \,, \tag{5.19a}$$

which, in dimensionless form is:

$$\frac{dp_D}{dt_D} = 2\left(\frac{r_e}{r_w}\right)^2 \,. \tag{5.19b}$$

Equation (5.19) allows us to calculate the pressure distribution $p(r)$ in the reservoir for any value of $t > t_{ss}$, provided we have one pressure profile, also measured at a $t > t_{ss}$, to start from.

The variation of the bottom hole flowing pressure p_{wf} during these three flow regime periods is shown schematically in Fig. 5.4.

Pseudo-steady state flow occurs when we have a "no-flow" (i.e. non-permeable, or closed) outer boundary condition. An alternative condition is the "constant pressure boundary" (i.e. fluid is replenished across the boundary, so that the pressure p_e remains constant). In this case the flow regime goes to *steady state* after the late transient period.

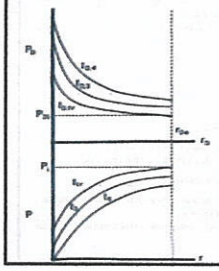

Fig. 5.3. *Pseudo-steady state pressure behaviour in the drainage area of a producing well with a no-flow boundary at $r = r_e$*

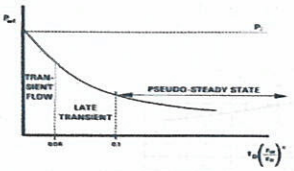

Fig. 5.4. *Bottom hole flowing pressure p_{wf} versus time*

From Darcy's equation:

$$q = \frac{2\pi r h k}{\mu}\frac{dp}{dr} \,, \tag{5.20a}$$

where $2\pi rh$ is the cross-sectional area to flow.

Integrating Eq. (5.20a) from r_w to r:

$$p - p_w = \frac{q\mu}{2\pi hk}\ln\frac{r}{r_w} \,, \tag{5.20b}$$

which is, in dimensionless form, for any value of t:

$$p_D(1) - p_D(r_D) = \ln r_D \,, \tag{5.20c}$$

where $r_D = 1$ is by definition [Eq. (5.14a)] the dimensionless wellbore radius.

5.6 Solutions to the Radial Diffusivity Equation for a Fluid of Constant Compressibility

5.6.1 Transient Flow

5.6.1.1 Treatment for an Ideal Well

Earlier in this chapter it was shown that during a certain initial period when the well is put on production ($t \leq t_{ss}$), the reservoir is *infinite acting* and the flow regime is *transient*.

The initial conditions are:

$$p = p_i \quad \text{at } t = 0 \text{ for all } r \tag{5.21a}$$

The boundary conditions are:

$$p = p_i \quad \text{at } r = \infty \text{ for all } t \tag{5.21b}$$

$$q = \frac{2\pi khr_w}{\mu}\left(\frac{\partial p}{\partial r}\right)_{r_w} = \text{constant for all } t \,. \tag{5.21c}$$

If we assume that r_w is negligibly small, Eq. (5.21c) simplifies to:

$$\lim_{r\to 0}\left(r\frac{\partial p}{\partial r}\right) = \frac{q\mu}{2\pi kh} = \text{constant} \,. \tag{5.21d}$$

The solution to the radial diffusivity equation under these conditions is referred to as the *line source solution for constant terminal rate*.

Using the Boltzmann transform

$$s = \frac{r^2}{4(k/\phi\mu c_t)t} = \frac{\phi\mu c_t r^2}{4kt} \tag{5.22a}$$

so that

$$\frac{\partial s}{\partial r} = \frac{\phi\mu c_t r}{2kt} \tag{5.22b}$$

and:

$$\frac{\partial s}{\partial t} = -\frac{\phi\mu c_t r^2}{4kt^2} \,, \tag{5.22c}$$

the radial diffusivity equation:

$$\frac{1}{r}\frac{\partial}{\partial r}\left(r\frac{\partial p}{\partial r}\right) = \frac{\phi\mu c_t}{k}\frac{\partial p}{\partial t} \tag{5.10}$$

becomes, through transforming the independent variables (r, t) to the independent variable s:

$$\frac{1}{r}\frac{d}{ds}\left(r\frac{dp}{ds}\frac{\partial s}{\partial r}\right)\frac{\partial s}{\partial r} = \frac{\phi\mu c_t}{k}\frac{dp}{ds}\frac{\partial s}{\partial t} \,, \tag{5.23a}$$

where $p = p(r, t)$ is now only a function of $s = s(r, t)$.

Substituting from Eqs. (5.22b) and (5.22c), Eq. (5.23a) becomes:

$$\frac{1}{r}\frac{\phi\mu c_t r}{2kt}\frac{d}{ds}\left(\frac{\phi\mu c_t r^2}{2kt}\frac{dp}{ds}\right) = -\frac{\phi\mu c_t}{k}\frac{\phi\mu c_t r^2}{4kt^2}\frac{dp}{ds} \tag{5.23b}$$

which, substituting from Equation (5.22a)

$$\frac{d}{ds}\left(s\frac{dp}{ds}\right) = -s\frac{dp}{ds} \tag{5.23c}$$

or:

$$\frac{dp}{ds} + s\frac{d}{ds}\left(\frac{dp}{ds}\right) = -s\frac{dp}{ds} \,. \tag{5.23d}$$

Equation (5.10), which is a partial differential equation in r and t, has been converted by means of Boltzmann's transform to an ordinary differential equation which is easy to solve. If we write:

$$\frac{dp}{ds} = p' \,. \tag{5.24a}$$

equation (5.23d) is now:

$$p' + s\frac{dp'}{ds} = -sp' \tag{5.24b}$$

or:

$$\frac{dp'}{p'} = -ds - \frac{ds}{s} \,, \tag{5.24c}$$

which, when integrated, results in the general equation:

$$\ln p' = -s - \ln s + C_1 \tag{5.25a}$$

so that:

$$p' = C_2\frac{e^{-s}}{s} \,, \tag{5.25b}$$

where $C_2 = e^{C_1}$.

For the calculation of C_2, we need to refer to the boundary conditions at the well. We already have that:

$$r\frac{\partial p}{\partial r} = r\frac{dp}{ds}\frac{\partial s}{\partial r} = r\frac{2\phi\mu c_t r}{4kt}\frac{dp}{ds} = 2s\frac{dp}{ds} = 2sC_2\frac{e^{-s}}{s} = 2C_2e^{-s} \tag{5.26}$$

and, from Eq. (5.21d):

$$\lim_{s\to 0}(2C_2e^{-s}) = 2C_2 = \frac{q\mu}{2\pi kh} \,, \tag{5.27}$$

since when $r \to 0$, $s \to 0$ as well.

Substituting from Eq. (5.25b) into Eq. (5.27) we now have:

$$p' = \frac{q\mu}{4\pi kh}\frac{e^{-s}}{s} \,. \tag{5.28}$$

Equation (5.28) is integrated, at radius r, between the pressures $p_i(t = 0)$ and $p(r, t)$ at time t. The corresponding values of s are [Eq. (5.22a)]:

$$s(t = 0) = \infty$$

and

$$s(r, t) = \frac{\phi\mu c_t r^2}{4kt} = x \,.$$

Therefore:

$$\int_{p_i}^{p(r,t)} dp = \frac{q\mu}{4\pi kh}\int_x^s \frac{e^{-s}}{s}ds \tag{5.29}$$

from which:

$$\frac{4\pi kh}{q\mu}[p_i - p(r, t)] = \int_s^x \frac{e^{-s}}{s}ds \,. \tag{5.30}$$

The integral in the right hand term of Eq. (5.30) is the well-known *exponential integral* $ei(x)$, whose behaviour is shown in Fig. 5.5.

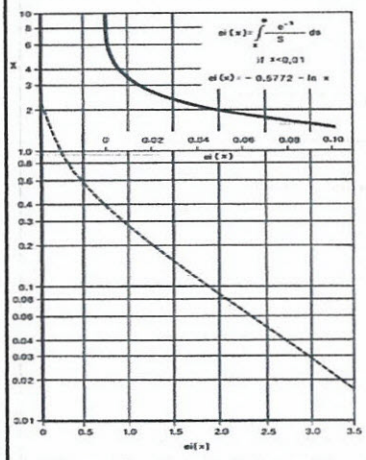

Fig. 5.5. *The exponential integral function ei(x), for the range x = 0.01 to x = 10*

$ei(x)$ can be developed as a series:

$$ei(x) = -0.57721 - \ln x - \sum_{n=1}^{\infty} \frac{(-1)^n x^n}{n\,n!} . \tag{5.31a}$$

For $x < 0.01$, ignoring the summation introduces only a very small error,[11] and the equation reduces to:

$$ei(x) = -0.57721 - \ln x \quad (x < 0.01) , \tag{5.31b}$$

where the 0.57721 is *Euler's constant*, and

$$e^{0.57721} = 1.781 = \gamma .$$

We can express Eq. (5.31b) alternatively as:

$$ei(x) = -\ln(\gamma x) \quad \text{for } x < 0.01 . \tag{5.31c}$$

Substituting this into Eq. (5.30) we obtain:

$$p_i - p(r,t) = -\frac{q\mu}{4\pi kh} \ln \frac{\gamma\phi\mu c_t r^2}{4kt} = \frac{q\mu}{4\pi kh} \ln \frac{4kt}{\gamma\phi\mu c_t r^2} . \tag{5.32a}$$

In dimensionless terms, this is:

$$p_D = \frac{1}{2}\ln\left[\frac{4}{\gamma}\left(\frac{r_w}{r}\right)^2 t_D\right] = \frac{1}{2}(\ln t_D - 2\ln r_D + 0.809) , \tag{5.32b}$$

where:

$$\ln\frac{4}{\gamma} = \ln 2.246 = 0.809 . \tag{5.32c}$$

At the well, where $r_D = 1$ ($r = r_w$), the relationship between pressure and time is given by:

$$p_D(1, t_D) = 0.5(\ln t_D + 0.809) , \tag{5.33a}$$

which, in real terms, is:

$$p_{wf} = p_i - \frac{q\mu}{4\pi kh}\left(\ln\frac{kt}{\phi\mu c_t r_w^2} + 0.809\right) . \tag{5.33b}$$

It is important to realise that Eqs. (5.33a) and (5.33b) are based on an approximation [Eq. (5.31b)] which is only valid when x (or its equivalent in the terms of the equations) < 0.01, i.e.:

$$\frac{\phi\mu c_t r_w^2}{4kt} < 0.01 \tag{5.34a}$$

otherwise stated as:

$$\frac{kt}{\phi\mu c_t r_w^2} > 25 . \tag{5.34b}$$

For values of t less than that required to satisfy Eq. (5.34), the solution containing the full exponential integral should be used.

In most cases, Eq. (5.34) is usually satisfied after a few minutes, or even seconds, after a well starts flowing.

5.6.1.2 *Treatment for a Real Well – Skin Effect*

Among the initial assumptions upon which we have based the derivation of the above equations, two are of particular importance:

- the porous medium is homogeneous and isotropic in permeability,
- the well is open to production over the entire thickness of the reservoir.

These conditions are not met in the following situations:

- damage to the near-wellbore formation by mud filtrate invasion, causing a reduction in permeability from k to k_s out to a distance r_s,
- well only drilled through a portion of the reservoir thickness ("partial penetration"),

- well completed with casing and cement, but only perforated over a portion of the reservoir interval,
- the reservoir interval consists of a number of layers of different permeabilities; this situation is further complicated if the well is only perforated in one or some of the layers,
- presence of fractures which intersect the well, resulting in a local increase in permeability.

Each of these factors will modify the flow pattern around the wellbore, so that Eq. (5.33) will not be a true representation of the situation (Fig. 5.6). Their influence is accounted for by introducing a quantity S, the *skin factor*, into the equation:

$$p_D(1, t_D) = 0.5(\ln t_D + 0.809) + S \tag{5.35}$$

from which we derive the following classical equations:

$$p_D(1, t_D) = 0.5(\ln t_D + 0.809 + 2S) , \tag{5.36a}$$

$$p_{wf} = p_i - \frac{q\mu}{4\pi kh}\left(\ln\frac{kt}{\phi\mu c_t r_w^2} + 0.809 + 2S\right) . \tag{5.36b}$$

S is a dimensionless parameter, and therefore *just a number*. Depending on conditions, the additional pressure drop Δp_s caused by the skin:

$$\Delta p_s = \frac{q\mu}{2\pi kh} S \tag{5.37}$$

may be *positive* [$(p_i - p_{wf})$ in the real well is *greater* than $(p_i - p_{wf})$ in the ideal well], or *negative* [$(p_i - p_{wf})$ in the real well is *less* than $(p_i - p_{wf})$ in the ideal well].

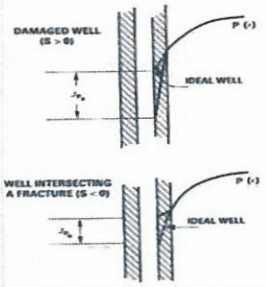

Fig. 5.6. *The pressure profile close to the wellbore in the case of formation damage (S > 0), and in the case of improved productivity due to fracturing (S < 0)*

Δp_s is positive in the case of blockage by mud filtrate,[10] partial penetration of the reservoir interval,[1,9] and partial perforation of the casing.[8]

In the case of filtrate damage, we have:

$$\Delta p_s = \frac{q\mu}{2\pi kh}\frac{k - k_s}{k_s}\ln\frac{r_s}{r_w} , \tag{5.38a}$$

which means that:

$$S = \frac{k - k_s}{k_s}\ln\frac{r_s}{r_w} \tag{5.38b}$$

This damage can be reduced by means of surfactant treatment, which facilitates the removal of the filtrate.

In a reservoir section consisting of zones of differing permeabilities, only some of which have been perforated, Δp_s may be positive or negative[3] depending on whether the zones open to flow have an average permeability which is lower or higher than the average of the entire interval.

Δp_s is always negative where the well is intercepted by fractures.[4]

Where the well has been drilled through an oil-bearing formation and an underlying aquifer, the section will obviously be only partially perforated, so as to avoid producing water. We might therefore expect the skin to be positive ($\Delta p_s > 0$).

However, we have two fluids present: oil (which flows towards the well), and water (which, although it does not flow, still transmits the pressure disturbance).

If the oil has a higher viscosity than the water, Chierici[5] has shown that it is possible to find a negative skin factor (Δp_s).

We shall return to the skin factor, and its estimation from well tests, in Chap. 6.

5.6.2 Pseudo-Steady State Flow

Once the pressure disturbance has reached the outer limits of the drainage area of the well, and after a relatively short "late transient" period which follows this, the flow regime enters pseudo-steady state, during which for q = constant, dp/dt is constant at all points in the drainage area (see Sect. 5.5).

To satisfy the conservation of mass:

(mass of fluid leaving the well per unit time) = (change per unit time of mass of fluid in the drainage area of the well)

we have the following relationship, which also allows for the rock compressibility:

$$q\rho = -\pi r_e^2 h \frac{\partial}{\partial t}(\rho\phi) = -\pi r_e^2 h \frac{d(\rho\phi)}{dp}\frac{\partial p}{\partial t} = -\pi r_e^2 h\phi\rho c_t \frac{\partial p}{\partial t} . \tag{5.39a}$$

from which it follows that:

$$\frac{\partial p}{\partial t} = -\frac{q}{\pi r_e^2 h\phi c_t} , \tag{5.39b}$$

From Eqs. (5.10) and (5.39b) we have:

$$\frac{1}{r}\frac{\partial}{\partial r}\left(r\frac{\partial p}{\partial r}\right) = -\frac{q\mu}{2\pi r_e^2 hk} \tag{5.40}$$

and, after first integrating with respect to r:

$$r\frac{\partial p}{\partial r} = -\frac{q\mu}{2\pi kh}\left(\frac{r}{r_c}\right)^2 + C_1 . \tag{5.41}$$

At $r = r_c$, $(\partial p/\partial r)_{r_c} = 0$, so that:

$$C_1 = \frac{q\mu}{2\pi kh} . \tag{5.42}$$

We therefore have:

$$\frac{\partial p}{\partial r} = \frac{q\mu}{2\pi kh}\left(\frac{1}{r} - \frac{r}{r_c^2}\right) . \tag{5.43}$$

which when integrated between r_w and r (equivalent to integration between p_{wf} and p) gives:

$$p - p_{wf} = \frac{q\mu}{2\pi kh}\left(\ln\frac{r}{r_w} - \frac{r^2 - r_w^2}{2r_c^2}\right) . \tag{5.44a}$$

The term $(r_w/r_c)^2$ is negligibly small, so that we can write, after introducing the skin factor S (see Sect. 5.6.1.2):

$$p_e - p_{wf} = \frac{q\mu}{2\pi kh}\left(\ln\frac{r_e}{r_w} - \frac{1}{2} + S\right) . \tag{5.44b}$$

This equation would enable us to calculate the bottom hole flowing pressure p_{wf} in a producing well at any time, given the outer boundary pressure p_e at the same instant. This latter term is not usually known, and it is more useful to write the equation in terms of the *average* drainage area pressure $\bar{p}$, since this can usually be estimated.

From the radial symmetry of the system we have:

$$\bar{p} = \frac{\int_{r_w}^{r_e} 2\pi r h p\, dr}{\pi(r_e^2 - r_w^2)h} \tag{5.45a}$$

or, ignoring the r_w^2 term (negligible relative to r_e^2) in the denominator:

$$\bar{p} = \frac{2}{r_e^2}\int_{r_w}^{r_e} pr\, dr . \tag{5.45b}$$

Substituting for p from Eq. (5.44a):

$$\bar{p} = \frac{2}{r_e^2}\left\{p_{wf}\int_{r_w}^{r_e} r\, dr + \frac{q\mu}{2\pi kh}\left[\int_{r_w}^{r_e} r\ln\frac{r}{r_w}dr - \frac{1}{2r_c^2}\int_{r_w}^{r_e} r^3 dr\right]\right\} , \tag{5.45c}$$

which, when we ignore r_w^2, becomes:

$$\bar{p} = p_{wf} + \frac{q\mu}{2\pi kh}\frac{2}{r_e^2}\left(\frac{r_e^2}{2}\ln\frac{r_e}{r_w} - \frac{r_e^2}{4} - \frac{r_e^2}{8}\right) . \tag{5.45d}$$

Finally, after simplifying and adding the skin factor we get:

$$\bar{p} = p_{wf} + \frac{q\mu}{2\pi kh}\left(\ln\frac{r_e}{r_w} - \frac{3}{4} + S\right) . \tag{5.46}$$

Now, Eq. (5.46) can be used to calculate the average pressure in a circular drainage area in pseudo-steady state flow. Other geometries can be handled by rewriting Eq. (5.46) in a more general form:

$$\begin{aligned}\bar{p} &= p_{wf} + \frac{q\mu}{2\pi kh}\left[\frac{1}{2}\ln\left(\frac{r_e}{r_w}\right)^2 - \frac{1}{2}\ln(e^{3/2}) + S\right] \\ &= p_{wf} + \frac{q\mu}{4\pi kh}\left[\ln\frac{\pi r_e^2}{\pi e^{3/2} r_w^2} + 2S\right] \\ &= p_{wf} + \frac{q\mu}{4\pi kh}\left(\ln\frac{A}{31.62\, r_w^2} + 0.809 + 2S\right) ,\end{aligned} \tag{5.47}$$

where A is the area of a circle of radius r_e, and the quantity 31.62 is the value of the *Dietz shape factor* C_A for a circular geometry.

We now assume that A represents any drainage area, regardless of shape. The geometry is taken into account via the shape factor; some of the values of C_A calculated by Dietz[6] for a wide range of geometries are listed in Fig. 5.7. In the same table there are also reported values of $t_D r_w^2/A = t_{DA}$, the dimensionless time at which, for a given geometry, pseudo-steady state flow can be assumed to have developed.

With Eq. (5.47) we are able to calculate $\bar{p}$ in fields where well placement leads to non-circular drainage areas, provided of course that we know S in the well under test (see Chap. 6).

For any distribution of wells in a field, once pseudo-steady state flow conditions are established, the size of the drainage area of each well is proportional to its production offtake per unit pay thickness, q/h. This assumes that there is no variation in permeability between the wells.

Consider the case of two wells a distance d apart (Fig. 5.8):

$$\frac{r_1}{q_1/h_1} = \frac{r_2}{q_2/h_2} \tag{5.48a}$$

and

$$r_1 + r_2 = d , \tag{5.48b}$$

$$r_1 = \frac{q_1 h_2}{q_1 h_2 + q_2 h_1} d , \tag{5.49a}$$

$$r_2 = \frac{q_2 h_1}{q_1 h_2 + q_2 h_1} d . \tag{5.49b}$$

The average pressure of the reservoir $\bar{p}_R$ can be calculated as the volume weighted mean of the average pressures $\bar{p}_i$ of the drainage areas of the wells, the volume being the volume of oil $V_{\mathrm{o}i,i}$ present in each area:

$$\bar{p}_R = \frac{\sum_i \bar{p}_i V_{\mathrm{o}i,i}}{\sum_i V_{\mathrm{o}i,i}} . \tag{5.50a}$$

To a first approximation, the production rate q_i from the ith well is proportional to the volume $V_{\mathrm{o}i,i}$ contained in its drainage area, so that we can simplify Eq. (5.50a

	C_A	$\ln C_A$	Exact for $t_{DA}>$	Less than 1% error for $t_{DA}>$	Use infinite system solution with less than 1% error for $t_{DA}<$
⊙	31.62	3.4538	0.1	0.06	0.10
⬡	31.6	3.4532	0.1	0.06	0.10
△	27.6	3.3178	0.2	0.07	0.09
▱	27.1	3.2995	0.2	0.07	0.09
1/2 ◻	21.9	3.0865	0.4	0.12	0.08
2 ⟨△⟩ 1	0.098	−2.3227	0.9	0.60	0.015
◻	30.8626	3.4302	0.1	0.05	0.09
⊞	12.9851	2.5638	0.7	0.25	0.03
⊞	4.5132	1.5070	0.6	0.30	0.025
⊞	3.3351	1.2045	0.7	0.25	0.01
1 ◻ 2	21.8369	3.0836	0.3	0.15	0.025

	C_A	$\ln C_A$	Exact for $t_{DA}>$	Less than 1% error for $t_{DA}>$	Use infinite system solution with less than 1% error for $t_{DA}<$
1 ◻ 2	10.8374	2.3830	0.4	0.15	0.025
1 ◻ 2	4.5141	1.5072	1.5	0.50	0.06
1 ◻ 2	2.0769	0.7309	1.7	0.50	0.02
1 ◻ 2	3.1573	1.1497	0.4	0.15	0.005
1 ◻ 2	0.5813	−0.5425	2.0	0.60	0.02
1 ◻ 2	0.1109	−2.1991	3.0	0.60	0.005
1 ◻ 4	5.3790	1.6825	0.8	0.30	0.01
1 ◻ 4	2.8896	0.9894	0.8	0.30	0.01
1 ◻ 4	0.2318	−1.4619	4.0	2.00	0.03
1 ◻ 4	0.1155	−2.1585	4.0	2.00	0.01
1 ◻ 3	2.3606	0.8589	1.0	0.40	0.025

Fig. 5.7. *Values of the shape factor for different drainage area shapes, and the time limits to the validity of Eqs. (5.36) and (5.47). From Ref. 6, 1965, Society of Petroleum Engineers of AIME, reprinted by permission of the SPE*

Fig. 5.8. *Drainage areas of two adjacent wells*

tor:

$$p_R = \frac{\sum_i p_i q_i}{\sum_i q_i}. \tag{5.50b}$$

5.6.3 Steady State Flow

Steady state flow conditions will occur in a reservoir only when there is an influx of water from a flanking aquifer sufficient to maintain the outer boundary pressure p_e constant with time; or when the reservoir is developed with injection of water or other fluid in such a way that the total volume of fluid (oil + injected fluid) is kept constant.

The boundary conditions applicable at the end of the transient period are:

$$p = p_e = \text{constant} \quad \text{at } r = r_e \tag{5.51a}$$

$$\frac{\partial p}{\partial t} = 0 \quad \text{for all } r \text{ and } t \tag{5.51b}$$

When these conditions apply, Eq. (5.10) becomes:

$$\frac{1}{r}\frac{\mathrm{d}}{\mathrm{d}r}\left(r\frac{\mathrm{d}p}{\mathrm{d}r}\right) = 0, \tag{5.52a}$$

$$r\frac{\mathrm{d}p}{\mathrm{d}r} = \frac{q\mu}{2\pi kh} = \text{const}. \tag{5.52b}$$

Integrating, and introducing the skin term:

$$p - p_{wf} = \frac{q\mu}{2\pi kh}\left(\ln\frac{r}{r_w} + S\right). \tag{5.53}$$

Following the same procedure as for pseudo-steady state flow in Sect. 5.6.2, we obtain the following equation:

$$\bar{p} = p_{wf} + \frac{q\mu}{2\pi kh}\left(\ln\frac{r_e}{r_w} - \frac{1}{2} + S\right). \tag{5.54}$$

Table 5.1 summarises the radial inflow equations for steady and pseudo-steady state flow introduced in the preceding pages.

The C term on the right-hand side is the units conversion coefficient.

If we adhere strictly to the SI units convention, with p in MPa, μ in mPa.s, then the value of C would be $10^{-6}/2\pi$. For practical metric and oilfield units systems, the values of C are listed in Table 5.1, along with the units for each parameter.

Table 5.1. *Radial inflow equations*

	Flow regime	
	Steady state	Pseudo-steady state
General equation	$p - p_{wf} = C\frac{q\mu}{kh}\left(\ln\frac{r}{r_w} + S\right)$	$p - p_{wf} = C\frac{q\mu}{kh}\left(\ln\frac{r}{r_w} - \frac{r^2}{2r_e^2} + S\right)$
Equation in terms of p_e	$p_e - p_{wf} = C\frac{q\mu}{kh}\left(\ln\frac{r_e}{r_w} + S\right)$	$p_e - p_{wf} = C\frac{q\mu}{kh}\left(\ln\frac{r_e}{r_w} - \frac{1}{2} + S\right)$
Equation in terms of $\bar{p}$	$\bar{p} - p_{wf} = C\frac{q\mu}{kh}\left(\ln\frac{r_e}{r_w} - \frac{1}{2} + S\right)$	$\bar{p} - p_{wf} = C\frac{q\mu}{kh}\left(\ln\frac{r_e}{r_w} - \frac{3}{4} + S\right)$

Parameter	Symbol	Units			
		Practical metric		Oilfield (US)	
Pay thickness	h	metres	(m)	feet	(ft)
Permeability	k	millidarcy	(md)	millidarcy	(md)
Downhole flow rate	q	cubic metres/day	(m^3/d)	barrels/day	(bbl/d)
Radii	r, r_e, r_w	metres	(m)	feet	(ft)
Viscosity	μ	centipoise	(cP)	centipoise	(cP)
Pressure	$p, p_e, p_{wf}, \bar{p}$	kilogram/square cm	(kg/cm^2)	pounds/square inch	(psi)
Constant	C	19.03		141.2	

5.7 The Principle of Superposition Applied to the Solution of the Diffusivity Equation

The linearised diffusivity equation, Eq. (5.10), and indeed all differential equations with constant coefficients, are amenable to Duhamel's theorem, which states that "a linear combination of the solutions of a differential equation is itself a solution to that equation".

In other words, if we combine – in a linear fashion – solutions to the diffusivity equation corresponding to different initial and boundary conditions, we will obtain another solution to the diffusivity equation. This is the so-called *principle of superposition*, which is so widely used in mathematical physics.

Consider the case of a well which is initially shut in ($q = 0$ at $t = 0$), with a constant pressure p_i over the whole of its drainage area.

The well is now put on production at a rate q, which is varied with time (Fig. 5.9) instead of being held constant. The flow schedule is as follows:

Flow rate	*Duration*
q_1	$t_1 - 0$
q_2	$t_2 - t_1$
q_3	$t_3 - t_2$
...	...
q_{j-1}	$t_{j-1} - t_{j-2}$
q_j	$t_j - t_{j-1}$
...	...
q_n	$t_n - t_{n-1}$

Equation (7.36) can be used to find the pressure drop $(p_i - p)$ that will have occurred at any radius about a flowing well after the well has flowed at a rate, q, for some time, t. For example, consider a reservoir where oil is flowing and $\mu_o = 0.72$ cp; $B_o = 1.475$ bbl/STB; $k = 100$ md; $h = 15$ ft; $c_t = 15 \times 10^{-6}$ psi^{-1}; $\phi = 23.4\%$; $p_i = 3000$ psia. After a well is produced at 200 STB/day for 10 days, the pressure at a radius of 1000 ft will be:

$$p = 3000 - \frac{70.6(200)(0.72)(1.475)}{100(15)}\left[-E_i\left(-\frac{0.234(0.72)15(10)^{-6}(1000)^2}{0.00105(100)(10)(24)}\right)\right]$$

Then

$$p = 3000 + 10.0\,E_i(-0.10)$$

From Fig. 7.11, $E_i(-0.10) = -1.82$. Therefore

$$p = 3000 + 10.0(-1.82) = 2981.8 \text{ psia}$$

Figure 7.12 shows this pressure plotted on the 10-day curve and shows the pressure distributions at 0.1, 1.0, and 100 days for the same flow conditions.

It has been shown that for values of the E_i function argument less than 0.01 the following approximation can be made:

$$-E_i(-x) = -\ln(x) - 0.5772$$

$$p(r,t) = p_i - \frac{70.6q\mu B}{kh}\left[-E_i\left(-\frac{\phi\mu c_t r^2}{0.00105\,kt}\right)\right]$$

r=1000,t=100*24, x=0.001,E= -4.027970186

r=100,t=10*24, x=0.001,E= -6.330555279

r=100,t=100*24, x=0.0001,E= -8.633140372

2937=3000-63

2914=3000-86

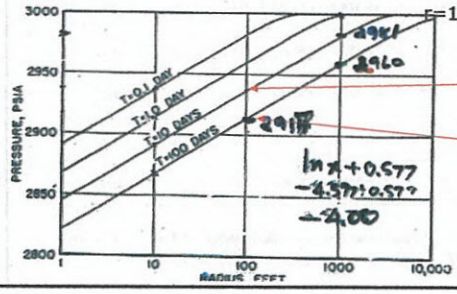

$$\frac{\phi\mu c_t r^2}{0.00105kt} < 0.01$$

rearranging the equation and solving for t, the time required to make this approximation valid for the pressure determination 1000 ft from the producing well can be found:

$$t > \frac{0.234(0.72)15(10)^{-6}(1000)^2}{0.00105(100)(0.01)} \approx 2400 \text{ hr} = 100 \text{ days}$$

To determine if the approximation to the E_i function is valid when calculating the pressure at the sandface of a producing well, it is necessary to assume a wellbore radius, r_w, (0.25 ft) and to calculate the time that would make the approximation valid. The following is obtained:

$$t > \frac{0.234(0.72)15(10)^{-6}(0.25)^2}{0.00105(100)(0.01)} \approx 0.0002 \text{ hours}$$

It is apparent from these calculations that whether the approximation can be used is a strong function of the distance from the pressure disturbance to the point at which the pressure determination is desired or, in this case, from the producing well. For all practical purposes, the assumption is valid when considering pressures at the point of the disturbance. Therefore, at the wellbore and wherever the assumption is valid, Eq. (7.36) can be rewritten as:

$$p(r, t) = p_i - \frac{70.6q\mu B}{kh}\left[-\ln\left(+\frac{\phi\mu c_t r^2}{0.00105kt}\right) - 0.5772\right]$$

Substituting the log base 10 into this equation for the ln term, rearranging and simplifying, one gets:

$$p(r, t) = p_i - \frac{162.6\ q\mu B}{kh}\left[\log\left(\frac{kt}{\phi\mu c_t r^2}\right) - 3.23\right] \quad (7.37)$$

6.2. Radial Flow of Compressible Fluids, Transient Flow

In Sect. 5, Eq. (7.32)

$$\frac{0.234}{r}\frac{\partial}{\partial r}\left(0.001127\frac{k}{\mu}\rho r\frac{\partial p}{\partial r}\right) = \rho\phi c_t\frac{\partial p}{\partial t} + \phi\frac{\partial \rho}{\partial t} \quad (7.32)$$

was developed to describe the flow of any fluid flowing in a radial geometry in porous media. To develop a solution to Eq. (7.32) for the compressible fluid, or gas, case, two additional equations are required: (1) an equation of state, usually the real gas law, which is Eq. (1.7); and (2) Eq. (1.19), which describes how the gas isothermal compressibility varies with pressure:

$$pV = znR'T \quad (1.7)$$

$$c_g = \frac{1}{p} - \frac{1}{z}\frac{dz}{dp} \quad (1.19)$$

These three equations can be combined to yield

$$\frac{1}{r}\frac{\partial}{\partial r}\left(r\frac{p}{\mu z}\frac{\partial p}{\partial r}\right) = \frac{\phi c_t p}{0.0002637kz}\frac{\partial p}{\partial t} \quad (7.38)$$

Al-Hussainy, Ramey, and Crawford and Russel, Goodrich, Perry, and Bruskotter introduced a transformation of variables to obtain a solution to Eq. (7.38).[7-8] The transformation involves the real gas pseudopressure, $m(p)$, which has units of psia^2/cp in standard field units and is defined as:

$$m(p) = 2\int_{p_b}^{p}\frac{p}{\mu z}dp \quad (7.39)$$

where p_R is a reference pressure, usually chosen to be 14.7 psia, from which the function is evaluated. Since μ and z are only functions of pressure for a given reservoir system, which we have assumed to be isothermal, Eq. (7.39) can be differentiated and the chain rule of differentiation applied to obtain the following relationships:

$$\frac{\partial m(p)}{\partial p} = \frac{2p}{\mu z} \tag{7.40}$$

$$\frac{\partial m(p)}{\partial r} = \frac{\partial m(p)}{\partial p}\frac{\partial p}{\partial r} \tag{7.41}$$

$$\frac{\partial m(p)}{\partial t} = \frac{\partial m(p)}{\partial p}\frac{\partial p}{\partial t} \tag{7.42}$$

Substituting Eq. (7.40) into Eq. (7.41) and (7.42) yields

$$\frac{\partial p}{\partial r} = \frac{\mu z}{2p}\frac{\partial m(p)}{\partial r} \tag{7.43}$$

$$\frac{\partial p}{\partial t} = \frac{\mu z}{2p}\frac{\partial m(p)}{\partial t} \tag{7.44}$$

Combining Eq. (7.43), (7.44), and (7.38) yields

$$\frac{\partial^2 m(p)}{\partial r^2} + \frac{1}{r}\frac{\partial m(p)}{\partial r} = \frac{\phi\mu c_t}{0.0002637k}\frac{\partial m(p)}{\partial t} \tag{7.45}$$

Equation (7.45) is the diffusivity equation for compressible fluids, and it has

Equation (7.45) is still a nonlinear differential equation because of the dependence of μ and c_t on pressure or the real gas pseudopressure. Thus, there is no analytical solution for Eq. (7.45). Al-Hussainy and Ramey, however, used finite difference techniques to obtain an approximate solution to Eq. (7.45).[9] The result of their studies for pressures at the wellbore (i.e., where the logarithm approximation to the E_i function can be made) is the following equation:

$$m(p_{wf}) = m(p_i) - \frac{1637(10)^3 qT}{kh}\left[\log\left(\frac{kt}{\phi\mu_i c_{ti} r_w^2}\right) - 3.23\right] \tag{7.46}$$

interest, p_1. The value of $m(p_1)$ that corresponds with pressure, p_1, is given by:

$$m(p_1) = 2\,(\text{area}_1)$$

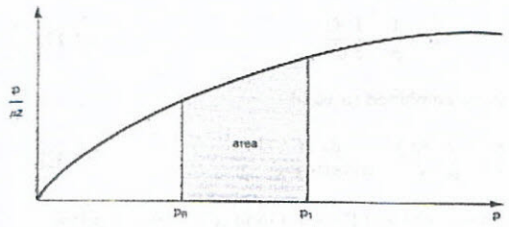

Fig. 7.13. Graphical determination of $m(p)$.

where

$$\text{area}_1 = \int_{p_R}^{p_1} \frac{p}{\mu z}\,dp$$

TABLE 7.2.
Shape factors for various single-well drainage areas (after Earlougher.[3])

In Bounded Reservoirs	C_A	$\ln C_A$	$1/2 \ln\left(\frac{2.2458}{C_A}\right)$	*Exact for* $t_{DA} >$	*Less than 1% Error for* $t_{DA} >$	*Use Infinite System Solution with Less than 1% Error for* $t_{DA} <$
	31.62	3.4538	−1.3224	0.1	0.06	0.10
	31.6	3.4532	−1.3220	0.1	0.06	0.10
	27.6	3.3178	−1.2544	0.2	0.07	0.09
	27.1	3.2995	−1.2452	0.2	0.07	0.09
	21.9	3.0865	−1.1387	0.4	0.12	0.08
	0.098	−2.3227	1.5659	0.9	0.60	0.015

	31.6	3.4532	−1.3220	0.1	0.06	0.10
	27.6	3.3178	−1.2544	0.2	0.07	0.09
	27.1	3.2995	−1.2452	0.2	0.07	0.09
	21.9	3.0865	−1.1387	0.4	0.12	0.08
	0.098	−2.3227	1.5659	0.9	0.60	0.015

	30.8828	3.4302	−1.3106	0.1	0.05	0.09
	12.9851	2.5638	−0.8774	0.7	0.25	0.03
	4.5132	1.5070	−0.3490	0.6	0.30	0.025
	3.3351	1.2045	−0.1977	0.7	0.25	0.01
	21.8369	3.0836	−1.1373	0.3	0.15	0.025
	10.8374	2.3830	−0.7870	0.4	0.15	0.025
	4.5141	1.5072	−0.3491	1.5	0.50	0.06
	2.0769	0.7309	0.0391	1.7	0.50	0.02
	3.1573	1.1497	−0.1703	0.4	0.15	0.005

7. PSEUDOSTEADY-STATE FLOW SYSTEMS

7.1. Radial Flow of Slightly Compressible Fluids, Pseudosteady-State Flow

condition used to find a solution to the radial diffusivity equation is that the outer boundary of the reservoir is a no-flow boundary. In mathematical terms,

Eq. 7.35

$$\frac{\partial p}{\partial r}=0 \qquad \text{at } r=r_e$$

$$\frac{\partial^2 p}{\partial r^2}+\frac{1}{r}\frac{\partial p}{\partial r}=\frac{\phi\mu c_t}{0.0002637k}\frac{\partial p}{\partial t} \qquad (7.35)$$

Continuity Eq.

Applying these conditions to Eq. (7.35), the solution for the pressure at the wellbore becomes

$$p_{wf}=p_i-\frac{162.6q\mu B}{kh}\log\left[\frac{4A}{1.781C_Ar_w^2}\right]-\frac{0.2339qBt}{Ah\phi c_t} \qquad (7.47)$$

where A is the drainage area of the well in square feet and C_A is a reservoir shape factor. Values of the shape factor are given in Table 7.2 for several

After reaching pseudosteady-state flow, the pressure at every point in the reservoir is changing at the same rate, which suggests that the average reservoir pressure is also changing at the same rate. The volumetric average reservoir pressure, which is usually designated as $\bar{p}$ and is the pressure used to calculate fluid properties in material balance equations, is defined as:

$$\bar{p}=\frac{\sum_{j=1}^{n}\bar{p}_jV_j}{\sum_{j=1}^{n}V_j} \qquad (7.48)$$

where p_j is the average pressure in the jth drainage volume and V_j is the volume of the jth drainage volume. It is useful to rewrite Eq. (7.47) in terms of the average reservoir pressure, $\bar{p}$:

$$p_{wf}=\bar{p}-\frac{162.6q\mu B}{kh}\log\left[\frac{4A}{1.781C_Ar_w^2}\right] \qquad (7.49)$$

$\ln(0.22\frac{r_e^2}{r_w^2})$

For a well in the center of a circular reservoir with a distance to the outer boundary of r_e, Eq. (7.49) reduces to:

$$p_{wf}=\bar{p}-\frac{70.6q\mu B}{kh}\left[\ln\left(\frac{r_e^2}{r_w^2}\right)-1.5\right]=\bar{p}-\frac{141.2q\mu B}{kh}\left[\ln\frac{r_e}{r_w}-0.75\right]$$

If this equation is rearranged and solved for q,

$$q=\frac{0.00708kh}{\mu B}\left[\frac{\bar{p}-p_{wf}}{\ln(r_e/r_w)-0.75}\right] \qquad (7.50)$$

7.2. Radial Flow of Compressible Fluids, Pseudosteady-State Flow

The differential equation for the flow of compressible fluids in terms of the real gas pseudopressure was derived in Eq. (7.45). When the appropriate boundary conditions are applied to Eq. (7.45), the pseudosteady-state solution rearranged and solved for q yields Eq. (7.51):

$$q=\frac{19.88(10)^{-6}khT_{sc}}{Tp_{sc}}\left[\frac{m(\bar{p})-m(p_{wf})}{\ln(r_e/r_w)-0.75}\right] \qquad (7.51)$$

$\frac{10^6\times 14.7}{19.88\times 520}=1422$

4.5 GAS FLOW EQUATION SUMMARY

Writing $C = 0.703\ kh/[\mu T z \ln(r_e/r_w)]$, and the power n is turbulent flow effect in steady state gas flow, Equation (4.27) becomes

$$Q_g = C(p_r^2 - p_{wf}^2)^n \tag{4.44}$$

This equation is normally called the empirical back pressure equation. The power n is the turbulent effect which is ranging from low flow rate = 1.00 to absolutely turbulent = 0.500. The equation is not especially helpful in predicting reservoir characteristics or in analyzing the components of pressure drops, although it may be useful in characterizing well performance.

When multirate data are available it is more useful to revert to one of the basis flow equations in field units:

$$\bar{p}_r^2 - P_{wf}^2 = \left(\frac{1422 Q_g \mu z T}{kh}\right)\left[\ln\left(\frac{r_e}{r_w}\right) - 0.75 + S\right] \tag{4.45}$$

Or

$$\bar{p}_r^2 - P_{wf}^2 = \left(\frac{1422 Q_g \mu z T}{kh}\right)\left[\ln\left(\frac{0.472 r_e}{r_w}\right) + S\right] + BQ^2 \tag{4.46}$$

(semi-steady state)

Or

$$\bar{p}_r^2 - P_{wf}^2 = \left(\frac{1422 Q_g \mu z T}{kh}\right)\left[\frac{1}{2}\ln(t_D + 0.809) + S\right] + BQ^2 \tag{4.47}$$

(transient)

$$\Delta(p^2) = AQ + BQ^2$$

Where

$$A = \left(\frac{1422 Q_g \mu z T}{kh}\right)\left[\ln\left(\frac{0.472 r_e}{r_w}\right) + S\right] \text{ (semi-steady state)}$$

$$= \left(\frac{1422 Q_g \mu z T}{kh}\right)\left[\frac{1}{2}\ln(t_D + 0.809) + S\right] \text{ (transient)}$$

And B = non-Darcy coefficient,

It is more appropriate to use the real gas pseudo-pressure $m(p)$ equation:

$$m(\bar{p}_r) - m(p_{wf}) = \left(\frac{1422 Q_g T}{kh}\right)\left[\ln\left(\frac{r_e}{r_w}\right) - 0.75 + S\right] + FQ^2$$

$$= \left(\frac{1422 Q_g T}{kh}\right)\left[\ln\left(\frac{r_e}{r_w}\right) - 0.75 + S + DQ\right] \tag{4.48}$$

Where

$$D = \left(\frac{Fkh}{1422T}\right)$$

And DQ is known as the rate dependent skin factor

8. PRODUCTIVITY INDEX (PI)

The ratio of the rate of production, expressed in STB/day for liquid flow, to the pressure drawdown at the midpoint of the producing interval, is called the *productivity index*, symbol J.

$$J = \frac{q}{\bar{p} - p_{wf}} \qquad (7.52)$$

In some wells, the PI remains constant over a wide variation in flow rate such that the flow rate is directly proportional to the bottom-hole pressure drawdown. In other wells, at higher flow rates the linearity fails, and the PI index declines, as shown in Fig. 7.14. The cause of this decline may be (a) turbulence at increased rates of flow, (b) decrease in the permeability to oil due to presence of free gas caused by the drop in pressure at the well bore, (c) the increase in oil viscosity with pressure drop below bubble point, and/or (d) reduction in permeability due to formation compressibility.

In depletion reservoirs, the productivity indexes of the wells decline as depletion proceeds, owing to the increase in oil viscosity as gas is released from solution and to the decrease in the permeability of the rock to oil as the oil saturation decreases. Since each of these factors may change from a few to several-fold during depletion, the PI may decline to a small fraction of the initial value. Also, as the permeability to oil decreases, there is a corresponding increase in the permeability to gas, which results in rising gas-oil ratios.

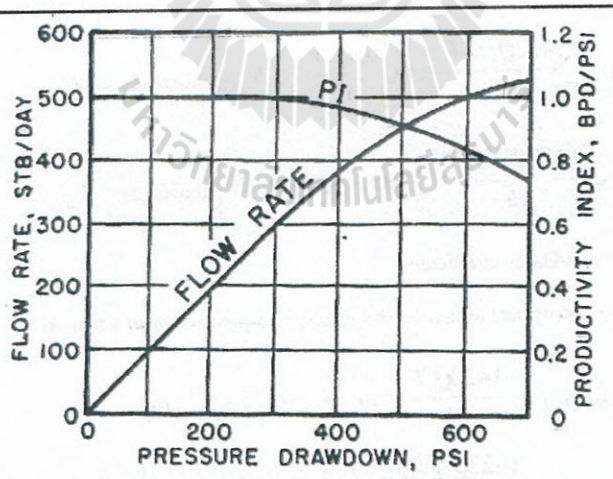

Fig. 7.14. Decline in productivity index at higher flow rates.

The *injectivity index* is used with salt water disposal wells and with *injection wells* for secondary recovery or pressure maintenance. It is the ratio of the injection rate in STB per day to the excess pressure above reservoir pressure that causes that injection rate, or

$$\text{Injectivity index} = I = \frac{q}{p_{wf} - \bar{p}} \text{ STB/day/psi} \qquad (7.53)$$

there is a variation in net productive thickness but when the other factors affecting the productivity index are essentially the same, the specific productivity index J_s is sometimes used, which is the productivity index divided by the net feet of pay, or,

$$\text{Specific productivity index} = J_s = \frac{J}{h} = \frac{q}{h(\bar{p} - p_{wf})} \text{ STB/day/psi/ft} \quad (7.54)$$

P.I

8.1. Productivity Ratio (PR)

In evaluating well performance, the standard usually referred to is the productivity index of an open hole that completely penetrates a circular formation normal to the strata, and in which no alteration in permeability has occurred the vicinity of the wellbore. Substituting Eq. (7.50) into Eq. (7.52) we get

$$J = 0.00708 \frac{kh}{\mu B[\ln(r_e/r_w) - 0.75]} \quad (7.55)$$

The PR then is the ratio of the PI of a well in any condition to the PI of this *standard* well:

$$PR = \frac{J}{J_w} \quad (7.56)$$

Thus, the productivity ratio may be less than one, greater than one, or equal one. Although the productivity index of the standard well is generally unknown, the relative effect of certain changes in the well system may be evaluated from theoretical considerations, laboratory models, or well tests. For example, the theoretical productivity ratio of a well reamed from an 8-in. borehole diameter to 16 in. is derived by Eq. (7.55):

$$PR = \frac{J_{16}}{J_8} = \frac{\ln(r_e/0.333) - 0.75}{\ln(r_e/0.667) - 0.75}$$

Assuming $r_e = 660$ ft,

$$PR = \frac{\ln(660/0.333) - 0.75}{\ln(660/0.667) - 0.75} = 1.11$$

9. SUPERPOSITION

SUPERPOSITION

$$\Delta p_t = \Delta p_1 + \Delta p_2$$

Each of the individual Δp terms is given by Eq. (7.36), or:

$$\Delta p = p_i - p(r, t) = \frac{70.6q\mu B}{kh}\left[-E_i\left(-\frac{\phi\mu c_t r^2}{0.00105kt}\right)\right]$$

To apply the method of superposition, pressure drops or changes are added. It is not correct simply to add or subtract individual pressure terms. It is obvious that if there are more than two flowing wells in the reservoir system, the procedure is the same, and the total pressure drop is given by the following.

$$\Delta p_t = \sum_{j=1}^{n} \Delta p_j \quad (7.57)$$

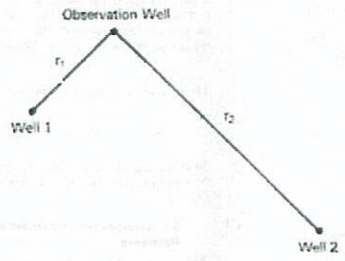

Fig. 7.15. Two flowing-well reservoir system to illustrate the principle of superposition.

at two flow rates. The change in the flow rate from q_1 to q_2 occurred at time t_1. Figure 7.17 shows that the total pressure drop is given by the sum of the pressure drop caused by the flow rate q_1 and the pressure drop caused by the change in flow rate $q_2 - q_1$. This new flow rate, $q_2 - q_1$, has flowed for time $t - t_1$.

The pressure drop for this flow rate, $q_2 - q_1$, is given by

$$\Delta p = p_i - p(r, t) = \frac{70.6(q_2 - q_1)\mu B}{kh}\left[-E_i\left(\frac{\phi\mu c_t r^2}{0.00105k(t - t_1)}\right)\right]$$

As in the case of the multiwell system just described, superposition can also be applied to multirate systems as well as the two rate examples depicted in Fig. 7.17.

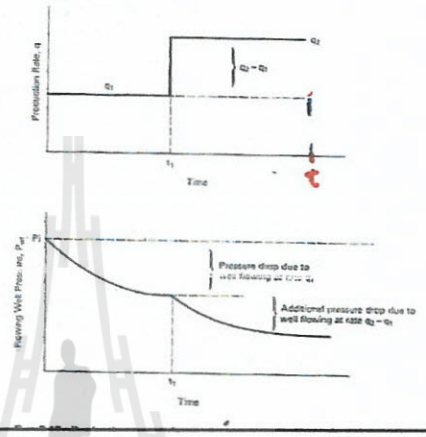

where N equals the number of flowing wells in the system. Example 7.1 illustrates the calculations involved when more than one well affects the pressure of a point in a reservoir.

Example 7.1. For the well layout shown in Fig. 7.16, calculate the total pressure drop as measured in the observation well (well 3) caused by the four flowing wells (wells 1, 2, 4, and 5) after 10 days. The wells were shut in for a long time before opening them to flow.

Given: The following data apply to the reservoir system:

oil viscosity = 0.40 cp
k = 47 md
porosity = 11.2%
B_o=1.50 bbl/STB
formation thickness = 50 ft
$c_t = 15 \times 10^{-6}$ psi^{-1}

Well	Flow Rate (STB/day)	Distance to Observation well (feet)
1	265	1700
2	270	1920
4	267	1870
5	260	1690

SOLUTION: The individual pressure drops can be calculated with Eq. (7.36), and the total pressure drop is given by Eq. (7.57). For well 1

$$\Delta p_1 = \frac{70.6(265)(0.40)(1.5)}{(47)(50)}\left[-E_i\left(\frac{(.112)(0.40)(15 \times 10^{-6})(1700)^2}{0.00105(47)(240)}\right)\right]$$

$$\Delta p_1 = 4.78[-E_i(-0.164)]$$

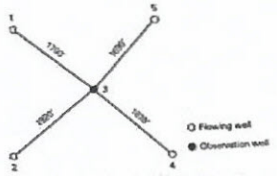

Fig. 7.16. Well Layout for Ex. Prob. 7.1.

From Fig. 7.11

$$-E_i(-0.164) = 1.39$$

Therefore

$$\Delta p_1 = 4.78(1.39) = 6.6 \text{ psi}$$

Similarly, for wells 2, 4, and 5

$$\Delta p_2 = 4.87[-E_i(-0.209)] = 5.7 \text{ psi}$$
$$\Delta p_4 = 5.14[-E_i(-0.198)] = 6.4 \text{ psi}$$
$$\Delta p_5 = 4.69[-E_i(-0.162)] = 6.6 \text{ psi}$$

Using Eq. (7.57) to find the total pressure drop at the observation well, Well 3, the individual pressure drops are added together to give the total:

$$\Delta p_t = \Delta p_1 + \Delta p_2 + \Delta p_4 + \Delta p_5$$

or

$$\Delta p_t = 6.6 + 5.7 + 6.4 + 6.6 = 25.3 \text{ psi}$$

The superposition principle can also be applied in the time dimension, as is illustrated in Fig. 7.17. In this case, one well (which means the position where the pressure disturbances occur remains constant) has been produced at two flow rates. The change in the flow rate from q_1 to q_2 occurred at time t_1. Figure 7.17 shows that the total pressure drop is given by the sum of the pressure drop caused by the flow rate q_1 and the pressure drop caused by the change in flow rate $q_2 - q_1$. This new flow rate, $q_2 - q_1$, has flowed for time $t - t_1$.

The pressure drop for this flow rate, $q_2 - q_1$, is given by

$$\Delta p = p_i - p(r, t) = \frac{70.6(q_2 - q_1)\mu B}{kh}\left[-E_i\left(\frac{\phi\mu c_t r^2}{0.00105k(t - t_1)}\right)\right]$$

As in the case of the multiwell system just described, superposition can also be applied to multirate systems as well as the two rate examples depicted in Fig. 7.17.

9.1. Superposition in Bounded or Partially Bounded Reservoirs

Although Eq. (7.36) applies to infinite reservoirs, it may be used in conjunction with the superposition principle to simulate boundaries of closed or partially closed reservoirs. The effect of boundaries is always to cause greater

9.1. Superposition in Bounded or Partially Bounded Reservoirs

Although Eq. (7.36) applies to infinite reservoirs, it may be used in conjunction with the superposition principle to simulate boundaries of closed or partially closed reservoirs. The effect of boundaries is always to cause greater pressure drops than those calculated for the infinite reservoirs. The method of *images* is useful in handling the effect of boundaries. For example, the pressure drop at point X (Fig. 7.18), owing to production in a well located a distance d from a sealing fault, will be the sum of the effects of the producing well and an image well that is superimposed at a distance d behind the fault. In this case the total pressure drop is given by Eq. (7.57), where the individual pressure drops are again given by Eq. (7.36), or for the case shown in Fig. 7.18:

$$\Delta p = \Delta p_1 + \Delta p_{image}$$

$$\Delta p_1 = \frac{70.6q\mu B}{kh}\left[-E_i\left(\frac{\phi\mu c_t r_1^2}{-0.00105kt}\right)\right]$$

$$\Delta p_{image} = \frac{70.6q\mu B}{kh}\left[-E_i\left(\frac{\phi\mu c_t r_2^2}{-0.00105kt}\right)\right]$$

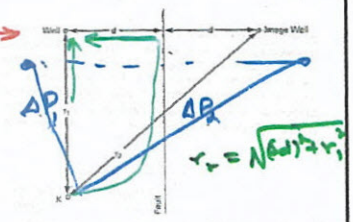

Fig. 7.18. Method of images used in the solution of boundary problems.

9.1. Superposition in Bounded or Partially Bounded Reservoirs

$$\Delta p = \Delta p_1 + \Delta p_{image}$$

$$\Delta p_1 = \frac{70.6q\mu B}{kh}\left[-E_i\left(\frac{\phi\mu c_t r_1^2}{-0.00105kt}\right)\right]$$

$$\Delta p_{image} = \frac{70.6q\mu B}{kh}\left[-E_i\left(\frac{\phi\mu c_t r_2^2}{-0.00105kt}\right)\right]$$

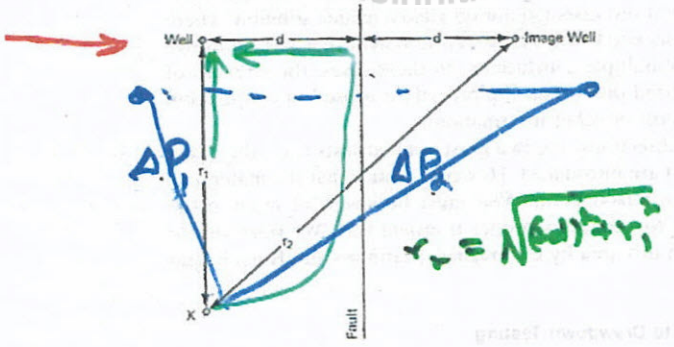

Fig. 7.18. Method of images used in the solution of boundary problems.

SHORTEN TERM

- Initial Reservoir Pressure/Temperature
- Permeability
- Active Pay thickness
- Skin Factor
- Fluid Type and properties
- Type of Flow System
- Production Rate/Problems

LONG TERM

1. Volume proving
2. Extended Investigation Radius
3. Reservoir Limits
4. Relative Reservoir shape
5. Boundary Type

Drill Stem Test

- RELATIVELY CHEAP AND FAST
- RESULTS MAY BE ADEQUATE
- WELL SAFETY NOT OPTIMUM

PACKER PERFORMANCE IN OPEN HOLE NOT RELIABLE
(CASED HOLE FLOATERS)

DRILLSTRING UNSUITABLE FOR HIGH GAS PRESSURE AND H_2S SERVICE

OFFSHORE VESSEL MOVEMENT INDUCES STRING MOVEMENT

- NO DST FROM FLOATERS WITH OPEN HOLE PACKERS
- HARDLY EVER USED IN GROUP ORCO'S

10.4.1 Well Testing Objective

SHORT TERM
- Initial Reservoir Pressure/Temperature
- Permeabilities
- Active Pay Thickness
- Skin Factor
- Fluid Type and Properties
- Type of Flow System
- Production Rate/Problems

LONG TERM
- Volume Proving
- Extended Investigation Radius
  - Reservoir Limits
  - Relative Reservoir Shape
  - Boundary Type

10-10

10.1. Introduction to Drawdown Testing

$$p(r,t) = p_i - \frac{162.6\,q\mu B}{kh}\left[\log\frac{k}{\phi\mu c_t r^2} - 3.23\right] \qquad (7.37)$$

which predicts the pressure at any radius, r, as a function of time for a given reservoir flow system during the transient period. If $r = r_w$, then $p(r, t)$ will be the pressure at the wellbore. For a given reservoir system, p_i, q, μ, B, k, h, ϕ, c_t, and r_w are constant, and Eq. (7.37) can be written as

$$p_{wf} = b + m\log(t) \qquad (7.58)$$

where,

p_{wf} = flowing well pressure in psia
b = constant
t = time in hrs

$$m = \text{constant} = -\frac{162.6\,q\mu B}{kh} \qquad (7.59)$$

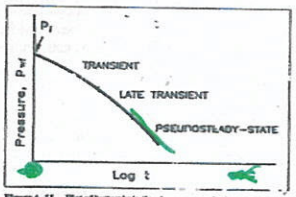

Figure 6-11. Plot of bottomhole flowing pressure (p_{wf}) vs log of producing time t.

1. Laminar, horizontal flow in a homogeneous reservoir.
2. Reservoir and fluid properties, k, ϕ, h, c_t, μ, and B are independent of pressure.
3. Single-phase liquid flow in the transient time region.
4. Negligible pressure gradients.

The expression for the slope, Eq. (7.59), can be rearranged to solve for the capacity, kh, of the drainage area of the flowing well. If the thickness is known, then the average permeability can be obtained by Eq. (7.60):

$$k = -\frac{162.6\,q\mu B}{mh} \qquad (7.60)$$

If the drawdown test is conducted long enough for the pressure transients to reach the pseudosteady-state period, then Eq. (7.47) is used to describe the pressure behavior:

$$p_{wf} = p_i - \frac{162.6\,q\mu B}{kh}\log\left[\frac{4A}{1.781\,C_A r^2}\right] - \frac{0.2339\,qBt}{Ah\phi c_t} \qquad (7.47)$$

Again grouping together the terms that are constant for a given reservoir system, Eq. (7.47) becomes

$$p_{wf} = b' + m't \qquad (7.61)$$

where

b' = constant

$$m' = \text{constant} = -\frac{0.2339\,qB}{Ah\phi c_t} \qquad (7.62)$$

Now a plot of pressure versus time on regular cartesian graph paper yields a straight line with slope equal to m' through the late time data that correspond to the pseudosteady-state period. If Eq. (7.62) is rearranged, an expression for the drainage volume of the test well can be obtained:

$$Ah\phi = -\frac{0.2339\,qB}{m'c_t} \qquad (7.63)$$

A damage zone yields an additional pressure drop because of the reduced permeability in that zone. Van Everdingen and Hurst developed an expression for this pressure drop and defined a dimensionless damage factor, S, called the skin factor[16,17]:

$$\Delta p_{skin} = \frac{141.2 q\mu B}{kh} S \tag{7.64}$$

or

$$\Delta p_{skin} = -0.87 mS \tag{7.65}$$

From Eq. (7.65), a positive value of S causes a positive pressure drop and therefore represents a damage situation. A negative value of S causes a negative pressure drop that represents a stimulated condition like a fracture. Notice that these pressure drops caused by the skin factor are compared to the pressure drop that would normally occur through this affected zone as predicted by Eq. (7.37). Combining Eq. (7.37) and (7.65), the following expression is obtained for the pressure at the wellbore:

$$p_{wf} = p_i - \frac{162.6 q\mu B}{kh}\left[\log\frac{kt}{\phi\mu c_t r_w^2} - 3.23 + 0.87S\right] \tag{7.66}$$

This equation can be rearranged and solved for the skin factor, S:

$$S = 1.151\left[\frac{p_i - p_{wf}}{\frac{162.6 q\mu B}{kh}} - \log\frac{kt}{\phi\mu c_t r_w^2} + 3.23\right]$$

The value of p_{wf} must be obtained from the straight line in the transient flow region. Usually a time corresponding to 1 hr is used, and the corresponding pressure is given by the designation, p_{1hr}. Substituting m into this equation and recognizing that the denominator of the first term within the brackets is actually $-m$,

$$S = 1.151\left[\frac{p_{1hr} - p_i}{m} - \log\frac{k}{\phi\mu c_t r_w^2} + 3.23\right] \tag{7.67}$$

Example 7.2. A drawdown test was conducted on a new oil well in a large reservoir. At the time of the test, the well was the only well that had been developed in the reservoir. Analysis of the data indicates that wellbore storage does not affect the pressure measurements. Use the data to calculate the

average permeability of the area around the well the skin factor, and the drainage area of the well.

Given:

$p_i = 4000$ psia	formation thickness = 20 ft
$q = 500$ STB/day	$c_t = 30 \times 10^{-6}$ psia^{-1}
$\mu_o = 1.5$ cp	porosity = 25%
$B_o = 1.2$ bbl/STB	$r_w = 0.333$ ft

Flowing pressure, p_{wf} psia	*time, t hrs*
3503	2
3469	5
3443	10
3417	20
3383	50
3368	75
3350	100
3306	150
3282	200
3250	300

SOLUTION: Figure 7.19 contains a semilog plot of the pressure data. The slope of the early time data, which are in the transient time region, was found to be -86 psi/cycle and the value of P_{1hr} was found to be 3526 psia. Equation (7.60) can now be used to calculate the permeability:

$$k = -\frac{162.6(500)(1.5)(1.2)}{-86(20)} = 85.1 \text{ md}$$

The skin factor is found from Eq. (7.67):

$$S = 1.151\left[\frac{3526 - 4000}{-86} - \log\left(\frac{85.1}{(0.25)(1.5)(30\times10^{-6})(0.333)^2}\right) + 3.23\right]$$

$$S = 1.04$$

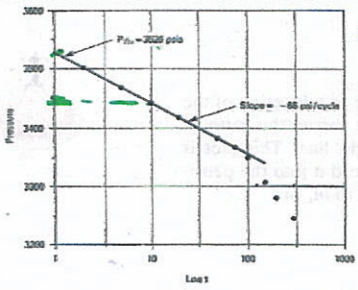

Fig. 7.19. Plot of pressure versus log time for the data of Ex. 7.2.

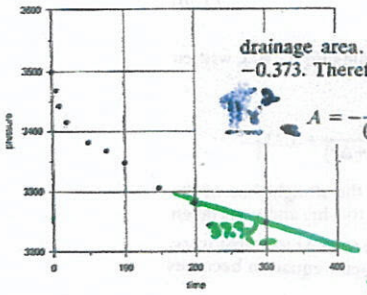

Fig. 7.20. Plot of pressure versus time for the data of Ex. 7.2.

drainage area. The slope of a line drawn through the last three points is −0.373. Therefore,

$$A = -\frac{0.2339(500)(1.2)}{(-.373)(30\times 10)^{-6}(20)(0.25)} = 2{,}508{,}000\ ft^2 = 57.6\ ac$$

10.2. Introduction to Buildup Testing

$$t_p = \frac{N_p}{q} \tag{7.68}$$

where, N_p = cumulative production that has occurred during the time before shut-in that the well was flowed at the constant flow rate q.

Equations (7.37) and (7.57) can be used to describe the pressure behavior of the shut-in well:

$$p_{ws} = p_i - \frac{162.6q\mu B}{kh}\left[\log\frac{k(t_p+\Delta t)}{\phi\mu c_t r_w^2} - 3.23\right] - \frac{162.6(-q)\mu B}{kh}\left[\log\frac{k\Delta t}{\phi\mu c_t r_w^2} - 3.23\right]$$

Expanding this equation and cancelling terms,

$$p_{ws} = p_i - \frac{162.6q\mu B}{kh}\left[\log\frac{(t_p+\Delta t)}{\Delta t}\right] \tag{7.69}$$

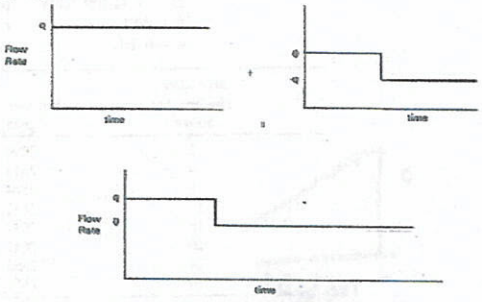

Fig. 7.21. Graphical simulation of pressure buildup test using superposition.

where,

p_{ws} = bottom-hole shut-in pressure

Equation (7.69) is used to calculate the shut-in pressure as a function of the shut-in time and suggests that a plot of this pressure versus the ratio of $(t_p + \Delta t)/\Delta t$ on semilog graph paper will yield a straight line. This plot is referred to as a Horner plot after the man who introduced it into the petroleum literature.[18] The slope of the Horner plot is equal to m, or

$$m = -\frac{162.6q\mu B}{kh}$$

This equation can be rearranged to solve for the permeability:

$$k = -\frac{162.6q\mu B}{mh} \tag{7.70}$$

The skin factor equation for buildup is found by combining Eq. (7.67), written for $t = t_p$ $(\Delta t = 0)$, and Eq. (7.69):

$$S = 1.151\left[\frac{p_{wf}(\Delta t = 0) - p_{ws}}{m} - \log\frac{kt_p\,\Delta t}{\phi\mu c_t r_w^2(t_p + \Delta t)} + 3.23\right]$$

The shut-in pressure, p_{ws}, can be taken at any Δt on the straight line of the transient flow period. For convenience, Δt is set equal to 1 hr, and p_{ws} is taken at that point. At a time of $\Delta t = 1$ hr, t_p is much larger than Δt for most tests, and $t_p + \Delta t \approx t_p$. With these considerations, the skin factor equation becomes

$$S = 1.151\left[\frac{p_{wf}(\Delta t = 0) - p_{1hr}}{m} - \log\frac{k}{\phi\mu c_t r_w^2} + 3.23\right] \tag{7.71}$$

Example 7.3. Calculation of permeability and skin from a pressure buildup test.

Given:

flow rate before shut in period = 280 STB/day

N_p during constant rate period before shut in = 2682 STB

p_{wf} at the time of shut-in = 1123 psia

From the foregoing data and Eq. (7.68), t_p can be calculated

$$t_p = \frac{N_p}{q} = \left(\frac{2682}{280}\right)24 = 230 \text{ hours}$$

Other given data are

$B_o = 1.31$ bbl/STB $\quad \mu_o = 2.0$ cp

$h = 40$ ft $\quad c_t = 15 \times 10^{-6}$ psi^{-1}

$\phi = 0.10$ $\quad r_w = 0.333$ ft

time after shut in, Δt, hours	*Pressure, p_{ws}, psia*	$\frac{t_p + \Delta t}{\Delta t}$
1	2254	
2	2290	116.0
4	2514	58.5
8	2584	29.8
12	2612	20.2
16	2632	15.4
20	2643	12.5
24	2650	10.6
30	2658	8.7

SOLUTION: The slope of the straight line region (notice the difficulty in identifying the straight line region) of the Horner plot in Fig. 7.22 is −170 psi/cycle. From Eq. (7.70)

$$k = -\frac{162.6(280)(2.0)(1.31)}{(-170)(40)} = 17.5 \text{ md}$$

Again from the Horner plot, p_{1hr} is 2435 psia and from Eq. (7.71)

$$S = 1.151\left[\frac{1123 - 2435}{-170} - \log\left(\frac{17.5}{(0.1)(2.0)(15\times10^{-6})(0.333)^2}\right) + 3.23\right]$$

$$S = 3.71$$

difficulty in identifying the straight line of the transient time region results wellbore storage and other anomalies that could affect the pressure transient data.

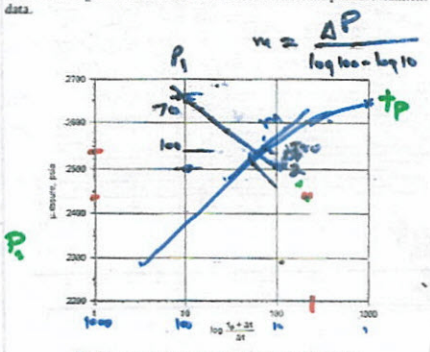

Fig. 7.22. Plot of pressure versus time ratio for Ex. 7.3.

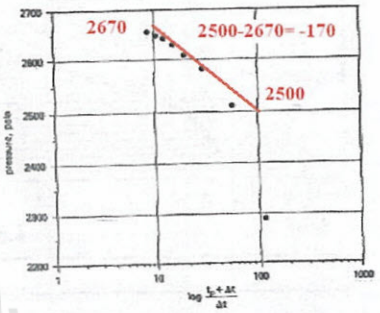

Fig. 7.22. Plot of pressure versus time ratio for Ex. 7.3.

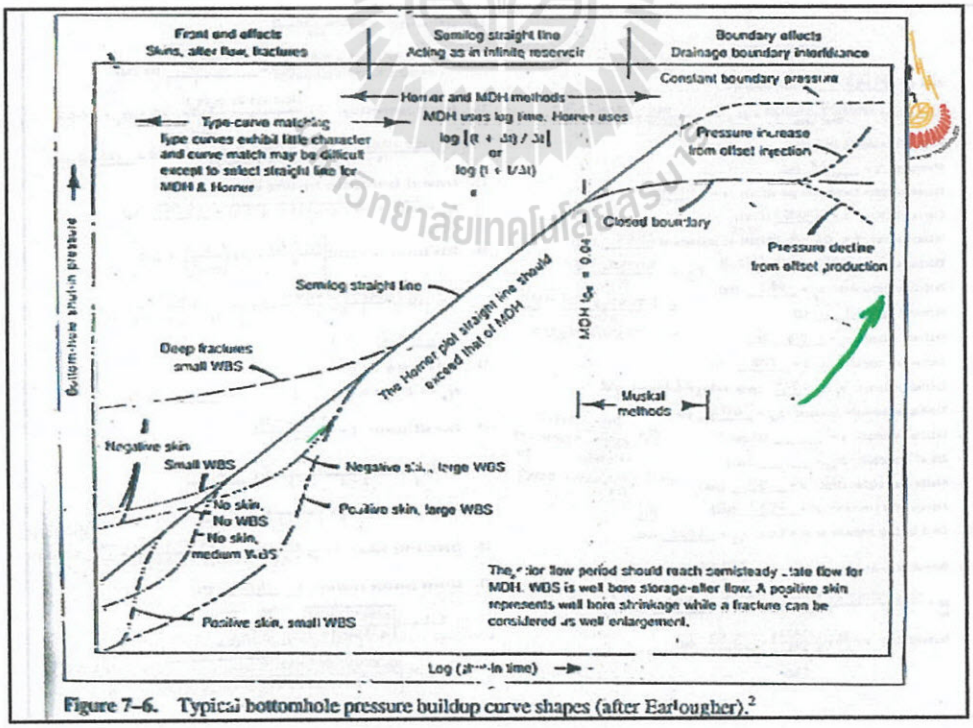

Figure 7–6. Typical bottomhole pressure buildup curve shapes (after Earlougher).[2]

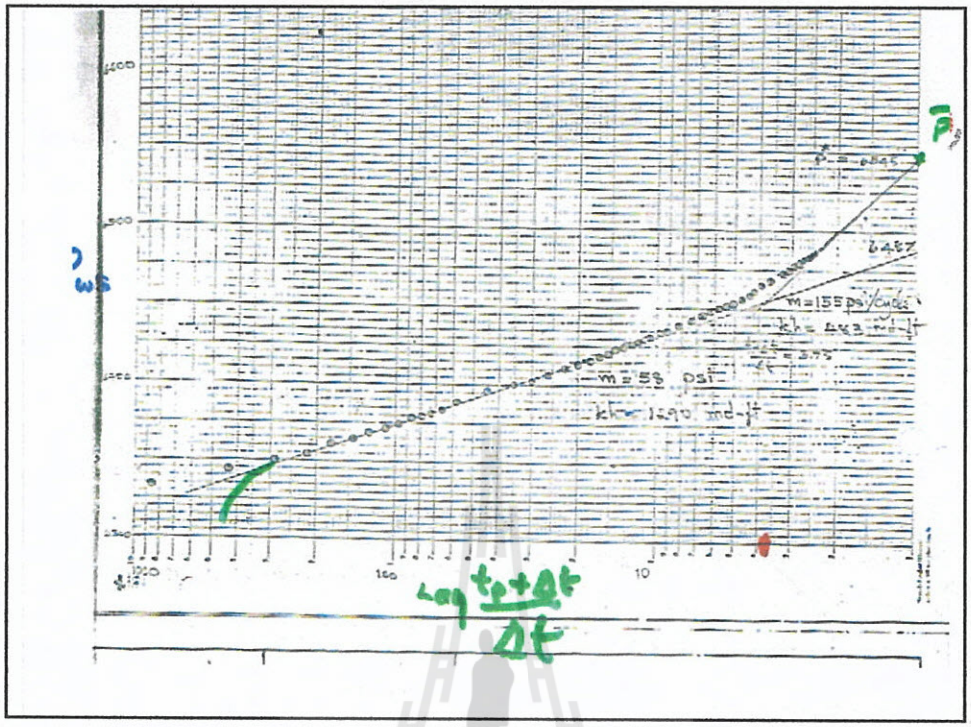

BUILDUP ANALYSIS

1. Rate q = 29343 (STB/D; MSCF/D)
2. Horner Time: $\frac{\text{Cumulative production}}{\text{Last rate}} = 24 \times \frac{(\text{STB})}{(\text{STB/D})}$ = 860 (hr)
3. Fluid and reservoir properties
   - Viscosity: μ = 0.027 (cp)
   - Compressibility factor (for gas wells): z = 1.1395
   - Compressibility: c = 0.000153 (1/psi)
   - Volume factor: B = 0.5809 (RB/STB) at pressure of 6545 (psi)
   - Thickness: h = 83% (ft) 35%/fcalc'd
   - Perforated thickness: h_p = 137 (ft)
   - Porosity: ϕ = 5 (%)
   - Wellbore radius: r_w = 0.3 (ft)
   - Bottom-hole temperature: T = 102 (°F)

$$B_g = \frac{0.00504\,T\,z}{P}$$

$$= \frac{0.00504 \times 662 \times 1.1395}{6545} = 0.0005409 \text{ RM/SCF}$$

4. Initial pressure: p_i = 6545 (psi) extrapolated Horner plot
5. Flowing bottom-hole pressure: p_{wf} = 6114 (psi)
6. Wellbore storage: C = _____ (RB/psi)
7. End of infinite-acting flow: Δt_{ef} = _____ (min)
8. Middle time region slope: m = 58 (psi)
9. Extrapolated pressure: p^* = 6487 (psi)
10. Ideal building pressure at Δt = 1 hr: p_{1ft} = 6420 (psi)
11. Permeability-thickness product: $kh = \frac{162.6\,q\mu B}{m}$

$$kh = \frac{162.6\,(29343)\,(0.027)\,(0.5809)}{58} = 1290.1 \text{ (md-ft)}$$

12. Permeability: $k = \frac{kh}{h} = \frac{(1290.1)}{(256)}$ = 5.52 (md)

Pg 1 of 2

13. Diffusivity: $\eta = \frac{2.637 \times 10^{-4}\,k}{\phi\mu c}$

$$= \frac{2.637 \times 10^{-4}\,(5.52)}{(0.05)\,(0.027)\,(0.000153)} = 6920 \text{ (ft}^2\text{/hr)}$$

14. Average permeability: $\bar{k} = \frac{141.2\,qB\mu \ln(r_e/r_w)}{h\,(p^* - p_{wf})}$ ($\ln r_e/r_w$ = 6.0–8.0)

$$kE = \frac{141.2\,(29343)\,(0.027)\,(0.5809)\,\ln(\quad/\quad)}{(\quad)\,((6487) - (6114))} = 1289.5 \text{ (md)}$$

15. Radius of investigation beginning of MTR:

$$R_{ib} = \sqrt{\eta\Delta t_{MTR}} = \sqrt{6920\,(14.33)} = 630 \text{ (ft)}$$

16. Skin factor: $s = 1.151\left[\frac{p_{1ft} - p_{wf}}{m} - \log\left(\frac{k}{\phi\mu c r_w^2}\right) + 3.23\right]$

$$s = 1.151\left[\frac{((6420) - (6114))}{(58)} - \log\frac{(5.52)}{(0.05)(0.027)(0.000153)(0.3)^2} + 3.23\right]$$

s = 0.072 ≈ 0

17. Pressure drop due to skin:

$\Delta p_s = 0.87\,ms$ = 0.87 (____)(____) = _____ (psi)

18. Flow efficiency: $E = \frac{p^* - p_{wf} - \Delta p_s}{p^* - p_{wf}}$

$E = \frac{(\quad) - (\quad) - (\quad)}{(\quad) - (\quad)}$ = 1

19. Damage ratio: $DR = \frac{1}{E} = \frac{1}{(\quad)}$ = 1

20. Productivity index: $J = \frac{q}{p^* - p_{wf}} = \frac{(29343)}{((6487) - (6114))}$ = 79 (MSCF/D/psi)

21. Closest possible boundary: L_{cb} 672 (ft)

$$L_{cb} = \sqrt{\frac{0.000237\,kt}{\phi\mu c\,[t_p/\Delta t/(r_w)^2]_{Fig.2}}}$$

$$= \sqrt{\frac{0.000237 \times 5.52 \times 14.33}{4 \times 0.05 \times 0.027 \times 0.000015 \times 1.4}}$$

= 672 ft

Pg 2 of 2

Reservoir Engineering I, 2012
HW NO 7 no.2, Due date: Friday, August 24, 2012
Unsteady State Flow
Chapter 7; 7.20, 7.21, 7.23, 7.25, 7.28

ANSWERS TO THE PROBLEMS

7.20; 32.23 psi
7.21; 22.5 psi
7.23; ΔP = 107 psi,
Pencounter = 4300-107= 4193 psia.
7.25 m = -57 psi/cycle, k = 14.3 md.
S = 0.01, Ahφ = 5,600,000 bbl
7.28 m = -14 psi/cycle, k = 226 md.
S = 14.5

Chapter 8

12. CHAPTER 8
11th week 20-24 AUGUST 2012

Water Influx

WATER INFLUX

I. INTRODUCTION

Many reservoirs are bounded on a portion or all of their peripheries by water-bearing rocks called *aquifers* (Latin:aqua—water, ferre—to bear). The aquifers may be so large compared with the reservoirs they adjoin as to appear infinite for all practical purposes, and they may range down to those so small as to be negligible in their effect on reservoir performance. The aquifer itself may be entirely bounded by impermeable rock so that the reservoir and aquifer together form a closed, or volumetric, unit (Fig. 8.1). On the other hand, the reservoir may outcrop at one or more places where it may be replenished by surface waters (Fig. 8.2). Finally, an aquifer may be essentially horizontal with the reservoir it adjoins, or it may rise, as at the edge of structural basins, considerably above the reservoir to provide some artesian kind of flow of water to the reservoir.*

In response to a pressure drop in the reservoir, the aquifer reacts to offset, or retard, pressure decline by providing a source of water influx or encroachment by (a) expansion of the water; (b) expansion of other known or unknown hydrocarbon accumulations in the aquifer rock; (c) compressibility

*References throughout the text are given at end of each chapter.

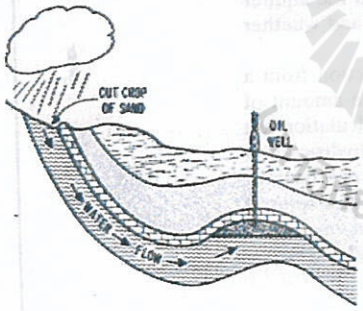

Fig. 68—Reservoir having artesian water drive.

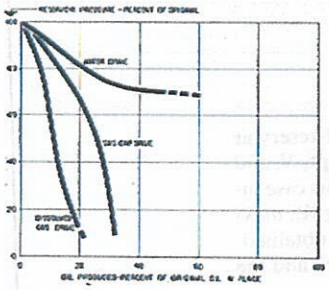

Fig. 69—Reservoir pressure trends for reservoirs under various drives.

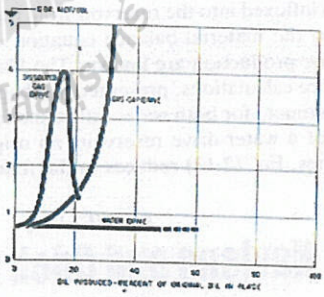

Fig. 70—Reservoir gas-oil ratio trends for reservoirs under various drives. (Courtesy API, Drilling and Production Practices—1943.)

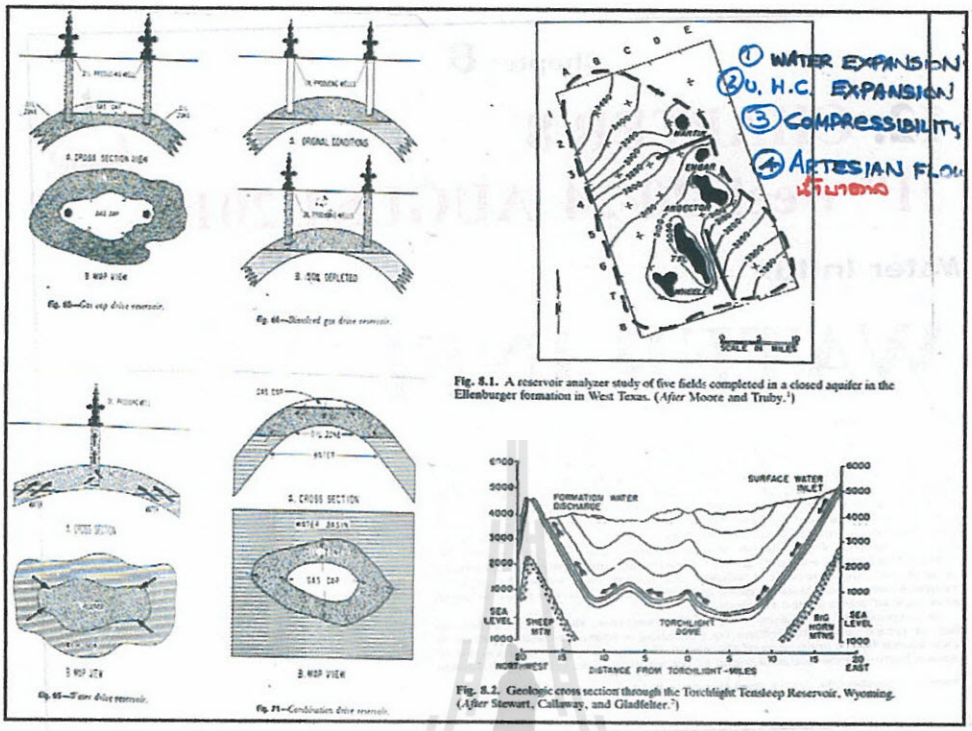

Fig. 8.1. A reservoir analyzer study of five fields completed in a closed aquifer in the Ellenburger formation in West Texas. (*After* Moore and Truby.[4])

Fig. 8.2. Geologic cross section through the Torchlight Tensleep Reservoir, Wyoming. (*After* Stewart, Callaway, and Gladfelter.[5])

of the aquifer rock; and/or (d) artesian flow, which occurs when the aquifer rises to a level above the reservoir, whether it outcrops or not, and whether or not the outcrop is replenished by surface water.

To determine the effect that an aquifer has on the production from a hydrocarbon reservoir, it is necessary to be able to calculate the amount of water that has influxed into the reservoir from the aquifer. This calculation can be made using the material balance equation when the initial hydrocarbon amount and the production are known. The Havlena and Odeh approach to material balance calculations, presented in Chapter 2, can sometimes be used to obtain an estimate for both water influx and initial hydrocarbon amount.[3,4] For the case of a water-drive reservoir, no original gas cap, and negligible compressibilities, Eq. (2.13) reduces to the following:

$$F = NE_o + W_e$$

or

Havlena and Odeh approach

$$\frac{F}{E_o} = N + \frac{W_e}{E_o}$$

If correct values of W_e are placed in this equation as a function of reservoir pressure, then the equation should plot as a straight line with intercept, N, and slope equal to unity. The procedure to solve for both W_e and N in this case involves assuming a model for W_e as a function of pressure, calculating W_e, making the plot of F/E_o versus W_e/E_o, and observing if a straight line is obtained. If a straight line is not obtained, then a new model for W_e is assumed and the procedure repeated.

2. STEADY-STATE MODELS

The simplest model we discuss is the Schilthuis steady-state model, in which the rate of water influx, dW_e/dt, is directly proportional to $(p_i - p)$, where the pressure, p, is measured at the original oil-water contact.[5] This model assumes that the pressure at the external boundary of the aquifer is maintained at the

Steady State Model (Schilthuis)

The simplest method for characterizing water influx is due to Schilthuis [3]. It is often a good idea to try this model first since the calculations are considerably less involved than with either of the other two methods.

The assumptions inherent in the Schilthuis model are many. First, it is assumed that the aquifer is gigantic and highly permeable. In fact, the aquifer is taken to have permeability so high that the pressure gradient across the aquifer itself is negligible. And the aquifer is so huge that the pressure within the aquifer never declines; i.e., the initial pressure, P_i, always exists at all locations within the aquifer. Consider the hydraulic analog to the Schilthuis steady state model shown below.

dW_e/dt directly propertional to (p_i-p)

Then $dW_e/dt = k^*(p_i-p)$

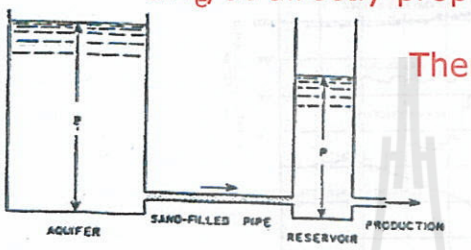

Hydraulic analog of steady-state water influx into a reservoir (from Craft & Hawkins[4]).

STEADY STATE MODELS

$dw/dt \propto (pi-p)$

Water Influx

initial value p_i and that flow to the reservoir is, by Darcy's Law, proportional to the pressure differential, assuming the water viscosity, average permeability, and aquifer geometry remain constant,

Schilthuis Model.

$\frac{F}{E_o} = N + \frac{W_e}{E_o}$

$$W_e = k' \int_0^t (p_i - p)dt \quad (8.1)$$

$$\frac{dW_e}{dt} = k'(p_i - p) \quad (8.2)$$

where k' is the water influx constant in barrels per day per pounds per square inch and $(p_i - p)$ is the boundary pressure drop in pounds per square inch. If the value of k' can be found, then the value of the cumulative water influx W_e can be found from Eq. (8.1), from a knowledge of the pressure history of the reservoir. If during any reasonably long period the rate of production and reservoir pressure remain substantially constant, it is obvious that the volumetric withdrawal rate, or *reservoir voidage rate*, must equal the water influx rate, or

$$\frac{dW_e}{dt} = \begin{bmatrix}\text{Rate of active}\\ \text{oil volumetric}\\ \text{voidage}\end{bmatrix} + \begin{bmatrix}\text{Rate of free}\\ \text{gas volumetric}\\ \text{voidage}\end{bmatrix} + \begin{bmatrix}\text{Rate of water}\\ \text{volumetric}\\ \text{voidage}\end{bmatrix}$$

In terms of single-phase oil volume factors

$$\frac{dW_e}{dt} = B_o\frac{dN_p}{dt} + (R - R_{so})\frac{dN_p}{dt}B_g + \frac{dW_e}{dt}B_w \quad (8.3)$$

where dN_p/dt is the daily oil rate in STB/day and $(R - R_{so})dN_p/dt$ is the daily free gas rate in SCF/day. The solution gas-oil ratio R_{so} is subtracted from the *net daily or current* gas-oil ratio R because the solution gas R_{so} is accounted for in the oil volume factor B_o of the oil voidage term. Equation (8.3) may be converted to an equivalent one using two-phase volume factors by adding and subtracting the term $R_{so}B_gdN_p/dt$, and grouping as

$$\frac{dW_e}{dt} = [B_o + (R_{so} - R_{so})B_g]\frac{dN_p}{dt} + (R - R_{so})B_g\frac{dN_p}{dt} + B_w\frac{dW_e}{dt}$$

and since $[B_o + (R_{so} - R_{so})B_g]$ is the two-phase volume factor B_t:

$$\frac{dW_e}{dt} = B_t\frac{dN_p}{dt} + (R - R_{so})B_g\frac{dN_p}{dt} + B_w\frac{dW_e}{dt} \quad (8.4)$$

When dW_e/dt has been obtained in terms of the voidage rates by Eqs. (8.3) or

2. STEADY-STATE MODELS

The simplest model we discuss is the Schilthuis steady-state model, in which the rate of water influx, dW_e/dt, is directly proportional to $(p_i - p)$, where the

Then $dW_e/dt = k^*(p_i-p)$

WATER INFLUX

Aquifer Description

The aquifer can be either of several types depending on the geometrical configuration:

(a) Linear

Schilthuis Steady State (Darcy)

$\frac{\Delta We}{\Delta t} = k'(P_i - P)$ or $We = k'\int_0^t (P_i - P)$

Hurst

$\frac{\Delta We}{\Delta t} = \frac{C'(P_i - P)}{\log t}$

(b) Radial

or it may be characterized depending on how the water encroaches.

B. Water production during the period was negligible. Example 8.1 he calculation of the water influx constant k' for the Conroe Field from r this period of stabilized pressure. If the pressure stabilizes and the awal rates are not reasonably constant, the water influx for the period ilized pressure may be obtained from the total oil, gas, and water es for the period.

P. stabilize แล้ว ค่าจะ

$$\Delta W_e = B_t \Delta N_p + (\Delta G_p - R_{soi} \Delta N_p) B_g + B_w \Delta W_p$$

ΔG_p, ΔN_p, and ΔW_p are the gas, oil, and water produced during the l in surface units. The influx constant is obtained by dividing ΔW_e by the ct of the days in the interval *and* the stabilized pressure drop $(p_i - p_s)$,

$$k' = \frac{\Delta W_e}{\Delta t (p_i - p_s)}$$

$\Delta w = k(\Delta P)\Delta t$

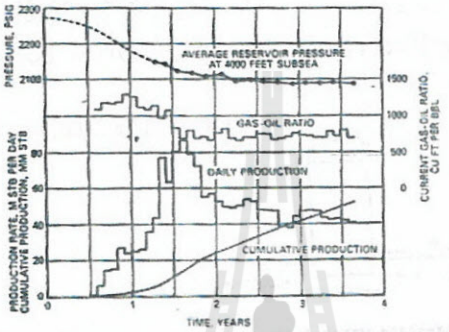

g. 8.3. Reservoir pressure and production data, Conroe Field. (*After* Schilthuis.[5])

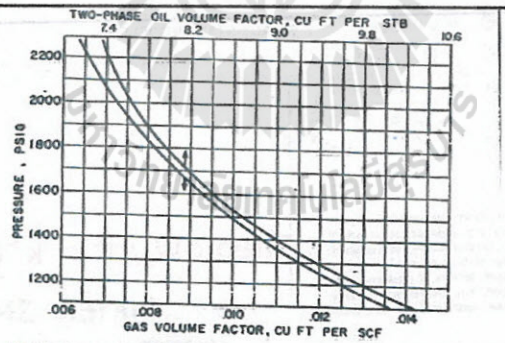

Fig. 8.4. Pressure volume relations for Conroe Field oil and original complement of dissolved gas. (*After* Schilthuis.[5])

Example 8.1. Calculating the water influx constant when reservoir pressure stabilizes.

Given:

.he PVT data for Conroe Field, Fig. 8.4:

$p_i = 2275$ psig

$p_s = 2090$ psig (stabilized pressure)

$B_t = 7.520$ cu ft/STB at 2090 psig

$B_g = 0.00693$ cu ft/SCF at 2090 psig

$R_{soi} = 600$ SCF/STB (initial solution gas)

$R = 825$ SCF/STB, from production data

$dN_p/dt = 44{,}100$ STB/day, from production data

$dW_p/dt = 0$

SOLUTION: At 2090 psig by Eq. (8.4) the daily voidage rate is

2. Steady-State Methods

$$\frac{dV}{dt} = 7.520 \times 44{,}100 + (825 - 600)0.00693 \times 44{,}100 + 0$$

$$= 401{,}000 \text{ cu ft/day}$$

Since this must equal the water influx rate at stabilized pressure conditions, by Eq. (8.2)

$$\frac{dV}{dt} = \frac{dW_e}{dt} = 401{,}000 = k'(2275 - 2090)$$

$$k' = 2170 \text{ cu ft/day/psi}$$

A water influx constant of 2170 cu ft/day/psi means that if the reservoir pressure suddenly drops from an initial pressure of 2275 to, say, 2265 psig (i.e., $\Delta p = 10$ psi) and remains there for 10 days, during this period the water influx will be

$$\Delta W_{e1} = 2170 \times 10 \times 10 = 217{,}000 \text{ cu ft}$$

If at the end of 10 days it drops to, say, 2255 (i.e., $\Delta p = 20$ psi) and remains there for 20 days, the water influx during this second period will be

$$\Delta W_{e2} = 2170 \times 20 \times 20 = 868{,}000 \text{ cu ft}$$

This is four times the influx in the second period because the influx rate was twice as great (because the pressure drop was twice as great) and because the interval was twice as long. The cumulative water influx at the end of 30 days, then, is

$$W_e = k' \int_0^{30} (p_i - p)\, dt = k' \sum_0^{30} (p_i - p)\Delta t$$

$$= 2170[(2275 - 2265) \times 10 + (2275 - 2255) \times 20]$$

$$= 1{,}085{,}000 \text{ cu ft}$$

In Fig. 8.5 the $\int_0^t (p_i - p)dt$ is represented by the area *beneath* the curve of *pressure drop*, $(p_i - p)$, plotted versus time; or it represents the area *above* the curve of *pressure* versus time. The areas may be found by graphical integration.

One of the problems associated with the Schilthuis steady-state model is that as the water is drained from the aquifer, the distance that the water has to travel to the reservoir increases. Hurst suggested a modification to the Schilthuis equation by including a logarithmic term to account for this increasing distance.* The Hurst method has met with limited application and is

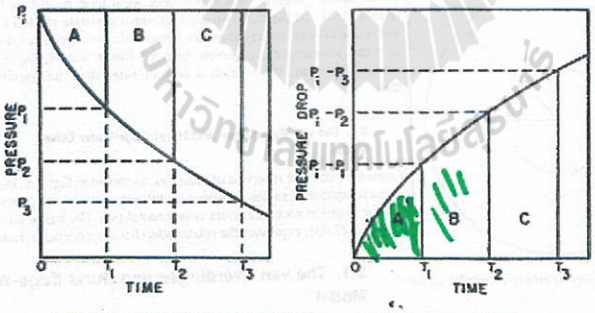

Fig. 8.5. Plot of pressure and pressure drop versus time.

Hurst modified To Schilthuis

$$W_e = c' \int_0^t \frac{(p_i - p)dt}{\log at}$$

$$\frac{dW_e}{dt} = \frac{c'(p_i - p)}{\log at}$$

where c' is the water influx constant in barrels per day per pounds per square inch, $(p_i - p)$ is the boundary pressure drop in pounds per square inch, and a is a time conversion constant that depends on the units of the time t.

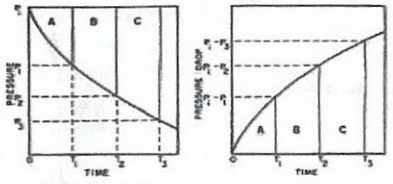

Fig. 8.5. Plot of pressure and pressure drop versus time.

$$W_e = c' \int_0^t \frac{(p_i - p)dt}{\log at}$$

$$\frac{dW_e}{dt} = \frac{c'(p_i - p)}{\log at}$$

where c' is the water influx constant in barrels per day per pounds per square inch, $(p_i - p)$ is the boundary pressure drop in pounds per square inch, and a is a time conversion constant that depends on the units of the time t.

3. UNSTEADY-STATE MODELS

In nearly all applications, the steady-state models discussed in the previous section are not adequate in describing the water influx. The transient nature of the aquifers suggests that a time-dependent term be included in the calculations for W_e. In the next two sections, unsteady-state models for both edge-water and bottom-water drives are presented. An edge-water drive is defined as water influxing the reservoir from its flanks with negligible flow in the vertical direction. In contrast, a bottom-water drive has significant vertical flow.

3.1. The van Everdingen and Hurst Edge-Water Drive Model

Consider a circular reservoir of radius r_R, as shown in Fig. 8.6, in a horizontal, circular aquifer of radius r_e, which is uniform in thickness, permeability, and porosity, and in rock and water compressibilities. The radial diffusivity equation, Eq. (7.35), expresses the relationship between pressure, radius, and time

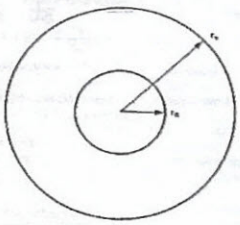

Fig. 8.6. Circular reservoir inside a circular aquifer.

for a radial system such as Fig. 8.6, where the driving potential of the system is the water expandibility and the rock compressibility:

$$\frac{\partial^2 p}{\partial r^2} + \frac{1}{r}\frac{\partial p}{\partial r} = \frac{\phi \mu c_t}{0.0002637k}\frac{\partial p}{\partial t} \tag{7.35}$$

This equation was solved in Chapter 7 for what is referred to as the *constant terminal rate case*. The constant terminal rate case requires a constant flow rate at the inner boundary, which was the wellbore for the solutions of Chapter 7. This was appropriate for the applications of Chapter 7 since it was desirous to know the pressure behavior at various points in the reservoir because a constant flow of fluid came into the wellbore from the reservoir.

In this chapter, the diffusivity equation is applied to the aquifer where the inner boundary is defined as the interface between the reservoir and the aquifer. With the interface as the inner boundary, it would be more useful to require the pressure at the inner boundary to remain constant and observe the flow rate as it crosses the boundary or as it enters the reservoir from the aquifer. Mathematically, this condition is stated as

$$p = \text{constant} = p_i - \Delta p \text{ at } r = r_R \tag{8.5}$$

where r_R is a constant and is equal to the outer radius of the reservoir (i.e., the original oil-water contact). The pressure p must be determined at this original oil-water contact. Van Everdingen and Hurst[7] solved the diffusivity equation for this condition, which is referred to as the *constant terminal pressure case*, and the following initial and outer boundary conditions:

3. UNSTEADY-STATE MODELS

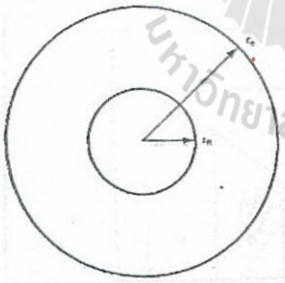

Fig. 8.6. Circular reservoir inside a circular aquifer.

for a radial system such as Fig. 8.6, where the driving potential of the system is the water expandibility and the rock compressibility:

$$\frac{\partial^2 p}{\partial r^2} + \frac{1}{r}\frac{\partial p}{\partial r} = \frac{\phi \mu c_t}{0.0002637k}\frac{\partial p}{\partial t} \tag{7.35}$$

This equation was solved in Chapter 7 for what is referred to as the *constant terminal rate case*. The constant terminal rate case requires a constant flow rate at the inner boundary, which was the wellbore for the solutions of Chapter 7. This was appropriate for the applications of Chapter 7 since it was desirous to know the pressure behavior at various points in the reservoir because a constant flow of fluid came into the wellbore from the reservoir.

In this chapter, the diffusivity equation is applied to the aquifer where the inner boundary is defined as the interface between the reservoir and the aquifer. With the interface as the inner boundary, it would be more useful to require the pressure at the inner boundary to remain constant and observe the flow rate as it crosses the boundary or as it enters the reservoir from the aquifer. Mathematically, this condition is stated as

$$p = \text{constant} = p_i - \Delta p \text{ at } r = r_R \tag{8.5}$$

where r_R is a constant and is equal to the outer radius of the reservoir (i.e., the original oil-water contact). The pressure p must be determined at this original oil-water contact. Van Everdingen and Hurst[7] solved the diffusivity equation for this condition, which is referred to as the *constant terminal pressure case*,

3.1. The van Everdingen and Hurst Edge-Water Drive Model

Unsteady State Model

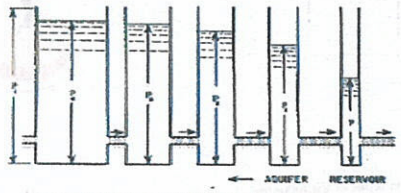

Fig. 5.2. Hydraulic analog of unsteady-state water influx into a reservoir.

tion rate in a manner such as that shown in Fig. 5.3 for a constant reservoir production rate, and Fig. 5.4 for constant reservoir pressure.

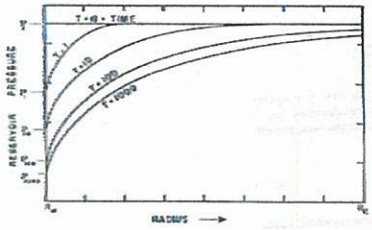

Fig. 5.3. Pressure distributions in an aquifer at several time periods, for a constant rate of water influx across a circumference of radius r_e.

From if there is an infinite number of aquifer tanks, it is evident that reservoir pressure can never fully stabilize at constant production rate, because an ever-increasing portion of the water influx must come from an ever-increasing distance. This will be reflected in a decline in the value of f_t in Eq. (5.1). This decline in the potential or activity of the aquifer is embodied in the water influx expressions Eq. (5.2) and (5.3).

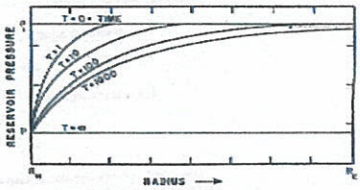

Fig. 5.4. Pressure distributions in an aquifer at several time periods, for a constant boundary pressure maintained at radius r_e.

3. Water Influx from Solutions to the Diffusivity Equation. Consider a circular reservoir of radius r_e in a horizontal, circular aquifer of radius r_e, which is uniform in thickness, permeability, and porosity, and in rock and water compressibilities. Such a system may be represented by the hydraulic analog of Fig. 5.2 if the aquifer is thought of as a series of concentric, cylindrical elements such as shown in Fig. 5.5. The volumes of the

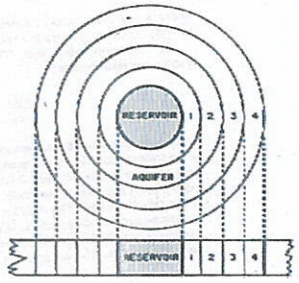

Fig. 5.5. Cylindrical elements in an aquifer surrounding a circular reservoir.

Unsteady

A Edge

(a) Edgewater

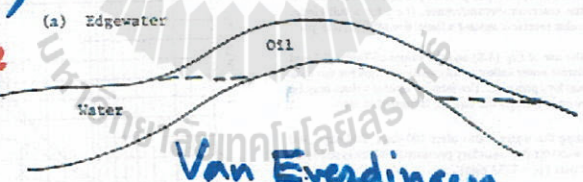

Van Everdingen + Hurst

(b) Bottom water:

B. Bottom

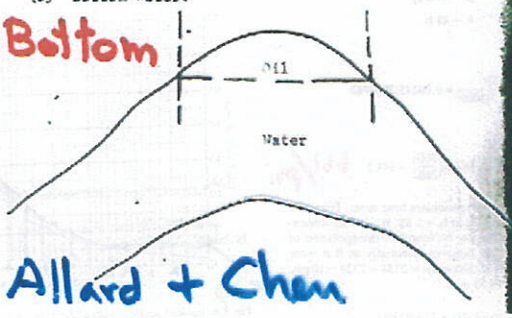

Allard + Chen